## Novel Mathematical Techniques for Scattering Amplitudes

#### Dissertation

zur

Erlangung des Doktorgrades (Dr. rer. nat.) der Mathematisch-Naturwissenschaftlichen Fakultät der Rheinischen Friedrich-Willhelms Universität Bonn

 ${\it vorgelegt\ von}$  Franziska Maria Porkert

aus

Mühldorf a. Inn

Bonn, März 2025

Angefertigt mit Genehmigung der Mathematisch-Naturwissenschaftlichen Fakultät der Rheinischen Friedrich-Willhelms-Universität Bonn

Gutachter/Betreuer: Prof. Dr. Claude Duhr Gutachter: Prof. Dr. Albrecht Klemm Gutachter: Prof. Dr. Pierpaolo Mastrolia

Tag der Promotion: 24.10.2025

Erscheinungsjahr: 2025

Il faut imaginer Sisyphe heureux. – Albert Camus

## Summary

In this thesis, we discuss mathematical methods to compute families of Feynman integrals. Central to our approach are two mathematical structures: the geometries underlying integral families, and their associated twisted (co-)homology groups. We use the latter to derive general relations among integrals and understand the so-called canonical form of a basis of master integrals better. Additionally, we present the analytic computation of several integral families: specific Lauricella integrals associated with hyperelliptic curves, the unequal-mass kite integral family, and two-dimensional (fishnet) integrals.

We begin by reviewing the physical and mathematical background. Starting with a brief summary of the role of Feynman integrals in perturbative quantum field theory, we introduce key tools such as their parametric representations, their cuts, and the method of differential equations, which relies on finding a so – called canonical basis of an integral family. Then we introduce the mathematical background: We discuss the geometries appearing in the integral families studied in this thesis – including hyperelliptic curves and Calabi–Yau varieties – and review the twisted (co-)homology groups, with an emphasis on the computation of intersection and period matrices.

We conclude the first part by discussing how a matrix of cuts of Feynman integrals can be interpreted as a period matrix of twisted (co-)homology groups. This interpretation provides a transition into one of the central results of this thesis: We explore what can be learned from the so-called twisted Riemann bilinear relations for the intersection and period matrices of twisted (co-)homology groups associated to a Feynman integral family. These relations not only explain known and provide new relations, but also enable us to gain a deeper understanding of the canonical basis. Then we use these insights to construct canonical differential equations for Lauricella integral families associated to genus-one and genus-two hyperelliptic curves which serve as models for hyperelliptic maximal cuts. Next we present the analytic computation of the unequal-mass kite integral family, which is related to two distinct elliptic curves. A key step is the parametrisation of the five kinematic variables on two elliptic tori, enabling the solution in terms of iterated integrals on these tori. Then we study single-valued Feynman integrals in two spacetime dimensions. We show how these integrals naturally are bilinear combinations – effectively, double copies – of twisted periods. This construction is equivalent to the one of the Kähler potential of a Calabi-Yau geometry, which we exploit to compute the conformal fishnet integrals directly from the data of their associated Calabi-Yau varieties.

The techniques developed here provide a conceptual bridge between the abstract mathematics of (twisted) periods and the analytic computation of Feynman integrals, e.g., for scattering amplitudes.

### List of Publications

This thesis contains the results of the following peer-reviewed and published papers:

- [1] Claude Duhr, Albrecht Klemm, Florian Loebbert, Christoph Nega, and Franziska Porkert. "Yangian-Invariant Fishnet Integrals in Two Dimensions as Volumes of Calabi-Yau Varieties". In: *Phys. Rev. Lett.* 130.4 (2023), p. 041602. DOI: 10.1103/PhysRevLett. 130.041602. arXiv: 2209.05291 [hep-th].
- [2] Claude Duhr and Franziska Porkert. "Feynman integrals in two dimensions and single-valued hypergeometric functions". In: *JHEP* 02 (2024), p. 179. DOI: 10 . 1007 / JHEP02(2024)179. arXiv: 2309.12772 [hep-th].
- [3] Claude Duhr, Albrecht Klemm, Florian Loebbert, Christoph Nega, and Franziska Porkert. "The Basso-Dixon formula and Calabi-Yau geometry". In: *JHEP* 03 (2024), p. 177. DOI: 10.1007/JHEP03(2024)177. arXiv: 2310.08625 [hep-th].
- [4] Mathieu Giroux, Andrzej Pokraka, Franziska Porkert, and Yoann Sohnle. "The soaring kite: a tale of two punctured tori". In: *JHEP* 05 (2024), p. 239. DOI: 10.1007/JHEP05(2024)239. arXiv: 2401.14307 [hep-th].
- [5] Claude Duhr, Albrecht Klemm, Florian Loebbert, Christoph Nega, and Franziska Porkert. "Geometry from integrability: multi-leg fishnet integrals in two dimensions". In: *JHEP* 07 (2024), p. 008. DOI: 10.1007/JHEP07(2024)008. arXiv: 2402.19034 [hep-th].
- [6] Claude Duhr, Franziska Porkert, Cathrin Semper, and Sven F. Stawinski. "Twisted Riemann bilinear relations and Feynman integrals". In: *JHEP* 03 (2025), p. 019. DOI: 10.1007/JHEP03(2025)019. arXiv: 2407.17175 [hep-th].
- [7] Claude Duhr, Franziska Porkert, Cathrin Semper, and Sven F. Stawinski. "Self-duality from twisted cohomology". In: *JHEP* 03 (2025), p. 053. DOI: 10.1007/JHEP03(2025) 053. arXiv: 2408.04904 [hep-th].
- [8] Claude Duhr, Franziska Porkert, and Sven F. Stawinski. "Canonical differential equations beyond genus one". In: *JHEP* 02 (2025), p. 014. DOI: 10.1007/JHEP02(2025)014. arXiv: 2412.02300 [hep-th].

Some of the content of [4] also appeared in the following conference proceedings:

[9] Mathieu Giroux, Andrzej Pokraka, Franziska Porkert, and Yoann Sohnle. "Looping the loops: a tale of elliptic dual Feynman integrals". In: *PoS* RADCOR2023 (2024), p. 033. DOI: 10.22323/1.432.0033. arXiv: 2309.04592 [hep-th].

Parts of the discussion in Subsection 4.2.3 are based on unpublished work:

[10] Axel Kleinschmidt, Franziska Porkert, and Oliver Schlotterer. "UUITP-xx/24 Towards Motivic Coactions at Genus One from Zeta Generators [In Progress]". In: (2025).

The following paper was published during the PhD, but its content is not included in this thesis:

- [11] Franziska Porkert and Oliver Schlotterer. "One-loop amplitudes in Einstein-Yang-Mills from forward limits". In: *JHEP* 02 (2023), p. 122. DOI: 10.1007/JHEP02(2023)122. arXiv: 2201.12072 [hep-th].
- ♠ We mention the papers the results presented in a given chapter/section are based on in their introductions.

# Contents

Li	List of Symbols 1			
1	Intr	oducti	ion	11
2	Fey	nman	Integrals	18
	2.1	Feynn	nan Integrals in High Energy Physics	20
	2.2	Feynn	nan Integrals: Representations	26
		2.2.1	Momentum Representation	27
		2.2.2	Schwinger and Feynman Parameter Representation	29
		2.2.3	Baikov Representation	31
	2.3	Feynn	nan Integrals: Cuts	32
	2.4		nan Integrals: Examples	33
		2.4.1	The Sunrise and Kite Integral Families	34
		2.4.2	The Non-planar Crossed Box Family	37
		2.4.3	Fishnet Integrals	40
	2.5	Feynn	nan Integrals: Differential Equations	43
		2.5.1	Linear Relations Between Feynman Integrals	44
		2.5.2	Differential Equations for Feynman Integrals	45
3	Geo	metrie	es and Special Functions for Feynman Integrals	52
J	3.1		Homology Groups and Periods	54
	3.2	,	ann Surfaces and Hyperelliptic Curves	58
	0.2	3.2.1	Basics on Hyperelliptic Curves	58
		3.2.2	Elliptic Curves and Tori	65
	3.3	_	i-Yau Varieties	71
	3.4		ed Integrals and Special Functions	75
	0.1	3.4.1	Multiple Polylogarithms	75
		3.4.2	Modular Forms and Iterated Eisenstein Integrals	77
		3.4.3	Elliptic Multiple Polylogarithms	82
		3.4.4	Siegel Modular Forms and Abelian Differentials	84
	3.5		etry And Feynman Integrals	90
4	$Tw^{i}$	isted a	nd Motivic (Co-)Homology Groups	94
_	4.1		w of Twisted (Co-)Homology Groups	
		4.1.1	Review: Twisted (Co-)homology	
		4.1.2	Review: Relative Twisted Cohomology	

### CONTENTS

	4.2	Review: Motivic Periods for Phycisists	115
		4.2.1 Motivic and de Rham Periods	115
		4.2.2 Single-valued Periods	118
		4.2.3 Coactions	121
	4.3	Aomoto-Gelfand Hypergeometric Functions	
		4.3.1 Definition of Aomoto-Gelfand Hypergeometric Functions	
		4.3.2 Single-valued Hypergeometric Functions	
	4.4	Feynman Integrals and Their Cuts as Twisted Periods	
5	$Tw^{i}$	isted Riemann Bilinear Relations and Cuts of Feynman Integrals	138
	5.1	Bilinear Relations for Feynman Integrals	140
		5.1.1 Classification of the TRBRs for Feynman Integrals	142
		5.1.2 Bilinear Relations for Maximal Cuts	
		5.1.3 Examples	
	5.2	The Intersection Matrix for Canonial Differential Equations	153
		5.2.1 Properties of Canonical Differential Equations	154
		5.2.2 Bases in C-Form and the Intersection Matrix	158
		5.2.3 Maximal Cuts in $C$ -Form	162
6	Нур	perelliptic Maximal Cuts	166
	6.1	DEQs for Hyperelliptic Lauricella Functions	168
		6.1.1 Review: Algorithm	168
		6.1.2 Elliptic Hypergeometric ${}_{2}F_{1}$ -function	171
		6.1.3 Three Parameter Lauricella Function	
		6.1.4 Four Parameter Lauricella Function	179
	6.2	Modular properties of the Canonical Differential Equation	183
		6.2.1 Modular Properties of the Connection Matrix $\mathbf{B}_{H,3}(\boldsymbol{\lambda},\varepsilon)$	
		6.2.2 Modular Properties of the Connection Matrix $\mathbf{B}_{H,5}(\boldsymbol{\lambda},\varepsilon)$	
7	The	e Kite Integral Family	188
	7.1	The Kite Integral Family	190
	7.2	The $\varepsilon$ -form Differential Equation	195
		7.2.1 Sunrise subtopology	196
		7.2.2 Eyeball subtopology	197
		7.2.3 Full Kite Family	203
	7.3	Pullback on the Tori	208
		7.3.1 Algorithmic Pullback	209
		7.3.2 Comments on the Forms	215
	7.4	Boundary Value and Integration	218
8	Mas	ssless Feynman Integrals in 2D	222
	8.1	Single-valued Hypergeometric Functions	224
	8.2	Conformal Fishnets as Kähler Potentials	229
		8.2.1 Conformal Fishnets in $2D$ as Kähler Potentials	229
		8.2.2 Fishnets as Quantum Volumes	234
		8.2.3 Relations Between One-Parameter Fishnets	235

### CONTENTS

9	Conclusion	<b>240</b>
$\mathbf{A}$	Basic Objects in Mathematics	244
$\mathbf{B}$	Computing Intersection Matrices	246
	B.1 Review: Computing Intersection Numbers	246
	B.1.1 Twisted Cohomology Intersection Numbers	246
	B.1.2 Twisted Homology Intersection Numbers	249
	B.2 Examples (Intersection Matrices)	256
	B.3 The $\varepsilon$ -Dependence of Specific Intersection Numbers	262
$\mathbf{C}$	Additional Relations for Kite Punctures	266
	C.1 Elliptic Integrals	266
	C.2 Relations Between the Punctures	267
$\mathbf{D}$	Extended Calculations	269
	D.1 Laurent Expansion of Differentials on a Hyperelliptic Curve	269
	D.2 Proof for the Linear Independence of Certain Iterated Integrals	270
$\mathbf{E}$	Representation Theory	274

# List of Symbols

Here, we collect the symbols that we use repeatedly throughout the thesis. Note that some of the symbols have different meanings in different contexts. We list those with  $\odot$  and give all meanings. Some symbols that are only used locally are not listed.

Symbol	Meaning
⟨⋅ ⋅]	Period pairing – (4.3)
$[\cdot \cdot\rangle$	Dual period pairing – (4.38)
$\langle \cdot   \cdot \rangle$	⊚ Inner product between de-Rham cohomology groups – (3.10) & (4.36)
	⊚ Bracket of QFT – only in Section 2.1
$[\cdot \cdot]$	Homology intersection pairing $-(4.34)$
(123)	Object related to (123)-sunrise or -torus of the kite integral family
(345)	Object related to (345)-sunrise or -torus of the kite integral family
$a_i$	$\odot$ a cycles of a hyperelliptic curve – figure 3.3
	⊚ Parameters of hypergeometric function – (4.173) & (4.182)
$\alpha_i$	⊚ Indicials in the Frobenius method −(3.23)
	$\odot$ Generic exponent of a factor $L_i(z)$ of the twist $-(4.2)$
	$\odot$ Data of Aomoto-Gelfand hypergeometric function - $(4.163)$
$\mathbf{A}(oldsymbol{\lambda},arepsilon)$	Connection matrix for a vector of master integrals – (2.98)
$\mathcal{A}$	Matrix of a-periods of the hyperelliptic curve $-(3.35)$
$ ilde{\mathcal{A}}$	Matrix of a-quasi-periods of the hyperelliptic curve – (3.46)
$\mathbb{A}_B$	K-algebra of functions – Section 5.2.1
$\mathbb{A}_{oldsymbol{B},arepsilon}$	$\mathbb{A}_{oldsymbol{B}}\otimes_{\mathbb{K}}\mathbb{K}(arepsilon)$
$\mathbb{A}(\epsilon_k;  au)$	Defines generating series for iterated Eisenstein integrals – (3.158)
$b_i$	$\odot$ b cycles of a hyperelliptic curve – figure 3.3
	⊚ Parameters of hypergeometric functions −(4.173) & (4.182)
	$\odot$ Betti number, dim $[H_i(X)]$
B(z,z')	Bidifferential $-(3.200)$
$\mathbf{B}(oldsymbol{\lambda})$	$\varepsilon$ -independent part of canonical connection matrix – (2.103)

Symbol	Meaning
$BF_k$	$\frac{B_k}{k!}$ with $B_k$ the k-th Bernoulli number
$\mathrm{B}^{\mathrm{n}}(\mathrm{M},\mathbb{C})$	$\{n - \text{forms } \varpi \mid \varpi = d\tilde{\varpi}, \text{ where } \tilde{\varpi} \text{ is an } (n-1) - \text{form } \}$
$B_n(M, \mathbb{Z})$	$\{\Delta_{\gamma} \text{ n-chain }   \Delta_{\gamma} = \partial \Delta_{\tilde{\gamma}} \}$
$B^n(X, \nabla_{\Phi})$	$\{n - \text{forms } \nabla_{\Phi} \tilde{\varphi} \mid \tilde{\varphi} \text{ a } n - 1 \text{-form}\}$
$B_n(X, \check{\mathcal{L}}_\Phi)$	{twisted $n - \text{cycles } \partial \gamma \mid \gamma = \Delta_{\gamma}^{c} \otimes \Phi _{\Delta_{\gamma}} \text{ with } \Delta_{\gamma}^{c} \text{ a } n + 1 \text{-cycle }}$
$\mathcal{B}(z)$	Baikov polynomial – (2.37)
$\mathcal{B}_B$	Basis of $\mathbb{E}_{\mathbf{B}}$ – Section 5.2.1
$\mathcal{B}$	Matrix of $b$ -periods of the hyperelliptic curve $-(3.35)$
$ ilde{\mathcal{B}}$	Matrix of $b$ -quasi-periods of the hyperelliptic curve – (3.46)
C	Cohomology intersection matrix – (4.37)
$C^n(M,\mathbb{C})$	$\{n\text{-form }\varpi \mathrm{d}\varpi=0\}$
$C_n(M, \mathbb{Z})$	$\{n - \operatorname{chains}\Delta_{\gamma} \mid \partial \Delta_{\gamma} = 0\}$
$C_n(X, \check{\mathcal{L}}_\Phi)$	$\{\gamma = \Delta_{\gamma}^c \otimes \Phi _{\Delta_{\gamma}^c} \mid \Delta_{\gamma}^c \text{ an } n - \text{cycle and } \partial(\gamma \otimes \Phi _{\gamma}) = 0\}$
$C^n(X, \nabla_{\Phi})$	$\{n - \text{forms } \varphi \text{ on } X \mid \nabla_{\Phi} \varphi = 0\}$
$C^{ ext{cl}}_{i_1,\cdots,i_L}$	Classical intersection numbers – (8.43)
$\mathcal{C}_{j}$	Integration contour in Baikov representation – (2.39)
$\mathfrak{c}_j$	$\exp(2\pi i\alpha_j) - (\mathrm{B.20})$
$\mathfrak{C}(x)$	$\cot(\pi x)$
$\operatorname{Cut}_{j_1,\ldots,j_r}\left[I_{\boldsymbol{\nu}}\right]$	Cut of a Feynman integral – (2.43)
$\mathrm{comp}_{X,\Phi}$	Comparison isomorphism $-(4.124)$
$\chi$ , $\chi_{ijkl}$	Conformal cross ratios – (2.87)
$\chi(X)$	Euler Number
D	Dimension
d	Integer part of the dimension
$D_j$	Propagator of a Feynman graph/integral
$D_{+}$	$\{\boldsymbol{z} \mid \Phi\varphi(\boldsymbol{z}) = 0\} - (4.91)$
$D_{-}$	$\{z \mid z \text{ is a pole of } \Phi \varphi(z) \text{ and } z \notin \Sigma\}$ (4.92)
$D_I^J$	Matrix of determinants of periods – (3.18)
$d_{\mathrm{ext}}$	Exterior derivative in the external coordinates
$d_{\mathrm{int}}$	Exterior derivative in the internal coordinates
d	$d_{int} + d_{ext}$
$\partial_z$	partial derivative in $z - (3.2)$

Symbol	Meaning	
dr	de Rham object	
$\mathfrak{d}_i$	$c_j - 1 - (B.20)$	
$\partial$	Operator that sends n-chain to its boundary (including twist)	
$\delta_i$	⊚ Symbols for Leray co-boundaries – (4.109)	
	⊚ Symbolic generic exponents in regularised poles of the twist	
$\Delta_{\gamma}$	Topological cycle	
$\Delta_{\gamma}^{c}$	Compactified topological cycle	
$\Delta \otimes \Phi _{\Delta}$	Twisted cycle – (4.21)	
$\Delta_p$	Coaction-like map $-(4.154)$	
$\Delta(z)$	Factor in modular forms – (3.147)	
$\Delta_j$	Conformal weights	
E	Linearly independent ext. points of Feynman graph, $E = n_{\text{ext}} - 1$	
$\mathrm{E}(\lambda)$	Elliptic integral $-(3.70)$	
$E(x,y \mathbf{\Omega})$	Prime form $-(3.198)$	
$\mathbb{E}_{\mathbf{B}}$	$\mathbb{K}$ -algebra of generating $e_{I,j}$ – Section 5.2.1	
$\mathbb{E}_{\mathcal{F}}$	$\mathcal{F}_{\mathbb{C}}\otimes \mathbb{E}_{m{B}}$	
$e_{\mathrm{I},i_{\mathrm{k}}}$	Letters of generating series for iterated integrals – (5.91)	
$\epsilon_k^{(j)}$	Tsunogai algebra generators – (3.161)	
$\epsilon$	Characteristics – (3.184)	
$\varepsilon$	Dimensional regulator for Feynman integrals	
$\mathcal{E}\left[egin{array}{cccc} j_1 & j_2 & \cdots & j_\ell \ k_1 & k_2 & \ldots & k_\ell \end{array};  au ight]$	Iterated Eisenstein integrals – (3.152)	
$\eta$	Metric	
$\eta( au)$	Dedekind $\eta$ function – (3.93)	
$\eta_1,\eta_2$	Quasi-periods of an elliptic curve – (3.48)	
$\eta_2(\tau), \eta_4(\tau)$	$\eta$ -function – (3.86)	
F	Second Symanzik Polynomial – (2.24)	
$F_G$	Prefactor with conformal weight	
$F(\lambda)$	Elliptic integral – (3.74)	
$F_{EK}(z, \eta, q)$	Kronecker-Eisenstein series – (3.170)	
$\mathcal{F}_{\mathbb{C}}$	$\operatorname{Frac}(\mathbb{C}\otimes_{\mathbb{K}}\mathbb{A}_{\boldsymbol{B}})$	
$_2F_1$	Gauss' hypergeometric $_2F_1$ function $-$ (4.2)	
$\mathcal{F}(oldsymbol{lpha} oldsymbol{\mu} oldsymbol{\lambda}_{ ext{AG}})$	Aomoto-Gelfand hypergeometric function –(4.163)	

Symbol	Meaning	
g	Genus of a hyperelliptic curve – (3.29)	
$g_2, g_3$	Coefficients in the Weierstrass form $-(3.67) \& (3.81)$	
$g^{(k)}\left(z, au ight)$	g-kernels – $(3.174)$	
$G_k(\tau)$	Eisenstein series – (3.85)	
$G(a_1,\ldots,a_n;x)$	Multiple polylogarithms – Definition (3.21)	
$\mathbb{G}_I$	Generating functional for iterated integrals – (5.91)	
$\mathbb{G}_G$	Generating functional for multiple poylogarithms $G-(3.132)$	
$\det \mathcal{G}(q_1,\ldots,q_n)$	Gram determinant – (2.36)	
$\Gamma_g$	Siegel modular group – (3.179)	
$\Gamma_0(N),\Gamma(N)$	Congruence subgroups – (3.139)	
$\tilde{\Gamma}\left(\begin{smallmatrix} n_1 n_2 \dots n_k \\ w_1 w_2 \dots w_k \end{smallmatrix}; w   \tau\right)$	Elliptic multiple polylogarithms – (3.171)	
$\Gamma\left(\begin{smallmatrix} n_1 n_2 \dots n_k \\ w_1 w_2 \dots w_k \end{smallmatrix}; w   \tau\right)$	Elliptic multiple polylogarithms – (3.177)	
$\gamma_E$	Euler-Mascheroni constant	
Н	Homology intersection matrix – (4.34)	
$H^n_{\mathrm{dR}}(X,\mathbb{C})$	de-Rham cohomology group on $X$ , $\mathrm{C}^{\mathrm{n}}(\mathrm{X},\mathbb{C})/\mathrm{B}^{\mathrm{n}}(\mathrm{X},\mathbb{C})$	
$H_n(X,\mathbb{Z})$	Betti homology group on $X$ , $C_n(X, \mathbb{Z})/B_n(X, \mathbb{Z})$	
$H^n_{\mathrm{dR}}(X,\nabla_\Phi)$	$C^{n}(X, \nabla_{\Phi})/B^{n}(X, \nabla_{\Phi})$	
$H_n(X, \check{\mathcal{L}}_\Phi)$	$C_n(X, \check{\mathcal{L}}_{\Phi})/B_n(X, \check{\mathcal{L}}_{\Phi})$	
$H_n^{lf}(X,\mathcal{L}_\Phi)$	Locally finite version of $H_n(X, \check{\mathcal{L}}_{\Phi})$ – (4.5)	
$H_n(X, D_+, \check{\mathcal{L}}_\Phi)$	Relative twisted homology group – (4.97)	
$H_n(X_+,D,\mathcal{L}_\Phi)$	Dual relative twisted homology group – (4.98)	
$\mathbb{H}_g$	Siegel upper half-space in $\mathbb{C}^{g \times g}$	
$\mathcal{H}_{X,\Phi}$	Tuple of (co-)homologies and comparison isomorphism	
$\mathscr{H}$	Hamiltonian density	
$I(a_0,\dots a_{n+1})$	Multiple polylogarithms – Definition 3.22	
$\mathbf{I}(oldsymbol{\lambda})$	Vector of master integrals	
$I_{\nu}(\{p_ip_j\},\{m_i^2\})$	Feynman integral in momentum representation – (2.12)	
$\mathbb{I}_{\mathcal{E},+}(\epsilon_k; au)$	Generating series for iterated Eisenstein integrals	
j	j-invariant of an elliptic curve – (3.68)	
J	⊚ Complex structure on a manifold	
	⊚ Matrix in Feynman representation – (2.22)	
$J^{\mathrm{a}},~\hat{\mathrm{J}}^{a}$	Yangian generator of level zero and one – (2.82)	

Symbol	Meaning
$K(\lambda)$	Elliptic integral of first kind– (3.70)
$K(\lambda)$	Kähler potential of a Calabi-Yau
K	Some algebraic number field – Definition in A.1
$\mathcal{K}_{ o}$	Kinematic space of the kite integral family – (7.2)
$\mathbf{K}_N$	Skew-diagonal matrix of ones – (5.99)
L	Loop number of a Feynman graph
$L_i(z)$	Factor of the twist $\Phi$
$\ell_i,\ell$	Loop momentum
$\operatorname{Li}_{\mathrm{n}}(\mathrm{z})$	Classical Polylogarithm – (3.20)
$\check{\mathcal{L}}_\Phi, \mathcal{L}_\Phi$	Local systems – (4.5) and Definition A.3
L	Lagrangian
$\Lambda, \Lambda_{\omega_1, \omega_2}, \Lambda_{ au}$	⊚ Lattice in the Jacobian – (3.7)
	⊚ Set of punctures
$oldsymbol{\lambda}, \lambda_i$	⊚ Generic external parameter
	⊚ Parameter of a hyperelliptic curve or Calabi-Yau family
$\lambda(a,b,c)$	Källén function $a^2 + b^2 + c^2 - 2ab - 2ac - 2bc$
$\lambda_{abc}$	$\lambda(X_a, X_b, X_c)$
$M, \mathcal{M}, M_G$	Variety
M	⊚ For fishnet integrals: Number of vertices on the vertical axis
	⊚ Matrix in Feynman representation – (2.22)
$m_i$	Internal mass in a Feynman graph
$\mathbb{M}_0^{\mathfrak{m}}$	Generating series for independent motivic $\zeta$ values – (4.133)
$\mathcal{M}_{ ext{cs}}$	Complex moduli space of a Calabi-Yau family
$\mathcal{M},\mathcal{M}_n$	${\rm Amplitude}-(2.10)$
m	Label for motivic object
$\mathfrak{m} \left[ egin{array}{cccc} j_1 & j_2 & & j_\ell \ k_1 & k_2 & & k_\ell \end{array}  ight]$	Multiple modular values $-(3.155)$
$\mu$	Data of a Aomoto-Gelfand hypergeometric function – (4.163)
$\mu_B(m{x})$	Holomorphic measure on a base space $B$ – used in eq. (3.219)
n	Dimension of space $X$ on which we define twisted (co-)homology groups
N	For fishnet integrals: Number of vertices on the horizontal axis
$n_{ m ext}$	Number of external legs of a Feynman graph
$n_{ m int}$	Number of internal propagators of a Feynman graph

Symbol	Meaning		
$n_{\rm isp}$	Number of irreducible scalar products		
$ u_i, oldsymbol{ u} $	Exponents of propagators in Feynman integral		
$\nu\begin{bmatrix}j\\k\end{bmatrix};\tau\end{bmatrix}$	Kernels for iterated Eisenstein integrals – (3.151)		
$\nabla_{\Phi}$	Twisted connection – (4.3)		
0	Differential operator (e.g., Picard-Fuchs operators)		
Ω	Unique holomorphic differential of a CY		
Ω	Normalised period matrix of a hyperelliptic curve – (3.36)		
$\Omega_{ m EK}(z,\eta)$	Combination of Kronecker Eisenstein forms – (3.176)		
$\Omega^n(M,\mathbb{C})$	Space of $n$ -forms on $M$ over $\mathbb{C}$		
$\Omega^1(\mathbb{A}_B)$	$\mathbb{K}$ -vector space of differential forms with coefficients in $\mathbb{A}_B$		
ω	Kähler form $-(3.94)$		
$\omega_G$	Kähler form of a fishnet graph $G$		
$\omega_1,  \omega_2$	Periods of holomorphic differential of an elliptic curve – (3.37)		
$\omega_n$	Form in hypergeometric functions – (4.165)		
$\omega^{(i)}$	Basis of $\mathrm{H}^{(1,1)}(\mathcal{W}_{\mathrm{G}})$		
$\omega_\Phi$	$\frac{\mathrm{d_{int}\Phi}}{\Phi} = \mathrm{d_{int}log}\Phi - (4.3)$		
$\omega_k(z, au)$	Kronecker Eisenstein forms – (3.175)		
p	Dimension of $C^1(\mathbb{A}_B)$ in Section 5.2.1		
$p_i$	⊚ External momentum of a Feynman diagram		
	$\odot$ Coefficients of differential operators $p_i(z) = \frac{q_i(z)}{q_{\text{deg}}(z)}$		
P	Period matrix – (4.4)		
$\mathbf{P}_{\Theta}^{\mathrm{log}}(oldsymbol{\lambda},arepsilon)$	Maximal cut sector in d log basis		
$\mathcal{P}$	Period matrix for a hyperelliptic curve		
П	Period vector of a (CY) manifold $M$		
$\mathbb{P}\exp$	Path-ordered exponential		
$\wp(z)$	Weierstraß $\mathfrak{p}$ -function – (3.79)		
Φ	Twist - (4.2)		
$\varphi$	Generic form in a twisted cohomology group		
$\phi(x)$	Scalar field in the Lagrangian		
$\phi_G(oldsymbol{\chi})$	Conformal part of the fishnet integrals – (2.86)		
$\phi_{\mathbb{G}_I}$	$\mathbb{E}_{\mathcal{F}}^* \to \mathcal{F}_{\mathbb{C}} \otimes_{\mathbb{K}} \mathcal{V}_{\mathbf{B}}, \ p^* \mapsto p^*(\mathbb{G}_I) = \sum_{w \in \mathcal{S}} f_w J(w)$		

Symbol	Meaning		
$\psi_i(x)$	$\odot$ Polynomials in second kind Abelian differentials – (3.45)		
	⊚ Series needed for the computation of intersection numbers – (B.3)		
$\Psi_j^{2,\mathrm{e}},\Psi_j^{2,\mathrm{o}}$	Polynomials second kind differentials – (3.53)		
$\overline{\omega}$	(p,q)-form		
$\overline{\omega}_i$	Basis element of $\mathbb{V}_{\boldsymbol{B}}$ in Section 5.2.1		
$\tilde{arpi}_i$	Basis element of $C^2(\mathbb{A}_B)$ in Section 5.2.1		
q	$\odot$ Exponential of period, $q = \exp(\pi i \tau) - (3.87)$		
	$\odot$ Dimension of $C^2(\mathbb{A}_B)$ in Section 5.2.1		
$q_i(z)$	⊚ Coefficients of a differential operator – (3.16)		
	$\odot$ Momenta in the propagators – (2.13)		
$\mathbf{R}(oldsymbol{\lambda},arepsilon)$	Dimensional shift matrix – (2.97)		
r	Number of factors in the twist $-(4.2)$		
$ ho_f$	Map between f alphabet and $\zeta$ values		
S	⊙ Physical action		
	⊚ Generator of the modular group – Definition 3.25		
$S_{\Lambda}$	Punctured Riemann sphere		
$\operatorname{Sp}(2g,\mathbb{Z})$	Symplectic group – (3.179)		
$\mathrm{Sol}(\mathbb{O})$	Solution space of an operator $\mathbb{O}-(3.109)$		
$S_{\epsilon}(x)$	$\varepsilon$ -sphere around point $x$		
$\mathcal{S}$	Semi-simple part of a period matrix		
S	Scattering matrix – (2.8)		
$s_2(r,k)$	Stirling number of second kind: $\frac{1}{k!} \sum_{i=0}^{k} {k \choose i} (k-i)^r$		
$ ilde{s}_k$	Symmetric polynomials – e.g., in (3.49)		
$\mathfrak{s}(x)$	$\sin(\pi x)$		
$\sigma$	Permutation		
$\Sigma_i$	Hypersurfaces defined from a twist: $\bigcup_{i=1}^{r} \{ \boldsymbol{z}   L_i(\boldsymbol{z}) = 0 \}$		
$\Sigma_{\lambda}$	Riemann surface family with parameters ${m \lambda}$		
Σ	Homology intersection matrix		
Т	Generator of the modular group – Definition 3.25		
T	Interaction part of the scattering matrix		

Symbol	Meaning
$t_i(z)$	Mirror map – Definition 3.15
$ig  t_{G,i}^{\mathbb{R}}$	Mirror map from fishnet graph $G$
τ	Normalised period of the elliptic curve, $\tau = \frac{\omega_2}{\omega_1}$
$\theta$	$\odot$ Differential operator $\theta_z = z\partial_z$
	⊚ Symbols that track boundaries – (4.109)
$\theta_j^R$	$\odot$ Riemann $\Theta$ constants – Definition 3.12
	$\odot$ Special Jacobi- $\theta$ -functions – (3.89)
$\theta[a,b](z \tau)$	Jacobi- $\theta$ -function – (3.88)
$\Theta_{ u}$	Sectors of Feynman integral family – (2.14)
$\Theta(oldsymbol{z}, oldsymbol{\Omega})$	Classical Riemann $\Theta$ function – Definition 3.38
$\Theta\left[oldsymbol{\epsilon} ight]\left(oldsymbol{z},\Omega ight)$	Riemann $\Theta$ function with characteristics – (3.184)
U	First Symanzik Polynomial – (2.23)
$\mathbf{U}(oldsymbol{\lambda},arepsilon)$	Transformation matrix between bases of Feynman integrals
U	Unipotent part of a period matrix
u	Abel's map $-(3.44)$
$u_i(\boldsymbol{\lambda}, \varepsilon)$	Entries in transformation ansatz to find canonical DEQ
$u_i^{(123)}, u_i^{(345)}$	Functions in the definition of the sunrise punctures – (7.21)
V	Number of propagators going into vertex in a fishnet theory
$V_G$	Number of vertices of a Feynman graph
$\mathbb{V}_B$	Space of differential forms generated by canonical differential equation
$\mathcal{V}_{B}$	$\langle J_{\gamma}(w)   w \in \mathcal{B}_{\boldsymbol{B}} \rangle_{\mathbb{K}} - (5.95)$
$W_G$	Mirror Calabi-Yau to CY $M_G$
$w_{1 j}$	Canonical first kind Abelian differential
$w_{2 w}^{(k)}$	Second kind Abelian differential – (3.208)
$w_{3 z_1,z_2}$	Third kind Abelian differential – (3.204)
$x, \boldsymbol{x}, x_i$	⊚ Coordinate of hyperelliptic curve – (3.28)
	⊚ Internal spacetime coordinates
X	Space on which we define the twisted cohomology groups
$X_i$	Scaleless kinematic parameters of the kite integral family $-$ (7.1)
$X_{\pm}$	$\mathbb{CP}^n - \Sigma - D_{\pm}$
$\xi_i$	Position space coordinates in $\mathbb{R}^2$
y	Coordinate of hyperelliptic curve – (3.28)

Symbol	Meaning
$oldsymbol{y}_{ ext{AG}}$	Data of a Aomoto-Gelfand hypergeometric function – (4.163)
$z_i, oldsymbol{z}$	⊙ Complex coordinate – (3.1)
	⊚ Baikov variables
$z_i^{(123)}, z_i^{(345)}$	Sunrise punctures – (7.20)
$ar{z}_i,ar{oldsymbol{z}}$	Conjugate complex coordinate
$\mathrm{d}_{oldsymbol{z}}$	Exterior derivative in $\boldsymbol{z}$
$\mathrm{d}_{\overline{z}}$	Complex conjugate exterior derivative
$\zeta_n$	$\zeta$ value – Definition 3.23

# List of Abbreviations

BD Basso Dixon

CY Calabi-Yau

DEQ Differential equation

eMPL Elliptic multiple polylogarithm

eq. Equation

LHC Large Hadron Collider

MPL Multiple polylogarithm

MMV Multiple modular value

MZV Multiple zeta value

PFI Picard Fuchs Ideal

QCD Quantum Chromodynamics

QED Quantum electrodynmamics

 $\mbox{QFT} \qquad \mbox{Quantum field theory}$ 

TRBR Twisted Riemann bilinear relations

# Chapter 1

# Introduction

One of the core ideas of modern theoretical physics is to describe the world using mathematical frameworks and to derive predictions from these frameworks that can be tested experimentally. In turn, this pursuit has also inspired various areas of mathematics and provided concrete applications and examples for abstract constructions. The interplay between physics and mathematics remains fascinating and fruitful in a wide variety of areas. Along these lines, this thesis focuses on a specific topic: a special class of integrals known as Feynman integrals, which arise in Quantum Field Theory (QFT). QFT is the theoretical framework of the standard model of particle physics, used to describe three of the four fundamental forces: the strong, weak, and electromagnetic interactions. The fourth force, gravity, is described within a different geometric framework – general relativity. Recently, however, integrals such as the ones we discuss are also used to study observables related to gravitational waves [1–5]. Additionally, these integrals appear in other contexts, such as string theory [6, 7], which plays a minor role in this work. Here, we extend this motivation to study Feynman integrals, explain the focus of this thesis, and outline its structure.

QFT is a framework used and developed in modern particle physics. Much of experimental particle physics is conducted in collider experiments, such as those at the Large Hadron Collider (LHC). In these experiments, incoming elementary particles with high energies scatter, and the outgoing particles are measured. To learn from these experiments, one must compare them with existing theories, which requires accurate theoretical predictions. The central theoretical framework is the Standard Model of particle physics, which has been remarkably successful in explaining a wide range of experimental results. The strongest of its forces is the strong interaction. Quantum Chromodynamics (QCD) governs this force and particles interacting with it in a self-contained way. To bridge experiment and theories, one must compute observables within these theories. However, since these are quantum theories, it is not possible to compute a single definitive value for an observable. Instead, one determines the probability distribution for a certain outcome. The probability distribution for a certain collision producing certain outgoing particles with specific momenta and masses is the so-called scattering amplitude. A highly successful method for computing scattering amplitudes is perturbation theory: The

#### Introduction

amplitude is computed as an expansion in the small coupling constants associated with each force. The coefficient at each order can be computed from Feynman integrals. One writes down all allowed Feynman diagrams for that order and particle content, extracts their mathematical expressions, and sums them up. Each additional term in the expansion corresponds to additional integrations over an internal momentum and these are represented with higher loop orders in the diagrams. The resulting integrals are known as Feynman integrals. This explains in a nutshell, how scattering amplitudes and their fundamental building blocks, Feynman integrals, play a central role in theoretical particle physics. Consequently, an entire research field is dedicated to their computation. The two primary goals of these studies are the following:

- Precision Physics. After the discovery of the Higgs boson and the so far widely observed predictability of the Standard model of particle physics, we are in the precision era of particle physics. The goal is now to measure the Standard Model's parameters with high accuracy. Small discrepancies from its predictions in experimental data could point to physics beyond the Standard Model.
- Structures in QFT. A better understanding of the scattering amplitudes the objects connecting a theory to observables in the real world is crucial for a better understanding of the theory. Non-trivial relations between theories have been found from studying their scattering amplitudes. An example is the so-called double-copy formalism, which says that a wide variety of gravity amplitudes can be built putting together building blocks of gauge theory amplitudes (such as the ones describing the strong and electroweak forces). Crucially, the study of Feynman integrals also revealed deep connections to various areas of mathematics, which are interesting in their own right.

In this thesis, we are especially interested in the mathematical structures, which, as noted earlier, also arises in integrals from other contexts. In string perturbation theory, certain amplitudes are given by integrals over punctured Riemann spheres – similarly to certain Feynman integrals related to tori or Riemann surfaces of genus two. Additionally, the use of amplitudes-based techniques in the study of gravitational wave observables and cosmology has revealed the appearance of integrals that are very similar to Feynman integrals.

One of the central objectives of this thesis is to obtain a deeper understanding how the geometries underlying Feynman integrals can be used to establish relations between them and to facilitate their analytical computation. Many Feynman integrals – in particular ones used for phenomenological applications – are expressible in so-called multiple polylogarithms and in that way trivially related to the punctured Riemann sphere. More complicated Feynman integrals – in particular ones involving higher loop orders with massive internal momenta – have also been found to involve periods of elliptic curves [8–10] and more recently even Calabi-Yau (CY) varieties [3–5, 11–28] and higher genus Riemann surfaces [27, 29–31]. While

methods for computing these specific Feynman integrals have rapidly advanced in recent years, open questions remain. In this thesis, we take steps toward addressing them by studying specific integral families and identifying general patterns along the way. In particular, we discuss an integral family related to two distinct elliptic curves [32, 33], functions that model maximal cuts which constitute specific limits of hyperelliptic Feynman integrals [34] as well as a class of Feynman integrals that are computed by single-valued versions of CY periods [35–38]. The second major theme of this thesis is the application of twisted intersection theory for similar purposes. Twisted intersection theory was introduced in the study of Feynman integrals to identify linear relations [39–46]. As a natural framework for integrals with multi-valued integrands, it can also be used to deduce further properties and relations [6, 47–49]. Specifically, we explore the implication of a set of bilinear relations between (twisted) periods, the so-called twisted Riemann bilinear relations (TRBR) for Feynman integrals [34, 50]. The results of this discussion are closely tied and directly applicable to the classes of integrals that we study because of their interesting geometric properties. In that sense and a multitude of specific ways, both objectives are intimately tied to each other. In more detail, we discuss the following content in this thesis:

#### Overview of the thesis

In Chapter 2, we introduce Feynman integrals and some common techniques and objects used in their computations. Specifically, we first review how they arise in QFT in Section 2.1. Then, in Section 2.2 we introduce different integral representations commonly used for Feynman integrals in different contexts. One of these contexts is the computation of so-called *cuts of Feynman integrals*, specific limits that preserve important properties and we discuss them in Section 2.3. In Section 2.4, we illustrate the concepts discussed up to this point with several examples. Finally, we discuss today's standard method for computing Feynman integrals, the method of differential equations, in Section 2.5.

In Chapter 3, we discuss all basic geometric notions that we need for the rest of the thesis. Specifically, we start with a general introduction of objects related to varieties such as their cohomology and homology group and the differential operators annihilating their periods – integrals between the cycles from the homology group and differentials from the cohomology group. Then we discuss specific varieties: Riemann surfaces and hyperelliptic curves in Section 3.2 and then Calabi-Yau varieties in Section 3.3. Our main interest are iterated integrals defined on these varieties, as they naturally appear in Feynman integrals. In Section 3.4, we explore these integrals, focusing on those over Riemann surfaces of varying genera. Finally, in Section 3.5, we establish the connection to Feynman integrals by discussing how a variety can be associated with a family of Feynman integrals, and do so with several examples relevant for this thesis.

In **Chapter 4**, we introduce another central mathematical framework for this thesis: The theory of twisted (co-)homology groups and their intersection numbers. In Section 4.1 we start with a review of these concepts (computational details can

#### Introduction

also be found in Appendix B). Here we distinguish between twisted cohomology groups for differentials without additional poles and relative twisted cohomology groups used to treat integrands that have unregulated poles. Then we briefly mention (twisted) motivic and de Rham periods in Section 4.2. We use these objects to review a construction of single-valued versions of twisted periods. As a prime example of twisted periods we introduce Aomoto-Gelfand hypergeometric functions in Section 4.3 and construct single-valued versions for several examples of these functions. Finally, in Section 4.4, we explain, how Feynman integrals can be interpreted as (relative) twisted periods.

In Chapter 5, we discuss how a good understanding of the concepts from Chapter 4 can be used to derive new relations for Feynman integrals: In Section 5.1 we explain how one can find bilinear relations (for maximal cuts) from the twisted Riemann bilinear relations from twisted intersection theory. In Section 5.2 we explain what else one can learn from these relations about the structure of the intersection matrix for a Feynman integral family in canonical form, i.e., with a basis particularly suited for solving with the differential equation approach. This is related to a concept of self-duality for maximal cuts and reveals interesting connections to representation theory.

In Chapter 6, we discuss canonical differential equations for a class of functions that form the prototype of a hyperelliptic maximal cut: Lauricella functions. In particular, we explain how to derive a canonical basis for families of Lauricella functions related to hyperelliptic curves of genus one and two in Section 6.1. In particular, we also use results of Section 5.2 to get a better understanding of the new functions arising in these canonical bases. In Section 6.2 we also discuss the modular properties of the iterated integrals we obtain as a solution for the canonical differential equations. We find that the appearing forms are partially Siegel quasimodular forms.

In Chapter 7, we discuss one specific integral family, the unequal mass kite integral family in  $D = 2 - 2\varepsilon$  dimensions. This integral family is related to two distinct tori and has five parameters, which makes it an interesting example for a multi-parameter Feynman integral family related to more than one non-trivial geometry. After introducing this integral family in Section 7.1, we explain how one can find its canonical differential equation in Section 7.2. Then, we discuss how to express this differential equation on the two tori in Section 7.3 and comment on the choice of boundary values and the integration in Section 7.4.

In Chapter 8, we discuss Feynman integrals in two integer dimensions. These are generally single-valued periods of some (twisted) (co-)homology groups. In that sense, one can compute them as single valued versions of twisted periods (which are all Aomoto-Gelfand hypergeometric functions), as we explain in Section 8.1. For specific parameter choices these single-valued versions of periods are at the same time special objects in the context of Calabi-Yau varieties, namely exponentials of their Kähler potentials. These can be written in bilinears of Calabi-Yau periods, which is analogous to the bilinear formula for single valued versions of twisted periods from twisted intersection theory. We discuss this connection in Section 8.2 and also consider its implications, including an interpretation of fishnet integrals

#### Introduction

as quantum volumes and special relations that one can derive in this framework.

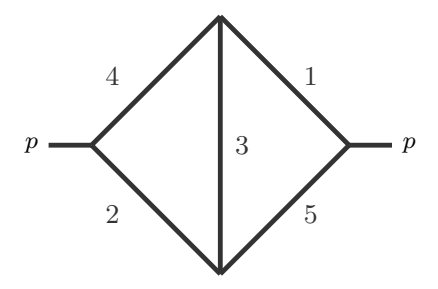
The main part of the thesis is accompanied by a set of **Appendices**:

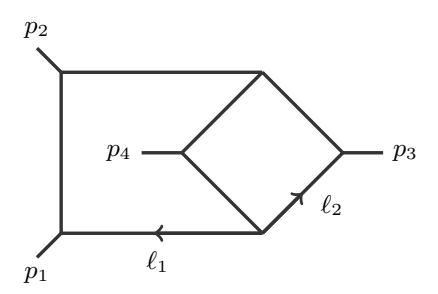
- In Appendix A we give definitions for various mathematical concepts we use throughout the thesis.
- In Appendix B we explain methods to compute intersection numbers in (relative) twisted (co-)homology groups and illustrate them with examples. Additionally, we give a proof for the ε-dependence of certain intersection numbers.
- In Appendix C we give additional relations for punctures related to the kinematic space of the unequal mass kite integral family of Chapter 7.
- In Appendix D we give extended calculations that were omitted in the main part of the thesis, in particular we give the proof of Theorem 5.1 and as well as several the Laurent expansions of basic differentials on hyperelliptic curves.
- In Appendix E we review some relevant aspects of representation theory.

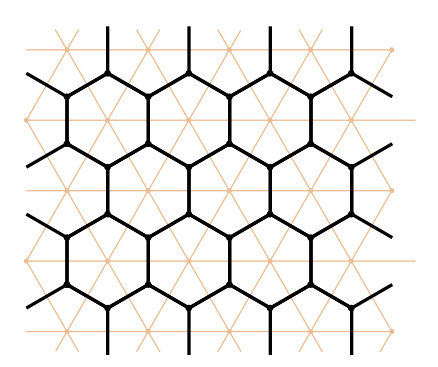
# Chapter 2

# Feynman Integrals

In this chapter, we provide the physical motivation for considering the types of integrals that are discussed in subsequent chapters.







In Section 2.1, we focus first on Feynman integrals that appear in scattering amplitudes computed in the context of particle physics. Then, we mention integrals with similar structures that appear in gravitational wave physics, cosmology and string theory. In Sections 2.2 and 2.3, we introduce all relevant definitions and ideas related to these (Feynman) integrals – such as different integral representations and limits – and illustrate them with several examples in Section 2.4. Finally, in Section 2.5, we introduce the method of differential equations, a standard method to compute Feynman integrals that we use throughout the thesis.

### This chapter reviews existing literature.

### Contents of this Chapter

2.1	Feyr	nman Integrals in High Energy Physics	20
2.2	Feynman Integrals: Representations		
	2.2.1	Momentum Representation	27
	2.2.2	Schwinger and Feynman Parameter Representation	29
	2.2.3	Baikov Representation	31
2.3	Feyr	nman Integrals: Cuts	<b>32</b>
2.4	Feyr	nman Integrals: Examples	33
	2.4.1	The Sunrise and Kite Integral Families	34
	2.4.2	The Non-planar Crossed Box Family	37
	2.4.3	Fishnet Integrals	40
2.5	Feyr	nman Integrals: Differential Equations	43
	2.5.1	Linear Relations Between Feynman Integrals	44
	2.5.2	Differential Equations for Feynman Integrals	45

# 2.1 Feynman Integrals in High Energy Physics

We provide a very brief review of how Feynman integrals arise in the calculation of observables in QFT, particularly in modern particle physics. For a more indepth treatment of the foundations of this topic, see the classic literature (e.g., [51–53]). For a modern, research-focused perspective, see e.g., [54, 55], or [8], which specifically focuses on Feynman integrals.

## Feynman Integrals in Quantum Field Theory

We begin by introducing the concept of an observable in QFT and then show how the computation of observables relies on the computation of scattering amplitudes, which in turn can be obtained perturbatively in the coupling constants with Feynman integrals appearing in the coefficients.

Observables From Scattering Amplitudes. The fundamental object defining a QFT is its Lagrangian density (or simply the Lagrangian)  $\mathcal{L}(\{\phi_i(\boldsymbol{x})\}, \{\partial_{\mu}\phi_i(\boldsymbol{x})\})$ , which is a function of fields  $\phi_i(\boldsymbol{x})$  – depending on local coordinates  $\boldsymbol{x}^1$  – and their derivatives  $\partial_{\mu}\phi_i(\boldsymbol{x})$ . Different types of fields exist and represent different types of particles. They are distinguished by their behaviour under Lorentz transformations. For all examples considered in this thesis, we only need scalar fields. The integral of the Lagrangian density over space-time is the action S:

$$S = \int \mathcal{L}(\{\phi_i(\boldsymbol{x})\}, \{\partial_{\mu}\phi_i(\boldsymbol{x})\}) d^D x.$$
 (2.1)

We denote by D the number of space-time dimensions. In general, the physical space-time dimension is D=4 in particle physics. However, in QFT, we generally use dimensional regularisation<sup>2</sup>, setting  $D=d+2\varepsilon$  with  $\varepsilon$  being a small perturbation from an integer space-time dimension d. The equation of motion for each field  $\phi_i$  is given by the *Euler-Lagrange* equation

$$\partial_{\mu} \left( \frac{\partial \mathcal{L}}{\partial (\partial_{\mu} \phi_i)} \right) - \frac{\partial \mathcal{L}}{\partial \phi_i} = 0, \qquad (2.2)$$

which can be derived by requiring  $\delta S = 0$  in accordance with the *principle of least action*.

**Example 2.1** ( $\phi^4$ -theory: Lagrangian). Possibly the simplest example is the Lagrangian of a single scalar field  $\phi(\mathbf{x})$  with mass  $m^3$ :

$$\mathcal{L} = \frac{1}{2} \left( \partial_{\mu} \phi(\boldsymbol{x}) \right)^{2} - \frac{1}{2} m^{2} \phi(\boldsymbol{x})^{2}.$$
 (2.3)

Its equation of motion is given by the Klein-Gordon equation

$$\left(\partial^{\mu}\partial_{\mu} + m^2\right)\phi(\mathbf{x}) = 0. \tag{2.4}$$

<sup>1</sup>Throughout this thesis, we denote vectors and matrices in boldface, e.g.,  $\mathbf{x} = (x_1, \dots, x_4)$  for a four-vector.

<sup>2</sup>That is because some Feynman integrals are divergent individually. Their divergence is captured by poles in  $\varepsilon$  which cancel against each other in the physical observable.

<sup>3</sup>The term  $\frac{1}{2} (\partial_{\mu} \phi(x))^2$  is called the *kinematic* term and the term  $\frac{1}{2} m^2 \phi(x)^2$  is called the mass term.

With an additional interaction term, we obtain the Lagrangian for the so-called  $\phi^4$ -theory.

$$\mathcal{L} = \frac{1}{2} \left( \partial_{\mu} \phi(x) \right)^{2} - \frac{1}{2} m^{2} \phi(x)^{2} - \frac{g}{4!} \phi(x)^{4}, \qquad (2.5)$$

where g is the coupling constant determining the strength of the interaction.

The beauty of the Lagrangian formulation lies in the fact that the Lagrangian contains all information on a theory of fundamental forces. A particularly compact example is the following:

**Example 2.2** (QED). The Lagrangian for quantum electrodynamics (QED), the quantum field theory of electromagnetism is:

$$\mathcal{L}_{QED} = \mathcal{L}_{Dirac} + \mathcal{L}_{Maxwell} + \mathcal{L}_{int} = \bar{\psi} \left( i \gamma^{\mu} \partial_{\mu} - m \right) \psi - \frac{1}{4} \left( F_{\mu\nu} \right)^{2} - e \bar{\psi} \gamma^{\mu} \psi A_{\mu} . \tag{2.6}$$

This Lagrangian contains the electromagnetic vector potential  $A_{\mu}$  (whose particles are photons), which also defines the electromagnetic field tensor  $F_{\mu\nu} = \partial_{\mu}A_{\nu} - \partial_{\nu}A_{\mu}$ , as well as a bispinor field  $\psi$  (whose particles are electrons). The coupling constant e is equal to the electric charge of the bispinor field, i.e. the electron.

Similarly, one can construct a Lagrangian for other established theories of particle physics or extended candidate theories. A particularly relevant theory for particle physics is QCD describing the strong interaction and QCD is itself part of the full standard model of particle physics which describes the electro-weak and strong interactions and all particles that interact with these forces. To test these theories in reality, one needs to compare their predictions with experimental measurements. In particle physics, parameters are measured through collider experiments. The theoretical description of a certain<sup>5</sup> scattering event (in a collider) is the following: We assume that we have a set of incoming particles described by the fields  $\{\phi_{\rm in}^1, \phi_{\rm in}^2, \dots\}$  in the (asymptotically) far past, where they can be considered free, i.e. non-interacting. Similarly, consider a set of outgoing particles described by the fields  $\{\phi_{\rm out}^1, \phi_{\rm out}^2, \dots\}$  in the far future, where they are free. The probability for this specific scattering event to happen in a certain theory containing the involved particles is denoted by

$$|\langle \phi_{\text{out}}^1 \phi_{\text{out}}^2 \dots | \phi_{\text{in}}^1 \phi_{\text{in}}^2 \dots \rangle|^2.$$
 (2.7)

In general, we work in momentum space, with the position space vectors  $\langle \phi_{\text{out}}^1 \phi_{\text{out}}^2 \dots \rangle$  and  $|\phi_{\text{in}}^1 \phi_{\text{in}}^2 \dots \rangle$  related to momentum space vectors  $\text{out} \langle \boldsymbol{p}_1 \boldsymbol{p}_2 |$  and  $|\boldsymbol{k}_1 \boldsymbol{k}_2 \dots \rangle_{\text{in}}$  via a Fourier transform.<sup>6</sup> In momentum space, we need to compute:

$$_{\text{out}}\langle \boldsymbol{p}_{1}\boldsymbol{p}_{2}\dots|\boldsymbol{k}_{1}\boldsymbol{k}_{2}\rangle_{\text{in}}=\langle \boldsymbol{p}_{1}\boldsymbol{p}_{2}\dots|\mathbf{S}|\boldsymbol{k}_{1}\boldsymbol{k}_{2}\dots\rangle. \tag{2.8}$$

This is equivalent to saying that we compute a matrix element of the limiting unitary operator S, describing the time-evolution between in- and out-states. In

<sup>&</sup>lt;sup>4</sup>A bispinor field transforms as an element of a four-dimensional complex vector space  $(\frac{1}{2},0)\oplus(0,\frac{1}{2})$  representation of the Lorentz group.

<sup>&</sup>lt;sup>5</sup>A certain scattering event means a scattering event with a specified set of incoming and outgoing particles.

<sup>&</sup>lt;sup>6</sup>We now attach the labels in and out to the brackets  $\langle$  and  $\rangle$  to avoid clutter.

#### Chapter 2

general, the time-evolution operator takes the form  $\mathbf{S} = N \exp(-i\mathcal{H}(2T))$  where T is the asymptotic time and  $\mathcal{H}$  the Hamiltonian density of the system. Commonly, one splits  $\mathbf{S}$  into

$$\mathbf{S} = \mathbf{1} + i\mathbf{T} \,, \tag{2.9}$$

where T captures the interactions and the limit S = 1 describes a history without interaction, where the particles just pass each other. In a scattering process, we are interested in the interaction part, which takes the form

$$\langle \boldsymbol{p}_1 \boldsymbol{p}_2 \dots | i \mathbf{T} | \boldsymbol{k}_1 \boldsymbol{k}_2 \dots \rangle = (2\pi)^4 \delta^{(4)} \left( \sum_i \boldsymbol{k}_i - \sum_i \boldsymbol{p}_i \right) i \mathcal{M} \left( \{ \boldsymbol{k}_i \} \to \{ \boldsymbol{p}_i \} \right) . \quad (2.10)$$

The  $\delta^{(4)}$  function guarantees that the momentum of in- and outgoing particles is conserved, and  $\mathcal{M}$  is the *scattering amplitude*. The cross section and the differential cross section, which can be measured in experiments are functions of the scattering amplitude, appearing in the form  $|\mathcal{M}|^2$ . Thus, the scattering amplitude is the quantity that needs to be computed to connect to experiments.

Scattering Amplitudes From Feynman Diagrams. In general, the matrix element of (2.8) cannot simplify be computed exactly. However, the exponential in S can be expanded in the one or multiple coupling constants of the theory (for simplicity we assume here that there is only one coupling constant) and then the amplitude can be computed perturbatively. In general, the full perturbative expansion diverges [56] and a full treatment of the amplitude must contain non-perturbative effects. Still, considering only the first few orders of the perturbative expansion has proven to produce valid results confirmed by experiments.

There is a systematic approach to computing the coefficients: One uses socalled Feynman diagrams. These are graphical representations of the terms in each coefficient, consisting of vertices connected by internal edges and attached to external ones. A vertex represents an interaction and is associated with the coupling constant(s), whereas the lines connecting vertices, the so-called *propagators*, represent terms due to the kinematic and mass terms in the Lagrangian/Hamiltonian. Depending on the explicit particle content, the propagators take different forms - graphically represented by differently structured lines and formally by the different kinematic and mass terms of the respective particles. The precise rules for which graphs are allowed in the given theory and which mathematical terms are associated to them are the so-called Feynman rules and can be read off from the Lagrangian. For more details and examples we refer to the standard literature, e.g., [51]. The full coefficient for the coupling constant at a specific order can be constructed by drawing all allowed Feynman diagrams with the respective order in the couplings and then summing up their mathematical expressions. The resulting expression can be decomposed in terms of expressions coming from scalar diagrams, with scalar products between the external momenta serving as coefficients – this decomposition originated from Passarino and Veltman [57]. It is a key step in reducing a scattering amplitude to its simplest components. Thus, we focus here on scalar diagrams.

**Example 2.3** ( $\phi^4$ -theory: Feynman Rules). Let us thus give as a first example the Feynman rules in  $\phi^4$ -theory (from example 2.1):

To account for higher order propagators  $(q^2-m^2+i\varepsilon)^{-\nu}$ , we put  $\nu-1$  dots on the propagator in the Feynman diagram. For each closed internal loop of propagators, we introduce an internal momentum, over which we integrate. The momenta for the internal propagators are assigned such that the overall incoming momentum is conserved at each vertex:

<sup>7</sup>This appears, e.g., in the kite integral family as depicted in figure 7.3.

Loop 
$$= \int \frac{\mathrm{d}^{\mathrm{D}} \ell}{(2\pi)^{D}}$$
 Vertex: 
$$\longrightarrow \text{ momentum conservation}$$

The integrals we obtain by imposing such rules (and specifically the integration for each loop) are called Feynman integrals. There are two types of physical singularities that Feynman integrals in QFT typically posses: ultra-violet (UV) singularities and infra-red (IR) singularities. UV divergences occur at large momenta, whereas IR divergences occur for low momenta or long distances. Specifically, the latter are classified as collinear and soft divergences. Both can be regularised by introducing dimensional regularisation, i.e., a dimension  $D = d - 2\varepsilon$ . In general, Feynman integrals have at most regular singularities in the kinematic variables and the scaling exponents near a singularity are linear in the space-time dimension D. In this thesis, we discuss Feynman integrals obtained from multi-loop Feynman graphs. To set the notation for the remainder of this thesis, let us summarise the parameters that identify a (multi-loop) Feynman graph:

**Definition 2.1** (Feynman graphs). We denote by a Feynman graph G a graph defined by the following sets:

- $V_G$ : the number of vertices
- $n_{int}$ : the number of internal edges (each attached to a vertex on either side)

•  $n_{ext}$ : the number of external legs (or half-edges).

This just defines the graph as a picture. To bring physics into this picture, we assign:

- to every external leg in  $n_{ext}$  a momentum  $p_i \in \mathbb{R}^D$  (or  $\mathbb{C}^D$ ),
- to every internal edge in  $n_{int}$  a mass  $m_i \in \mathbb{R}$  (or  $\mathbb{C}$ ) and a momentum  $q_i$ ,
- to every vertex some power of the coupling constant(s) appearing in the theory.

Note that due to momentum conservation, not all of the external momenta are linearly independent. We denote by E the number of linearly independent external momenta; generally  $E=n_{\rm ext}-1$  in four-dimensional spacetime.

**Example 2.4** ( $\phi^4$ -theory: Simple One-Loop Graphs). In a scalar theory, the simplest one-loop graphs are:

To conclude our discussion of Feynman graphs arising in QFT, let us summarise the relevant steps for computing a scattering amplitude from these graphs:

#### Review: Computing a scattering amplitude from Feynman graphs

We typically compute the scattering amplitude at a specific loop order, which corresponds to a particular order in the expansion of the coupling constant. For the L-th loop order and  $n_{\rm ext}$  external particles of a given species, the following steps can be applied:

- 1. Draw all allowed Feynman graphs. This can be done with existing software, e.g., the packages QGraf [58] (or FeynArts [59]).
- 2. Perform all spinor algebra to obtain a decomposition in only scalar Feyman integrals, e.g., with the packages FORM [60–62] (or FeynCalc [63–65]).
- 3. Write down the mathematical expressions for all appearing Feynman graphs and compute the Feynman integrals.
- 4. Put everything back together.

The focus of the next sections is on step 3, in particular on the computation of massive multi-loop Feynman integrals. Similar integrals also appear in other areas of physics, such as string theory. Moreover, the application of scattering amplitude-based techniques in gravitational wave physics and cosmology has further highlighted the importance of understanding and precisely computing these integrals.

## **String Integrals**

In the following chapters, we explore how connections to specific geometries can be leveraged to compute Feynman integrals. Such connections also exist in the context of string integrals, leading to an overlap in technical knowledge and computational methods between the two fields. Standard literature for string integrals is [66, 67].

String amplitudes are path integrals describing scattering between states coming in from infinity. Whilst the trajectory of a point particle is a worldline, strings sweep out two-dimensional worldsheets. We distinguish between open and closed strings: a closed string forms a loop, whereas an open string has endpoints. Notably, the graviton corresponds to an excitation of a closed string, while the gluon arises as an excitation of an open string. Consequently, in some theories, closed strings are associated with gravity, whereas open strings correspond to gauge theory. Any element of a string S-matrix is associated to some two dimensional worldsheet with insertion points from interactions. Due to physical constraints, these worldsheets take the form of Riemann surfaces with punctures. A Riemann surface with g handles is referred to as a genus g surface. As in QFT we can arrange a string amplitude by loops and the number of loops corresponds to this genus. For example, a closed string amplitude of n external strings,  $\mathcal{M}_n$ , can be expanded as

$$\mathcal{M}_n = \frac{1}{g_S^2} \mathcal{M}_n^{(0)} + \mathcal{M}_n^{(1)} + g_S^2 \mathcal{M}_n^{(2)} + \dots,$$
 (2.11)

where  $g_S$  is the string coupling constant. In contrast to QFT, in closed string theory there is only one integral per loop order. For open and unoriented strings there are more possibilities. In the former case, every L-loop string integral  $\mathcal{M}_n^{(L)}$  is an integral over a genus L Riemann surface:  $\mathcal{M}_n^{(0)}$  is an integral over a punctured Riemann sphere,  $\mathcal{M}_n^{(1)}$  is an integral over a punctured torus and for higher loops, one considers higher genus Riemann surfaces. This connects the study of string integrals to the study of Feynman integrals associated to Riemann surfaces, many of which can also be written order by order in  $\varepsilon$  in terms of integrals over punctured Riemann surfaces.

Additionally, closed string integrals are single-valued and connected to open string integrals by the Kawai-Lewellen-Tye (KLT) relations [68]. In that sense, the KLT relations are closely related to constructing single-valued versions of certain integrals, which are also relevant for certain Feynman integrals.

Finally, let us note that a large amount of knowledge on Calabi-Yau varieties in the Feynman integrals community, where it is used to compute Feynman integrals

#### See also:

We give a more in depth account of the appearing geometries in Chapter 3 and explain how they are associated to Feynman graphs in Section 3.5

#### See also:

We discuss examples for Feynman integrals associated to Riemann surfaces in Chapter 6 and Chapter 7. These also appear in many examples throughout other parts of this thesis.

#### See also:

We discuss the single-valued construction in Section 4.2 and we apply it to construct single-valued Feynman integrals in Chapter 8.

related to these varieties, is imported from the string theory literature. In superstring theory, Calabi-Yau (CY) varieties arise as the geometry of the additional space-time dimensions (in addition to the standard four dimensions in Minkowski space-time).

## Other Applications: Gravitational Waves and Cosmology

The success of methods and results from scattering amplitudes in particle physics has led to their application in other areas. Here, we provide a brief, incomplete overview of how these techniques are being applied in gravitational wave physics and cosmology.

Gravitational Waves. The first observation of gravitational waves [69] as well as subsequent observations [70] and the prospect of more sensitive gravitational wave detectors [71, 72], have led to significant efforts in computing the associated observables such as the gravitational waveform. Traditionally, these computations have relied on numerical relativity, but in recent years scattering amplitude-based techniques have been adopted. These involve a direct computation from appropriate amplitudes, different effective field theories as well as the worldline QFT approach [73–75]. In many cases, these computations involve Feynman-like integrals that can be solved with methods similar to the ones discussed later in this thesis. For example, high-precision computations in the WQFT formalism are performed with the differential equation method and by leveraging the Calabi-Yau variety associated to the appearing integrals [4]. This provides further motivation to better understand Feynman integrals associated with non-trivial geometries.

See also: intersection theory and specifically application Feynman integrals in discussed in Chapter

Twisted

4.

Cosmological Correlators. Cosmological correlators have recently also been computed with methods developed for Feynman integrals, such as the differential equations method [48, 76–82]. Specifically, these integrals can naturally be considered in the framework of twisted intersection theory, which has also been employed for Feynman integrals. Additionally, notions such as cuts and a coaction are being developed for cosmological correlators [83]. Another application in cosmology, which is closer to experimental observations, is the computation of loop integrals in the Effective Field Theory of Large Scale-Structure for the one-loop bispectrum analysis of the BOSS data, measuring cosmological parameters [84].

#### 2.2Feynman Integrals: Representations

The form of Feynman integral obtained by applying the Feynman rules in momentum space to a Feynman graph is referred to as the momentum representation. Other representations also exist and those are valuable for different applications. In particular, we review momentum representation, Schwinger and Feynman parameter representation and Baikov representation.

## 2.2.1 Momentum Representation

Let us begin by stating the form of a generic scalar multi-loop Feynman integral in momentum representation, as one would read it off from a Feynman graph. Similarly, one can also define a position space representation.

**Definition 2.2** (Feynman Integrals in Momentum Representation). A scalar L-loop Feynman integral with internal masses  $m_i$  and external momenta  $p_i$  in momentum representation is a function of the independent scalar products  $p_i \cdot p_j$  of the external momenta and the squared internal masses  $m_i^2$ :

$$I_{\nu}(\{p_i \cdot p_j\}, \{m_i^2\}) = e^{L\varepsilon\gamma_E} (\mu^2)^{\nu - \frac{LD}{2}} \int \left(\prod_{r=1}^L \frac{\mathrm{d}^D \ell_r}{i\pi^{\frac{D}{2}}}\right) \prod_{j=1}^{n_{int}} \frac{1}{D_j^{\nu_j}}$$
(2.12)

with propagators  $D_j = q_j^2 + m_j^2$  where

$$\nu = \sum_{j=1}^{n_{ext}} \nu_j \text{ and } q_j = \sum_{r=1}^{L} c_{jr} \ell_r + \sum_{r=1}^{n_{ext}-1} d_{jr} p_r.$$
 (2.13)

Here and henceforth, we denote by  $\ell_i$  the loop or internal momenta<sup>8</sup>, by L the loop number and  $\gamma_E$  is the Euler-Mascheroni constant. We call the entries  $\nu_j$  of  $\boldsymbol{\nu}$  the propagator powers. The renormalisation scale  $\mu$  is introduced to make the action dimensionless. Occasionally, we shorten  $I_{\boldsymbol{\nu}} := I_{\boldsymbol{\nu}}(\{p_i \cdot p_j\}, \{m_i^2\})$ .

In general, the physical spacetime is a four-dimensional Minkowski space, whereas the integral in eq. (2.12) is often initially considered in Euclidean space. One can translate between these spaces with a coordinate transformation called the Wick rotation. The integrals are labelled by  $\nu$ , the collection of their propagator powers. We can interpret a specific Feynman integral as a member of a family of Feynman integrals indexed by these propagator powers. The concept of collecting a set of Feynman integrals into a family will be useful because it allows us to interpret this family as a vector space and define a basis for it. Additionally, we partition such a family into sub-families or sectors. We characterise these sectors by introducing the object

$$\mathbf{\Theta}_{\nu} = (\theta_{\mathrm{H}}(\nu_{1}), \dots, \theta_{\mathrm{H}}(\nu_{n_{\mathrm{int}}})) \text{ with } \theta_{\mathrm{H}}(x) = \begin{cases} 1 & x > 0 \\ 0 & x \leq 0 \end{cases}, \tag{2.14}$$

the Heaviside step function. Every integral with the same value of  $\Theta_{\nu}$  is said to belong to the same sector. Those sectors can be (partially) ordered in a natural way by the prescription

$$\Theta_{\nu} \ge \Theta_{\mu} \text{ if } \theta_{H}(\nu_{i}) \ge \theta_{H}(\mu_{i}) \text{ for } 1 \le i \le n_{\text{int}}.$$
 (2.15)

Let us illustrate these concepts with the example of the bubble integral family, whose graph was given in Example 2.4.

<sup>8</sup>The linear combination of momenta in the  $q_i$  depends on the specific graph and needs to be chosen such that momentum is conserved at each vertex.

**Example 2.5** (Bubble integral family). In momentum representation, the bubble integral family with two distinct masses in D dimensions is

$$I_{\nu}^{\circ}(\{p^2\},\{m_1^2,m_2^2\}) = e^{\gamma_E \varepsilon} (\mu^2)^{\nu - \frac{D}{2}} (-1)^{\nu} \int \frac{\mathrm{d}^D \ell}{i\pi^{\frac{D}{2}}} \frac{1}{(\ell^2 - m_1^2)^{\nu_1} ((\ell - p)^2 - m_2^2)^{\nu_2}}.$$
(2.16)

The three relevant sectors are depicted in figure 2.1.

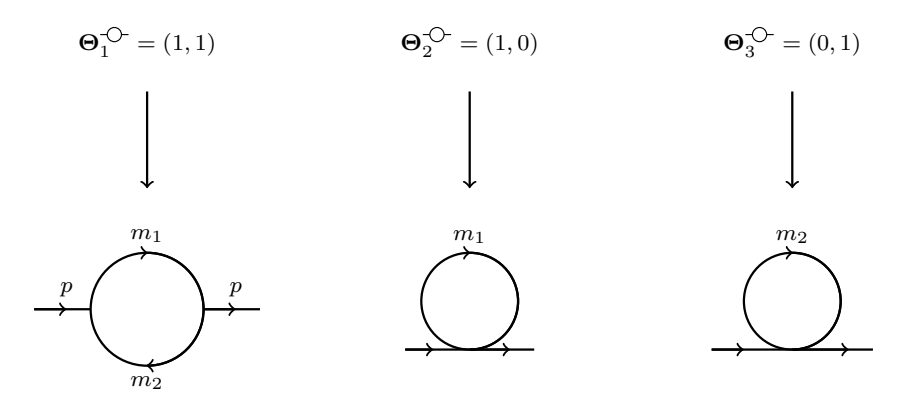


Figure 2.1: The bubble integral family has three master integrals, one in each sector. The top sector contains the unequal mass bubble [left] and the other two sectors contain tadpoles, each with one of the two masses of the full bubble integral [middle and right].

Their graphs are called the bubble and the tadpole graphs. These serve as simple examples for the remainder of this introductory chapter (and beyond).

Massless Feynman Integrals in D=2 Dimensions. We comment here specifically on massless Feynman integrals in D=2 dimensions. The propagators of eq. (2.13) for massless Feynman integrals take the following form:

$$D_{j} = q_{j}(\boldsymbol{u}, \boldsymbol{v})^{2} = \left(\sum_{r=1}^{L} c_{jr} u_{r} + \sum_{r=1}^{n_{\text{ext}}-1} d_{jr} v_{r}\right)^{2}, \qquad c_{jr}, d_{jr} \in \{-1, 0, 1\}. \quad (2.17)$$

Here  $u_r$  and  $v_r$  denote generic internal and external coordinates in  $\mathbb{R}^2$ . These can live either in position or in momentum space. In momentum space we set  $u_r = \ell_r$  to be the loop momenta and  $v_r$  to be the external momenta  $p_r$ . In any case, we can replace the two-dimensional real vectors  $u_r$  and  $v_r$  by complex variables, whose real and imaginary parts are the components of the real vectors. Explicitly, in position space, we write

$$x_i = u_i^1 + iu_i^2 \text{ and } \lambda_i = v_i^1 + iv_i^2.$$
 (2.18)

In these coordinates eq. (2.17) is

$$D_j = |q_j(\boldsymbol{x}, \boldsymbol{\lambda})|^2 \tag{2.19}$$

See also: We discuss Feynman

integrals in two dimensions in detail in Chapter 8.

and the full integral family for a Feynman graph G takes the form

$$I_{\nu}^{G}(\boldsymbol{\lambda}) = \left(-\frac{1}{2\pi i}\right)^{L} \int_{\mathbb{C}^{L}} \left(\bigwedge_{j=1}^{L} dx_{j} \wedge d\bar{x}_{j}\right) \prod_{j=1}^{n_{\text{int}}} \frac{1}{|q_{j}(\boldsymbol{x}, \boldsymbol{\lambda})|^{2\nu_{j}}}.$$
 (2.20)

Note that this from relies on the propagators being massless. We cannot trivially express massive propagators as squared absolute values in the same way.

## 2.2.2 Schwinger and Feynman Parameter Representation

Two closely connected standard representations are the Schwinger and Feynman parameter representations. Both of these are based on the Schwinger trick and their building blocks are the *graph polynomials*. The *Schwinger trick* relies on the formula

$$\frac{1}{A^{\nu}} = \frac{1}{\Gamma(\nu)} \int_{0}^{\infty} d\alpha \, \alpha^{\nu-1} e^{-\alpha A} \text{ for } A > 0 \text{ and } \operatorname{Re}(\nu) > 0.$$
 (2.21)

Applying it to each propagator of the form  $(-q_j^2 + m_j^2)$ , one finds:

$$I_{\boldsymbol{\nu}} = \frac{e^{L\varepsilon\gamma_E}(\mu^2)^{\boldsymbol{\nu}-\frac{LD}{2}}}{\prod_{j=1}^{n_{\mathrm{int}}}\Gamma(\nu_j)} \int_{\alpha_j>0} \mathrm{d}^{n_{\mathrm{int}}}\boldsymbol{\alpha} \left(\prod_{j=1}^{n_{\mathrm{int}}} \alpha_j^{\nu_j-1}\right) \int \left(\prod_{r=1}^L \frac{\mathrm{d}^D\ell_r}{i\pi^{\frac{D}{2}}}\right) e^{-\sum_{j=1}^{n_{\mathrm{int}}} \alpha_j \left(-q_j^2 + m_j^2\right)}.$$

The argument of the exponential function in the integrand can be expressed with the matrices M and J:

$$\sum_{j=1}^{n_{\text{int}}} \alpha_j \left( -q_j^2 + m_j^2 \right) = -\sum_{r=1}^{L} \sum_{s=1}^{L} \ell_r \cdot M_{rs} \cdot \ell_s + \sum_{r=1}^{L} 2\ell_r \cdot J_r + \tilde{J}.$$
 (2.22)

These matrices define the graph polynomials:

**Definition 2.3** (Graph Polynomials). The first Symanzik polynomial is

$$U = \det(M) \tag{2.23}$$

and the second Symanzik polynomial is

$$F = \frac{\det(M)}{\mu^2} \left( \tilde{J} + J^T M^{-1} J \right). \tag{2.24}$$

With these polynomials one can define the following two representations:

**Definition 2.4** (Feynman Integral in Schwinger Representation). A Feynman integral in Schwinger representation is

$$I_{\nu} = \frac{e^{L\varepsilon\gamma_E}}{\prod_{j=1}^{n_{\text{int}}} \Gamma(\nu_j)} \int_{\alpha_j > 0} d^{n_{\text{int}}} \boldsymbol{\alpha} \left( \prod_{j=1}^{n_{\text{int}}} \alpha_j^{\nu_j - 1} \right) \left[ \mathbf{U}(\boldsymbol{\alpha}) \right]^{-\frac{D}{2}} \exp\left( -\frac{\mathbf{F}(\boldsymbol{\alpha})}{\mathbf{U}(\boldsymbol{\alpha})} \right)$$
(2.25)

**Definition 2.5** (Feynman Integral in Feynman Parameter Representation). The Feynman parameter representation of a Feynman integral is given by

$$I_{\nu} = \frac{e^{L\varepsilon\gamma_{E}}\Gamma\left(\nu - \frac{LD}{2}\right)}{\prod_{j=1}^{n_{\text{int}}}\Gamma(\nu_{j})} \int_{\alpha_{j}\geq 0} d^{n_{\text{int}}}\boldsymbol{\alpha} \,\delta\left(1 - \sum_{j=1}^{n_{\text{int}}}\alpha_{j}\right) \left(\prod_{j=1}^{n_{\text{int}}}\alpha_{j}^{\nu_{j}-1}\right) \frac{\left[\mathrm{U}(\boldsymbol{\alpha})\right]^{\nu - \frac{(L+1)D}{2}}}{\left[\mathrm{F}(\boldsymbol{\alpha})\right]^{\nu - \frac{LD}{2}}}.$$
(2.26)

Note that by the Cheng-Wu theorem the delta distribution in the integrand can also be replaced by a reparametrisation with any delta distribution of the form

$$\delta\left(1 - \sum_{j \in \tilde{J} \subseteq \{1,\dots,n_{\text{int}}\}} \alpha_j\right). \tag{2.27}$$

As an example we consider the bubble integral of Example 2.5.

**Example 2.6** (The Bubble Integral in Feynman Parameter Representation). For the bubble integral family of Example 2.6, we find

$$\sum_{j=1}^{2} \alpha_j (-q_j^2 + m_j^2) = -(\alpha_1 + \alpha_2)\ell^2 + 2\alpha_2 \ell \cdot p + (\alpha_1 m_1^2 + \alpha_2 m_2^2 - \alpha_2 p^2)$$
 (2.28)

and thus

$$U(\boldsymbol{\alpha}) = \alpha_1 + \alpha_2 \text{ and } F(\boldsymbol{\alpha}) = \frac{1}{\mu^2} \left[ (\alpha_1 + \alpha_2) \left( \alpha_1 m_1^2 + \alpha_2 m_2^2 \right) - \alpha_1 \alpha_2 p^2 \right]. \quad (2.29)$$

Consequently, the Feynman parameter representation of this integral family is

$$I_{\boldsymbol{\nu}}^{\circ} = \frac{e^{\varepsilon \gamma_E} \Gamma\left(\nu - \frac{D}{2}\right)}{\prod_{j=1}^{2} \Gamma(\nu_j)} \int_{\alpha_j > 0} d\alpha_1 d\alpha_2 \, \delta\left(1 - \alpha_1 - \alpha_2\right) \alpha_1^{\nu_1 - 1} \alpha_2^{\nu_2 - 1} \frac{\left[U(\boldsymbol{\alpha})\right]^{\nu - D}}{\left[F(\boldsymbol{\alpha})\right]^{\nu - \frac{D}{2}}}. \quad (2.30)$$

<u>Massless case</u> In the massless limit, i.e., for  $m_1^2 = m_2^2 = 0$ , this is

$$I_{\nu}^{\circ}(\{p^2\},\{0,0\}) = \frac{e^{\varepsilon \gamma_E} \Gamma\left(\nu - \frac{D}{2}\right)}{\Gamma(\nu_1)\Gamma(\nu_2)} \left(-\frac{p^2}{\mu^2}\right)^{\frac{D}{2}-\nu} \int_{0}^{1} d\alpha_1 \, \alpha_1^{\frac{D}{2}-\nu_2-1} (1-\alpha_1)^{\frac{D}{2}-\nu_1-1} \,. \tag{2.31}$$

This integral is the integral representation of a  $\beta$  function as in Definition 4.1 for

$$\operatorname{Re}\left(\frac{D}{2}-\nu_2\right), \operatorname{Re}\left(\frac{D}{2}-\nu_1\right) > 0.$$

Thus, it can also be written as

$$I_{\nu}^{\mathcal{O}}(\{p^2\},\{0,0\}) = e^{\varepsilon \gamma_E} \frac{\Gamma\left(\nu - \frac{D}{2}\right)}{\Gamma(\nu_1)\Gamma(\nu_2)} \left(-\frac{p^2}{\mu^2}\right)^{\frac{D}{2}-\nu} \beta\left(\frac{D}{2} - \nu_2, \frac{D}{2} - \nu_1\right)$$
$$= e^{\varepsilon \gamma_E} \left(-\frac{p^2}{\mu^2}\right)^{\frac{D}{2}-\nu} \frac{\Gamma\left(\nu - \frac{D}{2}\right)\Gamma\left(\frac{D}{2} - \nu_1\right)\Gamma\left(\frac{D}{2} - \nu_2\right)}{\Gamma(\nu_1)\Gamma(\nu_2)\Gamma(D - \nu)}. \tag{2.32}$$

## 2.2.3 Baikov Representation

In *Baikov representation*[8, 85], we choose the propagators themselves (and irreducible scalar products) as integration variables.

**Definition 2.6** (Feynman Integral in Baikov Representation). The integral of eq. (2.12) in Baikov representation is

$$I_{\nu}(\{p_i \cdot p_j\}, \{m_i^2\}) = e^{L\varepsilon\gamma_E} (\mu^2)^{\nu - \frac{LD}{2}} \frac{\left[\det \mathcal{G}(p_1, \dots, p_E)\right]^{\frac{E+1-D}{2}}}{\pi^{\frac{1}{2}(n_{isp}-L)} \left[\det C\right] \prod_{j=1}^{L} \Gamma\left(\frac{D-E+1-j}{2}\right)} \mathbb{I}_{\nu} \quad (2.33)$$

 $with^9$ 

$$\mathbb{I}_{\nu} = \mathbb{I}_{\nu}(\{p_i \cdot p_j\}, \{m_i^2\}) = \int_{\mathcal{C}} d^{n_{isp}} z \left[\mathcal{B}(\boldsymbol{z})\right]^{\frac{D-L-E-1}{2}} \prod_{s=1}^{n_{isp}} z_s^{-\nu_s}.$$
 (2.34)

The

$$n_{isp} = \frac{1}{2}L(L+1) + EL.$$
 (2.35)

integration variables  $\mathbf{z} = (z_1, \dots, z_{n_{isp}})$  are linearly independent scalar products involving the loop momenta. In general, we choose  $n_{int}$  of these to be the propagators  $z_i = D_i$  of the graph. If  $n_{isp} > n_{int}$ , one can either add irreducible scalar products as additional variables or equivalently one considers a larger graph with a sufficient number of propagators and sets the powers  $\nu_i$  of these additional propagators to zero. The Gram determinants are defined as

$$\det \mathcal{G}(q_{1}, \dots, q_{n}) = \det \begin{pmatrix} -q_{1}^{2} & -q_{1} \cdot q_{2} & \dots & -q_{1} \cdot q_{n_{\text{isp}}} \\ -q_{2} \cdot q_{1} & -q_{2}^{2} & \dots & -q_{2} \cdot q_{n_{\text{isp}}} \\ \vdots & \vdots & \ddots & \vdots \\ -q_{n_{\text{isp}}} \cdot q_{1} & -q_{n_{\text{isp}}} \cdot q_{2} & \dots & -q_{n_{\text{isp}}}^{2} \end{pmatrix}$$
(2.36)

and the Baikov polynomial is

$$\mathcal{B}(z) = \det \mathcal{G}(\ell_1, \dots, \ell_L, p_1, \dots, p_E) . \tag{2.37}$$

The determinant  $\det C$  is independent of the integration variables  $z_i$  and encodes parts of the Jacobian due to the variable transformation. We denote regions where the ratios of Gram determinants are positive by

$$C_j = \left\{ \frac{\det \mathcal{G}(k_j, k_{j+1}, \dots, k_L, p_1, \dots, p_E)}{\det \mathcal{G}(k_{j+1}, \dots, k_L, p_1, \dots, p_E)} \ge 0 \right\}$$

$$(2.38)$$

and define the integration region as

$$C = C_1 \cap C_2 \cap \cdots \cap C_L. \tag{2.39}$$

<sup>9</sup>In this thesis, we refer to the integral eq. (2.34) as the Baikov integral to distinguish from the full Feynman integral in Baikov representation that contains the pre-factor in eq. (2.33).

In dimensional regularisation the exponent of the Baikov polynomial in the integrand of eq. (2.34) is non-integer and consequently the integrand is multi-valued. The factors  $z_s^{-\nu_s}$  introduce additional branch points for non-integer  $\nu_s$  and poles for integer positive  $\nu_s$ . In many higher loop cases, computing the Baikov representation for the full integral in this way gives unnecessarily bloated expressions which need to be simplified. In those cases, it is easier to transform the variables loop-by-loop, viewing the remaining graph as external [86, 87]<sup>10</sup>.

We give here a simple example to illustrate Baikov representation, but refer to Section 2.4 for further examples including ones where we use the loop-by-loop approach.

**Example 2.7** (Baikov Representation of Bubble Integral Family). We start with a rather trivial one-loop example and compute the Baikov representation for the bubble integral family of Example 2.5. It has two linearly independent scalar products,  $\ell^2$  and  $\ell \cdot p$  as well as two propagators. Thus, one can choose as variables

$$z_1 = \ell^2 - m_1^2 \text{ and } z_2 = (\ell - p)^2 - m_2^2.$$
 (2.40)

The Baikov polynomial is

$$\mathcal{B}_{-}(z_1, z_2) = p^2(m_1^2 + z_1) - \frac{1}{4} \left( p^2 + m_1^2 - m_2^2 + z_1 - z_2 \right)^2$$
 (2.41)

and we obtain:

$$\mathbb{I}_{\nu}^{\circlearrowright}(\{p^2\}, \{m_1^2, m_2^2\}) = \int_{\mathcal{C}_{\bigcirc}} \left[ p^2(m_1^2 + z_1) - \frac{1}{4} \left( p^2 + m_1^2 - m_2^2 + z_1 - z_2 \right)^2 \right]^{\frac{D-3}{2}} z_1^{-\nu_1} z_2^{-\nu_2}.$$
(2.42)

In this case, the integration region  $\mathcal{C}_{\bigcirc}$  is just the region of  $\mathbb{R}^2$  where the Baikov polynomial eq. (2.41) is positive.

# 2.3 Feynman Integrals: Cuts

Different notions of cuts exist in the physics literature, and they are reviewed concisely in [88] and we give a rather intuitive presentation here. They all have in common that a certain set of propagators is cut and generally cutting means replacing the propagators by some Dirac  $\delta$  function. Here, we define a cut integral as the original loop integral with the cut propagators put on-shell or equivalently, the contour replaced by a contour that encircles only the poles of the cut propagators. In momentum representation – see eq. (2.12) – cutting propagators  $j_1, \ldots, j_r$  yields the following expression:

$$\operatorname{Cut}_{j_1,\dots,j_r}[I_{\nu}] = e^{L\varepsilon\gamma_E}(\mu^2)^{\nu - \frac{LD}{2}} \operatorname{Res}_{D_{j_1} = 0\dots D_{j_r} = 0} \left[ \int \left( \prod_{r=1}^L \frac{\mathrm{d}^D \ell_r}{i\pi^{\frac{D}{2}}} \right) \prod_{j=1}^{n_{\text{int}}} \frac{1}{D_j^{\nu_j}} \right] . \quad (2.43)$$

<sup>10</sup>In mathematical terms, one can consider this approach to be the construction of a fibration. A precise definition and an extended discussion of cuts at one loop is given in [89]. Practically, it is often easier to compute cuts in Baikov representation, where the integration variables include the propagators themselves:

$$\operatorname{Cut}_{j_1,\dots,j_r} \left[ \mathbb{I}_{\nu}(\{p_i \cdot p_j\}, \{m_i^2\}) \right] \sim \operatorname{Res}_{z_{j_1} = 0 \dots z_{j_r} = 0} \left[ \int_{\mathcal{C}} d^{n_{\mathrm{isp}}} z \left[ \mathcal{B}(\boldsymbol{z}) \right]^{\frac{D - L - E - 1}{2}} \prod_{s = 1}^{n_{\mathrm{isp}}} z_s^{-\nu_s} \right].$$
(2.44)

The maximal cut is obtained by cutting all physical propagators. In general, the contour associated with a given residue is not unique, and there exist multiple linearly independent ways to take the maximal cut. A natural approach to defining a basis for these linearly independent maximal cuts is by considering them as periods of twisted (co-)homology groups (or their relative versions for non-maximal cuts). To lay the groundwork for this discussion, we first introduce the concept of cut integrands in an intuitive way.

Graphically, the cut propagators are denoted by slashed propagators and one can associate a Feynman rule in momentum space to them:

Combining this rule with the uncut Feynman rules, one can find a cut integrand. Again, this is often most conveniently done in Baikov representation, with the  $\delta$  function  $\delta(z_i)$  for each cut propagator  $D_i = z_i$ . The branch-points and poles of the resulting integrand (in the maximal cut, we generally have *only* branch points, no poles) can then be used to determine a variety. One can find a basis of independent contours and differentials on this space and compute their integrals. These integrals form a basis of maximal cuts and we collect them in a matrix that we call the *maximal cut matrix*.

This matrix preserves many of the (physical) properties of the full Feynman integral family. In particular, since cut integrals are obtained from uncut ones by taking a residue at  $z_i = 0$  for some values of i, all linear relations for uncut integrals also hold for cuts (with all integrals where non-existent propagators are cut set to zero) [90, 91].

# 2.4 Feynman Integrals: Examples

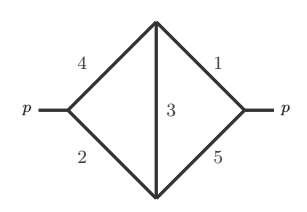
In this section we gather a number of examples to illustrate the concepts introduced in the previous sections. At the same time, we introduce in that way many of the Feynman integrals that we study in subsequent chapters.

#### See also:

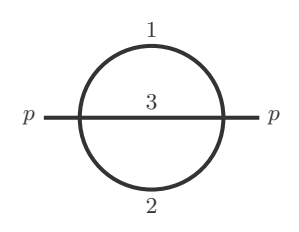
The mathematical background of this framework is introduced in Chapter 4, and we explain how to construct these maximal cuts within that context in Section 4.4.

# 2.4.1 The Sunrise and Kite Integral Families

## Kite graph:



## Sunrise graph:



#### See also:

We compute the unequal mass kite integral family in  $D=2-2\varepsilon$  in Chapter 7. The unequal mass sunrise integral family is solved in [92].

The sunrise integral family also appears in other examples throughout this thesis, e.g., in Examples 3.13 and 5.2.

In the previous sections we used the unequal mass bubble integral family as a simple yet generic example for a one-loop graph. In fact, one can easily see that the unequal mass bubble is the most generic two-point one-loop graph. As a natural next step, we now consider the most general two-loop two-point graph. A two-point graph with external momentum p and two loop-momenta  $\ell_1, \ell_2$  has five linearly independent irreducible scalar products:

$$\{\ell_1^2, \, \ell_2^2, \, \ell_1 \cdot \ell_2, \, \ell_1 \cdot p, \, \ell_2 \cdot p\}$$
. (2.45)

Thus, the most generic two-loop, two-point graph must have five internal propagators and it is given by the kite graph, depicted as the upper graph in figure 2.2 and in the margin here.

**Example 2.8** (The Kite Integral Family in Momentum Representation). In momentum representation, the kite integral family is

$$I_{\nu}^{-} = (-1)^{|\nu|} e^{2\gamma_{EM}\varepsilon} (\mu^2)^{|\nu|-D} \int \frac{\mathrm{d}^D \ell_1}{i\pi^{D/2}} \frac{\mathrm{d}^d \ell_2}{i\pi^{D/2}} \frac{1}{\mathbf{D}^{\nu}}, \qquad (2.46)$$

where  $\boldsymbol{\nu} \in \mathbb{Z}^5$ , **D** is a vector of the propagators

$$D_{1} = -\ell_{1}^{2} + m_{1}^{2} - i\epsilon, D_{2} = -(\ell_{2} - p)^{2} + m_{2}^{2} - i\epsilon,$$

$$D_{3} = -(\ell_{1} - \ell_{2})^{2} + m_{3}^{2} - i\epsilon,$$

$$D_{4} = -\ell_{2}^{2} + m_{4}^{2} - i\epsilon, D_{5} = -(\ell_{1} - p)^{2} + m_{5}^{2} - i\epsilon.$$

$$(2.47)$$

Note that we included the factor  $(-1)^{|\nu|}$  to match with the conventions in [32]. As in [32, 92], we choose  $\mu = m_3$ . The integral family has uniform transcendentality and all integrals (besides the trivial double-tadpoles) are finite in two dimensions.

The sunrise integral family is a sub-family of the kite integral family. In fact, there are two ways to obtain subtopologies belonging to sunrise families from the kite integral family. Setting  $\nu_4 = \nu_5 = 0$ , we obtain a sunrise integral family with propagators  $D_1, D_2, D_3$  – later denoted the (123)-sunrise – and setting  $\nu_1 = \nu_2 = 0$  we obtain a sunrise integral family with propagators  $D_3, D_4, D_5$  – later denoted the (345)-sunrise. The graphs for both of these families and their relation to the kite graph are depicted in figure 2.2.

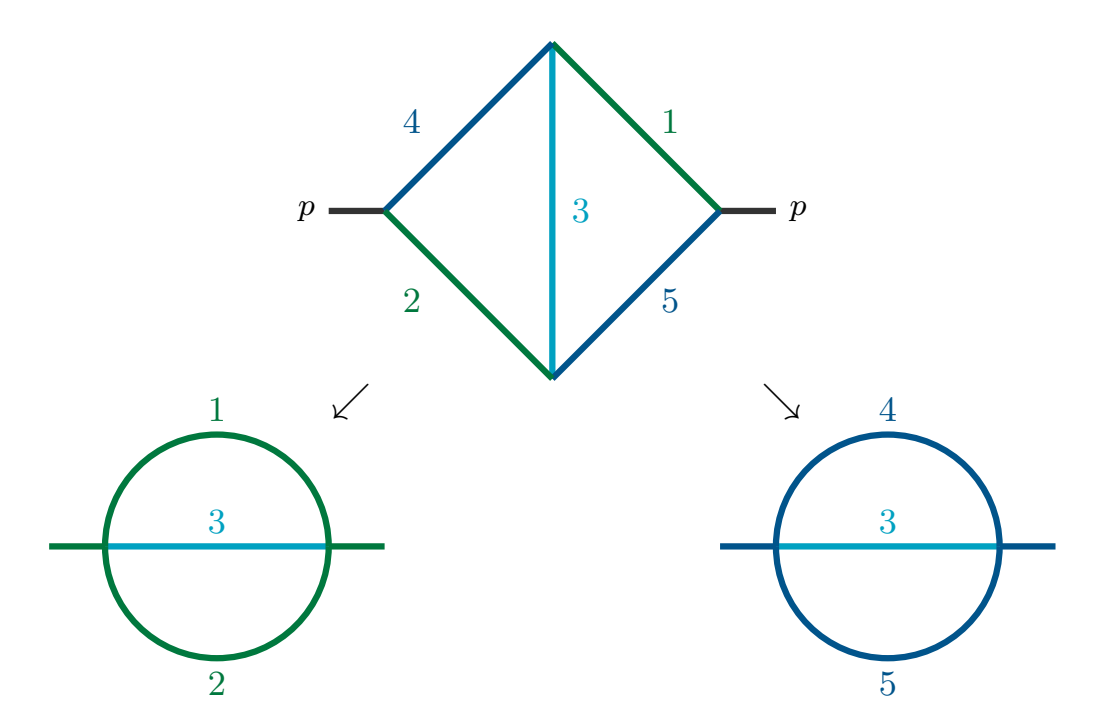


Figure 2.2: The upper graph is the kite graph with five propagators to which we associate distinct masses. Upon setting certain propagator weights to zero (or graphically *pinching* the propagators) one obtains two distinct sunrise graphs.

The kite integral and its sunrise sub-topology appears most prominently in self-energy computations at two-loops (e.g., the electron's or photon's self-energy) – see e.g., [28, 93–95]. The massive sunrise integral family is a thoroughly studied integral family in the physics [96–104] as well as mathematics literature [105, 106], as it is arguably the simplest Feynman integral in whose solution elliptic integrals appear and has been studied for a long time [93]. We will later see how this appearance of elliptic objects can be deduced from the maximal cut computed in Baikov representation. Let us therefore derive the Baikov representation for the sunrise integral family.

**Example 2.9** (The Kite Integral Family in Baikov Representation). By eq. (2.45), the sunrise integral family has five independent irreducible scalar products. Thus in the standard approach of computing Baikov representation, one needs to introduce two additional variables besides the three propagators – for example the two additional propagators that complete a sunrise integral family to the kite integral family. However, we choose to use the loop-by-loop approach, where we require only one additional variable. We split the diagram in two one-loop graphs as depicted in figure 2.3 and parametrise each of them separately. From the viewpoint of the first loop with loop momentum  $\ell_1$ , the second loop momentum  $\ell_2$  is an external momentum and thus the first loop can be parametrised as

$$\frac{\mathrm{d}^{D}\ell_{1}}{i\pi^{\frac{D}{2}}} = \frac{1}{2\sqrt{\pi}\Gamma\left(\frac{D-1}{2}\right)} \left[\det \mathcal{G}(\ell_{2})\right]^{1-\frac{D}{2}} \left[\det \mathcal{G}(\ell_{1},\ell_{2})\right]^{\frac{D-3}{2}} \mathrm{d}z_{1}\mathrm{d}z_{3}. \tag{2.48}$$

#### See also:

We discuss elliptic curves (for Feynman integrals) in Section 3.2.

<sup>&</sup>lt;sup>11</sup>This example was also discussed in [8].

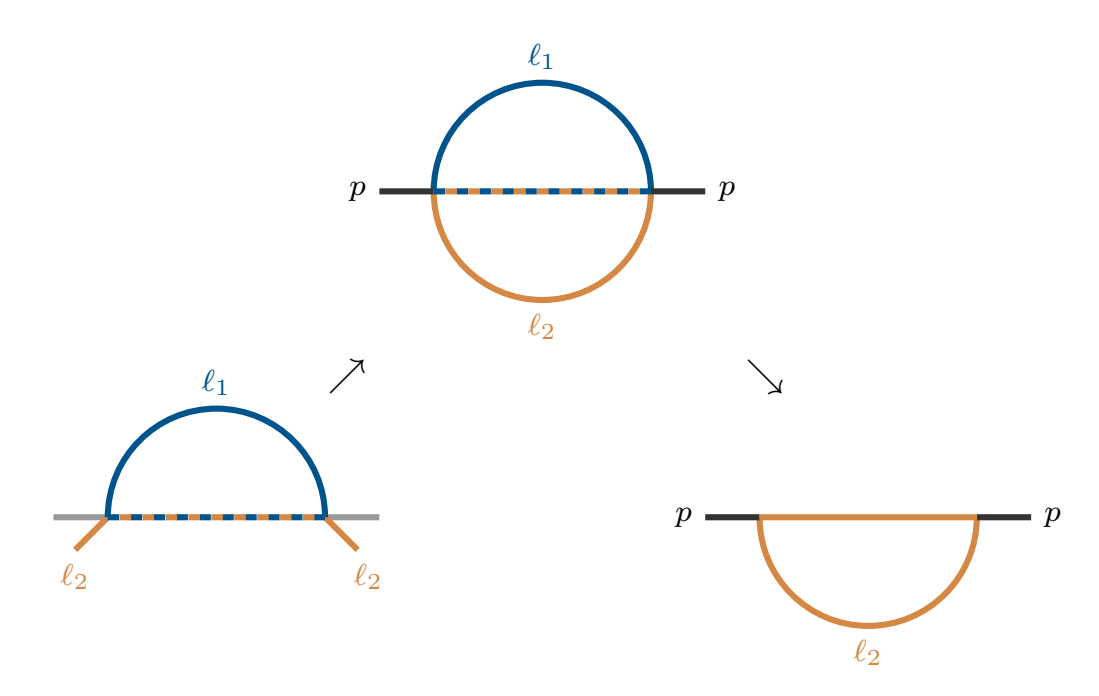


Figure 2.3: We illustrate the loop-by-loop approach for computing the Baikov representation of the sunrise integral family. The first loop has loop momentum  $\ell_1$  and the second loop has loop momentum  $\ell_2$ .

The two Gram determinants contain the three irreducible scalar products  $\ell_1^2, \ell_2^2, \ell_1 \cdot \ell_2$  and in addition to the two variables  $z_1$  and  $z_3$  we choose  $z_4 = D_4$  to express them all in Baikov variables. The second loop has loop momentum  $\ell_2$  and the loop momentum  $\ell_1$  has already been integrated out (see figure 2.3). Thus, for this loop the internal momentum is  $\ell_2$  and the external one is p. It is parametrised by

$$\frac{\mathrm{d}^{D} \ell_{2}}{i\pi^{\frac{D}{2}}} = \frac{1}{2\sqrt{\pi}\Gamma\left(\frac{D-1}{2}\right)} \left[\det \mathcal{G}(p)\right]^{1-\frac{D}{2}} \left[\det \mathcal{G}(\ell_{2}, p)\right]^{\frac{D-3}{2}} \mathrm{d}z_{2} \,\mathrm{d}z_{4} \,. \tag{2.49}$$

Since the Gram determinants in this expression contain the irreducible scalar products  $\ell_2^2$  and  $\ell_2 \cdot p$ , they can be expressed solely in  $z_2$  and  $z_4$ . Overall, we find for the sunrise integral family in Baikov representation:

$$I_{\nu}^{\oplus}(\{p_i \cdot p_j\}, \{m_i^2\}) = e^{2\varepsilon\gamma_E}(\mu^2)^{|\nu-D} \frac{(p^2)^{1-\frac{D}{2}}}{4\pi\Gamma\left(\frac{D-1}{2}\right)^2} \mathbb{I}_{\nu}^{\oplus}(\{p_i \cdot p_j\}, \{m_i^2\})$$
 (2.50)

with the Baikov integral

$$\mathbb{I}_{\nu}^{\oplus}(\{p_i \cdot p_j\}, \{m_i^2\}) = \int_{\mathcal{C}_{-}^{ll}} \mathcal{B}_{\oplus}^{ll}(\boldsymbol{z}) \cdot z_1^{-\nu_1} z_2^{-\nu_2} z_3^{-\nu_3} dz_1 dz_2 dz_3 dz_4, \qquad (2.51)$$

where

$$\mathcal{B}_{\oplus}^{ll}(z) = \left[\det \mathcal{G}(\ell_2)\right]^{1 - \frac{D}{2}} \left[\det \mathcal{G}(\ell_1, \ell_2)\right]^{\frac{D - 3}{2}} \left[\det \mathcal{G}(\ell_2, p)\right]^{\frac{D - 3}{2}} \tag{2.52}$$

is expressed in coordinates  $z_1, z_2, z_3, z_4$ . We take the maximal cut, i.e. the residues in  $z_1, z_2, z_3$  around 0, finding

$$MC\left[\mathbb{I}_{\boldsymbol{\nu}}^{\ominus}(\{p_i \cdot p_j\}, \{m_i^2\})\right] = \int \left[\mathcal{B}_{\ominus}^{ll}(\boldsymbol{z})|_{z_1, z_2, z_3 \to 0}\right] dz_4, \qquad (2.53)$$

where

$$\mathcal{B}_{\oplus}^{ll}(z)|_{z_1,z_2,z_3\to 0} \sim z_4^{\varepsilon} \left( (z_4 - \lambda_1^{\ominus})(z_4 - \lambda_2^{\ominus})(z_4 - \lambda_3^{\ominus})(z_4 - \lambda_4^{\ominus}) \right)^{-\frac{1}{2} - \varepsilon}$$
 (2.54)

with

$$\lambda_1^{\oplus} = -(m_1 + m_2)^2, \ \lambda_2^{\oplus} = -(m_3 + p)^2,$$
 (2.55)

$$\lambda_3^{\oplus} = -(m_3 - p)^2, \, \lambda_4^{\oplus} = -(m_1 - m_2)^2.$$
 (2.56)

The L-loop banana integral is the L-loop generalisation of the sunrise integral. Its one- and two-loop versions are the bubble (Example 2.5) and the sunrise integral.

**Example 2.10** (Banana Integral Family in Momentum Representation). In momentum representation, the banana integral family is

$$I_{\nu}^{\text{bananas}}(\{p^2\}, \{m_i^2\}) = e^{2\varepsilon\gamma_E} (\mu^2)^{\nu-D} \int \left( \prod_{k=1}^L \frac{\mathrm{d}^D \ell_k}{i\pi^{D/2}} \right) \delta^D \left( p - \sum_{i=1}^L \ell_i \right) \prod_{j=1}^{L+1} \frac{1}{D_j^{\nu_j}}$$
(2.5)

with

$$D_j = (-\ell_j + m_j^2). (2.58)$$

This integral family has been studied extensively in the literature as an example for integrals with Calabi-Yau varieties associated to them [16, 18, 19, 22, 107].

# 2.4.2 The Non-planar Crossed Box Family

The non-planar crossed box family has the following form in momentum representation:

$$I_{\nu}^{\text{npcb}}(\{\boldsymbol{p^2}\}, \{\boldsymbol{m^2}\}) = e^{2\varepsilon\gamma_E}(\mu^2)^{\nu-D} \int \frac{\mathrm{d}^D \ell_1}{i\pi^{D/2}} \frac{\mathrm{d}^D \ell_2}{i\pi^{D/2}} \prod_{i=1}^7 \frac{1}{D_i^{\nu_i}}, \qquad (2.59)$$

with

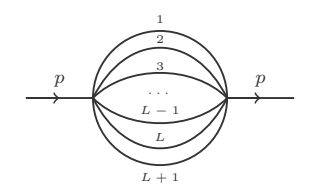
$$D_{1} = -\ell_{1}^{2} + m_{1}^{2} - i\epsilon, D_{2} = -(\ell_{1} - p_{1})^{2} + m_{2}^{2} - i\epsilon, D_{3} = -(\ell_{1} - p_{1} - p_{2})^{2} + m_{3}^{2} - i\epsilon,$$

$$D_{4} = -\ell_{2}^{2} + m_{4}^{2} - i\epsilon, D_{5} = -(\ell_{2} - p_{3})^{2} + m_{5}^{2} - i\epsilon, D_{6} = -(\ell_{1} + \ell_{2})^{2} + m_{6}^{2} - i\epsilon,$$

$$D_{7} = -(\ell_{1} + \ell_{2} - p_{1} - p_{2} - p_{3})^{2} + m_{7}^{2} - i\epsilon.$$
(2.60)

Here, we consider all external particles to be massless, i.e.,  $p_i^2 = 0$  and set  $D = 4 - 2\varepsilon$ . The integral only depends on the kinematic variables  $s = (p_1 + p_2)^2$ , t = 0

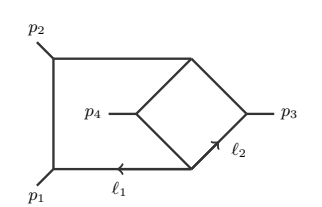
## Banana graph:



#### See also:

We compute the twodimensional and massless version of these integrals in Example 8.1.

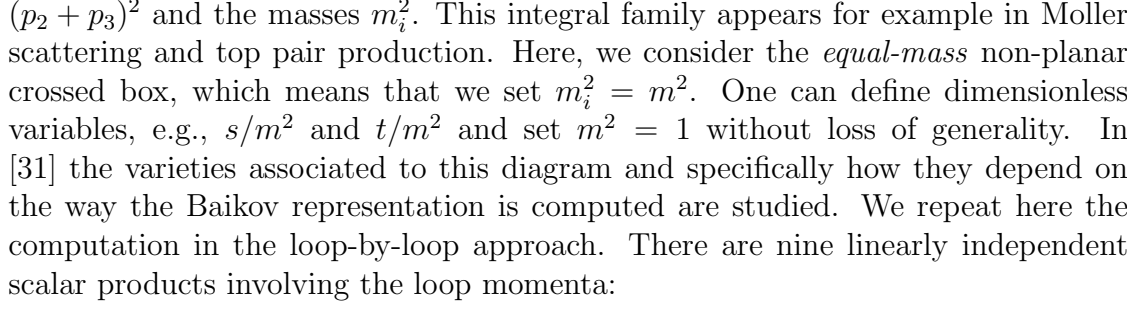
Non-Planar Crossed Box Graph:



 $(p_2+p_3)^2$  and the masses  $m_i^2$ . This integral family appears for example in Moller crossed box, which means that we set  $m_i^2 = m^2$ . One can define dimensionless variables, e.g.,  $s/m^2$  and  $t/m^2$  and set  $m^2 = 1$  without loss of generality. In [31] the varieties associated to this diagram and specifically how they depend on the way the Baikov representation is computed are studied. We repeat here the computation in the loop-by-loop approach. There are nine linearly independent

#### $\{\ell_1^2, \ell_2^2, \ell_1 \cdot \ell_2, \ell_1 \cdot p_1, \ell_1 \cdot p_2, \ell_1 \cdot p_3, \ell_2 \cdot p_1, \ell_2 \cdot p_2, \ell_2 \cdot p_3\}$ . (2.61)

We use as external momenta the independent set  $\{p_{12} = p_1 + p_2, p_2, p_3\}$  and split the graph in two loops as depicted in figure 2.4.



Feynman integrals in Section 3.5 and in particular, how to associate a hyperelliptic curve to this integral

See also:

We discuss how to as-

sociate geometries to

family.

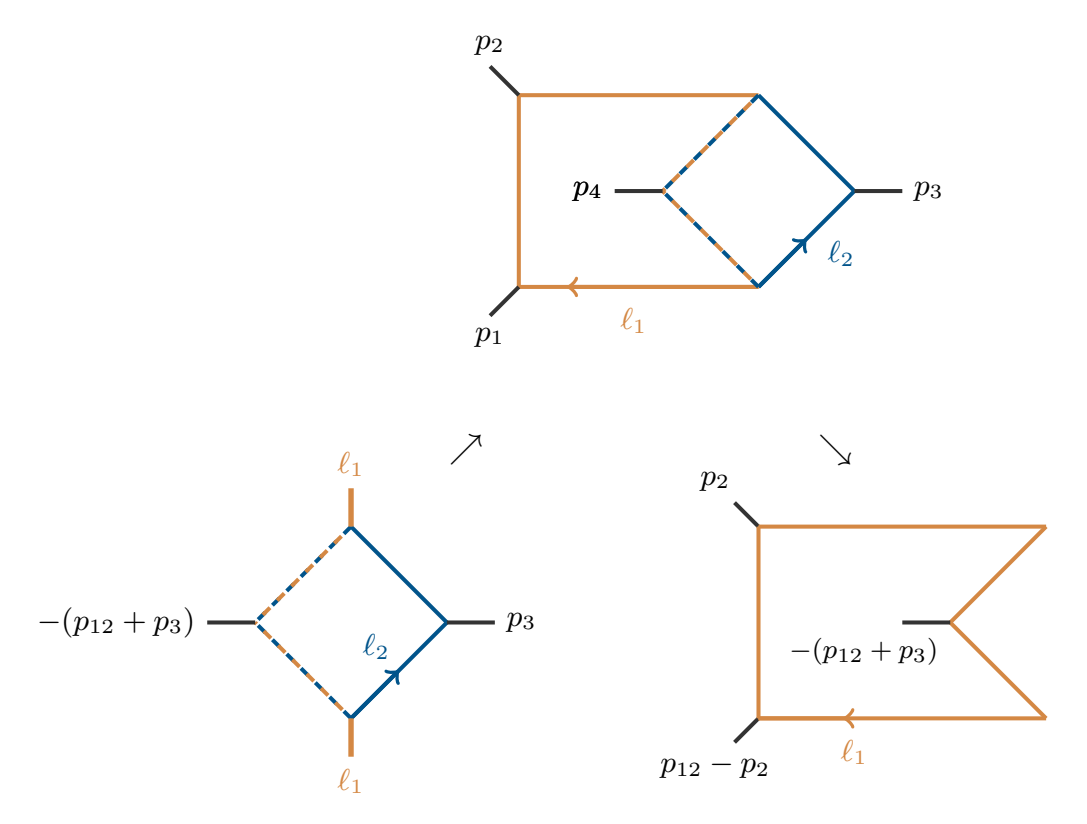


Figure 2.4: We illustrate the loop-by-loop approach for computing the Baikov representation of the sunrise integral family. The first loop has loop momentum  $\ell_2$ and the second loop has loop momentum  $\ell_1$ .

**Example 2.11** (Non-Planar Crossed Box: Baikov Representation). We take as the first loop the one spanned by the propagators 4, 5, 6, 7 and with loop momentum  $\ell_2$  (represented by the lower left graph in figure 2.4). The external parameters of this loop are  $p_{12}, p_3, \ell_1$  and we parametrise

$$d^{D}\ell_{2} \sim \mathcal{B}_{1}^{npcb}(\boldsymbol{z})^{\frac{4-D}{2}} \mathcal{B}_{2}^{npcb}(\boldsymbol{z})^{\frac{D-5}{2}} dz_{4} dz_{5} dz_{5} dz_{7}$$
 (2.62)

with 
$$\mathcal{B}_1^{npcb}(\mathbf{z}) = \det \mathcal{G}(p_{12}, p_3, \ell_1)$$
 and  $\mathcal{B}_2^{npcb} = \det \mathcal{G}(p_{12}, p_3, \ell_1, \ell_2)$ . (2.63)

The Gram determinants can be expressed in the seven propagators (denoted  $z_1, \ldots, z_7$  in their role as coordinates) and an additional irreducible scalar product  $z_8 = \frac{1}{2}\ell_1 \cdot p_3$ . In the following, we will be less precise concerning prefactors in the external variables, as we want to highlight the integrand in the coordinates  $z_i$ . The second loop is the one spanned by the propagators 1, 2, 3 and in a sense the additional one, 8 (represented by the lower right graph in figure 2.4). We parametrise:

$$d^{D}\ell_{1} \sim \mathcal{B}_{3}^{npcb}(\boldsymbol{z})^{\frac{4-D}{2}}\mathcal{B}_{3}^{npcb}(\boldsymbol{z})^{\frac{D-5}{2}}dz_{1}dz_{2}dz_{3}dz_{8}$$
 (2.64)

with 
$$\mathcal{B}_{3}^{npcb}(z) = \det \mathcal{G}(p_{12}, p_1, p_3)$$
 and  $\mathcal{B}_{4}^{npcb} = \det \mathcal{G}(p_{12}, p_1, p_3, \ell_1)$ . (2.65)

From these parametrisations of both loops, we obtain for the maximal cut:

$$Max-Cut \left[ \mathbb{I}_{\nu}^{npcb}(\{s,t\},\{m^{2}\}) \right]$$

$$\sim \operatorname{Res}_{z_{j_{1}},...,z_{j_{7}}=0} \left[ \mathcal{B}_{1}^{npcb}(\boldsymbol{z})^{\frac{4-D}{2}} \mathcal{B}_{2}^{npcb}(\boldsymbol{z})^{\frac{D-5}{2}} \mathcal{B}_{3}^{npcb}(\boldsymbol{z})^{\frac{4-D}{2}} \mathcal{B}_{4}^{npcb}(\boldsymbol{z})^{\frac{D-5}{2}} \left( \prod_{i=1}^{7} z_{i}^{-1} \right) \prod_{i=1}^{8} dz_{i} \right]$$

$$= \int \mathcal{B}_{1}^{npcb}(\boldsymbol{z})^{\frac{4-D}{2}} \mathcal{B}_{2}^{npcb}(\boldsymbol{z})^{\frac{D-5}{2}} \mathcal{B}_{3}^{npcb}(\boldsymbol{z})^{\frac{4-D}{2}} \mathcal{B}_{4}^{npcb}(\boldsymbol{z})^{\frac{D-5}{2}} \Big|_{z_{1},...,z_{7}\to 0} dz_{8}$$

$$= \int 2 \left( P_{2}^{npcb} \right)^{-\frac{1}{2}} \left( P_{4}^{npcb} \right)^{-\frac{1}{2}-\varepsilon} ,$$

$$(2.67)$$

where

$$P_2^{npcb} = (z - \lambda_1^{npcb})(z - \lambda_2^{npcb}) \tag{2.68}$$

$$P_4^{npcb} = (z - \lambda_3^{npcb})(z - \lambda_4^{npcb})(z - \lambda_5^{npcb})(z - \lambda_6^{npcb})$$
 (2.69)

with

$$\lambda_1^{npcb} = -\frac{s(s+t) + 2\sqrt{m^2 s t (s+t)}}{2s} \tag{2.70}$$

$$\lambda_2^{npcb} = \frac{-s(s+t) + 2\sqrt{m^2 s t (s+t)}}{2s} \tag{2.71}$$

$$\lambda_3^{npcb} = \frac{1}{4} \left( -s - \sqrt{-4m^2s + s^2} \right) \,, \tag{2.72}$$

$$\lambda_4^{npcb} = \frac{1}{4} \left( -s + \sqrt{-4m^2s + s^2} \right) \tag{2.73}$$

$$\lambda_5^{npcb} = \frac{1}{4} \left( -s - \sqrt{12m^2s + s^2} \right) \tag{2.74}$$

$$\lambda_6^{npcb} = \frac{1}{4} \left( -s + \sqrt{12m^2s + s^2} \right) \tag{2.75}$$

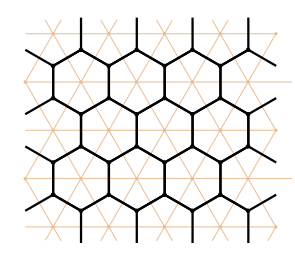
The maximal cut of this diagram was first computed directly in momentum space [108, 109]. In [31] different geometries arising from this maximal cut depending on the mode of calculation were analysed.

#### See also:

In Section 6.1.4 we discuss a normalised version of the Lauricella function with six parameters, which is a model for the maximal cut of the equal-mass non-planar crossed box.

# 2.4.3 Fishnet Integrals

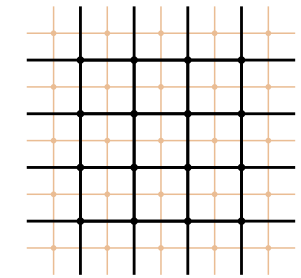
## Fishnet graphs:



Finally, we introduce a class of integrals known as fishnet integrals. These integrals derive their name from fishnet graphs. Those can be obtained by cutting a a regular tiling of the plane along a closed curve  $\mathcal{C}$  that intersects the edges of the tiling. This process defines a connected graph G, consisting of the external edges—those intersecting  $\mathcal{C}$ —and the interior edges, which lie within the enclosed region. An example – with a rectangular tiling – is depicted in figure 2.5. In particular, we consider the tiling in position space, where we denote the internal coordinates by  $\xi_i$  and they are related to the momentum space coordinates by:

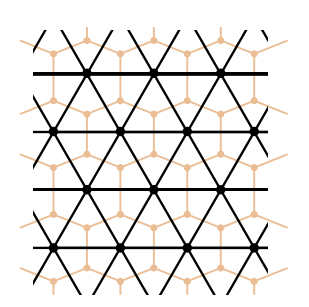
$$\ell_j^{\mu} = \xi_j^{\mu} - \xi_{j+1}^{\mu} \,. \tag{2.76}$$

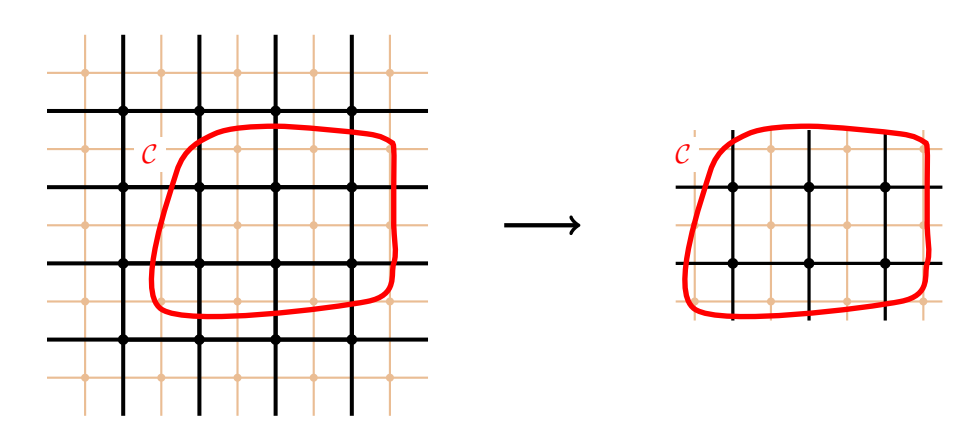
The Feynman rules for massless fishnet integrals in position space are:



$$\longrightarrow \int d^{D} \xi_{i}$$
 a  $\longrightarrow$  b  $\rightarrow [(a-b)^{2}]^{-\nu}$  . (2.77)

Each vertex denotes an integration over the D-dimensional position space (the number of vertices in position space equals the number of loops in momentum space).





See also:

We discuss how these integrals can be computed as single-valued versions of twisted periods or equivalently as Kähler potentials of certain Calabi-Yau varieties in Chapter 8.

Figure 2.5: An illustration of how one obtains a fishnet graph by cutting along a closed contour in a regular tiling. In this example, a 6-loop graph is cut from a rectangular tiling, where the black graph depicts the position space representation and the light-orange graph depicts the dual momentum space representation.

We consider vertices with 3,4 and 6 edges attached. The internal edges are propagators and we consider theories where they are raised to some (globally constant) power  $\nu$ . With these rules, we can associate to a fishnet graph G a Feynman integral

$$I_{\nu}^{G}(\boldsymbol{\sigma}) = \int \left[ \prod_{i} d^{D} \xi_{i} \right] \left[ \prod_{i,j} \frac{1}{[(\xi_{i} - \xi_{j})^{2}]^{\nu}} \right] \left[ \prod_{i,j} \frac{1}{[(\xi_{i} - \sigma_{j})^{2}]^{\nu}} \right].$$
 (2.78)

where  $\sigma$  are the external position space variables. We are particularly interested in two-dimensional massless fishnet integrals. As in eq. (2.20), we can write these integrals in D=2 dimensions in complex coordinates, where they take the form:

$$I_{\nu}^{G}(\boldsymbol{\lambda}) \sim \int \left[ \prod_{i} dx_{i} \wedge d\bar{x}_{i} \right] \left[ \prod_{i,j} \frac{1}{[|x_{i} - x_{j}|^{2}]^{\nu}} \right] \left[ \prod_{i,j} \frac{1}{[|x_{i} - \lambda_{j}|^{2}]^{\nu}} \right]. \tag{2.79}$$

Of particular interest are fishnet integrals exhibiting conformal symmetry in two dimensions. That means they are invariant under the operators of the conformal algebra, see the discussion below and specifically eq. (2.85). Conformality is ensured by assigning appropriate propagator powers. They have to be chosen, such that at each vertex with V incoming propagators

$$V \cdot \nu = D, \tag{2.80}$$

which means, we let  $\nu = \frac{D}{V}$ . We consider tillings with V = 3, 4, 6 (i.e., propagator powers  $\frac{2}{3}, \frac{1}{2}, \frac{1}{3}$  in D = 2) with a particular focus on square tilings V = 4. In general, fishnet integrals can be understood as correlation functions and in particular, for square tilings (V = 4), they belong to the bi-scalar fishnet theory, see refs. [110, 111]. For more details on fishnet integrals in integrability, see e.g., refs. [112–115].

#### Symmetries of Fishnet Integrals

Conformal fishnet integrals not only exhibit symmetry under the conformal algebra (as mentioned above) but also possess discrete symmetries. Moreover, there exist correspondences between graphs of different valencies—these are known as the startriangle relations.

**Yangian Symmetry.** Feynman integrals are called conformal if they are annihilated by the tensor product action of the Lie-algebra  $\mathfrak{so}(1, D+1)$ . The corresponding densities can be organised as *level-zero generators*  $J^a$  – which correspond to the original generators of  $\mathfrak{g}$  – and the *level-one generators*  $\hat{J}^a$  – which are constructed from the level-zero ones:

$$J^{a}I_{\nu}^{G} = \hat{J}^{a}I_{\nu}^{G} = 0. \tag{2.81}$$

These generators satisfy the following commutation relations:

$$\left[\mathbf{J}^{\mathbf{a}}, \mathbf{J}^{\mathbf{b}}\right] = f^{ab}{}_{c} \mathbf{J}^{\mathbf{c}}, \qquad \left[\mathbf{J}^{\mathbf{a}}, \hat{\mathbf{J}}^{\mathbf{b}}\right] = f^{ab}{}_{c} \hat{\mathbf{J}}^{c}, \qquad (2.82)$$

where  $f^{ab}{}_{c}$  are the structure constants of the algebra  $\mathfrak{g}$ . The action of these generators on the external labels  $\lambda_{i}$  is defined as follows:

$$J^{a} = \sum_{j=1}^{n} J_{j}^{a}, \qquad \qquad \hat{J}^{a} = \frac{1}{2} f^{a}_{bc} \sum_{j < k} J_{j}^{c} J_{k}^{b} + \sum_{j=1}^{n} \hat{s}_{j} J_{j}^{a}, \qquad (2.83)$$

where  $J_j^a$  represents a differential operator in the external variables  $\lambda_i$ . The constants  $\acute{s}_j$ , known as *evaluation parameters*, characterize an external automorphism of the Yangian algebra. Specifically, in D=2 dimensions, the Yangian splits into holomorphic and anti-holomorphic parts:

$$Y(\mathfrak{so}(1,3)) = Y(\mathfrak{sl}_2(\mathbb{R})) \oplus \overline{Y(\mathfrak{sl}_2(\mathbb{R}))}. \tag{2.84}$$

The generators  $J_i^a$  of  $Y(\mathfrak{sl}_2(\mathbb{R}))$  are

$$P_{j}^{\mu} = -i\partial_{\lambda_{j}}^{\mu}, \qquad K_{j}^{\mu} = -2i\lambda_{j}^{\mu} \left(\lambda_{j}^{\nu}\partial_{\lambda_{j},\nu} + \Delta_{j}\right) + i\lambda_{j}^{2}\partial_{\lambda_{j}}^{\mu},$$

$$L_{j}^{\mu\nu} = i\left(\lambda_{j}^{\mu}\partial_{\lambda_{j}}^{\nu} - \lambda_{j}^{\nu}\partial_{\lambda_{j}}^{\mu}\right), \qquad D_{j} = -i\left(\lambda_{j}^{\mu}\partial_{\lambda_{j},\mu} + \Delta_{j}\right). \qquad (2.85)$$

Here, the scaling dimension  $\Delta_j$  corresponds to the conformal dimension that tells how it transforms under dilations (scale changes), of the external leg j of the fishnet graph. Since these generators act as differential operators, eq. (2.81) leads to a set of partial differential equations satisfied by the fishnet integrals. Complete Yangian invariance can be inferred from invariance under the level-zero Lie algebra together with a single additional level-one generator—for example, the level-one momentum generator  $\hat{P}^{\mu}$ . Since the Yangian  $Y(\mathfrak{so}(1, D+1))$  contains the conformal algebra  $\mathfrak{so}(1, D+1)$  as a subalgebra, fishnet integrals are conformally invariant, with each external point  $\lambda_j$  carrying a conformal weight  $\Delta_j$ . Consequently, a fishnet integral associated with a given Feynman graph G can be expressed as

$$I_{\nu}^{G}(\lambda) = |F_{G}(\lambda)|^{2} \phi_{G}(\chi), \qquad (2.86)$$

where  $|F_G(\lambda)|^2$  is an algebraic function carrying the conformal weight, while  $\phi_G \chi$ ) depends solely on conformal cross ratios such as

$$\chi_{ijkl} := \frac{\lambda_{ij}^2 \lambda_{kl}^2}{\lambda_{ik}^2 \lambda_{il}^2}, \qquad \lambda_{ij} := \lambda_i - \lambda_j.$$
 (2.87)

**Permutation symmetries** In addition to Yangian symmetry, enforced by differential operators, fishnet integrals also exhibit discrete symmetries under permutations of the external points. In particular, for massless fishnet integrals there is considerable freedom in these permutations. We denote by  $Perm_G$  the subgroup of the permutation group of the external labels that leaves the integral invariant:

$$I_{\nu}^{G}(\sigma \cdot \lambda) = I_{\nu}^{G}(\lambda), \quad \text{for all } \sigma \in \text{Perm}_{G}.$$
 (2.88)

In particular, every automorphism of G induces a permutation of the external labels  $\lambda_j$  under which the fishnet integral remains invariant and  $\operatorname{Aut}(G)$  is a subgroup of  $\operatorname{Perm}_G$ . Unlike Yangian symmetry, which is implemented via differential operators, permutation symmetries act by exchanging labels. However, they can still be used to generate additional operators that annihilate the integral family: a permutation of the external points by  $\sigma \in \operatorname{Perm}_G$  corresponds to a corresponding permutation of the differential operators.

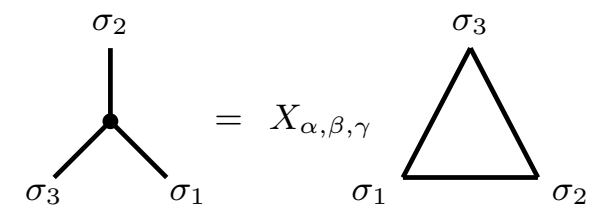
$$J_{\sigma}^{a} := \sigma J^{a} \sigma^{-1} \quad \text{and} \quad \hat{J}_{\sigma}^{a} := \sigma \hat{J}^{a} \sigma^{-1}.$$
 (2.89)

These operators define an alternative representation corresponding to a different ordering, which also annihilates the integral. The level-zero generators remain unchanged  $J_{\sigma}^{a} = J^{a}$  for all  $\sigma \in \operatorname{Perm}_{G}$  whereas the permuted level-one operators generally differ from the original ones. Since Yangian invariance follows from conformal invariance combined with the invariance under the level-one momentum operator  $\widehat{P}^{\mu}$ , it suffices to examine how permutations act on the latter. For a non-trivial reordering, the differential operator  $\widehat{P}^{\mu}_{\sigma}$  generally differs from  $\widehat{P}^{\mu}$ . In other words, there exists a set of level-one momentum operators  $\operatorname{Perm}_{G}$  that annihilate  $I_{G}^{(D)}$ .

$$\widehat{\mathbf{P}}^{\mu}_{\sigma}I^{G}_{\nu} = 0$$
, for every  $\sigma \in \operatorname{Perm}_{G}$ . (2.90)

**Star-Triangle Relations.** The star-triangle relations allow us relate different conformally-invariant integrals, in particular fishnet integrals. This allows a higher-loop fishnet integral to be computed from a lower-loop one with modified propagator weights. In particular we can relate certain graphs in triangular (V=3) and hexagonal (V=6) tilings. For  $\alpha + \beta + \gamma = D$ , these relations allow to identify an integration-star with a propagator-triangle,

$$\int \frac{\mathrm{d}^{D} \xi}{(\sigma_{1} - \xi)^{2\sigma} (\sigma_{2} - \xi)^{2\beta} (\sigma_{3} - \xi)^{2\gamma}} = \frac{X_{\sigma\beta\gamma}}{(\sigma_{1} - \sigma_{2})^{2\gamma'} (\sigma_{2} - \sigma_{3})^{2\sigma'} (\sigma_{3} - \sigma_{1})^{2\beta'}} \quad (2.91)$$



with

$$X_{\alpha\beta\gamma} = \pi^{D/2} \frac{\Gamma(\alpha')\Gamma(\beta')\Gamma(\gamma')}{\Gamma(\alpha)\Gamma(\beta)\Gamma(\gamma)}, \qquad (2.92)$$

where we use the notation x' = D/2 - x. Note that these relations do not provide a one-to-one map between graphs from triangular and hexagonal tilings.

# 2.5 Feynman Integrals: Differential Equations

Currently, the standard approach for computing Feynman integrals analytically — especially those with non-trivial underlying geometries or multiple parameters — is the method of differential equations [116–120]. In a nutshell, this method involves identifying a basis of so-called *master integrals* for a given family of Feynman integrals and solving the differential equation that this basis satisfies. A key step is transforming to a *canonical* basis of master integrals, where the solution can be expressed algorithmically in terms of iterated integrals.

#### See also:

In Chapters 7 and 6 we solve different families of (Feynman) integrals with this approach.

## 2.5.1 Linear Relations Between Feynman Integrals

As discussed near Definition 2.2, Feynman integrals in the same dimension D with the same set of propagators  $D_i$  form a Feynman integral family, parametrised by the values  $\nu$  and can be further divided into different sectors. Importantly, there exist linear relations among different members of the same family, and in fact, the integral family defines a vector space with a finite basis. This statement becomes precise when considering instead of the integrals themselves, their integrands as elements of a (relative) twisted cohomology group, as we explore in Section 4.4.<sup>12</sup> In the physics literature, linear relations between integrals of the same family manifest as integration-by-parts (IBP) relations [121, 122], dimensional shift identities, and symmetry-induced linear relations among Feynman graphs. We review all of these here, with particular emphasis on the IBP relations.

<sup>12</sup>Moreover, the IBP relations discussed below arise naturally from a basis decomposition in this framework [40, 41, 44–46].

**IBP** Relations. IBP relations can be derived from identities of the form

$$\int d^D \ell_i \frac{\partial}{\partial \ell_i^{\mu}} \left( \frac{v^{\mu}}{D_1^{\nu_1} \dots D_m^{\nu_m}} \right) = 0, \qquad (2.93)$$

with  $v^{\mu}$  being a linear combination of internal and external momenta. This identity stems from the Poincaré invariance of Feynman integrals, which requires Feynman integrals to be invariant under a shift of the loop momentum, i.e., under  $\ell \to \ell + p$ , where p is a constant momentum. This invariance implies the following relation

$$\int d^D \ell f(\ell + p) = \int d^D \ell f(\ell). \qquad (2.94)$$

Expanding the integrand for small p gives:

$$\int d^D \ell f(\ell + p) = \int d^D \ell f(\ell) + p^{\mu} \int d^D \ell \frac{\partial}{\partial \ell^{\mu}} f(\ell) + \mathcal{O}(p^2).$$
 (2.95)

From this expansion, it follows that all higher order terms and thus any total derivative must vanish, leading to the identity in eq. (2.93), where  $v^{\mu}$  is a combination of internal and external momenta. Based on this result, we can now derive linear relations for Feynman integrals within a family. Note that any derivative in a combination of internal and external momenta changes the powers of the appearing propagators and otherwise only introduces scalar products of the external momenta in the numerators, which are in particular independent of the loop momenta. In that sense, one obtains on the left-hand side of eq. (2.93) a linear combination of integrals from a particular family. Additionally, linear relations exist between different integrals within an integral family due to graph symmetries. Together, these relations allow for a recursive determination of a basis of so-called master integrals for the integral family. This standard recursive approach to find it is the so-called Laporta algorithm [123, 124]. There are different publicly available packages [125–128] that compute the IBP reduction of a family of master integrals based on the Laporta algorithm. For the integrals considered in this thesis we used primarily the

Mathematica Package LiteRed [129]. However, for many computations in particle phenomenology, but also in gravitational waves physics, the decomposition of multi-parameter Feynman integral families in terms of master integrals is still a bottleneck and thus its improvement is an active area of research. Different frameworks are being used, such as Gröbner bases [129–136], twisted cohomology [40, 41, 44–46] and machine learning [137]. Note that as indicated in eq. (2.15), there is a natural partial order for sectors of the family of Feynman integrals. We generally sort the master integrals in a way that respects this ordering. Additionally, note that the basis of master integrals is always finite and its dimension can be obtained via critical point counting or equivalently an Euler characteristic [138, 139].

**Dimensional Shift Relations.** Linear relations also exist between Feynman integrals of different dimensions, differing by multiples of two, known as dimensional shift relations. They can easily be derived in Baikov representation, where the dimension appears as an exponent of the integrand and a shift by  $D \to D + 2$  introduces an additional factor of  $\mathcal{B}(z)$  in the integrand:

$$\mathbb{I}_{\boldsymbol{\nu}}^{D+2}(\{p_i \cdot p_j\}, \{m_i^2\}) = \int_{\mathcal{C}} d^{n_{\text{isp}}} z \left[\mathcal{B}(\boldsymbol{z})\right]^{\frac{D-L-E-1}{2}} \mathcal{B}(\boldsymbol{z}) \prod_{s=1}^{n_{\text{isp}}} z_s^{-\nu_s}.$$
 (2.96)

Since  $\mathcal{B}(z)$  is a polynomial in the z, the left hand side can be written as a linear combination of integrals in D dimensions with shifted  $\nu_s$ . Conceptually, these relations resemble IBP relations, as both the spacetime dimension and the propagator exponents appear in the exponent and both classes of relations connect integrands with different exponents. The dimension-shift relations were derived in ref. [140] (see also ref. [141]). We denote the matrix encoding these dimensional shift relations by  $\mathbf{R}(\lambda, \varepsilon)$  and refer to it as the dimension shift matrix:

$$\mathbb{I}_{\nu}^{D+2}(\{p_i \cdot p_i\}, \{m_i^2\}) = \mathbf{R}(\lambda, \varepsilon) \,\mathbb{I}_{\nu}^D(\{p_i \cdot p_i\}, \{m_i^2\}). \tag{2.97}$$

One application of the dimension shift matrix is the following: Certain Feynman integrals are easier to compute in specific dimensions, such as d=2, while the desired result is in four physical dimensions. The dimensional shift relations allow us to translate results obtained in different dimensions.

# 2.5.2 Differential Equations for Feynman Integrals

Differentiating a Feynman integral with respect to an external parameter yields a linear combination of integrals from the same family with different propagator exponents. Any such derivative can be expressed as a linear combination of the basis of master integrals. Specifically, for the vector  $\mathbf{I}(\lambda, \varepsilon)$  of master integrals, this results in a linear differential equation of the form [116–120]:

$$d_{\text{ext}}\mathbf{I}(\boldsymbol{\lambda}, \varepsilon) = \mathbf{A}(\boldsymbol{\lambda}, \varepsilon)\mathbf{I}(\boldsymbol{\lambda}, \varepsilon) . \tag{2.98}$$

Note that we use both exterior derivatives with respect to the internal and the external variables in this paper. For that reason, we introduce a notation for

these derivatives and their sum:  $d_{int}$  is the exterior derivative with respect to the internal variables, e.g., the loop momenta,  $d_{ext}$  is the exterior derivative with respect to the external variables and  $d_{full} = d_{int} + d_{ext}$ . Often, we just write d, if the considered variables are obvious from the context. The connection matrix  $\bf A$  can be decomposed as

$$\mathbf{A}(\boldsymbol{x},\varepsilon) = \sum_{i=1}^{E} d\lambda_i \, \mathbf{A}_i(\boldsymbol{\lambda},\varepsilon) \,, \tag{2.99}$$

with the  $\mathbf{A}_i(\lambda, \varepsilon)^{13}$  consisting of rational functions in the external variables  $\lambda$  and  $\varepsilon$ . Note that if we sort the master integrals in a way that respects the partial ordering of eq.  $(2.15)^{14}$ , we obtain a matrix  $\mathbf{A}$  that is block lower-triangular. By construction, the matrix  $\mathbf{A}$  is integrable, i.e., it satisfies the constraint

$$d\mathbf{A} + \mathbf{A} \wedge \mathbf{A} = 0. \tag{2.100}$$

We have considerable freedom in choosing the basis of master integrals and two bases  $\mathbf{I}'$  and  $\mathbf{I}$  can be related via a transformation matrix  $\mathbf{U}(\lambda, \varepsilon)$ :

$$\mathbf{I}'(\boldsymbol{\lambda}, \varepsilon) = \mathbf{U}(\boldsymbol{\lambda}, \varepsilon) \mathbf{I}(\boldsymbol{\lambda}, \varepsilon). \tag{2.101}$$

The corresponding connection matrices are related by

$$\mathbf{A}' = \mathbf{U} \,\mathbf{A} \,\mathbf{U}^{-1} + d\mathbf{U} \,\mathbf{U}^{-1} \,. \tag{2.102}$$

It is natural to expect that the differential equations derived from some bases are easier to solve than others. Indeed, there exist specific bases, known as *canonical bases*, which seem to be particularly useful for solving their differential equations. The key properties we require of a canonical basis  $\mathbf{J}(\lambda, \varepsilon)$  are the following:

- The connection matrix of the differential equation  $\varepsilon$ -factorizes, i.e. it takes the form  $\mathbf{A}(\lambda, \varepsilon) = \varepsilon \cdot \mathbf{B}(\lambda)$  with  $\mathbf{B}(\lambda)$  independent of  $\varepsilon$ .
- $B(\lambda)$  has only simple poles.

While the first condition is straightforward, the interpretation of the second is case-dependent. The properties of the canonical differential equation be a recurring theme throughout this thesis. For now, we focus on the implications of the first property, which help us to identify a function space of iterated integrals and ultimately lead us back to the second condition. In ref. [142], it was observed that there exists a distinguished basis  $\mathbf{J}(\lambda, \varepsilon)$  such that

$$d\mathbf{J}(\lambda, \varepsilon) = \varepsilon \mathbf{B}(\lambda) \mathbf{J}(\lambda, \varepsilon) \text{ with } \mathbf{B}(\lambda) = \sum_{i} \mathbf{B}_{i} \omega_{i}, \qquad (2.103)$$

where the  $\omega_i$  are one-forms in  $\lambda$ . This differential equation can formally be solved by

$$\mathbf{J}(\boldsymbol{\lambda}, \varepsilon) = \mathbb{P}_{\gamma}(\boldsymbol{\lambda}, \varepsilon) \, \mathbf{J}_{0} \text{ with } \mathbb{P}_{\gamma}(\boldsymbol{\lambda}, \varepsilon) = \mathbb{P} \exp \left( \varepsilon \int_{\gamma} \mathbf{B} \right), \qquad (2.104)$$

<sup>13</sup>We often leave out the explicit dependence and shorten to  $\mathbf{A}$  and  $\mathbf{A}_{i}$ .

<sup>14</sup>With the largest integral in this ordering being the last one.

## See also:

In particular, we consider the properties of forms appearing in the canonical differential equation in Section 5.2 and discuss them with specific examples in Section 6.2.

where Pexp denotes the path-ordered exponential along some path  $\gamma$  from a point  $\lambda_0$  to a generic space in the kinematics. The integrability of the connection guarantees that the path-ordered exponential depends only on the homotopy class  $[\gamma]$ , i.e. on the chosen endpoints and not the specific path. To account for the lower boundary, the path-ordered exponential is multiplied with a boundary value  $J_0$ , i.e. with the vector of master integrals evaluated at the point  $\lambda_0$ , which needs to be computed separately. While the entries of  $A(\lambda, \varepsilon)$  are rational one-forms in  $\lambda$ , the entries of  $B(\lambda)$  may not be rational. The transformation matrix  $U(\lambda, \varepsilon)$  that expresses the change of basis to the canonical one generally involve the maximal cuts of the Feynman integrals in integer dimensions, and the latter often contain algebraic functions of the external kinematics and/or the periods and quasi-periods of some algebraic variety. This non-rational dependence then typically arises in the matrix  $B(\lambda)$ . In practice one only needs the first few terms in the Laurent expansion around  $\varepsilon = 0$ . The path-ordered exponential in the solution of the  $\varepsilon$ -form differential equation can easily be Laurent expanded:

$$\mathbf{J}(\boldsymbol{\lambda}, \varepsilon) = \left(\mathbf{1} + \varepsilon \int_{\gamma} \mathbf{B} + \varepsilon^{2} \int_{\gamma} \mathbf{B} \cdot \mathbf{B} + \mathcal{O}(\varepsilon^{3})\right) \cdot \mathbf{J}_{0}. \tag{2.105}$$

Note that the coefficients of this expansion are iterated integrals over the matrix **B**. More specifically, we can write them as iterated integrals of the one-forms  $\omega_i$ :

$$\mathbb{P}_{\gamma}(\boldsymbol{\lambda}, \varepsilon) = \mathbb{1} + \sum_{k=1}^{\infty} \varepsilon^{k} \sum_{1 \leq i_{1}, \dots, i_{k} \leq p} \mathbf{B}_{i_{1}} \cdots \mathbf{B}_{i_{k}} I_{\gamma}(\omega_{i_{1}}, \dots, \omega_{i_{k}}), \qquad (2.106)$$

where we defined the iterated integral:

$$I_{\gamma}(\omega_{i_{1}}, \dots, \omega_{i_{k}}) = \int_{\gamma} \omega_{i_{1}} \cdots \omega_{i_{k}} = \int_{0 \leq \xi_{k} \leq \dots \leq \xi_{1} \leq 1} d\xi_{1} f_{i_{1}}(\xi_{1}) d\xi_{2} f_{i_{2}}(\xi_{2}) \cdots d\xi_{k} f_{i_{k}}(\xi_{k}).$$
(2.107)

Therefore, understanding the function space of the Feynman integral in a perturbative expansion reduces to understanding these iterated integrals. Since these integrals are determined by the differential forms  $\omega_i$ , this naturally leads us back to the second condition imposed on the canonical basis: the requirement that the forms have only simple poles. In many cases, this property manifests through a decomposition the Feynman integrals in terms of multiple polylogarithms—a class of functions defined by iterated integrals over one-forms of the type  $\frac{dx}{x-c}$ . There are also examples where  $\mathbf{B}(\lambda)$  involves modular forms [5, 22, 102–104, 143–147], the coefficients of the Kronecker-Eisenstein series [92, 147] or periods of Calabi-Yau varieties and integrals thereof [5, 21, 22, 24, 107]. While the existence of a canonical form for the differential equation remains conjectural, there is now substantial evidence in its favour. In particular, in the case where the differential forms  $\omega_i$  are d log-forms, there is a solid understanding of how to find the canonical basis, see, e.g., refs. [116, 117, 148–152]. For cases where the canonical form cannot be expressed just in rational functions of the kinematic parameters  $\lambda$ , generic algorithms

#### See also:

We discuss these and other iterated integrals appearing in Feynman integrals in Section 3.4.

or packages do not exist, but there are different proposals for generic methods [24, 34, 107], which have been employed in many examples, some of which be discuss below. Here, we apply them to the simple example of the bubble, we used throughout the chapter to illustrate the above concepts:

**Example 2.12** (The Equal Mass Bubble Family: Differential Equations). We continue with the example introduced in Example 2.5. In that case an integral reduction with LiteRed gives three master integrals,  $I_{-} = \begin{pmatrix} I_{1,0}^{\circ}, I_{0,1}^{\circ}, I_{1,1}^{\circ} \end{pmatrix}^T$ . In D dimensions and the dimensionless coordinate  $\{\lambda_1 = \frac{m_1^2}{m_2^2}, \lambda_2 = \frac{p^2}{m_2^2}\}$  the initial differential equation takes the form

The functions in eq. (2.108) are:

$$\begin{split} a_1^1 &= \frac{D-2}{F(\lambda_1,\lambda_2)} \\ a_1^2 &= \frac{(2-D)(\lambda_1+\lambda_2-1)}{2\lambda_2F(\lambda_1,\lambda_2)} \\ a_2^1 &= \frac{(D-2)(\lambda_2-\lambda_1-1)}{2\lambda_1F(\lambda_1,\lambda_2)} \\ a_2^2 &= \frac{(D-2)(\lambda_1-\lambda_2-1)}{2\lambda_2F(\lambda_1,\lambda_2)} \\ a_3^1 &= \frac{(D-3)(\lambda_1-\lambda_2-1)}{F(\lambda_1,\lambda_2)} \\ a_3^2 &= -\frac{\left((D-2)(\lambda_1-1)^2\right)}{2\lambda_2F(\lambda_1,\lambda_2)} \\ &+ \frac{2(1+\lambda_1)\lambda_2+(D-4)\lambda_2^2}{2\lambda_2F(\lambda_1,\lambda_2)} \;. \end{split}$$

$$\mathbf{A}_{\sim} = \begin{pmatrix} 0 & 0 & 0 \\ 0 & \frac{(D-2)}{2\lambda_1} & 0 \\ a_1^1 & a_2^1 & a_3^1 \end{pmatrix} d\lambda_1 + \begin{pmatrix} 0 & 0 & 0 \\ 0 & 0 & 0 \\ a_1^2 & a_2^2 & a_3^2 \end{pmatrix} d\lambda_2, \qquad (2.108)$$

with the  $a_{i,j}^k$  in the margin and the function  $F(\lambda_1, \lambda_2)$ 

$$F(\lambda_1, \lambda_2) = \lambda_1^2 + (\lambda_2 - 1)^2 - 2\lambda_1(1 + \lambda_2). \tag{2.109}$$

Note that in  $D=2-2\varepsilon$  dimensions, all except for the lower right entry are already in  $\varepsilon$ -form and we choose to work in this dimension. Then with a simple transformation of the form

$$\boldsymbol{J}_{-} = \mathbf{U}_{-} \boldsymbol{I}_{-} \quad with \ \mathbf{U}_{-} = \begin{pmatrix} 1 & 0 & 0 \\ 0 & 1 & 0 \\ 0 & 0 & \sqrt{F(\lambda_{1}, \lambda_{2})} \end{pmatrix}$$
 (2.110)

we obtain a differential equation in  $\varepsilon$ -form,  $\mathrm{d} \boldsymbol{J}_{-\!\!\!\circlearrowleft} = \varepsilon \mathbf{B}_{-\!\!\!\circlearrowleft} \boldsymbol{J}_{-\!\!\!\circlearrowleft}$  with

$$\mathbf{B}_{\sim} = \begin{pmatrix} 0 & 0 & 0 \\ 0 & -\frac{d\lambda_1}{\lambda_1} & 0 \\ (\mathbf{B}_{\sim})_{3,1} & (\mathbf{B}_{\sim})_{3,2} & (\mathbf{B}_{\sim})_{3,3} \end{pmatrix}$$
 (2.111)

where

$$(\mathbf{B}_{\odot})_{3,1} = \frac{(\lambda_1 + \lambda_2 - 1)\lambda_1 d\lambda_2 - 2\lambda_1 \lambda_2 d\lambda_1}{\lambda_1 \lambda_2 \sqrt{F(\lambda_1, \lambda_2)}}$$
(2.112)

$$(\mathbf{B}_{-0})_{3,2} = \frac{(\lambda_1 - \lambda_2 + 1)\lambda_2 d\lambda_1 + (\lambda_2 - \lambda_1 + 1)\lambda_1 \lambda_2}{\lambda_1 \lambda_2 \sqrt{F(\lambda_1, \lambda_2)}}$$
(2.113)

$$(\mathbf{B}_{-})_{3,3} = \frac{2\lambda_2(1-\lambda_1+\lambda_2)d\lambda_1 + (1+\lambda_2-\lambda_2)(1-\lambda_2-\lambda_2)d\lambda_2}{\lambda_2 F(\lambda_1,\lambda_2)}.$$
 (2.114)

Thus, the differential equation is in  $\varepsilon$  form and only contains simple poles as well as the square-root  $\sqrt{F(\lambda_1, \lambda_2)}$ . Note that this square-root can be removed with an appropriate change of coordinates, see the standard literature [8]. Let us also shortly comment on the special functions that appear in the simplest integrals of the family

here: The tadpoles related to the upper left-block of the differential equation. Due to the structure of the differential equation matrix, these can only be iterated integrals over  $-\frac{\mathrm{d}\lambda_i}{\lambda_i}$ . Additionally, note that in the equal mass limit  $m_1 = m_2 = m$  with the single dimensionless parameter  $\lambda = \lambda_2 = \frac{p^2}{m^2}$ , the basis reduces to two master integrals with the initial basis being  $\mathbf{I}_{-\!\!\!-\!\!\!-}^{\mathrm{eq}} = \left(I_{1,0}^{-\!\!\!-\!\!-}, I_{1,1}^{-\!\!\!-\!\!-\!\!-}\right)^T$  and the canonical differential equation matrix reduces to

$$\mathbf{B}_{-}^{\text{eq}} = \begin{pmatrix} 0 & 0\\ \frac{1}{\sqrt{(\lambda - 4)\lambda}} & \frac{1}{4 - \lambda} \end{pmatrix} d\lambda. \tag{2.115}$$

In that case, there is a simple transformation of variables that rationalizes the square-root, which is

$$\lambda \mapsto \frac{(1+\chi)^2}{\chi}$$

and after this transformation, the matrix takes the form

$$\mathbf{B}_{\circlearrowleft}^{\mathrm{eq}} = \begin{pmatrix} 0 & 0 \\ \frac{1}{\gamma} & \frac{1}{\gamma} - \frac{2}{\gamma - 1} \end{pmatrix} \mathrm{d}\chi \,. \tag{2.116}$$

This differential equation matrix only has simple poles at  $\chi = \{0, 1, \infty\}$ .

This naturally raises several important questions, which we address through various examples and the general discussion presented throughout the thesis:

- How can we systematically find the canonical differential equation?
- What can we understand about the appearing forms in the canonical differential equation and the corresponding iterated integrals?

Naturally, these questions are deeply interconnected. A systematic approach to finding canonical differential equations depends on the specific properties we require. These properties, in turn, serve as a means to constrain the space of iterated integrals. Understanding these integrals is crucial not only for more efficient numerical evaluations in phenomenological applications but also for gaining deeper insight into the mathematical structures that arise in QFT.

# Geometries and Special Functions for Feynman Integrals

In this chapter, we introduce basic notions related to the geometries that we associate to Feynman integrals throughout the thesis. Those are depicted in figure 3.1.

#### See also:

- In Chapter 6 we discuss a class of functions that model maximal cuts of Feynman integrals related to hyperelliptic curves, specifically focusing on genus one and two.
- In Chapter 7 we solve the kite integral family related to two elliptic curves.
- In Chapter 8 we discuss fishnet integrals in two dimensions, which can be computed as special single-valued functions of periods related to Calabi-Yau varieties.

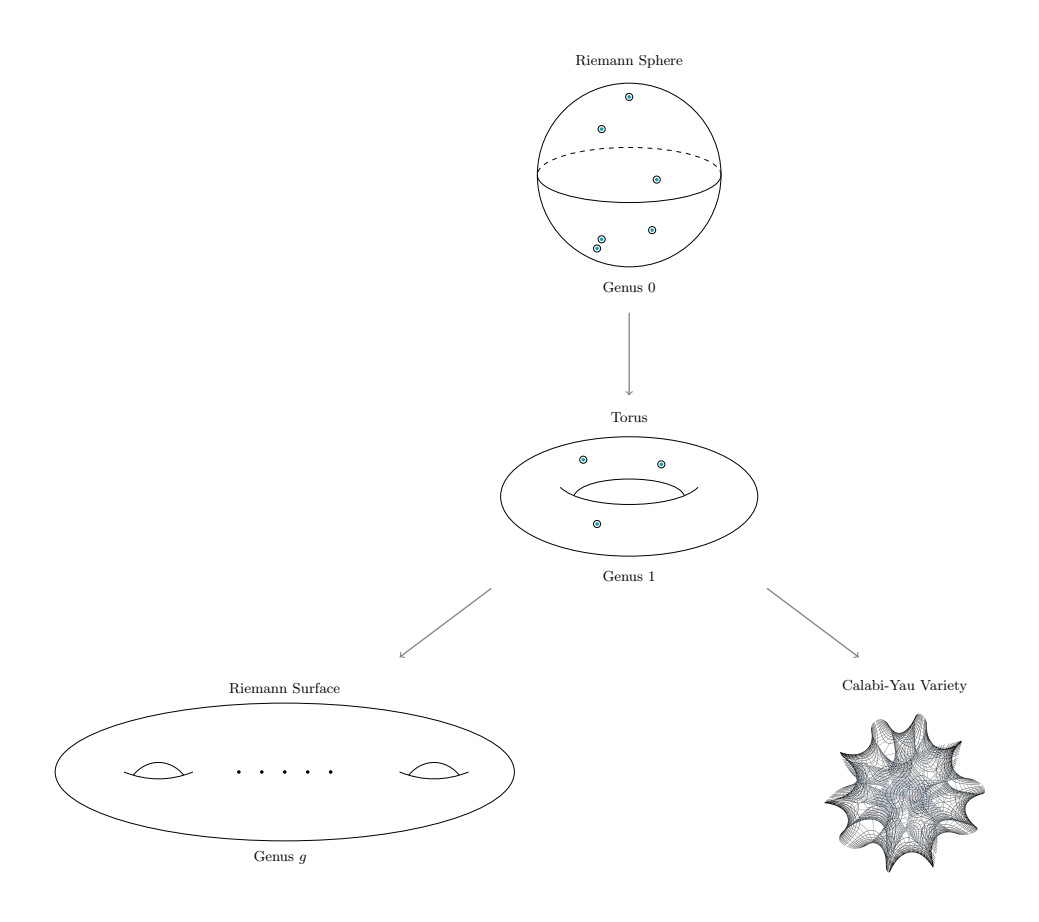


Figure 3.1: Varieties appearing in Feynman integrals.

First, in Section 3.1, we review objects related to varieties and in particular their (co-)homology groups and periods. Then we examine two specific classes of varieties: In Section 3.2 we focus on Riemann surface, in particular those arising from hyperelliptic curves and in Section 3.3 we briefly cover Calabi-Yau varieties. Next, in Section 3.4, we explore the iterated integrals associated with these geometric objects. Finally, in Section 3.5, we outline how varieties can be related to Feynman integrals, with a particular focus on examples that appear throughout the thesis.

Sections 3.1 to 3.3 and parts of Sections 3.4 and 3.5 are reviews based on the existing literature. The following results were obtained during the PhD and are already published:

- $\spadesuit$  The construction of Abelian differentials in terms of  $\Theta$  functions in Section 3.4 was already presented in an appendix of [34], which resulted from a collaboration with Claude Duhr and Sven Stawinski. The expressions can easily be derived from the existing literature on Riemann  $\Theta$  functions.
- ♠ The connection between conformal fishnet integrals in two dimensions and CY varieties of Section 3.5 was already presented in [35] which resulted from a collaboration with Claude Duhr, Florian Loebbert, Albrecht Klemm and Christoph Nega.

## Contents of this Chapter

3.1 (Co-)Homology Groups and Periods				
3.2 Riemann Surfaces and Hyperelliptic Curves				
3.2.1	Basics on Hyperelliptic Curves	58		
3.2.2	Elliptic Curves and Tori	65		
3.3 Calabi-Yau Varieties				
3.4 Iterated Integrals and Special Functions				
3.4.1	Multiple Polylogarithms	75		
3.4.2	Modular Forms and Iterated Eisenstein Integrals $\ . \ . \ .$ .	77		
3.4.3	Elliptic Multiple Polylogarithms	82		
3.4.4	Siegel Modular Forms and Abelian Differentials	84		
3.5 Geometry And Feynman Integrals				

# 3.1 (Co-)Homology Groups and Periods

Let us start by introducing the basic algebro-geometric definitions that we use throughout this chapter irrespective of the variety we consider. In particular, we characterise a variety by its (co-)homology groups and its periods.

# Cycles, Differentials and Periods

Let  $\mathcal{M}$  be a manifold with dimension D. In general, we work with complex manifolds and a D-dimensional complex manifold can also be expressed as a 2D-dimensional real manifold. We choose the complex coordinates  $\boldsymbol{z}=(z_1,\ldots,z_D)$  and their complex conjugates  $\boldsymbol{\bar{z}}=(\bar{z}_1,\ldots,\bar{z}_D)$ , where

$$z_k = z_{k,r} + i z_{k,i} \text{ and } \bar{z}_k = z_{k,r} - i z_{k,i},$$
 (3.1)

with  $z_{k,r}$  and  $z_{k,i}$  being the real and imaginary parts of the coordinate  $z_k^{-1}$ . Then, one can define the operators

$$\partial_k = \frac{\partial}{\partial z_k} = \frac{1}{2} \left( \frac{\partial}{\partial z_{k,r}} - i \frac{\partial}{\partial z_{k,i}} \right) \text{ and } \bar{\partial}_k = \frac{\partial}{\partial \bar{z}_k} = \frac{1}{2} \left( \frac{\partial}{\partial z_{k,r}} + i \frac{\partial}{\partial z_{k,i}} \right)$$
(3.2)

and from these the exterior derivatives

$$d_{z} = \sum_{k=1}^{D} dz_{k} \, \partial_{k} \text{ and } d_{\bar{z}} = \sum_{k=1}^{D} d\bar{z}_{k} \, \bar{\partial}_{k}$$
(3.3)

as well as

$$d = d_z + d_{\bar{z}}. \tag{3.4}$$

Any differential on  $\mathcal{M}$  can locally be expressed as a (p,q)-form

$$\varpi = f_{\varpi}(\boldsymbol{z}, \bar{\boldsymbol{z}}) \, \mathrm{d}z_{i_1} \wedge \cdots \wedge \mathrm{d}z_{i_p} \wedge \mathrm{d}\bar{z}_{i_1} \wedge \cdots \wedge \mathrm{d}\bar{z}_{i_q}$$
 (3.5)

with  $p, q \in \{0, ..., D\}$ . We denote the space of n-forms by  $\Omega^n(\mathcal{M}, \mathbb{C})$  and it can be decomposed into spaces of (p, q)-forms with p + q = n denoted by  $\Omega^{(p,q)}(\mathcal{M}, \mathbb{C})$ . The full exterior derivative of eq. (3.4) acts by  $d : \Omega^n(\mathcal{M}, \mathbb{C}) \to \Omega^{n+1}(\mathcal{M}, \mathbb{C})$ . Of particular interest are *closed* and *exact forms* on  $\mathcal{M}$ :

$$C^{n}(\mathcal{M}, \mathbb{C}) = \{ n \text{-form } \varpi \mid d\varpi = 0 \}$$
(3.6)

$$B^{n}(\mathcal{M}, \mathbb{C}) = \{n\text{-form } \varpi \mid \varpi = d\tilde{\varpi}, \text{ where } \tilde{\varpi} \text{ is an } n-1\text{-form}\}.$$
 (3.7)

**Definition 3.1** (de-Rham Cohomology Group). The n-th de Rham cohomology group of  $\mathcal{M}$  is

$$H^n_{dR}(\mathcal{M}, \mathbb{C}) = C^n(\mathcal{M}, \mathbb{C})/B^n(\mathcal{M}, \mathbb{C}), \qquad (3.8)$$

i.e., it consists of equivalence classes of closed forms modulo exact forms.

#### See also:

We collect basic definitions of complex and Kähler manifolds in Appendix A.

<sup>1</sup>Note that we could take the  $z_{k,r}$  and  $z_{k,i}$  as coordinates for the space in 2D real dimensions.

Naturally, one can split the cohomology group into subgroups of (p, q)-type and obtain a Hodge decomposition:

$$H_{dR}^{n}(\mathcal{M}, \mathbb{C}) = \bigoplus_{p+q=n} H_{dR}^{p,q}(\mathcal{M}, \mathbb{C}). \tag{3.9}$$

In the middle cohomology, we can define an intersection form

$$\langle \cdot, \cdot \rangle : \mathrm{H}^{\mathrm{n},0}_{\mathrm{dR}}(\mathcal{M}, \mathbb{C}) \times \mathrm{H}^{\mathrm{n},0}_{\mathrm{dR}}(\mathcal{M}, \mathbb{C}) \to \mathbb{C}, \text{ with } \langle \alpha, \beta \rangle = \int_{\mathcal{M}} \alpha \wedge \beta.$$
 (3.10)

Similarly to the de-Rham cohomology groups of differentials, we consider the singular or Betti homology groups of contours. The elements of the n-th singular homology group on  $\mathcal{M}$  are equivalence classes of closed n-chains  $\Delta$  taken modulo boundaries. In particular, these n-chains are linear combinations of oriented simplical subsets (i.e. one can think of them as oriented smooth submanifolds). More specifically, we let  $\partial$  be the operator that maps the n-chain to its boundary and

- $C_n(\mathcal{M}, \mathbb{Z})$  is the set of *n*-chains  $\Delta$ , that fulfil  $\partial \Delta = 0$ ,
- $B_n(\mathcal{M}, \mathbb{Z})$  is the set of *n*-chains  $\Delta$ , that are boundaries, i.e.  $\Delta = \partial \tilde{\Delta}$ .

**Definition 3.2** (Betti Homology Group). The n-th singular or Betti homology group of the manifold is

$$H_n(\mathcal{M}, \mathbb{Z}) = C_n(\mathcal{M}, \mathbb{Z})/B_n(\mathcal{M}, \mathbb{Z}).$$
 (3.11)

Its dimension  $b_n = \dim (H_n(\mathcal{M}, \mathbb{Z}))$  is called the Betti number.

There exists a natural intersection pairing

$$H_p(\mathcal{M}, \mathbb{Z}) \times H_{D-p}(\mathcal{M}, \mathbb{Z}) \to \mathbb{C},$$
 (3.12)

which computes the oriented topological intersection of cycles. We denote the matrix of intersections between a basis of cycles by  $\Sigma$  in this context. The *period pairing* maps tuples of Betti and de Rham (co-)cycles to complex numbers by integration:

$$(\Delta, \varpi) \mapsto \int_{\Lambda} \varpi.$$
 (3.13)

These integrals are the *periods* of the manifold. Here, we collect these periods of basis elements in vectors and matrices. In particular, we denote by  $\Pi$  a vector of the middle cohomology basis element integrated over the basis cycles (in particular for a CY, where the middle cohomology is one-dimensional) and by  $\mathcal{P}$  the *period matrix* that contains all basis differentials integrated against basis cycles (in particular for hyperelliptic curves).

## Picard-Fuchs Ideals

The computation of Feynman integrals as described in Section 2.5 is based on Gauss-Manin differential equations. In general the periods defined by these integrals also satisfy higher-order inhomogeneous differential equations, particularly in the limit  $\varepsilon \to 0$ . We discuss these differential equations facilitated by the so-called *Picard-Fuchs operators* in the context of CY periods and follow the discussion in ref. [19]. The Picard-Fuchs ideal of a CY variety (or any other algebraic variety) is the ideal of operators  $\mathbb O$  that annihilate the periods, i.e.,

$$\mathbb{O}\mathbf{\Pi} = 0. \tag{3.14}$$

Here we review some basic notions related to Picard-Fuchs operators and their solutions. In particular, we write the Picard-Fuchs operators in the differential operators

$$\theta_z = z\partial_z \text{ and } \bar{\theta}_z = \bar{z}\partial_{\bar{z}}.$$
 (3.15)

Single-Parameter Operators. A single-parameter differential operator of degree deg has the form

$$\mathbb{O} = q_{\text{deg}}(z)\partial_z^{\text{deg}} + q_{\text{deg}-1}(z)\partial_z^{\text{deg}-1} + \dots + q_0(z)$$
(3.16)

$$= \tilde{q}_{\text{deg}}(z)\theta_z^{\text{deg}} + \tilde{q}_{\text{deg}-1}(z)\theta^{\text{deg}-1} + \dots + \tilde{q}_0(z), \qquad (3.17)$$

where  $q_k(z)$  and  $\tilde{q}_k(z)$  are polynomials in z. The leading coefficient  $q_{\text{deg}}(z)$  is called the discriminant of  $\mathbb{O}$  and also denoted by  $\text{Disc}(\mathbb{O})$ . We let  $p_i(z) = \frac{q_i(z)}{q_{\text{deg}}(z)}$ . Note, that  $\theta_z$  and  $\partial_z$  are related by

$$\theta_z^r = \sum_{i=1}^k s_2(r,k) z^k \partial_z^k$$
 or equivalently  $z^r \partial_z^r = \prod_{j=0}^{r-1} (\theta - j)$ . (3.18)

This relation includes the Stirling number of second kind:

$$s_2(r,k) = \frac{1}{k!} \sum_{i=0}^{k} (-1)^i {k \choose i} (k-i)^r.$$

The singularities of a Picard-Fuchs operator can be classified into three categories:

**Definition 3.3.** Ordinary, regular singular and irregular singular points

- The differential equation has an ordinary point at  $z = z_0$  if the coefficient functions  $p_i(z)$  are analytic in a neighbourhood of  $z_0$  for all  $0 \le i \le \deg$ .
- The differential equation as a regular singular point if  $(z z_0)^{\text{deg-i}} p_i(z)$  is analytic in a neighbourhood of  $z_0$  for all  $0 \le i \le \text{deg}$ .
- A point that is neither an ordinary nor a regular singular point is called a irregular singular point.

All singular points are zeroes of the discriminant.

**Definition 3.4** (Fuchsian differential equation). A differential equation without irregular singular points is called a Fuchsian differential equation.

To solve Fuchsian differential equations locally around a point  $z_0$ , we generally use the *Frobenius method*.

## Review: Frobenius Method in One Variable

- 1. Choose a point  $z_0$  and determine whether it is an ordinary or a regular singular point. In general, we perform a coordinate transformation, such that  $z_0 = 0$ .
- 2. The starting point is the indicial equation

$$\tilde{q}_{\text{deg}}(0)\alpha^{\text{deg}} + \tilde{q}_{\text{deg}-1}(0)\alpha^{\text{deg}-1} + \dots + \tilde{q}_0(0)\alpha = 0.$$
 (3.19)

The solutions  $\alpha$  of this equation are the *indicials* or *local exponents* near  $z_0 = 0$ .

3. Make ansätze for the independent solutions of the differential equation

$$\mathbb{O}f(z) = 0, \tag{3.20}$$

near  $z_0 = 0$ . There are deg independent solutions and they take the following form:

• Ordinary: There are deg solutions  $\alpha_1, \ldots, \alpha_n$  to the indicial equation eq. (3.19) and the solution space of  $\mathbb{O}$  near  $z_0 = 0$  is spanned by

$$z^{\alpha_i} F_{i,0}(z) = z^{\alpha_i} \sum_{k=0}^{\infty} c_{i,k} z^k \text{ for } 1 \le i \le \text{deg with } a_{i,0} \ne 0.$$
 (3.21)

In general, we choose the normalisation  $c_{i,0} = 1$ .

• Regular singular: The indicials come with some multiplicity:

$$\left\{ \underbrace{\alpha_1, \dots, \alpha_1, \alpha_2, \dots, \alpha_2}_{\deg_1}, \dots, \underbrace{\alpha_m, \dots, \alpha_m}_{\deg_m} \right\}, \tag{3.22}$$

where  $\deg_1 + \deg_2 + \cdots + \deg_m = \deg$ . A singular point, where all indicials are equal is called a *point of maximal unipotent monodromy* or short *MUM-point*. One can collect the information of the singular points  $z_1, \ldots, z_s$  in the so-called *Riemann*  $\mathcal{P}$  *symbol*:

$$\begin{cases}
z_1 & z_2 & \dots & z_s \\
\alpha_1^{(1)} & \alpha_1^{(2)} & \dots & \alpha_1^{(s)} \\
\vdots & \vdots & \vdots & \vdots \\
\alpha_{\text{deg}}^{(1)} & \alpha_{\text{deg}}^{(2)} & \dots & \alpha_{\text{deg}}^{(s)}
\end{cases}$$
(3.23)

#### See also:

In Example 3.10 we apply the Frobenius method to the Legendre curve family.

Each of the distinct indicials  $\alpha_i$  comes with deg<sub>i</sub> solutions. The solutions have branch cuts, which are reflected by the appearance of log functions in the solution. Explicitly, the k-th solution with indicial  $\alpha_i$  takes the form

$$z^{\alpha_i} \sum_{j=0}^k \frac{1}{(k-j)!} \log^{k-j}(z) F_{i,j}(z) \text{ for } 0 \le k \le \deg_{i-1}.$$
 (3.24)

In particular, the lowest orders are:

$$z^{\alpha_i} F_{i,0}(z) \tag{3.25}$$

$$z^{\alpha_i} \left[ \log(z) F_{i,0}(z) + F_{i,1}(z) \right] \tag{3.26}$$

$$z^{\alpha_i} \left[ \log(z) F_{i,0}(z) + F_{i,1}(z) \right]$$

$$z^{\alpha_i} \left[ \frac{1}{2} \log^2(z) F_{i,0}(z) + \log(z) F_{i,1}(z) + F_{i,2}(z) \right]$$
(3.26)

4. Apply the operator  $\mathbb{O}$  to the ansätze and solve for the  $F_{i,j}(z)$ . Generally, we normalise by  $F_{i,i}(0) = 1$ .

Multi-Parameter Operators Similarly, one can build Picard-Fuchs operators in m variables from the operators  $\theta_{z_1}, \ldots, \theta_{z_m}$ . Their solution can also be obtained with the Frobenius method around singular points  $z_0$ . For more details on the form of the solutions and subtleties in that case, see e.g., refs. [19, 38].

#### 3.2 Riemann Surfaces and Hyperelliptic Curves

In this chapter, we discuss Riemann surfaces, i.e. one-dimensional complex oriented manifolds. They are distinguished by their genus q, which generally amounts to the number of holes in the surface. We restrict the discussion to Riemann surfaces that are hyperelliptic curves. We start by reviewing central objects related to hyperelliptic curves and specifically discuss their periods in Subsection 3.2.1. For more details, we refer to the standard literature on Riemann surfaces and their special functions [153–157] (see also [158, 159] for recent reviews in the physics literature). Then we focus on the genus one case, which is particularly relevant for Feynman integrals, in Subsection 3.2.2.

#### 3.2.1Basics on Hyperelliptic Curves

All hyperelliptic curves are Riemann surfaces (but not all Riemann surfaces are hyperelliptic curves).

**Definition 3.5** (Riemann surface). A Riemann surface is a connected one-dimensional complex analytic manifold or equivalently, a connected two-dimensional real mani-

See also:

We discuss the special functions in Sections 3.4.3 and 3.4.4.



fold  $\mathcal{R}$  with a complex structure on it, i.e. an atlas of charts to the open unit disc such that the transition functions are holomorphic.

In particular, we consider compact Riemann surfaces:

**Theorem 3.1.** Any compact Riemann surface is homeomorphic to a sphere with handles. The number of handles is called the genus of the surface.

We illustrate a Riemann surface as described in Theorem 3.1 in 3.2.

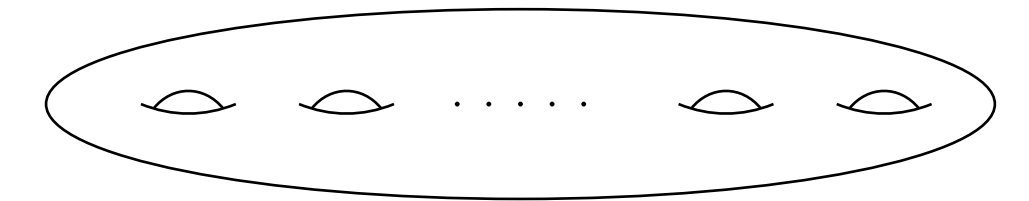


Figure 3.2: We can picture a Riemann surface of genus g as a sphere with g handles.

A hyperelliptic curve is defined by the polynomial equation

$$y^{2} = P_{n_{g}+2}(x) = \prod_{i=1}^{n_{g}+2} (x - \lambda_{i}), \qquad (3.28)$$

where the genus g of the curve is given by

$$g = \begin{cases} \frac{n_g}{2}, & \text{if } n_g \text{ is even,} \\ \frac{n_g+1}{2}, & \text{if } n_g \text{ is odd.} \end{cases}$$
 (3.29)

A hyperelliptic curve is referred to as *even* or *odd*, depending on whether  $n_g$  is even or odd.<sup>2</sup> The hyperelliptic curve in eq. (3.28) has branch points at

$$\boldsymbol{\lambda} = (\lambda_1, \dots, \lambda_{n_q+2}).$$

We typically set  $\lambda_1 = 0$  and  $\lambda_2 = 1$ . The points  $(x, \pm y)$  satisfying the condition in eq. (3.28) fulfil

$$y_{\pm} = \pm \sqrt{\prod_{i=1}^{2g+2} (x - \lambda_i)},$$
 (3.30)

and thus define two Riemann sheets, which can be glued together along g+1 branch cuts. We choose these cuts as

$$[\lambda_1, \lambda_2], [\lambda_3, \lambda_4], \dots, [\lambda_{2g-1}, \lambda_{2g}], \text{ and } \begin{cases} [\lambda_{2g+1}, \lambda_{2g+2}], & \text{if } n_g \text{ is even,} \\ [\lambda_{2g+1}, \infty], & \text{if } n_g \text{ is odd.} \end{cases}$$
 (3.31)

The resulting Riemann surface  $\Sigma_{\lambda}$  is topologically equivalent to a Riemann sphere with g handles. Notably, any Riemann surface of genus two is necessarily hyperelliptic, meaning that restricting to hyperelliptic curves is only a limitation for  $g \geq 3$ .

<sup>2</sup>Most of the notions described in this section apply similarly in both cases, and any differences will be specifically pointed out.

## Canonical Cycles for a Hyperelliptic Curve

In general, the homology group  $H_1(\Sigma_{\lambda}, \mathbb{Z})$  is 2g dimensional. That means there are no non-trivial cycles for the (genus zero) Riemann sphere (Section 3.4.1) and two cycles for the (genus one) torus (Section 3.2.2). If we consider a punctured Riemann surface, the number of basis cycles generally increases. In general, a canonical basis for the homology group  $H_1(\Sigma_{\lambda}, \mathbb{Z})$  of a hyperelliptic curve of genus g (without punctures) can be split into g g-cycles, denoted by g, and g g-cycles, denoted by g. Here, canonical refers to the fact that the topological intersection numbers of the cycles, as given by the intersection pairing  $[\bullet]$ , adopt the following simple (symplectic) form:

$$[a_i|a_j] = 0,$$
  $[b_i|b_j] = 0,$   $[a_i|b_j] = -[b_i|a_j] = \delta_{ij}.$  (3.32)

A canonical basis of cycles for an even hyperelliptic curve of genus g is depicted in figure 3.3. The figure looks the same for an odd hyperelliptic curve of genus g, with  $\lambda_{2g+2}$  replaced by  $\infty$ . Note that for a *punctured* Riemann surface, one needs to add cycles encircling each of the punctures.

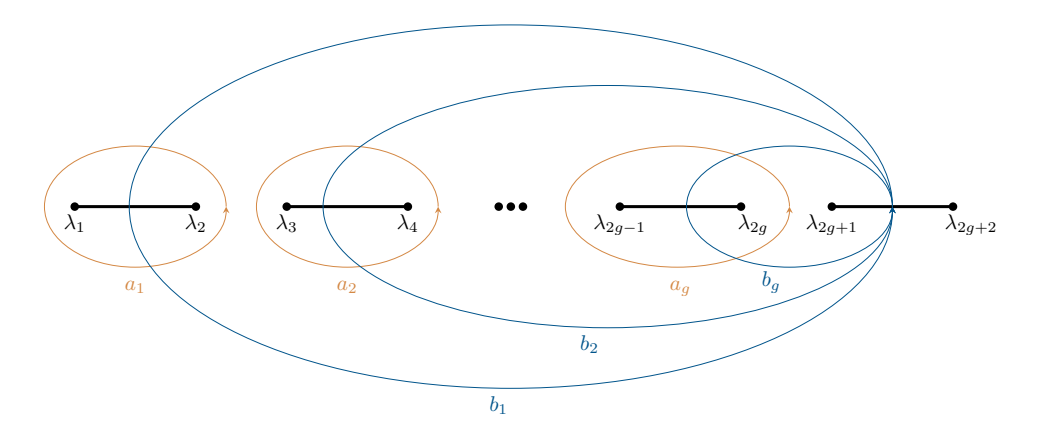


Figure 3.3: There are 2g canonical cycles for an *even* hyperelliptic curve of genus g. Note that the canonical cycles for an *odd* hyperelliptic curve of genus g can be chosen in a very similar way, with the point  $\lambda_{2g+2}$  replaced by  $\infty$ .

In figure 3.4 we illustrate how these cycles can be drawn on the corresponding Riemann surface of genus g depicted as a sphere with handles.

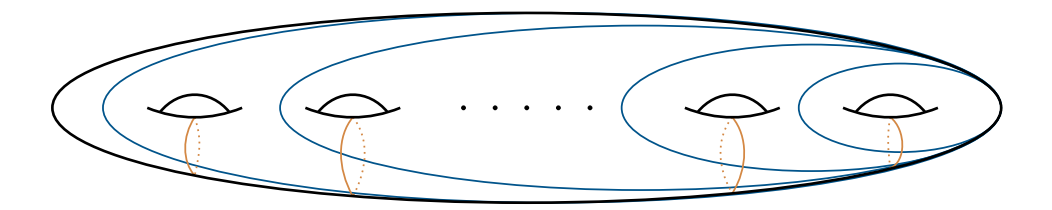


Figure 3.4: The canonical cycles on a Riemann surface of generic genus g wind around the holes.

## Abelian Differentials and Periods on the Hyperelliptic Curve

All rational differentials on a hyperelliptic curve – in algebraic coordinates x, y or geometric coordinate z – can be classified into three classes of so-called Abelian differentials:

**Definition 3.6** (Abelian differentials).

- Abelian differentials of the first kind are holomorphic differentials.
- Abelian differentials of the second kind are meromorphic differentials with vanishing residues at the poles.
- Abelian differentials of the third kind are meromorphic differentials with nonvanishing residues.

In the following paragraphs, we construct bases for these classes of differentials using linear combinations of the simple forms:

$$\frac{x^i \, \mathrm{d}x}{y} \,. \tag{3.33}$$

This construction is based on determining the residues of the simple differentials via a Laurent expansion. Notably, since the Laurent series for differentials on even and odd hyperelliptic curves differ, the construction depends on whether we consider an even or an odd hyperelliptic curve.

Abelian Differentials of the First Kind & the Normalized Period Matrix. As a basis for the holomorphic or first kind Abelian differentials of an (even or odd) hyperelliptic curve, we can choose the g one-forms

$$\varpi_i = \frac{x^{i-1} dx}{y}, \qquad 1 \le i \le g. \tag{3.34}$$

The integrals of the first kind basis differentials over the a or b-cycles are the a- $and\ b$ -period matrices,

$$\mathcal{A}_{ij} = \int_{a_j} \frac{x^{i-1} dx}{y}, \qquad \mathcal{B}_{ij} = \int_{b_j} \frac{x^{i-1} dx}{y}, \qquad i, j = 1, \dots, g.$$
 (3.35)

The (normalized) period matrix, is the quotient of the a- and b-period matrices:

$$\Omega = \mathcal{A}^{-1}\mathcal{B}. \tag{3.36}$$

This normalized period matrix is a symmetric  $g \times g$  matrix with positive definite imaginary part.

#### See also:

We give the Laurent expansions of these monomials in Appendix D.1.

**Example:** A basis of holomorphic differentials for hyperelliptic curves of genus zero to two is given by the following sets:

Genus  $0:\{\}$ 

Genus 1 :  $\left\{ \frac{\mathrm{d}x}{y} \right\}$ 

Genus 2:  $\left\{\frac{\mathrm{d}x}{y}, \frac{x\mathrm{d}x}{y}\right\}$ .

#### See also:

In Example 3.8, we give explicit expressions for these periods for a family of elliptic curves in terms of elliptic integrals.

**Example 3.1** (Period Matrix for Hyperelliptic Curves of Genus *One*). For an elliptic curve, the a- and b-periods are commonly denoted as

$$\omega_1 = \int_a \frac{\mathrm{d}x}{y} \,, \qquad \omega_2 = \int_b \frac{\mathrm{d}x}{y} \,. \tag{3.37}$$

The normalized period matrix reduces to a single scalar, commonly denoted the modular parameter:

$$\tau = \frac{\omega_2}{\omega_1} \,. \tag{3.38}$$

**Example 3.2** (Period Matrix for Hyperelliptic Curves of Genus Two). At genus two the a- and b-periods are  $2 \times 2$  matrices

$$\mathbf{A} = \begin{pmatrix} \int_{a_1} \frac{\mathrm{d}x}{y} & \int_{a_2} \frac{\mathrm{d}x}{y} \\ \int_{a_1} \frac{x\mathrm{d}x}{y} & \int_{a_2} \frac{x\,\mathrm{d}x}{y} \end{pmatrix}, \qquad \mathbf{B} = \begin{pmatrix} \int_{b_1} \frac{\mathrm{d}x}{y} & \int_{b_2} \frac{\mathrm{d}x}{y} \\ \int_{b_1} \frac{x\mathrm{d}x}{y} & \int_{b_2} \frac{x\,\mathrm{d}x}{y} \end{pmatrix}. \tag{3.39}$$

The normalized period matrix allows us to define the Jacobian of the hyperelliptic curve:

**Definition 3.7** (Jacobian variety). Let

$$\Lambda = \{2\pi i N + \Omega M | N, M \in \mathbb{Z}^g\}. \tag{3.40}$$

The complex torus

$$\operatorname{Jac}(\Sigma_{\lambda}) = \mathbb{C}^{g}/\Lambda \tag{3.41}$$

is called the Jacobian variety.

A Riemann surface of genus one is conformally equivalent to its Jacobian variety. The canonical differentials  $w_1 = \{w_{1|1}, \dots, w_{1|g}\}$  on the Riemann surface are defined by the normalization

$$\int_{a_i} w_{1|j} = \delta_{ij} . \tag{3.42}$$

They can be related to the basis choice of eq. (3.34) in algebraic coordinates by

$$\overline{\omega}_i = \sum_{j=1}^g \mathcal{A}_{ij} \, w_{1|j} \,. \tag{3.43}$$

We denote by  $\mathfrak{u}$  the Abel map:

$$\mathfrak{u}: \Sigma_{\lambda} \to \operatorname{Jac}(\Sigma_{\lambda}), \quad \mathfrak{u}(x,y) = \int_{x}^{y} w_{1} = \left(\int_{y}^{x} w_{1|1}, \dots, \int_{y}^{x} w_{1|g}\right).$$
(3.44)

**Abelian Differentials of the Second Kind.** For the Abelian differentials of the second kind in algebraic coordinates, we choose forms

$$\frac{\Psi_i(x)}{y} dx, \quad \text{with} \quad \Psi_i(x) = \sum_{j=1}^{2g} c_j x^j, \qquad (3.45)$$

where the coefficients  $c_j$  are such that they have poles at infinity, but their residues vanish. To construct a basis, one must find g linearly independent differentials of this form, which we denote by  $\varpi_{g+1}, \ldots, \varpi_{2g}$ . The construction depends on whether the underlying hyperelliptic curve is even or odd and we use the Laurent expansions given in Appendix D.1. For instance, in the case of an odd hyperelliptic curve, the differentials  $\frac{x^i dx}{y}$  for  $i \geq g$  have a pole but no residue at  $\infty$ . In contrast, for an even hyperelliptic curve, they have a residue at  $\infty$ , which must be cancelled by adding appropriate counter-terms. It is important to note that there is considerable freedom in choosing the basis: clearly we can add any linear combination of differentials of the first kind (which are holomorphic) without affecting the residue. The integrals of the second kind differentials over the a and b cycles are the a- and b-quasi-period matrices,

$$\tilde{\mathcal{A}}_{ij} = \int_{a_i} \frac{\mathrm{d}x \, \Psi_i(x)}{y} \,, \qquad \tilde{\mathcal{B}}_{ij} = \int_{b_i} \frac{\mathrm{d}x \, \Psi_i(x)}{y} \,, \qquad i, j = 1, \dots, g \,. \tag{3.46}$$

Let us illustrate this with some examples:

**Example 3.3** (Second Kind Abelian Differentials at Genus One). At genus one, for an <u>odd</u> elliptic curve, a basis of second kind differentials is given by the single element

$$\frac{x \, \mathrm{d}x}{y} \,. \tag{3.47}$$

The quasi-periods are

$$\eta_1 = \int_a \frac{x \, \mathrm{d}x}{y}, \qquad \eta_2 = \int_b \frac{x \, \mathrm{d}x}{y}.$$
(3.48)

For an even elliptic curve of genus one, we can choose for example:

$$\left(x^2 - \frac{\tilde{s}_1}{2} + \frac{\tilde{s}_2}{6}\right) \frac{\mathrm{d}x}{y},\tag{3.49}$$

where we denote by  $\tilde{s}_k$  the  $k^{th}$  elementary symmetric polynomial in the branch points  $\lambda_i$  (including for the choice  $\lambda_1 = 0, \lambda_2 = 1$ ) – e.g.,  $\tilde{s}_1 = \sum_{i=1}^{n_g+2} \lambda_i, \tilde{s}_2 = \sum_{i,j=1,i< j}^{n_g+2} \lambda_i \lambda_j, \ldots$ 

**Example 3.4** (Second Kind Abelian Differential at Genus Two). For a genus two hyperelliptic curve we need two second kind differentials. For an <u>odd</u> hyperelliptic curve, we choose:

$$\frac{\Psi_1^{2,o}(x)dx}{v}, \quad \frac{\Psi_2^{2,o}(x)dx}{v},$$
 (3.50)

with the polynomials

$$\Psi_1^{2,o}(x) = (3x^3 - 2\tilde{s}_1 x^2 + \tilde{s}_2 x) \quad and \quad \Psi_2^{2,o}(x) = x^2.$$
 (3.51)

For an <u>even</u> hyperelliptic curve, we choose:

$$\frac{\mathrm{d}x}{y}, \quad \frac{x\mathrm{d}x}{y}, \quad \frac{\Psi_1^{2,\mathrm{e}}(x)\mathrm{d}x}{y}, \quad \frac{\Psi_2^{2,\mathrm{e}}(x)\mathrm{d}x}{y}, \quad \frac{x^2\mathrm{d}x}{y} \tag{3.52}$$

with the polynomials

$$\Psi_1^{2,e}(x) = 4\left(x^4 - \frac{3}{4}\tilde{s}_1x^3 + \frac{1}{2}\tilde{s}_2x^2 - \frac{1}{4}\tilde{s}_3x\right) \quad and \quad \Psi_2^{2,e}(x) = 2\left(x^3 - \frac{1}{2}\tilde{s}_1x^2\right). \tag{3.53}$$

Abelian Differentials of the Third Kind. To complete the basis of Abelian differentials, one must include an Abelian differential of the third kind for each puncture of a punctured Riemann surface. An even hyperelliptic curve always has a puncture at  $\infty$ , meaning that at least one third-kind differential must be added in this case. We choose this differential to be

$$\varpi_{2g+1} = \frac{x^g \mathrm{d}x}{y} \,. \tag{3.54}$$

For any additional puncture at a point c, we add another third kind Abelian differential of the form

$$\varpi^c = \frac{\mathrm{d}x}{y(x-c)} \,. \tag{3.55}$$

These have simple poles at  $(x, y) = (c, \pm y_c)$  with  $y_c = \sqrt{P_g(c)}$  for a fixed choice of branch.

**Summary.** The basis of Abelian differentials for a hyperelliptic curve of genus g with punctures at the points  $\{c_1, c_2, \dots\}$  has the following elements:

first kind second kind third kind 
$$\overline{\omega}_1, \dots, \overline{\omega}_g, \overline{\omega}_{g+1}, \dots, \overline{\omega}_{2g}, \overline{\omega}_{2g+1}, \dots$$
 (3.56)

Computing the periods between these differentials and the basis cycles, we obtain the period matrix

$$\mathcal{P} = \left( \int_{\gamma_j} \varpi_i \right) = \begin{pmatrix} \mathcal{A} & \mathcal{B} & \star \\ \tilde{\mathcal{A}} & \tilde{\mathcal{B}} & \star \\ \star & \star & \star \end{pmatrix} , \qquad (3.57)$$

where the upper-left blocks are the already discussed a- and b-cycle (quasi-)periods. For an odd hyperelliptic curve with no punctures, these blocks make up the full period matrix. The elements  $\star$  are periods from (co-)cycles related to punctures,

Example: For even hyperelliptic curves of low genus, the third kind differentials with residue at  $\infty$  are

Genus 1 : 
$$\frac{x dx}{y}$$
  
Genus 2 :  $\frac{x^2 dx}{y}$ .

including the puncture at  $\infty$ . The entries of the (quasi-)period matrices can be expressed in terms of Lauricella D functions. These matrices satisfy quadratic relations, specifically the classical Riemann bilinear relations:

$$\sum_{i=1}^{2} \left[ \int_{a_i} \omega \int_{b_i} \eta - \int_{b_i} \omega \int_{a_i} \eta \right] = \int_{\partial \mathcal{C}} f \eta, \qquad (3.58)$$

where  $\omega, \eta$  are one-forms and f is a primitive of  $\omega$ , i.e.,  $\mathrm{d}f = \omega$ , see, e.g., [160] for details. The integral on the right-hand side is taken over the boundary of the fundamental domain  $\mathcal{C}$ , which is obtained by cutting the hyperelliptic curve along all homology cycles. This integral can be interpreted as a sum of residues on the hyperelliptic curve. Alternatively, these relations can also be derived by considering the limit  $\varepsilon \to 0$  of the twisted Riemann bilinear relations [50].

**Example 3.5** (Bilinear Relations for Odd Hyperelliptic Curve of Genus *One*). The periods of Example 3.1 and the quasi-periods of Example. 3.3 satisfy the Legendre relation,

$$\omega_1 \eta_2 - \omega_2 \eta_1 = -8\pi i \,. \tag{3.59}$$

**Example 3.6** (Bilinear Relations for Hyperelliptic Curves of Genus Two). Choosing the bases of Abelian differentials as in the examples above, one can obtain the following simple relations, referred to as generalized Legendre relations, from the Riemann bilinear relations [161] (see also [160])

$$\begin{pmatrix} \mathcal{A} & \mathcal{B} \\ \tilde{\mathcal{A}} & \tilde{\mathcal{B}} \end{pmatrix} \begin{pmatrix} \mathbf{0} & \mathbb{1} \\ -\mathbb{1} & \mathbf{0} \end{pmatrix} \begin{pmatrix} \mathcal{A} & \mathcal{B} \\ \tilde{\mathcal{A}} & \tilde{\mathcal{B}} \end{pmatrix}^{T} = 8\pi i \begin{pmatrix} \mathbf{0} & \mathbb{1} \\ -\mathbb{1} & \mathbf{0} \end{pmatrix}. \tag{3.60}$$

More explicitly, these provide three independent quadratic relations between  $2 \times 2$  matrices,

$$\mathcal{B}\mathcal{A}^T - \mathcal{A}\mathcal{B}^T = 0, \qquad (3.61)$$

$$\tilde{\mathcal{B}}\tilde{\mathcal{A}}^T - \tilde{\mathcal{A}}\tilde{\mathcal{B}}^T = 0, \qquad (3.62)$$

$$\tilde{\mathcal{B}}\mathcal{A}^T - \tilde{\mathcal{A}}\mathcal{B}^T = 8\pi i \mathbb{1} . \tag{3.63}$$

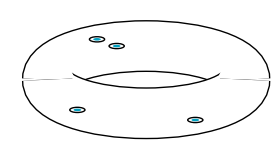
By taking the inverse of the above matrix equation (3.60) we find two additional relations

$$\mathcal{A}^{T}\tilde{\mathcal{A}} - \tilde{\mathcal{A}}^{T}\mathcal{A} = 0,$$

$$\mathcal{B}^{T}\tilde{\mathcal{B}} - \tilde{\mathcal{B}}^{T}\mathcal{B} = 0.$$
(3.64)

# 3.2.2 Elliptic Curves and Tori

Now we discuss in some more detail the genus one case, i.e. elliptic curves or tori. We already learned that a hyperelliptic curve is related to different objects (i.e. the curve itself, the Jacobian variety, a double-cover of a higher genus Riemann



We define the Lauricella *D* function in Definition 4.174. Additionally note that due to their special role in period matrices of hyperelliptic curves, families of Lauricella functions are a model for hyperelliptic maximal cuts, which we discuss in Chapter 6.

surface). For the genus one case, these are particularly well-studied and we only scratch the surface here. For some more mathematical background, we refer to the standard literature [162] as well as different reviews in the physics literature [8, 144, 163]. In the integrals we discuss in later chapters of this thesis, elliptic curves generally arise via their polynomial equations, i.e. as (odd) cubics

$$y^{2} = (x - \lambda_{1})(x - \lambda_{2})(x - \lambda_{3})$$
(3.65)

and (even) quartics

$$y^{2} = (x - \lambda_{1})(x - \lambda_{2})(x - \lambda_{3})(x - \lambda_{4}).$$
(3.66)

**Definition 3.8** (Elliptic Curve). More specifically, any elliptic curve can be written as the locus of a cubic equation in  $\mathbb{P}^2_{\mathbb{C}}$  with only one point, the base point, on the line at  $\infty$  and every elliptic curve has an equation of the form

$$y^2 = 4x^3 - g_2x - g_3 (3.67)$$

written in non-homogenous coordinates  $x = \frac{X}{Z}$  and  $y = \frac{Y}{Z}$  (where the base point in homogenous coordinates is at [0,1,0]). This form is called the Weierstrass normal form.

Note that despite the Weierstrass standard form being a cubic, any quartic with distinct roots can be brought in Weierstrass form by a specific transformation and therefore we can call both even and odd curves *elliptic*. At this point, we already observe that different polynomial equations might define the *same* elliptic curve. To uniquely classify the curve, one can compute the so-called *j*-invariant:

$$j = \frac{1728g_2}{g_2^3 - 27g_3} \,. \tag{3.68}$$

**Example 3.7** (Legendre form). A Weierstrass equation is in Legendre form, if it can be written as

$$y^{2} = x(x-1)(x-\lambda). (3.69)$$

By choosing  $\lambda$  as a parameter and considering the moduli space of Legendre curves, one has a simple example for a family of elliptic curves and we come back to this example repeatedly. The (co-)homology groups for even and odd elliptic curves were already given in Examples 3.1 and 3.3. We depict the cycles again for this specific case in figure 3.5.

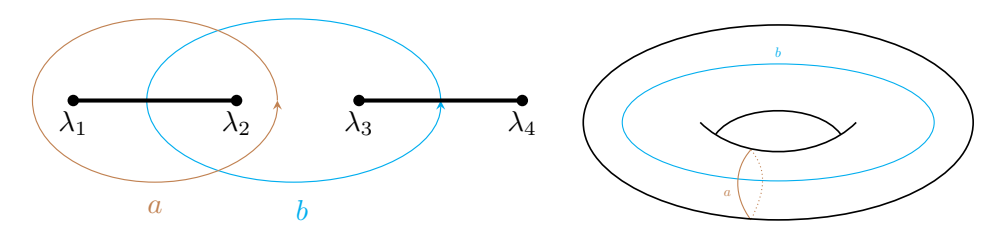


Figure 3.5: The elliptic curve has two cycles, which are realised as two independent contours wrapping the hole of the torus.

An elliptic curve is characterised by its modular parameter  $\tau$ , which is computed as a ratio of the individual periods. Generally, the periods evaluate to linear combinations of elliptic integrals. The complete elliptic integrals of the first and second kind are defined as

$$K(\lambda) = \int_0^1 \frac{dx}{\sqrt{(1 - \lambda x^2)(1 - x^2)}}$$
 and  $E(\lambda) = \int_0^1 dx \sqrt{\frac{1 - \lambda x^2}{1 - x^2}}$ . (3.70)

**Example 3.8** (Periods and Quasi-Periods of the Legendre Curve). For the basis choice of Example 3.1 and the Legendre curves of Example 3.7 labelled by the parameter  $\lambda$ , we find

$$\omega_1 = 2 \int_0^1 \frac{\mathrm{d}x}{y} = \frac{4}{\sqrt{\lambda}} K(\lambda^{-1}) \text{ and } \omega_2 = 2 \int_{\lambda}^1 \frac{\mathrm{d}x}{y} = \frac{4}{\sqrt{\lambda}} K(1 - \lambda^{-1}),$$
 (3.71)

$$\eta_1 = 4\sqrt{\lambda} \left( K \left( \lambda^{-1} \right) - E \left( \lambda^{-1} \right) \right) . \tag{3.72}$$

Consequently, the Legendre relations of eq. (3.59) give relations between elliptic integrals. In particular, those can be reduced to the generic relation

$$K(u)E(1-u) + E(u)K(1-u) - K(u)K(1-u) = \frac{\pi}{2}$$
. (3.73)

Additionally, we use the incomplete elliptic integrals such as

$$F(\arcsin(\sqrt{X})|Y) = \int_0^{\sqrt{X}} \frac{dx}{\sqrt{(1 - Yx^2)(1 - x^2)}}.$$
 (3.74)

#### The Lattice and the Torus

The periods  $\omega_1, \omega_2$  of an elliptic curve define a lattice

$$\Lambda_{\omega_1,\omega_2} = \omega_1 \mathbb{Z} \oplus \omega_2 \mathbb{Z} = \{ n_1 \omega_1 + n_2 \omega_2 | n_1, n_2 \in \mathbb{Z} \}. \tag{3.75}$$

Often, one defines it with the normalised period  $\tau$  as:

$$\Lambda_{\tau} = \mathbb{Z} \oplus \tau \mathbb{Z} = \{ n_1 + n_2 \tau | n_1, n_2 \in \mathbb{Z} \}. \tag{3.76}$$

We picture the lattice  $\Lambda_{\omega_1,\omega_2}$  in figure 3.6.

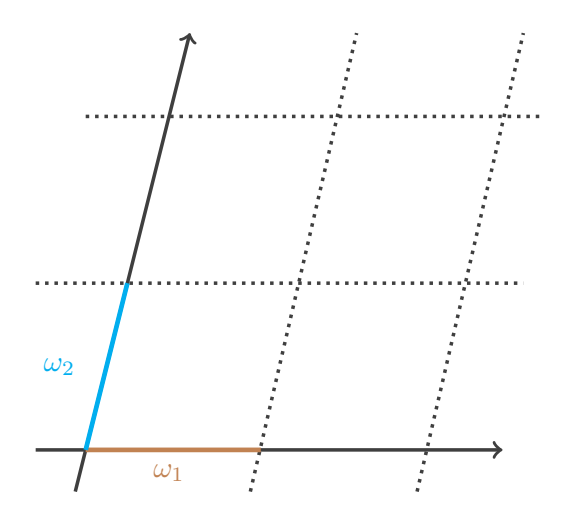


Figure 3.6: The periods  $\omega_1$  and  $\omega_2$  define the lattice  $\Lambda_{\omega_1,\omega_2}$ .

Then  $\mathbb{C}/\Lambda_{\omega_1,\omega_2}$  is equivalent to  $\mathbb{C}/G_{\omega_1,\omega_2}^3$  with the group  $G_{\omega_1,\omega_2}$  generated by the translations

$$z \to z + \omega_1, \ z \to z + \omega_2 \,. \tag{3.77}$$

In particular, one obtains

$$\Sigma_{\tau} = \mathbb{C}/\Lambda_{\omega_1,\omega_2} = \{ z \in \mathbb{C} | z = a\omega_1 + b\omega_2 \text{ with } a, b \in [0,1) \}, \qquad (3.78)$$

which is called the fundamental parallelogram. We represent it in figure 3.6. The basis a- and b-cycles are the boundaries of the rectangle. Topologically, one can obtain a torus from this parallelogram by identifying opposite sides, i.e. gluing them together.

**Translating between torus and curve** So far, we have discussed objects on the elliptic curve in terms of the coordinates x, y. Alternatively, one can work on the torus with a single complex coordinate z. We now explain how to translate between these coordinates by first introducing the following function on the torus:

**Definition 3.9** (Weierstrass'  $\wp(z)$ -function).

$$\wp(z) = \frac{1}{z^2} + \sum_{Y \in \Lambda_{\omega_1, \omega_2} - \{0\}} \left( \frac{1}{(z+Y)^2} - \frac{1}{Y^2} \right). \tag{3.79}$$

By definition, this function is periodic with periods  $\omega_1, \omega_2$  and additionally it is even, i.e.  $\wp(-z) = \wp(z)$ .

The Weierstrass'  $\wp(z)$  function fulfils the following equation:

$$(\wp(z)')^2 = 4\wp(z)^3 - q_2\wp(z) - q_3, \qquad (3.80)$$

<sup>3</sup>Note that due the uniformisation theorem (e.g. [164]all compact Riemann surfaces can be obtained as quotients the form $\Delta/G$ with  $\Delta$  a domain in  $\mathbb{C}$  and Ga group that acts properly discontinuously.

any function on the fundamental parallelogram/torus must have this periodicity.

Note that in order

well-defined,

be

where

$$g_2 = 60 \sum_{Y \in \Lambda - \{0\}} \frac{1}{Y^4} \text{ and } g_3 = 140 \sum_{Y \in \Lambda - \{0\}} \frac{1}{Y^6}$$
 (3.81)

and thus

$$(x,y) = (\wp'(z), \wp(z)) \tag{3.82}$$

is a point on the elliptic curve with Weierstrass normal form (3.67). In that way, we can translate from a point z on the torus to a point (x, y) on the elliptic curve in Weierstrass form. To define differentials on the torus, we see:

$$\frac{\mathrm{d}x}{y} = \frac{\mathrm{d}\wp(z)}{\wp(z)'} = \mathrm{d}z. \tag{3.83}$$

To translate in the other direction – from the curve to the torus – we use Abel's map, which makes the isomorphism between the elliptic curve and the torus explicit:<sup>4</sup>

**Definition 3.10** (Abel's map). Abel's map is defined as

$$\mathfrak{u}: (x, \pm y) \mapsto z^{\pm} = \pm \frac{1}{\omega_1} \int_{\lambda_1}^x \frac{\mathrm{d}x}{y} \mod \Lambda_{\omega_1, \omega_2}. \tag{3.84}$$

On the moduli space of elliptic curves At this point, we want to again explicitly. We generally do not work with one elliptic curve, but with a moduli space of elliptic curves<sup>5</sup>. That means, the parameter we are interested in (e.g. physical parameters like momenta and masses) are the parameters that define the elliptic curve, in general by combining to the branch points  $\lambda_i$ . As we also want to vary with respect to these parameters (to compute differential equations) we have to work with the moduli space of elliptic curves. In particular, as soon as we have more than E > 1 parameter (that can be represented in some way by  $\tau$  through a change of variables), we need to work with the moduli space of elliptic curves with E marked points, commonly denoted by  $\mathcal{M}_{1,E}$ . Note that every even elliptic curve has one marked point, so we just add E-1 that correspond to the remaining parameters.

<sup>5</sup>And the same is true also for the other geometries we work with

**Special Functions on the Torus** Let us introduce some special functions on the torus. A particularly important class of functions are Eisenstein series, which we discuss in more detail as modular forms in Section 3.4.2.

**Definition 3.11** (Eisenstein Series). We define holomorphic Eisenstein series of  $SL(2,\mathbb{Z})$  by

$$G_k(\tau) = \sum_{(m,n)\in\mathbb{Z}^2 - \{(0,0)\}} \frac{1}{(m\tau + n)^k} \text{ for } k \ge 4, \text{ even } .$$
 (3.85)

These is the standard examples for modular forms in the following paragraph. Additionally, we define special combinations of Eisenstein series, that are modular forms and appear in the sunrise integral family:

$$\eta_2(\tau) = [G_2(\tau) - 2G_2(2\tau)] \frac{\mathrm{d}\tau}{2\pi i},$$
(3.86a)

$$\eta_4(\tau) = G_4(\tau) \frac{\mathrm{d}\tau}{(2\pi i)^3}.$$
(3.86b)

Often it is useful to expand a  $\tau$ -dependent quantity as a function of

$$q = \exp(\pi i \tau) \tag{3.87}$$

instead of working directly with  $\tau$ .

**Definition 3.12** (Jacobi- $\theta$ -function). In general, the Jacobi- $\theta$ -function is defined as

$$\theta[a,b](z|\tau) = \theta[a,b](z,q) = \sum_{n=-\infty}^{\infty} q^{(n+\frac{1}{2}a)^2} e^{2i(n+\frac{1}{2}a)(z-\frac{1}{2}\pi b)}.$$
 (3.88)

Due to the symmetry of these functions<sup>6</sup> we only need the following four  $\theta$  functions and their q-expansions:

$$\theta_1(z,q) = \theta[1,1](z,q) = 2\sum_{n=0}^{\infty} (-1)^n q^{(n+\frac{1}{2})^2} \sin((2n+1)z)$$
(3.89)

$$\theta_2(z,q) = \theta[1,0](z,q) = 2\sum_{n=0}^{\infty} q^{(n+\frac{1}{2})^2} \cos((2n+1)z)$$
(3.90)

$$\theta_3(z,q) = \theta[0,0](z,q) = 1 + 2\sum_{n=1}^{\infty} q^{n^2} \cos(2nz)$$
(3.91)

$$\theta_4(z,q) = \theta[0,1](z,q) = 1 + 2\sum_{n=1}^{\infty} (-1)^n q^{n^2} \cos(2nz).$$
 (3.92)

Additionally, we use the following function:

**Definition 3.13** (Dedekind  $\eta$  function). The Dedekind  $\eta$  function is defined for  $\tau \in \mathbb{H}$ :

$$\eta(\tau) = e^{\frac{i\pi\tau}{12}} \prod_{n=1}^{\infty} (1 - e^{2\pi i n \tau}) = q^{-\frac{1}{24}} \prod_{n=1}^{\infty} (1 - \bar{q}^n).$$
 (3.93)

 $\begin{array}{ll} \theta[a & + & 2n, b](z|\tau) & = \\ \theta[a, b](z|\tau) & \theta[a, b & + & 2n](z|\tau) & = \\ e^{-n\pi i a}\theta[a, b](z|\tau) & = \end{array}$ 

## 3.3 Calabi-Yau Varieties

For completeness, let us start with the definition of a Calabi-Yau manifold:

**Definition 3.14** (Calabi-Yau geometry). A Calabi-Yau n-fold is the quadruple  $(\mathcal{M}, \omega, \Omega)$  where  $\mathcal{M}$  is a compact n-dimensional Kähler manifold (with a Kähler metric  $\eta$  and complex structure J),  $\omega$  is the Kähler form and  $\Omega$  is a non-vanishing holomorphic (n, 0) form. The latter forms are linked by the following relation:

$$\frac{\omega^n}{n!} = (-1)^{\frac{n(n-1)}{2}} \left(\frac{i}{2}\right)^n \Omega \wedge \bar{\Omega}. \tag{3.94}$$

Note that besides the existence of the non-trivial (n,0) form there are several equivalent definitions for Calabi-Yau n-folds and we refer for these as well as proofs of their equivalence to the standard literature [165, 166]. One such definition is the vanishing of the canonical class. This condition allows us to derive an explicit condition for a space to be Calabi-Yau: The families of Calabi-Yau n-folds we encounter in this thesis, specifically in Chapter 8, are defined as covers of a base space B. That means we consider a polynomial constraint  $y^{n_c} = P(x, \lambda)$  in an n-dimensional base space B with coordinate  $x = (x_1, \ldots, x_n)$ . The variables  $\lambda$  appear in the coefficients of the polynomial and parametrise the family of n-folds. In order for such a polynomial constraint to define a Calabi-Yau family, its degree needs to be such that the canonical class vanishes and this condition is captured in the so-called adjunction formula [165]. The unique holomorphic L-form of this family is

$$\Omega = \frac{\mu_B(\boldsymbol{x})}{P(\boldsymbol{x}, \boldsymbol{\lambda})^{\frac{1}{n_c}}},$$
(3.95)

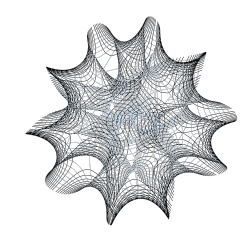
where  $\mu_B$  is the holomorphic measure on B. Note that, at this point, we have already encountered and studied in detail the simplest Calabi-Yau geometries: tori. Here, we begin by examining them explicitly as Calabi-Yau varieties and in particular use as an example the Legendre family of Example 3.7.

**Example 3.9** (Legendre Elliptic Family as a Calabi-Yau Family). As discussed in Example 3.1, the basis of holomorphic differentials for an elliptic curve is one-dimensional. In particular, the unique holomorphic (1,0) differential in coordinates (x,y) is  $\Omega = \frac{dx}{y}$ . From eq. (3.94) we see that the volume form in the coordinate z is  $\omega = \frac{i}{2} dz \wedge d\bar{z}$ .

#### Calabi-Yau Periods

We denote by

$$\mathbf{\Pi} = \left( \int_{\Delta_1} \Omega, \dots, \int_{\Delta_{b_n}} \Omega \right), \quad b_n = \dim \mathcal{H}_n(\mathcal{M}, \mathbb{Z})$$
 (3.96)



#### See also:

More details on definitions of basic objects in the context of Kähler manifolds can be found in Appendix A.

#### See also:

We discuss how the fishnet integrals define Calabi-Yau n-folds in eq. (3.218).

the vector of periods that are integrals of the basis element  $\Omega$  of the one-dimensional middle cohomology  $H^n_{dR}(\mathcal{M})$  along the basis cycles  $\Delta_i$ . In general, we characterise the Calabi-Yau geometry by its Picard-Fuchs ideal that annihilates the periods and compute these with the Frobenius method as explained in Section 3.1. We illustrate this using the Legendre curve from Example 3.10.

**Example 3.10** (Picard-Fuchs Operator for Legendre Curves). For the Legendre curves, the Picard-Fuchs operator takes the form

$$\mathbb{O}_L(\lambda) = \theta_\lambda^2 - \lambda \left(\theta + \frac{1}{2}\right)^2 \tag{3.97}$$

$$= \lambda^{2} (1 - \lambda) \frac{\partial^{2}}{\partial \lambda^{2}} + \lambda (1 - 2\lambda) \frac{\partial}{\partial \lambda} - \frac{1}{4} \lambda.$$
 (3.98)

Now, we apply the Frobenius method to obtain the solutions of this operator, which correspond to the periods of the Legendre family. Specifically, we compute it around the singular point  $\lambda_0 = 0$ .

- 1. The indicial equation is simply  $\alpha^2 = 0$ . Thus,  $\lambda_0 = 0$  is a MUM point with indicial zero.
- 2. At this MUM point, we can make the following ansätze for the two periods:

$$\Pi_{L,1} = \sum_{i=0}^{\infty} c_{1,i} \lambda^i \tag{3.99}$$

$$\Pi_{L,2} = \log(\lambda) \sum_{i=0}^{\infty} c_{1,i} \lambda^{i} + \sum_{i=0}^{\infty} c_{2,i} \lambda^{i}.$$
 (3.100)

3. We choose the order  $n_{max}$  up to which we want to determine the coefficients and apply the operator to solve for the coefficients:

$$\mathbb{O}_L \Pi_{L,1} = 0 \text{ and } \mathbb{O}_L \Pi_{L,2} = 0.$$
 (3.101)

Choosing additinoally the normalisation  $c_{1,0} = c_{2,0} = 1$ , we find:

$$c_{1,1} = \frac{1}{4}, c_{1,2} = \frac{9}{64}, c_{1,3} = \frac{25}{256}, \dots$$
 (3.102)

$$c_{2,1} = \frac{3}{4}, c_{2,2} = \frac{15}{32}, c_{2,3} = \frac{65}{192}, \dots$$
 (3.103)

We can read off from the coefficients in eq. (3.102) that the first period is

$$\Pi_{L,1} = {}_{2}F_{1}\left(\frac{1}{2}, \frac{1}{2}, 1; \lambda\right) \tag{3.104}$$

with  $_2F_1$  being Gauss hypergeometric function as defined in eq. (4.2). This fits with our assumption that the periods of elliptic curves should be elliptic integrals, as

$$_{2}F_{1}\left(\frac{1}{2}, \frac{1}{2}, 1; \lambda\right) = \frac{2}{\pi} K(\lambda).$$
 (3.105)

In this case, we started with the Picard-Fuchs operator and found its periods. However, there are situations where we have one period of a Calabi-Yau variety and must determine the corresponding operators to determine the remaining periods. In general, determining the Picard-Fuchs operator from a single period  $\Pi_{G,0}$  given in integral representation is a non-trivial task. However, in some cases, the Picard-Fuchs ideal can be found using the following method:

We mention this again in Section 8.2.1 where we also present results partially obtained in this way.

<sup>7</sup>For more details, we refer to the standard lit-

erature [165, 166].

## Review: Finding the Picard-Fuchs Ideal

- 1. Obtain a series representation of  $\Pi_{G,0}$ .
- 2. Make an ansatz for the operators in the Picard-Fuchs ideal.
- 3. Solve for the coefficients in the ansatz by requiring that they annihilate the initial period  $\Pi_{G,0}$ .

Note that confirming whether the full ideal has been found is non-trivial, as the dimension of the homology group is not necessarily known. However, if we identify a MUM point and obtain the expected solution structure using the Frobenius method, this provides a strong indication.

**Bilinear Relations** Due to Griffiths transversality<sup>7</sup>, the periods of a Calabi-Yau n-fold satisfy relations, which take the form

$$\mathbf{\Pi}(\boldsymbol{\lambda})^T \boldsymbol{\Sigma} \, \partial_{\boldsymbol{z}}^{\boldsymbol{k}} \mathbf{\Pi}(\boldsymbol{\lambda}) = \int_{M_n} \Omega \wedge \partial_{\boldsymbol{z}}^{\boldsymbol{k}} \Omega = \begin{cases} 0 & \text{for } 0 \le r \le n \\ C_{\boldsymbol{k}}(\boldsymbol{\lambda}) & \text{for } |\boldsymbol{k}| = n \end{cases}, \tag{3.106}$$

where the  $C_k(\lambda)$  are rational functions in the complex structure parameters. Specifically, we obtain bilinear relations, called the *Hodge-Riemann bilinear relations*:

$$\mathbf{\Pi}(\mathbf{z})^T \mathbf{\Sigma} \mathbf{\Pi}(\mathbf{z}) = \mathbf{0}. \tag{3.107}$$

Due to their origin, these relations appear in the literature with the name *Griffiths* transversality relations.

# **Picard-Fuchs Operators**

For the remainder of this chapter, we discuss properties of Picard-Fuchs operators. We restrict the discussion here to single-parameter operators: We consider operators as in eq. (3.16) and specifically ones in a single coordinate  $\lambda$ , that take the form

$$\mathbb{O} = \partial_{\lambda}^{n} + a_{n-1}\partial_{\lambda}^{n-1} + \ldots + a_{1}\partial_{\lambda} + a_{0}, \text{ with } a_{i} \in \mathbb{C}(\lambda) , \qquad (3.108)$$

for some coefficients  $a_i$ . We denote the *n*-dimensional  $\mathbb{C}$ -vector space of its solutions by

$$Sol(\mathbb{O}) = \{f(\lambda) : \mathbb{C} \to \mathbb{C} : \mathbb{O} f(\lambda) = 0\}.$$
(3.109)

This solution space is spanned by the periods  $\Pi_i(\lambda)$  of the associated Calabi-Yau variety.

**Definition 3.15** (Mirror Map). In general, the mirror map is defined by

$$t_i(\lambda) = \frac{1}{2\pi i} \frac{\Pi_{G,i}(\lambda)}{\Pi_{G,0}(\lambda)}, \quad i = 1, \dots, b_n - 1,$$
 (3.110)

where the  $\Pi_{G,i}(\lambda)$  exhibit a logarithmic divergence at the MUM-point and  $b_n$  is the dimension of the CY's homology group.

Let us now assume, that  $\mathbb{O}$  is a differential operator of degree L+1 with only regular-singular points and  $\lambda_0 = 0$  is a MUM point. Thus, near this point the differential equation  $\mathbb{O}f(\lambda) = 0$  admits solutions of the form

$$\Pi_k(\lambda) = \Pi_0(\lambda) \frac{1}{k!} \log^k z + \mathcal{O}(\log^{k-1}(\lambda), z), \qquad 0 \le k \le \ell.$$
(3.111)

If  $b_n = 2$ , the mirror-map is

$$t(\lambda) = t_1(\lambda) = \frac{1}{2\pi i} \frac{\Pi_1(\lambda)}{\Pi_0(\lambda)} = \frac{\log z}{2\pi i} + \mathcal{O}(\lambda).$$
 (3.112)

Its exponential is a holomorphic function of  $\lambda$ :

$$q(\lambda) = e^{2\pi i t(\lambda)} = z + \mathcal{O}(\lambda^2). \tag{3.113}$$

We consider two Picard-Fuchs operators  $\mathbb{O}$  and  $\tilde{\mathbb{O}}$  to be equivalent,  $\tilde{\mathbb{O}} \sim \mathbb{O}$ , if there is a function  $\alpha(\lambda) \in \overline{\mathbb{Q}(\lambda)}$ , so that

$$\widetilde{\mathbb{O}} = \alpha(\lambda) \mathbb{O} \alpha(\lambda)^{-1} \text{ with } \alpha(\lambda) \in \overline{\mathbb{Q}(\lambda)}.$$
(3.114)

In order to relate Picard-Fuchs operators related to different Feynman graphs, we need certain operations on these operators and we define these here.

**Definition 3.16** (Hadamard product). Let us consider two holomorphic functions (at  $\lambda_0 = 0$ ), denoted f and g, whose expansion in  $\lambda$  around 0 takes the form

$$f(\lambda) = \sum_{i=0}^{\infty} f_i \lambda^i \quad and \quad g(\lambda) = \sum_{i=0}^{\infty} g_i \lambda^i.$$
 (3.115)

Then, their Hadamard product is defined as

$$(f * g)(\lambda) := \oint_{|\lambda| = \epsilon} \frac{\mathrm{d}t}{2\pi i t} f(t) g(\lambda/t) = \sum_{i=0}^{\infty} f_i g_i \lambda^i.$$
 (3.116)

Based on the definition of the Hadamard product of functions, one can define the Hadamard product of operators. Namely, let  $\mathbb{O}_f$  and  $\mathbb{O}_g$  be the operators of minimal degree that annihilate f and g, respectively. Then, their Hadamard product is

$$\mathbb{O}_f * \mathbb{O}_g = \mathbb{O}_{f*g}. \tag{3.117}$$

Similarly,  $m^{\text{th}}$  symmetric and anti-symmetric power representations respectively be denoted by  $\text{Sym}^{\text{m}}\mathbb{O}$  and  $\wedge^{m}\mathbb{O}$ . Again, these operations are defined by operations on the solution space.

**Definition 3.17** (Symmetric Product). Sym<sup>m</sup> $\mathbb{O}$  is the operator of minimal degree that annihilates all products of m solutions of  $\mathbb{O}$ , i.e., it is defined by its solution space

$$Sol(Sym^{m}\mathbb{O}) = \langle y_{i_{1}} \cdots y_{i_{m}} | y_{i_{k}} \in Sol(\mathbb{O}) \rangle_{\mathbb{C}}.$$
(3.118)

**Definition 3.18** (Anti-Symmetric Product). Let  $J = (j_1, \ldots, j_m)$  and  $A_{m,n}$  the set of  $\binom{n}{m}$  m-tuples J. For a given choice, of tuples I, J we define

$$D_I^J := \det \begin{pmatrix} \theta_z^{j_1} y_{i_1} & \dots & \theta_z^{j_1} y_{i_m} \\ \theta_z^{j_2} y_{i_1} & & \theta_z^{j_2} y_{i_m} \\ \vdots & \ddots & \vdots \\ \theta_z^{j_m} y_{i_1} & \dots & \theta_z^{j_m} y_{i_m} \end{pmatrix}$$
(3.119)

with elements  $(W)_{ij} = \theta_z^j y_i$ , i, j = 0, ..., n-1 and  $y_i \in Sol(\mathbb{O})$ . We also define  $D_I = D_I^{(0, ..., m-1)}$ . The  $m^{th}$  anti-symmetric power of  $\mathbb{O}$  is then defined as the irreducible operator of minimal degree with solution space

$$Sol(\wedge^{m}\mathbb{O}) = \langle D_{I} | I \in A_{m,n} \rangle_{\mathbb{C}}. \tag{3.120}$$

Finally, we introduce the statement of mirror-symmetry:

**Definition 3.19** (Mirror Symmetry). Mirror symmetry states that CY L-folds come in pairs  $(\mathcal{M}_G, \mathcal{W}_G)$  such that the cohomology groups  $H^{p,q}(\mathcal{M}_G)$  and  $H^{\ell-p,q}(\mathcal{W}_G)$  are interchanged. Mirror symmetry exchanges the complex structures encoded in  $H^{L-1,1}(\mathcal{M}_G)$  with the Kähler structures from  $H^{1,1}(\mathcal{W}_G)$ .

# 3.4 Iterated Integrals and Special Functions

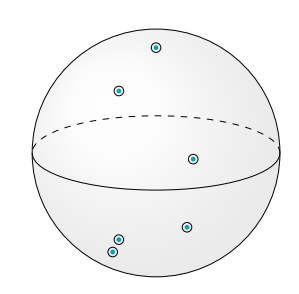
In the following section we discuss iterated integrals. In particular we focus on iterated integrals that can be expressed on Riemann surfaces or are in other ways related to these.

# 3.4.1 Multiple Polylogarithms

The simplest Riemann surface is the genus zero surface, the punctured Riemann sphere  $\mathbb{S}_{\Lambda} = \hat{\mathbb{C}} - \Lambda$ , where  $\Lambda$  is the set of punctures. A basis for its homology group  $H_1(\mathbb{S}_{\Lambda})$  simply consists of a circle around each of the punctures and its de Rham cohomology group  $H^1_{dR}(\mathbb{S}_{\Lambda})$  is spanned by the differentials

$$\frac{\mathrm{d}z}{z - \lambda_i} \text{ for } \lambda_i \in \Lambda \tag{3.121}$$

and z a coordinate on  $\mathbb{S}_{\Lambda}$ . The iterated integrals over these simple differentials are the multiple polylogarithms. The classical version of multiple polylogarithms is defined by a series expansion:



**Definition 3.20** (Classical (Multiple-)Polylogarithm  $\mathrm{Li}_n(x)$ ). The classical polylogarithm is defined as

$$\operatorname{Li}_{n}(z) = \int_{0}^{z} \frac{\mathrm{d}t}{t} \operatorname{Li}_{n-1}(t) = \sum_{k=1}^{\infty} \frac{z^{k}}{k^{n}}.$$
 (3.122)

The series definition of eq. (3.122) can also be generalised to the case with multiple parameters<sup>8</sup>

$$\operatorname{Li}_{m_1,\dots,m_k}(z_1,\dots,z_k) = \sum_{0 < n_1 < n_2 < \dots < n_k} \frac{z_1^{n_1} z_2^{n_2} \dots z_k^{n_k}}{n_1^{m_1} n_2^{m_2} \dots n_k^{m_k}}.$$
 (3.123)

In the context of Feynman integrals, we want to define multiple polylogarithms iteratively by integrating the basis differentials with simple poles of eq. (3.121).

**Definition 3.21** (Multiple Poylogarithms G). The standard convention for multiple polylogarithms (MPLs) in physics is

$$G(a_1, \dots, a_n; x) = \int_0^x \frac{dt}{t - a_1} G(a_2, \dots, a_n; t).$$
 (3.124)

The recursion starts with G(x) = 1 and the  $a_i$  are constants in x. The weight of the MPL is the number of integrations n. If  $a_n = 0$ , the integral diverges. In that case one regularises it by taking the lower boundary to be one, e.g.,

$$G(0, ..., 0; x) = \frac{1}{n!} \log^n(x) \text{ since } \log x = \int_1^x \frac{dt}{t}.$$
 (3.125)

The classical version of multiple polylogarithms is contained in this definition [167]:

$$Li_{m_1,\dots,m_k}(z_1,\dots,z_k) = (-1)^k G\left(\underbrace{0,\dots,0}_{m_k-1},z_k^{-1},\dots,\underbrace{0,\dots,0}_{m_1-1},(z_1,\dots,z_k)^{-1},1\right).$$

An alternative notation that is commonly used for the class of functions spanned by the G is the following

**Definition 3.22** (Multiple Poylogarithms I). Multiple polylogarithms as commonly used in the mathematics literature are defined as the iterated integrals

$$I(a_0, a_1, \dots, a_n; a_{n+1}) = \int_{a_0}^{a_{n+1}} \frac{dt}{t - a_n} I(a_0, a_1, \dots, a_{n-1}, t).$$
 (3.126)

The functions G and I are related by

$$G(a_n, \dots, a_1; a_{n+1}) = I(0, a_1, \dots, a_n, a_{n+1}). \tag{3.127}$$

We mostly use the functions G and only refer to Li and I when necessary. In any case, multiple polylogarithms satisfy many relations. For example, the G form a shuffle algebra, which means that we can express products of G of weight  $n_1$  and  $n_2$  as sums of G of weight  $n_1 + n_2$ . For a comprehensive review, see e.g., [168, 169].

<sup>8</sup>Note that this series may not be defined for some values of  $z_i$  and  $m_i$ . We use this definition within its domain of convergence.

**Multiple Zeta Values** Multiple  $\zeta$  values are defined as the values of the Li functions at  $z_i = 1$ :

**Definition 3.23** (MZVs). The  $\zeta$  values are

$$\zeta_n = \operatorname{Li}_{\mathbf{n}}(1) \text{ for } \mathbf{n} > 1. \tag{3.128}$$

For  $n_1, \ldots, n_k > 1$ , we can also compute the multiple  $\zeta$  values<sup>9</sup>

$$\zeta_{n_1,\dots,n_r} = \operatorname{Li}_{n_1,\dots,n_r}(1,\dots,1) = \sum_{0 < k_1 < \dots < k_r} k_1^{-n_1} k_2^{-n_2} \dots k_r^{-n_r}$$
(3.129)

$$= (-1)^r G(\underbrace{0, \dots, 0}_{n_r-1}, 1, \dots, \underbrace{0, \dots, 0}_{n_2-1}, 1, \underbrace{0, \dots, 0}_{n_1-1}, 1; 1).$$
 (3.130)

All even values, i.e. values of the form  $\zeta_{2n}$ , evaluate to powers of  $\pi$ . More specifically:

$$\zeta_{2n} = (-1)^{n+1} \frac{(2\pi)^{2n} B_{2n}}{2(2n)!}.$$
(3.131)

The relations that hold for MPLs are translated to MZVs and conjecturally there are no relations between MZVs of different weights.

Generating Series for MPLs One can also obtain MPLs as coefficients of the generating series [170]

$$\mathbb{G}_{G}(e_{i};z) = \sum_{w=0}^{\infty} \sum_{a_{1},\dots,a_{w}=0,1} e_{a_{1}} e_{a_{2}} \dots e_{a_{w}} G(a_{w},\dots,a_{2},a_{1};z),$$

which solves the Knizhnik-Zamalodchikov equation and involves the non-commuting variables  $e_0, e_1$ . Note that also here we have endpoint singularities that are regularised by the choices of eq. (3.125), see [171–173].

# 3.4.2 Modular Forms and Iterated Eisenstein Integrals

Next we discuss iterated integrals in the modular parameter  $\tau$ . In particular, we consider ones whose kernels are modular forms. Additionally, we need the concept of *modularity* to obtain a canonical basis for the kite integral family in Chapter 7.

## Modular forms

**Definition 3.24** ( $\mathrm{SL}_2(\mathbb{K})$ ). Let  $\mathbb{K} \subset \mathbb{C}$  a ring.  $\mathrm{SL}_2(\mathbb{K})$  is the group of matrices

$$\begin{pmatrix} a & b \\ c & d \end{pmatrix} \tag{3.132}$$

with  $a, b, c, d \in \mathbb{K}$  and ad - bc = 1. It acts on  $t \in \mathbb{K} \cup \{\infty\}$  by

$$gt = \frac{at+b}{ct+d} \text{ for } g \in SL_2(\mathbb{K}).$$
 (3.133)

<sup>9</sup>We say that these  $\zeta$  values have depth r and weight  $n_1 + \cdots + n_r$ , where  $n_i \in \mathbb{N}$  and  $n_r \geq 2$ .

#### See also:

We briefly discuss motivic and de-Rham versions of the MPLs in Example 4.12.

**Definition 3.25** (Modular Group). The group  $SL_2(\mathbb{Z})/\{\pm 1\}$  is the modular group. It is spanned by

$$S = \begin{pmatrix} 0 & -1 \\ 1 & 0 \end{pmatrix} \text{ and } T = \begin{pmatrix} 1 & 1 \\ 0 & 1 \end{pmatrix}. \tag{3.134}$$

Their action on the upper half-plane is given by

$$St = -\frac{1}{t} \text{ and } Tt = t + 1.$$
 (3.135)

They satisfy the identities

$$S^2 = 1 \text{ and } (ST)^3 = 1.$$
 (3.136)

**Example 3.11.** In general, the normalised period  $\tau$  of an elliptic curve is chosen such that it lives in  $\mathbb{H}$  and thus its modular transformation takes the form

$$\tau \mapsto g\tau = \frac{a\tau + b}{c\tau + d} \,. \tag{3.137}$$

For a point z on a torus, a modular transformation acts as

$$z \mapsto gz = \frac{z}{c\tau + d} \,. \tag{3.138}$$

Of particular importance are special subgroups of the modular group, namely:

**Definition 3.26** (Principal Congruence Subgroups). The principle congruence subgroups are

$$\Gamma_0(N) := \left\{ \begin{pmatrix} a & b \\ c & d \end{pmatrix} \in \operatorname{SL}_2(\mathbb{Z}) \mid c = 0 \pmod{N} \right\}$$
(3.139)

$$\Gamma(N) := \left\{ \begin{pmatrix} a & b \\ c & d \end{pmatrix} \in \operatorname{SL}_2(\mathbb{Z}) \mid b = c = 0 \pmod{N} \ \text{and } a = d = 1 \pmod{N} \right\}$$

for  $N \in \mathbb{Z}$ .

**Definition 3.27** (Weakly Modular Functions). Let k be an integer. We say that a function f is weakly modular of weight k if f is meromorphic on the upper half plane  $\mathbb{H}$  and satisfies the relation

$$f\left(\frac{at+b}{ct+d}\right) = (ct+d)^k f(t) \text{ for all } \begin{pmatrix} a & b \\ c & d \end{pmatrix} \in SL_2(\mathbb{Z}).$$
 (3.140)

Since  $-1 \in SL_2(\mathbb{Z})$ , each modular function of weight k satisfies  $f(t) = (-1)^k f(t)$ , from which it follows that all modular functions of odd weight vanish.

**Definition 3.28** (Modular Form). A modular function is called modular form if it is holomorphic everywhere including at  $\infty$ . If the function is zero at  $\infty$  it is called a cusp form.

Modular forms of different weights are linearly independent and so

$$\mathcal{M} = \bigoplus_{k > 2} \mathcal{M}_k \,, \tag{3.141}$$

where  $\mathcal{M}_k$  denotes the space of modular forms of weight k. Note that the Eisenstein series of Definition 3.11 is a modular form and more specifically:

$$G_k(\tau) \in \mathcal{M}_k. \tag{3.142}$$

In fact, the Eisenstein series can be used to classify all modular forms. More specifically: 10

$$\mathcal{M}_0 = \mathbb{C}, \, \mathcal{M}_2 = 0, \, \mathcal{M}_4 = G_4(z)\mathbb{C}, \, \mathcal{M}_6 = G_6(z)\mathbb{C}$$
 (3.143)

$$\mathcal{M}_8 = G_4(z)^2 \mathbb{C} \,, \, \mathcal{M}_{10} = G_4(z)G_6(z)\mathbb{C}$$
 (3.144)

$$\mathcal{M}_{k>12} = \Delta(z)\mathcal{M}_{k-12} \oplus G_k \mathbb{C} \tag{3.145}$$

$$\mathcal{M}_{2k+1} = 0 \text{ for all } k \tag{3.146}$$

where

$$\Delta(z) = g_2(z)^3 - 27g_3(z)^2 \tag{3.147}$$

with

$$g_2(z) = \frac{(2\pi)^4}{12} \left[ 1 + 240 \sum_{n=1}^{\infty} \sigma_3(n) \exp(2\pi i n z) \right]$$
 (3.148)

$$g_3(z) = \frac{(2\pi)^6}{216} \left[ 1 - 504 \sum_{n=1}^{\infty} \sigma_5(n) \exp(2\pi i n z) \right]$$
 (3.149)

and  $\sigma_s(n) = \sum_{d|n} d^s$ . In the context of Feynman integrals, we also encounter the following generalizations of modular forms:<sup>11</sup>

**Definition 3.29** (Quasi-Modular Form). A quasi-modular form of quasi-modular weight k and depth p is a function whose image under a modular transformation takes the form

$$f(z,\tau) \to \sum_{i=0}^{p} (c\tau + d)^{k-2} \left(\frac{cz}{cz+d}\right)^{i} f_i(z,\tau),$$
 (3.150)

where the functions  $f_i$  are holomorphic on the upper-half plane  $\mathbb{H}$ .

## Iterated Eisenstein Integrals

The iterated integrals over Eisenstein series of Definition 3.11 are the so-called *iterated Eisenstein integrals*. Those related to modular graph forms, which appear in the expansion of closed one-loop string amplitudes [174, 175].

<sup>10</sup>Note that we chose a convention for the weight so that it does <u>not</u> agree with quasi-modular weight chosen quasi-modular forms in Definition 3.150. That is because we choose the latter to match the definitions in the physics literature e.g. [32, 92].Thus, a weakly modular form in the conventions here a quasi-modular form of weight k+2.

the definition of the quasi-modular weight in Definition 3.29 is the one commonly used in the physics literature whereas the definition of modular weight in Definition 3.27 is the one in the mathematics literature.

**Definition 3.30** (Iterated Eisenstein Integrals). More specifically, we define the following integration kernels

$$\nu\begin{bmatrix} j\\k \end{bmatrix} = (2\pi i)^{1+j-k} \tau^j G_k(\tau) d\tau \text{ and } \overline{\nu\begin{bmatrix} j\\k \end{bmatrix}} = (-2\pi i)^{1+j-k} \overline{\tau}^j \overline{G_k(\tau)} d\overline{\tau}$$
 (3.151)

to define the iterated integrals

$$\mathcal{E}\begin{bmatrix} j_1 & j_2 & \dots & j_\ell \\ k_1 & k_2 & \dots & k_\ell \end{bmatrix} := \int_{\tau}^{i\infty} \nu \begin{bmatrix} j_\ell \\ k_\ell \end{bmatrix} \cdot \tau \int_{\tau_3}^{i\infty} \nu \begin{bmatrix} j_2 \\ k_2 \end{bmatrix} \cdot \tau_2 \int_{\tau_2}^{i\infty} \nu \begin{bmatrix} j_1 \\ k_1 \end{bmatrix} \cdot \tau_1 \end{bmatrix}$$

$$= (2\pi i)^{1+j_\ell-k_\ell} \int_{\tau}^{i\infty} \tau_\ell^{j_\ell} G_{k_\ell}(\tau_\ell) \, \mathcal{E}\begin{bmatrix} j_1 & \dots & j_{\ell-1} \\ k_1 & \dots & k_{\ell-1} \end{bmatrix} \cdot \tau_\ell d\tau_\ell \qquad (3.152)$$

and their complex conjugates. The two simplest example are

$$\mathcal{E}\left[\begin{smallmatrix} j\\k \end{smallmatrix}; \tau\right] = (2\pi i)^{1+j-k} \int_{\tau}^{i\infty} d\tau_1 \tau_1^j G_k(\tau_1)$$
(3.153)

$$\mathcal{E}\left[\begin{smallmatrix} j_1 & j_2 \\ k_1 & k_2 \end{smallmatrix}; \tau\right] = (2\pi i)^{2+j_1+j_2-k_1-k_2} \int_{\tau}^{i\infty} d\tau_2 \tau_2^{j_2} G_{k_2}(\tau_2) \int_{\tau_2}^{i\infty} d\tau_1 \tau_1^{j_1} G_{k_1}(\tau_1) . \quad (3.154)$$

In discussing iterated Eisenstein integrals  $\mathcal{E}\begin{bmatrix} j \\ k \end{bmatrix}$  we denote the number of integrations the modular depth of the iterated Eisenstein integral and the number  $\sum_{i=1}^{\ell} k_i$  the degree.

Any endpoint divergences due to  $\tau_{\ell} \to i\infty$  are regularised by tangential-base-point regularisation as in [176]. Specifically:

$$\int_{\tau}^{i\infty} \tau_k^j \mathrm{d}\tau_k = -\frac{1}{j+1} \tau^{j+1} \,.$$

Additionally, we define the multiple modular values, which are obtained by taking the limit  $\tau \to 0$ .

**Definition 3.31** (Multiple modular values).

$$\mathfrak{m}\begin{bmatrix} j_1 & j_2 & \dots & j_\ell \\ k_1 & k_2 & \dots & k_\ell \end{bmatrix} = \int_0^{i\infty} \tau_\ell^{j_\ell} G_{k_\ell}(\tau_\ell) d\tau_\ell \int_{\tau_\ell}^{i\infty} \dots \int_{\tau_3}^{i\infty} \tau_2^{j_2} G_{k_2}(\tau_2) d\tau_2 \int_{\tau_2}^{i\infty} \tau_1^{j_1} G_{k_1}(\tau_1) d\tau_1,$$
(3.155)

Intuitively, we can consider the MMVs to be genus zero objects. At depth one, they are given by  $\zeta$ -values:

$$\mathfrak{m}\begin{bmatrix} j \\ k \end{bmatrix} := \int_0^{i\infty} \tau_1^j G_k(\tau_1) \, d\tau_1 = \begin{cases} -\frac{2\pi i \zeta_{k-1}}{k-1} & : j = 0, \\ \frac{2(-1)^{j+1} j! (2\pi i)^{k-1-j}}{(k-1)!} \zeta_{j+1} \zeta_{j+2-k} & : 0 < j \le k-2. \end{cases}$$
(3.156)

Beyond depth one, the multiple modular values contain additional periods such as L-values of holomorphic cusp forms. For more details and many examples, see [177]. In this thesis, we only consider MMVs from a subclass that can be expressed in  $\mathbb{Q}[2\pi i]$ -linear combinations of MZVs and these can be considered genus zero objects.

## **Generating Series**

A generating series whose coefficients are the iterated Eisenstein integrals of Definition 3.30 is [177]

$$\mathbb{I}_{\mathcal{E},+}(\epsilon_k;\tau) = \mathbb{P}\exp\left[\int_{\tau}^{i\infty} \mathbb{A}(\epsilon_k;\tau_1)\right], \qquad (3.157)$$

with

$$\mathbb{A}(\epsilon_k; \tau) = \sum_{k=4}^{\infty} \sum_{j=0}^{k-2} (-1)^j \frac{(k-1)}{j!} \nu \begin{bmatrix} j \\ k \end{bmatrix}; \tau \epsilon_k^{(j)}. \tag{3.158}$$

Specifically, the first few orders of the expansion of the path-ordered exponential is

$$\mathbb{I}_{\mathcal{E},+}(\epsilon_k;\tau) = 1 + \sum_{k_1=4}^{\infty} \sum_{j_1=0}^{k_1-2} (-1)^{j_1} \frac{(k_1-1)}{j_1!} \mathcal{E}\left[\frac{j_1}{k_1};\tau\right] \epsilon_{k_1}^{(j_1)}$$
(3.159)

$$+\sum_{k_1=4}^{\infty}\sum_{j_1=0}^{k_1-2}\sum_{k_2=4}^{\infty}\sum_{j_2=0}^{k_2-2}(-1)^{j_1+j_2}\frac{(k_1-1)(k_2-1)}{j_1!j_2!}\mathcal{E}\left[\begin{smallmatrix}j_1&j_2\\k_1&k_2\end{smallmatrix};\tau\right]\epsilon_{k_1}^{(j_1)}\epsilon_{k_2}^{(j_2)}+\ldots$$

with iterated Eisenstein integrals eq. (3.152) of modular depth  $\geq 3$  in the ellipsis and  $\tau$  derivative

$$\partial_{\tau} \mathbb{I}_{\mathcal{E},+}(\epsilon_k; \tau) d\tau = -\mathbb{I}_{\mathcal{E},+}(\epsilon_k; \tau) \mathbb{A}(\epsilon_k; \tau). \tag{3.160}$$

The non-commuting variables

$$\epsilon_k^{(j)} = \operatorname{ad}_{\epsilon_0}^j(\epsilon_k) \tag{3.161}$$

are elements of Tsunogai's derivation algebra, which is generated by  $\epsilon_0, \epsilon_2, \epsilon_4, \ldots$  and has been explored from various viewpoints in the mathematical literature [178–191]. The algebra generated by these letters is not free but rather they fulfill homogenous relations, the so-called Pollack relations [185, 186, 192]. Those arise at higher degrees<sup>12</sup>, starting from degree 14 with the relation

$$0 = [\epsilon_4, \epsilon_{10}] - 3[\epsilon_6, \epsilon_8]. \tag{3.162}$$

We can also express modular transformations in the language of generating series. Specifically, the S transformation of (3.135) acts on  $\mathbb{I}_{\mathcal{E},+}(\epsilon_k;\tau)$  by

$$\mathcal{S}\left[\mathbb{I}_{\mathcal{E},+}\left(\epsilon_{k};\tau\right)\right] = \mathbb{I}_{\mathcal{E},+}\left(\epsilon_{k};-\frac{1}{\tau}\right) = \mathbb{S}(\epsilon_{k})U_{S}^{-1}\mathbb{I}(\epsilon_{k};\tau)U_{S}. \tag{3.163}$$

The integration kernels of eq. (3.151) are transformed by the operators  $U_S$  which are defined by their action

$$U_S^{-1} \epsilon_k^{(j)} U_S = (-1)^j (2\pi i)^{k-2-2j} \frac{j!}{(k-j-2)!} \epsilon_k^{(k-j-2)}. \tag{3.164}$$

<sup>12</sup>In accordance with the associated iterated Eisenstein integrals in eq. (3.159) , the derivations  $\epsilon_k^{(j)}$  are given degree k and modular depth one and concatenation products  $\epsilon_{k_1}^{(j_1)}\epsilon_{k_2}^{(j_2)}\dots\epsilon_{k_\ell}^{(j_\ell)}$  are defined to have modular depth  $\ell$ .

The generating series  $\mathbb{S}(\epsilon_k)$  is the tangentially regulated S-cocycle

$$\mathbb{S}(\epsilon_k) := \mathbb{P}\exp\left(\int_0^{i\infty} \mathbb{A}(\epsilon_k; \tau_1)\right)$$
 (3.165)

$$= \mathbb{I}_{\mathcal{E},+}(e_k;\tau)|_{\tau \to 0} \tag{3.166}$$

$$=1+\sum_{k_1=4}^{\infty}\sum_{j_1=0}^{k_1-2}(-1)^{j_1}\frac{(k_1-1)}{j_1!}(2\pi i)^{j_1+1-k_1}\mathfrak{m}\left[\begin{smallmatrix}j_1\\k_1\end{smallmatrix}\right]\epsilon_{k_1}^{(j_1)}$$

$$+\sum_{k_1=4}^{\infty}\sum_{j_1=0}^{k_1-2}\sum_{k_2=4}^{\infty}\sum_{j_2=0}^{k_2-2}(-1)^{j_1+j_2}\frac{(k_1-1)(k_2-1)}{j_1!j_2!}(2\pi i)^{j_1+j_2+2-k_1-k_2}\mathfrak{m}\left[\begin{smallmatrix}j_1&j_2\\k_1&k_2\end{smallmatrix}\right]\epsilon_{k_1}^{(j_1)}\epsilon_{k_2}^{(j_2)}+\ldots.$$

Similarly, the modular T-transformation operates on  $\tau$  by  $\tau \to \tau + 1$  can be calculated from

$$\mathcal{T}\left[\mathbb{I}_{\mathcal{E},+}(\varepsilon_k;\tau)\right] = \mathbb{I}_{\mathcal{E},+}(\varepsilon_k;\tau+1) = \exp(2\pi i N)\mathbb{I}(\epsilon_k;\tau)U_T, \qquad (3.167)$$

The operation of  $U_T$  is defined by its action on the letters

$$U_T^{-1} \epsilon_k^{(j)} U_T = \sum_{p=0}^{k-2-j} \frac{(-2\pi i)^p}{p!} \epsilon_k^{(j+p)}$$
(3.168)

and [177, 193]

$$N = N_{+} - \epsilon_{0}$$
 with  $N_{+} = \sum_{k=4}^{\infty} (k-1)BF_{k}\varepsilon_{k}$ . (3.169)

where  $BF_k = \frac{B_k}{k!}$  with  $B_k$  the k-th Bernoulli number.

# 3.4.3 Elliptic Multiple Polylogarithms

Elliptic multiple polylogarithms can be equivalently defined on both the torus and the elliptic curve. We review their definition on the torus and refer to the literature for their definition directly on the elliptic curve in algebraic coordinates x, y. The integration kernels for elliptic multiple polylogarithms on the torus are built from the so-called g-kernels arising in the Kronecker Eisenstein series.

**Definition 3.32** (Kronecker-Eisenstein-series). The Kronecker-Eisenstein-series is defined as [163, 194, 195] (following conventions of [8])

$$F_{EK}(x,y,q) = \pi \frac{\theta_1'(0,q)\theta_1(\pi(x+y),q)}{\theta_1(\pi x,q)\theta_1(\pi y,q)} = \sum_{\alpha=0}^{\infty} y^{\alpha-1}g^{(\alpha)}(x,q), \qquad (3.170)$$

where  $\theta'_1(z,\tau) = \partial_z \theta_1(z,\tau)$  and  $\theta_1(z,\tau)$  is the odd Jacobi  $\theta$  function as defined in eq. (3.89).

See also: In Section 7.3.1, we express the forms of the kite integral family's canonical connection matrix in the kernels defined here. The coefficients of the Kronecker–Eisenstein series are the g-kernels  $g^{(\alpha)}(z,\tau)$ , which exhibit simple poles in z at lattice points, i.e., at  $z=a+b\tau$  with  $a,b\in\mathbb{Z}$  and  $b\neq 0$ . For  $k=1, g^{(1)}(z,\tau)$  has a simple pole at all lattice points, including those with b=0. These kernels serve as the elliptic analogs of d log forms, in the sense that they can be used as integration kernels for elliptic multiple polylogarithms.

**Definition 3.33** (Elliptic Multiple Polylogarithms on the Torus). *Iterated integrals over the g-kernels in z-space are* elliptic multiple polylogarithms [8, 195–197]

$$\tilde{\Gamma}\left({}_{w_{1}w_{2}...w_{k}}^{n_{1}n_{2}...n_{k}};w|\tau\right) = \int_{0}^{w} dw' \, g^{(n_{1})}(w'-w_{1},\tau) \tilde{\Gamma}\left({}_{w_{2}...w_{k}}^{n_{2}...n_{k}};w'|\tau\right) \,. \tag{3.171}$$

If we integrate along a path in  $\tau$ -space, we obtain integrals and series of the form

$$\mathfrak{M}(f_{1}, f_{2}, ..., f_{k} | \tau) = \int_{i\infty}^{\tau} f_{1}(t_{1}) \int_{i\infty}^{t_{1}} f_{2}(t_{2}) ... \int_{i\infty}^{t_{k-1}} f_{k}(t_{k}) , \qquad (3.172a)$$

$$\operatorname{ELi}_{n_{1}, ..., n_{\ell}; m_{1}, ..., m_{\ell}; \sigma_{1}, ..., \sigma_{\ell-1}}^{x_{1}, ..., y_{\ell}; \bar{q}} = \prod_{\alpha=1}^{\ell} \sum_{\substack{j_{\alpha}=1\\k_{\alpha}=1}}^{\infty} \frac{x_{\alpha}^{j_{\alpha}}}{j_{\alpha}^{n_{\alpha}}} \frac{y_{\alpha}^{k_{\alpha}}}{k_{\alpha}^{m_{\alpha}}} \bar{q}^{j_{\alpha}k_{\alpha}} \prod_{i=1}^{\ell-1} (j_{i}k_{i} + ... + j_{\ell}k_{\ell})^{-\sigma_{i}/2} .$$

$$(3.172b)$$

Their convergence properties are summarised in [197]. The g-kernels transform under  $SL(2, \mathbb{Z})$  as quasi-modular forms (see (3.150))

$$g^{(k)}\left(\frac{z}{c\tau+d}, \frac{a\tau+b}{c\tau+d}\right) = (c\tau+d)^k \sum_{j=0}^k \frac{(2\pi i \ c \ z)^j}{j!(c\tau+d)^j} g^{(k-j)}(z,\tau). \tag{3.173}$$

We give the q-expansions around q = 0 for k = 0, ..., 4 explicitely:

$$g^{(0)}(z,\tau) = 1$$

$$g^{(1)}(z,\tau) = \pi \cot(\pi z) + 4\pi \sin(2\pi z)q^{2} + \mathcal{O}(q^{4}),$$

$$g^{(2)}(z,\tau) = -\frac{\pi^{2}}{3} + 8\pi^{2} \cos(2\pi z)q^{2} + \mathcal{O}(q^{4}),$$

$$g^{(3)}(z,\tau) = -8\pi^{3} \sin(2\pi z)q^{2} + \mathcal{O}(q^{4}),$$

$$g^{(4)}(z,\tau) = -\frac{\pi^{4}}{45} - \frac{16\pi^{4}}{3} \cos(2\pi z)q^{2} + \mathcal{O}(q^{4}).$$
(3.174)

In Feynman integrals, the g-kernels often appear in the following combinations:

**Definition 3.34** (Kronecker-Eisenstein form).

$$\omega_k(z,\tau) = (2\pi)^{2-k} \left( g^{(k-1)}(z,\tau) dz + (k-1)g^{(k)}(z,\tau) \frac{d\tau}{2\pi i} \right). \tag{3.175}$$

These forms are quasi-modular forms with quasi-modular weight k as defined in Definition 3.29.

There is an alternative notion of elliptic multiple polylogarithms on the torus, which is defined with the so-called f-kernels. Those are the coefficients of the following generating series:

$$\Omega_{\text{EK}}(x, y, q) = \exp\left[2\pi i \frac{\text{Im}(z)}{\text{Im}(\tau)}\right] F_{\text{EK}}(x, y, q) = \frac{1}{y} \sum_{\alpha \ge 0} f^{(\alpha)}(x) y^{\alpha}. \tag{3.176}$$

The kernels  $f^{(n)}$  are invariant under translations in  $\omega_1$  and  $\omega_2$  but they explicitly depend on the anti-holomorphic variable  $\bar{z}$ . Their iterated integrals are

$$\Gamma\left({}_{w_{1}w_{2}...w_{k}}^{n_{1}n_{2}...n_{k}};w|\tau\right) = \int_{0}^{w} dw' f^{(n_{1})}(w'-w_{1},\tau)\Gamma\left({}_{w_{2}...w_{k}}^{n_{2}...n_{k}};w'|\tau\right). \tag{3.177}$$

One can also define a class of elliptic multiple polylogarithms on the elliptic curve, i.e. with kernels in the coordinates x, y and this was explicitly done in [163, 198–200]. The definitions of kernels on the torus and on the elliptic curve can be matched by comparing poles and residues.

## 3.4.4 Siegel Modular Forms and Abelian Differentials

In this section, we extend our discussion of functions and iterated integrals on elliptic curves to higher-genus hyperelliptic curves. In particular, we introduce Riemann  $\Theta$  functions as a generalisation of Jacobi  $\theta$  functions, Siegel modular forms as an extension of classical modular forms, and finally, we explore the concept of hyperelliptic polylogarithms on hyperelliptic curves and surfaces. For further details on Siegel modular forms, we refer to the classical textbook [201] (in German) as well as the more recent reviews [202–204].

#### Siegel-modular Forms

In the previous section, we considered modular forms in terms of the normalised period  $\tau$ , which lives in the upper half-plane  $\mathbb{H}$ . To generalize this concept, we classify the space where the normalised period  $\Omega$  lives and the transformations that act on it.

**Definition 3.35** (Siegel Upper Half Space and the Siegel Modular Group). The Siegel upper half space is the space<sup>13</sup>:

$$\mathbb{H}_g = \left\{ \mathbf{\Omega} \in \mathbb{C}^{g \times g} : \mathbf{\Omega} = \mathbf{\Omega}^T, \operatorname{Im} \mathbf{\Omega} > 0 \right\}. \tag{3.178}$$

The Siegel modular group  $\Gamma_q$ , is the symplectic group

$$\Gamma_g = \operatorname{Sp}(2g, \mathbb{Z}) = \left\{ \begin{pmatrix} \mathbf{A} & \mathbf{B} \\ \mathbf{C} & \mathbf{D} \end{pmatrix} \in \mathbb{Z}^{2g \times 2g} \middle| \begin{pmatrix} \mathbf{A} & \mathbf{B} \\ \mathbf{C} & \mathbf{D} \end{pmatrix}^T \begin{pmatrix} \mathbf{0} & \mathbb{1} \\ -\mathbb{1} & \mathbf{0} \end{pmatrix} \begin{pmatrix} \mathbf{A} & \mathbf{B} \\ \mathbf{C} & \mathbf{D} \end{pmatrix} = \begin{pmatrix} \mathbf{0} & \mathbb{1} \\ -\mathbb{1} & \mathbf{0} \end{pmatrix} \right\}.$$
(3.179)

Here g is some positive integer, that we generally identify with the genus.

<sup>13</sup>Note that  $\mathbb{H} = \mathbb{H}_1$ .

The Siegel modular group acts on the Siegel upper half space in the following way:

$$\gamma \cdot \Omega = (\mathbf{A}\Omega + \mathbf{B})(\mathbf{C}\Omega + \mathbf{D})^{-1} \text{ for } \gamma = \begin{pmatrix} \mathbf{A} & \mathbf{B} \\ \mathbf{C} & \mathbf{D} \end{pmatrix} \in \Gamma_g, \ \Omega \in \mathbb{H}_g.$$
 (3.180)

Now we can define the central object of this section:

**Definition 3.36** (Siegel Modular Forms). A Siegel modular form of weight  $\rho$  – where  $\rho$ :  $GL(g,\mathbb{C}) \to GL(V)$  is a finite-dimensional complex representation with representation space V – is a holomorphic map  $f: \mathbb{H}_g \to V$ , such that

$$f(\gamma \cdot \Omega) = \rho(C\Omega + D)f(\Omega), \qquad (3.181)$$

for all 
$$\Omega \in \mathbb{H}_g$$
 and  $\gamma = \begin{pmatrix} \mathbf{A} & \mathbf{B} \\ \mathbf{C} & \mathbf{D} \end{pmatrix} \in \Gamma_g$ .

As in the genus-one case, where the congruence subgroups in eq. (3.26) take a special role, we are particularly interested in functions that transform covariantly under subgroups. To this end, we define the principle congruence subgroups of the Siegel modular group.

**Definition 3.37** (Principle Congruence Subgroup). The principle congruence subgroup of level  $N \in \mathbb{Z}_{>0}$  is defined as

$$\Gamma_g(N) = \{ \mathbf{M} \in \Gamma_g \mid \mathbf{M} \equiv 1 \mod N \} \subset \Gamma_g. \tag{3.182}$$

A general congruence subgroup of  $\Gamma_g$  of level N is then any subgroup that contains the principle congruence subgroup  $\Gamma_g(N)$ , see the lecture notes [205] for some examples.

Riemann  $\Theta$  Functions and Constants Next, we introduce the Riemann  $\Theta$ -function, which simultaneously serves as a fundamental example of a Siegel modular form and as a key building block for the hyperelliptic multiple polylogarithms discussed in the second part of this section. For further details, we refer to the textbooks [153, 156, 157] and the lecture notes [164].

**Definition 3.38** (Riemann  $\Theta$  Function). The classic Riemann  $\Theta$  function is defined by the series representation

$$\Theta(\boldsymbol{z}, \boldsymbol{\Omega}) = \sum_{\boldsymbol{n} \in \mathbb{Z}^g} \exp\left[i\pi \boldsymbol{n}^T \boldsymbol{\Omega} \boldsymbol{n} + 2\pi i \boldsymbol{n}^T \boldsymbol{z}\right], \qquad (3.183)$$

where  $\mathbf{z} = (z_1, \dots, z_g) \in \mathbb{C}^g$ ,  $\mathbf{\Omega} \in \mathbb{H}_g$  and g is a positive integer. We let  $\mathbf{\epsilon}_1, \mathbf{\epsilon}_2 \in \mathbb{Z}^g$  be a pair of vectors and call the matrix  $\mathbf{\epsilon} = \begin{bmatrix} \mathbf{\epsilon}_1 \\ \mathbf{\epsilon}_2 \end{bmatrix}$  the matrix of characteristics. These characteristics are referred to as odd or even if their scalar product  $\mathbf{\epsilon}_1^T \mathbf{\epsilon}_2$  is odd or even. The  $\Theta$  function with characteristics is then defined as

$$\Theta\left[\boldsymbol{\epsilon}\right]\left(\boldsymbol{z},\boldsymbol{\Omega}\right) = \sum_{\boldsymbol{n}\in\mathbb{Z}^g} \exp\left[i\pi\left(\frac{\boldsymbol{\epsilon}_1}{2} + \boldsymbol{n}\right)^T \boldsymbol{\Omega}\left(\frac{\boldsymbol{\epsilon}_1}{2} + \boldsymbol{n}\right) + 2\pi i\left(\boldsymbol{n} + \frac{\boldsymbol{\epsilon}_1}{2}\right)^T \left(\boldsymbol{z} + \frac{\boldsymbol{\epsilon}_2}{2}\right)\right].$$
(3.184)

#### See also:

Since they define the weight of a Siegel modular form, finite-dimensional complex representations of  $GL(g, \mathbb{C})$  play an important role here and we give some remarks on such representations in Appendix E.

Note that at genus one, i.e. for  $\Omega = \tau$ , the Riemann  $\Theta$  function reduces to the Jacobi  $\theta$  function of eq. (3.88), albeit with different conventions.

Under translations of  $\boldsymbol{z}$  by a linear function in  $\Omega$ , the Riemann  $\Theta$  function transforms as

$$\Theta\left[\boldsymbol{\epsilon}\right]\left(\boldsymbol{z}+\boldsymbol{\Omega}\boldsymbol{\lambda}_{1}+\boldsymbol{\lambda}_{2},\boldsymbol{\Omega}\right) = \exp\left[2\pi i\left(\frac{1}{2}(\boldsymbol{\epsilon}_{1}^{T}\boldsymbol{\lambda}_{2}-\boldsymbol{\lambda}_{1}^{T}\boldsymbol{\epsilon}_{2})-\boldsymbol{\lambda}_{1}^{T}\boldsymbol{z}-\frac{1}{2}\boldsymbol{\lambda}_{1}^{T}\boldsymbol{\Omega}\boldsymbol{\lambda}_{1}\right)\right]\Theta\left[\boldsymbol{\epsilon}\right]\left(\boldsymbol{z},\boldsymbol{\Omega}\right).$$
(3.185)

Under a parity transformation of  $\boldsymbol{z}$ , the Riemann  $\Theta$  functions obey the following identity:

$$\Theta[\epsilon](-z,\Omega) = (-1)^{\epsilon_1 \cdot \epsilon_2} \Theta[\epsilon](z,\Omega). \tag{3.186}$$

Under translations of the characteristics  $\epsilon_i \to \epsilon_i + 2\nu_i$  with  $\nu_1, \nu_2 \in \mathbb{Z}^g$ , the Riemann  $\Theta$  function transforms as

$$\Theta\begin{bmatrix} \epsilon_1 + 2\nu_1 \\ \epsilon_2 + 2\nu_2 \end{bmatrix}(\boldsymbol{z}, \boldsymbol{\Omega}) = \exp\left(i\pi\boldsymbol{\epsilon}_1^T\boldsymbol{\nu}_2\right)\Theta\begin{bmatrix} \epsilon_1 \\ \epsilon_2 \end{bmatrix}(\boldsymbol{z}, \boldsymbol{\Omega}). \tag{3.187}$$

This allows one to restrict to  $\epsilon_1, \epsilon_2 \in \{0, 1\}^g$  and consequently there are only  $2^{2g}$  independent choices of (half) characteristics. For example, at genus one, there are four distinct characteristics and their Jacobi  $\theta$  functions are listed in eq. (3.89).<sup>14</sup>At genus two, there are 16 characteristics, 10 of which are even. The Riemann  $\Theta$  functions evaluated at z = 0 are called  $Riemann \Theta$  constants and can be interpreted as functions  $\Theta[\epsilon](\Omega) \equiv \Theta[\epsilon](0,\Omega)$  in  $\Omega$  on  $\mathbb{H}_g$ . Note that due to eq. (3.186), the  $\Theta$  constants vanish for odd characteristics. Similarly, one can define derivative (Riemann)  $\Theta$  constants  $\partial_i \Theta[\epsilon](\Omega) \equiv \partial_{z_i} \Theta[\epsilon](z,\Omega)|_{z=0}$ . As an example, we list below the 10  $\Theta$  constants and the 6 derivative  $\Theta$  constants for genus two.

**Example 3.12** ( $\Theta$  Constants for Genus Two). The 10 Riemann  $\Theta$  constants at genus two associated to the 10 even characteristics are:

$$\theta_{1}^{R} = \Theta \begin{bmatrix} 1,1 \\ 1,1 \end{bmatrix} (\mathbf{\Omega}), \qquad \theta_{2}^{R} = \Theta \begin{bmatrix} 0,0 \\ 1,1 \end{bmatrix} (\mathbf{\Omega}), \qquad \theta_{3}^{R} = \Theta \begin{bmatrix} 0,0 \\ 1,0 \end{bmatrix} (\mathbf{\Omega}), \\
\theta_{4}^{R} = \Theta \begin{bmatrix} 0,1 \\ 1,0 \end{bmatrix} (\mathbf{\Omega}), \qquad \theta_{5}^{R} = \Theta \begin{bmatrix} 0,0 \\ 0,1 \end{bmatrix} (\mathbf{\Omega}), \qquad \theta_{6}^{R} = \Theta \begin{bmatrix} 0,0 \\ 0,0 \end{bmatrix} (\mathbf{\Omega}), \\
\theta_{7}^{R} = \Theta \begin{bmatrix} 0,1 \\ 0,0 \end{bmatrix} (\mathbf{\Omega}), \qquad \theta_{8}^{R} = \Theta \begin{bmatrix} 1,1 \\ 0,0 \end{bmatrix} (\mathbf{\Omega}), \qquad \theta_{9}^{R} = \Theta \begin{bmatrix} 1,0 \\ 0,0 \end{bmatrix} (\mathbf{\Omega}), \\
\theta_{10}^{R} = \Theta \begin{bmatrix} 1,0 \\ 0,1 \end{bmatrix} (\mathbf{\Omega}). \qquad (3.188)$$

The six derivative  $\Theta$  constants are

$$\partial_{i}\theta_{11}^{R} = \partial_{i}\Theta\begin{bmatrix}0,1\\0,1\end{bmatrix}(\mathbf{\Omega}), \qquad \partial_{i}\theta_{12}^{R} = \partial_{i}\Theta\begin{bmatrix}0,1\\1,1\end{bmatrix}(\mathbf{\Omega}), \qquad \partial_{i}\theta_{13}^{R} = \partial_{i}\Theta\begin{bmatrix}1,0\\1,1\end{bmatrix}(\mathbf{\Omega}), \\
\partial_{i}\theta_{14}^{R} = \partial_{i}\Theta\begin{bmatrix}1,0\\1,0\end{bmatrix}(\mathbf{\Omega}), \qquad \partial_{i}\theta_{15}^{R} = \partial_{i}\Theta\begin{bmatrix}1,1\\1,0\end{bmatrix}(\mathbf{\Omega}), \qquad \partial_{i}\theta_{16}^{R} = \partial_{i}\Theta\begin{bmatrix}1,1\\0,1\end{bmatrix}(\mathbf{\Omega}).$$
(3.189)

The  $\Theta$  constants are (classical) Siegel modular forms with weight  $\rho_{\det,\frac{1}{2}}^{15}$  for a congruence subgroup of  $\Gamma_g$  of level 2, at least up to a multiplicative complex phase [206, 207]. By Thomae's formula one can also express the parameters of the polynomial defining a hyperelliptic curve in Riemann  $\Theta$  functions, see e.g. [208–210].

<sup>14</sup>Note that we the conventions we use for the Jacobi  $\theta$  and Riemann  $\Theta$  functions are distinct, so they cannot be obtained from each other, so  $\Theta[\epsilon](z,\tau) \neq \theta[\epsilon](z,\tau)$ , but there is a non-trivial relation between these functions.

<sup>15</sup>We define  $\rho_{\text{det},\frac{1}{2}}$  and other weights in appendix E.

(Quasi-)periods as Siegel (Quasi-)modular Forms. Let us consider a family of hyperelliptic curves with parameters  $\lambda$ . If we perform a closed loop in parameter space, the hyperelliptic curve remains the same but the integration cycles and consequently also the periods change due to the monodromy transformation. Specifically, the a and b-periods undergo a linear transformation and thus the periods are transformed by a constant  $2g \times 2g$  matrix M with integer values, the so-called  $monodromy\ matrix^{16}$ 

$$\begin{pmatrix} \mathbf{\mathcal{B}}^T \\ \mathbf{\mathcal{A}}^T \end{pmatrix} \to \mathbf{M} \begin{pmatrix} \mathbf{\mathcal{B}}^T \\ \mathbf{\mathcal{A}}^T \end{pmatrix} . \tag{3.190}$$

The monodromy matrix is an element of  $Sp(2g, \mathbb{Z})$  as it preserves the symplectic structure of the homology basis. The group of all transformations due to independent closed loops forms a subgroup of  $Sp(2g, \mathbb{Z})$ , i.e. a subgroup  $\Gamma$  of the Siegel modular group  $\Gamma_q$ , which is always some congruence subgroup [211]. By eq. (3.190) we find the action on the a-period matrix to be

$$\mathbf{M} \cdot \mathbf{A} = \mathbf{A} (\mathbf{C} \mathbf{\Omega} + \mathbf{D})^T \text{ for } \mathbf{M} = \begin{pmatrix} \mathbf{A} & \mathbf{B} \\ \mathbf{C} & \mathbf{D} \end{pmatrix} \in \Gamma_g,$$
 (3.191)

which shows that  $\mathcal{A}$  is a Siegel modular form with respect to  $\Gamma$  with weight  $1 \otimes \rho_{\rm F}^{17}$ , <sup>17</sup>We define  $1 \otimes \rho_{\rm F}$  and where 1 refers to the trivial representation. Additionally, we find for the normalised period matrix

$$\mathbf{M} \cdot \mathbf{\Omega} = (\mathbf{A}\mathbf{\Omega} + \mathbf{B})(\mathbf{C}\mathbf{\Omega} + \mathbf{D})^{-1}.$$
 (3.192)

We can also determine how the quasi-period matrix  $\tilde{\mathcal{A}}$  transforms under modular transformations. Note that the period matrix  $\mathcal{P}$  of eq. (3.57) fulfils some linear differential equation in the parameters  $\lambda$  and in particular this leads to a differential equation for the a-period matrix:

$$\partial \mathcal{A} = \mathbf{Q}_1 \mathcal{A} + \mathbf{Q}_2 \tilde{\mathcal{A}}, \tag{3.193}$$

where  $\mathbf{R}_i$  are  $q \times q$  matrices that depend on the choice of  $\partial$ . Consequently, we can express the matrix of a-quasi-periods in a-periods and their derivatives:

$$\tilde{\mathcal{A}} = \mathbf{R}_1 \mathcal{A} + \mathbf{R}_2 \partial \mathcal{A}, \qquad (3.194)$$

where  $\mathbf{R}_1 = -\mathbf{Q}_2^{-1}\mathbf{Q}_1$  and  $\mathbf{R}_2 = -\mathbf{Q}_2^{-1}$ . An analogous equation holds for the b (quasi-)periods and for  $\Omega = \mathcal{A}^{-1}\mathcal{B}$ . In particular, using also the quadratic identities (3.61) and (3.63), we can find [34]:

$$\mathbf{R}_2 \mathbf{A} \partial \mathbf{\Omega} = 8\pi i \mathbf{A}^{-1T} \,. \tag{3.195}$$

Using (3.194) and the transformation behavior of  $\mathcal{A}$  and  $\Omega$ , we find

$$\mathbf{M} \cdot \tilde{\mathbf{A}} = \tilde{\mathbf{A}} (\mathbf{C}\Omega + \mathbf{D})^T + \mathbf{R}_2 \mathbf{A} \partial \Omega \mathbf{C}^T.$$
 (3.196)

Inserting (3.194) in this relation, we finally obtain:

$$\mathbf{M} \cdot \tilde{\mathbf{A}} = \tilde{\mathbf{A}} (\mathbf{C}\Omega + \mathbf{D})^T + 8\pi i \mathbf{A}^{-1T} \mathbf{C}^T.$$
 (3.197)

Since  $\tilde{\mathcal{A}}$  does not transform as a Siegel modular form but rather as the derivative of one, we refer to it as a Siegel quasi-modular form; see [212] for a formal definition. Furthermore, the period matrix can also be expressed in terms of Riemann  $\Theta$ functions using the Rosenhain formula [213].

<sup>16</sup>The transposes are due to our convention to label the columns and not the rows of the  $\mathcal{A}, \mathcal{B}$  matrices by the cycles.

other weights in appendix E.

#### Abelian Differentials in Riemann $\Theta$ Functions

In this section, we comment on how to relate the Abelian differentials on the hyperelliptic curves in the algebraic coordinates (x, y) to differentials in the geometric coordinate z.<sup>18</sup> The change of coordinates from (x, y) to the coordinate z is obtained by the so-called *Schottky parametrisation*[216], see [154] for more details or [159] for a recent review in the physics literature. Numerically this coordinate change can e.g., be performed using the Myrberg algorithm [217], see for example [218–221] for further discussions and an implementation. We will see, that all Abelian differentials can be written in terms of first kind differentials and Riemann  $\Theta$  functions.

**Abelian Differentials of First Kind.** We already discussed how to relate the canonical first kind differentials  $w_{1|j}$  on the Riemann surface to the differentials  $\varpi_i$  in (3.43). Together with the Riemann  $\Theta$  functions, these are the building blocks for the second and third kind differentials.

The additional objects we require are the prime form and the bidifferential. The prime form is defined as (see, e.g., [155, 156, 222, 223])

$$E(x,y|\mathbf{\Omega}) = \frac{\Theta[\epsilon](\mathfrak{u}(x,y),\mathbf{\Omega})}{\eta_{\epsilon}(x)\eta_{\epsilon}(y)},$$
(3.198)

where  $\epsilon = (\epsilon_1, \epsilon_2)$  is an odd (half-)characteristic and  $\eta_{\epsilon}(x)$  is the holomorphic function defined by

$$\eta_{\epsilon}(x)^{2} = \sum_{i=1}^{g} w_{1|i} \partial_{i} \Theta[\epsilon](0, \mathbf{\Omega}). \qquad (3.199)$$

We commonly shorten  $E(x,y) = E(x,y|\mathbf{\Omega})$ .<sup>19</sup> The prime form is independent of the chosen characteristic. The fundamental bi-differential is defined by, see, e.g., [164],

$$B(z, z') = d_z d_{z'} \log E(z, z' | \mathbf{\Omega}) = d_z d_{z'} \log \Theta[\epsilon](\mathfrak{u}(z, z'), \mathbf{\Omega}). \tag{3.200}$$

We can explicitly write this as

$$B(z,z') = (2\pi)^2 \left[ \frac{\Theta\langle z,z'\rangle(\mathfrak{u}(z,z')+c_{\epsilon})}{\Theta(\mathfrak{u}(z,z')+c_{\epsilon})} - \frac{\Theta\langle z\rangle(\mathfrak{u}(z,z')+c_{\epsilon})\Theta\langle z'\rangle(\mathfrak{u}(z,z')+c_{\epsilon})}{\Theta(\mathfrak{u}(z,z')+c_{\epsilon})^2} \right] dz \wedge dz',$$
(3.201)

where we introduced the following notation for derivatives of  $\Theta$  functions

$$\Theta\langle z_1, \dots, z_k \rangle(x) = \sum_{n \in \mathcal{Z}^g} n^T w_1(z_1) \dots n^T w_1(z_k) \exp\left[i\pi n^T \mathbf{\Omega} n + 2\pi i n^T x\right], \quad (3.202)$$

and

$$c_{\epsilon} = \frac{1}{2} \left( \mathbf{\Omega} \epsilon_1 + \epsilon_2 \right) . \tag{3.203}$$

<sup>18</sup>Such considerations might also be a first step to relate hyperelliptic iterated integrals to the iterated integrals on genus g Riemann surfaces introduced in [159, 214, 215].

<sup>19</sup>Note that we also often drop the explicit dependence of the  $\Theta$  functions on  $\Omega$  to keep the expressions shorter.

**Abelian Differentials of Third Kind.** The normalised Abelian differential of third kind with poles at  $z_1, z_2$  is defined as [155]:

$$w_{3|z_1,z_2} = d_z \log \frac{E(z,z_1)}{E(z,z_2)} = dz \left[ \frac{\partial_z E(z,z_1)}{E(z,z_1)} - \frac{\partial_z E(z,z_2)}{E(z,z_2)} \right].$$
(3.204)

The normalisation here means that

$$\int_{a_i} w_{3|z_1,z_2} = 0, \qquad \operatorname{res}_{z=z_1} w_{3|z_1,z_2} = 1, \qquad \operatorname{res}_{z=z_2} w_{3|z_1,z_2} = -1. \tag{3.205}$$

In terms of Riemann  $\Theta$  functions this differential is

$$w_{3|z_1,z_2} = \left[ \frac{w_{1|i}(z)\partial_i \Theta(\mathfrak{u}(z,z_1), \mathbf{\Omega})}{\Theta(\mathfrak{u}(z,z_1), \mathbf{\Omega})} - \frac{w_{1|i}(z)\partial_i \Theta(\mathfrak{u}(z,z_2), \mathbf{\Omega})}{\Theta(\mathfrak{u}(z,z_2), \mathbf{\Omega})} \right] dz.$$
(3.206)

To relate these differentials to the third kind differentials of (3.54) and (3.55), we just match the respective poles and residues. For the third kind differential with pole at  $\infty$ , we find

$$\frac{x^g dx}{y} = -w_{3|z_{\infty}^+, z_{\infty}^-} + \sum_{i=1}^g \left( \oint_{a_i} \frac{x^g dx}{y} \right) w_{1|i}.$$
 (3.207)

Here  $z_{\infty}^+$  and  $z_{\infty}^-$  are the values of the global variable related to  $\infty$  on the two sheets.

**Abelian Differentials of Second Kind.** The normalised differential of the second kind with pole at  $\tilde{z}$  of order k+1 is given by a residue of the fundamental bi-differential [164],

$$w_{2|\tilde{z}}^{(k)} = -\frac{1}{k} \text{Res}_{z'=\tilde{z}} \left[ \frac{1}{(z'-\tilde{z})^k} B(z,z') \right],$$
 (3.208)

which satisfies

$$\oint_{a_i} w_{2|\tilde{z}}^{(k)} = 0, \qquad \text{res}_{z=\tilde{z}} \left[ w_{2|\tilde{z}}^{(k)} \right] = 0.$$
(3.209)

In particular, we find for a finite pole  $\tilde{z}$ :

$$w_{2|\tilde{z}}^{(k)} = \frac{(2\pi)^2}{k!} \left. \frac{\partial^{k-1}}{\partial z'^{k-1}} \left[ \frac{\Theta\langle z, z' \rangle (\mathfrak{u}(z, z') + c_{\epsilon})}{\Theta(\mathfrak{u}(z, z') + c_{\epsilon})} - \frac{\Theta\langle z \rangle (\mathfrak{u}(z, z') + c_{\epsilon}) \Theta\langle z' \rangle (\mathfrak{u}(z, z') + c_{\epsilon})}{\Theta(\mathfrak{u}(z, z') + c_{\epsilon})^2} \right] \right|_{z'=\tilde{z}} dz.$$
(3.210)

For a pole at  $\infty$ , we obtain (focusing on an even hyperelliptic curve for definiteness)

$$\omega_{2|\infty}^{(k)} = \frac{(2\pi)^2}{k!} \frac{\partial^{k-1}}{\partial u'^{k-1}} \frac{1}{u'^2} \left[ \frac{\Theta\langle z \rangle (\mathfrak{u}(z, 1/u') + c_{\epsilon}) \Theta\langle 1/u' \rangle (\mathfrak{u}(z, 1/u') + c_{\epsilon})}{\Theta(\mathfrak{u}(z, 1/u') + c_{\epsilon})^2} - \frac{\Theta\langle z, 1/u' \rangle (\mathfrak{u}(z, 1/u') + c_{\epsilon})}{\Theta(\mathfrak{u}(z, 1/u') + c_{\epsilon})} \right]_{u'=0}^{k} dz. \quad (3.211)$$

Using these expressions, one can match the second kind differentials on the curve and the surface again by comparing poles and residues.

#### See also:

In Appendix D.1 we give explicit expressions for the expansion of differentials of the basic differential forms around  $\infty$  for even and odd hyperelliptic curves.

# 3.5 Geometry And Feynman Integrals

Let us conclude the chapter by returning to the Feynman integrals we are interested in and reviewing different approaches to associate a family of varieties with a family of these integrals. Specifically, we focus on the integral families treated in the remainder of the thesis.

# From the Maximal Cut in Baikov Representation

As given in eq. (2.44), a non-trivial maximal cut is generally an integral

$$MC = \int \left( \prod_{i=1}^{L_{MC}} dx_i \right) \prod_j \mathcal{B}_j^{\nu_j}(\boldsymbol{x})$$
 (3.212)

after taking all residues.<sup>20</sup> In general and in particular for all examples considered in this thesis, the exponents  $\nu_j$  take the form  $\nu_j = \frac{\mu_j}{2} \pm \varepsilon$  with  $\mu_j \in \mathbb{Z}$ . The  $\varepsilon \to 0$  limit of the integrand can be used to define a polynomial equation

$$y^2 = \prod_j \mathcal{B}_j^{\nu_j}(\boldsymbol{x})|_{\varepsilon \mapsto 0} \tag{3.213}$$

and we can define a variety via this polynomial constraint in  $\mathbb{P}^{L_{\text{MC}}}_{\mathbb{C}}$ . We illustrate this with the prominent examples of this thesis and start with the sunrise integral family:

**Example 3.13** (The Sunrise's Elliptic Curve). We reviewed the Baikov representation and subsequently the maximal cut of the unequal mass sunrise integral in the loop-by-loop approach in Example 2.9. We gave the Baikov polynomial in the maximal cut limit in eq. (2.54). In the limit  $\varepsilon \to 0$ , it reduces to

$$\mathcal{B}_{\oplus}^{ll}(z) = \left( (z_4 - \lambda_1^{\oplus})(z_4 - \lambda_2^{\oplus})(z_4 - \lambda_3^{\oplus})(z_4 - \lambda_4^{\oplus}) \right)^{-\frac{1}{2}}.$$
 (3.214)

From this integrand we can define a quartic elliptic curve with the polynomial equation

$$y^{2} = (x - \lambda_{1}^{\ominus})(x - \lambda_{2}^{\ominus})(x - \lambda_{3}^{\ominus})(x - \lambda_{4}^{\ominus}), \qquad (3.215)$$

with the branch points  $\lambda_i^{\oplus}$  depending on the masses and the external momentum.

This procedure relied on the integral family being considered in  $D=2-2\varepsilon$ . If we considered the same integral family in three  $(\pm \varepsilon)$  dimensions, we would not find this curve. Similarly, we consider an integral family related to a hyperelliptic curve with genus two.

**Example 3.14** (A Hyperelliptic Curve of Genus Two from the Non-Planar Crossed Box). We use the expressions from Example 2.11. In the limit  $\varepsilon \to 0$ , the integrand of eq. (2.67) defines a hyperelliptic curve of genus two via the polynomial

$$y^{2} = (x - \lambda_{1}^{\text{npcb}})(x - \lambda_{2}^{\text{npcb}})(x - \lambda_{3}^{\text{npcb}})(x - \lambda_{4}^{\text{npcb}})(x - \lambda_{5}^{\text{npcb}})(x - \lambda_{6}^{\text{npcb}}), \quad (3.216)$$
as discussed in [29, 31].

<sup>20</sup>Note that in some cases this is non-trivial and we have additional poles besides  $z_i = 0$ . We need to also take their residues before using the integral expression to determine the associated geometry.

See also:

We discuss hyperelliptic curves in Section 3.2 and the integral family of this example in Section 6.1.4. In the two examples given here, the remaining integral of eq. (3.212) after taking all residues is one-dimensional. There also exist cases, where more than one integration variable remains and we can associate higher dimensional manifolds to Feynman integral families. Specifically, there are different examples of Feynman integral families related to CYs appearing in the literature [5, 19, 20, 24, 28, 95]. At this point we make an important remark: The geometries associated with a Feynman integral family need not necessarily arise from its top sector, as illustrated in the example above. The varieties related to a Feynman integral family may instead be associated with one or more of its sub-sectors. A notable example is the kite integral family from Example 2.8: while its top sector has a trivial maximal cut, simply corresponding to a punctured Riemann sphere, it contains two distinct sunrise sub-sectors, each associated with a different torus, as illustrated in figure 7.1.

## Special Case: Fishnet Integrals

We consider as a special case, the massless fishnet integrals of eq. (2.78) in D=2, which take the form

$$I_{\boldsymbol{\nu}}^{G}(\boldsymbol{\lambda}) \sim \int \left[ \prod_{i} \mathrm{d}x_{i} \wedge \mathrm{d}\bar{x}_{i} \right] \left[ \prod_{i,j} \frac{1}{[|x_{i} - x_{j}|^{2}]^{\nu}} \right] \left[ \prod_{i,j} \frac{1}{[|x_{i} - \lambda_{j}|^{2}]^{\nu}} \right]$$
$$\sim \int \prod_{i,j,k,l,m} \left( \frac{\mathrm{d}x_{i}}{(x_{j} - x_{k})^{\nu} (x_{l} - \lambda_{m})^{\nu}} \right) \wedge \left( \frac{\mathrm{d}\bar{x}_{i}}{(\bar{x}_{j} - \bar{x}_{k})^{\nu} (\bar{x}_{l} - \bar{\lambda}_{m})^{\nu}} \right).$$

As described in Section 3.3 a family of Calabi-Yau manifolds can be defined by a polynomial equation and an ambient space. For specific parameter and dimension choices, these data defining a CY L-fold family can be read off from the integrals of eq. (2.78) in position space representation. The integrand of eq. (2.78) is defined with coordinates  $\boldsymbol{x}$  in  $\mathbb{C}^L$ . The natural compactification of this space is an L-fold product of  $\mathbb{P}_{\mathbb{C}}$ , i.e., we choose the base space  $B = \mathbb{P}_{\mathbb{C}}^L = \underset{i=1}{\overset{L}{\searrow}} \mathbb{P}_{\mathbb{C},i}$ . The polynomial equation in this space – which we can read off from the half-integrand in holomorphic coordinates – is:<sup>21</sup>

$$y^{d_c} = P_G(\mathbf{x}, \lambda) = \prod_{j,k,l,m} (x_j - x_k)^{\nu} \prod_{i,j} (x_l - \lambda_m)^{\nu}.$$
 (3.217)

We consider a  $d_c$ -fold covering over the base space and in particular, we often choose a double cover  $d_c = 2$ . The adjunction formula [165] implies that for this polynomial equation to define a CY L-fold, the parameters need to fulfill the condition

$$\frac{d_c}{d_c - 1} = V \cdot \nu \,. \tag{3.218}$$

For  $d_c = D = 2$  this is equal to the condition of (2.80) – the conformal massless fishnet integrals in two dimensions define CY *L*-folds. Specifically, we consider the tilings with V = 3, 4, 6 and propagator powers  $\frac{2}{3}, \frac{1}{2}, \frac{1}{3}$  respectively. The unique

#### See also:

We discuss these integrals in detail in Section 8.2.

<sup>&</sup>lt;sup>21</sup>Note, that we use the same name for the coordinates in  $\mathbb{C}^L$  and  $\mathbb{P}_L$  here for simplicity. Of course the transition to  $\mathbb{P}_L$  requires a homogenisation of coordinates.

holomorphic differential is given in the homogeneous coordinates  $[x_i:w_i]$  of each  $\mathbb{P}_{\mathbb{C}}$  by

$$\Omega_G(\boldsymbol{x}, \boldsymbol{\lambda}) = \frac{\bigwedge_{i=1}^{\ell} (w_i \, \mathrm{d}x_i - x_i \, \mathrm{d}w_i)}{\mathrm{P}_G(\boldsymbol{x}, \boldsymbol{\lambda})^{\frac{\mathrm{d}-1}{\mathrm{d}}}}.$$
 (3.219)

For more subtle explanations related to this association, we refer to [35, 37, 38].

## Other Approaches

As we have seen in Section 3.3, the periods of a Calabi-Yau variety are determined as the solutions of an ideal of differential operators, the Picard Fuchs ideal. Thus, this ideal of operators also determines the Calabi-Yau family that is associated to the integral family. One can find the Picard-Fuchs ideal for the maximal cut from the linear differential equations it satisfies algorithmically. Another way to obtain a family of varieties from a Feynman integral family is via the Symanzik representation, more specifically by taking a quotient of the Symanzik polynomials [224, 225] in the proper embedding space. One example, where this has been shown to give the same variety as the polynomial equation defined from the maximal cut in Baikov representation is the sunrise integral family [92]. Lastly, let us remind again of the fact that in different contexts, the integrals take different forms and for example in string integrals, the integration space is always a punctured Riemann surface of genus L with L the loop number, see the discussion in Section 2.1.

# Twisted and Motivic (Co-)Homology Groups

#### See also:

- In Chapter 5 we study bilinear relations between twisted periods and their implications for relations between (cuts of) Feynman integrals. We also understand the role of the intersection matrix of twisted cohomology in canonical bases.
- In Chapter 6 we study hyperelliptic maximal cuts, modelled by hypergeometric Lauricella functions. We use results derived from from twisted intersection theory and particularly the results of Chapter 5
- In Chapter 8 we discuss Feynman integrals in two dimensions, as single-valued versions of twisted periods, which can be constructed as a double copy of twisted periods, as described in Subsection 4.3.2.

Many of the integrals we consider in this thesis have multi-valued integrands — most importantly Feynman integrals in dimensional regularisation and the special hypergeometric functions with generic parameters that arise in them. As such, one natural way to study them is as twisted periods, i.e., periods of twisted (co-)homology groups, which form are (co-)homology groups with coefficients. This viewpoint and the insights from twisted intersection theory that it allows us to use are relevant for many results presented in this thesis. Some of them are listed in the margin here. They require a solid understanding of the basics of twisted intersection theory, which we provide in this chapter. In addition to twisted (co-)homology groups, we will also — more briefly — introduce some results from motivic cohomology and comment on their appearance in the context of Feynman integrals. Additionally, the motivic framework is where the construction for single-valued versions of twisted periods we apply stems from.

In particular, brief reviews on twisted (co-)homology groups as well as motivic cohomology are presented in Sections 4.1 and 4.2. In the latter our focus is on constructing single-valued versions of periods in Subsection 4.2.2 and on the motivic coaction for special classes of functions in Subsection 4.2.3. We supplement these introductions with a class of examples in Section 4.3, where we discuss Aomoto-Gelfand hypergeometric functions. Finally, we explain in Section 4.4 how one can interpret Feynman integrals as twisted periods. This chapter is further complemented with Appendix B, where we explain how to practically compute some of the objects introduced throughout the chapter.

Section 4.1 and parts of Section 4.2 are reviews based on the existing literature and resemble similar reviews in [36, 50, 226]. The following results were obtained during the PhD and many of them are already published:

- ♠ In Section 4.2.3 we present preliminary results on a coaction-like map, which was obtained during a collaboration with Axel Kleinschmidt and Oliver Schlotterer. A publication on this construction is in preparation [227].
- ♠ The discussion of (single-valued) Aomoto-Gelfand hypergeometric functions in Section 4.3 was already presented in [36], which resulted from a collaboration with Claude Duhr.
- ♠ The discussion on how to interpret Feynman integrals as twisted periods is partially taken from similar discussions in [50, 226], which resulted from collaborations with Claude Duhr, Cathrin Semper and Sven Stawinski.

# Contents of this Chapter

4.1	Revi	ew of Twisted (Co-)Homology Groups	96	
	4.1.1	Review: Twisted (Co-)homology	98	
	4.1.2	Review: Relative Twisted Cohomology	110	
4.2	Revi	ew: Motivic Periods for Phycisists	115	
	4.2.1	Motivic and de Rham Periods	115	
	4.2.2	Single-valued Periods	118	
	4.2.3	Coactions	121	
4.3 Aomoto-Gelfand Hypergeometric Functions 124				
	4.3.1	Definition of Aomoto-Gelfand Hypergeometric Functions	124	
	4.3.2	Single-valued Hypergeometric Functions	128	
4.4	Feyn	man Integrals and Their Cuts as Twisted Periods	130	

# 4.1 Review of Twisted (Co-)Homology Groups

In this section, we discuss the cohomology and homology groups whose period pairings evaluate to multi-valued integrals of the form

$$\int_{\gamma} \Phi \varphi . \tag{4.1}$$

More specifically:

•  $\Phi$  is a multi-valued function – the twist – and here, we assume that the twist takes the form

$$\Phi = \prod_{i=0}^{r} L_i(\boldsymbol{z})^{\alpha_i}, \qquad (4.2)$$

where the  $L_i(z)$  are polynomials in the variables  $z \in X^1$  and  $\alpha_i \in \mathbb{C}$  in the most general case.

- $\varphi$  is a rational *n*-form on X. In general, we define the twist such that all poles of  $\varphi$  appear as a zero of one of the  $L_i(z)$ . That might be achieved by including factors  $L_i(z)^0$  in the twist.
- $\gamma$  is a closed integration contour on X. For the integral in eq. (4.1) to be well-defined, we attach a choice for the branch of  $\Phi$  to  $\gamma$ .

Starting from some integral of interest, the data extracted from these objects can be used to define (relative) twisted (co-)homology groups.<sup>2</sup>. In particular, we define a connection and the corresponding systems of its local sections. The *twisted connection* and the *dual twisted connection* are

$$\nabla_{\Phi} = d_{int} + \omega_{\Phi} \wedge \cdot \text{ and } \check{\nabla}_{\Phi} = d_{int} - \omega_{\Phi} \wedge \cdot \text{ with } \omega_{\Phi} = \frac{d_{int}\Phi}{\Phi} = d_{int}\log\Phi, \quad (4.3)$$

where the term with  $\omega_{\Phi}$  account for the multi-valuedness of the integrands. The spaces these are defined on also depend on the particular integrals we want to consider and will be specified below. Note that at this point we explicitly use the exterior derivative with respect to the (physically) internal variables. The distinction between the derivatives  $d_{int}$  and  $d_{ext}$  is particularly relevant in this chapter. Acting with the connection  $\nabla_{\Phi}$  on  $\varphi$  is equivalent to acting with the exterior derivative on the full integrand  $\Phi\varphi$ :

$$d_{int} \left( \Phi \varphi \right) = \Phi d_{int} \varphi + d_{int} \Phi \wedge \varphi = \Phi \left( d_{int} \varphi + \frac{d_{int} \Phi}{\Phi} \wedge \varphi \right) = \Phi \nabla_{\Phi} \varphi \,. \tag{4.4}$$

The  $local systems^3$  defined by the twist are

$$\check{\mathcal{L}}_{\Phi} = \{ f(\boldsymbol{z}) \, | \, \check{\nabla}_{\Phi} f(\boldsymbol{z}) = 0 \} \text{ and } \mathcal{L}_{\Phi} = \{ f(\boldsymbol{z}) \, | \, \nabla_{\Phi} f(\boldsymbol{z}) = 0 \}. \tag{4.5}$$

<sup>1</sup>Typically  $X = \mathbb{P}_{\mathbb{C}}^n - \Sigma$  here with  $\Sigma$  a union of hypersurfaces specified by the branch points and poles of  $\Phi \varphi$  as detailed later. But one can also define twisted cohomology groups on other varieties.

<sup>2</sup>Twisted (co-)homology groups form a subset of (co-)homology groups with coefficients, with the coefficients defined by values of the twist.

<sup>&</sup>lt;sup>3</sup>A proper definition of the local system can be found in Definition A.3.

If  $\Phi\varphi$  has branch points, but no poles or zeroes (i.e.  $\alpha_i \notin \mathbb{Z}$  for all i and  $\sum_{i=0}^r \alpha_i \notin \mathbb{Z}$ ), the definition of the twisted (co-)homology groups defined by the data is straightforward and we review it in Subsection 4.1.1. In situations relevant for physics, we typically have additional poles in  $\Phi\varphi$  that are not regulated by  $\Phi$  – meaning they are not branch points of the twist. One can regulate these either by working relative to some hypersurfaces – using relative twisted (co-)homology groups – or by introducing a generic parameter and performing a limit. We review these modes of regularisation in Section 4.2, but also make some comments on how the two approaches are equivalent for the objects we care about. Throughout this discussion, we keep referring to the example of Euler's  $\beta$ -function as well as Gauss hypergeometric  ${}_2F_1$  function. Let us start by introducing these here to illustrate the discussion so far.

**Example 4.1** (Euler's  $\beta$  function: An Example for a Multivalued Function). Euler's  $\beta$  function is defined by

$$\beta(a,b) = \int_0^1 x^{a-1} (1-x)^{b-1} dx = \frac{\Gamma(a)\Gamma(b)}{\Gamma(a+b)} \text{ for Re(a), Re(b)} > 0.$$
 (4.6)

We define the twist

$$\Phi = x^a (1 - x)^b \tag{4.7}$$

and the form  $\varphi = \frac{dx}{x(1-x)}$  such that

$$\beta(a,b) = \int_0^1 \Phi \, \varphi \,. \tag{4.8}$$

**Example 4.2** (Gauss Hypergeometric  ${}_{2}F_{1}$  function: An Example for a Multivalued Function). The integral representation of the hypergeometric  ${}_{2}F_{1}$  function is

$${}_{2}F_{1}(a,b,c;\lambda^{-1}) = \frac{\Gamma(c)}{\Gamma(b)\Gamma(c-b)} \int_{0}^{1} z^{b-1} (1-z)^{c-b-1} (1-\lambda^{-1}z)^{-a} dz$$
 (4.9)

and we also use its normalised version

$${}_{2}\mathcal{F}_{1}(a,b,c;\lambda^{-1}) = \frac{\Gamma(b)\Gamma(c-b)}{\Gamma(c)} {}_{2}F_{1}(a,b,c;\lambda^{-1})$$
(4.10)

and assume that the parameters a, b, c are generic. Then we can write

$$_{2}\mathcal{F}_{1}(a,b,c;\lambda^{-1}) = (-\lambda)^{a} \int_{\gamma=[0,1]} \Phi \,\varphi$$
 (4.11)

with 
$$\Phi = z^b (1-z)^{c-b} (z-\lambda)^{-a}$$
 and  $\varphi = \frac{dz}{z(1-z)}$  (4.12)

Due to the generic choice of a, b, c the function  $\Phi$  is multi-valued on  $X = \mathbb{P}_{\mathbb{C}} - \{0, 1, \lambda, \infty\}$  and  $\varphi$  is a single-valued and holomorphic form on X. In this example, the connection of eq. (4.3) is defined with

$$\omega_{\Phi} = d_{\text{int}} \log \Phi = \frac{b - cz}{z(1 - z)} + \frac{a}{\lambda - z}. \tag{4.13}$$

# 4.1.1 Review: Twisted (Co-)homology

Here, we follow mostly the notion of twisted cohomology from [228–230] as commonly done in the physics community [39, 44]. Within the current subsection, we restrict the exponents in the twist of eq. (4.2) by the condition

$$\alpha_i \notin \mathbb{Z}$$
 and  $\sum_{i=0}^r \alpha_i \notin \mathbb{Z}$ . (4.14)

In that case,  $\varphi$  is a single-valued, holomorphic form on the space

$$X = \mathbb{P}_{\mathbb{C}}^{n} - \Sigma \text{ where } \Sigma = \bigcup_{i=1}^{r} \Sigma_{i} = \bigcup_{i=1}^{r} \{ \boldsymbol{z} | L_{i}(\boldsymbol{z}) = 0 \}.$$
 (4.15)

We call the components  $\Sigma_i$  the regulated boundaries. X needs not be the punctured Riemann sphere, one could just as well consider twisted cohomology on other varieties, as it was for example done in [6], but the examples we consider here are covered by the choice of eq. (4.15).

#### Twisted (Co-)Homology Groups and Their Pairings

One can understand twisted (co-)homology groups using what we know about standard (co-)homology groups from Section 3.1 but replacing the exterior derivative d with the connection  $\nabla_{\Phi}$ . In particular, that means that we also consider the notions of closed ( $\nabla_{\Phi}\varphi = 0$ ) and exact ( $\varphi = \nabla_{\Phi}\tilde{\varphi}$ ) with respect to this connection  $\nabla_{\Phi}$ . Here, we elaborate the consequences of this in detail.

We are still primarily interested in integrals of the form eq. (4.1) – here with the restriction of eq. (4.14) – and we work modulo differentials that vanish upon integration. Consequently, we want to work modulo exact forms and to that end define an equivalence relation  $\varphi + \nabla \tilde{\varphi}^{4}$  That means, we want to consider differentials from a twisted de-Rham cohomology group:

**Definition 4.1** (Twisted de Rham Cohomology Group). The twisted version of a de Rham cohomology group is defined as

$$H_{dR}^{k}(X, \nabla_{\Phi}) = C^{k}(X, \nabla_{\Phi})/B^{k}(X, \nabla_{\Phi}), \qquad (4.16)$$

with

$$C^{k}(X, \nabla_{\Phi}) = \{k - forms \varphi \ on \ X \mid \nabla_{\Phi}\varphi = 0\}, \qquad (4.17)$$

$$B^{k}(X, \nabla_{\Phi}) = \{k - forms \ \nabla_{\Phi} \tilde{\varphi} \mid \tilde{\varphi} \ a \ k - 1 \text{-} form\}.$$
 (4.18)

All twisted cohomology groups we consider here are finite-dimensional and specifically [231]:

$$\sum_{k=0}^{2n} (-1)^k \dim \left[ \mathcal{H}^k_{\mathrm{dR}} \left( \mathbf{X}, \nabla_{\Phi} \right) \right] = \chi(X) , \qquad (4.19)$$

<sup>4</sup>This is equivalent to the approach of working modulo IBP relations in the context of Feynman integrals [40]. where  $\chi(X)$  is the Euler number of the underlying space, see Definition A.8. Practically, one can obtain the dimension of a given cohomology group  $H^k_{dR}(X, \nabla_{\Phi})$  by counting the critical points of  $d_{int} \log \Phi$ . For n=1 this can be done by computing the number of solutions of  $d_{int} \log \Phi = 0$ . For n > 1, the dimension can be found iteratively [232]. In fact, only the middle cohomology group  $H^n_{dR}(X, \nabla_{\Phi})$  is non-zero [231]. Thus, we only consider k=n. The elements of  $C^n(X, \nabla)$  are called twisted co-cycles. In a similar way, we consider closed modulo exact contours. That means we consider contours that are taken from equivalence classes of so-called twisted cycles (or loaded cycles) in

$$C_{n}(X, \check{\mathcal{L}}_{\Phi}) = \{ \gamma = \Delta_{\gamma}^{c} \otimes \Phi|_{\Delta_{\gamma}^{c}} \mid \Delta_{\gamma}^{c} \text{ an } n - \text{cycle and } \partial(\gamma \otimes \Phi|_{\gamma}) = 0 \}.$$
 (4.20)

We denote these cycles by<sup>5</sup>

$$\gamma = \Delta_{\gamma}^{c} \otimes \Phi|_{\gamma} = \sum_{\Delta}^{\text{finite}} a_{\Delta} \Delta \otimes \Phi|_{\Delta}. \tag{4.21}$$

Here,  $\Delta_{\gamma}^{c}$  is a compactified topological n-cycle that can be decomposed into a finite number of simplices embedded in X – denoted by  $\Delta$  – with coefficients  $a_{\Delta} \in \mathbb{R}$ . They always come with a branch choice of  $\Phi|_{\Delta}$  (loaded onto  $\Delta$ ). Practically, this means that every twisted cycle comes with a local choice of branch for  $\Phi$ . This branch is taken from the local system  $\check{\mathcal{L}}_{\Phi}$ . The operation  $\partial(\Delta_{\gamma}^{c}\otimes\Phi|_{\gamma})$  restricts both the contour and the branch of  $\Phi$  to the boundary (of the contour). We denote the space of boundaries by

$$B_{n}(X, \check{\mathcal{L}}) = \{ \text{twisted } n - \text{cycles } \partial \gamma \, | \, \gamma = \Delta_{\gamma}^{c} \otimes \Phi|_{\Delta_{\gamma}} \text{ with } (n+1) \text{-cycles } \Delta_{\gamma}^{c} \}$$

$$(4.22)$$

and define the twisted homology group:

**Definition 4.2** (Twisted Homology Group). The twisted version of a Betti homology group is defined as

$$H_n(X, \check{\mathcal{L}}_{\Phi}) = C_n(X, \check{\mathcal{L}}_{\Phi}) / B_n(X, \check{\mathcal{L}}_{\Phi}). \tag{4.23}$$

In some contexts, we put the twisted cycles and co-cycles into brackets, denoting by  $\langle \varphi |$  the twisted co-cycle and by  $|\gamma|$  the twisted cycle. These brackets already hint at a vector space structure and pairings between the objects, the first of which we define promptly:

**Definition 4.3** (Period Pairing). The period pairing pairs twisted cycles and cocycles via integration. The periods evaluate to integrals such as the one in eq. (4.1):

$$\langle \cdot | \cdot | : H_n(X, \check{\mathcal{L}}_{\Phi}) \times H^n_{dR}(X, \nabla_{\Phi}) \to \mathbb{C}$$
 (4.24)

$$\langle \gamma | \varphi ] = \int_{\gamma} \Phi \varphi \,. \tag{4.25}$$

<sup>5</sup>Note that including only a finite number of simplices is a *choice* and serves as a regularisation. We comment on this in more details below when defining also the dual twisted homology group as well as in the appendix R

Applying this pairing to basis elements  $\gamma_i$  of  $H_n(X, \check{\mathcal{L}}_{\Phi})$  and  $\varphi_j$  of  $H^n_{dR}(X, \nabla_{\Phi})$ , we obtain the period matrix  $\mathbf{P}$ :

**Definition 4.4** (Twisted Period Matrix). The entries of the twisted period matrix **P** are

$$P_{ij} = \langle \varphi_i | \gamma_j ] = \int_{\gamma_j} \Phi \varphi_i . \tag{4.26}$$

For all objects introduced up to here – specifically the twisted (co-)homology groups and periods – one can define dual<sup>6</sup> versions. In principle,<sup>7</sup> one can think of these as elements of the twisted (co-)homology groups with the inverse twist  $\Phi^{-1}$  or equivalently, with the connection  $\check{\nabla}_{\Phi}$ . Practically, the pairings that define the dualities require that at least one of the two objects that are paired is regularised, since we always want to pair two elements with at least one of them being compactly supported so that the pairings are well-defined. Implicitly, we already defined the twisted cycles to be regularised by taking only finite linear combinations of simplices, so the dual twisted cycles do not need to be compactly supported in our conventions.

**Definition 4.5** (Dual Twisted Homology Group). The (locally-finite) dual twisted homology group is defined by

$$H_n^{lf}(X, \mathcal{L}_{\Phi}) = \{ \check{\eta} = \Delta_{\check{\eta}} \otimes \Phi^{-1}|_{\check{\eta}} \mid \Delta_{\check{\eta}} \text{ locally finite}, \ \partial \check{\eta} = 0 \} / \{ \text{boundaries } \partial \tilde{\eta} \},$$

$$(4.27)$$

with the elements  $\check{\eta}$  taking the form

$$\Delta_{\check{\eta}} \otimes \Phi|_{\check{\eta}}^{-1} = \sum_{\square}^{locally finite} b_{\square} \square \otimes \Phi^{-1}|_{\square}, \qquad (4.28)$$

where the  $\square$  are embeddings of simplices and  $b_{\square} \in \mathbb{R}$ .

In general<sup>8</sup>, these locally finite dual cycles are generated by a set of bounded chambers – specifically for linear factors  $L_i(z)$  – whose boundaries are the zero loci of the factors  $L_i(z)$  of the twist  $\Phi$ . Often, we deform the chambers, so that they lie in X and do not intersect points lying outside of X. Their regularised versions generate the cycles of the twisted homology group in 4.23 and they are obtained by taking tubings around the boundaries. Note that the particular feature of restricting with eq. (4.14) allows us to take in principle the same basis choice for the homology group and its dual, albeit one of them being regularised. In that case, we denote both bases by the letter  $\gamma_i$ , distinguishing the contour  $\Delta_{\tilde{\gamma}_i}$  from its regularised version  $\Delta \gamma_i$ .

**Example 4.3** (Twisted Homology Bases for Twist with Only Linear Factors in 1D). We consider here as a simple example the univariate case with a twist built from r+1 linear factors of the form  $L_i(x) = (\lambda_i - x)$ . The zero loci of these linear

<sup>6</sup>In particular, the duality is facilitated by the intersection pairings.

<sup>7</sup>As long as there are no poles to regularise and one needs to be even more careful.

<sup>8</sup>Though, keeping in mind that throughout this discussion the restriction of eq. (4.14) holds.

See also:

This become more clear in the examples, with the first one being Example 4.3.

equations simply define a set of points  $\Sigma = \{\lambda_i \mid 0 \leq i \leq r\}$  that we assume to be ordered  $\lambda_i < \lambda_j$  for i < j and real. In this situation, a basis of locally-finite dual cycles can be chosen to be supported on r independent open intervals between these points  $\lambda_i$ . Two examples for natural choices of this basis are

$$\check{\gamma}_j = \Delta_{\check{\gamma}_j} \otimes \Phi^{-1}|_{\check{\gamma}_j} \text{ with } \Delta_{\check{\gamma}_j} = (0, \lambda_j) \text{ for } j = 1, \dots, r$$

$$(4.29)$$



Figure 4.1: The dual cycle  $\check{\gamma}_j$  of eq. (4.29) is supported on the interval  $(0, \lambda_j)$  as illustrated here.

and

$$\check{\eta}_j = \Delta_{\check{\eta}_j} \otimes \Phi^{-1}|_{\check{\eta}_j} \text{ with } \Delta_{\check{\eta}_j} = (\lambda_{j-1}, \lambda_j), \text{ for } j = 1, \dots, r.$$
 (4.30)



Figure 4.2: The dual cycle  $\check{\eta}_j$  of eq. (4.30) is supported on the interval  $(\lambda_{j-1}, \lambda_j)$  as illustrated here.

These choices<sup>9</sup> are depicted with their orientations in figures 4.1 and 4.2. The intervals are deformed into the lower half-plane so that they do not intersect the other punctures  $\lambda_i$  that are taken out of X. This amounts to analytically continuing the twist on the lower-half plane and is equivalent to choosing the following branch for each factor locally:

<sup>9</sup>Note that we here generally write intervals (x, y) and mean the deformed path from x to y that lies in X.

$$\arg[L_{j}(z)] = \begin{cases} 0 & \text{if } 1 \leq j \leq k \\ -\pi & \text{if } k+1 \leq j \leq m \end{cases} \text{ on the interval } (\lambda_{k}, \lambda_{k+1}). \tag{4.31}$$

For the (non-dual) twisted cycles we need to construct the compactly supported version  $\Delta_{\gamma}^{c}$  of the topological cycles  $\Delta_{\tilde{\gamma}}$ . In particular, the regularised versions of the dual twisted cycles  $\tilde{\gamma}_{j}$  are <sup>10</sup>

The factors  $\mathfrak{d}_i$  and  $\mathfrak{c}_i$  are defined by:  $\mathfrak{c}_j = \exp(2\pi i \alpha_j)$   $\mathfrak{d}_j = \mathfrak{c}_j - 1$ as in eq. (B.20).

$$\gamma_{j} = \Delta_{\gamma_{j}}^{c} \otimes \Phi|_{\Delta_{\gamma_{j}}^{c}} = \frac{S_{\epsilon}(0)}{\mathfrak{d}_{0}} \otimes \Phi|_{S_{\epsilon}(0)} + (\epsilon, \lambda_{j} - \epsilon) \otimes \Phi|_{(0+\epsilon, \lambda_{j} - \epsilon)} - \frac{S_{\epsilon}(\lambda_{j})}{\mathfrak{d}_{j}} \otimes \Phi|_{S_{\epsilon}(\lambda_{j})}.$$

$$(4.32)$$

Their support is depicted in figure 4.3.

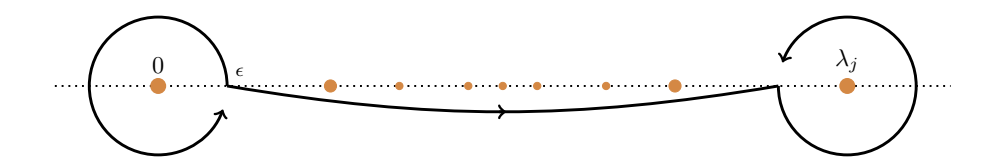


Figure 4.3: The cycle  $\gamma_j$  of eq. (4.32) is supported on a regularised version of the interval  $(0, \lambda_i)$  as illustrated here.

The  $S_{\epsilon}(x)$  are oriented positively (anti-clockwise)  $\varepsilon$ -circles around x and the branches are chosen by analytically continuation along these circles, taking into account the branch choices of eq. (4.31). The boundary of these cycles vanishes due to the normalising factors  $\mathfrak{d}_i$ :

$$\partial \left( \Delta_{\gamma_j}^c \otimes \Phi |_{\Delta_{\gamma_j}^c} \right) = \frac{\epsilon}{\mathfrak{d}_0} \left( \mathfrak{c}_0 - 1 \right) + \left( \lambda_j - \epsilon - \epsilon \right) - \frac{\lambda_j - \epsilon}{\mathfrak{d}_j} \left( \mathfrak{c}_j - 1 \right) = 0. \tag{4.33}$$

For multi-variable cases, the intervals are replaced with multi-dimensional chambers and the regularisation can be obtained similarly.

In some contexts, we denote the dual twisted cycles by  $|\check{\eta}|$ , in particular, when they are part of a pairing. The intersection pairing between a twisted cycle  $\gamma$  and a dual twisted cycle  $\check{\xi}$  – which we denote by  $[\cdot|\cdot]$  – counts the (topological) intersections of the two cycles, taking into account their orientations as well as the branch choices for  $\Phi$  and  $\Phi^{-1}$  loaded onto them at each of the intersecting points. More details on their computation are given in appendix B or can be found in refs. [36, 228, 233].

**Definition 4.6** (Homology Intersection Matrix **H**). If  $\{\beta_1, \beta_2, ...\}$  is a basis of the homology group  $H_n(X, \check{\mathcal{L}}_{\Phi})$  and  $\{\check{\alpha}_1, \check{\alpha}_2, ...\}$  is a basis of a dual homology group  $H_n(X, \mathcal{L}_{\Phi})$ , the intersection matrix **H** for these bases has the entries

$$H_{ij} = \left[\check{\alpha}_j | \beta_i\right]. \tag{4.34}$$

Let us turn our attention to the dual differentials, i.e. the co-cycles in the dual cohomology group. We regularise the elements of the dual twisted cohomology group, which is:

$$H_{dR,c}^{n}\left(X,\check{\nabla}_{\Phi}\right) = \left\{\text{compactly supported } n - \text{forms } \check{\varphi} \mid \check{\nabla}_{\Phi} \, \check{\varphi} = 0\right\} / \left\{\text{exact forms}\right\}. \tag{4.35}$$

Since in general X is not compact and the forms  $\varphi \in H^k_{dR}(X, \nabla_{\Phi})$ , compactified dual co-cycles  $\check{\chi}$  are necessary, so that the intersection pairing

$$\langle \varphi | \check{\chi} \rangle = \int_X \varphi \wedge \check{\chi} \tag{4.36}$$

is well-defined. Note that within this pairing and in related contexts, we often denote the dual co-cycles by  $|\check{\chi}\rangle$ . Due to the restriction in eq. (4.14), we can use a compactified version of the twisted cohomology basis for the dual twisted cohomology basis. These compactified differentials are denoted by  $\check{\varphi}_c$ , but often we omit the label c explicitly as the dual differentials are always compactified.<sup>11</sup>

<sup>&</sup>lt;sup>11</sup>This particular feature is important for the results of Chapter 5.

**Definition 4.7** (Cohomology intersection matrix **H**). Given bases  $\varphi_i$  and  $\check{\chi}_{d,j}$  of the twisted cohomology and its compactified dual, we define the cohomology intersection matrix **C** with entries

$$C_{ij} = \frac{1}{(2\pi i)^n} \langle \varphi_i | \check{\chi}_j \rangle. \tag{4.37}$$

We explain an algorithm for computing intersection numbers in Appendix B. Additionally, we define the dual period matrix:

**Definition 4.8** (Dual Period Matrix). The dual period matrix is the matrix  $\dot{\mathbf{P}}$  with entries

$$\check{P}_{ij} = [\check{\gamma}_j | \check{\varphi}_i \rangle = \int_{\check{\gamma}_j} \Phi^{-1} \check{\varphi}_i \,. \tag{4.38}$$

Thus, we have reviewed pairings between all four twisted (co-)homology groups. Applied on bases of these spaces, the resulting matrices are all non-degenerate, i.e. have full rank. Poincaré duality implies the isomorphisms [231]:

$$H_{dR}^k(X, \nabla_{\Phi}) \cong H_{2n-k}^{lf}(X, \mathcal{L}_{\Phi}) \text{ and } H_{dR,c}^k(X, \check{\nabla}_{\Phi}) \cong H_{2n-k}(X, \check{\mathcal{L}}_{\Phi}).$$
 (4.39)

We summarise the groups and the pairings that facilitate the dualities in figure 4.4.

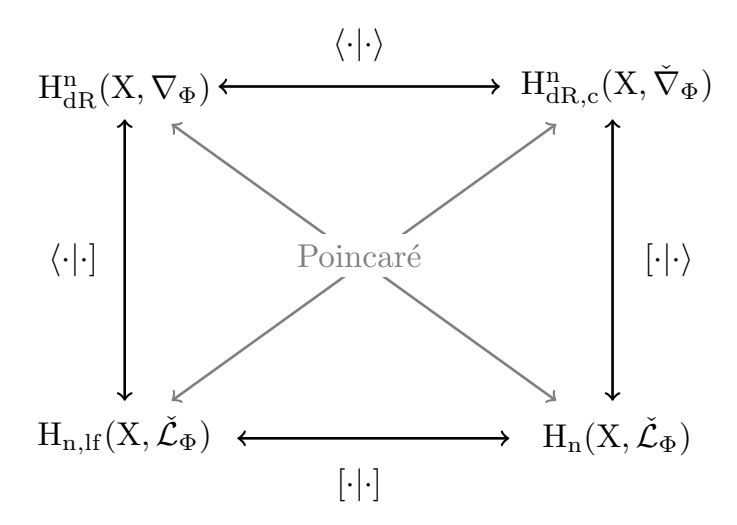


Figure 4.4: There are four twisted (co-)homology groups we can associate to a space X and a twist  $\Phi$  and for each pair of them we can associate a pairing.

We illustrate these objects and pairings with two simple examples.

**Example 4.4** (Euler  $\beta$  function: (Co-)Homology Groups and Their Bases). This example is a continuation of example 4.1. Here, we assume that 0 < a, b < 1 are non-integer. The (co-)homology groups defined by the twist  $\Phi$  of eq. (4.7) on the space  $X = \mathbb{C} - \{0, 1, \infty\}$  are one-dimensional. We choose for  $H^1_{dR}(X, \nabla_{\Phi})$  the basis

If a > 1 or b > 1, we just split the respective parameter into an integer part and a non-integer part that is smaller than one and takes the role of the a, b in this example.

element  $\varphi = \frac{dx}{x(1-x)}$ . We can choose the same representation for the basis of the dual cohomology group  $H^1_{dR}(X, \check{\nabla_{\Phi}})$ . The corresponding intersection matrix is

$$\mathbf{C} = (\langle \varphi | \check{\varphi} \rangle) = \left(\frac{a+b}{ab}\right). \tag{4.40}$$

The homology group  $H_1(X, \check{\mathcal{L}}_{\Phi})$  is spanned by  $\gamma = \Delta_{\gamma}^c \otimes \Phi_{\Delta_{\gamma}}$ , where  $\Delta_{\gamma}^c$  is the regularised version of the interval  $\Delta_{\tilde{\gamma}} = (0,1)$  – with the regularisation as in eq. (4.32). For the dual homology group we choose this interval to be the support of the single basis element. The corresponding homology intersection matrix is

$$\mathbf{H} = ([\check{\gamma}|\gamma]) = \left(-\frac{\exp(\pi i a) \exp(2\pi i b) - 1}{(\exp(2\pi i a - 1) (\exp(2\pi i b) - 1))}\right) \tag{4.41}$$

$$= -\frac{1}{2\pi i} \left( \frac{\Gamma(1-a)\Gamma(a)\Gamma(1-b)\Gamma(b)}{\Gamma(1-a-b)\Gamma(a+b)} \right). \tag{4.42}$$

The period matrix is

$$\mathbf{P} = (\langle \varphi | \gamma]) = (\beta(a, b)) \tag{4.43}$$

and the dual period matrix is  $\check{\mathbf{P}} = \mathbf{P}|_{\{a,b\} \to -\{a,b\}}$ .

**Example 4.5** ( ${}_2F_1$  function: (Co-)homology Groups and Their Bases). We continue with the conventions of Example 4.2, assuming that  $a, b, c, c - a \notin \mathbb{Z}$ . For the dual homology, we choose a basis with supports  $\Delta_{\tilde{\gamma}_1} = (\lambda, \infty)$  and  $\Delta_{\tilde{\gamma}_2} = (0, 1)$ . These are depicted in figure 4.5.



Figure 4.5: The basis elements  $\check{\gamma}_1$  and  $\check{\gamma}_2$  of the dual homology group  $H_1(X, \mathcal{L}_{\Phi})$  are supported on the intervals  $(\lambda, \infty)$  and (0, 1).

For the homology group  $H_1(X, \check{\mathcal{L}}_{\Phi})$  we choose a basis supported on the regularised versions of these intervals. The homology intersection matrix is

$$\mathbf{H}(\lambda) = \begin{pmatrix} \frac{i}{2} \csc[a\pi] \csc[(a-c)\pi] \sin[c\pi] & 0\\ 0 & -\frac{i}{2} \csc[b\pi] \csc[(b-c)\pi] \sin[c\pi] \end{pmatrix}.$$
(4.44)

One can choose a standard d log basis for  $H^1_{dR}(X, \nabla_{\Phi})$ :

$$\chi_1 = d \log \left( \frac{z}{1-z} \right) = \frac{dz}{z(1-z)} \text{ and } \chi_2 = d \log \left( \frac{z}{z-\lambda} \right) = \frac{\lambda dz}{z(z-\lambda)}.$$
(4.45)

See also:

We use the bases  $\chi, \tilde{\chi}$  in Example 4.10, whereas we use the bases  $\varphi, \tilde{\varphi}$  in Section 6.1.2.

The dual cohomology group  $H^1_{dR}(X, \check{\nabla}_{\Phi})$  is generated by the same basis  $\check{\chi}_i = \chi_i$ . Another basis choice is

$$\varphi_1 = \mathrm{d}z \ and \ \varphi_2 = z\mathrm{d}z \tag{4.46}$$

and

$$\check{\varphi}_1 = \left[\frac{\varphi_1}{z(1-z)(z-\lambda)}\right]_c \text{ and } \check{\varphi}_2 = \left[\frac{\varphi_2}{z(1-z)(z-\lambda)}\right]_c. \tag{4.47}$$

Explicitly, the cohomology intersection matrices are:

$$\mathbf{C}_{\chi}(\lambda) = \begin{pmatrix} -\frac{c}{b(b-c)} & \frac{1}{b} \\ \frac{1}{b} & \frac{a-b}{ab} \end{pmatrix} \quad and \quad \mathbf{C}_{\varphi}(\lambda) = \begin{pmatrix} 0 & \frac{1}{1-a+c} \\ \frac{1}{2-a+c} & \frac{1-a+b+\lambda(1+c)}{(1-a+c)(2-a+c)} \end{pmatrix}$$
(4.48)

The period matrix in the  $\varphi$  basis is

$$P_{11}^{\varphi}(\lambda) = e^{i\pi(c-b)}\lambda^{1-a+c}{}_{2}\mathcal{F}_{1}\left(b-c, a-c-1, -c; \lambda^{-1}\right)$$
(4.49)

$$P_{12}^{\varphi}(\lambda) = e^{-i\pi a} \lambda^{-a} {}_{2}\mathcal{F}_{1}\left(1 + b, a, 2 + c; \lambda^{-1}\right)$$
(4.50)

$$P_{21}^{\varphi}(\lambda) = e^{i\pi(c-b)}\lambda^{2+c-a}{}_{2}\mathcal{F}_{1}\left(b-c, a-2-c, -1-c; \lambda^{-1}\right)$$
(4.51)

$$P_{22}^{\varphi}(\lambda) = e^{-i\pi a} \lambda^{-a} {}_{2}\mathcal{F}_{1}\left(2+b,a,3+c;\lambda^{-1}\right). \tag{4.52}$$

The dual period matrix can be obtained by mapping  $a \to -a+1, b \to -b-1, c \to -c-1$  in the period matrix entries. These shifts invert the twist and adjust for the different choice of dual basis and basis. Note that for a twist

$$\Phi = z^{-\frac{1}{2} + a_1 \varepsilon} (1 - z)^{-\frac{1}{2} + a_2 \varepsilon} (z - \lambda)^{-\frac{1}{2} + a_3 \varepsilon}$$
(4.53)

that shift simply amounts to  $\varepsilon \to -\varepsilon$  and consequently, as a function of  $\varepsilon$ :  $\check{\mathbf{P}}(\varepsilon) = \mathbf{P}(-\varepsilon)$ . We motivate why choices such as this one lead to particular intersection matrices in Chapter 5. The period matrix in the basis  $\chi$  can also be expressed in hypergeometric  ${}_2F_1$  functions and we do not explicitly state it here. The corresponding dual period matrix in the basis  $\check{\chi}$  can be obtained by mapping  $(a,b,c) \to -(a,b,c)$ . Explicitly:

$$\check{\mathbf{P}}_{\chi}(a,b,c) = \mathbf{P}_{\chi}(-a,-b,-c). \tag{4.54}$$

#### Twisted Riemann Bilinear Relations

There are *completeness relations* for the homology and the cohomology basis respectively:

$$(2\pi i)^{-n} |\check{\varphi}_i\rangle(\boldsymbol{C}^{-1})_{ij}\langle\varphi_j| = \mathbf{1} \text{ and } |\gamma_i|(\boldsymbol{H}^{-1})_{ji}[\check{\gamma}_j| = \mathbf{1}.$$
 (4.55)

These completeness relations can be used to decompose period integrals in the co-cycles or cycles respectively:

$$\langle \varphi | \gamma \rangle = (2\pi i)^{-n} \sum_{j=1}^{d} \langle \varphi | \varphi_i \rangle \left( \mathbf{C}^{-1} \right)_{ij} \langle \varphi_j | \gamma \rangle$$
(4.56)

#### See also:

Note that we spell out the calculation of the cohomology intersection matrix in Example B.1 and of the homology intersection matrix in Subsection B.1.2 of Appendix B.

#### See also:

More examples can be found, e.g., in:
bullet Examples 5.2 & 5.3
bullet Section 6.1.3 & 6.1.4
bullet Appendix B.2

# $\langle \varphi | \gamma \rangle = \sum_{j=1}^{d} \langle \varphi | \gamma_i \rangle \left( \mathbf{H}^{-1} \right)_{ji} \left[ \gamma_j | \gamma \right]. \tag{4.57}$

See also:

In Section 5 we discuss what one can learn from the twisted Riemann bilinear relations about (maximal cuts of) Feynman integrals.

By inserting a completeness relation into the homology and cohomology intersection pairing one obtains the twisted Riemann bilinear relations [230]:

$$\frac{1}{(2\pi i)^n} \mathbf{P} \left( \mathbf{H}^{-1} \right)^T \check{\mathbf{P}}^T = \mathbf{C} \,, \tag{4.58}$$

$$\frac{1}{(2\pi i)^n} \mathbf{P}^T \left( \mathbf{C}^{-1} \right)^T \check{\mathbf{P}} = \mathbf{H}. \tag{4.59}$$

**Example 4.6** ( $_2F_1$  function: Twisted Riemann Bilinear Relations). We continue the discussion of the hypergeometric  $_2F_1$  function of Examples 4.2 and 4.5. The Riemann bilinear relations in that example are bilinear relations between hypergeometric  $_2F_1$  functions. An example for such a relation obtained with the basis eq. (4.46) is:

$$(a-c-2)_{2}\mathcal{F}_{1}\left(1-b,1-a,1-c;\lambda^{-1}\right)_{2}\mathcal{F}_{1}\left(-b,1-a,-c;\lambda^{-1}\right) + (a-1-c)_{2}\mathcal{F}_{1}\left(1+b,a,2+c;\lambda^{-1}\right)_{2}\mathcal{F}_{1}\left(1-b,1-a,1-c;\lambda^{-1}\right) + (1-a+b+\lambda(1+c))_{2}\mathcal{F}_{1}\left(-b,1-a,-c;\lambda^{-1}\right)_{2}\mathcal{F}_{1}\left(-b,1-a,-c;\lambda^{-1}\right) = 0$$

$$(4.60)$$

Note that for specific parameter choices, these relations can become quadratic. Generally, they reduce to known relations for this class of functions.

#### **Differential Equations**

Generally, the differentials in the period integrals depend on some parameters  $\lambda$ . In applications in physics these are the physical parameters, such as the masses and momenta. As outlined in Section 2.5, we use differential equations with respect to these parameters to compute Feynman integrals. The differential equations can also be derived using the cohomology intersection numbers. The period matrix  $\mathbf{P}(\lambda)$  and the dual period matrix  $\check{\mathbf{P}}(\lambda)$  as functions of the *physical* parameters are the fundamental solutions of the differential equations

$$d_{\text{ext}} \mathbf{P}(\lambda) = \mathbf{A}(\lambda) \mathbf{P}(\lambda), \qquad (4.61)$$

$$d_{ext}\check{\mathbf{P}}(\lambda) = \mathbf{C}(\lambda)\check{\mathbf{P}}(\lambda). \tag{4.62}$$

Similarly, the intersection matrix C is the unique – up to constant prefactors – rational solution of the differential equation [234–237]

$$d_{\text{ext}}\mathbf{C}(\lambda) = \mathbf{A}(\lambda)\mathbf{C}(\lambda) + \mathbf{C}(\lambda)\dot{\mathbf{A}}(\lambda)^{T}.$$
 (4.63)

The connection matrix  $\mathbf{A}(\lambda)$  for the differential equation for a basis of differentials  $\varphi_i$  can also be computed from intersection numbers<sup>12</sup>:

$$A_{i,k} = \frac{1}{(2\pi i)^n} \sum_{l,k} \langle \eta_i | \check{\chi}_l \rangle \left( \mathbf{C}(\boldsymbol{\lambda}, \boldsymbol{\alpha})^{-1} \right)_{lk}$$
 (4.64)

<sup>12</sup>As in eq. (4.37), we use  $C_{ij}(\boldsymbol{\lambda}, \boldsymbol{\alpha}) = \frac{1}{(2\pi i)^n} \langle \varphi_i | \check{\chi}_j \rangle.$ 

with the  $\check{\chi}_l$  being elements of some dual basis and

$$\eta_i = d_{\text{ext}}\varphi_i + d_{\text{ext}}\log\Phi \wedge \varphi_i. \tag{4.65}$$

C is the intersection matrix between the two bases  $\varphi$  and  $\check{\chi}$ .

**Example 4.7** ( $_2F_1$  function: Differential Equations). We continue in the conventions of Examples 4.2, 4.5 and 4.6 and compute the connection matrix for the period matrix defined with the basis  $\varphi$  of eq. (4.46) using eq. (4.64):

$$d\mathbf{P}^{\varphi}(\lambda) = \mathbf{A}^{\varphi}(\lambda)\mathbf{P}^{\varphi}(\lambda) \text{ with } \mathbf{A} = \begin{pmatrix} \frac{1-a+b-a\lambda}{\lambda(1-\lambda)} & \frac{2-a+c}{\lambda(\lambda-1)} \\ \frac{1+b}{1-\lambda} & \frac{2-a+c}{\lambda-1} \end{pmatrix}.$$
(4.66)

d log bases: For specific basis choices, we can deduce additional properties and symmetries of the connection matrix. We do so specifically for so-called d log bases. A common basis choice for the homology group are chambers bounded by the hypersurfaces defined by the zeroes of the factors  $L_i(z)$  in the twist, as discussed, e.g., in Example 4.3. The analogous basis choice for the differentials is a d log basis. The defining property of this basis is, that it has only d log singularities and these are located only on the boundaries of the hypersurfaces. While such a d log basis is expected to exist quite generally, explicit constructions are only known in cases where at most one of the factors  $L_i(z)^{13}$  of the twist is a polynomial of degree larger than one and the remaining factors define hyperplanes [40]. For instance, if  $\Sigma$  is a union of linear hyperplanes only, it is possible to choose a dlog basis of the form

$$\varphi_I = \operatorname{dlog}\left(\frac{L_{i_0}}{L_{i_1}}\right) \wedge \operatorname{dlog}\left(\frac{L_{i_1}}{L_{i_2}}\right) \wedge \dots \wedge \operatorname{dlog}\left(\frac{L_{i_{h-1}}}{L_{i_h}}\right),$$
(4.67)

where  $I = (i_0, i_1, \dots, i_h)$  [231]. For bases of this form, the following theorem holds [50]:

**Theorem 4.1.** We consider a twisted cohomology group with twist

$$\Phi = \prod_{k=1}^{r} L_k(\boldsymbol{z})^{a_k \mu}, \qquad a_k \in \mathbb{Q},$$
(4.68)

where  $\mu$  is a formal variable, and assume that the period matrix  $\mathbf{P}(\lambda, \mu)$  is defined from a d log basis as in eq. (4.67) such that it satisfies the differential equation

$$d_{\text{ext}} \mathbf{P}(\lambda, \mu) = \mathbf{A}(\lambda, \mu) \mathbf{P}(\lambda, \mu)$$
(4.69)

with respect to the variables  $\lambda$ . Then the connection matrix takes the form

$$\mathbf{A}(\lambda, \mu) = \mu \, \mathbf{B}(\lambda) \,. \tag{4.70}$$

Moreover, it is possible to pick d log bases such that  $\mathbf{B}(\lambda) = \mathbf{B}(\lambda)^T$  is a symmetric matrix.

<sup>13</sup>Below we repeatedly shorten these to  $L_i := L_i(z)$ .

#### See also:

We gave an example for a d log basis in eq. (4.45).

*Proof.* We prove the  $\mu$ -dependence and the symmetry separately, following the proof already given in [50].

#### $\mu$ -dependence

We choose a d log basis  $\varphi_I$  as specified in eq. (4.67), along with a corresponding dual basis  $\check{\varphi}_I = [\varphi_I]_c$ . The matrix  $\mathbf{A}(\lambda, \mu)$  can be computed in terms of intersection numbers from eq. (4.64). Our first goal is to see that the dependence of  $\mathbf{A}(\lambda, \mu)$  on  $\mu$  is as given in eq. (4.70) and we do so by analysing the  $\mu$ -dependence of the intersection numbers used to compute  $\mathbf{A}(\lambda, \mu)$ :

• Given that we use a d log basis, a result from ref. [238] (see Theorem B.1 in Appendix B.3) implies that

$$C_{KL}(\boldsymbol{\lambda}, \mu) = \frac{1}{(2\pi i)^n} \langle \varphi_K | \check{\varphi}_L \rangle = \frac{1}{\mu^n} a_{KL}, \qquad (4.71)$$

for some rational numbers  $a_{KL}$ . Equivalently

$$\mathbf{C}(\lambda,\mu) = \frac{1}{\mu^n} \widetilde{\mathbf{C}} \,, \tag{4.72}$$

where  $\widetilde{\mathbf{C}}$  is a constant matrix.

• In appendix B.3 we prove that for  $\eta_I$  as in eq. (4.65):

$$\langle \eta_I | \check{\varphi}_L \rangle = \frac{(2\pi i)^n}{\mu^{n-1}} \, \tilde{a}_{IL}(\boldsymbol{\lambda}) \,,$$
 (4.73)

for some constants  $\tilde{a}_{IL}$  in  $\mu$ .

Thus, we find that the entries of  $\mathbf{A}(\lambda, \mu)$  as computed from eq. (4.64) are linear in  $\mu$ :

$$\mathbf{A}(\lambda, \mu) = \mu \, \widetilde{\mathbf{A}}(\lambda) \widetilde{\mathbf{C}}^{-1} \,, \tag{4.74}$$

with  $\tilde{\mathbf{A}}$  a matrix that is constant in  $\mu$ .

## Symmetry

Note that it is always possible to select a d log basis  $\varphi_I$  such that the matrix  $\mathbf{C}(\lambda,\mu)$ , is diagonal. If  $\mathbf{C}(\lambda,\mu)$  is not diagonal in some basis  $\varphi_I$ , we can transform to an orthogonal basis with entries  $\tilde{\varphi}_I$  using the Gram-Schmidt procedure<sup>14</sup>:

$$\tilde{\varphi}_I = \varphi_I - \sum_{J=1}^{I-1} \frac{\langle \tilde{\varphi}_J | \check{\varphi}_I \rangle}{\langle \tilde{\varphi}_J | \check{\tilde{\varphi}}_J \rangle} \tilde{\varphi}_J, \qquad I = 1, \dots, M,$$
(4.75)

and we have  $\langle \tilde{\varphi}_I | \check{\tilde{\varphi}}_J \rangle = 0$  for  $I \neq J$ . Let us write the change of basis from  $\varphi_I$  to  $\tilde{\varphi}_I$  as

$$\tilde{\varphi}_I = \sum_{J=1}^M U_{IJ} \varphi_J \,, \tag{4.76}$$

<sup>14</sup>The Gram-Schmidt algorithm can be used since the cohomology intersection pairing is symmetric and non-degenerate for our specific choice of bases.

transforming the dual basis in the same way. A priori, the transformation matrix  $\mathbf{U}$  depends on  $\boldsymbol{\lambda}$  and  $\mu$ . However, from eq. (4.75) we know (inductively) that the entries of  $\mathbf{B}$  are built from ratios of intersection numbers of the form  $\langle \varphi_I | \check{\varphi}_J \rangle$ . It follows from eq. (4.71) that these ratios, and therefore the entries of the matrix  $\mathbf{U}$ , are constant in  $\mu$ . The matrix of intersection numbers in this basis is

$$\mathbf{UC}(\lambda, \varepsilon)\mathbf{U}^T = \mu^{-n} \mathbf{U\widetilde{C}}\mathbf{U}^T = \mu^{-n} \operatorname{diag}(c_1, \dots, c_M),$$
 (4.77)

with the constants  $c_I$  given by

$$c_I = (2\pi i)^{-n} \mu^n \langle \tilde{\varphi}_I | \dot{\tilde{\varphi}}_I \rangle . \tag{4.78}$$

The period matrix in the basis  $\tilde{\varphi}_I$  is  $\tilde{\mathbf{P}}(\boldsymbol{\lambda}, \mu) = \mathbf{U}\mathbf{P}(\boldsymbol{\lambda}, \mu)$ , and by construction the dual period matrix is  $\tilde{\boldsymbol{P}}(\boldsymbol{\lambda}, \mu) = \tilde{\mathbf{P}}(\boldsymbol{\lambda}, -\mu)$ . Since  $\mathbf{U}$  is constant, the differential equation for  $\tilde{\mathbf{P}}(\boldsymbol{\lambda}, \mu)$  is still in  $\mu$ -factorised form,

$$d_{\text{ext}}\widetilde{\mathbf{P}}(\boldsymbol{\lambda}, \mu) = \mu \, \mathbf{U}\mathbf{B}(\boldsymbol{\lambda})\mathbf{U}^{-1}\widetilde{\mathbf{P}}(\boldsymbol{\lambda}, \mu) \,. \tag{4.79}$$

At this point we can even renormalise the bases so that they are orthonormal

$$\psi_I = \sqrt{(2\pi i)^{-n} \,\mu^n \,c_I^{-1}} \,\tilde{\varphi}_I \quad \text{and} \quad \check{\psi}_I = \sqrt{(2\pi i)^{-n} \,\mu^n \,c_I^{-1}} \,\check{\tilde{\varphi}}_I \,.$$
 (4.80)

For this basis, the intersection matrix is  $\langle \psi_I | \check{\psi}_J \rangle = \delta_{IJ}$ . Consequently, we have constructed bases that are simultaneously orthonormal and exhibit a differential equation in  $\mu$ -factorised form. Let us assume, we have chosen such bases from the beginning. We can obtain the differential equation for the dual period matrix  $\check{\mathbf{P}}$  in two ways. It can be found by replacing  $\mu$  by  $-\mu$  in the differential equation for the period matrix  $\mathbf{P}$ :

$$d_{\text{ext}}\check{\mathbf{P}}(\lambda,\mu) = d_{\text{ext}}\mathbf{P}(\lambda,-\mu) = -\mu\mathbf{B}(\lambda)\mathbf{P}(\lambda,-\mu) = -\mu\mathbf{B}(\lambda)\check{\mathbf{P}}(\lambda,\mu). \tag{4.81}$$

On the other hand, since the intersection matrix  $\mathbf{C}$  is the identity matrix in this case, eq. (4.63) implies that  $\mathbf{B}(\lambda)^T = -\check{\mathbf{B}}(\lambda)$  and consequently

$$d_{\text{ext}}\check{\mathbf{P}}(\lambda,\mu) = -\mathbf{B}(\lambda,\mu)^T\check{\mathbf{P}}(\lambda,\mu) = -\mu\mathbf{B}(\lambda)^T\check{\mathbf{P}}(\lambda,\mu). \tag{4.82}$$

Comparing eqs. (4.81) and (4.82), we see that 
$$\mathbf{B}(\lambda)^T = \mathbf{B}(\lambda)$$
.

Relations Between Periods and Dual Periods We conclude this subsection by focusing on relations between the periods and the dual periods that are due to the restriction of eq. (4.14) before lifting this restriction in the following subsection. If we choose the dual basis elements to be  $\tilde{\varphi}_i = [\varphi_i]_c$ , i.e., the compactified versions of the basis elements, the period matrix and the dual period matrix are related by

$$\check{P}_{ij}(\boldsymbol{\lambda}, \boldsymbol{\alpha}) = \int_{\check{\gamma}_j} \Phi^{-1} \check{\varphi}_i = \int_{\check{\gamma}_j} \Phi^{-1} [\varphi_i]_c = \int_{[\check{\gamma}_j]_c} \Phi^{-1} \varphi_i = \int_{\gamma_j} \Phi^{-1} \varphi_i = P_{ij}(\boldsymbol{\lambda}, -\boldsymbol{\alpha}).$$
(4.83)

#### See also:

We already had an example with this property in eq. (4.54).

We can always define the bases in such a way as long as the restriction of eq. (4.14) holds, i.e., it is always possible to choose

$$\check{\mathbf{P}}(\lambda, \alpha) = \mathbf{P}(\lambda, -\alpha)$$
, if condition (4.14) holds. (4.84)

We interpret this as a self-duality property of the periods. This self-duality property is also realised on the level of the connection matrix  $\mathbf{B}$  of eq. (4.61):

$$\check{\mathbf{B}}(\lambda, \alpha)\check{\mathbf{P}}(\lambda, \alpha) = d_{\text{ext}}\check{\mathbf{P}}(\lambda, \alpha) = d_{\text{ext}}\mathbf{P}(\lambda, -\alpha) = \mathbf{B}(\lambda, -\alpha)\mathbf{P}(\lambda, -\alpha)$$
(4.85)

or

See also:

Sec-

We discuss in

tion 4.4 how maximal

cuts of Feynman integrals are twisted peri-

ods with specific exponents of the form  $\alpha_i =$ 

 $\frac{\mu_i}{2} \pm \varepsilon$  and also have

this property.

$$\check{\mathbf{B}}(\lambda, \alpha) = \mathbf{B}(\lambda, -\alpha). \tag{4.86}$$

Note that if we have additional poles that are not regulated by the twist  $\Phi$  in the periods, this choice will in general not be possible and thus we also generally don't have the self-duality property. Note also that in the applications in this thesis, we might not always be interested in the dependence on the full  $\alpha$  by itself, but instead  $\alpha$  has entries of the form  $\alpha_i = \frac{\mu_i}{2} \pm \varepsilon$ . In that case, we can also choose a basis with the self-duality property

$$\check{\mathbf{P}}(\lambda,\varepsilon) = \mathbf{P}(\lambda,-\varepsilon). \tag{4.87}$$

In particular, the dual basis that allows for this is

$$\check{\varphi}_i = \left[ \varphi_i \prod_{j=1}^r L_j(\boldsymbol{z})^{-1} \right]_c. \tag{4.88}$$

In this case, we find similarly to eq. (4.86), that

$$\check{\mathbf{B}}(\lambda,\varepsilon) = \mathbf{B}(\lambda,-\varepsilon). \tag{4.89}$$

# 4.1.2 Review: Relative Twisted Cohomology

If condition (4.14) does not hold, additional subtleties need to be considered: Additional poles in the integrand need to be regulated. One way to do so is by using relative twisted (co-)homology groups. We discuss these, mostly based on [47, 49, 229] in this subsection. An alternative way to regulate the poles is by introducing factors into the twist, whose exponents  $\delta_i$  we set to zero at the end of any calculation. We also comment on this regularisation and compare the two methods.

# Relative Twisted (Co-)Homology Groups

Whilst the definitions for the connections in eq. (4.3) and the local systems in eq. (4.5) in spirit remain the same, the spaces we define them on need to be chosen more carefully. From the data imposed by the integral (4.1), we define the following hypersurfaces of branch points, poles and zeroes:

$$\Sigma = \{ \boldsymbol{z} \mid L_i(\boldsymbol{z}) = 0 \land \alpha_i \notin \mathbb{Z} \} \cup \{ \infty \}, \qquad (4.90)$$

$$D_{+} = \{ \boldsymbol{z} \mid \Phi \varphi(\boldsymbol{z}) = 0 \}, \tag{4.91}$$

$$D_{-} = \{ \boldsymbol{z} \mid \boldsymbol{z} \text{ is a pole of } \Phi \varphi(\boldsymbol{z}) \text{ and } \boldsymbol{z} \notin \Sigma \}. \tag{4.92}$$

Additionally, we define

$$X_{\pm} = \mathbb{P}_{\mathbb{C}}^{n} - (\Sigma \cup D_{\pm}). \tag{4.93}$$

Relative Twisted Homology Groups Since  $D_+$  contains the zeroes of  $\Phi\varphi$ , we can work relative to this set, i.e., consider cycles with boundaries on  $D_+$  as closed – we are interested in differential forms that vanish on  $D_+$ , so we can allow for cycles with boundaries on  $D_+$  and still consider them *closed*. Explicitly, we define relative twisted cycles as elements of

$$C_{n}(X_{-}, D_{+}, \check{\mathcal{L}}_{\Phi}) = C_{n}(X_{-}, \check{\mathcal{L}}_{\Phi}) / C_{n}(D_{+}, \check{\mathcal{L}}_{\Phi}),$$
 (4.94)

with

$$C_n(D_+, \check{\mathcal{L}}_{\Phi}) = C_n(X_-, \check{\mathcal{L}}_{\Phi})|_{D_+}. \tag{4.95}$$

Similarly, we define

$$B_{n}(X_{-}, D_{+}, \check{\mathcal{L}}_{\Phi}) = B_{n}(X_{-}, D_{+}, \check{\mathcal{L}}_{\Phi}) / B_{n}(D_{+}, \check{\mathcal{L}}_{\Phi})$$
(4.96)

and the relative twisted homology group

$$H_n(X_-, D_+, \check{\mathcal{L}}_{\Phi}) = C_n(X_-, D_+, \check{\mathcal{L}}_{\Phi}) / B_n(X_-, D_+, \check{\mathcal{L}}_{\Phi}).$$
 (4.97)

In practice, the cycles generating this homology group are supported on

- either regularised versions of chambers bounded by the  $\Sigma_i$  (as for non-relative twisted homology groups) or
- on tubings around the surfaces in  $D_{-}$  (as for non-twisted homology groups).

The cycles may look like they have non-vanishing boundaries, as long as these (seeming) boundaries lie in  $D_+$ , which we work relative to. The dual homology group is defined with the inverse twist  $\Phi^{-1}$  and thus the roles of poles and zeroes are interchanged on the dual side. We define the dual relative twisted homology group very similarly to the definition in eq. (4.97), albeit exchanging  $X_+ \leftrightarrow X_-$  and  $D_+ \leftrightarrow D_-$ :

$$H_n(X_+, D_-, \mathcal{L}_{\Phi}) = C_n(X_+, D_-, \mathcal{L}_{\Phi}) / B_n(X_+, D_-, \mathcal{L}_{\Phi}).$$
 (4.98)

The (basis) cycles of the dual twisted homology group are allowed to end at poles of  $\Phi\varphi$  and thus the generators look like bounded chambers with the boundaries being from  $\Sigma$  or  $D_-$ . We shortly discuss the computation of homology intersection numbers in relative twisted homologies in Appendix B.1.2.

**Example 4.8** ( $_2F_1$  function: Relative Twisted Homology Group). Let us return to the  $_2F_1$  function of Examples 4.2 and 4.5, but this time we do not take the parameters a, b, c to be generic and instead choose a configuration that introduces poles. More specifically, we set  $b, c \notin \mathbb{Z}$  to be generic and a = 0 so that the integrand has a pole at  $\lambda$ . We assume  $0 < 1 < \lambda$  and define the spaces

$$\Sigma = \{0, 1, \infty\}, D_{+} = \emptyset \text{ and } D_{-} = \{\lambda\}.$$
 (4.99)

Consequently

$$X_{+} = \mathbb{CP} - \{0, 1, \infty\} \text{ and } X_{-} = \mathbb{CP} - \{0, 1, \lambda, \infty\}.$$
 (4.100)

The relative twisted homology group is  $H_1(X_-, D_+ = \emptyset, \check{\mathcal{L}}_{\Phi}) \cong H_1(X_-, \check{\mathcal{L}}_{\Phi})$ . Since the integrand has no zeroes, the surface we are working relative to vanishes and since the integrand is not multi-valued near the point  $\lambda$ , we choose the first basis cycle to be supported on the  $\epsilon$ -ball around  $\lambda$ . As a second basis element of the homology group we choose one supported on the regularised interval (0,1):

$$\Delta_{\gamma_1} = (2\pi i)^{-1} S_{\epsilon}(\lambda) \text{ and } \Delta_{\gamma_2} = (0,1)^c.$$
 (4.101)

For the dual basis we choose cycles supported on the following intervals bounded by points from  $\Sigma \cup D_-$ :

$$\Delta_{\tilde{\gamma}_1} = (\lambda, \infty) \text{ and } \Delta_{\tilde{\gamma}_2} = (0, 1). \tag{4.102}$$

We depict both, the support of the basis and the support of the dual basis in figure 4.6.

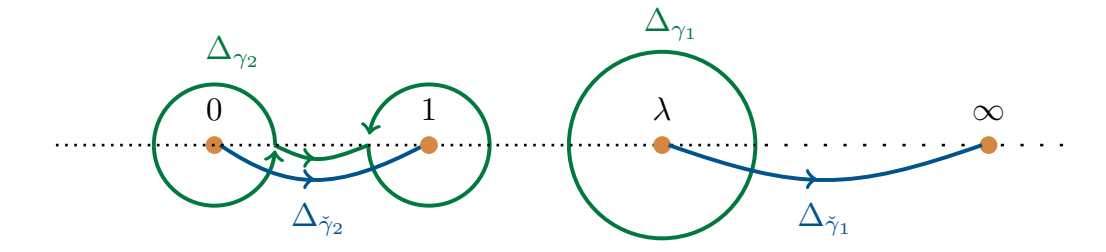


Figure 4.6: The basis cycles of basis cycles of eq. (4.101) are depicted on a regularized interval  $(0,1)^c$  and a  $\epsilon$ -ball around  $\lambda$ . The dual basis cycles of eq. (4.102) are supported on the intervals (0,1) and  $(\lambda,\infty)$ .

The homology intersection matrix of these bases is

$$\mathbf{H}_{R} = \begin{pmatrix} -\frac{i}{2\pi} & 0\\ 0 & -\frac{i}{2}\csc[b\pi]\csc[(b-c)\pi]\sin[c\pi] \end{pmatrix}. \tag{4.103}$$

We review how to compute this intersection matrix in Example B.5 of Appendix B.

Relative Twisted Cohomology Groups In the same way, one can define the relative twisted cohomology group

$$H_{dR}^{n}(X_{-}, D_{+}, \nabla_{\Phi}) = C^{n}(X_{-}, D_{+}, \nabla_{\Phi}) / B^{n}(X_{-}, D_{+}, \nabla_{\Phi}), \qquad (4.104)$$

with

$$C^{n}(X_{-}, D_{+}, \nabla_{\Phi}) = C^{n}(X_{-}, \nabla)/C^{n}(D_{+}, \nabla).$$
 (4.105)

In cases where we consider integrands that have only poles but no zeroes – i.e.,  $D_{+} = \emptyset$  – the relative twisted cohomology reduces to the *non-relative* version presented in the previous section [229]

$$H_{dR}^{n}(X_{-}, D_{+}, \nabla_{\Phi}) \cong H_{dR}^{n}(X_{-}, \nabla_{\Phi}),$$
 (4.106)

albeit defined on the space  $X_{-} = X - D_{-}$ . Due to the presence of these poles, the dual relative twisted cohomology group – which our conventions should be compactly supported – looks significantly different than the dual twisted cohomology without poles:

$$H_{dR}^{n}(X_{+}, D_{-}, \check{\nabla}_{\Phi}) = C^{n}(X_{+}, D_{-}, \check{\nabla})/B^{n}(X_{+}, D_{-}, \check{\nabla}_{\Phi}). \tag{4.107}$$

Its elements can be written in the form [47, 49]

$$\check{\varphi} = \theta \psi + \delta_1(\theta \psi_1) + \dots + \delta_{1,2}(\theta \psi_{1,1}) + \dots, \tag{4.108}$$

where  $\theta$  is a symbol that tracks the possible boundary terms. The sum is taken over all (intersections of) sub-boundaries of  $D_-$ . The form  $\delta_{i_1,\dots,i_p}(\phi_{i_1,\dots,i_p})$  is the Leray coboundary [47, 49, 231] of a form  $\phi_{i_1,\dots,i_p}$  that is defined on the boundary  $\{\Sigma_{i_1}=0\}\cup\dots\cup\{\Sigma_{i_p}=0\}$ . Explicitly, it can be expressed as

$$\delta_{i_1,\dots,i_p}(\phi_{i_1,\dots,i_p}) = \frac{\Phi}{\Phi|_{i_1,\dots,i_p}} d\theta_{i_1} \wedge \dots d\theta_{i_p} \wedge \phi_{i_1,\dots,i_p}, \qquad (4.109)$$

where  $d\theta$  can be thought of as the derivative of the Heaviside  $\theta$  function

$$\theta_H(x) = \left\{ \begin{array}{l} 1, & x > 0, \\ 0, & x < 0. \end{array} \right\}. \tag{4.110}$$

More details on the meaning of the symbols  $\delta$  and  $\theta$  are given in refs. [47, 49], where they are constructed. For one-forms, i.e., for forms in  $H^1_{dR}(X_+, D_-, \check{\nabla})$ , we can explicitly construct a basis from forms

$$\delta_{z_i}(1) = \frac{\Phi}{\Phi|_{z_i=0}} d\theta(z - z_i), \quad \text{for } z_i \text{ a pole},$$
(4.111)

and compactifications of twisted co-cycles  $\phi_{reg}$  with 'regulated' singularities,

$$[\phi_{\text{reg}}]_c^{\text{rel}} = \phi_{\text{reg}} \prod_i \theta(z - z_i) + \sum_i \psi_i \, d\theta(z - z_i), \qquad (4.112)$$

with  $\phi_{\text{reg}}$  chosen as in the non-relative case and  $z_i \in D_+ \cup \Sigma$ . The functions  $\psi_i$  are the local primitives defined by  $\check{\nabla}_{\Phi} \psi_i = \phi_{\text{reg}}$ .

**Example 4.9** ( $_2F_1$  function: Relative Twisted Cohomology Group). We continue the discussion of Example 4.8, focusing now on the twisted cohomology group rather than the homology group. Since the example we consider has no zeroes in the integrand,  $H^1_{dR}(X_-, D_+ = \emptyset, \nabla_{\Phi}) \cong H^1_{dR}(X_-, \nabla_{\Phi})$  can be treated exactly as in the non-relative case and consequently, we can also choose the  $d \log basis$  of eq. (4.45):  $\chi_{R,i} = \chi_i$ . The dual relative twisted cohomology group is  $H^1_{dR}(X_+, \{\lambda\}, \nabla_{\Phi})$  and we can choose for its basis the following classes of differentials

$$\check{\chi}_{R,1} = \chi_{R,1} \text{ and } \check{\chi}_{R,2} = -\delta_{\lambda}(1) = -\frac{\Phi}{\Phi|_{z \mapsto \lambda}} d\theta(z - \lambda). \tag{4.113}$$

Note that the first basis element is the same as in the non-relative or non-dual basis and only the element  $\check{\chi}_{R,2}$  is distinct due to the non-regulated pole at  $\lambda$ . The period matrices of these bases and the homology bases of Example B.1 are 15

$$\mathbf{P}_{R} = \begin{pmatrix} 0 & \frac{\Gamma(b)\Gamma(c-b)}{\Gamma(c)} \\ -(1-\lambda)^{c-b}\lambda^{b} & {}_{2}\mathcal{F}_{1}\left(b,1,1+c,\frac{1}{\lambda}\right) \end{pmatrix}$$
(4.114)

$$\mathbf{P}_{R} = \begin{pmatrix} 0 & \frac{\Gamma(b)\Gamma(c-b)}{\Gamma(c)} \\ -(1-\lambda)^{c-b}\lambda^{b} & {}_{2}\mathcal{F}_{1}\left(b,1,1+c,\frac{1}{\lambda}\right) \end{pmatrix}$$

$$\mathbf{\tilde{P}}_{R} = \begin{pmatrix} e^{i\pi(b-c)}\beta\left(\frac{1}{\lambda},1+c,b-c\right) & \frac{\Gamma(-b)\Gamma(b-c)}{\Gamma(-c)} \\ -e^{i\pi(b-c)}(\lambda-1)^{b-c}\lambda^{-b} & 0 \end{pmatrix} .$$

$$(4.114)$$

The cohomology intersection matrix is

$$\mathbf{C}_R = \begin{pmatrix} -\frac{c}{b(b-c)} & 0\\ \frac{1}{b} & -1 \end{pmatrix}. \tag{4.116}$$

## Regulating with Limits

As already noted, we include every pole of  $\Phi\varphi$  in the twist, albeit possibly with an exponent that is zero. But, we can also take that exponent to be a generic factor  $\delta_i$  to zero, so that we have no more unregulated poles and work with standard twisted cohomology groups. In the end, we set the generic  $\delta_i$ . This limit needs to be taken carefully, i.e., potentially after an additional rotation, to avoid producing degeneracies or spurious poles. A discussion of this procedure can also be found in [239]. Instead of going into detail about this procedure, we illustrate it with an example, the hypergeometric  ${}_{2}F_{1}$  function of Example 4.8.

**Example 4.10** ( ${}_{2}F_{1}$  Functions: Regulating with Limits). We consider the twist as a function of the exponent a, with the aim of setting  $a \to 0$  in the end of the calculation:

$$\Phi(a) = z^b (1 - z)^{b-c} (1 - \lambda z)^{-a} , \qquad a \neq 0.$$
 (4.117)

In the generic case  $a \neq 0$ , the condition (4.14) is satisfied and we can consider the corresponding twisted (co-)homology groups as described in Section 4.1.1. In particular, in that case we can choose the twisted homology basis of Example 4.3 and the twisted cohomology basis  $\chi$  of Example 4.5. In these examples, we computed

<sup>15</sup>The function  $\beta(a,b,c)$ denotes the incomplete  $\beta$  function with upper integration limit a.

the period and intersection matrices. We Laurent expand the intersection matrices of eq. (B.8) and eq. (4.44) in the parameter a, finding:

$$\mathbf{H}(a) = \begin{pmatrix} -\frac{i}{2\pi} \frac{1}{a} + \mathcal{O}(a^0) & 0\\ 0 & -\frac{i}{2} \csc[b\pi] \csc[(b-c)\pi] \sin[c\pi] \end{pmatrix}$$
(4.118)

$$\mathbf{C}_{\chi}(a) = \begin{pmatrix} -\frac{c}{b(b-c)} & \frac{1}{b} \\ \frac{1}{b} & -\frac{1}{a} + \frac{1}{b} + \mathcal{O}(a) \end{pmatrix}. \tag{4.119}$$

Both matrices diverge in the limit  $a \to 0.16$  On the other hand, if we just take the global lowest order, we obtain matrices that does not have full rank, i.e., that cannot be the intersection matrices of non-degenerate bases. We can perform a rotation so that the intersection matrices are non degenerate in the limit – which is equivalent to considering the local lowest order in each entry of the matrices in eq. (4.118). Taking the limit in that specific way, we also find intersection matrices that are exactly the same as the ones we obtain using relative twisted (co-)homology groups: 18

$$^{17}$$
The corresponding rotation matrices  $\mathbf{U}_H$  and  $\mathbf{U}_C$  can be read

<sup>16</sup>Taking  $\alpha \rightarrow 0$  we

would obtain  $\infty$  in the entry (1,1) of  $\mathbf{H}(a)$  and

the (2,2) entry of  $\mathbf{C}(a)$ .

and 
$$\mathbf{U}_C$$
 can be read off easily.

$$\mathbf{H}_{R} = \left[\mathbf{U}_{H}(a)\mathbf{H}(a)\right]|_{a\to 0} \text{ with } \mathbf{U}_{H}(a) = \begin{pmatrix} a & 0\\ 0 & 1 \end{pmatrix}$$
(4.120)

$$\mathbf{C}_{R} = \left[\mathbf{C}_{\chi}(a)\mathbf{U}_{C}(a)\right]|_{a\to 0} \text{ with } \mathbf{U}_{C}(a) = \begin{pmatrix} 1 & 0\\ 0 & a \end{pmatrix}. \tag{4.121}$$

Taking the same rotation of the homology basis and the dual cohomology basis, one can also recover the period matrices of eq. (4.114) after the limit:

$$\mathbf{P}_{R} = \left[\mathbf{P}_{\chi}(a) \cdot \mathbf{U}_{H}(a)\right]|_{a \to 0} \text{ and } \check{\mathbf{P}}_{R} = \left[\mathbf{U}_{C}(a) \cdot \check{\mathbf{P}}_{\chi}(a)\right]|_{a \to 0}. \tag{4.122}$$

Thus, by taking the correct limit we can recover the same results as we obtain in the relative framework. Taking this limit correctly (i.e., after the additional rotation imposed by the matrices  $\mathbf{U}_{H/C}$ ) changes the dependence of the period matrix and the dual period matrix on a, b, c and consequently, in general relations such as eq. (4.54) do not hold after the limit.

# 4.2 Review: Motivic Periods for Phycisists

In this section, we give a rather brief and conceptual review of *motivic* and *de Rham* periods from a physicist's perspective. In particular, we discuss the construction of single-valued periods from de Rham periods and give some comments on iterated Eisenstein integrals. For a more detailed introduction of motivic and de Rham periods tailored to a physics audience, see [240, 241]. The following summary constitutes a brief intuitive review of relevant parts of these references.

#### 4.2.1 Motivic and de Rham Periods

As established before, we interpret *periods* as pairings between a contour  $\sigma$  and a differential  $\omega$  by integration<sup>19</sup>:

<sup>19</sup>We extend here the notation of the previous section to include twisted as well as non-twisted periods and for the latter  $\Phi = 1$ .

$$\langle \omega | \sigma ] = \int_{\sigma} \Phi \, \omega \,. \tag{4.123}$$

In general we take  $\omega$  to be an element of a (twisted) de-Rham cohomology group  $H^n_{dR}(X, \nabla_{\Phi})$  and  $\sigma$  to be an element of a (twisted) Betti homology group  $H_{n,B}(X, \check{\mathcal{L}}_{\Phi})$  group. They are related by the Grothendieck-de Rham comparison isomorphism:

$$comp_{X,\Phi}: H^n_{dR}(X, \nabla_{\Phi}) \otimes \mathbb{C} \to H_{n,B}(X, \check{\mathcal{L}}_{\Phi}) \otimes \mathbb{C}. \tag{4.124}$$

The comparison isomorphism is practically computed by integration when it makes sense, i.e., by integrals such as the one in eq. (4.123). We collect the (co-)homology groups and their comparison isomorphism in a tuple

$$\mathcal{H} = \mathcal{H}_{X,\Phi} = (H_{n,B}(X, \check{\mathcal{L}}_{\Phi}), H_{dB}^{n}(X, \nabla_{\Phi}), comp_{X,\Phi}) . \tag{4.125}$$

Here, we think about a *motivic period* via its realisations that can be written as a tuple

$$[\mathcal{H}_{X,\Phi}, \sigma, \omega]^{\mathfrak{m}} \tag{4.126}$$

with  $\sigma$  and  $\omega$  representing equivalence classes of elements in  $H_{n,B}(X, \mathcal{L}_{\Phi})$  and  $H^n_{dR}(X, \nabla_{\Phi})$  respectively. The motivic periods of  $\mathcal{H}_{X,\Phi}$  form a ring, which we denote by  $\mathcal{P}_{\mathcal{H}}$  and there is a homomorphism [241]

per : 
$$\mathcal{P}_{\mathcal{H}} \to \mathbb{C}$$
,  $[\mathcal{H}_{X,\Phi}, \sigma, \omega]^{\mathfrak{m}} \mapsto \langle \omega | \sigma] = \int_{\sigma} \Phi \omega$  (4.127)

called the period map. Due to this map, the notation

$$[\mathcal{H}_{X,\Phi}, \sigma, \omega]^{\mathfrak{m}} = \langle \omega | \sigma ]^{\mathfrak{m}} = \int_{\sigma}^{\mathfrak{m}} \Phi \omega \tag{4.128}$$

is justified, i.e., occasionally we just write motivic periods as the period integrals they evaluate to under the period map labelled with  $\mathfrak{m}$ .

**Example 4.11** (Motivic Logarithm). Let  $X = \mathbb{P}^1_{\mathbb{C}} - \{0, \infty\}$ . We consider the relative (non-twisted) (co-)homology groups  $H^1_{dR}(X \mod \{1, \lambda\})$  and  $H_1(X \mod \{1, \lambda\})$ . Choosing  $[1, \lambda] \in H_1(X \mod \{1, \lambda\})$  and  $\frac{dt}{t} \in H^1_{dR}(X \mod \{1, \lambda\})$ , the motivic logarithm is

$$\log^{\mathfrak{m}}(\lambda) = \left[\mathcal{H}_X, (1, \lambda), \frac{\mathrm{d}t}{t}\right] \tag{4.129}$$

and its period map evaluates to the logarithm

$$\operatorname{per}\left[\log^{\mathfrak{m}}(\lambda)\right] = \int_{1}^{\lambda} \frac{\mathrm{dt}}{\mathrm{t}} = \log(\lambda). \tag{4.130}$$

Similarly, de Rham periods can be thought of via their realisations

$$[\mathcal{H}_{X,\Phi}, \tilde{\omega}, \omega]^{\mathfrak{dr}}$$
 or here shortly  $\langle \tilde{\omega}, \omega \rangle^{\mathfrak{dr}}$  (4.131)

where in some sense,  $\tilde{\omega}$  can be viewed as a representative of an element of a dual version of the de Rham cohomology group  $H_{n,dR}(X, \nabla_{\Phi})$ , also called a de Rham homology. Thus, rather than pairing Betti and de Rham representatives, we now consider pairings between de Rham representatives and their dual counterparts. Unlike for the motivic periods there is no natural period map that uniquely relates these representatives to integrals. However, one can construct a single-valued map acting on de Rham periods, which provides a way to evaluate them as elements in  $\mathbb{C}$ . With this framework in place, we can turn to the motivic coaction and the construction of single-valued versions of periods. These constructions are particularly well understood for multiple polylogarithms and their constants. For these cases, there also exist generating series from which one can read them off [170] and we shortly review them below in order to lead up to similar constructions that are being developed for iterated Eisenstein integrals and that are presented in Subsection 4.2.3.

Example 4.12 (MZVs: Motivic and de-Rham versions). In Subsection 3.4.1 we introduced MPLs. There are motivic  $G^{\mathfrak{m}}$ ,  $\zeta^{\mathfrak{m}}$  and de Rham versions  $G^{\mathfrak{dr}}$ ,  $\zeta^{\mathfrak{dr}}$  of both, the MPLs and the MZVs [225, 241–243]. As already mentioned, the  $\zeta_{n_1,\ldots,n_r}$  fullfill relations and so do their motivic versions. There is a representation of these motivic  $\zeta^{\mathfrak{m}}$  values, in which all of these  $\mathbb{Q}$ -relations are already inherent: the f-alphabet [243, 244]. The f-alphabet consists of non-commuting letters  $f_{2k+1}$  for  $k \in \mathbb{N}_{>0}$ , along with a commuting letter  $f_2$ . The map  $\rho_f$  relates MZVs to elements of the f-alphabet. This map is an isomorphism for  $\mathbb{Q}$ -independent  $\zeta^{\mathfrak{m}}$  values, but it is not unique<sup>20</sup>. <sup>20</sup>This As a normalisation condition, it is assigned to act on depth-one MZVs by

$$\rho_{\rm f}(\zeta_{2k+1}^{\mathfrak{m}}) = {\rm f}_{2k+1} \ and \ \rho_{\rm f}(\zeta_{2}^{\mathfrak{m}}) = {\rm f}_{2}.$$
(4.132)

There is a generating series for the preimages of words in f, that is, the  $\mathbb{Q}$ -independent multiple zeta values:

$$\mathbb{M}_{0}^{\mathfrak{m}} = \sum_{r=0}^{\infty} \sum_{i_{1}, \dots, i_{r} \in 2\mathbb{N}+1} \rho^{-1}(f_{i_{1}} \dots f_{i_{r}}) M_{i_{1}} \dots M_{i_{r}}$$

$$= 1 + \sum_{i_{1} \in 2\mathbb{N}+1} \zeta_{i_{1}}^{\mathfrak{m}} M_{i_{1}} + \sum_{i_{1}, i_{2} \in 2\mathbb{N}+1} \rho^{-1}(f_{i_{1}} f_{i_{2}}) M_{i_{1}} M_{i_{2}} + \dots$$

$$(4.133)$$

Inserting the motivic and de Rham versions of the MZVs appearing in the series of eq. (4.133), one can also define motivic and de Rham versions of this generating series that we denote by  $\mathbb{M}_0^{\mathfrak{m}}$  and  $\mathbb{M}_0^{\mathfrak{dr}}$  respectively. We also use MZV series with a different set of generators  $\sigma_w$  that replace the  $M_w$ , i.e.,

$$\mathbb{M}_{\sigma} = \mathbb{M}_{0} \big|_{M_{w} \to \sigma_{w}} = \sum_{r=0}^{\infty} \sum_{i_{1}, \dots, i_{r} \in 2\mathbb{N}+1} \rho^{-1}(f_{i_{1}} \dots f_{i_{r}}) \sigma_{i_{1}} \dots \sigma_{i_{r}}.$$
 (4.134)

The genus-one zeta generators  $\sigma_w$  contain an arithmetic component  $z_w$  and a geometric component  $\sigma_w - z_w$ .

This map is not unique, and its ambiguities are well understood as being linked to a basis of irreducible MZVs [243, 244]. A canonical choice is provided in [245].

## 4.2.2 Single-valued Periods

In general, the periods we consider in this chapter are twisted periods – that is, they are multi-valued functions in the entries of some set of parameters  $\lambda$ . Such functions naturally arise as Feynman integrals, correlators or string integrals. But in many applications, the object of interest are single-valued objects – as physical observables should be in the end. A small number of examples, where the construction of single-valued periods was explicitly used in physics include:

- amplitudes in the multi-Regge limit of  $\mathcal{N}=4$  SYM built from single-valued versions of multiple polylogarithms [246, 247],
- closed string integrals, that are single-valued versions of periods defined on Riemann surfaces (or models thereof, as in [6]) and
- Feynman integrals in two dimensions, as we discuss in detail in Chapter 8 based on [35–38].

The diversity of these few examples indicates, how a good understanding of single-valued periods can be used in physics. We review below how to associate to a twisted period its single-valued version. This procedure is generally non-trivial and we do not go into the details. Unless stated otherwise, we assume that we are working with twisted (motivic or de Rham) cohomology groups on the punctured Riemann sphere, where computations tend to be more tractable. In particular, we do not claim that the statements and constructions discussed here extend to (co-)homology groups defined on more complex varieties (or their moduli spaces), such as the torus. The so-called single-valued maps is particularly well-understood for punctured Riemann spheres, see e.g., [7, 248, 249]. It assigns to a de-Rham period defined from equivalence classes of (dual) n-forms  $\check{\nu}$  and  $\omega$  a single-valued period:

$$\operatorname{sv}\left(\left[\mathcal{H}_{X,\Phi},\check{\nu},\omega\right]^{\mathfrak{dr}}\right) = (2\pi i)^{-n} \int_{X} \omega \wedge \operatorname{conj}^{*}(\check{\nu}) = (-2\pi i)^{-n} \int_{X} \operatorname{conj}^{*}(\omega) \wedge \check{\nu}, \quad (4.135)$$

where is induced by complex conjugation as described in  $\text{conj}^*: X \to X$  [248]. When we explicitly include the twist<sup>21</sup>, this amounts to

$$\operatorname{sv}\left(\left[\mathcal{H}_{X,\Phi},\check{\nu},\omega\right]^{\mathfrak{dr}}\right) = (-2\pi i)^{-n} \int_{X} |\Phi|^{2} \ \omega \wedge \overline{\check{\nu}} \ . \tag{4.136}$$

In going back to the notation of Section 4.1 we can express this as<sup>22</sup>

$$\operatorname{sv}\left(\left[\mathcal{H}_{X,\Phi},\check{\nu},\omega\right]^{\mathfrak{dr}}\right) = (-2\pi i)^{-n} \langle \omega | \overline{\check{\nu}} \rangle \tag{4.137}$$

and using the Riemann bilinear relations of eq. (4.58) (or equivalently, inserting a completeness relation), we find:

$$\operatorname{sv}\left(\left[\mathcal{H}_{X,\Phi},\check{\nu},\omega\right]^{\mathfrak{dr}}\right) = (-2\pi i)^{-n} \langle \omega | \overline{\check{\nu}} \rangle = (-2\pi i)^{-n} \sum_{i,j} \langle \omega | e_i \right] \left[\check{e}_i | \check{e}_j \right] \left[\check{e}_j | \overline{\check{\nu}} \right) \tag{4.138}$$

<sup>21</sup>Additionally, we assume that the forms  $\check{\omega}$  and  $\omega$  are algebraic.

<sup>22</sup>Note that this is a slight abuse of notation. Additionally, the argument presented here is rather an intuitive reasoning and not a proper derivation of the results. For a more rigorous treatment see [7, 248].

for bases  $e_i$ ,  $\check{e}_j$  of the twisted cohomology group and the dual group respectively. Using eq. (4.138) we can find the single-valued version of a particular de-Rham period defined by the co-cycles  $\check{\nu}$  and  $\omega$ . We can also define an object that we denote the single-valued version of the twisted period matrix for a given basis<sup>23</sup>:

$$\mathbf{P}^{\text{sv}} = (-2\pi i)^{-n} \mathbf{P} \left( \mathbf{H}^{-1} \right)^{T} \overline{\mathbf{P}}^{T} = \mathbf{P} \left[ \overline{\mathbf{P}}^{-1} \overline{\mathbf{C}} \right] |_{\boldsymbol{\alpha} \mapsto -\boldsymbol{\alpha}}, \tag{4.139}$$

with  $\alpha$  the exponents of the twist. This single-valued version of the period matrix can only be related to a certain period matrix canonically (and uniquely) if it arises from *separated* de Rham groups. For the applications in physics discussed here, it is sufficient to know that this condition is always fulfilled when X is the punctured Riemann sphere, i.e., whenever we work with genus zero objects, but not, when we work with higher genus or higher dimensional objects. In those cases, there exists a natural map, the so-called de Rham projection

$$\check{c}_0: \mathcal{H}_{1,\mathcal{B}}(\mathcal{X}, \check{\mathcal{L}}_{\Phi}) \to \mathcal{H}^1_{\mathrm{dR}}(\mathcal{X}, \nabla_{\Phi}), \qquad (4.140)$$

which uniquely maps a cycle to a dual co-cycle. In that way, one can relate a period to a de Rham period and then to a single-valued period:

$$\int_{\gamma} \omega \longrightarrow \left[ \mathcal{H}_{X,\Phi}, \check{c}_0(\gamma), \omega \right]^{\mathfrak{dr}} \longrightarrow (2\pi i)^{-n} \int_{X} \omega \wedge \overline{\check{c}_0(\gamma)}$$
 (4.141)

This single-valued period can be computed explicitly with the double-copy formula of eq. (4.139). The matrix  $\mathbf{P}^{\text{sv}}$  satisfies the same holomorphic differential equation as the period matrix  $\mathbf{P}$ . Indeed, since  $\mathbf{P}$  is the only holomorphic factor in eq. (4.139), we have

$$\partial \mathbf{P}^{\text{sv}} = (\partial \mathbf{P}) \left[ \overline{\mathbf{P}}^{-1} \overline{\mathbf{C}} \right] |_{\alpha \mapsto -\alpha} = \mathbf{A} \mathbf{P}^{\text{sv}} \text{ for } \partial \mathbf{P} = \mathbf{A} \mathbf{P}.$$
 (4.142)

To confirm that the single-valued version of the period matrix that we gave in eq. (4.139) is actually single-valued, we observe that it behaves under a monodromy transformation as

$$\mathbf{P}^{\mathrm{sv}} \to \mathbf{P} \mathbf{M}_{\alpha}(\delta) \overline{\mathbf{M}}_{-\alpha}(\delta)^{-1} \left[ \overline{\mathbf{P}}^{-1} \overline{\mathbf{C}} \right] |_{\alpha \mapsto -\alpha} = \mathbf{P}^{\mathrm{sv}},$$
 (4.143)

i.e. it is invariant.

**Example 4.13** ( $\beta$  function: Single-valued Version). Let us start by reviewing the single-valued analogue of the Euler  $\beta$  function from Example 4.1. It admits the integral representation:

$$\beta^{sv}(\alpha_1, \alpha_2) = -\frac{1}{2\pi i} \int_{\mathbb{C}} |z|^{2\alpha_1} |1 - z|^{2\alpha_1} \frac{\mathrm{d}z \wedge \mathrm{d}\bar{z}}{|z|^2 |1 - z|^2}. \tag{4.144}$$

An expression for  $\beta^{sv}$  in terms of Gamma functions can be obtained from the period and intersection matrix computed in Example 4.4:

$$\beta^{sv}(\alpha_1, \alpha_2) = -\frac{1}{2\pi i} \mathbf{P}_{\alpha} \mathbf{H}_{\alpha}^{-1} \overline{\mathbf{P}}_{\alpha} = \frac{\Gamma(\alpha_1) \Gamma(\alpha_2) \Gamma(1 - \alpha_1 - \alpha_2)}{\Gamma(\alpha_1 + \alpha_2) \Gamma(1 - \alpha_1) \Gamma(1 - \alpha_2)}, \qquad (4.145)$$

where we dropped the transposition of all matrices, because they are one-dimensional. This was also derived in ref. [7, 248].

 $^{23}\mathrm{Note}$ that  $_{
m in}$ applications of this, we consider non-relative twisted (co-)homology groups and the intersection numbers between twisted cycles rational with rational tions coefficients of  $e^{2\pi i a_j}$ . which implies that  $\overline{\mathbf{H}}|_{\alpha \to -\alpha} = \mathbf{H}_{\alpha}$  for  $\alpha$ the exponents of the twist.

Again, this map is particularly well-understood for the single-valued versions of MPLs and MZVs. We give as an example the generating series for single-valued versions of words in the f-alphabet of Example 4.12.

**Example 4.14** (MZVs: Single-Valued Versions). As a second example, we continue the discussion of Example 4.12. In particular, we note, that the single-valued map acts on words in the f-alphabet by shuffle products [250, 251]

$$sv(f_2^n f_{i_1} \dots f_{i_r}) = \delta_{n,0} \sum_{i=0}^r f_{i_j} \dots f_{i_2} f_{i_1} \gg f_{i_{j+1}} \dots f_{i_r}, \quad i_1, \dots, i_r \in 2\mathbb{N} + 1. \quad (4.146)$$

From this expression, one can also deduce the action of the single-valued map on the generating series  $\mathbb{M}_0$ :

$$\operatorname{sv} \mathbb{M}_{0} = \sum_{r=0}^{\infty} \sum_{i_{1}, \dots, i_{r} \in 2\mathbb{N}+1} \rho^{-1} \left( \operatorname{sv} \left( f_{i_{1}} \dots f_{i_{r}} \right) \right) M_{i_{1}} \dots M_{i_{r}}$$

$$= 1 + 2 \sum_{i_{1} \in 2\mathbb{N}+1} \zeta_{i_{1}} M_{i_{1}} + 2 \sum_{i_{1}, i_{2} \in 2\mathbb{N}+1} \zeta_{i_{1}} \zeta_{i_{2}} M_{i_{1}} M_{i_{2}} + \dots$$

$$(4.147)$$

From this expression, we can read off the single-valued versions of independent combinations of MZVs by taking the coefficients of the respective words in the  $M_{ij}$ .

Similarly there exists a generating series for equivariant and single-valued versions of iterated Eisenstein integrals as defined in eq. (3.157).

**Example 4.15** (Iterated Eisenstein Integrals: Equivariant and Single-Valued Versions). Equivariant versions of iterated Eisenstein integrals were constructed in [252] and this construction was translated into explicit generating series in [177]:

$$\mathbb{I}^{\text{eqv}}(\epsilon_k; \tau) = (sv \,\mathbb{M}_z)^{-1} \,\overline{\mathbb{I}(\epsilon_k; \tau)^T} \,(sv \,\mathbb{M}_\sigma) \,\mathbb{I}_{\mathcal{E}, +}(\epsilon_k; \tau) \,. \tag{4.148}$$

This combination of Eisenstein integrals fulfils the condition<sup>24</sup>

$$\mathbb{I}^{\text{eqv}}\left(\epsilon_k; -\frac{1}{\tau}\right) = U_S^{-1} \mathbb{I}^{\text{eqv}}(\epsilon_k; \tau) U_S , \qquad \mathbb{I}^{\text{eqv}}(\epsilon_k; \tau+1) = U_T^{-1} \mathbb{I}^{\text{eqv}}(\epsilon_k; \tau) U_T \qquad (4.149)$$

so that it to transform under  $SL(2,\mathbb{Z})$  in the same manner as the connection eq. (3.158), without introducing any cocycles. Analogously to eq. (4.148) one derives a generating series for single-valued iterated Eisenstein integrals [177, 252].

$$sv\mathbb{I}(\epsilon_k;\tau) = (sv\mathbb{M}_{\sigma})^{-1}\overline{\mathbb{I}(\epsilon_k;\tau)^T}(sv\mathbb{M}_{\sigma})\mathbb{I}_{\mathcal{E},+}(\epsilon_k;\tau). \tag{4.150}$$

Unlike the equivariant iterated Eisenstein integrals in eq. (4.148), their single-valued counterparts in eq. (4.150) align with the general concept of single-valued periods [252].

 $^{24}{
m The}$ single-valued map of  $\operatorname{sv} \mathbb{M}_z$  and  $\operatorname{sv} \mathbb{M}_{\sigma}$ simply on the MZVs in the expansion eq. (4.134)via eq. (4.146), and the series  $\mathbb{M}_z = \mathbb{M}_{\sigma}|_{\sigma_w \to z_w}$ only retains the arithmetic parts of the genus-one zeta generators.

#### 4.2.3 Coactions

The general version of the motivic coaction is given by [240, 253]

$$\Delta_{\text{mot}} \langle \sigma | \omega ]^{\mathfrak{m}} = \sum_{e_i} \langle \sigma | e_i ]^{\mathfrak{m}} \otimes \langle \check{e}_i | \omega \rangle^{\mathfrak{dr}}, \qquad (4.151)$$

where the  $e_i$  form a basis of the de Rham cohomology group and  $\check{e}_i$  is the dual basis (i.e. the basis of the de Rham homology). To use this operation in physics, we want to interpret both sides of the  $\otimes$  as (iterated) integrals, when possible. For the motivic period, this can be done with the period map. For the de Rham periods such an interpretation – due to the single-valued map of (4.136) – only exists in the genus zero case in a well-defined way due to the de Rham projection. Different notions of the coaction map and the closely related symbol calculus have been widely studied in the physics literature [168, 169, 250, 254–271]. In particular, the polylogarithmic case is well understood and for polylogarithmic Feynman integrals, the coaction is used to connect and simplify their expressions, see [173] for a review. The connection between the coaction prescriptions used by physicists and the motivic Galois coaction studied by mathematicians [242–244, 272–275] is well understood for MPLs [249, 264]. We give an example for a well-understood and simple case, the coaction of motivic MZVs in the f-alphabet.

**Example 4.16** (MZVs: Coaction). We continue the discussion of Examples 4.12 and 4.14. Words in the alphabet f of motivic MZVs admit a simple expression for their motivic coaction [242–244, 274], given by a deconcatenation formula:

$$\Delta \left( f_2^n f_{i_1} \dots f_{i_r} \right)^{\mathfrak{m}} = \sum_{j=0}^r \left( f_2^n f_{i_1} \dots f_{i_j} \right)^{\mathfrak{m}} \left( f_{i_{j+1}} \dots f_{i_r} \right)^{\mathfrak{dr}}, \quad i_1, \dots, i_r \in 2\mathbb{N} + 1. \quad (4.152)$$

Note that we often shorten the notation  $x^{\mathfrak{m}} = x^{\mathfrak{m}} \otimes \mathbf{1}$  and  $x^{\mathfrak{dr}} = \mathbf{1} \otimes x^{\mathfrak{dr}}$  to indicate by the labels  $\mathfrak{m}$  and  $\mathfrak{dr}$  also the position within the tensor product. From this formula, one can deduce:

$$\Delta \mathbb{M}_0^{\mathfrak{m}} = \mathbb{M}_0^{\mathfrak{m}} \mathbb{M}_0^{\mathfrak{dr}} \,. \tag{4.153}$$

Simple expressions for the coaction and single-valued version of the generating series  $\mathbb{G}_G$  also exist [170]. Beyond that, there has been significant effort to identify a simple representation for an elliptic coaction [198, 276, 277], see e.g., [278–280] for applications in particle physics. In particular a mathematically rigorous treatment of the motivic coaction for the sunrise integral family has been given in [105, 264]. Nevertheless, establishing a connection between the mathematical results [105, 264] and the coaction prescriptions proposed in the physics literature remains an open problem. In the remainder of Subsection 4.2.3, we give some ideas in this direction for a specific class of elliptic iterated integrals, the iterated Eisenstein integrals as defined in eq. (3.157).

We collect qualitative expressions for the generating series of the coaction and single-valued versions of multiple polylogarithms – which are genus zero objects –

<sup>25</sup>This is only possible in a canonical way, if the de Rham projection exists. Even if it does not – i.e., beyond genus zero – one can still assign *some* contour to a dual co-cycle, if one can find a consistent prescription and in that way make sense of the motivic coaction.

on the left-hand side of figure 4.7. Additionally, we review a generating series for single-valued iterated Eisenstein integrals in eq. (4.150), which we depict in the lower-right corner of figure 4.7.

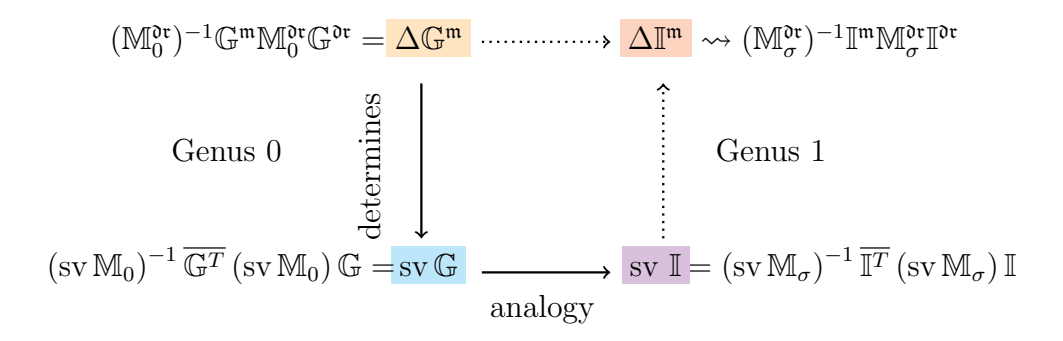


Figure 4.7: The single-valued map (lower-right) and coaction (upper-right) for the generating series of multiple polylogarithms as well as their relation is well understood. Additionally there exists a single-valued map for the generating series of iterated Eisenstein integrals. By analogy, we define a map  $\Delta$  acting on the generating series for iterated Eisenstein integrals.

Note that the generating series for single-valued iterated Eisenstein integrals is structurally very similar to the one for single-valued MPLs. In particular, genus-one construction can be derived from the genus-zero construction by interchanging the roles of genus-zero and genus-one quantities as follows:

- meromorphic MPLs  $\rightarrow$  by iterated Eisenstein integrals of eq. (3.152)
- non-commutative elements  $e_0, e_1 \to \text{Tsunogai derivations } \epsilon_k^{(j)}$
- genus-zero zeta generators  $M_w \to \text{genus-one generators } \sigma_w$ .

This analogy is depicted by the solid horizontal arrow at the bottom of figure 4.7. By applying the same analogy to the motivic coaction of MPLs, as indicated by the dashed horizontal arrow in the top row of figure 4.7 we obtain the following expression:

$$\Delta_{p} \mathbb{I}_{\mathcal{E},+}^{\mathfrak{m}}(\epsilon_{k};\tau) = (\mathbb{M}_{\sigma}^{\mathfrak{dr}})^{-1} \mathbb{I}_{\mathcal{E},+}^{\mathfrak{m}}(\epsilon_{k};\tau) \mathbb{M}_{\sigma}^{\mathfrak{dr}} \mathbb{I}_{\mathcal{E},+}^{\mathfrak{dr}}(\epsilon_{k};\tau) . \tag{4.154}$$

We denote the map defined in this way by  $\Delta_p$  to signify that it is a proposal and we do not claim that it is equal to the motivic coaction for these objects. In particular, a better understanding of the de-Rham periods appearing in  $\mathbb{I}^{\mathfrak{dr}}_{\mathcal{E},+}(\epsilon_k;\tau)$  is necessary to write down the motivic coaction of these objects explicitly. Since the objects in  $\mathbb{I}^{\mathfrak{dr}}_{\mathcal{E},+}(\epsilon_k;\tau)$  are written as iterated Eisenstein integrals labelled by  $\mathfrak{dr}$  whereas de Rham periods are generally tuples of de Rham co-cycles and dual co-cycles, one needs a prescription to map the dual co-cycles to cycles of iterated Eisenstein integrals in a unique way (which involves a choice). Whilst an understanding of this prescription has not been obtained yet, the map  $\Delta_p$  still allows for simple closed expressions at low depth and has interesting properties. Differentiation with  $\tau$  acts

only on the  $\mathfrak{dr}$  entry of  $\Delta_p \mathbb{I}^{\mathfrak{m}}(\epsilon_k; \tau)$ . Thus, the genus-zero property  $\Delta \partial_z = (\mathbf{1} \otimes \partial_z) \Delta$  naturally extends to

$$\Delta_p \partial_\tau = (\mathbf{1} \otimes \partial_\tau) \, \Delta_p$$

for the iterated Eisenstein integrals appearing in the expansion of  $\mathbb{I}_{\mathcal{E},+}^{\mathfrak{m}}(\epsilon_{k};\tau)$ . All non-trivial iterated Eisenstein integrals (3.152) vanish in the regularized limit  $\tau \to i\infty$  and thus  $\lim_{\tau \to i\infty} \mathbb{I}_{\mathcal{E},+}(\epsilon_{k};\tau) = \mathbf{1}$ . This allows us to derive, that  $\Delta_{p}$  commutes with the limit at  $\tau \to i\infty$ . In the limit  $\tau \to 0$  – which can in principle be thought of as a limit to genus zero – the generating series of iterated Eisenstein integrals reduces to that of MMVs (3.165) and

$$\lim_{\tau \to 0} \mathbb{I}_{\mathcal{E},+}(\epsilon_k;\tau) = \mathbb{S}(\epsilon_k). \tag{4.155}$$

The assumption that the limit  $\tau \mapsto 0$  commutes with  $\Delta_p$ , i.e.,

$$\Delta_p \left( \lim_{\tau \to 0} \mathbb{I}_{\mathcal{E},+}^{\mathfrak{m}}(\epsilon_k; \tau) \right) = \lim_{\tau \to 0} \Delta_p \left( \mathbb{I}_{\mathcal{E},+}^{\mathfrak{m}}(\epsilon_k; \tau) \right), \tag{4.156}$$

is equivalent to it acting on  $\mathbb{S}^{m}$  by

$$\Delta_{p} \mathbb{S}^{\mathfrak{m}}(\epsilon_{k}) = \left(\mathbb{M}_{\sigma}^{\mathfrak{dr}}\right)^{-1} \mathbb{S}^{\mathfrak{m}}(\epsilon_{k}) \mathbb{M}_{\sigma}^{\mathfrak{dr}} \mathbb{S}^{\mathfrak{dr}}(\epsilon_{k}). \tag{4.157}$$

One can show, that the motivic coaction  $\Delta$  acts on  $\mathbb{S}^{\mathfrak{m}}$  in exactly that way [193], implying that when applied to multiple modular values,  $\Delta_p$  agrees with the motivic coaction. To verify this assertion, we inserted known multiple modular values in the f-alphabet into  $\mathbb{S}^{\mathfrak{m}}$  and computed the deconcatenation coaction for each coefficient. One can compare these to the coefficients on the right-hand side of (4.157) to confirm, that it gives the motivic coaction. We performed this check for the following depths and weights:

The advantage of the expression in eq. (4.157) is that it allows us to practically compute the motivic coaction of multiple modular values explicitly from the generating series. At genus zero, the coaction exhibits a particular behaviour under discontinuities [168]: de Rham periods (on the right-hand side of the coproduct) are only defined up to discontinuities. More generally, any de Rham period is defined by two de Rham representatives (as in (4.131)) and thus does not know how an integration cycle changes under a modular transformation. Instead, under a modular transformation  $\gamma$ , it is only sensitive to how  $\gamma$  acts on differential forms. To make this precise, we introduce an operation pre $\gamma$  that acts on differentials without affecting integration contours. Specifically, for the S- and T-transformations, we define

$$\operatorname{pre} \mathcal{S} \left[ \mathbb{Y} \right] = U_S^{-1} \mathbb{Y} U_S, \tag{4.158}$$

$$\operatorname{pre} \mathcal{T} \left[ \mathbb{Y} \right] = U_T^{-1} \mathbb{Y} U_T, \tag{4.159}$$

The translation between the motivic coaction in [193] and the action of  $\Delta_p$  on  $\mathbb{S}^{\mathfrak{m}}$  is obtained by the following translations:  $C_{\mathfrak{s}}^{\mathfrak{m}} \mapsto \mathbb{S}^{\mathfrak{m}}$   $\phi^{\mathfrak{m}} \mathbb{Y} \mapsto \mathbb{M}_{z}^{\mathfrak{m}} \mathbb{Y} \left(\mathbb{M}_{z}^{\mathfrak{m}}\right)^{-1}$   $b^{\mathfrak{m}} \mapsto \mathbb{M}_{z}^{\mathfrak{m}} \left(\mathbb{M}_{\sigma}^{\mathfrak{m}}\right)^{-1}$   $\mathbb{Y}|_{\gamma} \mapsto U_{\gamma} \mathbb{Y} U_{\gamma}^{-1}$   $s_{S} \mapsto \mathbb{X}_{S}.$ 

where  $U_S$  and  $U_T$  are given in (3.164) and (3.168). Notably,

$$pre S[A] = S[A]. \tag{4.160}$$

By explicitly performing S and T transformations to the generating series  $\mathbb{I}_{\mathcal{E},+}$  we find, that  $\Delta_p$  interacts with modular transformations  $\gamma$  by

$$\Delta_p\left(\gamma \mathbb{I}_{\mathcal{E},+}\left(\epsilon_k;\tau\right)\right) = \left(\gamma \otimes \operatorname{pre}\gamma\right)\left(\Delta_p \mathbb{I}_{\mathcal{E},+}\left(\epsilon_k;\tau\right)\right) \pm \mathbb{M}_{\sigma}^{\mathfrak{dr}} U_{\gamma} \mathbb{M}_{\sigma}^{\mathfrak{dr}} U_{\gamma}^{-1} \,. \tag{4.161}$$

The properties discussed here align with ones one would expect the motivic coaction to have, though to explicitly compare to the latter as defined in [193], one still needs to understand the appearing de Rham periods.

# 4.3 Aomoto-Gelfand Hypergeometric Functions

In Examples 4.1 and 4.2 as well as subsequent examples featuring these functions, we have already encountered Euler's  $\beta$  function and the hypergeometric  ${}_2F_1$  function. Those are the first two examples of Aomoto-Gelfand hypergeometric functions appearing in this thesis. Aomoto-Gelfand hypergeometric functions constitute a very general class of hypergeometric functions and were first introduced by Gelfand [281, 282] and then further studied by Aomoto [231, 283]. As these functions constitute a large class of examples for twisted periods and appear frequently in Feynman integrals as well as other physical objects, we explore them in more detail in this section and specifically consider several examples that arise again throughout this thesis. This section is supplemented with appendix B.2, where we give intersection matrices of twisted (co-)homology groups that one can associate to certain of these hypergeometric functions.

# 4.3.1 Definition of Aomoto-Gelfand Hypergeometric Functions

We primarily define the Aomoto-Gelfand hypergeometric functions<sup>26</sup> via their integral representation to get an immediate connection to their twisted (co-)homology groups [228]. We do not discuss other definitions or the general properties of Aomoto-Gelfand hypergeometric functions in detail here, but we refer to the literature (cf., e.g., refs. [228, 231, 281–283]).

**Definition 4.9** (Aomoto-Gelfand Hypergeometric Function). An Aomoto-Gelfand hypergeometric function of type (n+1,r+1) is defined by the data  $(\boldsymbol{\alpha}|\boldsymbol{\mu}|\boldsymbol{y}_{AG})$ , where<sup>27</sup>

•  $\alpha = (\alpha_0, \dots, \alpha_r) \in \mathbb{C}^r$  and  $\mu = (\mu_0, \dots, \mu_r) \in \mathbb{Z}^r$  are r + 1 dimensional vectors

<sup>26</sup>The same class of functions is also known with different names, including: Generalized Euler integrals, Mellin Integrals, A-hypergeometric integrals.

<sup>27</sup>In our examples, we keep the restriction of eq. (4.14), which means:  $\alpha_i \notin \mathbb{Z}, \sum_{i=0}^r \alpha_i \notin \mathbb{Z}.$ 

• and  $y_{AG}$  is an  $(n+1) \times (r+1)$  matrix of parameters:

$$\boldsymbol{y}_{\mathrm{AG}} = \begin{pmatrix} y_{00} & \dots & y_{0r} \\ \vdots & \ddots & \vdots \\ y_{n0} & \dots & y_{nr} \end{pmatrix} . \tag{4.162}$$

From this data we define:

$$\mathcal{F}(\boldsymbol{\alpha}|\boldsymbol{\mu}|\boldsymbol{y}_{AG}) = \int_{\Gamma} \Phi_{AG} \,\omega = \int_{\Gamma} \Phi_{AG} \,f \,\omega_n \,, \tag{4.163}$$

where

$$\Phi_{AG} = \prod_{j=0}^{r} (y_{0j}\tau_0 + y_{1j}\tau_1 + \dots + y_{nj}\tau_n)^{\alpha_j}$$
(4.164)

and the integrand involves the holomorphic n-form in the homogenous coordinates  $[\tau_0:\ldots:\tau_n]$  on  $\mathbb{P}^n_{\mathbb{C}}$ 

$$\omega_n = \sum_{i=0}^n (-1)^i \tau_i \, d\tau_0 \wedge \dots \wedge \widehat{d\tau_i} \wedge \dots \wedge d\tau_n , \qquad (4.165)$$

where the hat indicates that the corresponding element has been omitted. The rational function f takes the form

$$f = \prod_{j=0}^{r} (y_{0j}\tau_0 + y_{1j}\tau_1 + \dots + y_{nj}\tau_n)^{\mu_j} . \tag{4.166}$$

If  $\mu_i = 0$  for all i, then f = 1. We generally use the affine coordinate chart  $z_i = \frac{\tau_i}{\tau_0}$ ,  $1 \le i \le n$  in which the twist and the n-form are

$$\Phi_{AG} = \prod_{j=0}^{r} (y_{0j} + y_{1j}z_1 + \dots + y_{nj}z_n)^{\alpha_j} \text{ and } \omega_n = \bigwedge_{i=1}^{n} dz_i.$$
 (4.167)

The data  $(\alpha | \mu | y_{AG})$  also defines twisted (co-)homology groups: We take the twist from eq. (4.164) and define the space<sup>28</sup>

 $^{28}\mathrm{We}$  are working with the affine coordinates

$$X_{AG} = \mathbb{C}^n - \bigcup_{j=1}^r \{ z | y_{0j} + y_{1j} z_1 + \dots + y_{nj} z_n = 0 \}.$$
 (4.168)

Then we can interpret  $f\omega_n$  as an element of  $H_{dR}^n(X_{AG}, \nabla_{AG})$  and  $\Gamma$  as an element of  $H_n(X_{AG}, \check{\mathcal{L}}_{AG})$ . Finally, the Aomoto-Gelfand hypergeometric functions are twisted periods

$$\mathcal{F}(\boldsymbol{\alpha}|\boldsymbol{\mu}|\boldsymbol{y}_{\mathrm{AG}}) = \langle f\omega_n|\Gamma] \tag{4.169}$$

of these groups. One consequence of this interpretation is, that we can decompose any Aomoto-Gelfand hypergeometric functions into a *basis* of Aomoto-Gelfand hypergeometric functions via the completeness relations of eq. (4.55):

$$\mathcal{F}(\boldsymbol{\alpha}|\boldsymbol{\mu}|\boldsymbol{y}_{\mathrm{AG}}) = \boldsymbol{c}^{T} \mathbf{C}_{\mathrm{AG}}^{-1} \mathbf{P}_{\mathrm{AG}} \left(\mathbf{H}_{\mathrm{AG}}^{-1}\right)^{T} \boldsymbol{h}$$
(4.170)

with

$$\mathbf{c} = (2\pi i)^{-n} \left( \langle f \, \omega_n | \check{\varphi}_1 \rangle, \dots, \langle f \, \omega_n | \check{\varphi}_{d_{\mathbf{H}}} \rangle \right)^T, \tag{4.171}$$

$$\boldsymbol{h} = ([\check{\gamma}_1 | \Gamma], \dots, [\check{\gamma}_{d_{\mathrm{H}}} | \Gamma])^T, \tag{4.172}$$

where  $d_{\rm H}$  is the dimension of the (co-)homology group. All information on these functions is encoded in the period and intersection matrices. As is commonly done in the literature, we simply refer to the Aomoto-Gelfand hypergeometric functions as hypergeometric functions from here on.

# Lauricella functions $F_D^{(R)}$

The Lauricella functions  $F_D^{(R)}$  are defined by the hypergeometric series

$$F_D^{(R)}(a, \boldsymbol{b}, c; \boldsymbol{y}) = \sum_{i_1, \dots, i_r = 0}^{\infty} \frac{(a)_{i_1 + \dots + i_r} (b_1)_{i_1} \dots (b_r)_{i_r}}{(c)_{i_1 + \dots + i_r} i_1! \dots i_r!} y_1^{i_1} \dots y_r^{i_r}, \qquad (4.173)$$

where  $\boldsymbol{b} = (b_1, \dots, b_R)$  and  $\boldsymbol{y} = (y_1, \dots, y_R) \in \mathbb{C}^R$ . The Lauricella  $F_D^{(R)}$  admit the integral representation

$$F_D^{(R)}(a, \boldsymbol{b}, c; \boldsymbol{y}) = \frac{\Gamma(c)}{\Gamma(a)\Gamma(c-a)} \int_0^1 z^a (1-z)^{c-a} \prod_{j=1}^R (1-y_j z)^{-b_j} \frac{\mathrm{d}z}{z(1-z)} . \quad (4.174)$$

Additionally, we define the normalised version of the Lauricella functions  $F_D^{(R)}$  by

$$\mathcal{F}_{D}^{(R)}(a, \mathbf{b}, c; \mathbf{y}) = \beta(c - a, a) F_{D}^{(R)}(a, \mathbf{b}, c; \mathbf{y}).$$
 (4.175)

From the previous equation, we can recognise them as Aomoto-Gelfand hypergeometric functions of type (2, R + 2) with

$$\mathbf{y} = \begin{pmatrix} 0 & 1 & 1 & \dots & 1 \\ 1 & -1 & -y_1 & \dots & -y_R \end{pmatrix} . \tag{4.176}$$

For R = 0, we recover Euler's b function and for R = 1, 2 we obtain the hypergeometric functions of Gauss and Appell:

$$\beta(a,c) = F_D^{(0)}(a,c) \tag{4.177}$$

$$_{2}F_{1}(a,b_{1},c;y_{1}) = F_{D}^{(1)}(a,b_{1},c;y_{1}),$$

$$(4.178)$$

$$F_1(a, b_1, b_2, c; y_1, y_2) = F_D^{(2)}(a, b_1, b_2, c; y_1, y_2).$$

We also introduce their normalized versions:

$$_{2}\mathcal{F}_{1}(a,b_{1},c;y_{1}) = \beta(c-a,a)_{2}F_{1}(a,b_{1},c;y_{1}),$$

$$(4.179)$$

$$\mathcal{F}_1(a, b_1, b_2, c; y_1, y_2) = \beta(c - a, a) F_1(a, b_1, b_2, c; y_1, y_2). \tag{4.180}$$

From the integrand in eq. (4.174), we can read off the twist:

$$\Phi = z^a (1-z)^{c-a} \prod_{j=1}^R (1-y_j z)^{-b_j}. \tag{4.181}$$

In general<sup>29</sup>, we consider cases, where  $0 < |a|, |b_j|, |c-a| < 1$ . If this condition is not fulfilled, we can split the respective parameter into an integer part and a non-integer part that is smaller than one and proceed in the same way. To get the Lauricella function with the respective parameters, we just need to choose a form  $\varphi$  with a higher pole (regulated by the twist). Of course we can in principle also have exponents larger than one in the twist. The Lauricella functions  $F_D^{(R)}$  have been discussed in detail in [253] in the framework of twisted cohomology groups.

# define the twist to be $z^{a}(1-z)^{c-a}\prod_{j=1}^{R}(y_{j}^{-1}-z)^{-b_{j}}.$ We still define the

<sup>29</sup>Note that we can also

We still define the same (co-)homology groups, the specific hypergeometric functions just need prefactors to have the correct normalization.

#### Generalised hypergeometric $_{p+1}F_p$ functions

The generalised hypergeometric p+1 $F_p$  functions are defined by the series

$${}_{p+1}F_p(a_0, a_1, \dots, a_p, b_1, \dots, b_p, y) = \sum_{n=0}^{\infty} \frac{(a_0)_n \dots (a_p)_n}{(b_1)_n \dots (b_p)_n} \frac{y^n}{n!}, \qquad (4.182)$$

which converge on |y| < 1, and the  $b_i$  are not allowed to be negative integers. Additionally we assume that  $a_i - b_j \notin \mathbb{Z}$  and  $b_i - b_j \notin \mathbb{Z}$  for any i, j. For p = 1, we recover the definition of Gauss' hypergeometric function  ${}_2F_1$ . The generalised hypergeometric functions admit the integral representation:

$$_{p+1}F_p(a_0, a_1, \dots, a_p, b_1, \dots, b_p, y) = b(a_p, b_p - a_p)^{-1}$$
 (4.183)

$$\times \int_0^1 dt_p \, t_p^{a_p - 1} (1 - t_p)^{b_p - a_p - 1} {}_p F_{p-1}(a_0, \dots, a_{p-1}, b_1, \dots, b_{p-1}, yt_p) \tag{4.184}$$

$$= \left(\prod_{i=1}^{p} b(a_i, b_i - a_i)^{-1} \int_0^1 dt_i \, t_i^{a_i - 1} (1 - t_i)^{b_i - a_i - 1}\right) (1 - yt_1 \dots t_p)^{-a_0}, \quad (4.185)$$

with  ${}_{1}F_{0}(a_{0},y)=(1-y)^{-a_{0}}$ . We also define the normalised versions

$$_{p+1}\mathcal{F}_{p}\left(\boldsymbol{a},\boldsymbol{b},y\right) = _{p+1}F_{p}\left(\boldsymbol{a},\boldsymbol{b},y\right) \prod_{i=1}^{p} b(a_{i},b_{i}-a_{i})$$

$$(4.186)$$

$$= \left(\prod_{i=1}^{p} \int_{0}^{1} dt_{i} t_{i}^{a_{i}-1} (1-t_{i})^{b_{i}-a_{i}-1}\right) (1-yt_{1} \dots t_{p})^{-a_{0}}.$$
 (4.187)

where we set  $\mathbf{a} = (a_0, a_1, \dots, a_p)$  and  $\mathbf{b} = (b_1, \dots, b_p)$ . The zeros of the twist are located at the hyperplanes  $t_i = 0$  and  $t_i = 1$ , along with the hypersurface

 $1-yt_1 ldots t_p$ . For p>1, this hypersurface is not a hyperplane, which seems to imply that the generalised hypergeometric functions  $_{p+1}F_p$  do not directly fit into the category of Aomoto-Gelfand hypergeometric functions. However, by introducing a variable change  $t_i = \frac{z_i}{z_{i-1}}$  (where  $z_0 = 1$ ), we obtain

$$1 - t_i = \frac{z_{i-1} - z_i}{z_{i-1}} \quad \text{and} \quad 1 - yt_1 \dots t_p = 1 - z_p y. \tag{4.188}$$

In these new variables, the zeros of the twist appear at the hyperplanes  $z_i = 0$ ,  $z_i = z_{i-1}$ , and  $1-yz_p = 0$ . Consequently, the generalised hypergeometric functions  $p+1F_p$  are in fact Aomoto-Gelfand hypergeometric functions. The twisted (co-)homology groups associated with the generalised  $p+1F_p$  function are explored in detail in [284, 285]. The first non-trivial instance beyond the Gauss hypergeometric function occurs at p=2 with the hypergeometric  ${}_3F_2$  function:

$${}_{3}\mathcal{F}_{2}(\boldsymbol{a},\boldsymbol{b};y)$$

$$= \int_{0}^{1} \int_{0}^{1} t_{2}^{a_{2}-1} (1-t_{2})^{b_{2}-a_{2}-1} t_{1}^{a_{1}-1} (1-t_{1})^{b_{1}-a_{1}-1} (1-yt_{1}t_{2})^{-a_{0}} dt_{1} \wedge dt_{2}$$

$$= \int_{D_{1}} z_{1}^{a_{1}-b_{2}} z_{2}^{a_{2}-1} (1-z_{1})^{b_{1}-a_{1}-1} (1-yz_{2})^{-a_{0}} (z_{1}-z_{2})^{b_{2}-a_{2}-1} dz_{1} \wedge dz_{2}.$$

$$(4.189)$$

The integration region is  $D_1 = \{0 < x_2 < x_1 < 1\}$ . From the integrand in eq. (B.55), we read off the twist:

$$\Phi = z_1^{a_1 - b_2} z_2^{a_2} (1 - z_1)^{b_1 - a_1} (1 - y z_2)^{-a_0} (z_1 - z_2)^{b_2 - a_2}. \tag{4.190}$$

In general, we consider cases, where the exponents in the twist are between zero and one but as for the Lauricella function, other cases can also be treated equivalently. We provide the period and intersection matrices for this case in Appendix B, which is partially based on [285].

# 4.3.2 Single-valued Hypergeometric Functions

The single-valued version of an Aomoto-Gelfand hypergeometric function as in eq. (4.163) is

$$\mathcal{F}^{\text{sv}}(\boldsymbol{\alpha}|\boldsymbol{\mu}|\boldsymbol{y}_{\text{AG}}) = \int_{\Gamma} |\Phi_{\text{AG}}|^2 f \,\omega_n \wedge \overline{f\omega_n}, \qquad (4.191)$$

In the remainder of this section, we construct single-valued versions of special hypergeometric functions as bilinears in the respective class of functions – which is possible due to the double copy formula of (4.139).

**Example 4.17** (Single-valued Lauricella functions.). The single-valued analogues of the Lauricella  $F_D$  functions have been studied in detail in ref. [253]. They admit the integral representation:

$$\mathcal{F}_{D}^{sv}(a, \boldsymbol{b}, c; \boldsymbol{y}) = -\frac{1}{2\pi i} \int_{\mathbb{C}} dx \wedge d\bar{x} |x|^{2(a-1)} |1 - x|^{2(c-a-1)} \prod_{i=1}^{r} |1 - y_i x|^{-2b_i}. \quad (4.192)$$

We can express  $\mathcal{F}_D^{sv}(a, \mathbf{b}, c; \mathbf{y})$  as a bilinear combination of holomorphic Lauricella functions by utilizing eq. (4.139). The period and intersection matrices needed for this construction are provided in eq. (B.54) and eq. (B.52). Here, we specifically present the formulas for the cases r = 1 and r = 2, which correspond to Gauss' hypergeometric  $_2F_1$  function and the Appell  $F_1$  function, respectively (see eq. (4.177). For the single-valued analogue of Gauss' hypergeometric function, we find

$${}_{2}\mathcal{F}_{1}^{sv}(a,b_{1},c;y) = \frac{\mathfrak{s}(a)\mathfrak{s}(c-a)}{\pi\mathfrak{s}(c)}{}_{2}\mathcal{F}_{1}(a,b_{1},c;y){}_{2}\mathcal{F}_{1}(a,b_{1},c;\bar{y})$$
(4.193)

$$-\frac{\mathfrak{s}(b_1)\mathfrak{s}(c-b_1)}{\pi\mathfrak{s}(c)}{}_{2}\mathcal{G}_{1}(a,b_1,c;y){}_{2}\mathcal{G}_{1}(a,b_1,c;\overline{y}), \qquad (4.194)$$

where we introduced the abbreviation  $\mathfrak{s}(x) = \sin(\pi x)$ . The function  ${}_2\mathcal{F}_1(a,b_1,c;y)$  is the normalised Gauss hypergeometric function introduced in eq. (4.179), and the function  ${}_2\mathcal{G}_1(a,b_1,c;y)$  is given by

$$_{2}\mathcal{G}_{1}(a,b_{1},c;y) = (-1)^{c-a-b_{1}}y^{1-c}{}_{2}\mathcal{F}_{1}(1+a-c,1+b_{1}-c,2-c;y)$$
. (4.195)

This expression agrees with the one given in ref. [253]. The single-valued Appell  $F_1$  given by

$$\begin{split} \mathcal{F}_{1}^{sv}(a,b_{1},b_{2},c;y_{1},y_{2}) &= y_{1}^{-a}y_{2}^{-a} \frac{\mathbf{s}(a)\mathbf{s}(b_{1})\mathbf{s}(b_{2})\mathbf{s}(a-c)}{\mathbf{s}(b_{1}+b_{2}-c)} \\ \left\{ 2\mathcal{F}_{1}(a,b_{1},b_{2},c;\bar{y}_{1},\bar{y}_{2}) \left[ \frac{y_{1}^{a}y_{2}^{a}}{\mathbf{s}} \frac{\mathbf{s}(a-b_{1}-b_{2})}{\mathbf{s}(a)\mathbf{s}(b_{1})\mathbf{s}(b_{2})} \mathcal{F}_{1}(a,b_{1},b_{2},c;y_{1},y_{2}) \right. \\ &+ y_{1}^{a}(i+\mathfrak{C}(a))(1-i\mathfrak{C}(b_{1}))\mathcal{F}_{1}\left(a,1+a-c,b_{1},1+a-b_{2};\frac{1}{y_{2}},\frac{y_{1}}{y_{2}}\right) \\ &- y_{2}^{a}(i+\mathfrak{C}(a))(1+i\mathfrak{C}(b_{2}))\mathcal{F}_{1}\left(a,1+a-c,b_{2},1+a-b_{1};\frac{1}{y_{1}},\frac{y_{2}}{y_{1}}\right) \right] \\ &- \frac{e^{-i\pi(2(a+b_{1})+c)}y_{2}^{a}\bar{y}_{2}^{-a}}{\mathbf{s}(a)\mathbf{s}(a-c)} \mathcal{F}_{1}\left(a,1+a-c,b_{1},1+a-b_{2};\frac{1}{\bar{y}_{2}},\frac{\bar{y}_{1}}{\bar{y}_{2}}\right) \\ &\times \left[ \frac{y_{1}^{a}\left(e^{i\pi(2a+b_{1})}-e^{i\pi(b_{1}+2c)}\right)}{\mathbf{s}(b_{1})} \mathcal{F}_{1}(a,b_{1},b_{2},c;y_{1},y_{2}) \right. \\ &+ 2ie^{2i\pi(a+b_{1})}\mathcal{F}_{1}\left(a,1+a-c,b_{2},1+a-b_{1};\frac{1}{y_{1}},\frac{y_{2}}{y_{1}}\right) \right] \\ &- 2i\frac{e^{-i\pi(a-b_{2})}y_{1}^{a}\bar{y}_{1}^{-a}}{\mathbf{s}(a)} \mathcal{F}_{1}\left(a,1+a-c,b_{2},1+a-b_{1};\frac{1}{y_{1}},\frac{\bar{y}_{2}}{\bar{y}_{1}}\right) \\ &\times \left[ \frac{y_{2}^{a}}{\mathbf{s}(b_{2})}\mathcal{F}_{1}(a,b_{1},b_{2},c;y_{1},y_{2}) + \frac{e^{i\pi(a-b_{2}+c)}}{\mathbf{s}(a-c)}\mathcal{F}_{1}\left(a,1+a-c,b_{1},1+a-b_{2};\frac{1}{y_{2}},\frac{y_{1}}{y_{2}}\right) \right] \\ &+ \left[ \frac{2iy_{1}^{a}\bar{y}_{2}^{-a}\mathbf{s}(b_{1}-c)}{\mathbf{s}(a)\mathbf{s}(b_{1})\mathbf{s}(a-c)} \right| \mathcal{F}_{1}\left(a,1+a-c,b_{1},1+a-b_{2};\frac{1}{y_{2}},\frac{y_{1}}{y_{2}}\right) \right|^{2} + (y_{1},b_{1}\leftrightarrow y_{2},b_{2}) \right] \right\}, \end{split}$$

with  $\mathfrak{C}(x) = \cot(\pi x)$  and  $\mathfrak{s}(x) = \sin(\pi x)$ . For the construction of the analytic continuations of the Appell  $F_1$  function necessary to evaluate this function, we refer to ref. [286].

**Example 4.18** (Single-valued Generalized Hypergeometric  $_{p+1}F_p$  functions). The generalized hypergeometric  $_{p+1}F_p$  functions has been discussed in refs. [284, 285]. In Appendix B.2 we give the intersection and period matrices necessary to construct the single-valued versions of the functions with the double copy formula. This single-valued analogue is given by the integral (we use the conventions of Section 4.3.1):

$$\mathcal{F}_{p+1}^{sv}(\boldsymbol{a}, \boldsymbol{b}; y) = \left(-\frac{1}{2\pi i}\right)^{p} \int_{\mathbb{C}^{p}} dx_{1} \wedge \dots \wedge dx_{p} \wedge d\bar{x}_{1} \wedge \dots \wedge d\bar{x}_{p} |x_{p}|^{2(a_{p}-1)} \\
\times |1 - x_{1}|^{2(b_{1} - a_{1} - 1)} |1 - yx_{p}|^{-2a_{0}} \prod_{k=1}^{p-1} |x_{k}|^{2(a_{k} - b_{k+1})} |x_{k} - x_{k+1}|^{2(b_{k+1} - a_{k+1} - 1)},$$
(4.197)

(4.198)

which is equal to the following sum of bilinears of  $_{p+1}\mathcal{F}_p$  functions:

$$P_{p+1}\mathcal{F}_{p}^{sv}(\boldsymbol{a},\boldsymbol{b};y) = \left|_{p+1}\mathcal{F}_{p}(\boldsymbol{a},\boldsymbol{b};y)\right|^{2} \prod_{i=1}^{p} \frac{\mathfrak{s}(a_{i})\mathfrak{s}(b_{i}-a_{i})}{\pi\mathfrak{s}(b_{i})}$$

$$-\sum_{i=1}^{p} |y|^{2(1-b_{i})} \left|_{p+1}\mathcal{F}_{p}(\boldsymbol{a}_{i},\boldsymbol{b}_{i};y)\right|^{2} \frac{\mathfrak{s}(a_{0})\mathfrak{s}(b_{i}-a_{0})}{\pi\mathfrak{s}(b_{i})} \prod_{j=1,j\neq i}^{p} \frac{\mathfrak{s}(b_{i}-a_{j})\mathfrak{s}(b_{j}-a_{j})}{\pi\mathfrak{s}(b_{i}-b_{j})},$$

$$(4.199)$$

where we defined

$$\mathbf{a}_{i} = (1 + a_{i} - b_{i}, 1 + a_{1} - b_{i}, \dots, 1 + \widehat{a_{i}} - b_{i}, \dots, 1 + a_{p} - b_{i}, 1 + a_{0} - b_{i}),$$

$$(4.200)$$

$$\mathbf{b}_{i} = (1 + b_{1} - b_{i}, \dots, 1 + \widehat{b_{i}} - b_{i}, \dots, 1 + b_{p} - b_{i}, 2 - b_{i}).$$

$$(4.201)$$

We come back to these single-valued versions of hypergeometric functions when discussing two dimensional Feynman integrals in Chapter 8.

# 4.4 Feynman Integrals and Their Cuts as Twisted Periods

We conclude this chapter by explaining explicitly how one can interpret Feynman integrals as (relative) twisted periods. In particular, we discuss this interpretation for Feynman integrals in Baikov representation, as defined in eq. (2.34).<sup>30</sup> We focus on the Baikov integral  $\mathbb{I}_{\nu}$  of eq. (2.33) and do not take the prefactors arising in

<sup>&</sup>lt;sup>30</sup>It is also possible to interpret Feynman integrals as twisted periods starting from different representations and this was done e.g. in [47, 49].

Baikov representation into account. Obtained in the loop-by-loop approach, these integrals  $\mathbb{I}_{\nu}$  have the form

$$\mathbb{I}_{\boldsymbol{\nu}}(\{p_i \cdot p_j\}, \{m_j^2\}) = \int_{\mathcal{C}} \Phi \,\varphi_{\boldsymbol{\nu}} \text{ with } \Phi = \mathcal{B}_1(\boldsymbol{z})^{\alpha_1} \dots \mathcal{B}_K(\boldsymbol{z})^{\alpha_K}. \tag{4.202}$$

with C as given in eq. (2.39). The exponents of the twist depend on the dimension D and in particular in dimensional regularisation, they have the form

$$\alpha_i = \frac{\mu_i}{2} \pm \varepsilon \text{ with } \mu_i \in \mathbb{Z},$$

$$(4.203)$$

and the rational differential form is

$$\varphi_{\nu} = \mathrm{d}^{N} z \prod_{i=1}^{N} z_{i}^{-\nu_{i}} \,.$$
 (4.204)

This information defines (relative) twisted cohomology groups, from which we can construct a period matrix.<sup>31</sup> The product of Baikov polynomials raised to some non-integer powers containing the dimensional regulator  $\varepsilon$  defines the multi-valued twist  $\Phi$  and consequently a collection of bounding surfaces  $\Sigma$ . Additional poles not regulated by the twist arise due to the form  $\varphi_{\nu}$  and are located at the surfaces  $\{z_i=0\}$ . They can be gathered in  $D_-$  as described in eq. (4.92). Assuming the set of zeroes  $D_+$  is empty, we obtain the groups  $H_n(X_-, \check{\mathcal{L}}_{\Phi})$  and  $H^n_{dR}(X_-, \nabla_{\Phi})$  as well as their duals  $H_n(X_+, D_-, \mathcal{L}_{\Phi})$  and  $H^n_{dR}(X_+, D_-, \check{\nabla}_{\Phi})$  associated to the Feynman integral family. In general, we need to use relative twisted (co-)homology groups – i.e.  $D_- \neq \emptyset$  – for uncut Feynman integrals as not all poles of  $\varphi_{\nu}$  are regulated by the twist. As discussed in Subsection 4.2, the dual forms are qualitatively different in this situation. Though these dual Feynman integrands still carry valuable information and have been studied [47, 49, 288].

Let us start by making more comments on the forms spanning the cohomology group and repeat some properties we discussed for Feynman integrals but this time stated in the twisted cohomology framework: First of all, the forms can be split in different sectors. More specifically, every rational form  $\varphi_{\nu} \in H^{N}_{dR}(X_{-}, \nabla_{\Phi})$ that we consider a Feynman integrand is associated to a sector  $\Theta_{\nu} \in \{0,1\}^N$ , as defined in eq. (2.14).<sup>32</sup> The sectors have a natural partial order as defined in eq. (2.15). This partial order induces a partial order on the Feynman integrands – as it did for the master integrals. A sector is called reducible if every twisted cocycle belonging to this sector can be expressed as a linear combination of co-cycles from a lower sector. A top-sector is an irreducible sector that is maximal for the partial ordering. We denote the irreducible sectors of the family by  $\Theta_1, \ldots, \Theta_S$ and  $M_i$  is the number of master integrands in the irreducible sector  $\Theta_i$  – i.e. the number of basis elements needed to span the top sector. Note<sup>33</sup> that the overall number of master integrands of course must be equal to the dimension of the twisted cohomology group  $H^n_{dR}(X_-, \nabla_{\Phi})$  and in principle finding the basis of master integrands is equivalent to finding a basis for this group. Similarly, the IBP relations are just projections of elements of the cohomology group onto this basis, which can

<sup>&</sup>lt;sup>31</sup>Some ideas on period matrices for Feynman integrals were also presented in refs. [19, 287].

<sup>&</sup>lt;sup>32</sup>For simple reference, we state it here again:  $\Theta_{\nu} = (\theta_H(\nu_1), \dots, \theta_H(\nu_N))$  where  $\theta_H(\nu)$  is the Heaviside step function from eq. (4.110).

<sup>&</sup>lt;sup>33</sup>For some Feynman integral families, the dimension one obtains for the twisted cohomology group is smaller than the one found via IBP reduction, because the latter includes physical symmetries.

be done via intersection numbers. This fact has been used to compute IBP relations from intersection numbers [39, 40, 42, 44, 45, 239, 289]. We can always choose the basis to only consist of integrands from irreducible sectors.<sup>34</sup>

Integrating the master integrands along appropriate contours, we obtain the

Integrating the master integrands along appropriate contours, we obtain the master integrals. Integrating along all basis cycles, we obtain a generating set of periods that we collect in the period matrix. Note that integrating over a basis of cycles is equivalent to integrating over contours that encircle different poles, which means we compute cuts as described in eq. (2.44). We now give more details of this construction.

 $^{35}$ Here we give the sector a single number or letter T to name it.

ner: It is defined on

boundaries i.e. on cuts.

So we can build it cut-

by-cut as described in

[47, 49].

The full period matrix We start from the top-sector of the integral family and denote it by  $\Theta_T^{35}$  This sector is associated with  $M_T$  independent master integrands, which share the same propagators raised to a non-integer power. This is equivalent to seeing that there are  $M_T$  maximal cuts with each maximal cut corresponding to an independent contour encircling the propagators of the sector. These contours can be identified by determining a basis of (regularised) chambers bounded by the planes in  $\Sigma$  or in other words by analysing the zeroes of the Baikov polynomials. This is discussed in the physics literature cf., e.g., refs. [86, 290–292]. If we integrate the  $M_T$  master integrands from the sector  $\Theta_T$  around these  $M_T$  contours we obtain the  $M_T \times M_T$  matrix of maximal cuts. Similarly, one can find the master integrands and contours for each of the  $k_S$  sectors, where  $k_S$  is the number of sectors needed to fill the full basis, and order them sector by sector:

$$H_{n}(X_{-}, \check{\mathcal{L}}_{\Phi}) = \langle \underbrace{\gamma_{1,1}, \dots, \gamma_{1,M_{1}}}_{\text{Sector 1}} \dots \underbrace{\gamma_{k_{S},1}, \dots, \gamma_{k_{S},M_{k_{S}}}}_{\text{top sector}} \rangle.$$

$$(4.206)$$

Integrating a differential from a lower sector along a contour from a higher sector means integrating a rational form around a pole absent in this form. Thus, these integrals vanish. On the other hand, integrating a differential from a higher sector along a contour from a lower sector gives some twisted period that does not necessarily vanish and which is in general a (non-maximal) cut. Consequently, if we order the periods sector by sector in the period matrix – as indicated by eq. (4.205)— vectors associated to different sectors in the differentials automatically are linearly independent as they have zeroes at different positions. Vectors whose differentials are associated to the same sector are already linearly independent as the differentials chosen from a basis. Of course this linear independence is necessary for the period matrix to be non-degenerate. The preceding discussion should illuminate the properties related to the sectors. Before we continue this discussion, let us consider a simple example:

**Example 4.19** (Bubble Integral Family: The Period Matrix). We consider again the example of the bubble, from Example 2.5, with the integral defined in 2.16 and its sectors  $\Theta_1^{\circ} = (1,1), \Theta_2^{\circ} = (1,0)$  and  $\Theta_3^{\circ} = (0,1)$ . Each sector has one

master integral associated to it and we choose  $I_{1,1}^D$ ,  $I_{1,0}^D$  and  $I_{0,1}^D$ . We can write down a period matrix for the one-loop bubble integral as follows:

$$\mathbf{P}_{\circ} = \begin{pmatrix} m_1 & & & & \\ & \circ & 0 & 0 & \\ & m_2 & & \\ 0 & & \circ & 0 & \\ & m_1 & m_1 & m_1 & \\ & & \ddots & & \ddots & \\ & m_2 & m_2 & m_2 & \end{pmatrix} . \tag{4.207}$$

Analytic results for all the cut integrals entering the period matrix can be found in ref. [287].

Now that we have understood, how to interpret the cuts as twisted periods and how to construct the full period matrix from them, let us summarise some properties of this period matrix:

- 1. **P** has full rank, because all columns (and also the rows) are linearly independent.
- 2. Each column satisfies the differential equation (2.98) for this basis of master integrals.
- 3. If the master integrals and the maximal cut contours are ordered in a way that respects the natural partial ordering on the sectors, then  $\mathbf{P}$  is block lower-triangular. The blocks on the diagonal are the maximal cuts for the irreducible sectors, while the entries below the diagonal are non-maximal cuts.
- 4. All non-zero entries are cut Feynman integrals.

The first two properties indicate that the matrix we have just constructed is the fundamental solution to the differential equation governing the Feynman integral family. This is to be expected. Specifically, this implies that every solution to eq. (2.98) can be expressed as  $\mathbf{P}\hat{\mathbf{I}}_0$ , where  $\hat{\mathbf{I}}_0$  is a constant vector of boundary values. In particular, for every vector of master integrals  $\hat{\mathbf{I}}^{\text{uncut}}$  (evaluated on the contour defining the uncut integral) there is a boundary vector  $\hat{\mathbf{I}}_0^{\text{uncut}}$  such that  $\hat{\mathbf{I}}^{\text{uncut}} = \mathbf{P}\hat{\mathbf{I}}_0^{\text{uncut}}$ . As a result, each Feynman integral can be written as a linear combination of its cuts, as stated in the Feynman tree theorem [293, 294]. The existence of a spanning set of cuts with this property was also proposed as a conjecture in ref. [287].

The Maximal Cuts Let us now repeat this discussion for only the maximal cut (or the top sector). Note that, since taking the maximal cut is equivalent to integrating around all poles, the integrals in the maximal cut all take the form<sup>36</sup>

$$MC\left(\mathbb{I}_{\nu}(\{p_i \cdot p_j\}, \{m_j^2\}) \sim \int \Phi|_{z_1 \dots z_N \mapsto 0} dz_{N+1} \wedge \dots \wedge dz_n.$$
 (4.208)

 $^{36}$ Here we assume without loss of generality, that the parameters are ordered so that the physical propagators are the first N.

In this case, the integrand consists only of the multivalued twist and potentially forms with poles at the branch points of the twist. Thus,  $D_{-} = \emptyset$  and we work with twisted (co-)homology without requiring any regularisation. This case is important in the next chapter. We conclude this section with another example, this time one with a maximal cut that is associated to a twisted cohomology group with dimension larger than one.

**Example 4.20** (Unequal mass sunrise integral family: Period Matrix). As a second example we consider the unequal-mass sunrise integral in  $D = 2 - 2\varepsilon$  dimensions as introduced in Section 2.4.1. Its integral form was given is in eq. (2.46) and it has four irreducible sectors:

$$\Theta_1^{\oplus} = (1, 1, 1), \quad \Theta_2^{\oplus} = (0, 1, 1), \quad \Theta_3^{\oplus} = (1, 0, 1), \quad \Theta_4^{\oplus} = (1, 1, 0).$$
(4.209)

The subsectors  $\Theta_2^{\oplus}$ ,  $\Theta_3^{\oplus}$ ,  $\Theta_4^{\oplus}$  each have one master integral, all simply given by two-loop tadpole integrals. The top sector,  $\Theta_1^{\oplus}$  has four master integrals. Equivalently we also have four independent maximal cuts and can give a  $4 \times 4$  matrix for the maximal cut period matrix. Structurally, the period matrix for the unequal mass sunrise family looks as depicted in figure 4.8.

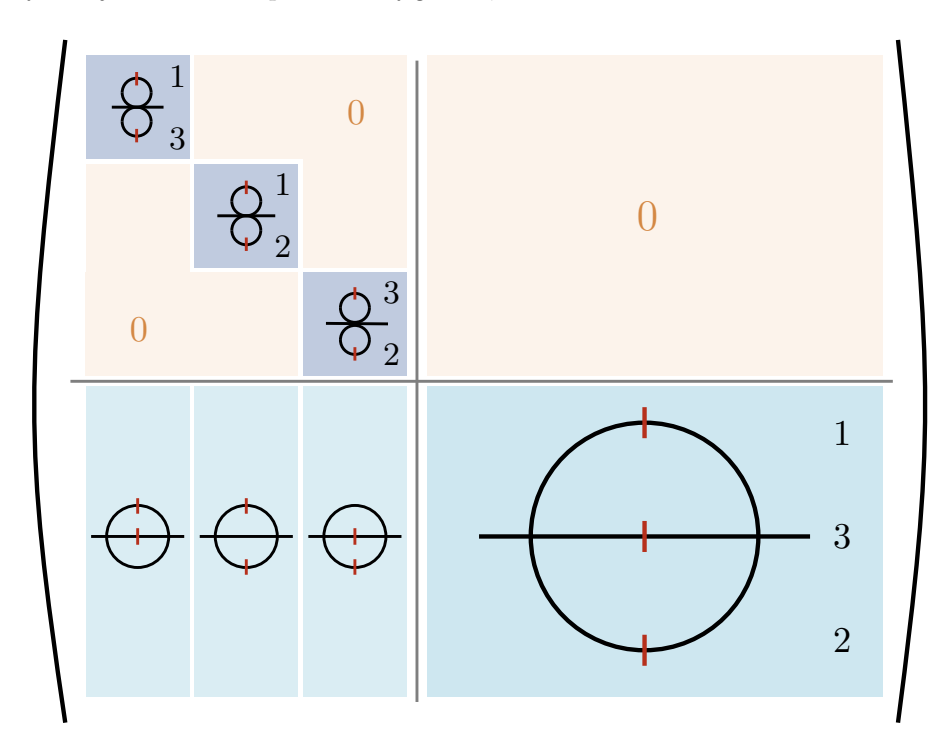


Figure 4.8: The unequal mass sunrise integral family has seven master integrals and four of these are in the top sector.

Here the lower right block is a  $4 \times 4$  matrix of integrals involving the four independent maximal cut contours and master integrands of the top sector  $\Theta_1^{\odot}$ . This block is the maximal cut period matrix and as promised above we discuss it separately in detail here. We already found, that the integrand of a maximal cut for the

unequal mass sunrise integral takes the form given in eq. (2.54) of Example 2.9. Now, we can extract a multivalued twist from this expression, which takes the form

$$\Phi_{\oplus} = z^{\varepsilon} \left[ (z - \lambda_1)(z - \lambda_2)(z - \lambda_3)(z - \lambda_4) \right]^{-\frac{1}{2} - \varepsilon} . \tag{4.210}$$

Additionally, we define the space  $X_{\oplus} = \mathbb{C} - \{0, \lambda_1, \lambda_2, \lambda_3, \lambda_4, \infty\}$  and we define the twisted (co-)homology groups  $H^1_{dR}(X_{\oplus}, \nabla_{\oplus})$  and  $H_1(X_{\oplus}, \check{\mathcal{L}}_{\oplus})$  as well as their duals. We choose for the basis of  $H^1_{dR}(X_{\oplus}, \nabla_{\ominus})$  the following differentials:

$$\varphi_1^{\oplus} = \mathrm{d}z\,,\tag{4.211}$$

$$\varphi_2^{\oplus} = \left(z^2 - \frac{s_1}{2}z + \frac{s_2}{6}\right) dz,$$
 (4.212)

$$\varphi_3^{\oplus} = z \, \mathrm{d}z \,, \tag{4.213}$$

$$\varphi_4^{\Leftrightarrow} = \frac{\mathrm{d}z}{z} \,, \tag{4.214}$$

with  $s_i$  elementary symmetric polynomials in the branch points  $\lambda_1, \ldots, \lambda_4$ . The differentials  $\varphi_1^{\oplus}, \varphi_2^{\oplus}, \varphi_3^{\oplus}$  are inspired by the natural Abelian differentials of the elliptic curve related to this integral. For the dual basis of  $H_{dR}^n(X, \nabla_{\ominus})$  we choose

$$\check{\varphi}_i^{\oplus} = \left[ \varphi_i^{\oplus} \left( \Phi_{\oplus}^2 |_{\varepsilon \to 0} \right) \right]_c, \qquad i = 1, \dots, 4.$$
 (4.215)

For the dual homology basis we choose cycles supported on

$$\Delta_{\check{\gamma}_1, \oplus} = [\lambda_2, \lambda_3], \tag{4.216}$$

$$\Delta_{\tilde{\gamma}_2, \oplus} = [\lambda_2, \lambda_3] \tag{4.217}$$

$$\Delta_{\check{\gamma}_3, \oplus} = [\lambda_1, \lambda_2] + [\lambda_3, \lambda_4], \qquad (4.218)$$

$$\Delta_{\tilde{\gamma}_4, \oplus} = [\lambda_4, 0]. \tag{4.219}$$

This basis is depicted in figure 4.9, together with the canonical cycles a and b of the elliptic curve. Additionally, we choose the basis of the twisted homology group to be supported on the regularised version of the dual cycles.

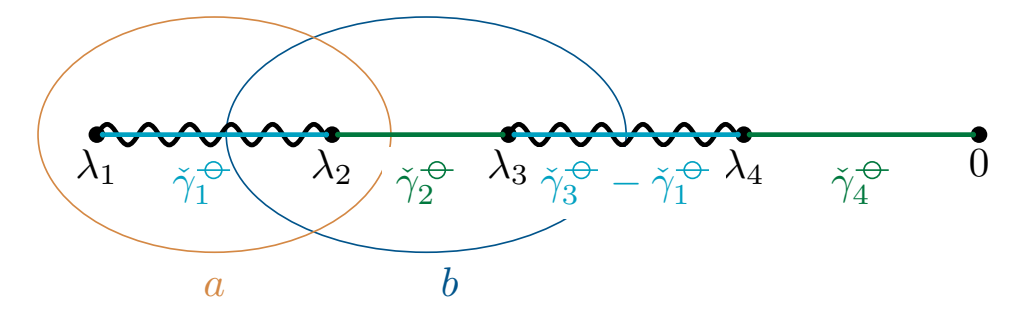


Figure 4.9: We derive the twisted cycles that we choose for the basis of the sunrise's homology group by choosing the intervals related to the sunrise's elliptic curve's a and b cycles .

The period matrix only contains Lauricella functions with five branch points and fulfils:

$$\check{\mathbf{P}}_{\oplus}(\boldsymbol{x},\varepsilon) = \mathbf{P}_{\oplus}(\boldsymbol{x},-\varepsilon). \tag{4.220}$$

# Twisted Riemann Bilinear Relations and Cuts of Feynman Integrals

TRBRs:

$$\begin{split} \mathbf{P} \left( \mathbf{H}^{-1} \right)^T \check{\mathbf{P}}^T \, \sim \mathbf{C} \,, \\ \mathbf{P}^T \left( \mathbf{C}^{-1} \right)^T \check{\mathbf{P}} \, \sim \mathbf{H} \,. \end{split}$$

#### See also:

- In Chapter 4 we introduced the basics on twisted (co-)homology groups.
- In Chapter 6 we use the insights of Section 5.2 to obtain canonical differential equations for models of hyperelliptic maximal cuts.

This chapter builds directly on the discussion of Section 4.4, where we explored the interpretation of (cuts of) Feynman integrals as twisted periods and explained how one can write down a period matrix of cuts for a given Feynman integral family. In particular, this allows us to take advantage of relations for twisted (co-)homology groups. Here, we focus on the implications of one specific (set of) relations: the twisted Riemann bilinear relations of eq. (4.58), as established in [230]. The first natural question that arises in this context is the following:

Do we obtain new relations for (cuts of) Feynman integrals from the twisted Riemann bilinear relations?

We explore this question in Section 5.1. Despite finding that we only obtain meaningful relations on the level of maximal cuts, we can leverage these in finding the canonical differential equation for a Feynman integral family. In particular, we also find that there is a deeper connection between the canonical basis and properties of the intersection matrices that one can derive using the twisted Riemann bilinear relations. We do so in Section 5.2, where we also understand how a notion of self-duality for Feynman integrals arises from their properties as entries of a twisted period matrix and explain how to practically use these insights in finding the canonical basis.

♠ This chapter closely follows previously published results [50, 226], which were obtained in collaborations with Claude Duhr, Cathrin Semper and Sven Stawinski.

# Contents of this Chapter

	US OI U	ms Chapter
5.	.1 Biliı	near Relations for Feynman Integrals 140
	5.1.1	Classification of the TRBRs for Feynman Integrals $142$
	5.1.2	Bilinear Relations for Maximal Cuts
	5.1.3	Examples
5.	2 The	Intersection Matrix for Canonial Differential Equa-
	${f tion}$	s
	5.2.1	Properties of Canonical Differential Equations 154
	5.2.2	Bases in $C$ -Form and the Intersection Matrix 158
	5.2.3	Maximal Cuts in $C$ -Form

# 5.1 Bilinear Relations for Feynman Integrals

In this section, we primarily put together everything we have understood about (cuts of) Feynman integral and twisted cohomology so far to answer the question asked in the introduction of this chapter. To contextualise our results, we start by reviewing bilinear relations for cuts of Feynman integrals that have appeared in the literature. In all cases, those take the form:

$$\mathbf{P}(\lambda, -\varepsilon)^T \mathbf{M}_1(\lambda, \varepsilon) \mathbf{P}(\lambda, \varepsilon) = \mathbf{M}_2(\varepsilon), \qquad (5.1)$$

where  $\mathbf{P}(\lambda, \varepsilon)$  and  $\mathbf{M}_i(\lambda, \varepsilon)$  are matrices. The matrix  $\mathbf{M}_2(\varepsilon)$  is independent of the kinematic variables. Specifically,  $\mathbf{P}(\lambda, \varepsilon)$  contains (cuts of) Feynman integrals<sup>1</sup>. In particular, the following types of bilinear relations for cuts exist in the literature:

- Quadratic relations for Feynman integrals were first studied for maximal cuts of equal-mass banana integrals with parameters  $p^2 = m^2$  [295]. Further discussions related to these relations can be found in [296–300].
- Maximal cuts of certain Feynman integrals evaluate to periods of Calabi-Yau varieties in the limit  $\varepsilon \to 0$ . These fulfill the Hodge-Riemann bilinear relations of eq. (3.107) as discussed in [12–16, 18–20, 277, 301].
- In [302, 303] quadratic relations for maximal cuts beyond the limit  $\varepsilon \to 0$  were observed and studied.

Throughout this section, we see how all of these relations can be derived from the TRBRs. At a first glance, it seems that the quadratic relations in eq. (5.1) and the twisted Riemann bilinear relations in eq. (4.58) take different forms: Instead of two copies of the period matrix, the latter involve the period matrix and the dual period matrix. Its entries are dual Feynman integrals, which are – in the fully general case – not related to the Feynman integrals themselves in a non-trivial way – except through the TRBRs themselves. Thus, a necessary condition for deriving quadratic relations for Feynman integrals from the TRBRs is that the entries of the dual period matrix  $\check{\mathbf{P}}$  are linear combinations of those of  $\mathbf{P}$  with  $\varepsilon \to -\varepsilon$ . Before we extend Let us start with a simple example that already illustrates many of the generic structures we discuss throughout this chapter.

**Example 5.1** (The Massive Bubble in  $D = 2 - 2\varepsilon$  Dimensions: TRBR). Let us take as a simple example the one-loop bubble integral from examples 2.5, 2.6 and 4.19 with  $m_1 = m$  and  $m_2 = 0$ . Since one propagator is massless this integral family has only two master integrals – the massless tadpole is scaleless and thus vanishes. The period matrix of cuts is the following sub-matrix of the one in eq. (4.207):

$$\mathbf{P}_{\diamondsuit} = \begin{pmatrix} m_1 \\ \diamondsuit & 0 \\ m_1 & m_1 \\ -\diamondsuit & -\diamondsuit \\ m_2 & m_2 \end{pmatrix} . \tag{5.2}$$

<sup>1</sup>We already denote the matrix of cuts by  $\mathbf{P}(\lambda,\varepsilon)$  as we saw in Section 4.4 how to define a period matrix of cuts, which this matrix will turn out to be. But for now, we just assume they are some matrices of Feynman integrals that fulfill such relations. Analytic expressions for the cuts in this period matrix in the region  $p^2 > m^2 > 0$  are (cf. ref. [260]):

$$\diamondsuit = e^{\gamma_E \varepsilon} \frac{(-m^2)^{-\varepsilon}}{\Gamma(1-\varepsilon)} \,, \tag{5.3}$$

$$-\!\!\!\!\!-- = e^{\gamma_E \varepsilon} \frac{(-m^2)^{-\varepsilon}}{p^2 \Gamma(1-\varepsilon)} {}_2F_1\left(1, 1+\varepsilon; 1-\varepsilon; \frac{m^2}{p^2}\right), \tag{5.4}$$

Note that the period matrix of eq. (5.2) can be obtained from the period matrix  $\mathbf{P}_R$  in eq. (4.114) by a specific parameter choice and a simple rotation in the homology and cohomology bases

$$\mathbf{P}_{\circlearrowleft} = \mathbf{T}_c \, \mathbf{P}_R \mathbf{T}_h \tag{5.6}$$

with the parameter choice  $b=1+\varepsilon$ ,  $c=-\varepsilon$  and  $\lambda=\frac{p^2}{m^2}$  in  $\mathbf{P}_R$  and the rotations

$$\mathbf{T}_{c} = e^{\gamma_{E}\varepsilon} m^{-2\varepsilon} \begin{pmatrix} \frac{1}{\pi\varepsilon} \frac{\Gamma(-\varepsilon)}{(\cot(\pi\varepsilon)+i)\Gamma(-1-2\varepsilon)} & 0\\ 0 & \frac{e^{-i\pi\varepsilon}}{p^{2}\Gamma(1-\varepsilon)} \end{pmatrix} \text{ and } \mathbf{T}_{h} = \begin{pmatrix} 0 & -\frac{2e^{3\pi i\varepsilon}\Gamma(1-\varepsilon)^{2}}{\Gamma(1-2\varepsilon)}\\ 1 & 0 \end{pmatrix}.$$

For the dual forms (and cycles) we are free to choose bases and natural choices for dual Feynman integrands have been discussed in [47, 49]. We make a particular choice to obtain bilinear relations between some entries. Namely we rotate the bases from Example 4.8, so that the bubble's dual period matrix is

$$\check{\mathbf{P}}_{--} = \check{\mathbf{T}}_c \check{\mathbf{P}}_R \check{\mathbf{T}}_h \tag{5.7}$$

with  $\check{\mathbf{P}}_R$  from eq. (4.114) and the same parameter choice as below eq. (5.6) and

$$\check{\mathbf{T}}_h = \begin{pmatrix} 0 & 1 \\ 1 & 0 \end{pmatrix} \ and \ \check{\mathbf{T}}_c = \begin{pmatrix} \frac{e^{i\pi\varepsilon}m^{2\varepsilon}(1+\varepsilon)\Gamma(\varepsilon)\sin(\pi\varepsilon)}{\pi\Gamma(1+2\varepsilon)} & 0 \\ 0 & -\frac{2e^{-2i\pi\varepsilon}p^2m^{2\varepsilon}\Gamma(1+\varepsilon)}{(m^2-p^2)^2\Gamma(1+2\varepsilon)} \,. \end{pmatrix} \,.$$

For this basis choice the dual bubble period matrix is

$$\check{\mathbf{P}}_{\circ} = \begin{pmatrix} - -e^{3\pi i \varepsilon} m^{2\varepsilon} (1+\varepsilon) \beta \left( \frac{m^2}{p^2}, 1-\varepsilon, 1+2\varepsilon \right) \frac{\Gamma(\varepsilon) \sin(\pi \varepsilon)}{\pi \Gamma(1+2\varepsilon)} \\ 0 - -e^{3\pi i \varepsilon} m^{2\varepsilon} (1+\varepsilon) \beta \left( \frac{m^2}{p^2}, 1-\varepsilon, 1+2\varepsilon \right) \frac{\Gamma(\varepsilon) \sin(\pi \varepsilon)}{\pi \Gamma(1+2\varepsilon)} \end{pmatrix}$$
(5.8)

and in particular the diagonal entries are related to the maximal cuts by a transformation<sup>2</sup>  $\varepsilon \to -\varepsilon$ . On the other hand, the off-diagonal entries are distinct objects, not related to linear combinations of the periods in a non-trivial way. The intersection matrices are

<sup>2</sup>We later discuss this to be a generic feature of the diagonal blocks.

$$\mathbf{C}_{\bigcirc} = \mathbf{T}_c \, \mathbf{C}_R \check{\mathbf{T}}_c^T = \begin{pmatrix} -\frac{\sin(\pi\varepsilon)\sin(2\pi\varepsilon)}{\pi^2\varepsilon} & 0\\ \frac{\Gamma(\varepsilon)\sin(\pi\varepsilon)}{p^2\pi\Gamma(1-\varepsilon)\Gamma(1+2\varepsilon)} & \frac{2\Gamma(1+\varepsilon)}{(m^2-p^2)^2\Gamma(1-\varepsilon)\Gamma(1+2\varepsilon)} \end{pmatrix}$$
(5.9)

$$\mathbf{H}_{-} = \check{\mathbf{T}}_{h}^{T} \mathbf{H}_{R} \mathbf{T}_{h} = \begin{pmatrix} \frac{i \csc(2\pi\varepsilon)}{2} & 0\\ 0 & \frac{1}{i\pi} \frac{\Gamma(1-\varepsilon)^{2}}{\Gamma(1-2\varepsilon)} \end{pmatrix}.$$
 (5.11)

Inserting these period and intersection matrices into the TRBRs, we find two relations that are bilinear in the maximal cuts in our conventions:

$$- - \left( - - - \right) = \frac{4\cos(\pi\varepsilon)}{(m^2 - p^2)^2}, \qquad (5.12)$$

$$\diamondsuit \left( \diamondsuit |_{\varepsilon \to -\varepsilon} \right) = \frac{\sin(\pi \varepsilon)}{\pi \varepsilon}.$$
(5.13)

One can use the third relation, for the off-diagonal non-trivial entry in the TRBRs to determine:

$$\left(\check{\mathbf{P}}_{-\bigcirc}\right)_{1,2} = \frac{1}{-\bigcirc} \frac{\sin(2\pi\varepsilon)}{p^2\pi^2\varepsilon} \left(\pi + p^2\Gamma(1-\varepsilon)^2\Gamma(1+2\varepsilon)\sin(2\pi\varepsilon) - \bigcirc\left(\bigcirc\right|_{\varepsilon \to -\varepsilon}\right)\right). \tag{5.14}$$

As expected the TRBRs can be split into two groups: one which allows us to write the off-diagonal elements of the dual period matrix in terms of Feynman integrals, and the other which give bilinear relations between maximal cuts evaluated at  $\varepsilon$  and  $-\varepsilon$  respectively.

In this example, the only relations between Feynman integrals appear on the diagonal, whilst off-diagonal entries involve objects unrelated to Feynman integrals, except via the twisted Riemann bilinear relations themselves. In the next section we explore this as a general feature and identify where non-trivial relations do appear.

# 5.1.1 Classification of the TRBRs for Feynman Integrals

What distinguishes the diagonal entries (or blocks) of the period matrix is that they correspond to maximal cuts. In general, maximal cuts are defined by integrals whose integrands have no poles that are not regulated by the Baikov polynomial (which plays the role of the twist). We observe that this property — and, in particular, the specific form taken by the twist defined through the Baikov polynomial in the maximal cut limit — enables us to identify non-trivial relations between Feynman integrals and their duals. We interpret this as the self-duality of the maximal cut period matrix. This feature is what allows us to extract non-trivial bilinear relations from the TRBRs, as in Example 5.1.

All poles regulated by the twist As long as we define twisted (co-)homology groups, so that the condition in eq. (4.14) holds – which is whenever all poles of the integrand are regulated by the twist – the *self-duality* condition of eq. (4.87) also holds. Then we can choose bases so that  $\check{\mathbf{P}}(\lambda, \alpha) = \mathbf{P}(\lambda, -\alpha)$ , with  $\alpha$  being the

exponents in the twist. In particular, this relation relies on choosing the *same* bases for the twisted (co-)homology group and its dual – or rather regularised versions of each other.<sup>3</sup> In that case the TRBRs turn into relations that are bilinear in the period matrix, albeit with one copy evaluated with  $\alpha_i \to -\alpha_i$ :

<sup>3</sup>As we can easily see in eq. (4.83).

$$\frac{1}{(2\pi i)^n} \mathbf{P}^T \left( \mathbf{C}^{-1} \right)^T \left( \mathbf{P} |_{\alpha_i \to -\alpha_i} \right) = \mathbf{H}, \quad \text{if condition (4.14) holds.}$$
 (5.15)

Maximal cuts always define twisted (co-)homology groups where all poles are regulated by the twist when all residues have been taken – see, e.g., eq. (4.208). Thus, for maximal cuts we can always choose a basis such that the TRBRs reduce to bilinear relations in periods. Beyond that, we can actually find bases such that instead of relating the period matrix and its dual via  $\alpha_i \to -\alpha_i$  – which by itself doesn't have much physical meaning – we can relate them via  $\varepsilon \to -\varepsilon$ : Consider a family of Feynman integrals and a sector  $\Theta$ , which we assume without loss of generality to be of the form

$$\Theta = (\underbrace{1, \dots, 1}_{m}, \underbrace{0, \dots, 0}_{N-m}). \tag{5.16}$$

We consider its maximal cut, i.e. the cut in all of the first m propagators. The cut Baikov-polynomials define a twist :

$$\Phi =: \left(\prod_{k=1}^{K} \mathcal{B}_{i}^{\text{m.c.}}(\boldsymbol{z})^{\frac{\mu_{k}}{2} \pm \varepsilon}\right) = \left(\prod_{k=1}^{K} \mathcal{B}_{i}(\boldsymbol{z})^{\frac{\mu_{k}}{2} \pm \varepsilon}\right) |_{z_{1}=\dots,=z_{m}=0} \text{ with } \mu_{k} \in \{0, \pm 1\}.$$

$$(5.17)$$

Then – as described in Section 4.4 – we define a twisted cohomology group  $H^1_{dR}(X, \nabla_{\Phi})$  and choose some basis

$$\varphi_i = f_i(z_{m+1}, \dots, z_N) \wedge_{i=m+1}^N dz_i \text{ with } i = 1, \dots, M_{\Theta},$$
 (5.18)

where the  $f_i(z)$  are rational functions in the  $z_{m+1}, \ldots, z_N$ . Additionally, we choose a basis of cycles  $\gamma_i$  for  $H_1(X, \check{\mathcal{L}}_{\Phi})$  and the entries of the corresponding period matrix are

$$P_{ij}(\boldsymbol{\lambda}, \varepsilon) = \int_{\gamma_j} \varphi_i \prod_{k=1}^K \mathcal{B}_i^{\text{m.c.}}(\boldsymbol{z})^{\frac{\mu_k}{2} + \sigma_k \varepsilon}.$$
 (5.19)

For the basis of  $H^1_{dR}(X, \check{\nabla}_{\Phi})$  we choose

$$\check{\varphi}_i = \left[ (\varphi_i|_{\varepsilon \to -\varepsilon}) \cdot \left( \Phi_{\varepsilon \to 0}^2 \right) \right]_c. \tag{5.20}$$

Since in the limit  $\varepsilon \to 0$ , all factors of the twist have exponents  $\frac{\mu_k}{2}$  with  $\mu_k$  an integer, the factor  $\Phi_{\varepsilon\to 0}^2$  in eq. (5.20) is a rational function and not multi-valued. This choice allows us to obtain the relation

$$\check{P}_{ij}(\boldsymbol{\lambda}, \varepsilon) = \int_{\gamma_j} \check{\varphi}_i \left( \prod_{k=1}^K \mathcal{B}_i^{\text{m.c.}}(\boldsymbol{z})^{\frac{\mu_k}{2} + \sigma_k \varepsilon} \right)^{-1}$$
(5.21)

$$= \int_{\gamma_j} \varphi_i \prod_{k=1}^K \mathcal{B}_i^{\text{m.c.}}(\boldsymbol{z})^{\mu_k} \left( \prod_{k=1}^K \mathcal{B}_i^{\text{m.c.}}(\boldsymbol{z})^{\frac{\mu_k}{2} + \sigma_k \varepsilon} \right)^{-1}$$
(5.22)

$$= \int_{\gamma_j} \varphi_i \prod_{k=1}^K \mathcal{B}_i^{\text{m.c.}}(\boldsymbol{z})^{\frac{\mu_k}{2} - \sigma_k \varepsilon} = P_{i,j}(\boldsymbol{\lambda}, -\varepsilon).$$
 (5.23)

between the period matrix and the dual period matrix. Then, the TRBRs in eq. (4.58) are

$$\frac{1}{(2\pi i)^h} \mathbf{P}(\boldsymbol{\lambda}, \varepsilon)^T (\mathbf{C}(\boldsymbol{\lambda}, \varepsilon)^{-1})^T \mathbf{P}(\boldsymbol{\lambda}, -\varepsilon) = \mathbf{H}(\varepsilon), \qquad (5.24)$$

or equivalently

$$\frac{1}{(2\pi i)^h} \mathbf{P}(\boldsymbol{\lambda}, \varepsilon) \left( \mathbf{H}(\varepsilon)^{-1} \right)^T \mathbf{P}(\boldsymbol{\lambda}, -\varepsilon)^T = \mathbf{C}(\boldsymbol{\lambda}, \varepsilon).$$
 (5.25)

These relations have the form anticipated in eq. (5.1). We discuss further implications of these relations for maximal cuts in the following subsection. In general we do not obtain such relations for non-maximal cuts, but there are special cases where they still apply: There are Feynman integral families where a sector has no sub-sectors in the natural partial ordering. In this case, all Feynman integrals and cuts from that sector can be expressed as linear combinations of maximal cuts, which satisfy condition (4.14). A trivial example for this scenario is the tadpole integral. One can also generate non-trivial examples: We begin with a Feynman graph that has no self-loops (i.e., no banana subgraph). Each edge is then replaced either by a banana graph with at least two loops and at most one massive propagator or by a one-loop massless bubble graph. It is straightforward to verify that such a graph has no subsectors, as contracting any propagator results in a graph containing a detachable massless tadpole integral, which vanishes in dimensional regularization. For these graphs, Feynman integrals without cut propagators decompose into linear combinations of maximal cuts, allowing the TRBRs to yield quadratic relations. So far, we have generalized the observation we have made in example 5.1 concerning the diagonal entries of the period matrix: Namely, that we can obtain bilinear relations for those and even for diagonal blocks that are maximal cuts. Now we also generalize the behaviour of the off-diagonal entries.

Additional poles In general, condition (4.14) is not satisfied for non-maximal cuts and the Feynman integral family defines relative twisted (co-)homology groups.<sup>4</sup> Consequently, the dual period matrix consists of dual periods that are qualitatively distinct from the standard periods which are the Feynman integrals and cannot be directly identified with those in a non-trivial way. But the twisted Riemann bilinear relations can in principle be used to connect these distinct objects to periods and intersection numbers:

$$\check{\mathbf{P}} = (2\pi i)^n \, \mathbf{C}^T \, (\mathbf{P}^{-1})^T \, \mathbf{H} \,. \tag{5.26}$$

<sup>4</sup>Alternatively, one can work with a regulator as in Example 4.10, but this does not change the outcome of the discussion here as we briefly outline below.

The intersection number are rational in the kinematic variables  $\lambda$  and the inverse of the period matrix is

$$(\mathbf{P}^{-1})_{ji} = (\det \mathbf{P})^{-1} (-1)^{i+j} \mathbf{M}_{ij},$$
 (5.27)

where  $\mathbf{M}_{ij}$  is the minor of  $\mathbf{P}$  obtained by deleting the  $i^{\text{th}}$  row and  $j^{\text{th}}$  column of  $\mathbf{P}$ .  $\mathbf{P}$  is lower triangular, so its determinant is

$$\det \mathbf{P} = \prod_{i=1}^{S} \det \mathbf{P}_{\mathbf{\Theta}_i}, \qquad (5.28)$$

where  $\mathbf{P}_{\Theta_i}$  is the period matrix of maximal cut associated to the master integrals in the sector  $\Theta_i$ . So, dual periods can be expressed as cuts multiplied with determinants of maximal cuts via the TRBRs.

Let us briefly comment on another approach to work with a generic Feynman integral family as in eq. (4.202). The poles in its integrand arise due to the factors  $z_i^{-\nu_i}$  in eq. (4.204), that are not regulated by the twist. To address this, we include them in the twist with exponents<sup>5</sup>  $\delta_i$ , which we ultimately set to zero but treat as generic for now<sup>6</sup>:

$$\mathbb{I}_{\boldsymbol{\nu},\boldsymbol{\delta}}(\{p_i \cdot p_j\}, \{m_j^2\}) = \int_{\mathcal{C}} \left[ \Phi\left(\prod_{i=1}^N z_i^{\delta_i}\right) \right] \prod_{i=1}^N z_i^{-\nu_i} d^N z \text{ with } \Phi = \mathcal{B}_1^{\alpha_1} \dots \mathcal{B}_K^{\alpha_K}.$$
(5.29)

For simplicity, we choose  $\delta_i = \delta \, \forall i$ . This choice of regulator is equivalent to shifting all propagators weights by  $\nu_i \to \nu_i - \delta_i$ . We include these factors with generic exponent in an alternative twist

$$\tilde{\Phi} = \Phi\left(\prod_{i=1}^{N} z_i^{\delta_i}\right) \tag{5.30}$$

and consider the integral family as periods of the twisted (co-)homology groups defined from this twist. All poles are regulated by this twist and we do not need to use relative twisted cohomology. In particular, we can choose bases such that

$$\check{\mathbf{P}}(\lambda, \alpha, \delta) = \mathbf{P}(\lambda, -\alpha, -\delta) \tag{5.31}$$

or even

$$\check{\mathbf{P}}(\lambda, \varepsilon, \delta) = \mathbf{P}(\lambda, -\varepsilon, -\delta). \tag{5.32}$$

With the latter basis choice, we also find bilinear relations

$$\frac{1}{(2\pi i)^N} \mathbf{P}(\boldsymbol{\lambda}, \varepsilon, \delta)^T (\mathbf{C}(\boldsymbol{\lambda}, \varepsilon, \delta)^{-1})^T \mathbf{P}(\boldsymbol{\lambda}, -\varepsilon, -\delta) = \mathbf{H}(\varepsilon, \delta), \qquad (5.33)$$

where  $\mathbf{C}(\lambda, \varepsilon, \delta)$  and  $\mathbf{H}(\varepsilon, \delta)$  are intersection matrices for the co-cycles and cycles with deformed propagators. Thus, we again obtain bilinear relations in the periods

<sup>5</sup>Note that these are not the  $\delta$  symbols of the relative approach, but rather symbols representing generic noninteger exponents.

<sup>6</sup>Note that, in principle, according to the conventions of this thesis, we *always* include the poles in the twist for bookkeeping. However, we do not generally treat their zero exponents as generic.

as long as the regulator remains generic. However, to recover the Feynman integral cuts, we must take the limit. It is important to note that this procedure is non trivial, as the result may contain poles in  $\delta$ . We obtain quadratic relations as long as the regulator remains generic. To recover the Feynman integrals, we must take the limit in the correct way and as we already saw in Example 4.10, this procedure is non-trivial:

- 1. If we take the limit by choosing the overall leading order terms in the matrices, the relations in eq. (5.33) hold and are bilinear in a set of integrals. But, we generally obtain non-invertible matrices in the relations i.e., the objects after the limit are degenerate and not associated to an actual basis. The entries giving bilinear relations are at most the ones associated to maximal cuts.
- 2. Another alternative is to rotate the bases with a constant diagonal matrix that has orders of  $\varepsilon$  on the diagonal such that the leading order term of the intersection matrices is  $\varepsilon^0$  (it might be 0) in every entry, as we did in eq. (4.120) of Example 4.10. As detailed in ref. [239], this approach yields the same results as a direct computation of the intersection matrices within a relative framework for an appropriate choice of basis. That means, we obtain valid objects, but at the same time the rotation needed for this has destroyed the symmetry and again, the dual period matrix is not related to the period matrix of cuts in a non-trivial way.

#### 5.1.2 Bilinear Relations for Maximal Cuts

As shown in the previous subsection, the twisted Riemann bilinear relations provide non-trivial relations for the maximal cut. We now explore these relations further, showing that the bilinear relations in the literature discussed in the introduction of this section are special cases of these relations.

#### **One-Parameter Case**

Ref. [302] explored canonical bases and differential equations for one-parameter Feynman integral families, identifying quadratic relations for the maximal cut experimentally. Here, we show how these results naturally emerge from the TRBRs and how they can be generalized. For that purpose, let us consider a family of Feynman integrals depending on a single dimensionless parameter  $\lambda$ . We denote here by  $\mathbf{P}(\lambda,\varepsilon)$  the matrix of maximal cuts, i.e., a matrix whose only non-zero entries are all maximal cut blocks on the diagonal. Then we can express the conjectures of [302] in the following way:

Conjecture 1 ( $\mu$ -form). When the twist related to a matrix of maximal cuts can be written as

$$\Phi = (\mathcal{B}^{m.c.}(z))^{-\mu} \text{ with } \mu \in \{\varepsilon, \frac{1}{2} + \varepsilon\},,$$
 (5.34)

there is a basis such that

$$d_{\text{ext}} \mathbf{P}(\lambda, \varepsilon) = \mu \cdot \mathbf{B}(\lambda) \mathbf{P}(\lambda, \varepsilon), \qquad (5.35)$$

where  $\mathbf{B}(\lambda)^T = \mathbf{B}(\lambda)$  is a symmetric matrix.

**Conjecture 2** (Quadratic Relations). The matrix  $\mathbf{P}(\lambda, \varepsilon)$  satisfies a set of quadratic relations:

•  $\mu = \varepsilon$ : The fundamental solution of eq. (5.35) is a path ordered exponential (as defined in eq. (2.104)):

$$\mathbf{P}(\lambda, \varepsilon) = \mathbb{P} \exp \left[ \varepsilon \int_{\gamma} \mathbf{B}(\lambda) \right]. \tag{5.36}$$

Since  $\mathbf{B}(\lambda)$  is symmetric by conjecture 1, this implies:

$$\mathbf{P}(\lambda, -\varepsilon)^T \mathbf{P}(\lambda, \varepsilon) = 1. \tag{5.37}$$

•  $\mu = \frac{1}{2} + \varepsilon$ : In that case, one can still find quadratic relations of the form:

$$\mathbf{P}(x, -\varepsilon)^{T} \mathbf{R}(x, \varepsilon) \mathbf{P}(x, \varepsilon) = \widetilde{\mathbf{H}}(\varepsilon), \qquad (5.38)$$

where  $\widetilde{\boldsymbol{H}}(\varepsilon)$  is independent of x, and  $\boldsymbol{R}(x,\varepsilon)$  is the dimension-shift matrix from eq. (2.97).

We proof these relations using our knowledge of the TRBRs.

On the  $\mu$ -form: Proof of Conjecture 1 Since  $\mathbf{P}(\lambda, \varepsilon)$  is block-diagonal, it is sufficient to prove the statement for one of the diagonal blocks, i.e., the maximal cut matrix of one sector. Since the blocks are independent, each can be treated in the same way. Thus, we consider the period matrix  $\mathbf{P}_{\Theta}(\lambda, \varepsilon)$  of a maximal cut with entries as in eq. (5.19). In particular, we start from the Baikov representation and from the assumption, it can be used to derive a twist of the form<sup>7</sup>

$$\Phi = (\mathcal{B}^{\text{m.c.}}(z))^{-\mu} , \qquad (5.39)$$

where  $\mu \in \{\varepsilon, \frac{1}{2} + \varepsilon\}$ . At this point, we make a specific choice of basis and define the period matrix  $\mathbf{P}_{\Theta}^{\log}(\lambda, \varepsilon)$  with a d log basis as defined in eq. (4.67). Notably, the examples presented in ref. [302] can be expressed in d log bases. Then, we can apply Theorem 4.1 and find:

$$d_{\text{ext}} \mathbf{P}_{\Theta}^{\log}(\lambda, \varepsilon) = -\mu \, \mathbf{B}(\lambda) \mathbf{P}_{\Theta}^{\log}(\lambda, \varepsilon) \,, \quad \text{with} \quad \mathbf{B}(\lambda)^T = \mathbf{B}(\lambda) \,. \tag{5.40}$$

Thus, there is a basis such that Conjecture 1 is satisfied and it is the d log basis. The first conjecture of ref. [302] is naturally fulfilled when considering the maximal cuts as twisted periods and just requires the existence of a d log basis. In particular, the result is not restricted to the single-parameter case in this framework.

<sup>&</sup>lt;sup>7</sup>A twist of this form can also be obtained in the loop by loop approach, if all polynomials in the product have the same exponent  $\mu$  and we gather them in one factor  $\mathcal{B}^{\text{m.c.}}$ .

Note that for  $\mu = \epsilon$ , eq. (5.40) is already in  $\varepsilon$ -form. In contrast, when  $\mu = \frac{1}{2} + \epsilon$ , there is still a non-vanishing  $\mathcal{O}(\epsilon^0)$  contribution in the connection matrix  $-\mu \mathbf{B}(\lambda)$ . Generally, this situation appears when the family of Feynman integrals is associated with a non-trivial geometry beyond the Riemann sphere. We observe again that, at least on the maximal cut, the d log basis serves as the canonical basis as long as no geometry beyond the Riemann sphere is involved. This has also been explored in the twisted intersection theory framework in the literature, see e.g., [47, 304, 305].

Quadratic relations for maximal cuts: Proof of Conjecture 2 We have already established the existence of bilinear relations derived from the TRBRs in Section 5.1 and here we confirm their specific form as in Conjecture 2 for the two cases  $\mu = \varepsilon, \frac{1}{2} + \varepsilon$  in the assumption. Our argument follows the lines of ref. [302], but in the framework of twisted intersection theory where they do not rely on being in the single-variable case and so we perform the proof with a vector of parameters  $\lambda$ .

Quadratic relations for  $\mu = \varepsilon$ : In this case, the period matrix can be written as the path-ordered differential of eq. (5.36), more specifically:

$$\mathbf{P}_{\Theta}^{\log}(\lambda,\varepsilon) = \mathbf{U}_{\mathbf{P}}(\lambda,\varepsilon) \, \mathbf{P}_{\Theta,0}^{\log}(\varepsilon) \,, \tag{5.41}$$

where

$$\mathbb{P}_{\mathbf{P}}(\boldsymbol{\lambda}, \varepsilon) = \mathbb{P} \exp \left[ \varepsilon \int_{\boldsymbol{\lambda}_0}^{\boldsymbol{\lambda}} \mathbf{B}(\boldsymbol{\lambda}') \right] = \left( \mathbb{P}_{\mathbf{P}}(\boldsymbol{\lambda}, -\varepsilon)^T \right)^{-1}, \tag{5.42}$$

where the last step follows from the symmetry of  $\mathbf{B}(\lambda)$  [302].<sup>8</sup> Due to this relation, the path-ordered exponential fulfils the bilinear relation:

$$\mathbb{P}_{\mathbf{P}}(\boldsymbol{\lambda}, \varepsilon)^T \mathbb{P}_{\mathbf{P}}(\boldsymbol{\lambda}, -\varepsilon) = 1.$$
 (5.43)

Combining this with eq. (5.41), we find the quadratic relation

$$\mathbf{P}_{\Theta}^{\log}(\boldsymbol{\lambda}, \varepsilon)^{T} \mathbf{P}_{\Theta}^{\log}(\boldsymbol{\lambda}, -\varepsilon) = \mathbf{P}_{\Theta, 0}^{\log}(\varepsilon)^{T} \mathbf{P}_{\Theta, 0}^{\log}(-\varepsilon).$$
 (5.44)

This relation has the expected form of the Riemann bilinear relations for maximal cuts of eq. (5.24) with  $\mathbf{C}(\boldsymbol{\lambda}, \varepsilon) = (2\pi i)^{-h}\mathbf{1}$  and  $\mathbf{H}(\varepsilon) = \mathbf{P}_{\Theta,0}^{\log}(\varepsilon)^T \mathbf{P}_{\Theta,0}^{\log}(-\varepsilon)$ . That  $\mathbf{C}(\boldsymbol{\lambda}, \varepsilon)$  is a normalized version of the identity matrix is in agreement with what we find in the proof of Theorem 4.1. Whilst this specific form of the bilinear relations relies on the choice of the d log basis, we can derive bilinear relations in other bases of differentials: Consider another period matrix  $\tilde{\mathbf{P}}_{\Theta}(\boldsymbol{\lambda}, \varepsilon)$ , which is relate do  $\mathbf{P}_{\Theta}^{\log}(\boldsymbol{\lambda}, \varepsilon)$  by

$$\tilde{\mathbf{P}}_{\Theta}(\lambda, \varepsilon) = \mathbf{U}(\lambda, \varepsilon) \mathbf{P}_{\Theta}^{\log}(\lambda, \varepsilon). \tag{5.45}$$

Then  $\tilde{\mathbf{P}}_{\Theta}(\boldsymbol{\lambda}, \varepsilon)$  satisfies the quadratic relation

$$\frac{1}{(2\pi i)^h} \tilde{\mathbf{P}}_{\Theta}(\boldsymbol{\lambda}, \varepsilon)^T (\mathbf{C}(\boldsymbol{\lambda}, \varepsilon)^{-1})^T \tilde{\mathbf{P}}_{\Theta}(\boldsymbol{\lambda}, \varepsilon) = \mathbf{P}_{\Theta, 0}^{\log}(\varepsilon)^T \mathbf{P}_{\Theta, 0}^{\log}(-\varepsilon) = \mathbf{H}(\varepsilon), \quad (5.46)$$

<sup>8</sup>Note that,  $\lambda_0$ coincides with one the logarithmic singularities in the integrand, we employ a tangential base-point regularisation as in cf., e.g., refs. [176, 306].

with 
$$\mathbf{C}(\boldsymbol{\lambda}, \varepsilon) = (2\pi i)^{-h} \mathbf{U}(\boldsymbol{\lambda}, \varepsilon) (\mathbf{U}(\boldsymbol{\lambda}, -\varepsilon))^T$$
.

Quadratic relations for  $\mu = \frac{1}{2} + \varepsilon$ . Again, we choose the period matrix of maximal cuts  $\mathbf{P}_{\Theta}^{\log}(\boldsymbol{\lambda}, \varepsilon)$  computed from a d log basis so that Conjecture 1 is satisfied. Note that shifting the exponent of the Baikov-polynomial is akin to changing the spacetime dimension D and in particular,  $\mathbf{P}_{\Theta}^{\log}(\boldsymbol{\lambda}, \varepsilon - 1)$  is the fundamental solution matrix of maximal cuts computed in D+2 dimensions, which is related to  $\mathbf{P}_{\Theta}^{\log}(\boldsymbol{\lambda}, \varepsilon)$  by the dimension-shift matrix (see eq. (2.97)):

$$\mathbf{P}_{\Theta}^{\log}(\lambda, \varepsilon - 1) = \mathbf{R}(\lambda, \varepsilon) \mathbf{P}_{\Theta}^{\log}(\lambda, \varepsilon). \tag{5.47}$$

On the other hand, one can obtain the period matrix  $\mathbf{P}_{\Theta}^{\log}(\boldsymbol{\lambda}, \varepsilon - 1)$  by explicitly changing the basis of forms: If  $\varphi_i$  and  $\gamma_j$  are the cohomology and homology basis elements used to compute  $\mathbf{P}_{\Theta}^{\log}(\boldsymbol{\lambda}, \varepsilon)$ , then

$$\left(\mathbf{P}_{\Theta}^{\log}(\boldsymbol{\lambda}, \varepsilon - 1)\right)_{ij} = \langle \varphi_i^+ | \gamma_j ] \text{ with } \varphi_i^+ = \varphi_i \left(\mathbf{B}^{\text{m.c.}}(\boldsymbol{\lambda}) |_{\varepsilon \to 0}\right).$$
 (5.48)

In particular, these entries are related to the entries of the original dlog basis by

$$\left(\mathbf{P}_{\Theta}^{\log}(\boldsymbol{\lambda}, \varepsilon - 1)\right)_{ij} = \sum_{k=1}^{M} \langle \varphi_i^+ | \check{\varphi}_k \rangle \langle \varphi_k | \gamma_j] = \sum_{k=1}^{M} \langle \varphi_i^+ | \check{\varphi}_k \rangle \left(\mathbf{P}_{\Theta}^{\log}(\boldsymbol{\lambda}, \varepsilon)\right)_{kj}, \quad (5.49)$$

Comparing eq. (5.49) to eq. (5.47), we find the following expression for the entries of the dimensional shift matrix:

$$R_{ij}(\lambda, \varepsilon) = \langle \varphi_i^+ | \check{\varphi}_j \rangle .$$
 (5.50)

So far we have discussed this matrix to facilitate a dimension change or equivalently a shift in  $\varepsilon$ . But  $\varepsilon$  appears as a term in  $\mu$ , the exponent of the twist. So, one can also interpret the matrix to shift  $\mu \mapsto \mu - 1$ . In particular, when viewing the period matrix as a function  $\mathbf{P}_{\Theta}^{\log,\mu}(\boldsymbol{\lambda},\mu) = \mathbf{P}_{\Theta}^{\log}(\boldsymbol{\lambda},\varepsilon)$  of  $\mu$  we know that we can choose dual bases so that

$$\check{\mathbf{P}}_{\Theta}^{\log,\mu}(\lambda,\mu) = \mathbf{P}_{\Theta}^{\log,\mu}(\lambda,-\mu). \tag{5.51}$$

Then we find that  $\mathbf{R}(\lambda, \varepsilon)$  also allows us to make a basis change so that

$$\mathbf{P}_{\Theta}^{\log}(\lambda, -\varepsilon) = \mathbf{R}(\lambda, -\varepsilon)^{-1} \mathbf{P}_{\Theta}^{\log}(\lambda, -\varepsilon - 1)$$
 (5.52)

$$= \mathbf{R}(\boldsymbol{\lambda}, -\varepsilon)^{-1} \mathbf{P}_{\Theta}^{\log, \mu}(\boldsymbol{\lambda}, -\mu)$$
 (5.53)

$$= \mathbf{R}(\boldsymbol{\lambda}, -\varepsilon)^{-1} \check{\mathbf{P}}_{\boldsymbol{\Theta}}^{\log, \mu}(\boldsymbol{\lambda}, \mu). \tag{5.54}$$

Then the TRBRs take the form

$$\mathbf{H}(\varepsilon) = \mathbf{P}_{\Theta}^{\log,\mu}(\boldsymbol{\lambda},\mu)^T \mathbf{P}_{\Theta}^{\log,\mu}(\boldsymbol{\lambda},-\mu) = \mathbf{P}_{\Theta}^{\log}(\boldsymbol{\lambda},\varepsilon)^T \mathbf{R}(\boldsymbol{\lambda},-\varepsilon) \mathbf{P}_{\Theta}^{\log}(\boldsymbol{\lambda},-\varepsilon).$$
 (5.55)

#### Relations for $\varepsilon \to 0$

As discussed in Section 3.5, taking the limit  $\varepsilon \to 0$  in the integrand of the maximal cut (after taking all residues) provides insight into the geometry associated with the Feynman integral family. We have established here that this limit generally yields expressions where the Baikov polynomials come with integer or half-integer exponents, see eq. (5.17). In particular, we can write the twist as

$$\Phi = P(z)^{-\frac{1}{2} - \varepsilon} \tilde{P}(z)^{\pm \varepsilon}, \qquad (5.56)$$

with P(z) is a polynomial of degree 2n+1 or 2n+2 and  $\tilde{P}(z)^{\pm\varepsilon}$  vanishes for  $\varepsilon \to 0$ . One can define a variety from the polynomial P(z) as discussed in Section 3.5. In the limit  $\varepsilon \to 0$ , the period matrix should contain the periods of this variety. More specifically: In many cases, the period matrix for the twisted cohomology defined by  $\Phi$  splits into blocks that contain the periods of the variety (in the  $\varepsilon \to 0$  limit) and entries that are related to punctures and do not appear in the  $\varepsilon \to 0$  limit. So, the TRBRs we obtain on the maximal cut should also contain quadratic relations for the periods of the variety in the  $\varepsilon \to 0$  limit. Indeed, this is what happens and the relations obtained in this limit are well-known relations for the appearing varieties. The geometries studied in the context of Feynman integrals so far include Riemann surfaces of genus g as well as Calabi-Yau varieties. We have already observed that both types of varieties have natural quadratic relations: for Riemann surfaces, these are the generalised Legendre relations eq. (3.58), while for Calabi-Yau varieties, they arise from the Hodge-Riemann bilinear relations derived via Griffiths transversality in eq. (3.107).

Generalized Legendre Relations Hyperelliptic curves can arise in the maximal cut, when it is an integral of only a single variable z and P(z) is a polynomial of degree 2n+1 or 2n+2 – defining an odd or even hyperelliptic curve in the  $\varepsilon \to 0$  limit. Their bilinear relations are the generalized Legendre relations of eq. (3.58).

Quadratic Relations for CY Periods As already mentioned in the introduction, quadratic relations in the  $\varepsilon \to 0$  limit of maximal cuts related to CY varieties have been studied in the literature and used to compute certain Feynman integral families [19, 20]. These are derived from the so-called Riemann-Hodge bilinear relations, that are commonly also denoted the *Griffiths transversality relations*, as they are due to the Griffiths transversality condition. Periods of Calabi-Yau geometries generally appear in Feynman integral families, whose Baikov-polynomial contains a polynomial P(z) with a half-integer exponent and multiple variables  $z^9$ . The unique holomorphic differential associated to such a CY family is  $\Omega = \frac{\mathrm{d}z}{\sqrt{P(z)}}^{10}$  and the maximal cut at  $\varepsilon \to 0$  contains the periods and quasi-periods of the CY family, which fulfill the aforementioned Hodge-Riemann bilinear relations of eq. (3.106). In matrix form, those are

$$\mathbf{P}(\lambda, \varepsilon = 0) \mathbf{\Sigma} \mathbf{P}(\lambda, \varepsilon = 0)^{T} = \mathbf{Z}(\lambda), \qquad (5.57)$$

See also:

We give examples for hyperelliptic maximal cuts in Examples 3.13 and 3.14.

<sup>9</sup>Of course, the torus which is defined from a polynomial in a single variable is also a Calabi-Yau variety.

<sup>10</sup>Where dz denotes a suitable differential form in the base space B.

where  $\mathbf{Z}(\mathbf{x})$  is a matrix of rational functions of the kinematic variables (which correspond to the independent moduli of the family of CY varieties), and  $\Sigma$  is (the inverse of) the matrix of intersection numbers between generators of the middle homology of the CY variety. In particular, the integrals in the period matrix have the form

$$P_{ij}(\boldsymbol{\lambda}, \varepsilon = 0) = \int_{\mathcal{C}_i} \frac{\mathrm{d}^n z}{\sqrt{P(\boldsymbol{z})}} f_i^{\text{m.c.}}(\boldsymbol{z}), \qquad (5.58)$$

where  $C_j$  is some basis cycle and  $f_i^{\text{m.c.}}(z)$  is a polynomial. These integrals can also be interpreted as twisted periods, even for  $\varepsilon = 0$ . In that case, the twist is  $\Phi_{\text{CY}} = P(z)^{-\frac{1}{2}}$ , a basis of twisted cycles and co-cycles is given by  $C_j$  and  $\psi_i = d^n z f_i^{\text{m.c.}}(z)$  and a basis of dual co-cycles is  $\tilde{\psi}_i = [d^n z f_i^{\text{m.c.}}(z) P^{-1}(z)]_c$ . In this basis, the TRBRs are equivalent to the quadratic relations arising in CY geometry. A comprehensive discussion on the relationship between TRBRs for a particular hypergeometric function and the Riemann (in-)equality of the corresponding K3 surface can be found in ref. [228].

# 5.1.3 Examples

We conclude this subsection with two examples of maximal cuts of Feynman integrals related to hyperelliptic curves: the sunrise integral family and the non-planar crossed box family.

**Example 5.2** (The Sunrise Integral Family: TRBRs). We first discussed the sunrise integral family in Section 2.4.1 and also considered the period matrix of its maximal cut in Example 4.20. Here, we fix  $\lambda_1 < \lambda_2 < \lambda_3 < \lambda_4 < 0$  and we choose the twisted cohomology basis of eq. (4.211) and the dual basis of eq. (4.215), such that the period matrix is related to the dual period matrix by  $\varepsilon \to -\varepsilon$ , see eq. (4.220). These period matrices fulfill the TRBRs

$$\frac{1}{2\pi i} \mathbf{P}_{\oplus}(\boldsymbol{\lambda}, \varepsilon)^{T} \left( \mathbf{C}_{\oplus}(\boldsymbol{\lambda}, \varepsilon)^{-1} \right)^{T} \mathbf{P}_{\oplus}(\boldsymbol{\lambda}, -\varepsilon) = \mathbf{H}_{\oplus}(\varepsilon)$$
 (5.59)

with the intersection matrices  $\mathbf{C}_{\oplus}$  and  $\mathbf{H}_{\oplus}$  given in eq. (B.79) and eq. (B.80) respectively. We numerically confirm that eq. (5.59) holds, using analytic continuations of the periods. First, we expand eq. (5.59) in  $\varepsilon$  and observe that  $H_{\oplus,44}(\varepsilon)$  has a leading term of order  $\mathcal{O}(\varepsilon^{-1})$ . To take a finite limit, we introduce the rotation

$$\mathbf{T}_{\oplus}(\varepsilon) = \begin{pmatrix} 1 & 0 & 0 & 0 \\ 0 & 1 & 0 & 0 \\ 0 & 0 & 1 & 0 \\ 0 & 0 & 0 & \varepsilon \end{pmatrix} , \tag{5.60}$$

and define

$$\widetilde{\mathbf{P}}_{\oplus}(\boldsymbol{\lambda}, \varepsilon) = \mathbf{P}_{\oplus}(\boldsymbol{\lambda}, \varepsilon) \mathbf{T}_{\oplus}(\varepsilon), \qquad (5.61)$$

$$\widetilde{\mathbf{H}}_{\oplus} = \mathbf{T}_{\oplus}(\varepsilon)\mathbf{H}_{\oplus}(\varepsilon)\mathbf{T}_{\oplus}(-\varepsilon)$$
. (5.62)

After this change in the homology basis, the TRBRs of eq. (5.59) take the form:

$$\frac{1}{2\pi i} \widetilde{\mathbf{P}}_{\oplus}(\boldsymbol{\lambda}, \varepsilon)^{T} \left( \mathbf{C}_{\oplus}(\boldsymbol{\lambda}, \varepsilon)^{-1} \right)^{T} \widetilde{\mathbf{P}}_{\oplus}(\boldsymbol{\lambda}, -\varepsilon) = \widetilde{\mathbf{H}}_{\oplus}(\varepsilon) . \tag{5.63}$$

This equation is finite in the limit  $\varepsilon \to 0$  and we can derive from it the relation

where the left-hand side involves the periods and quasi-periods of the elliptic curve in the chosen basis:

$$\omega_1 = \frac{1}{c_4} K(\lambda) , \qquad (5.65)$$

$$\omega_2 = \frac{i}{c_4} K(1 - \lambda), \qquad (5.66)$$

$$\eta_1 = -2c_4 \left[ \mathcal{E}(\lambda) - \frac{2-\lambda}{3} \mathcal{K}(\lambda) \right] , \qquad (5.67)$$

$$\eta_2 = 2ic_4 \left[ E(1-\lambda) + \frac{1+\lambda}{3} K(1-\lambda) \right],$$
(5.68)

with  $\lambda = \frac{(\lambda_1 - \lambda_4)(\lambda_2 - \lambda_3)}{(\lambda_1 - \lambda_3)(\lambda_2 - \lambda_4)}$  and  $c_4 = \frac{1}{2}\sqrt{(\lambda_1 - \lambda_3)(\lambda_2 - \lambda_4)}$ . We find that eq. (5.64) is equivalent to the Legendre relations. Consequently, at leading order in  $\varepsilon$ , the TRBRs in eq. (5.63) reduce to the Legendre relations in this basis.

**Example 5.3** (The Non-planar Crossed Box Family: TRBR). We introduced the non-planar crossed box integral family in Section 2.4.2 and discussed the hyperelliptic curve one can obtain from its maximal cut in eq. (3.14). Here, we set  $m^2 = 1$ . The integrand of eq. (2.67) defines the twist

$$\Phi_{\text{npcb}}(z) = \left[ (z - \lambda_1^{npcb})(z - \lambda_2^{npcb}) \right]^{-\frac{1}{2}} \left[ (z - \lambda_3^{npcb})(z - \lambda_4^{npcb})(z - \lambda_5^{npcb})(z - \lambda_6^{npcb}) \right]^{-\frac{1}{2} - \varepsilon},$$
(5.69)

with the roots  $\lambda_i^{npcb}$  as given in eq. (2.70). In the limit  $\varepsilon \to 0$  of  $\Phi_{npcb}(z)$ , we obtain the polynomial of eq. (3.216). For the twisted cohomology group  $H^1_{dR}(X, \nabla_{npcb})$ , where  $X = \mathbb{C} - \{\lambda_1, \ldots, \lambda_6\}$  we choose the basis

$$\varphi_1^{\text{npcb}} = dz, \quad \varphi_2^{\text{npcb}} = z \, dz, \quad \varphi_3^{\text{npcb}} = -\left(z^4 - \frac{3}{4}s_1z^3 + \frac{s_2}{2}z^2 - \frac{s_3}{4}z\right) dz$$
 (5.70)

$$\varphi_4^{\text{npcb}} = -\frac{1}{2} \left( z^3 - \frac{s_1}{2} z^2 \right) dz, \quad \varphi_5^{\text{npcb}} = z^2 dz,$$
(5.71)

where the  $s_k$  are elementary symmetric polynomials in the branch points  $\lambda_1, \ldots \lambda_6$ . This basis is chosen, such that its differentials reduce to Abelian differentials on the hyperelliptic curve in the  $\varepsilon \to 0$  limit. In order to obtain a simple relation between the periods and dual periods, we choose the dual basis

$$\check{\varphi}_i^{\text{npcb}} = \left[\frac{1}{p_{\text{npcb}}(z)}\varphi_i^{\text{npcb}}\right]_c, \quad i = 1, \dots, 6,$$
(5.72)

See also: We discuss hyperellip-

tic curves in Section 3.2.

where  $y^2 = p_{\text{npcb}}(z) = (z - \lambda_1) \cdots (z - \lambda_6)$  is the defining equation for the hyperelliptic curve of eq. (3.216). The intersection matrix derived from these bases is denoted as  $C_{nocb}(\lambda, \varepsilon)$ . A natural choice for canonical basis cycles of a hyperelliptic curve is shown in Figure 3.3 and from this choice, we deduce our choice for the topological supports of the dual twisted homology group  $H_1(X, \mathcal{L}_{npcb})$ .<sup>11</sup>

$$\check{\Delta}_{\text{npcb}}^{1} = \left[\lambda_{1}^{npcb}, \lambda_{2}^{npcb}\right], \quad \check{\Delta}_{\text{npcb}}^{2} = \left[\lambda_{3}^{npcb}, \lambda_{4}^{npcb}\right], \tag{5.73}$$

$$\check{\Delta}_{\text{npcb}}^{3} = \left[\lambda_{2}^{npcb}, \lambda_{3}^{npcb}\right] + \left[\lambda_{4}^{npcb}, \lambda_{5}^{npcb}\right], \quad \check{\Delta}_{\text{npcb}}^{4} = \left[\lambda_{4}^{npcb}, \lambda_{5}^{npcb}\right], \qquad (5.74)$$

$$\check{\Delta}_{\text{npcb}}^{5} = \left[\lambda_{1}^{npcb}, \lambda_{2}^{npcb}\right] + \left[\lambda_{3}^{npcb}, \lambda_{4}^{npcb}\right] + \left[\lambda_{5}^{npcb}, \lambda_{6}^{npcb}\right], \qquad (5.75)$$

$$\check{\Delta}_{\text{npcb}}^{5} = \left[\lambda_{1}^{npcb}, \lambda_{2}^{npcb}\right] + \left[\lambda_{3}^{npcb}, \lambda_{4}^{npcb}\right] + \left[\lambda_{5}^{npcb}, \lambda_{6}^{npcb}\right], \tag{5.75}$$

For the basis of the twisted homology group  $H_1(X, \check{\mathcal{L}}_{npcb})$  we choose cycles supported on regularised versions of these intervals. In the  $\varepsilon \to 0$  limit,  $\check{\gamma}_1^{npcb}$  and  $\check{\gamma}_2^{npcb}$  correspond to the a-cycles, while  $\check{\gamma}_3^{npcb}$  and  $\check{\gamma}_4^{npcb}$  correspond to the b-cycles of the hyperelliptic curve. An additional basis element is required for  $\varepsilon \neq 0$  and is chosen such that the differential one-forms  $\Phi_{\rm npcb}\varphi_i^{\rm npcb}$  (for  $i=1,\ldots,4$ ) integrate to zero at  $\varepsilon = 0$ , resulting in a block structure of the period matrix. The intersection matrix corresponding to these bases is denoted by  $\mathbf{H}_{npcb}(\varepsilon)$ . Finally, we rotate the basis of forms again, so that the leading order in the matrices agree:

$$\mathbf{C}_{\text{npcb}}(\boldsymbol{\lambda}, \varepsilon) = \boldsymbol{U}(\varepsilon)\tilde{\mathbf{C}}_{\text{npcb}}(\boldsymbol{\lambda}, \varepsilon)\boldsymbol{U}(-\varepsilon),$$
 (5.76)

$$\mathbf{P}_{\text{npcb}}(\boldsymbol{\lambda}, \varepsilon) = \boldsymbol{U}(\varepsilon) \tilde{\mathbf{P}}_{\text{npcb}}(\boldsymbol{\lambda}, \varepsilon), \qquad (5.77)$$

with  $U(\varepsilon) = \operatorname{diag}(1,1,1,1,\varepsilon)$ . In this basis, the twisted Riemann bilinear relations are

$$\mathbf{P}_{\text{npcb}}(\boldsymbol{\lambda}, \varepsilon) \left( \mathbf{H}_{\text{npcb}}(\varepsilon)^{-1} \right)^T \mathbf{P}_{\text{npcb}}^T(\boldsymbol{\lambda}, -\varepsilon) = 2\pi i \, \mathbf{C}_{\text{npcb}}(\boldsymbol{\lambda}, \varepsilon) \,. \tag{5.78}$$

After expanding these relations in  $\varepsilon$  isolating the order  $\mathcal{O}(\varepsilon^0)$  terms, we find

$$\begin{pmatrix} \mathcal{B}\mathcal{A}^{T} - \mathcal{A}\mathcal{B}^{T} & \mathcal{B}\tilde{\mathcal{A}}^{T} - \mathcal{A}\tilde{\mathcal{B}}^{T} & 0\\ \tilde{\mathcal{B}}\mathcal{A}^{T} - \tilde{\mathcal{A}}\mathcal{B}^{T} & \tilde{\mathcal{B}}\tilde{\mathcal{A}}^{T} - \tilde{\mathcal{A}}\tilde{\mathcal{B}}^{T} & 0\\ 0 & 0 & 0 \end{pmatrix} = \begin{pmatrix} 0 & -i\pi\mathbf{1} & 0\\ i\pi\mathbf{1} & 0 & 0\\ 0 & 0 & 0 \end{pmatrix},$$
(5.79)

where  $\mathcal{A}, \mathcal{B}, \overline{\mathcal{A}}, \overline{\mathcal{B}}$  are the 2 × 2 a- and b-(quasi-)period block matrices in the period matrix for  $\varepsilon = 0$  eq. (3.57). These relations are the generalisations of the Legendre relations discussed in eq. (3.6). Expanding the second version of the twisted Riemann bilinears (the version solved for  $\mathbf{H}$ ),

$$\mathbf{P}_{\text{npcb}}(\boldsymbol{\lambda}, \varepsilon)^T \left( \mathbf{C}_{\text{npcb}}(\boldsymbol{\lambda}, \varepsilon)^{-1} \right)^T \mathbf{P}_{\text{npcb}}(\boldsymbol{\lambda}, -\varepsilon) = 2\pi i \, \mathbf{H}_{\text{npcb}}(\varepsilon)$$
 (5.80)

we also find the relation

$$\tilde{\mathcal{A}}^T \mathcal{B} - \mathcal{A}^T \tilde{\mathcal{B}} = -i\pi \mathbb{1}. \tag{5.81}$$

# The Intersection Matrix for Canonial Differ-5.2 ential Equations

So far, we have explored the relations imposed on cuts of Feynman integrals by the TRBRs. In proving Conjecture 2, we also observed that for  $\mu = \varepsilon$  a d log basis has

<sup>11</sup>Since crossing the branch cut merely flips the sign of the chosen one-forms (for  $\varepsilon = 0$ ), integrations around these cycles reduce to simple integrals along (sums of) intervals.

Orthogonality conditions between canonical bases and dual bases were also discussed in [47, 49,

307, 308].

In the literature the names  $\varepsilon$ -factorised systems and systems in canonical form are often used interchangeably. Here we keep them distinct.

<sup>12</sup>In the context of Feynman integrals, these  $\varpi_i$  are the *letters*.

a differential equation in  $\varepsilon$ -form, which can be considered canonical and that for this basis choice the cohomology intersection matrix is proportional to the identity matrix. Bases for which the intersection matrix is diagonal can be considered orthogonal. In this section, we generalise the observation that the intersection matrix has a specific form for canonical bases.

# 5.2.1 Properties of Canonical Differential Equations

We begin this section with a more detailed discussion of the properties of canonical differential equations. Our first goal is to introduce a property closely related to being in canonical form that is more precisely defined, enabling us to prove our statements — we refer to this property as being in C-form. All known examples of canonical differential equations in the literature that we are aware of have this property. We also explore the iterated integrals appearing in C-form Feynman integrals and in particular discuss when they are linearly independent. Additionally, we briefly mention a self-duality property for (cuts of) Feynman integrals. This subsection serves to define and specify the properties we connect in the following sections.

# C-Form for Differential Equations

We consider a vector  $\mathbf{J}(\lambda, \varepsilon)$  of master integrals whose differential equation is in  $\varepsilon$ -form, i.e.  $d_{\mathrm{ext}}\mathbf{J}(\lambda, \varepsilon) = \varepsilon \mathbf{B}(\lambda)\mathbf{J}(\lambda, \varepsilon)$ . The entries of the matrix  $\mathbf{B}(\lambda)$  are closed one-forms in the coordinates  $\lambda$ . Let  $\mathbb{K}$  be an algebraic number field – see Definition A.1 – and  $\mathbb{A}_{\mathbf{B}}$  a  $\mathbb{K}$ -algebra of functions chosen so that around every point we can find a local coordinate chart  $\lambda$  such that the entries of  $\mathbf{B}(\lambda)$  take the form

$$B_{ij}(\boldsymbol{\lambda}) = \sum_{k=1}^{d_{\text{ext}}} d\lambda_k \, b_{ijk}(\boldsymbol{\lambda}) \text{ with } b_{ijk}(\boldsymbol{\lambda}) \in \mathbb{A}_{\mathbf{B}}.$$
 (5.82)

We denote the K-vector space of differential forms with coefficients in  $\mathbb{A}_{\mathbf{B}}$  by  $\Omega^1(\mathbb{A}_B)$ , and the subspace of closed forms by  $C^1(\mathbb{A}_B) = \{\omega \in \Omega^1(\mathbb{A}_B) \mid d\omega = 0\}$ . The subspace of  $C^1(\mathbb{A}_B)$  that is generated by the entries of  $\mathbf{B}(\lambda)$  is generally finite dimensional and we denote it by  $\mathbb{V}_{\mathbf{B}}$ . We denote by  $\varpi_1, \ldots, \varpi_p$  a basis of  $\mathbb{V}_{\mathbf{B}}^{12}$  and we can expand the differential equation in this basis

$$\mathbf{B}(\lambda) = \sum_{i=1}^{p} \mathbf{B}_{i} \varpi_{i}, \qquad (5.83)$$

where the  $\mathbf{B}_i$  are constant  $M \times M$  matrices with entries in  $\mathbb{K}$ . Additionally, we define  $\mathbb{A}_{\mathbf{B},\varepsilon} := \mathbb{A}_{\mathbf{B}} \otimes_{\mathbb{K}} \mathbb{K}(\varepsilon)$  and  $\mathcal{F}_{\mathbb{C}} := \operatorname{Frac}(\mathbb{C} \otimes_{\mathbb{K}} \mathbb{A}_{\mathbf{B}})$ , the field of fractions of the complexification of the algebra  $\mathbb{A}_{\mathbf{B}}$ . We define the following property of a differential equation to which we can attach the above objects:

**Definition 5.1.** An  $\varepsilon$ -factorised differential equation is in C-form if

$$\mathbb{V}_{\mathbf{B}} \cap \mathrm{d}\mathcal{F}_{\mathbb{C}} = \{0\} \tag{5.84}$$

with  $\mathcal{F}_{\mathbb{C}}$  defined by an algebra  $\mathbb{A}_{\mathbf{B}}$  that fulfils the following properties

- $\mathbb{A}_{\mathbf{B}}$  is differentially closed: For all  $f \in \mathbb{A}_{\mathbf{B}}$ , we have  $\partial_{\lambda_i} f \in \mathbb{A}_{\mathbf{B}}$ , for all  $1 \leq i \leq r$  (if  $\mathbb{A}_{\mathbf{B}}$  is not differentially closed, we can enlarge it by adding the necessary derivatives).
- The field of constants of  $\mathbb{A}_{\mathbf{B}}$  is  $\mathbb{K}$ ,

$$Const(\mathbb{A}_{\mathbf{B}}) = \left\{ f \in \mathbb{A}_{\mathbf{B}} : \partial_{\lambda_i} f = 0, \text{ for all } 1 \le i \le r \right\} = \mathbb{K}.$$
 (5.85)

We illustrate these definitions with a simple example: Feynman integrals which can be brought into d log form in the kinematic parameters, i.e., where the canonical basis can be found using only algebraic transformations. Specifically, we focus on the example of the massive bubble integral family in  $D = 2 - 2\varepsilon$  dimensions that we already encountered in Examples 2.5, 2.6, 4.19 and 5.1.

**Example 5.4** (Feynman Integrals in d log Form – The Bubble Integral Family). We choose  $\mathbb{K} = \mathbb{Q}[i, \pi, \pi^{-1}]$ .<sup>13</sup> The algebra  $\mathbb{A}_{\mathbf{B}}$  defined by the connection matrix of a canonical differential equation in d log form is a ring of rational functions with a prescribed set of poles to which one adjoins a finite number of rationalisable square roots of polynomials. Because the derivative of an algebraic function is algebraic,  $\mathbb{A}_{\mathbf{B}}$  is differentially closed. By our assumption, the letters of the canonical differential equation are d log forms (potentially with square roots) and those generate  $\mathbb{V}_{\mathbf{B}}$ .

<sup>13</sup>We need to attach  $\pi$  due to the standard normalisations of Feynman integrals. The arguments still hold.

Let us make this more explicit with the example of the equal mass bubble integral family. In the coordinate  $\chi$ , the only finite poles of the connection matrix are located at  $\{0,1\}$ . Then,  $\mathbb{A}_{\bigcirc}$  is the algebra of rational functions with those poles and by definition  $\mathcal{F}_{\mathbb{C}}^{\bigcirc}$  is the field of fractions of its complexification. All entries of  $\mathbf{B}_{\bigcirc}^{\mathrm{eq}}$  can be expanded in the letters

$$\varpi_{-}^{1} = \frac{\mathrm{d}\chi}{\chi} \text{ and } \varpi_{-}^{2} = \frac{\mathrm{d}\chi}{\chi - 1},$$
 (5.86)

so these letters generate  $\mathbb{V}_{\mathbb{Q}}$ . Next, we show that the differential equation is in C-form: Since  $\mathbb{V}_{\mathbb{Q}}$  is generated by the forms in eq. (5.86), all elements of  $\mathbb{V}_{\mathbb{Q}}$  have only simple poles. On the other hand, the elements of  $d\mathcal{F}_{\mathbb{C}}^{\mathbb{Q}}$  cannot have simple poles as they are obtained as exterior derivatives of rational forms, so they have either no poles or higher order poles. For that reason, we find

$$\mathbb{V}_{\circ} \cap d\mathcal{F}_{\circ}^{\circ} = \{0\} \tag{5.87}$$

and the differential equation is in C-form. In this case, we find that for Feynman integrals without square roots or more complex special functions, being in C-form simply means having only simple poles—precisely the property we want a canonical differential equation to have.

The same criterion can be used to classify differential equations involving more complicated special functions, such as (quasi-)modular forms. We discuss several examples of this in the remainder of the thesis particularly for integral families related to (hyper-)elliptic curves.

#### See also:

- In Section 6.2, we discuss the forms appearing in the C-form differential equations of hyperelliptic Lauricella function families.
- In Section 7.3.2 we discuss the forms appearing in a C-form basis for the kite integral family.

# Linear independence of iterated integrals

See also:

In Section 2.5 we discussed how iterated integrals are the coefficients of  $\varepsilon$ -expansion of the solution of canonical differential equations.

The integrals solving the C-form differential equation are obtained as path-ordered exponentials over the connection matrix  $\mathbf{B}(\lambda)$  and thus, at each order in  $\varepsilon$ , we obtain iterated integrals over the basis forms  $\varpi_i$  of  $V_{\mathbf{B}}$ . We want to understand, which of these iterated integrals are linearly independent over the field  $\mathcal{F}_{\mathbb{C}}$ . By our assumption that the differential equation for a Feynman integral family should be integrable (explicitly expressed by the flatness condition of eq. (2.100), we expect only homotopy invariant combinations to appear. Inserting the expansion of eq. (5.83), we can expand the flatness condition in wedges of the basis differentials  $\varpi_i$ :

$$0 = \mathbf{B} \wedge \mathbf{B} = \sum_{i,j=1}^{p} [\mathbf{B}_i, \mathbf{B}_j] \, \varpi_i \wedge \varpi_j \,. \tag{5.88}$$

These wedge products  $\varpi_i \wedge \varpi_j$  are elements of the vector space  $C^2(\mathbb{A}_{\mathbf{B}})$  of closed two-forms, for which one can choose a basis  $\tilde{\boldsymbol{\varpi}}$ . Since we obtain finitely many  $\varpi_i$  from a connection matrix  $\mathbf{B}$ , the basis  $\tilde{\boldsymbol{\varpi}}$  is also finite dimensional and we denote its dimension by q here. Consequently, we can write the flatness condition in this basis as

$$\sum_{k=1}^{q} \tilde{\omega}_k \sum_{i,j=1}^{p} a_{ijk} \left[ \mathbf{B}_i, \mathbf{B}_j \right] = 0$$
 (5.89)

with the coefficients  $a_{ijk}$  defined by the decomposition  $\varpi_i \wedge \varpi_j = \sum_{k=1}^q a_{ijk} \tilde{\varpi}_k$ . Since  $\tilde{\varpi}$  is a basis, we obtain the condition

$$\sum_{i,j=1}^{p} a_{ijk} \left[ \mathbf{B}_{i}, \mathbf{B}_{j} \right] = 0 \text{ for } 1 \le k \le q.$$
 (5.90)

Next we translate this condition form the forms into a condition for the iterated integrals as defined in eq. (2.107). To do so, we interpret the iterated integrals as coefficients in a a generating functional with non-commuting letters  $e_{I,i}$ :<sup>14</sup>

$$\mathbb{G}_I = 1 + \sum_{k=1}^{\infty} \sum_{1 \le i_1, \dots, i_k \le n} e_{I, i_1} \cdots e_{I, i_k} I_{\gamma}(\varpi_{i_1}, \dots, \varpi_{i_k}) . \tag{5.91}$$

By definition, this generating functional fulfils the differential equation

$$d\mathbb{G}_I = \left(\sum_{i=1}^p e_{I,i} \varpi_i\right) \mathbb{G}_I. \tag{5.92}$$

Additionally, the letters  $e_I$  satisfy the same relations as the matrices  $\mathbf{B}_i$  and specifically, they satisfy the relations of eq. (5.90), i.e.,

$$\sum_{i,j=1}^{p} a_{ijk} \left[ e_{I,i}, e_{I,j} \right] = 0, \qquad 1 \le k \le q.$$
 (5.93)

 $^{14}$ Note, that the letters  $e_i$  here are not the ones  $\mathbb{G}G$ , but generic free letters.

The non-commuting letters  $e_{I,i}$  generate a  $\mathbb{K}$ -algebra that we denote by  $\mathbb{E}_{\mathbf{B}}$ . Due to the flatness of the connection as expressed in eq. (5.92) a basis of  $\mathbb{E}_{\mathbf{B}}$  corresponds to a basis of homotopy invariant iterated integrals. We can find such a basis algorithmically <sup>15</sup> and denote it by  $\mathcal{B}_{\mathbf{B}}$ . The generating functional decomposed in this basis is

<sup>15</sup>In Appendix A of [226] the construction of such a basis is explained in detail.

$$\mathbb{G}_I = \sum_{w \in \mathcal{B}_{\mathbf{B}}} w J_{\gamma}(w) , \qquad (5.94)$$

with  $J_{\gamma}(w)$  denoting a combination of iterated integrals that is homotopy-invariant. We denote the space that these integrals generate by

$$\mathcal{V}_{\mathbf{B}} = \langle J_{\gamma}(w) \, | \, w \in \mathcal{B}_{\mathbf{B}} \rangle_{\mathbb{K}} \,. \tag{5.95}$$

Next, we show how the C-form property of a differential equation and the linear dependence of the iterated integrals in its solution are connected.

# **Theorem 5.1.** The following statements are equivalent:

- 1. The differential equation defining  $\mathbb{A}_{\mathbf{B}}$  is in C-form, i.e ,it has the properties listed in Definition 5.1<sup>16</sup> and  $\mathbb{V}_{\mathbf{B}} \cap d\mathcal{F}_{\mathbb{C}} = \{0\}$ .
- 2. The iterated integrals  $J_{\gamma}(w)$ ,  $w \in \mathcal{B}_{\mathbf{B}}$ , are linearly independent over  $\mathcal{F}_{\mathbb{C}}$ .

 $^{16}\mathbb{A}_{\mathbf{B}}$  is differentially closed and all of its constants lie in  $\mathbb{K}$ .

In Appendix D.2 we repeat the proof given in [226], which closely follows the proof for the single-variable version of the statement given in [309].

# Lie Algebras for Differential Equations in C-Form

Let  $\mathfrak{g}_{\mathbf{B}}$  be the Lie algebra obtained as the quotient of the free Lie algebra over  $\mathbb{K}$  with generators  $e_{\mathbf{I},i}$ ,  $1 \leq i \leq p$  and the Lie ideal generated by (cf. eq. (5.93))

$$\sum_{i,j=1}^{p} a_{ijk} \left[ e_{I,i}, e_{I,j} \right], \qquad 1 \le k \le q.$$
(5.96)

The quadratic algebra  $\mathbb{E}_{\mathbf{B}}$  defined below eq. (5.93) is the universal enveloping algebra of  $\mathfrak{g}_{\mathbf{B}}$ . The matrices  $\mathbf{B}_i$  of eq. (5.83) provide an N-dimensional representation of  $\mathfrak{g}_{\mathbf{B}}$ ,

$$\rho: \mathfrak{g}_{\mathbf{B}} \to \operatorname{End}(\mathbb{C}^N), \quad e_{\mathrm{I},\mathrm{i}} \mapsto \mathbf{B}_{\mathrm{i}}.$$
(5.97)

Thus, to an algebra  $V_{\mathbf{B}}$  we can associate a Lie-Algebra  $\mathfrak{g}_{\mathbf{B}}$  and the differential equation provides a representation via the matrices  $\mathbf{B}_i$ . Note that different families of Feynman integrals might share the same Lie-algebra but of course their canonical differential equation is not the same, thus they provide different representations of this Lie-algebra.

<sup>&</sup>lt;sup>17</sup>Note that if there is a single variable (r=1), the flatness condition is trivially satisfied, and the Lie algebra  $\mathfrak{g}_{\mathbf{B}}$  is a free Lie algebra.

## **Self-Duality**

A self-duality property of Feynman integral differential equations arises as a symmetry of the  $\varepsilon$ -form connection matrix  $\mathbf{B}(\lambda)$ . In particular, by the definition of ref. [310] the matrix  $\mathbf{B}(\lambda)$  is self dual if there is a constant matrix  $\mathbf{M}$  such that  $\widetilde{\mathbf{B}}(\lambda) = \mathbf{M}^{-1}\mathbf{B}(\lambda)\mathbf{M}$  is persymmetric, i.e., it is symmetric with respect to the anti-diagonal. This is equivalent to saying that  $\widetilde{\mathbf{B}}$  fulfils

$$\widetilde{\mathbf{B}}(\lambda) = \mathbf{K}_N \widetilde{\mathbf{B}}(\lambda)^T \mathbf{K}_N^{-1}, \qquad (5.98)$$

with

$$\mathbf{K}_{N} = \mathbf{K}_{N}^{T} = \mathbf{K}_{N}^{-1} = \begin{pmatrix} 0 & 0 & \cdots & 0 & 1 \\ 0 & 0 & \cdots & 1 & 0 \\ \vdots & \ddots & \ddots & \vdots \\ 0 & 1 & \cdots & 0 & 0 \\ 1 & 0 & \cdots & 0 & 0 \end{pmatrix} . \tag{5.99}$$

It was observed in [21, 22, 107] that the differential equation for multi-loop equalmass banana integrals satisfies this property. These integrals are related to oneparameter families of Calabi-Yau varieties, where self-duality is expected to be a feature of the Gauss-Manin connection at  $\varepsilon \to 0$ . A more detailed discussion of this property was given in [310].

# 5.2.2 Bases in C-Form and the Intersection Matrix

The main aim of this section is to establish a connection between properties of the differential equation (being in C and  $\varepsilon$ -form) and the intersection matrix for certain bases of (cuts of) Feynman integrals. The crucial result needed for this is the following theorem of [226]:

**Theorem 5.2.** Consider two systems  $G_i(\lambda, \varepsilon)$  in  $\varepsilon$  and C-form for the same algebra  $A_B$  and of the same dimension N. They fulfill differential equations

$$d_{\text{ext}}\mathbf{G}_i(\boldsymbol{\lambda},\varepsilon) = \varepsilon \mathbf{B}^{(i)}(\boldsymbol{\lambda})\mathbf{G}_i(\boldsymbol{\lambda},\varepsilon), \qquad i = 1, 2.$$
 (5.100)

Assume that there are matrices of full rank,

$$\Delta(\lambda, \varepsilon) \in GL(N, \mathbb{A}_{\mathbf{B}} \otimes \mathbb{K}(\varepsilon)) \quad and \quad \mathbf{H}(\varepsilon) \in GL(N, \mathbb{C}(\varepsilon)),$$
 (5.101)

such that

$$\mathbf{G}_1(\lambda, \varepsilon) (\mathbf{H}(\varepsilon)^{-1})^T \mathbf{G}_2(\lambda, \varepsilon)^T = \Delta(\lambda, \varepsilon).$$
 (5.102)

Then  $d\Delta(\lambda, \varepsilon) = 0$ .

*Proof.* By eq. (2.104) we know that  $\varepsilon$ -form differential equations can be solved with path ordered exponentials

$$\mathbf{G}_{i} = \mathbb{P}_{\gamma}^{(i)}(\boldsymbol{\lambda}, \varepsilon) \cdot \mathbf{G}_{0,i}(\varepsilon), \qquad (5.103)$$

where the  $\mathbf{G}_{i,0}(\varepsilon)$  are constant in  $\mathbb{K}^{N\times N}$ . Then eq. (5.102) takes the form

$$\Delta(\lambda, \varepsilon) = \mathbb{P}_{\gamma}^{(1)}(\lambda, \varepsilon) \left( \mathbf{H}_{12}(\varepsilon)^{-1} \right)^{T} \mathbb{P}_{\gamma}^{(2)}(\lambda, \varepsilon)^{T}, \qquad (5.104)$$

with

$$\mathbf{H}_{12}(\varepsilon) = \left(\mathbf{G}_{0,1}(\varepsilon)^{-1}\right)^T \mathbf{H}(\varepsilon) \mathbf{G}_{0,2}(\varepsilon)^{-1}. \tag{5.105}$$

We expand  $\Delta(x,\varepsilon)$  in  $\varepsilon$ ,

$$\Delta_{ij}(\boldsymbol{\lambda}, \varepsilon) = \sum_{k=k_0}^{\infty} \varepsilon^k \, \Delta_{ij}^{(k)}(\boldsymbol{\lambda})$$
 (5.106)

and consider each of the coefficients  $\Delta_{ij}^{(k)}(\lambda)$  separately as a function of  $\lambda$ . By our assumption, we know that  $\Delta_{ij}^{(k)}(\lambda) \in \mathbb{A}_{\mathbf{B}} \subseteq \mathcal{F}_{\mathbb{C}}$ . On the other hand, due to eq. (5.104), we know that  $\Delta_{ij}^{(k)}(\lambda) \in \mathbb{E}_{\mathbf{B}}^{\mathbb{C}} = \mathbb{C} \otimes_{\mathbb{K}} \mathbb{E}_{\mathbf{B}}$  and thus takes the form

$$\Delta_{ij}^{(k)}(\lambda) = \sum_{w \in \mathcal{B}_{\mathbb{R}}} c_{\Delta,w}^{ijk} J(w)$$
 (5.107)

with  $c_{\Delta,w}^{ijk} \in \mathbb{C}$  and  $J(w) \in \mathbb{E}_{\mathbf{B}}$ . Due to Theorem 5.1, this trivially implies, that

$$0 = \sum_{\emptyset \neq w \in \mathcal{B}_{\mathbb{A}}} c_{\Delta,w}^{ijk} J(w) + (c_{\Delta,\emptyset}^{ijk} - \Delta_{ij}^{(k)}(\lambda)) J(\emptyset).$$
 (5.108)

Since we assumed that both differential equations are in C-form, the J(w) are linearly independent over  $\mathcal{F}_{\mathbb{C}}$ , by Theorem 5.1. Thus,  $c_{\Delta,w}^{ijk}=0$  for all  $w\neq\emptyset$  and

$$\Delta_{ij}^{(k)}(\lambda) = c_{\Delta,\emptyset}^{ijk} \in \mathbb{C}. \tag{5.109}$$

The matrix  $\Delta$  is constant in  $\lambda$ .

Towards Feynman Integrals Whilst this statement is generic for two systems in  $\varepsilon$  and C-form, we want to apply it for systems of (cuts of) Feynman integrals (which can always be interpreted as (relative) twisted periods). In general, we aim to compute a vector of master integrals  $\mathbf{I}(\lambda, \varepsilon)$  that fulfils a differential equation of the form  $d_{\text{ext}}\mathbf{I}(\lambda, \varepsilon) = \mathbf{A}(\lambda, \varepsilon)\mathbf{I}(\lambda, \varepsilon)$ , as given in eq. (2.98). One can choose a basis of the (relative) twisted cohomology group defined by the integral family, so that:

$$\mathbf{I}(\boldsymbol{\lambda}, \varepsilon) = \left(\int_{\gamma} \Phi \varphi_{I,i}\right)_{i=1,\dots,M} \tag{5.110}$$

where  $\gamma$  is some cycle. One can also choose a basis  $\{\gamma_i\}_{i=1,\dots,M}$  for the twisted homology group and define a period matrix  $\mathbf{P}_I(\boldsymbol{\lambda},\varepsilon)$ , which satisfies the same differential equation as  $\mathbf{I}(\boldsymbol{\lambda},\varepsilon)$ , besides simple boundary terms. As described in

#### See also:

In Section 4.4 we explained how to associate (relative) twisted (co-)homology group to a Feynman integral family.

Subsection 2.5.2, we first bring the basis in canonical form (which here we replace with  $\varepsilon$ -form and C-form) via a transformation

$$\mathbf{J}(\boldsymbol{\lambda}, \varepsilon) = \mathbf{U}(\boldsymbol{\lambda}, \varepsilon)\mathbf{I}(\boldsymbol{\lambda}, \varepsilon) \tag{5.111}$$

(or equivalently  $\varphi_J = \mathbf{U}\varphi_I$  or  $\mathbf{P}_J = \mathbf{U}\mathbf{P}_I$ ), so that the new basis fulfils a differential equation in  $\varepsilon$ - and C-form that we denote by

$$d_{\text{ext}} \mathbf{J}(\lambda, \varepsilon) = \varepsilon \mathbf{B}(\lambda) \mathbf{J}(\lambda, \varepsilon) . \tag{5.112}$$

We assume here, that this transformation to C-form can be found for the given integral family. The entries of the connection matrix  $\mathbf{B}(\lambda)$  define the related algebra  $\mathbb{A}_{\mathbf{B}}$ . Similarly, we can define the respective dual objects by considering the dual twisted cohomology group defined by the integral family. Starting with some basis of dual master integrals  $\check{\mathbf{I}}(\lambda,\varepsilon)$  that is defined by integrating the dual basis of cocycles  $\check{\boldsymbol{\varphi}}_I$  along some dual cycle and fulfills a differential equation  $\mathbf{d}_{\mathrm{ext}}\check{\mathbf{I}}(\lambda,\varepsilon) = \check{\mathbf{A}}(\lambda,\varepsilon)\check{\mathbf{I}}(\lambda,\varepsilon)$ , we assume that we can find a change of the dual basis

$$\check{\mathbf{J}}(\lambda,\varepsilon) = \check{\mathbf{U}}(\lambda,\varepsilon)\check{\mathbf{I}}(\lambda,\varepsilon) \tag{5.113}$$

so that the new basis fulfils the  $\varepsilon$  and C-form differential equation

$$d_{\text{ext}}\check{\mathbf{J}}(\lambda,\varepsilon) = \varepsilon \check{\mathbf{B}}(\lambda)\check{\mathbf{J}}(\lambda,\varepsilon). \tag{5.114}$$

Differential equations and their canonical form for dual integrands were studied in detail in [47, 49, 308]. Again, we assume that the differential equation is in C-form and the algebra it defines is the same as the one defined by the non-dual connection,  $A_{\mathbf{B}}$ . We can also choose some basis of dual cycles  $\check{\gamma}_i$  and define a dual twisted period matrix related to the Feynman integrals family  $\check{\mathbf{P}}_J(\lambda, \varepsilon)$ . From the starting bases and the canonical bases we compute intersection matrices:<sup>18</sup>

$$\mathbf{C}_{I} = \frac{1}{(2\pi i)^{n}} \int_{Y} \boldsymbol{\varphi}_{I} \wedge \check{\boldsymbol{\varphi}}_{I} \tag{5.115}$$

$$\mathbf{C}_J = \frac{1}{(2\pi i)^n} \int_X \boldsymbol{\varphi}_J \wedge \check{\boldsymbol{\varphi}}_J. \tag{5.116}$$

In general, for a simple choice of initial basis (e.g. the d log basis) the entries of the intersection matrix  $\mathbf{C}_I(\lambda, \varepsilon)$  are rational functions of  $\varepsilon$  and the kinematic parameters  $\lambda$ . Algebraic functions are generally introduced due to the transformation to an  $\varepsilon$ - and C-form basis. The intersection matrices are related by

$$\mathbf{C}_{I} = \mathbf{U}(\boldsymbol{\lambda}, \varepsilon) \, \mathbf{C}_{I}(\boldsymbol{\lambda}, \varepsilon) \, \check{\mathbf{U}}(\boldsymbol{\lambda}, \varepsilon)^{T} \,. \tag{5.117}$$

The entries of  $C_j(\lambda, \varepsilon)$  lie in  $A_B \otimes \mathbb{K}(\varepsilon)$ . The twisted Riemann bilinear relations of eq. (4.58) in the  $\varepsilon$ - and C-form basis take the form

$$(2\pi i)^{-n} \mathbf{P}_J(\boldsymbol{\lambda}, \varepsilon) \left( \mathbf{H}(\varepsilon)^{-1} \right)^T \check{\mathbf{P}}_{\mathbf{J}}(\boldsymbol{\lambda}, \varepsilon)^T = \mathbf{C}_J(\boldsymbol{\lambda}, \varepsilon). \tag{5.118}$$

Note that in some due to physicases cal symmetries in the Feynman integral family that doe not appear in the twisted cohomology group, the dimension of the Feynman integral family is smaller than the dimension of the twisted cohomology group. Let us assume here that the dimension of the twisted cohomology group and the Feynman integral family agree. Even if this assumption does not hold we can still apply many of the results in practice in many cases.

<sup>18</sup>We use here the notation  $\int_X \varphi \wedge \check{\varphi}$  to indicate a matrix with entries  $\int_X \varphi_i \wedge \check{\varphi}_j$ .

This relation has exactly the form that the relation required for Theorem 5.102 to be fulfilled need to have, considering that both intersection matrices necessarily have full rank. Thus, we can conclude that

$$d_{\text{ext}} \mathbf{C}_J(\lambda, \varepsilon) = 0, \qquad (5.119)$$

i.e. the intersection matrix is constant in the external parameters if it is computed from C- and  $\varepsilon$ -form bases.

**Theorem 5.3.** The matrix  $C_J(\varepsilon)$  computed from canonical ( $\varepsilon$ -form and C-form) bases can be written as a product

$$\mathbf{C}_{J}(\varepsilon) = \mathbf{C}_{J}^{0} \widetilde{\mathbf{C}}_{J}(\varepsilon) , \qquad (5.120)$$

where  $\mathbf{C}_J^0 \in \mathrm{GL}(N, \mathbb{K})$  is a constant matrix of full rank and  $\widetilde{\mathbf{C}}_J(\varepsilon) \in \mathrm{GL}(N, \mathbb{K}(\varepsilon))$  is a matrix of full rank that commutes with  $\check{\mathbf{B}}(\lambda)^T$ .

*Proof.* Using eq. (4.63), we give differential equation for the intersection matrix  $C_J$ :

$$d_{\text{ext}} \mathbf{C}_J(\boldsymbol{\lambda}, \varepsilon) = \varepsilon \mathbf{B}(\boldsymbol{\lambda}) \, \mathbf{C}_J(\boldsymbol{\lambda}) + \varepsilon \mathbf{C}(\boldsymbol{\lambda}) \, \check{\mathbf{B}}(\boldsymbol{\lambda})^T \,. \tag{5.121}$$

From eq. (5.119), we know that  $d_{\text{ext}}\mathbf{C}_J(\boldsymbol{\lambda},\varepsilon) = 0$ . Thus:

$$\mathbf{B}(\lambda) \, \mathbf{C}_J(\lambda) = -\mathbf{C}_J(\lambda) \, \check{\mathbf{B}}(\lambda)^T \,. \tag{5.122}$$

Both,  $\mathbf{B}(\lambda)$  and  $\check{\mathbf{B}}(\lambda)$  can be written in the basis of  $V_{\mathbf{B}}$  and we can expand the intersection matrix in  $\varepsilon$  around zero:

$$\mathbf{C}_{J}(\varepsilon) = \varepsilon^{m} \sum_{k=0}^{\infty} \mathbf{c}_{J,k} \varepsilon^{k}$$
 (5.123)

for some integer m. Then eq. (5.122) is equivalent to the set of equations

$$\mathbf{B}_{i} \mathbf{c}_{J,k} = -\mathbf{c}_{J,k} \check{\mathbf{B}}_{i}^{T}, \qquad 1 \le i \le p, k \ge 0.$$
 (5.124)

Since for generic  $\varepsilon$  the intersection matrix is non-degenerate, there must be some specific  $\varepsilon_0 \in \mathbb{C}$ , such that  $\mathbf{C}_J(\varepsilon_0)$  has full rank. We define  $\mathbf{C}_J^0 = \mathbf{C}_J(\varepsilon_0)$  and  $\mathbf{C}_J(\varepsilon) = \mathbf{C}_J^0 \tilde{\mathbf{C}}_J(\varepsilon)$ . The values of  $\varepsilon$  for which  $\mathbf{C}_J(\varepsilon)$  fails to have full rank are those for which  $\det \mathbf{C}_J(\varepsilon)$  is either zero or infinity. Since  $\det \mathbf{C}_J(\varepsilon)$  is a rational function of  $\varepsilon$ , it has a discrete and finite set of zeroes and singularities. Consequently, there exists a neighbourhood U around  $\varepsilon = 0$  such that  $\mathbf{C}_J(\varepsilon)$  maintains full rank for all  $\varepsilon \in U - \{0\}$ . The set  $U - \{0\}$  contains infinitely many rational numbers, from which we can choose one to be  $\varepsilon_0$ . Given that  $\mathbf{C}(\varepsilon) \in \mathbb{K}(\varepsilon)^{N \times N}$ , it follows that every entry of  $\mathbf{C}_0$  belongs to  $\mathbb{K}$ . Then, eq. (5.122) evaluated at  $\varepsilon = \varepsilon_0$  takes the form

$$\mathbf{B}(\lambda) = -\mathbf{C}_J^0 \, \check{\mathbf{B}}(\lambda)^T \, \left(\mathbf{C}_J^0\right)^{-1} \,. \tag{5.125}$$

We insert this back into eq. (5.122) for generic  $\varepsilon$  and find:

$$\check{\mathbf{B}}(\lambda)^T \tilde{\mathbf{C}}_J(\varepsilon) = \tilde{\mathbf{C}}_J(\varepsilon) \, \check{\mathbf{B}}(\lambda)^T \,. \tag{5.126}$$

Thus, we see that  $\check{\mathbf{B}}(\lambda)$  and  $\tilde{\mathbf{C}}_J(\varepsilon)$  commute.

Let us make some comments on what we have found in this section:

- The fact that the intersection matrix between a  $\varepsilon$ -form and C-form basis and dual basis needs to be constant confirms the observations made in the study of dual differential equations in [47, 49]. In those cases, the canonical dual basis that was constructed turned out to be orthogonal to the known canonical basis in the sense that  $\mathbf{C}_J \sim \mathbf{1}$ .
- The assertion that the canonical basis and the canonical dual basis are orthogonal or related in a simple way allows one to use knowledge of one of the two to construct the other. Additionally, the assertion that the intersection matrix should be constant in the  $\varepsilon$  and C-form bases gives us additional relations that one can use to find these bases. We comment on this specifically within the context of the algorithm of [24], that we review in Subsection 6.1.1: In the last step of this algorithm, one makes an ansatz for a rotation that removes  $\varepsilon^0$  entries of the connection matrix. To solve for the entries of this ansatz, one needs to solve the differential equations that result from the requirement of  $\varepsilon$ -form. But, one can also compute the intersection matrix after this rotation-ansatz and require it to be constant. This requirement generally leads to a number of algebraic relations for the entries of the ansatz (new functions). We confirm that this works experimentally with several examples in Chapter 6.

Thus, practically we have two ways to make use of the results of this section: We can interpret the constant intersection matrix as an informal check for having obtained a canonical basis<sup>19</sup>. On the other hand, we can use the assumption, that in the correct basis the intersection matrix *should* be constant to determine this basis. This is particularly useful for maximal cut families and that is because for maximal cuts, we have the discussed self-duality property of the period matrix that allows us to relate period matrices and dual period matrices and reduce the amount of *new objects* in the TRBRs.

# 5.2.3 Maximal Cuts in C-Form

In Section 5.1.2 we found that we obtain bilinear relations for maximal cuts from the TRBRs due to their self-duality property. Here, we explore how this self-duality property can be used to further restrict the form of the intersection matrix for canonical bases and establish a link to the self-duality discussed in [310]. The self-duality property of a twisted (co-)homology group implies that one can chose a dual basis so that the connection matrix of the period matrix and its dual are related by  $\varepsilon \to -\varepsilon$ , see eq. (4.89). In that case, if the basis of the twisted cohomology group is chosen such that its differential equation is in  $\varepsilon$ - and C-form, the same is true for the dual basis and

$$\check{\mathbf{A}}(\varepsilon, \lambda) = \varepsilon \check{\mathbf{B}}(\lambda) = -\varepsilon \mathbf{B}(\lambda) = \mathbf{A}(-\varepsilon, \lambda). \tag{5.127}$$

<sup>19</sup>Note that we do not claim, that the inverse direction is correct. In particular there are many bases that have constant intersection matrices but are not the canonical ones.

A family of Feynman integrals and its dual family share the same algebra  $\mathbb{A}_{\mathbf{B}}$ , they correspond to different representations of the same Lie algebra  $\mathfrak{g}_{\mathbf{B}}$ ,

$$\rho(\mathbf{e}_{\mathrm{I},i}) = \mathbf{B}_{\mathrm{i}} \quad \text{and} \quad \check{\rho}(\mathbf{e}_{\mathrm{I},i}) = \check{\mathbf{B}}_{\mathrm{i}}.$$
(5.128)

For any representation  $\rho$  of a Lie algebra, there exists a corresponding dual representation given by  $\rho^* = -\rho^T$ . Two representations  $\rho_1$  and  $\rho_2$  are equivalent, if there is an invertible matrix  $\mathbf{M}$ , such that  $\rho_2 = \mathbf{M}\rho_1\mathbf{M}^{-1}$ . Thus, the representation induced by the dual C-form differential equation coincides with the dual representation  $\check{\rho} = \rho^*$  as we see using eq.  $(5.125)^{20}$ :

<sup>20</sup>We label by J the  $\varepsilon$ and C-form basis.

$$\check{\rho}(e_{I,i}) = \check{\mathbf{B}}_{i} = -\left(\mathbf{C}_{J}^{0}\right)^{T} \mathbf{B}_{i}^{T} \left(\left(\mathbf{C}_{J}^{0}\right)^{-1}\right)^{T} = \left(\mathbf{C}_{J}^{0}\right)^{T} \rho^{*}(e_{I,i}) \left(\left(\mathbf{C}_{J}^{0}\right)^{T}\right)^{-1}. \tag{5.129}$$

Schur's Lemma (see eq.(2) in Appendix E) characterizes key properties of irreducible representations. Here, we present a version particularly suited for the analysis of C-form differential equations [226].

**Lemma 1.** Let  $\mathbf{B}(\lambda)$  be the matrix describing an irreducible system in C-form, and  $\mathbf{M}(\varepsilon) \in \mathbb{K}(\varepsilon)^{N \times N}$ . Then  $\mathbf{B}(\lambda)$  and  $\mathbf{M}(\varepsilon)$  commute if and only if  $\mathbf{M}(\varepsilon)$  is a multiple of the identity, i.e., there is a rational function  $f \in \mathbb{K}(\varepsilon)$  such that  $\mathbf{M}(\varepsilon) = f(\varepsilon)\mathbb{1}$ .

*Proof.* We express  $\mathbf{B}(\lambda)$  in terms of the basis  $\varpi_i$  and expand  $\mathbf{M}(\varepsilon)$  as a series in  $\varepsilon$ ,

$$\mathbf{M}(\varepsilon) = \sum_{k=k_0}^{\infty} \mathbf{M}_k \varepsilon^k \,. \tag{5.130}$$

Then  $\mathbf{B}(\lambda)$  and  $\mathbf{M}(\varepsilon)$  commute if and only if

$$[\mathbf{B}_i, \mathbf{M}_k] = 0, \qquad 1 \le i \le p, \quad k \ge k_0.$$
 (5.131)

Given that the system is assumed to be irreducible, the representation  $\rho(t_i) = \mathbf{B}_i$  is irreducible over  $\mathbb{C}$ . By Schur's lemma, any operator that commutes with an irreducible representation of a Lie algebra over an algebraically closed field must be a scalar multiple of the identity. Hence, we have  $\mathbf{M}_k = \lambda_k \mathbb{1}$  for some  $\lambda_k \in \mathbb{K}$ , which confirms the claim.

That means that if  $\rho$  is irreducible, so is its dual  $\rho^*$ . By applying Theorem 5.3 together with Schur's lemma, we conclude that  $\mathbf{C}(\varepsilon) = f(\varepsilon)\mathbf{C}_0$  for some rational function f. In general, the representation associated with the C-form differential equation of Feynman integrals is not necessarily irreducible. However, we observe that irreducible representations arise from the diagonal blocks. Specifically, for the  $\varepsilon$ -form and C-form canonical bases of the differential equation governing the maximal cut and its dual, equation eq. (5.127) holds and leads to

$$\mathbf{B}(\lambda) = \left(\mathbf{C}_J^0\right)^T \mathbf{B}(\lambda)^T \left(\left(\mathbf{C}_J^0\right)^{-1}\right)^T$$
 (5.132)

in the limit  $\varepsilon \to 0$ . That means, in  $\varepsilon \to 0$ , the representation is self-dual. If we additioanly assume that the representation is irreducible <sup>21</sup>, we can show [226]:

<sup>&</sup>lt;sup>21</sup>If this condition fails, then the statement holds for all irreducible blocks individually.

**Theorem 5.4.** If the representation of  $\mathfrak{g}_{\mathbf{B}}$  is both self-dual (in the above sense) and irreducible, then we have  $\mathbf{C}(\varepsilon) = f(\varepsilon) \mathbf{C}_J^0$ , where  $f \in \mathbb{K}(\varepsilon)$  is a rational function of  $\varepsilon$  and  $\mathbf{C}_J^0 \in \mathrm{GL}(N,\mathbb{K})$  is either symmetric or antisymmetric.

*Proof.* By the version of Schur's lemma applicable to our case, we know that  $\mathbf{C}(\varepsilon) = f(\varepsilon) \mathbf{C}_0$ . So, we just need to show the symmetry of  $\mathbf{C}_0$ . In a self-dual system, equation (5.132) must be satisfied. We interpret eq. (5.132) as an equation for  $\mathbf{C}_0$ , which is linear in  $\mathbf{C}_0$ . Moreover, if  $\mathbf{C}_0$  is a solution, then  $\mathbf{C}_0^T$  is also a solution. Schur's lemma implies that the solution is unique up to a multiplicative constant, so

$$\mathbf{C}_0^T = k \, \mathbf{C}_0 \,, \tag{5.133}$$

for some  $k \in \mathbb{K}$ . Taking the transpose of this equation, we find that k must satisfy  $k^2 = 1$ , leading to the conclusion that  $k = \pm 1$  and consequently  $\mathbf{C}_0$  is symmetric or antisymmetric.

More details on the symmetric and antisymmetric cases and when either arises can be found in [226]. Here, we just note that in the symmetric case, we can always change to another canonical basis so that the self-duality property of eq. (5.98) from [310] is fulfilled.

# Hyperelliptic Maximal Cuts

#### See also:

In this chapter, we make extensive use of the mathematical foundations introduced in Chapter 3, particularly in Sections 3.2 and 3.4. Additionally, we use the results on the intersection matrix for canonical bases that were introduced in Section 5.2.

In this chapter, we discuss canonical differential equations for maximal cuts of hyperelliptic Feynman integral families, using specific families of Lauricella functions as defined in eq. (4.175) as a model. The parameters are chosen such that, in the  $\varepsilon \to 0$  limit, their integrand defines the polynomial equation of a hyperelliptic curve.

In Section 6.1 we review a method for finding a canonical differential equation, following [24] and then explain how the transformation to a canonical basis can be determined for a genus-one example, as well as for both even- and odd-genus two cases. These considerations should naturally extend to any genus. In Section 6.2 we examine the forms that appear in the resulting differential equation.

♠ This chapter closely follows previously published results [34], which were obtained in collaborations with Claude Duhr and Sven Stawinski.

# Contents of this Chapter

6.1 DEQs for Hyperelliptic Lauricella Functions 168		
6.1.1	Review: Algorithm	
6.1.2	Elliptic Hypergeometric $_2F_1$ -function 171	
6.1.3	Three Parameter Lauricella Function	
6.1.4	Four Parameter Lauricella Function 179	
6.2 Modular properties of the Canonical Differential Equa-		
${f tion}$		
6.2.1	Modular Properties of the Connection Matrix $\mathbf{B}_{H,3}(\lambda,\varepsilon)$ 183	
6.2.2	Modular Properties of the Connection Matrix $\mathbf{B}_{H,5}(\lambda,\varepsilon)$ 184	

In this chapter, we consider families of integrals of the form

$$\mathcal{F}_{H}^{\nu}(\lambda,\varepsilon) = \int_{\lambda_{n}}^{\infty} dx \, x^{-\frac{1}{2}+\beta_{1}} (x-1)^{-\frac{1}{2}+\beta_{2}} (x-\lambda_{1})^{-\frac{1}{2}+\beta_{3}} \dots (x-\lambda_{n})^{-\frac{1}{2}+\beta_{n+2}} . \quad (6.1)$$

Here  $\beta_i = \nu_1 + a_i \varepsilon$ , where  $\nu$  is a vector of integers,  $a_i$  are some rational numbers,  $\lambda$  takes the role of the kinematic parameters and  $\varepsilon$  is a generic parameter resembling the dimensional regulator. Up to a prefactor in the  $\lambda$ , these integrals are linear combinations of Lauricella  $\mathcal{F}_D$  functions. For appropriate values of  $\nu$ ,  $\alpha$ , and  $\lambda$ , the maximal cut of the non-planar crossed box in eq. (2.67) contains only integrals of this form with n=4. This motivates considering the class of integrals in eq. (6.1) as a model for maximal cuts of Feynman integrals. In Example 3.14 we already noted that the non-planar crossed box is related to a hyperelliptic curve of genus two via the polynomial equation defined by the  $\varepsilon \to 0$  limit of the maximal cut's integrand. This argument can be extended to all integrals of the form in eq. (6.1). Taking  $\nu_i = 0$  and setting  $\varepsilon \to 0$ , the integrand defines the polynomial equation

$$y^2 = x(x-1)(x-\lambda_1)\dots(x-\lambda_n), \qquad (6.2)$$

which defines a hyperelliptic curve of genus g as given in eq. (3.28). We can also interpret the Aomoto-Gelfand hypergeometric functions eq. (6.1) as periods of twisted (co-)homology groups. In particular, the twist of eq. (6.1) is:

$$\Phi_H = x^{-\frac{1}{2} + a_1 \varepsilon} (x - 1)^{-\frac{1}{2} + a_2 \varepsilon} (x - \lambda_1)^{-\frac{1}{2} + a_3 \varepsilon} \dots (x - \lambda_n)^{-\frac{1}{2} + a_{n+2} \varepsilon}$$
(6.3)

and it defines the twisted cohomology group  $H^1_{dR}(X_H, \nabla_{\Phi_H})$ , the twisted homology group  $H_1(X_H, \check{\mathcal{L}}_{\Phi_H})$  and their duals with

$$X_H = \mathbb{CP} - \{0, 1, \lambda_1, \dots, \lambda_n, \infty\}.$$
(6.4)

Thus, one can compute a period matrix, its dual and the intersection matrices associated to a specific basis for this integral family, as explained in Appendix B. Note also that choosing a basis of differentials for  $H^1_{dR}(X_H, \nabla_{\Phi_H})$  is equivalent to choosing a basis of master integrals.<sup>1</sup>

# 6.1 DEQs for Hyperelliptic Lauricella Functions

In this first section of the chapter we focus on obtaining the canonical differential equation.

# 6.1.1 Review: Algorithm

Here, we provide a partial review of the algorithm in [24]. We only cover the steps relevant for the maximal cut while omitting detailed discussions of its full intricacies. Instead, we focus on the key concepts needed for the discussion below, with an emphasis on hyperelliptic Feynman integrals. For further details, we refer to [24]. Additionally, we highlight where ideas discussed in Chapter 5 can complement the method.

See also: c curves

Hyperelliptic curves are reviewed in Section 3.2.

### See also:

Twisted cohomology is reviewed in Section 4.1 and a specific discussion on Aomoto-Gelfand hypergeometric integrals in this context can be found in Section 4.3.

<sup>1</sup>Thus, as before, when we say basis of integrands or master integrands below we always refer to this basis of the twisted cohomology. Step 1: Initial basis We consider a family of integrals that define the maximal cut of a Feynman integral family. To set up the differential equation, we first choose an initial basis of master integrals. A good choice of initial integrals significantly simplifies the subsequent steps. It seems that selecting a basis of integrals that satisfy the Hodge filtration of the underlying geometry is a particularly suitable choice [8, 24, 107, 311, 312]. Practically, this requirement is often fulfilled if one chooses as the first (set of) master integrands<sup>2</sup> holomorphic ones, and then adds a set of their derivatives with respect to the external parameters. The remaining basis elements are completed with integrands that introduce additional poles (punctures on the geometry). This choice of initial basis is referred to as the derivative basis. Let us make this more clear by considering specifically maximal cuts of hyperelliptic integrals.

**Example 6.1** (Initial Basis for Hyperelliptic Maximal Cuts). In this case, the integrand should always contain a factor similar to the one in eq. (6.3). In the discussion below, we consider exclusively this factor.<sup>3</sup> Naturally, one can choose a basis of integrands as indicated in eq. (3.56), i.e., select g first-kind differentials, g second-kind differentials, and any additional differentials required by extra branch points. We find that this is not a good initial basis that simplifies the next steps. Instead, we choose for the second kind differentials independent derivatives of the first kind differentials. In particular, each second-kind differential can be taken as the derivative of one of the first-kind differentials. Naturally, there is some freedom in the choice of differentiation variables and we make a symmetric choice by summing over all derivatives:

$$\frac{\text{first kind}}{\varpi_1, \dots, \varpi_g}, \sum_{\lambda} \frac{\text{second kind}}{\partial_{\lambda_i} \varpi_1 \cdots \sum_{\lambda} \partial_{\lambda_i} \varpi_g}, \overline{\varpi^{c_1}, \varpi^{c_2}, \dots}.$$
(6.5)

In Feynman integrals related to Calabi-Yau varieties instead of Riemann surfaces, the notion of *Abelian differential* does not exist and one has only one holomorphic differential. In that case, one can build a derivative basis by also considering higher order derivatives of the holomorphic differentials [18, 107].

Step 2: Semi-simple Rotation. The crucial step of the method is the rotation by the inverse of  $a^4$  semi-simple part  $\mathcal{S}$  of the period matrix at  $\varepsilon \to 0$ . It appears that this rotation with  $\mathcal{S}^{-1}$  ensures that, after correctly performing the subsequent steps, we obtain an  $\varepsilon$ -form basis that is in C-form, in contrast to simply rotating with the inverse of the full period matrix at  $\varepsilon \to 0$ . Note that at this stage, there may still be hidden relations between the periods in the new differential equations (e.g., spurious zeroes). To see that the differential equation is fully simplified, it is necessary to also account for quadratic relations between the variety's periods. We discussed how these relations can be derived for *any* geometry using a limit of the twisted Riemann bilinear relations in Section 5.1.2.

Obtaining the canonical basis from a rotation with  $S^{-1}$  was first advocated for Feynman integrals related to elliptic curves in [163, 313] and was later systematised

#### See also:

Examples for genus one and two can be found in eq. (6.17), eq. (6.44), and eq. (6.79).

<sup>&</sup>lt;sup>2</sup>Note again that we use the term basis of master integrands to refer to the basis of twisted cohomology, and translating this into a basis of master integrals is straightforward.

<sup>&</sup>lt;sup>3</sup>In general, maximal cuts of hyperelliptic Feynman integrals might contain additional factors of the form  $(x - \xi_i)^{\varepsilon}$ . These vanish in the limit  $\varepsilon \to 0$  but necessitate additional punctures on the Riemann surface.

<sup>&</sup>lt;sup>4</sup>This involves a choice of semi-simple and unipotent part.

and applied to various Examples of Feynman integrals associated with higher-dimensional Calabi-Yau varieties in [24].

**Example 6.2.** For hyperelliptic Feynman integrals, the period matrix at  $\varepsilon \to 0$  generally takes the form

$$\mathcal{P}_{H}(\boldsymbol{\lambda}) = \begin{pmatrix} \boldsymbol{\mathcal{A}} & \boldsymbol{\mathcal{B}} & \star \\ \tilde{\boldsymbol{\mathcal{A}}} & \tilde{\boldsymbol{\mathcal{B}}} & \star \\ 0 & 0 & \star \end{pmatrix} = \begin{pmatrix} \boldsymbol{\mathcal{A}} & 0 & 0 \\ \tilde{\boldsymbol{\mathcal{A}}} & C_{N} \boldsymbol{\mathcal{A}}^{-1T} & 0 \\ 0 & 0 & 1 \end{pmatrix} \begin{pmatrix} \mathbf{1} & \Omega & \star \\ 0 & \mathbf{1} & \star \\ 0 & 0 & \star \end{pmatrix} \equiv \boldsymbol{\mathcal{S}}_{H} \boldsymbol{\mathcal{U}}_{H}, \quad (6.6)$$

with the entries  $\star$  denoting entries related to master integrands due to the additional punctures and the (quasi-)period matrices  $\mathcal{A}, \tilde{\mathcal{A}}, \mathcal{B}, \tilde{\mathcal{B}}$  as defined in Section 3.2.  $C_N$  is some normalization factor.

Step 3: Rescaling with  $\varepsilon$  and Reordering. After the second step, generally some entries are not yet in  $\varepsilon$ -form. To integrate them out in the final step, we first need to find a transformation that moves all such entries below the diagonal, i.e., we aim for a lower-triangular  $\varepsilon^0$  part in the connection matrix. In general, this is achieved by rescaling the master integrands with functions of  $\varepsilon$  and appropriately reordering them.

Step 4: Integrating out. After step three, the non- $\varepsilon$ -form entries are in the lower-triangular part of the connection matrix. In the final step, we aim to eliminate these entries *and* obtain a C-form differential equation. To achieve this, we make an ansatz for the final transformation, which takes the form

$$\mathbf{U}_t = \mathbf{1} + \mathbf{U}_t^a. \tag{6.7}$$

with the only non-zero entries of  $\mathbf{U}_t^a$  being undetermined functions  $u_i(\boldsymbol{\lambda}, \varepsilon)$  where we have  $\varepsilon^0$  terms in the differential equation. To determine these, we transform the differential equation using this ansatz and impose the condition that the resulting equation must be in  $\varepsilon$ -form. This requirement leads to a set of coupled differential equations<sup>5</sup> for the  $u_i(\lambda, \varepsilon)$ . In general, these differential equations can be solved formally by integration. Initially, one has to consider these integrals as new functions: functions that are not rational in the kinematic variables  $\lambda$  and the periods appearing in the differential equation. In order the result in a minimal amount of special functions, it is useful to understand these functions explicitly and to minimise the number of independent new functions that we do not understand how to express in rational functions of each other, the kinematic parameters and the periods. At the same time, we seek to obtain a differential equation in canonical form, not just in  $\varepsilon$ -form. We have classified the C-form of Definition 5.1 as a conjectural generalization of the canonical form and have an explicit criterion to verify this property for maximal cuts. Specifically, if both the basis of integrands and the dual integrands (which can be obtained directly from the integrands in the maximal cut case) are in C-form, then the cohomology intersection matrix is constant, see eq. (5.119). This criterion can be applied to ensure that the resulting

<sup>5</sup>To decouple them, one can also perform the transformations step by step. differential equation is in C-form while simultaneously revealing relations among the new functions. To achieve this, we compute the cohomology intersection matrix of the basis after the final transformation (which still contains the undetermined functions  $u_i(\lambda, \varepsilon)$ ) and impose the condition that it must remain constant in  $\lambda$  while being  $\varepsilon$ -factorised.<sup>6</sup>

This requirement provides a set of algebraic relations for the  $u_i(\lambda, \varepsilon)$  in addition to the differential equations obtained from the  $\varepsilon$ -form condition. These algebraic relations are generally simpler to solve and allow us to express a subset of the new functions  $u_i(\lambda, \varepsilon)$  as rational functions of the remaining new functions,  $\lambda$ , the periods, and  $\varepsilon$ .

# **6.1.2** Elliptic Hypergeometric $_2F_1$ -function

We start with an example related to an odd elliptic curve, i.e., a hyperelliptic curve of genus one: the normalised  ${}_{2}F_{1}$  family and in particular integrals of the form

$$\mathcal{F}_{H,3}^{\nu}(\lambda,\varepsilon) = \int_0^1 dx \, x^{-\frac{1}{2}+\nu_1+a_1\varepsilon} (x-1)^{-\frac{1}{2}+\nu_2+a_2\varepsilon} (x-\lambda)^{-\frac{1}{2}+\nu_3+a_3\varepsilon} \,. \tag{6.8}$$

Twisted Cohomology: The twist is

$$\Phi_{H,2} = x^{-\frac{1}{2} + a_1 \varepsilon} (x - 1)^{-\frac{1}{2} + a_2 \varepsilon} (x - \lambda)^{-\frac{1}{2} + a_3 \varepsilon}. \tag{6.9}$$

We start with the basis of master integrands

$$\varphi_{H3}^1 = 1 \text{ and } \varphi_{H3}^2 = x.$$
 (6.10)

This choice is inspired by the canonical Abelian differentials of first kind in eq. (3.34) and second kind in eq. (3.47) kind on the elliptic curve and we choose for the dual basis the differentials  $\check{\varphi}_{H,3}^i = \varphi_{H,3}^i \left(\Phi_{H,3}|_{\varepsilon\to 0}\right)^2$ . The initial intersection matrix of the twisted cohomology group  $H^1_{dR}(X_{H,1}, \Phi_{H,1})$  is

$$\mathbf{C}_{H,1}^{(0)} = \begin{pmatrix} 0 & \frac{2}{-1+2\varepsilon(a_1+a_2+a_3)} \\ \frac{2}{1+2\varepsilon(a_1+a_2+a_3)} & \frac{4\varepsilon((1+\lambda)a_1+\lambda a_2+a_3)}{(-1+2\varepsilon(a_1+a_2+a_3))(1+2\varepsilon(a_1+a_2+a_3))} \end{pmatrix}.$$
(6.11)

Elliptics: The choice eq. (6.10) correspond to an initial basis of master integrals  $\overline{\mathbf{I}_{H,3}^{(0)}(\lambda,\varepsilon)} = \left(\mathcal{F}_H^{0,0,0}(\lambda),\mathcal{F}_H^{1,0,0}(\lambda)\right)$ . The odd elliptic curve defined by the integrand takes the form

$$y^{2} = x(x-1)(x-\lambda)$$
 (6.12)

As discussed above, the period matrix  $\mathcal{P}_{H,3}$  is central to the method and we compute it with the basis eq. (6.10) of differential and the canonical a and b cycles. As in Examples 3.1 and 3.3 we denote its entries by  $\omega_1, \omega_2, \eta_1, \eta_2$ . We split the period matrix into a *semi-simple* and a *unipotent* part,

$$\mathbf{C}P_{H,3} = \mathbf{S}_{H,3} \mathbf{\mathcal{U}}_{H,3} = \begin{pmatrix} \omega_1 & 0 \\ \eta_1 & \frac{2\pi i \lambda}{\omega_1} \end{pmatrix} \begin{pmatrix} 1 & \tau \\ 0 & 1 \end{pmatrix}. \tag{6.13}$$

<sup>6</sup>In fact, since we only proved one direction, it is not clear that the DEQ is in Cform when the intersection matrix is constant. But we found that we can practically still use this restriction. Practically, to compute the intersection matrix after the transformations, one can first compute the intersection matrix  $\mathbf{C}_0$  of the initial basis and then apply the full transformation, including the ansatz U:

 $\mathbf{C}_t = \mathbf{U}(\varepsilon)\mathbf{C}_0\mathbf{U}(-\varepsilon)^T.$ 

Note that in this basis choice, the a-cycle (quasi-)periods are explicitly given by the expressions in Example 3.8.

<u>Initial differential equation:</u> This vector of master integrals satisfies the differential equation

$$d\mathbf{I}_{H,3}^{(0)}(\lambda,\varepsilon) = d\lambda \left[ \mathbf{A}_{H,3}(\lambda,\varepsilon) \right] \mathbf{I}_{H,3}^{(0)}(\lambda,\varepsilon) = d\lambda \left[ \mathbf{A}_{H,3}^{(0)}(\lambda) + \varepsilon \mathbf{A}_{H,3}^{(1)}(\lambda) \right] \mathbf{I}_{H,3}^{(0)}(\lambda,\varepsilon) ,$$
(6.14)

with

$$\mathbf{A}_{H,3}^{(0)}(\lambda) = \begin{pmatrix} -\frac{1}{2(\lambda-1)} & \frac{1}{2\lambda(\lambda-1)} \\ -\frac{1}{2(\lambda-1)} & \frac{1}{2(\lambda-1)} \end{pmatrix}, \quad \mathbf{A}_{H,3}^{(1)}(\lambda) = \begin{pmatrix} -\frac{a_1 - (\lambda-1)a_3}{\lambda(\lambda-1)} & \frac{a_1 + a_2 + a_3}{\lambda(\lambda-1)} \\ -\frac{a_1}{\lambda-1} & \frac{a_1 + a_2 + a_3}{\lambda-1} \end{pmatrix}.$$
(6.15)

For evaluating the integral after obtaining the canonical form, we also need a boundary value and we choose as a boundary point  $\lambda = 1$ , where

$$\mathcal{F}_{H,3}^{\nu}(1) = (-1)^{\nu_{23} + \varepsilon a_{23}} \frac{\Gamma\left(\frac{1}{2} + a_1 \varepsilon + \nu_1\right) \Gamma\left(\nu_{23} + \varepsilon a_{23}\right)}{\Gamma\left(\frac{1}{2} + \nu_{123} + \varepsilon a_{123}\right)}$$
(6.16)

for Re  $(\nu_1 + \varepsilon a_1) > -\frac{1}{2}$  and Re  $(\nu_{23} + \varepsilon a_{23}) > 0$ . A canonical differential equation for this family was first obtained in [144] and we rederive it with the algorithm reviewed in Section 6.1.1.

**Step 1: Derivative Basis.** As a first step, we rotate the starting basis of eq. (6.10) to a *derivative basis* as described in eq. (6.5). That means, we rotate with the matrix

$$\mathbf{U}_{H,3}^{(1)} = \begin{pmatrix} 1 & 0 \\ (\mathbf{A}_{H,3})_{1,1} & (\mathbf{A}_{H,3})_{1,2} \end{pmatrix} = \begin{pmatrix} 1 & 0 \\ -\frac{\lambda + 2\varepsilon[a_1 + (1-\lambda)a_3]}{2\lambda(\lambda - 1)} & \frac{\lambda + 2\varepsilon[a_1 + a_2 + a_3]}{2\lambda(\lambda - 1)} \end{pmatrix}$$
(6.17)

such that

$$\mathbf{I}_{H,3}^{(1)}(\lambda,\varepsilon) = \mathbf{U}_{H,3}^{(1)} \mathbf{I}_{H,3}^{(0)}(\lambda,\varepsilon) = \begin{pmatrix} \mathcal{F}_{H}^{0,0,0}(\lambda) \\ \partial_{\lambda} \mathcal{F}_{H}^{0,0,0,0}(\lambda) \end{pmatrix}$$
(6.18)

and 
$$\mathbf{B}_{H,3}^{(1)}(\lambda,\varepsilon) = d\mathbf{U}_{H,3}^{(1)} \left(\mathbf{U}_{H,3}^{(1)}\right)^{-1} + \mathbf{U}_{H,3}^{(1)} \mathbf{A}_{H,3} \left(\mathbf{U}_{H,3}^{(1)}\right)^{-1}$$
.

Step 2: Semi-simple Rotation. Since we already transformed the basis in the first step, we also need to rotate with the transformed semi-simple part, which is

$$\mathbf{S}_{H,3}^{(1)} = \mathbf{U}_{H,3}^{(1)} \, \mathbf{S}_{H,3}|_{\varepsilon \to 0} \tag{6.19}$$

and consequently the second transformation matrix is  $\mathbf{U}_{H,3}^{(2)} = \left(\boldsymbol{\mathcal{S}}_{H,3}^{(1)}\right)^{-1}$ . After this rotation, the differential equation takes the form

$$\mathbf{B}_{H,3}^{(2)}(\lambda,\varepsilon) = d\mathbf{U}_{H,3}^{(2)} \left(\mathbf{U}_{H,3}^{(2)}\right)^{-1} + \mathbf{U}_{H,3}^{(2)} \mathbf{B}_{H,3}^{(1)} \left(\mathbf{U}_{H,3}^{(2)}\right)^{-1}$$

$$= \begin{pmatrix} 0 & \bullet \\ 0 & 0 \end{pmatrix} + \begin{pmatrix} 0 & 0 \\ \bullet & \bullet \end{pmatrix} \varepsilon + \begin{pmatrix} 0 & 0 \\ \bullet & 0 \end{pmatrix} \varepsilon^{2}.$$

$$(6.20)$$

The shaded entries indicate non-zero entries that are too large to display explicitly and/or whose precise form is irrelevant for the discussion.

Step 3: Rescaling and Reordering. In order to get rid of the  $\varepsilon^2$  entry, we rescale the entries by powers of  $\varepsilon$ . The corresponding transformation matrix is

$$\mathbf{U}_{H,3}^{(3)} = \begin{pmatrix} \varepsilon & 0\\ 0 & 1 \end{pmatrix} . \tag{6.21}$$

After this transformation, the connection matrix has the form

$$\mathbf{B}_{H,3}^{(3)}(\lambda,\varepsilon) = d\mathbf{U}_{H,3}^{(3)} \left(\mathbf{U}_{H,3}^{(3)}\right)^{-1} + \mathbf{U}_{H,3}^{(3)} \mathbf{B}_{H,3}^{(2)} \left(\mathbf{U}_{H,3}^{(3)}\right)^{-1}$$
$$= \begin{pmatrix} 0 & 0 \\ \bullet & 0 \end{pmatrix} + \begin{pmatrix} 0 & \bullet \\ \bullet & \bullet \end{pmatrix} \varepsilon,$$

with the matrices explicitly given by

$$\mathbf{B}_{\varepsilon}^{(0)}(\lambda) = \begin{pmatrix} 0 & 0 \\ p(\lambda) & 0 \end{pmatrix}, \tag{6.22}$$

$$\mathbf{B}_{\varepsilon}^{(1)}(\lambda) = \begin{pmatrix} 0 & \frac{\pi i}{(\lambda - 1)\lambda\omega_1^2} \\ -\frac{a_3(a_1 + a_2 + a_3)\omega_1^2}{\pi i} & \frac{(\lambda - 1)a_1 + \lambda a_2 + (2\lambda - 1)a_3}{\lambda(\lambda - 1)} \end{pmatrix}, \tag{6.23}$$

where  $p(\lambda)$  is a function quadratic in the (quasi-)periods

$$p(\lambda) = \frac{1}{2\pi i} \frac{\omega_1}{\lambda(\lambda - 1)} \left[ -\lambda \omega_1(a_2 + a_3) + \eta_1 \left( (\lambda - 1)a_1 + \lambda a_2 + (2\lambda - 1)a_3 \right) \right]. \quad (6.24)$$

Step 4: Integrating out. We now rotate away the  $\varepsilon^0$  part in eq. (6.22) and obtain the canonical differential equation. To this end, we make the ansatz

$$\mathbf{U}_{H,3}^{(4)}(\lambda) = \begin{pmatrix} 1 & 0 \\ u(\lambda) & 1 \end{pmatrix}, \tag{6.25}$$

and define

$$\mathbf{U}_{H,3} = \mathbf{U}_{H,3}^{(4)} \mathbf{U}_{H,3}^{(3)} \mathbf{U}_{H,3}^{(2)} \mathbf{U}_{H,3}^{(1)}. \tag{6.26}$$

Here, we fix  $u(\lambda)$  by requiring that the ensuing connection matrix

$$\mathbf{B}_{H,3}^{(4)}(\lambda,\varepsilon) = d\mathbf{U}_{H,3}^{(4)} \left(\mathbf{U}_{H,3}^{(4)}\right)^{-1} + \mathbf{U}_{H,3}^{(4)} \mathbf{B}_{H,3}^{(3)} \left(\mathbf{U}_{H,3}^{(4)}\right)^{-1} = \varepsilon \mathbf{B}_{H,3}(\lambda)$$
(6.27)

is in  $\varepsilon$ -form and the intersection matrix takes the form

$$\mathbf{C}_{H,3}^{(4)} = \mathbf{U}_{H,3} \cdot \mathbf{C}_{H,3}^{(0)} \left( \mathbf{U}_{H,3}^T \big|_{\varepsilon \to -\varepsilon} \right) = f(\varepsilon) \Delta_{H,3}$$
(6.28)

with  $\Delta_{H,3}$  a matrix that is constant in  $\lambda$  and  $\varepsilon$ . The first requirement in eq. (6.27) implies the differential equation

$$du(\lambda) + p(\lambda)d\lambda = 0, \qquad (6.29)$$

whose formal solution is

$$u_{\lambda_0}(\lambda) = -\int_{\lambda_0}^{\lambda} d\lambda' \, u(\lambda') \,, \tag{6.30}$$

for some choice of basepoint  $\lambda_0$ . The second requirement in eq. (6.28) is

$$\mathbf{C}_{H,3} = \begin{pmatrix} 0 \\ \frac{\varepsilon}{i\pi} & -\frac{\varepsilon}{\pi^2} \left[ 2\pi i u(\lambda) - \omega_1^2 (a_1(\lambda - 1) + \lambda a_2 + a_3(2\lambda - 1)) \right] \end{pmatrix} = f(\varepsilon) \Delta_{H,3}.$$
(6.31)

One can immediately deduce, that we can choose

$$f(\varepsilon) = \frac{\varepsilon}{i\pi} \tag{6.32}$$

and that requiring the  $\lambda$ -dependent (2,2) entry to vanish is equivalent to requiring that

$$2\pi i u(\lambda) - \omega_1^2(a_1(\lambda - 1) + \lambda a_2 + a_3(2\lambda - 1)) = 0, \qquad (6.33)$$

which implies that

$$u(\lambda) = \frac{i\omega_1^2}{2\pi} (a_1(\lambda - 1) + \lambda a_2 + a_3(2\lambda - 1)).$$
 (6.34)

This solution also fulfills eq. (6.29). We define the basis for this choice of  $u(\lambda)$  to be

$$\mathbf{J}_{H,3} = \mathbf{U}_{H,3} \, \mathbf{I}_{H,3}^{(0)} \tag{6.35}$$

and its differential equation takes the form

$$\varepsilon \mathbf{B}_{H,3}(\lambda,\varepsilon) = d\mathbf{U}_{H,3} (\mathbf{U}_{H,3})^{-1} + \mathbf{U}_{H,3} \mathbf{A}_{H,3} (\mathbf{U}_{H,3})^{-1}$$
 (6.36)

(6.37)

The intersection matrix of this bases and the corresponding dual canonical basis is

$$\mathbf{C}_{H,3} = \frac{\varepsilon}{i\pi} \mathbf{K}_2 \,. \tag{6.38}$$

# 6.1.3 Three Parameter Lauricella Function

Next, we present our first genus two example, namely the family of integrals

$$\mathcal{F}_{H,5}^{\nu}(\lambda,\varepsilon) = \int_0^1 x^{\alpha_1} (x-1)^{\alpha_2} (x-\lambda_1)^{\alpha_3} (x-\lambda_2)^{\alpha_4} (x-\lambda_3)^{\alpha_5} dx$$
with  $\alpha_i = -\frac{1}{2} + a_i \varepsilon + \nu_i$ ,

which depends on the three parameters  $\lambda = (\lambda_1, \lambda_2, \lambda_3)$  that we consider to be real and ordered as  $\lambda_3 > \lambda_2 > \lambda_1 > 1$ . As our initial basis of master integrals we choose

$$\mathbf{I}_{H,5}^{(0)} = \left( \int_{\gamma} \frac{\mathrm{d}x}{y} \chi_{H,5}(x), \int_{\gamma} \frac{x \mathrm{d}x}{y} \chi_{H,5}(x), \int_{\gamma} \frac{\Psi_{1}^{2,o}(x) \mathrm{d}x}{y} \chi_{H,5}(x), \frac{\Psi_{2}^{2,o}(x) \mathrm{d}x}{y} \chi_{H,5}(x) \right)^{T}$$
(6.39)

with  $\gamma = (0, 1)$ . Here, we introduced the abbreviations

$$\chi_{H.5}(x) = x^{a_1\varepsilon}(x-1)^{a_2\varepsilon}(x-\lambda_1)^{a_3\varepsilon}(x-\lambda_2)^{a_4\varepsilon}(x-\lambda_3)^{a_5\varepsilon}, \tag{6.40}$$

and the functions  $\Psi_i^{2,o}(x)$  were defined in eq. (3.51). The differentials in (6.74) also define a basis<sup>7</sup> of the twisted cohomology group with the twist  $\Phi = \chi_{H,5}(x)/y$ . We denote the initial intersection matrix obtained from this basis by  $\mathbf{C}_{H,5}^{(0)}$ . Again, the basis of differentials is inspired by the Abelian differentials of a hyperelliptic curve, namely the one defined by the polynomial equation

$$y^{2} = x(x-1)(x-\lambda_{1})(x-\lambda_{2})(x-\lambda_{3}).$$
(6.41)

Explicitly that means that the integrands of the master integrals reduce to the Abelian differentials for  $\varepsilon \to 0$ . In particular, the a- and b-periods reduce to the  $\mathcal{A}$  and  $\mathcal{B}$  periods in that limit. Again, we decompose the full period matrix into a semi-simple and a unipotent part:

$$\mathcal{P}_{H,5} = \begin{pmatrix} \mathcal{A} & \mathcal{B} \\ \tilde{\mathcal{A}} & \tilde{\mathcal{B}} \end{pmatrix} = \begin{pmatrix} \mathcal{A} & 0 \\ \tilde{\mathcal{A}} & 8\pi i \mathcal{A}^{-1T} \end{pmatrix} \begin{pmatrix} \mathbf{1} & \Omega \\ 0 & \mathbf{1} \end{pmatrix} \equiv \mathcal{S}_{H,5} \mathcal{U}_{H,5}.$$
(6.42)

The initial differential equation is

$$d\mathbf{I}_{H,5}^{(0)}(\lambda,\varepsilon) = \mathbf{A}_{H,5}(\lambda,\varepsilon)\mathbf{I}_{H,5}^{(0)}(\lambda,\varepsilon) = \left[\mathbf{A}_{H,5}^{(0)}(\lambda) + \varepsilon\mathbf{A}_{H,5}^{(1)}(\lambda)\right]\mathbf{I}_{H,5}^{(0)}(\lambda,\varepsilon), \quad (6.43)$$

where  $d = \sum_{i=1}^{3} d\lambda_i \partial_{\lambda_i}$ . The matrix  $\mathbf{A}_{H,5}(\lambda, \varepsilon)$  consists of one-forms in these variables and the corresponding functions are rational in the  $\lambda$ .

**Step 1:** As a first step, we rotate the starting basis of eq. (6.10) to a derivative basis as described in eq. (6.5). Specifically, we transform to a basis

$$\mathbf{I}_{d} = \left( \int_{\gamma} \frac{\mathrm{d}x}{y} \chi(x) , \int_{\gamma} \frac{x \mathrm{d}x}{y} \chi(x) , \sum_{i=1}^{3} \partial_{\lambda_{i}} \left[ \int_{\gamma} \frac{\mathrm{d}x}{y} \chi(x) \right] , \sum_{i=1}^{3} \partial_{\lambda_{i}} \left[ \int_{\gamma} \frac{x \mathrm{d}x}{y} \chi(x) \right] \right).$$

$$(6.44)$$

To transform to that basis, we rotate with the matrix

$$\mathbf{U}_{H,5}^{(1)} = \begin{pmatrix} 1 & 0 & 0 & 0\\ 0 & 1 & 0 & 0\\ (\hat{\mathbf{A}}_{H,5})_{1,1} & (\hat{\mathbf{A}}_{H,5})_{1,2} & (\hat{\mathbf{A}}_{H,5})_{1,3} & (\hat{\mathbf{A}}_{H,5})_{1,4}\\ (\hat{\mathbf{A}}_{H,5})_{2,1} & (\hat{\mathbf{A}}_{H,5})_{2,2} & (\hat{\mathbf{A}}_{H,5})_{2,3} & (\hat{\mathbf{A}}_{H,5})_{2,4} \end{pmatrix}$$
(6.45)

with  $\mathbf{A} = \mathbf{A}|_{\mathrm{d}\lambda_i \to 1}$ . The differential equation after this rotation is

$$\mathbf{B}_{H,5}^{(1)}(\lambda,\varepsilon) = d\mathbf{U}_{H,5}^{(1)} \left(\mathbf{U}_{H,5}^{(1)}\right)^{-1} + \mathbf{U}_{H,5}^{(1)} \mathbf{A}_{H,5} \left(\mathbf{U}_{H,5}^{(1)}\right)^{-1}.$$
 (6.46)

<sup>7</sup>Explicitly this basis is given by

 $\varpi_1 = \mathrm{d}x,$ 

 $\varpi_2 = x \, \mathrm{d}x,$   $\varpi_3 = \Psi_1^{2,\mathrm{o}}(x) \, \mathrm{d}x,$   $\varpi_4 = \Psi_2^{2,\mathrm{o}}(x) \, \mathrm{d}x.$ 

**Step 2:** As for the elliptic Example, in the second step we rotate with the inverse of the semi-simple part of the period matrix of the hyperelliptic curve, which is

$$\mathbf{S}_{H,5}^{(1)} = \mathbf{U}_{H,5}^{(1)} \, \mathbf{S}_{H,5}|_{\varepsilon \to 0}. \tag{6.47}$$

We define a new basis by

$$\mathbf{I}_{H5}^{(2)} = \mathbf{U}_{H5}^{(2)} \mathbf{I}_{H5}^{(1)}, \tag{6.48}$$

with

$$\mathbf{U}_{H,5}^{(2)} = \left(\mathbf{\mathcal{S}}_{H,5}^{(1)}\right)^{-1} \tag{6.49}$$

The shaded entries indicate non-zero entries.

and new the differential equation is

$$\mathbf{B}_{H,5}^{(2)}(\lambda,\varepsilon) = d\mathbf{U}_{H,5}^{(2)} \left(\mathbf{U}_{H,5}^{(2)}\right)^{-1} + \mathbf{U}_{H,5}^{(2)} \mathbf{B}_{H,5}^{(1)} \left(\mathbf{U}_{H,5}^{(2)}\right)^{-1}$$

$$= \begin{pmatrix} 0 & 0 & \bullet & \bullet \\ 0 & 0 & \bullet & \bullet \\ 0 & 0 & 0 & 0 \\ 0 & 0 & 0 & 0 \end{pmatrix} + \begin{pmatrix} \bullet & \bullet & 0 & 0 \\ \bullet & \bullet & 0 & 0 \\ \bullet & \bullet & \bullet & \bullet \end{pmatrix} \varepsilon + \begin{pmatrix} 0 & 0 & 0 & 0 \\ 0 & 0 & 0 & 0 \\ \bullet & \bullet & 0 & 0 \\ \bullet & \bullet & 0 & 0 \end{pmatrix} \varepsilon^{2}.$$

$$(6.51)$$

Step 3: In order to get rid of the  $\varepsilon^2$  terms, we use the transformation matrix

$$\mathbf{U}_{H,5}^{(3)} = \begin{pmatrix} \varepsilon & 0 & 0 & 0 \\ 0 & \varepsilon & 0 & 0 \\ 0 & 0 & 1 & 0 \\ 0 & 0 & 0 & 1 \end{pmatrix} . \tag{6.52}$$

We define a new basis by

$$\mathbf{I}_{H,5}^{(3)} = \mathbf{U}_{H,5}^{(3)} \mathbf{I}_{H,5}^{(2)}, \tag{6.53}$$

and the differential equation

$$\mathbf{B}_{H,5}^{(3)}(\lambda,\varepsilon) = d\mathbf{U}_{H,5}^{(3)} \left(\mathbf{U}_{H,5}^{(3)}\right)^{-1} + \mathbf{U}_{H,5}^{(3)} \mathbf{B}_{H,5}^{(2)} \left(\mathbf{U}_{H,5}^{(3)}\right)^{-1}$$
(6.54)

The entries of the connection matrices are:

$$\mathbf{B}_{H,5}^{(3,0)}(\lambda) = \begin{pmatrix} 0 & 0\\ \Xi(\boldsymbol{\lambda}) & 0 \end{pmatrix}, \tag{6.56}$$

$$\mathbf{B}_{H,5}^{(3,1)}(\lambda) = \begin{pmatrix} \mathbf{A}^{-1} \boldsymbol{\beta}_1(\lambda) \mathbf{A} & \mathbf{A}^{-1} \boldsymbol{\beta}_2(\lambda) (\mathbf{A}^{-1})^T \\ \mathbf{A}^T \boldsymbol{\beta}_3(\lambda) \mathbf{A} & \mathbf{A}^T \boldsymbol{\beta}_4(\lambda) (\mathbf{A}^{-1})^T \end{pmatrix}, \tag{6.57}$$

where  $\Xi(\lambda)$  is a 2 × 2 matrix of differential one-forms, which can schematically be written as

$$\Xi(\lambda) = \mathcal{A}^T \Xi_1(\lambda) \mathcal{A} + \mathcal{A}^T \Xi_2(\lambda) \mathcal{A}t + \tilde{\mathcal{A}}^T \Xi_3(\lambda) \mathcal{A}, \qquad (6.58)$$

with each  $\Xi_i(\lambda)$  a matrix of rational one-forms in the parameter  $\lambda$ .

**Step 4:** To remove the remaining  $\varepsilon^0$  terms we make an ansatz for the final transformation that takes the form

$$\mathbf{U}_{H,5}^{(4)} = \begin{pmatrix} \mathbf{1} & \mathbf{0} \\ \mathbf{u}_{H,5}(\boldsymbol{\lambda}) & \mathbf{1} \end{pmatrix}, \tag{6.59}$$

where  $\mathbf{u}_{H,5}(\boldsymbol{\lambda})$  is a  $2 \times 2$  matrix of undetermined entries. We obtain them by requiring  $\varepsilon$ -form and a constant intersection matrix. For this, it is useful to decompose  $\mathbf{u}_{H,5}(\boldsymbol{\lambda})$  into a symmetric and an antisymmetric part,

$$\mathbf{u}_{H,5}(\boldsymbol{\lambda}) = \begin{pmatrix} u_{\sigma,5}^1(\boldsymbol{\lambda}) & u_{\sigma,5}^2(\boldsymbol{\lambda}) \\ u_{\sigma,5}^2(\boldsymbol{\lambda}) & u_{\sigma,5}^3(\boldsymbol{\lambda}) \end{pmatrix} + \begin{pmatrix} 0 & u_{a,5} \\ -u_{a,5} & 0 \end{pmatrix}.$$
(6.60)

The differential equation imposed by requiring the differential equation to be in  $\varepsilon$ -form is

$$d\mathbf{u}_{H,5}(\boldsymbol{\lambda}) + \Xi(\lambda) = 0. \tag{6.61}$$

It is significantly harder to solve than the algebraic equations imposed by requiring a constant intersection matrix. Those are obtained by first defining

$$\mathbf{U}_{H,5} = \mathbf{U}_{H,5}^{(4)} \, \mathbf{U}_{H,5}^{(3)} \, \mathbf{U}_{H,5}^{(2)} \, \mathbf{U}_{H,5}^{(1)} \tag{6.62}$$

and then computing

$$\mathbf{C}_{H,5}^{(4)}(\boldsymbol{\lambda},\varepsilon) = \mathbf{U}_{H,5}\boldsymbol{C}_{H,5}^{(0)}(\boldsymbol{\lambda},\varepsilon) \left(\mathbf{U}_{H,5}|_{\varepsilon \to -\varepsilon}\right) = -\frac{\varepsilon}{8\pi^2} \begin{pmatrix} 0 & 0 & 1 & 0\\ 0 & 0 & 0 & 1\\ 1 & 0 & v_1 & v_2\\ 0 & 1 & v_2 & v_3 \end{pmatrix} , \quad (6.63)$$

where  $v_1, v_2, v_3$  are some rational combinations of the parameters  $\lambda$ , the periods and the unknown functions. Requiring that this matrix takes the form  $f(\varepsilon)\Delta_{H,5}$  with  $\Delta_{H,5}$  constant, we read off

$$f_{H,5}(\varepsilon) = \frac{\varepsilon}{\pi^2} \tag{6.64}$$

and impose that the  $v_i$  vanish. We find

$$\begin{pmatrix} u_{\sigma,5}^{1}(\boldsymbol{\lambda}) & u_{\sigma,5}^{2}(\boldsymbol{\lambda}) \\ u_{\sigma,5}^{2}(\boldsymbol{\lambda}) & u_{\sigma,5}^{3}(\boldsymbol{\lambda}) \end{pmatrix} = \boldsymbol{\mathcal{A}}^{T} \boldsymbol{M}_{H,5}^{S}(\boldsymbol{\lambda}) \boldsymbol{\mathcal{A}},$$
(6.65)

where  $M_{H,5}^S(\lambda)$  is a symmetric  $2 \times 2$  matrix of rational functions. For  $a_i = 1$  it takes the form

$$\mathbf{M}_{H,5}^{S} = \frac{1}{8\pi i} \begin{pmatrix} 2(\tilde{s}_2 - \tilde{s}_3) & 1 - \tilde{s}_1 - \tilde{s}_2 \\ 1 - \tilde{s}_1 - \tilde{s}_2 & 4s_1 - 6 \end{pmatrix}. \tag{6.66}$$

The  $\tilde{s}_k$  are the  $k^{\text{th}}$  elementary symmetric polynomials in the branch points  $\lambda_1, \lambda_2, \lambda_3$ . In that way, we have used the four relations obtained from requiring a constant

intersection matrix to fix the four symmetric parts of the new functions. The intersection matrix now takes the simple form

$$\mathbf{C}_{H,5}^{(4)}(\boldsymbol{\lambda},\varepsilon) = f_{H,5}(\varepsilon)\boldsymbol{\Delta}_{H,5} \text{ with } \boldsymbol{\Delta}_{H,5} = -\frac{1}{8} \begin{pmatrix} 0 & 0 & 1 & 0 \\ 0 & 0 & 0 & 1 \\ 1 & 0 & 0 & 0 \\ 0 & 1 & 0 & 0 \end{pmatrix}, \tag{6.67}$$

which is proportional to the exchange matrix  $K_4$  after swapping the third and fourth basis elements. The antisymmetric function is still only defined by the differential equation

$$\mathbf{M}_{H,5}^{A} \equiv \begin{pmatrix} 0 & u_{a,5}(\boldsymbol{\lambda}) \\ -u_{a,5}(\boldsymbol{\lambda}) & 0 \end{pmatrix} = -\int_{\boldsymbol{\lambda}_{0}}^{\boldsymbol{\lambda}} \mathbf{P}^{A}, \qquad (6.68)$$

i.e. there is one remaining new function. For more details on the solution of the differential equation, see [34]. This feature is different to the elliptic case we considered in the previous example: For the odd elliptic curve we could express all (one) entries of the ansatz as rational functions of periods and branch points  $\lambda$ , now we obtain one proper new function  $u_{a,5}$ , which we cannot determine by the algebraic equations we obtain from requiring a constant intersection matrix. Of course, we cannot exclude that there might still be some way that the function can also be expressed in rational functions of periods and branch points, but we have excluded some general forms in [34].

Canonical Differential Equation We define the basis after the final rotation to be

$$\mathbf{J}_{H,5} = \mathbf{U}_{H,5} \mathbf{I}_{H,5}^{(0)} \tag{6.69}$$

and its connection matrix is

$$\varepsilon \mathbf{B}_{H,5}(\lambda) = d\mathbf{U}_{H,5} (\mathbf{U}_{H,5})^{-1} + \mathbf{U}_{H,5} \mathbf{A}_{H,5} (\mathbf{U}_{H,5})^{-1}$$

$$= \begin{pmatrix} \mathbf{A}^{-1} (\beta_{1} - \beta_{2} \mathbf{M}_{H,5}^{S}) \mathbf{A} & \mathbf{A}^{-1} \beta_{2} \mathbf{A}^{-1T} \\ \mathbf{A}^{T} (\beta_{3} + \mathbf{M}_{H,5}^{S} \beta_{1} - \mathbf{M}_{H,5}^{S} \beta_{2} \mathbf{M}_{H,5}^{S} - \beta_{4} \mathbf{M}_{H,5}^{S}) \mathbf{A} & \mathbf{A}^{T} (\beta_{4} + \mathbf{M}_{H,5}^{S} \beta_{2}) \mathbf{A}^{-1T} \end{pmatrix}$$

$$+ \begin{pmatrix} -\mathbf{A}^{-1} \beta_{2} \mathbf{A}^{-1T} \mathbf{M}_{H,5}^{A} & 0 \\ \mathbf{M}_{H,5}^{A} \mathbf{A}^{-1} (\beta_{1} - \beta_{2} \mathbf{M}_{H,5}^{S}) \mathbf{A} - \mathbf{A}^{T} (\mathbf{M}_{H,5}^{S} \beta_{2} + \beta_{4}) \mathbf{A}^{-1T} \mathbf{M}_{H,5}^{A} & \mathbf{M}_{H,5}^{A} \mathbf{A}^{-1} \beta_{2} \mathbf{A}^{-1T} \end{pmatrix}$$

$$+ \begin{pmatrix} 0 & 0 \\ -\mathbf{M}_{H,5}^{A} \mathbf{A}^{-1} \beta_{2} \mathbf{A}^{-1T} \mathbf{M}_{H,5}^{A} & 0 \end{pmatrix},$$

where we decomposed the matrix according to the degree in the new function  $M_{H,5}^A$ . We investigate the properties of the functions that enter  $\mathbf{B}_{H,5}(\lambda)$  in more detail in Section 6.2.

# 6.1.4 Four Parameter Lauricella Function

As a second genus two Example we consider the integral family

$$\mathcal{F}_{H,6}^{\nu}(\lambda,\varepsilon) = \int_0^1 x^{\alpha_1} (x-1)^{\alpha_2} (x-\lambda_1)^{\alpha_3} (x-\lambda_2)^{\alpha_4} (x-\lambda_3)^{\alpha_5} (x-\lambda_4)^{\alpha_6} dx$$
with  $\alpha_i = -\frac{1}{2} + a_i \varepsilon + \nu_i$ , (6.73)

which depends on the four parameters  $\lambda = (\lambda_1, \lambda_2, \lambda_3, \lambda_4)$  that we consider to be real and ordered:  $\lambda_4 > \lambda_3 > \lambda_2 > \lambda_1 > 1.^8$  As an initial basis of master integrals we choose

$$\mathbf{I}_{H,6}^{(0)} = \left(\int_{\gamma} \chi(x) \frac{\mathrm{d}x}{y}, \int_{\gamma} \chi(x) \frac{x \mathrm{d}x}{y}, \int_{\gamma} \chi(x) \frac{\Psi_{1}^{2,e}(x) \mathrm{d}x}{y}, \int_{\gamma} \chi(x) \frac{\Psi_{2}^{2,e}(x) \mathrm{d}x}{y}, \int_{\gamma} \chi(x) \frac{x^{2} \mathrm{d}x}{y}\right)^{\frac{1}{2}}$$

$$(6.74)$$

with  $\Psi_i^{2,e}(x)$  defined in eq. (3.53) and

$$\chi(x) = x^{a_1 \varepsilon} (x - 1)^{a_2 \varepsilon} (x - \lambda_1)^{a_3 \varepsilon} (x - \lambda_2)^{a_4 \varepsilon} (x - \lambda_3)^{a_5 \varepsilon} (x - \lambda_4)^{a_6 \varepsilon}, \tag{6.75}$$

The differentials in (6.74) also define a basis<sup>9</sup> of the twisted cohomology group with the twist  $\Phi_{H,6} = \chi(x)/y$ . We denote the initial intersection matrix obtained from this basis and its self-dual by  $\mathbf{C}_{H,6}^{(0)}$ . The integrand defines the following even hyperelliptic curve of genus two:

$$y^{2} = x(x-1)(x-\lambda_{1})(x-\lambda_{2})(x-\lambda_{3})(x-\lambda_{4}).$$
(6.76)

Since the hyperelliptic curve is even, it has a puncture at  $\infty$ . The period matrix of this hyperelliptic curve can be decomposed into semi-simple and unipotent parts in the following way:

$$\mathcal{P}_{H,6} = \begin{pmatrix} \mathcal{A} & \mathcal{B} & \star \\ \tilde{\mathcal{A}} & \tilde{\mathcal{B}} & \star \\ 0 & 0 & 1 \end{pmatrix} = \begin{pmatrix} \mathcal{A} & 0 & 0 \\ \tilde{\mathcal{A}} & 8\pi i \mathcal{A}^{-1T} & 0 \\ 0 & 0 & 1 \end{pmatrix} \begin{pmatrix} \mathbf{1} & \Omega & \star \\ 0 & \mathbf{1} & \star \\ 0 & 0 & 1 \end{pmatrix} \equiv \mathcal{S}_{H,6} \mathcal{U}_{H,6} . \quad (6.77)$$

The entries  $\star$  represent integrals over the additional cycle around  $\infty$  that was not present in the odd case. The initial differential equation is

$$d\mathbf{I}_{H,6}^{(0)}(\lambda,\varepsilon) = \mathbf{A}_{H,6}(\lambda,\varepsilon)\mathbf{I}_{H,6}^{(0)}(\lambda,\varepsilon) = \left[\mathbf{A}_{H,6}^{(0)}(\lambda) + \varepsilon\mathbf{A}_{H,6}^{(1)}(\lambda)\right]\mathbf{I}_{H,6}^{(0)}(\lambda,\varepsilon), \quad (6.78)$$

where  $d = \sum_{i=1}^{4} d\lambda_i \partial_{\lambda_i}$ . The matrix  $\mathbf{A}_{H,6}(\lambda, \varepsilon)$  consists of one-forms in these variables and the corresponding functions are rational in the  $\lambda$ .

Step 1: The first transformation – which is facilitated by the matrix  $\mathbf{U}_{H,6}^{(1)}$  that is a straightforward generalization of the matrix  $\mathbf{U}_{H,5}^{(1)}$  in eq. (6.45) – leads to the derivative basis

$$\mathbf{I}_{H,6}^{(1)} = \left( \int_{\gamma} \frac{\mathrm{d}x}{y} \chi(x) \right), \int_{\gamma} \frac{x \mathrm{d}x}{y} \chi(x) \right), \sum_{i=1}^{4} \partial_{\lambda_{i}} \left[ \int_{\gamma} \frac{\mathrm{d}x}{y} \chi(x) \right], \sum_{i=1}^{4} \partial_{\lambda_{i}} \left[ \int_{\gamma} \frac{x \mathrm{d}x}{y} \chi(x) \right], \int_{\gamma} \frac{x^{2} \mathrm{d}x}{y} \chi(x) \right). \tag{6.79}$$

<sup>8</sup>Note that this integral family is equivalent to T the maximal cut of the crossed box for specific choices of the  $\lambda_i$  as discussed in Section 2.4.2. Here we consider the fully general version with generic parameters  $\lambda_i$ .

<sup>9</sup>Explicitly, this basis is given by

$$\varpi_{H,6}^1 = \mathrm{d}x, 
\varpi_{H,6}^2 = x \,\mathrm{d}x 
\varpi_{H,6}^3 = \Psi_1^{2,e}(x) \,\mathrm{d}x 
\varpi_{H,6}^4 = \Psi_2^{2,e}(x) \,\mathrm{d}x 
\varpi_{H,6}^5 = x^2 \,\mathrm{d}x$$

The differential equation for this basis is

$$\mathbf{B}_{H,6}^{(1)}(\boldsymbol{\lambda},\varepsilon) = \left(d\mathbf{U}_{H,6}^{(1)}(\boldsymbol{\lambda},\varepsilon)\right) \left(\mathbf{U}_{H,6}^{(1)}(\boldsymbol{\lambda},\varepsilon)\right)^{-1} + \mathbf{U}_{H,6}^{(1)}(\boldsymbol{\lambda},\varepsilon)\mathbf{B}_{H,6}^{(0)}(\boldsymbol{\lambda},\varepsilon) \left(\mathbf{U}_{H,6}^{(1)}(\boldsymbol{\lambda},\varepsilon)\right)^{-1}.$$
(6.80)

**Step 2:** In the second step, we transform with the inverse of the semi-simple part of the new period matrix at  $\varepsilon \to 0$ ,

$$\mathbf{I}_{H.6}^{(2)}(\boldsymbol{\lambda},\varepsilon) = \mathbf{U}_{H.6}^{(2)}(\boldsymbol{\lambda})\mathbf{I}_{H.6}^{(1)}(\boldsymbol{\lambda},\varepsilon)$$
(6.81)

with 
$$\mathbf{U}_{H,6}^{(2)}(\boldsymbol{\lambda}) = \left(\boldsymbol{\mathcal{S}}_{H,6}^{(1)}(\boldsymbol{\lambda})\right)^{-1} = \left(\mathbf{U}_{H,6}^{(1)}(\boldsymbol{\lambda},0)\boldsymbol{\mathcal{S}}_{H,6}^{(0)}\right)^{-1}$$
, (6.82)

and this change of basis leads to the new connection matrix

$$\mathbf{B}_{H,6}^{(2)}(\lambda,\varepsilon) = \left(d\mathbf{U}_{H,6}^{(2)}(\lambda)\right) \left(\mathbf{U}_{H,6}^{(2)}(\lambda)^{-1}\right) + \mathbf{U}_{H,6}^{(2)}(\lambda)\mathbf{B}_{H,6}^{(1)} \left(\mathbf{U}_{H,6}^{(2)}(\lambda)\right)^{-1}, \quad (6.83)$$

which takes the form

The upper left  $4\times 4$  block has the same structure as the connection matrix  $\mathbf{B}_{H,5}^{(2)}(\boldsymbol{\lambda},\varepsilon)$  at this point. This makes sense: Those are the sectors which in both cases reduce to a- and b-(quasi-)periods of the hyperelliptic curve in the  $\varepsilon\to 0$  limit. The entries in the fifth row and column are related to the additional puncture at  $\infty$  and we obtain new structures from these.

**Step 3:** In order to get rid of the  $\varepsilon^2$  terms and bring all  $\varepsilon^0$  terms under the diagonal, we perform the simple rotation

$$\mathbf{I}_{H,6}^{(3)}(\boldsymbol{\lambda},\varepsilon) = \mathbf{U}_{H,6}^{(3)}(\varepsilon)\mathbf{I}_{H,6}^{(2)}(\boldsymbol{\lambda},\varepsilon) \quad \text{with} \quad \mathbf{U}_{H,6}^{(3)}(\varepsilon) = \begin{pmatrix} 1 & 0 & 0 & 0 & 0 \\ 0 & 1 & 0 & 0 & 0 \\ 0 & 0 & 0 & 0 & 1 \\ 0 & 0 & 0 & \frac{1}{\varepsilon} & 0 \\ 0 & 0 & \frac{1}{\varepsilon} & 0 & 0 \end{pmatrix} . \quad (6.85)$$

After this rotation, the new connection matrix

$$\mathbf{B}_{H,6}^{(3)}(\lambda,\varepsilon) = \left(d\mathbf{U}_{H,6}^{(3)}(\varepsilon)\right) \left(\mathbf{U}_{H,6}^{(3)}(\varepsilon)\right)^{-1} + \mathbf{U}_{H,6}^{(3)}(\varepsilon)\mathbf{B}_{H,6}^{(2)}(\lambda,\varepsilon)(\lambda,\varepsilon) \left(\mathbf{U}_{H,6}^{(3)}(\varepsilon)\right)^{-1},$$
(6.86)

takes the form

**Step 4:** We make the following ansatz for the final rotation:

$$\mathbf{U}_{H,6}^{(4)}(\boldsymbol{\lambda}) = \begin{pmatrix} 1 & 0 & 0 & 0 & 0\\ 0 & 1 & 0 & 0 & 0\\ u_{3,1} & u_{3,2} & 1 & 0 & 0\\ u_{4,1} & u_{4,2} & u_{4,3} & 1 & 0\\ u_{5,1} & u_{5,2} & u_{5,3} & 0 & 1 \end{pmatrix}$$
(6.88)

with the unknown entries  $u_{i,j}$  chosen such that the new differential equation matrix

$$\varepsilon \mathbf{B}_{H,6}(\boldsymbol{\lambda}) = \left( d\mathbf{U}_{H,6}^{(4)}(\boldsymbol{\lambda}) \right) \left( \mathbf{U}_{H,6}^{(4)}(\boldsymbol{\lambda}) \right)^{-1} + \mathbf{U}_{H,6}^{(4)}(\boldsymbol{\lambda}) \mathbf{B}_{H,6}^{(3)}(\boldsymbol{\lambda}, \varepsilon) \left( \mathbf{U}_{H,6}^{(4)}(\boldsymbol{\lambda}) \right)^{-1}$$
(6.89)

factorises in  $\varepsilon$ . To obtain the  $u_{i,j}$  from this condition one needs to solve eight coupled differential equations for the eight undetermined entries. Again, it is a lot easier to obtain a subset of the new functions by requiring that the intersection matrix is constant. We define

$$\mathbf{U}_{H,6} = \mathbf{U}_{H,6}^{(4)} \, \mathbf{U}_{H,6}^{(3)} \, \mathbf{U}_{H,6}^{(2)} \, \mathbf{U}_{H,6}^{(1)} \tag{6.90}$$

to obtain

$$\mathbf{C}_{H,6}^{(4)} = \mathbf{U}_{H,6} \mathbf{C}_{H,6}^{(0)} \left( \mathbf{U}_{H,6} |_{\varepsilon \to -\varepsilon} \right) = \begin{pmatrix} 0 & 0 & 0 & 0 & -\frac{i}{4\pi\varepsilon} \\ 0 & 0 & 0 & -\frac{i}{4\pi\varepsilon} & 0 \\ 0 & 0 & -\frac{1}{\varepsilon \sum_{i=1}^{6} a_{i}} & v_{3,4} & v_{3,5} \\ 0 & -\frac{i}{4\pi\varepsilon} & v_{4,3} & v_{4,4} & v_{4,5} \\ -\frac{i}{4\pi\varepsilon} & 0 & v_{5,3} & v_{5,4} & v_{5,5} \end{pmatrix},$$

$$(6.91)$$

where the entries  $v_{i,j}$  are rational functions of the branch points  $\lambda_i$ , the periods  $\mathcal{A}$  and quasi-periods  $\tilde{\mathcal{A}}$  and the entries  $u_{i,j}$  of eq. (6.88). We require that  $\mathbf{C}_{H,6}$  has non-zero entries only on the skew-diagonal and the other entries are zero. From this condition, we derive eight algebraic equations that can be solved for the  $u_{i,j}$ . However, owing to the symmetry of the intersection matrix, only five of these equations are linearly independent. We opt to determine the entries  $\{u_{3,1}, u_{3,2}, u_{4,2}, u_{5,1}, u_{5,2}\}$  in terms of the branch points, periods, and the three remaining unknown functions  $\{u_{4,1}, u_{4,3}, u_{5,3}\}$ . The intersection matrix then has the particularly elegant form

$$\mathbf{C}_{J} = -\frac{1}{\varepsilon} \begin{pmatrix} 0 & 0 & 0 & 0 & \frac{i}{4\pi} \\ 0 & 0 & 0 & \frac{i}{4\pi} & 0 \\ 0 & 0 & \frac{1}{\sum_{i=1}^{6} a_{i}} & 0 & 0 \\ 0 & \frac{i}{4\pi} & 0 & 0 & 0 \\ \frac{i}{4\pi} & 0 & 0 & 0 & 0 \end{pmatrix} . \tag{6.92}$$

<sup>10</sup>It should be noted that there is considerable flexibility in selecting which functions to solve for. Specifically, we identified 24 different sets that allow for a solution. At this stage, we have not discovered any symmetry or natural preference, as was the case in the three-parameter scenario.

We cannot rule out the possibility that the remaining components  $u_{4,1}, u_{4,3}, u_{5,3}$  (or a subset of them) can be expressed purely in terms of the periods and branch points.<sup>10</sup> Regardless, they are determined by the differential equation, and given the imposed constraints we have assume the differential equation is both in  $\varepsilon$ - and C-form.

Relation to the Non-Planar-Crossed Box Before concluding this chapter with an analysis of the modular properties of the forms arising in the five-branch-point case, let us briefly return to the non-planar crossed box, which originally motivated the study of the integrals examined here and we discussed the non-planar crossed box in Section 2.4.2. Its maximal cut has entries of the form:

Max-Cut 
$$\left[\mathbb{I}_{\boldsymbol{\nu}}^{\text{npcb}}(\{p_i \cdot p_j\}, \{m_i^2\})\right] = \int 2\left[P_2^{\text{npcb}}(z)\right]^{-\frac{1}{2}}\left[P_4^{\text{npcb}}(z)\right]^{-\frac{1}{2}-\varepsilon} dz$$

where the polynomials  $P_i^{\rm npcb}(z)$  are as defined in eq. (2.68) and the branch points are given in eq. (2.70) and the following equations. These entries can be expressed in the functions of eq. (6.73) by making specific parameter choices. In particular, one can write the maximal cut in twisted periods of the form

$$\mathcal{F}_{\text{npcb}}(s, t, \varepsilon) = \tilde{\lambda}^{-(2-4\varepsilon)} \int_{\gamma} x^{-\frac{1}{2}} (x - 1)^{-\frac{1}{2}} \prod_{i=1}^{4} (x - \tilde{\lambda}_i)^{-\frac{1}{2} + \varepsilon} dx$$

with

$$\tilde{\lambda} = \lambda_2^{\text{npcb}} - \lambda_1^{\text{npcb}}, \quad \tilde{\lambda}_i = (\lambda_i^{\text{npcb}} - \lambda_1^{\text{npcb}})\tilde{\lambda}.$$
 (6.93)

This representation introduces distinct features compared to previous considerations:

- 1. The integrals depend only on two parameters, s and t, which determine  $\tilde{\lambda}$  and the  $\tilde{\lambda}_i$ .
- 2. A prefactor  $\tilde{\lambda}^{-(2-4\varepsilon)}$  appears.

Both of these features are not obstacles. If we use the same initial basis as in eq. (6.79) but with the prefactor of the second feature incorporated and denote it by  $\tilde{\mathbf{I}}_{\rm npcb}^{(0)}$ , the resulting differential equation takes the form:

$$d\tilde{\mathbf{I}}_{\text{npcb}}^{(0)} = \left[ \mathbf{B}_{H,6}^{(0)}(\tilde{\boldsymbol{\lambda}}, \varepsilon) + (-2 + 4\varepsilon) \frac{d\tilde{\boldsymbol{\lambda}}}{\tilde{\boldsymbol{\lambda}}} \right] \tilde{\mathbf{I}}_{\text{npcb}}^{(0)}.$$
 (6.94)

This modifies the  $\varepsilon$ -dependence compared to the generic case without the prefactor. However, we can rescale the basis by  $\tilde{\lambda}^2$  and find for the rescaled vector of master integrals the following differential equation:

$$d\mathbf{I}_{\text{npcb}}^{(0)} = \mathbf{B}_{\text{npcb}}^{(0)}(\tilde{\boldsymbol{\lambda}}, \varepsilon)\mathbf{I}_{\text{npcb}}^{(0)} \text{ with } \mathbf{B}_{\text{npcb}}^{(0)}(\tilde{\boldsymbol{\lambda}}, \varepsilon) = \mathbf{B}_{H,6}^{(0)}(\tilde{\boldsymbol{\lambda}}, \varepsilon) + \left(\sum_{i=3}^{6} a_{i}\varepsilon\right) \frac{d\tilde{\lambda}}{\tilde{\lambda}} \mathbf{1}.$$
(6.95)

The additional term is already in  $\varepsilon$ -form and since the identity matrix commutes with all matrices, any transformation that renders  $\mathbf{B}_{H,6}^{(0)}(\boldsymbol{\lambda},\varepsilon)$  canonical also does so for  $\mathbf{B}_{H,6}^{(0)}(\tilde{\boldsymbol{\lambda}},\varepsilon)$ . Additionally, writing the differential equation in the physical variables (s,t) instead of the generic variables  $\{\lambda_1,\ldots,\lambda_4\}$  does not change the  $\varepsilon$ -structure and features of the canonical differential equation.

# 6.2 Modular properties of the Canonical Differential Equation

Finally, we discuss the modular properties of the canonical differential equations we found in the first part of this chapter, specifically for the elliptic example  $\mathbf{B}_{H,3}(\lambda,\varepsilon)$  and the genus two example  $\mathbf{B}_{H,5}(\lambda,\varepsilon)$ .

# 6.2.1 Modular Properties of the Connection Matrix $B_{H,3}(\lambda, \varepsilon)$

One can change from variable  $\lambda$  to the variable  $\tau$  in the differential equation  $\mathbf{B}_{H,3}(\lambda,\varepsilon)$  with

$$d\tau = \frac{4\pi \, d\lambda}{\lambda (1 - \lambda)\omega_1^2} \tag{6.96}$$

or equivalently

$$d\lambda(\tau) = \frac{4}{\pi} (\lambda(\tau) - 1) K \left(\lambda(\tau)^{-1}\right)^2 d\tau$$
 (6.97)

for our basis choice. In the variable  $\tau$  the canonical differential equation is

$$\mathbf{B}_{H,3}(\tau) = \begin{pmatrix} 0 & 1 \\ 0 & 0 \end{pmatrix} \varpi_{H,3}^1 + \begin{pmatrix} 1 & 0 \\ 0 & 1 \end{pmatrix} \varpi_{H,3}^2 + \begin{pmatrix} 0 & 0 \\ 1 & 0 \end{pmatrix} \varpi_{H,3}^3, \tag{6.98}$$

where

$$\overline{\omega}_{H,3}^1 = \frac{i}{4} \mathrm{d}\tau \tag{6.99}$$

$$\varpi_{H,3}^2 = \frac{2}{\pi} K(\lambda(\tau)^{-1})^2 \left[ \left( 1 - \lambda(\tau)^{-1} \right) a_1 + a_2 + \lambda(\tau)^{-1} a_3 \right] d\tau$$
 (6.100)

$$\varpi_{H,3}^3 = -\frac{16i}{\pi^2} K(\lambda(\tau)^{-1})^4 \left[ \frac{(a_1 + a_3)^2}{\lambda(\tau)^3} - 2 \frac{a_1^2 - a_2 a_3 + a_1(a_2 + a_3)}{\lambda(\tau)^2} + \frac{(a_1 + a_2)^2}{\lambda(\tau)} \right] d\tau.$$
(6.101)

We can now show,<sup>11</sup> that this canonical differential equation is an example for a differential equation in C-form with  $\mathbb{K} = \mathbb{Q}[i, \pi, \pi^{-1}]$ . By partial fractioning the connection matrix  $\mathbf{B}_{H,3}(\lambda)$  we see that  $\mathbb{A}_{\mathbf{B}}$  is the differential closure of the algebra

$$\mathbb{Q}\left[i\pi^{\pm}\right]\left[\frac{1}{\lambda(\tau)},\lambda(\tau),K(\lambda(\tau)^{-1}),\frac{1}{K(\lambda(\tau)^{-1})},E(\lambda(\tau)^{-1})\right]$$
(6.102)

<sup>11</sup>Since the derivatives of  $K(\lambda)$  and  $E(\lambda)$  can again be expressed in these elliptic functions as well as the rational functions  $\frac{1}{\lambda}$ ,  $\frac{1}{1-\lambda}$ , the differential closure only needs to contain rational functions with higher order poles in 0,1, but no new elliptic functions.

More precisely, one finds that  $\mathbb{A}_{\mathbf{B}}$  corresponds to the algebra of weakly holomorphic quasi-modular forms associated with the congruence subgroup  $\Gamma(2)$ , with  $i\pi^{\pm}$  included. The above differential forms  $\varpi^{i}_{H,3}$  generate the vector space  $\mathbb{V}_{\mathbf{B}}$ . Furthermore, following the approach used in [314, 315], one can verify that  $\mathbb{V}_{\mathbf{B}} \cap d\mathcal{F}_{\mathbb{C}} = \{0\}$ , where  $\mathcal{F}_{\mathbb{C}} = \operatorname{Frac}(\mathbb{C} \otimes_{\mathbb{K}} \mathbb{A}_{\mathbf{B}})$ , which confirms that this system is in C-form. The general strategy relies on demonstrating the linear independence of the specific iterated integrals under consideration, an approach we will also employ later when proving certain results about the C-form. Additionally, it is worth noting that the connection matrix  $\mathbf{B}_{H,5}$  has only simple poles in  $\lambda$ .

# 6.2.2 Modular Properties of the Connection Matrix $B_{H,5}(\lambda, \varepsilon)$

As discussed in eq. (3.191), the a-period  $\mathcal{A}$  is a Siegel modular form with weight  $1 \otimes \rho_F^{12}$  for an appropriate congruence subgroup  $\Gamma \subset \Gamma_2 = \operatorname{Sp}(4, \mathbb{Z})$ . Since the hyperelliptic curves are in Rosenhain normal form, the relevant congruence subgroup is known to lie in the principal congruence subgroup of level two  $\Gamma_2(2)$ , see e.g., [316]. In particular, we find that  $\mathcal{A}$  transforms as a Siegel modular form up to a sign

$$\mathbf{A} \to -\mathbf{A}(\mathbf{C}\Omega + \mathbf{D})^T$$
, for  $\begin{pmatrix} \mathbf{A} & \mathbf{B} \\ \mathbf{C} & \mathbf{D} \end{pmatrix} \in \Gamma_2(2)$ , (6.103)

and consequently the square  $\mathcal{A}^2$  transforms as a Siegel modular form.<sup>13</sup>

Matrix eq. (6.72) Without New Function  $\mathbf{M}_{H,5}^A$ 

The first matrix of  $\mathbf{B}_{H,5}(\lambda, \varepsilon)$ , given in eq. (6.72), which does not contain the new function, consists of four blocks, all of which are Siegel modular forms of a certain weight. These blocks correspond to representations

$$\rho_{ij}: GL(2, \mathbb{C}) \to GL(V_{ij}), \quad \mathbf{M} \to \rho_{ij}(\mathbf{M}).$$
(6.104)

where  $GL(2,\mathbb{C})$  acts on appropriate representation spaces. Each  $\rho_{ij}$  is a rank-two tensor representation, explicitly given by (for  $\mathbf{M} \in GL(2,\mathbb{C})$ )

$$\rho_{11} = \rho_{D} \otimes \rho_{F} : GL(2, \mathbb{C}) \to GL(V \otimes V), \quad \rho_{11}(\mathbf{M}) \cdot \mathbf{T} = (\mathbf{M}^{-1})^{T} \mathbf{T} \mathbf{M}^{T}$$
(6.105)

$$\rho_{12} = \rho_{\mathrm{D}} \otimes \rho_{\mathrm{D}} : \mathrm{GL}(2, \mathbb{C}) \to \mathrm{GL}(V \otimes V), \quad \rho_{12}(\mathbf{M}) \cdot \mathbf{T} = (\mathbf{M}^{-1})^T \mathbf{T} \mathbf{M}^{-1} \quad (6.106)$$

$$\rho_{21} = \rho_{\rm F} \otimes \rho_{\rm F} : \mathrm{GL}(2, \mathbb{C}) \to \mathrm{GL}(V \otimes V), \quad \rho_{21}(\mathbf{M}) \cdot \mathbf{T} = \mathbf{M} \mathbf{T} \mathbf{M}^T$$
(6.107)

$$\rho_{22} = \rho_{\rm F} \otimes \rho_{\rm D} : \operatorname{GL}(2, \mathbb{C}) \to \operatorname{GL}(V \otimes V), \quad \rho_{22}(\mathbf{M}) \cdot \mathbf{T} = \mathbf{M} \mathbf{T} \mathbf{M}^{-1},$$
(6.108)

where  $V = \mathbb{C}^2$ . Since all these representations are reducible, we can further decompose the Siegel modular forms into components with irreducible weights:

$$\rho_{11} = \rho_{\rm D} \otimes \rho_{\rm F} \simeq ({\rm Sym}^2 \otimes {\rm det}^{-1}) \oplus 1 \tag{6.109}$$

$$\rho_{12} = \rho_{\rm D} \otimes \rho_{\rm D} \simeq ({\rm Sym}^2 \otimes {\rm det}^{-2}) \oplus {\rm det}^{-1}$$
(6.110)

$$\rho_{21} = \rho_{\rm F} \otimes \rho_{\rm F} \simeq {\rm Sym}^2 \oplus \det$$
(6.111)

<sup>12</sup>We define  $1 \otimes \rho_{\rm F}$  and other weights in Appendix E.

<sup>13</sup>In the elliptic case the period of the elliptic curve is not a modular form for  $\Gamma(2)$ , but its square is.

### See also:

For details on the representation theory discussed here and the appearing representations  $\rho_i$ , see Appendix E.

$$\rho_{22} = \rho_{\rm F} \otimes \rho_{\rm D} \simeq \left( {\rm Sym}^2 \otimes {\rm det}^{-1} \right) \oplus 1, \qquad (6.112)$$

These decompositions can also be applied to the modular forms appearing in the matrix of eq. (6.72). To demonstrate this, we first introduce the local definition

$$\tilde{\mathbf{B}} = \begin{pmatrix} \boldsymbol{\beta}_1 - \boldsymbol{\beta}_2 \mathbf{M}_{H,5}^S & \boldsymbol{\beta}_2 \\ \boldsymbol{\beta}_3 + \mathbf{M}_{H,5}^S \boldsymbol{\beta}_1 - \mathbf{M}_{H,5}^S \boldsymbol{\beta}_2 \mathbf{M}_{H,5}^S - \boldsymbol{\beta}_4 \mathbf{M}_{H,5}^S & \boldsymbol{\beta}_4 + \mathbf{M}_{H,5}^S \boldsymbol{\beta}_2 \end{pmatrix}, \tag{6.113}$$

so that the matrix in eq. (6.72) takes the form

$$\begin{pmatrix} \mathcal{A}^{-1}\tilde{\mathbf{B}}_{11}\mathcal{A} & \mathcal{A}^{-1}\tilde{\mathbf{B}}_{12}\mathcal{A}^{-1T} \\ \mathcal{A}^{T}\tilde{\mathbf{B}}_{21}\mathcal{A} & \mathcal{A}^{T}\tilde{\mathbf{B}}_{22}\mathcal{A}^{-1T} \end{pmatrix}.$$
(6.114)

We consider in detail the (1,1)-block and define

$$\tilde{\epsilon} = \begin{pmatrix} 0 & 1 \\ -1 & 0 \end{pmatrix}. \tag{6.115}$$

We decompose the block into a symmetric and an antisymmetric part:

$$\mathcal{A}^{-1}\tilde{\mathbf{B}}_{11}\mathcal{A} = \tilde{\boldsymbol{\epsilon}}^{-1}\tilde{\boldsymbol{\epsilon}}\mathcal{A}^{-1}\tilde{\mathbf{B}}_{11}\mathcal{A}$$

$$= \tilde{\boldsymbol{\epsilon}}^{-1} \left[ \frac{1}{2} \left( \tilde{\boldsymbol{\epsilon}}\mathcal{A}^{-1}\tilde{\mathbf{B}}_{11}\mathcal{A} + \mathcal{A}^T\tilde{\mathbf{B}}_{11}^T\mathcal{A}^{-1T}\tilde{\boldsymbol{\epsilon}}^T \right) + \frac{1}{2} \left( \tilde{\boldsymbol{\epsilon}}\mathcal{A}^{-1}\tilde{\mathbf{B}}_{11}\mathcal{A} - \mathcal{A}^T\tilde{\mathbf{B}}_{11}^T\mathcal{A}^{-1T}\tilde{\boldsymbol{\epsilon}}^T \right) \right],$$
(6.116)

The first term within the square brackets transforms under the symmetric representation, up to an inverse determinant factor, whereas the second term transforms under the trivial representation, meaning it remains modular invariant. Consequently, the  $2 \times 2$  block that appears in the canonical differential equation matrix has been decomposed in terms of Siegel modular forms with irreducible weights, up to a constant factor of  $\tilde{\epsilon}^{-1}$ . A similar analysis can be performed for the other blocks. These observations confirm that the modular properties of the genus-one canonical differential equation naturally extend to Siegel modularity at higher genus – at least for the contributions without the new function.

# Matrices with new function $u_{a,5}(\lambda)$

Next, we also consider the other two matrices in eq. (6.70), i.e. the ones that contain powers of  $u_{a,5}(\lambda)$ . We find that, due to this new function, the respective terms cannot be interpreted as linear combinations of Siegel modular forms, irrespective of the explicit value of  $u_{a,5}(\lambda)$  as a function. As defined in eq. (6.68), the matrix  $\mathbf{M}_{H,5}^A$  in which the new function  $u_{H,5}(\lambda)$  appears is determined by the differential equation

$$d\mathbf{M}_{H,5}^A + \Xi^A = 0, (6.117)$$

We assume now that  $\mathbf{M}_{H,5}^A$  transforms in the same way as the symmetric part of the matrix of *new* functions given in eq. (6.65), i.e., as a Siegel modular form of weight  $\rho_{21}$ ; see (6.109). This would be necessary for Siegel modularity of the full differential equation matrix. Applying a Siegel modular transformation to eq. (6.117) as first

proposed in [308] we obtain two constraints. These two constraints contradict each other, i.e. they cannot be solved at the same time. Thus, unlike in the elliptic case, the entries of the full differential equation matrix cannot be entirely interpreted as Siegel modular forms; only certain parts of the entries exhibit this property. The terms that disrupt the modular properties involve the new function  $u_{H,5}(\lambda)$ , which explains why this issue did not arise at genus one.

# The Kite Integral Family

#### See also:

- In Section 2.4.1 we introduced the kite and sunrise integral families.
- In Example 3.13 we discussed the sunrise's elliptic curve.
- In Sections 3.2 and 3.4.3 introduced all objects related to tori that are needed for the computations of the kite integral family.

In this chapter, we derive the canonical differential equation for the unequal-mass kite integral family. This family is characterised by its five distinct parameters and the two elliptic curves related to its two sunrise subtopologies.

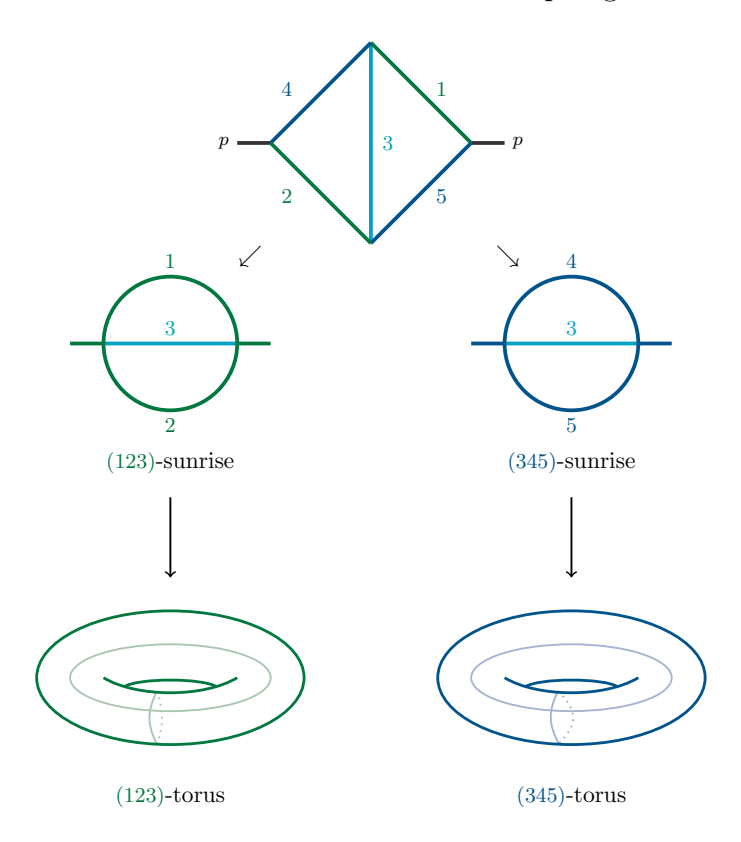


Figure 7.1: The Kite integral with its two sunrises and two tori.

These features require new ideas for the solution of the integral family. Specifically, we develop a systematic approach to parametrise the kinematics on the two tori. Finally, we express the canonical differential equation in Kronecker forms.

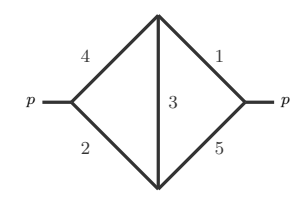
In Section 7.1 we give an extended discussion on the kite integral family, its master integrals and elliptic curves. In Section 7.2 we explain the derivation of its punctures and the canonical differential equation. In Section 7.3 we explain how to express these differential equations on the two tori and finally we give some comments on their integration and boundary values in Section 7.4.

♠ This chapter closely follows previously published results [32, 33], which were obtained in collaborations with Mathieu Giroux, Andrzej Pokraka and Yoann Sohnle.

# Contents of this Chapter

7.1 The	e Kite Integral Family	
7.2 The	$\epsilon$ $\epsilon$ -form Differential Equation 195	
7.2.1	Sunrise subtopology	
7.2.2	Eyeball subtopology	
7.2.3	Full Kite Family	
7.3 Pullback on the Tori		
7.3.1	Algorithmic Pullback	
7.3.2	Comments on the Forms	
7.4 Boundary Value and Integration 218		

# 7.1 The Kite Integral Family



We previously introduced the kite integral family  $I_{\nu}^{\uparrow}$  in Subsection 2.4.1. Here, we provide additional details necessary for its computation. Throughout this chapter, we fix the dimension at  $D=2-2\epsilon$ . To compute the integral in another dimension with even integer part, one can use dimensional shift relations[317–319], as explained in Section 2.5. The even dimensional case (specifically of course D=4) that we consider here is the one relevant for particle physics. The case of  $D=3-2\epsilon$  is also relevant in certain cosmological applications [84], but not covered by the discussion given here. Additionally, in the following sections we choose  $\mu=m_3$  and work with the dimensionless parameters

$$X_0 = p^2/m_3^2$$
,  $X_1 = m_1^2/m_3^2$ ,  $X_2 = m_2^2/m_3^2$ ,  $X_4 = m_4^2/m_3^2$ ,  $X_5 = m_5^2/m_3^2$ . (7.1)

which parametrise the kinematic space

$$\mathcal{K}_{---} = \{ \mathbf{X} = (X_0, X_1, X_2, X_4, X_5) \in \mathbb{C}^5 \} - \{ \text{Landau loci} \}.$$
 (7.2)

The solutions of the Landau equations for the kite integral were derived in [320]. <sup>1</sup> These conditions ensure, that the expressions in elliptic integrals match the generic integral expressions we give. Note also the branch choice given in eq. (7.14).

The initial basis We use LiteRed to perform the IBP reduction of this integral family and find a basis of master integrals. The initial basis we obtain takes the following form

$$\mathbf{I}^{\top} = (I_{1,1,0,0,0}, I_{1,0,1,0,0}, I_{0,1,1,0,0}, I_{0,0,1,1,0}, I_{0,0,1,0,1}, I_{0,0,0,1,1}, I_{1,0,0,1,0}, I_{0,1,0,0,1}, I_{1,1,1,0,0}, I_{1,1,1,0,0}, I_{1,2,1,0,0}, I_{1,1,2,0,0}, I_{0,0,1,1,1}, I_{0,0,2,1,1}, I_{0,0,1,2,1}, I_{0,0,1,1,2}, I_{1,0,1,1,0}, I_{1,1,0,1,0}, I_{1,1,0,0,1,1}, I_{0,1,0,1,1}, I_{0,1,1,0,1}, I_{1,1,0,0,1}, I_{1,0,1,0,1}, I_{1,0,1,1,1,0}, I_{1,1,1,1,0}, I_{1,1,1,1,0}, I_{1,1,1,1,1}, I_{1,0,1,1,1}, I_{1,1,0,1,1}, I_{1,1,0,1,1}, I_{1,1,1,1,1}).$$
(7.3)

These basic integrals are presented diagrammatically in figures 7.2, 7.3 and 7.6.

<sup>1</sup>For numerical implementations of the computations presented here, we always use points that fulfill the following restrictions:

$$X_{1} < (\sqrt{X_{0}} - \sqrt{X_{5}})^{2},$$

$$X_{1} < (1 - \sqrt{X_{4}})^{2},$$

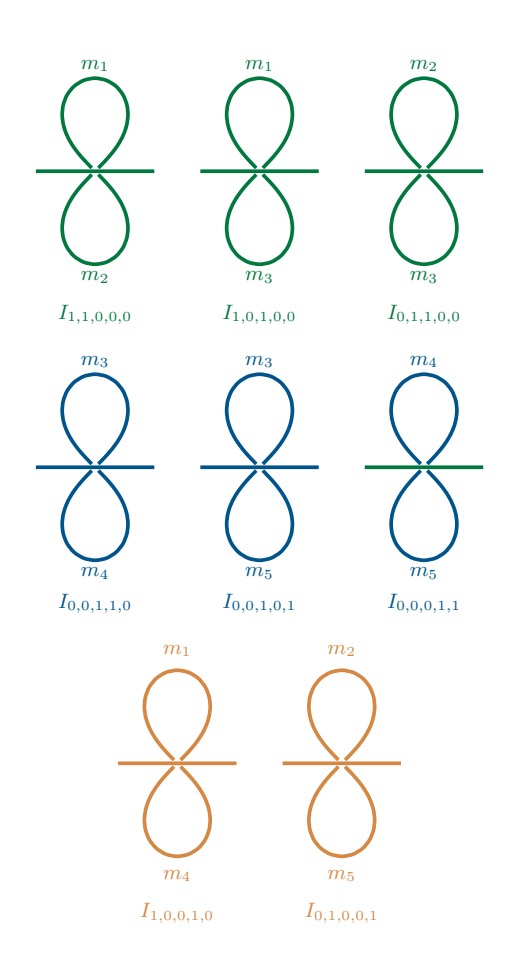
$$X_{2} < (\sqrt{X_{0}} - \sqrt{X_{4}})^{2},$$

$$X_{2} < (1 - \sqrt{X_{5}})^{2},$$

$$X_{4} > (\sqrt{X_{0}} + \sqrt{X_{2}})^{2},$$

$$X_{5} > (\sqrt{X_{0}} + \sqrt{X_{1}})^{2},$$

$$X_{5} > (1 + \sqrt{X_{2}})^{2}.$$



Diagrams in green are subtopologies of the (123)-sunrise or have that sunrise as their subtopology.

Diagrams in blue are subtopologies of the (123)-sunrise or have that sunrise as their subtopology.

Diagrams in orange are related to neither of the sunrises.

The single diagram in turquoise has both sunrises as its subtopologies, it is the top sector, the full kite integral itself.

Figure 7.2: Graphical representation of all Feynman diagrams from the basis eq. (7.3) that have two propagators.

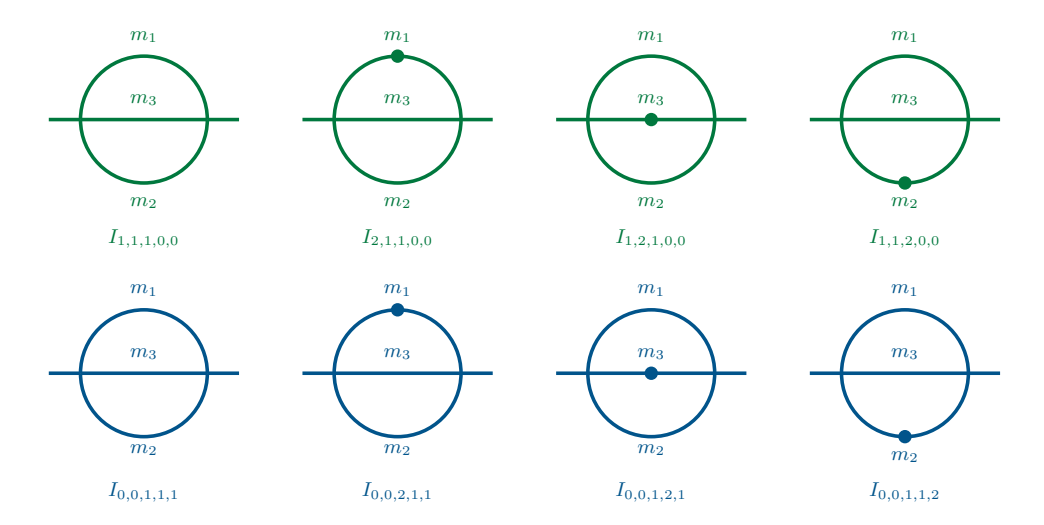


Figure 7.3: Graphical representation of all Feynman diagrams from the basis in eq. (7.3) that are in the sunrises' top sectors.

Diagrams in green are subtopologies of the (123)-sunrise or have that sunrise as their subtopology.

Diagrams in blue are subtopologies of the (123)-sunrise or have that sunrise as their subtopology.

Diagrams in orange are related to neither of the sunrises.

The single diagram in turquoise has both sunrises as its subtopologies, it is the top sector, the full kite integral itself.

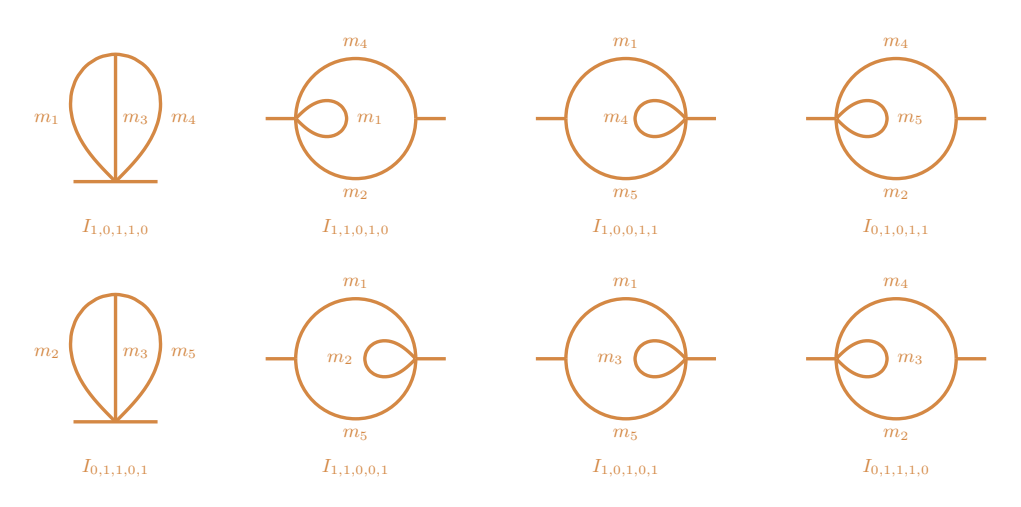


Figure 7.4: Graphical representation of all Feynman diagrams from the basis in eq. (7.3) that are not the sunrises' top sectors but have three propagators.

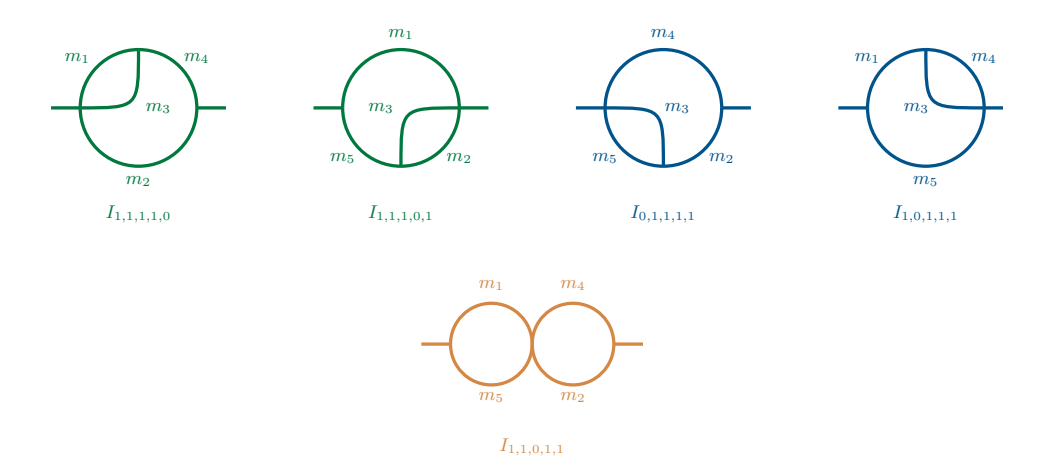


Figure 7.5: In the top line we give graphical representations of all Feynman diagrams from the basis in eq. (7.3) that contain *one* sunrise as their subtopology and have four propagators. We denote these the *eyeballs*. In the bottom line we give the single diagram that has four propagators and no sunrise subtopologies.

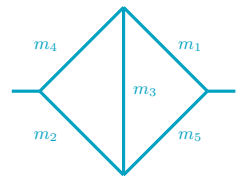


Figure 7.6: A diagrammatic representation of the top sector of the kite integral family, which contains only  $I_{1,1,1,1,1}$ .

As already mentioned in Example 2.8, the kite integral has two sunrise subtopologies: One with propagators  $D_1, D_2$  and  $D_3$  that we call the (123)-sunrise and one with propagators  $D_3$ ,  $D_4$  and  $D_5$  that we call the (345)-sunrise. We use the following colours: diagrams in green or blue either contain the (123)-sunrise or (345)-sunrise as a subtopology or are a subtopology of the (123)-sunrise [or (345)sunrise. The only exception to this colour coding is the kite (given in turquoise) since it contains both the (123)-sunrise and (345)-sunrise as subtopologies. All other topologies that do not contain a sunrise as a subtopology and are not a subtopology of a sunrise are coloured orange. These are not associated with any of the two elliptic curves and are polylogarithmic.

The Two Elliptic Curves As explained in Example 3.13 the massive sunrise integral is associated to an elliptic curve. Thus, there are two elliptic curves related to the kite integral family<sup>2</sup> and we call them the (123)-curve and the (345)-curve. In particular, we label all objects related to either curve by (123) or (345) respectively. According to eq. (2.55) the branch points for the two sunrise subtopologies in the parameters  $X_i$  are:

 $^{2}\mathrm{We}$ illustrate this graphically in figure 7.1.

$$\lambda_1^{(123)} = -(\sqrt{X_1} + \sqrt{X_2})^2 \qquad \lambda_1^{(345)} = -(\sqrt{X_4} + \sqrt{X_5})^2 \tag{7.4}$$

$$\lambda_2^{(123)} = -(1 + \sqrt{X_0})^2 \qquad \qquad \lambda_2^{(345)} = -(1 + \sqrt{X_0})^2 \tag{7.5}$$

$$\lambda_2^{(123)} = -(1 + \sqrt{X_0})^2 \qquad \lambda_2^{(345)} = -(1 + \sqrt{X_0})^2 \qquad (7.5)$$

$$\lambda_3^{(123)} = -(1 - \sqrt{X_0})^2 \qquad \lambda_3^{(345)} = -(1 - \sqrt{X_0})^2 \qquad (7.6)$$

$$\lambda_4^{(123)} = -(\sqrt{X_1} - \sqrt{X_2})^2 \qquad \lambda_4^{(345)} = -(\sqrt{X_4} - \sqrt{X_5})^2 . \qquad (7.7)$$

$$\lambda_4^{(123)} = -(\sqrt{X_1} - \sqrt{X_2})^2 \qquad \lambda_4^{(345)} = -(\sqrt{X_4} - \sqrt{X_5})^2. \tag{7.7}$$

Note that we consider the roots to be ordered:  $\lambda_i^{\alpha} < \lambda_j^{\alpha}$  for i < j for both  $\alpha \in$  $\{(123), (345)\}$ . We define the periods of these elliptic curves  $(\alpha \in \{(123), (345)\})$ with the standard canonical basis as in Section 3.2.2, albeit with a slightly different normalization:

$$\omega_1^{\alpha} = 2 \int_{\lambda_2^{\alpha}}^{\lambda_3^{\alpha}} \frac{\mathrm{d}x_{\alpha}}{y_{\alpha}} = \frac{2\mathrm{K}(\mathrm{k}_{\alpha}^2)}{c_4^{\alpha}} \text{ and } \omega_2^{\alpha} = 2 \int_{\lambda_4^{\alpha}}^{\lambda_3^{\alpha}} \frac{\mathrm{d}x_{\alpha}}{y_{\alpha}} = \frac{2i\mathrm{K}(1 - \mathrm{k}_{\alpha}^2)}{c_4^{\alpha}}, \tag{7.8}$$

where

$$c_4^{\alpha} = \frac{1}{2} \sqrt{(\lambda_3^{\alpha} - \lambda_1^{\alpha})(\lambda_4^{\alpha} - \lambda_2^{\alpha})} \text{ and } 0 \le k_{\alpha}^2 = \frac{(\lambda_3^{\alpha} - \lambda_2^{\alpha})(\lambda_4^{\alpha} - \lambda_1^{\alpha})}{(\lambda_3^{\alpha} - \lambda_1^{\alpha})(\lambda_4^{\alpha} - \lambda_2^{\alpha})} \le 1.$$
 (7.9)

In general, we consider the normalised period, which in this case takes is

$$\tau^{\alpha} = \frac{\omega_2^{\alpha}}{\omega_1^{\alpha}} = \frac{iK(1 - k_{\alpha}^2)}{K(k_{\alpha}^2)} \in \mathbb{H}.$$
 (7.10)

Explicitly, we obtain for the *elliptic moduli*  $k_{\alpha}^{2}$  of the two curves:

$$k_{(123)}^2 = -\frac{16\sqrt{X_0}\sqrt{X_1}\sqrt{X_2}}{X_0^2 - 2\left(X_1 + X_2 + 1\right)X_0 + X_1^2 + \left(X_2 - 1\right){}^2 - 8\sqrt{X_0}\sqrt{X_1}\sqrt{X_2} - 2X_1\left(X_2 + 1\right)}\,, \tag{7.11a}$$

$$k_{(345)}^{2} = -\frac{16\sqrt{X_{0}}\sqrt{X_{4}}\sqrt{X_{5}}}{X_{0}^{2} - 2(X_{4} + X_{5} + 1)X_{0} + X_{4}^{2} + (X_{5} - 1)^{2} - 8\sqrt{X_{0}}\sqrt{X_{4}}\sqrt{X_{5}} - 2X_{4}(X_{5} + 1)}}.$$
(7.11b)

The two curves are each isomorphic to a complex torus  $\mathcal{T}_{\alpha} = \mathbb{C}/\Lambda_{\alpha}$  defined by the lattice  $\Lambda_{\alpha} = \mathbb{Z} \oplus \tau_{\alpha}\mathbb{Z}$  respectively. To translate from the coordinates  $(x_{\alpha}, y_{\alpha})$  on the elliptic curves to points  $z_{\alpha}$  on the tori, we use Abel's map as given in Definition 3.10. In particular, for the (123) and (345)- curves they are

$$(x_{\alpha}, y_{\alpha}) \mapsto z_{\alpha}^{\pm} = \pm \left[ e^{i[\arg(x_{\alpha} - \lambda_{1}^{\alpha}) - \arg(x_{\alpha} - \lambda_{2}^{\alpha})]} \frac{F(\sqrt{u_{x}^{\alpha}}, k_{\alpha}^{2})}{2K(k_{\alpha}^{2})} + \frac{\tau_{\alpha}}{2} \right] \quad \text{for} \quad x_{\alpha} \in \mathbb{R} ,$$

$$(7.12)$$

where F is the incomplete elliptic integral of the first kind as defined in eq. (3.74) and

$$u_x^{\alpha} = \frac{x - \lambda_2^{\alpha}}{x - \lambda_1^{\alpha}} \frac{\lambda_1^{\alpha} - \lambda_3^{\alpha}}{\lambda_2^{\alpha} - \lambda_3^{\alpha}}.$$
 (7.13)

For the expression in eq. (7.11) to be compatible with the integral expression for the Abel's map we make the branch choice

$$\frac{y_{\alpha}}{|y_{\alpha}|} = \begin{cases}
-1 & x \leq \lambda_1^{\alpha} \text{ or } x > \lambda_4^{\alpha}, \\
-i & \lambda_1^{\alpha} < x_1 \leq \lambda_2^{\alpha}, \\
1 & \lambda_2^{\alpha} < x_1 \leq \lambda_3^{\alpha}, \\
i & \lambda_3^{\alpha} < x_1 \leq \lambda_4^{\alpha}.
\end{cases}$$
(7.14)

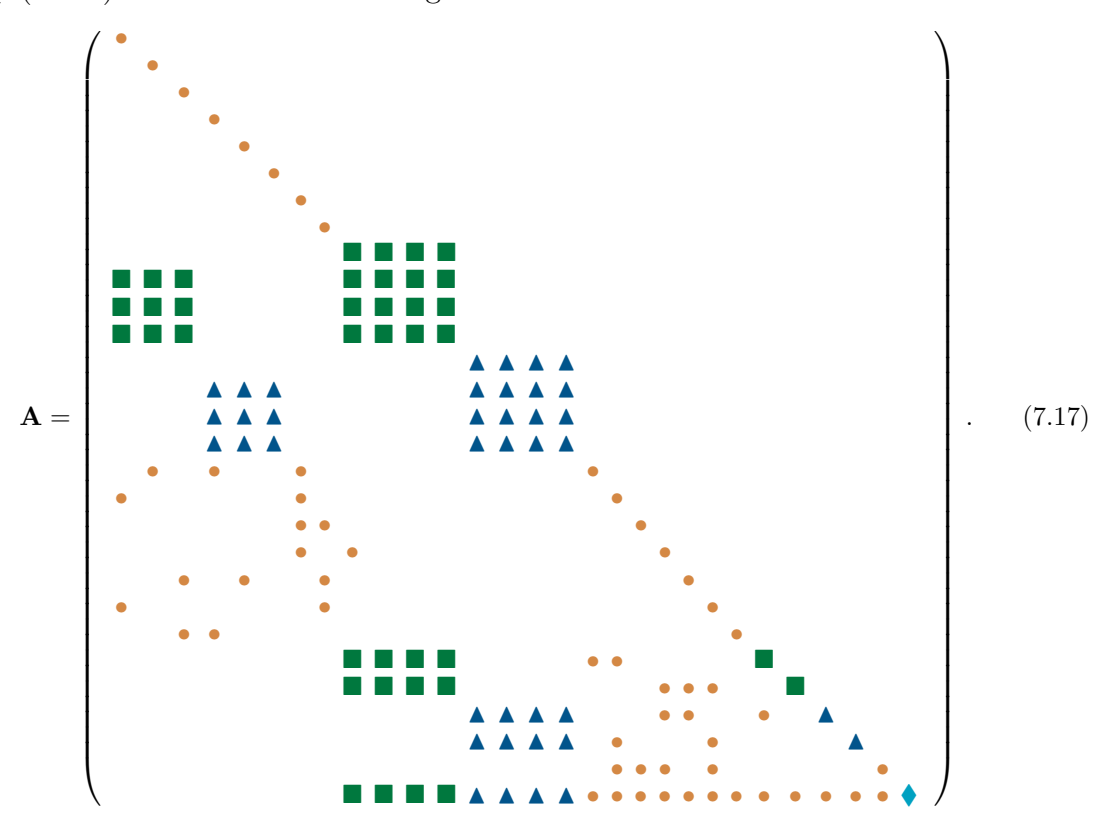
As we consider a space of five kinematic parameters,  $\mathcal{K}_{-\Phi}$ , we also need five parameters on the tori. One of them is the normalised period  $\tau_{\alpha}$  and the remaining degrees of freedom are accounted for by four punctures. More specifically, we do not work on the tori themselves, but on the moduli spaces of tori with five punctures,  $\mathcal{M}_{1,5}^{\alpha}$ , where one of the punctures is the fixed point of the elliptic curve and the other four are punctures  $z_{\alpha,i}$ . A suitable choice of these punctures  $z_{\alpha,i}$  for our computation is one of the central problems solved in this chapter (as presented in [32]). Because of the translation invariance on the torus, the punctures are best understood as differences of points mapped via Abel's map. Explicitly, we define them as:

$$z_i = z_i^+ - z_i^- = 2z_i^+. (7.15)$$

**The Initial Differential Equation** We denote the differential equation that the initial basis of eq. (7.3) fulfils by

$$d\mathbf{I} = \mathbf{A}\mathbf{I}, \tag{7.16}$$

where d is the exterior derivative on  $\mathcal{K}_{\rightarrow}$  and the components of **A** are differential one-forms on  $\mathcal{K}_{\rightarrow}$ . The connection matrix **A** fulfils the integrability condition of



eq. (2.100) and takes the following schematic form:

Here and in the subsequent sections we use the following colour/shape-code for the entries related to the two sunrise subtopologies/tori: Entries related to the (123)-sunrise are denoted by  $\blacksquare$ , entries related to the (345)-sunrise are denoted by  $\blacktriangle$ , the single entry that has both as a subtopology is denoted by  $\blacklozenge$  and entries related to neither are denoted by  $\blacklozenge$ . All empty entries are zero.

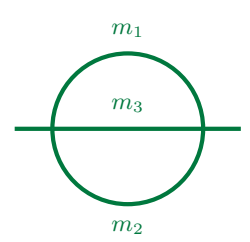
# 7.2 The $\varepsilon$ -form Differential Equation

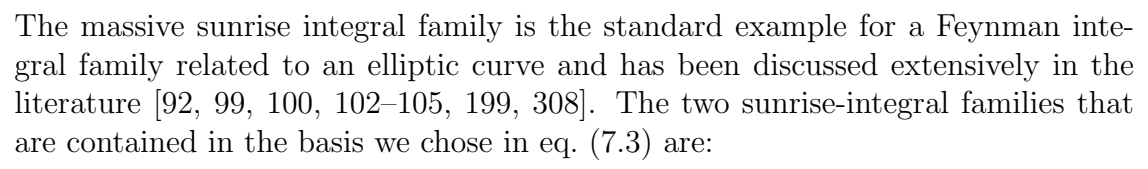
Our aim in this section is to construct a canonical basis J that fulfils a differential equation of the form given in eq. (2.103). We start with the sunrise subtopologies, where we use existing results [92]. Then we consider the four four-parameter eyeball subtopologies before finally constructing the transformation for the full kite integral family. Beyond the sunrise integral family the construction will always follow the same scheme:

- 1. We insert the known transformations for the sunrise subtopologies.
- 2. We normalise the remaining diagonal entries by the inverse of their maximal cuts in  $\varepsilon \to 0$  to remove  $\mathcal{O}(\varepsilon^0)$  entries on the diagonal.
- 3. We integrate out the remaining off-diagonal  $\varepsilon^0$  terms.

The final step is the crucial one in this construction and relies on understanding the coordinates of the integral family on the tori.

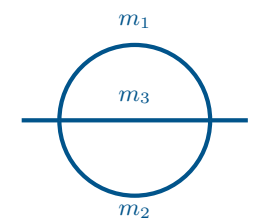
# 7.2.1 Sunrise subtopology





$$\mathbf{I}_{(123)}^T = (I_{1,1,0,0,0}, I_{1,0,1,0,0}, I_{0,1,1,0,0}, I_{1,1,1,0,0}, I_{2,1,1,0,0}, I_{1,2,1,0,0}, I_{1,1,2,0,0})$$
(7.18)

$$\mathbf{I}_{(345)}^{T} = (I_{0,0,1,1,0}, I_{0,0,1,0,1}, I_{0,0,0,1,1}, I_{0,0,1,1,1}, I_{0,0,2,1,1}, I_{0,0,1,2,1}, I_{0,0,1,1,2}). \tag{7.19}$$



In the equal mass case, these integral families can be expressed on the moduli spaces  $\mathcal{M}_{1,1}^{\alpha}$ , i.e., the differential equations can be written with the normalized period  $\tau_{\alpha}$  as its single parameter. In the multi-parameter case, the two additional parameters of  $\mathcal{M}_{1,3}^{\alpha}$  are given by two punctures:

$$z_i^{(123)} = \frac{F\Big(\arcsin\sqrt{u_i^{(123)}}, k_{(123)}^2\Big)}{K\Big(k_{(123)}^2\Big)} \text{ and } z_i^{(345)} = \frac{F\Big(\arcsin\sqrt{u_i^{(345)}}, k_{(345)}^2\Big)}{K\Big(k_{(345)}^2\Big)} \,, \quad (7.20)$$

where we have dropped a  $\tau=2\frac{\tau}{2}\sim0$  in the difference (7.15) when using (3.84) and

$$u_1^{(123)} = \frac{\left(\sqrt{X_0} + \sqrt{X_1}\right)^2 - \left(\sqrt{X_2} - 1\right)^2}{4\sqrt{X_2}}, \quad u_2^{(123)} = \frac{\left(\sqrt{X_0} + \sqrt{X_2}\right)^2 - \left(\sqrt{X_1} - 1\right)^2}{4\sqrt{X_1}}, \quad (7.21)$$

$$u_4^{(345)} = \frac{\left(\sqrt{X_0} + \sqrt{X_4}\right)^2 - \left(\sqrt{X_5} - 1\right)^2}{4\sqrt{X_5}}, \quad u_5^{(345)} = \frac{\left(\sqrt{X_0} + \sqrt{X_5}\right)^2 - \left(\sqrt{X_4} - 1\right)^2}{4\sqrt{X_4}}.$$

$$(7.22)$$

One can also define a third puncture  $z_3^{\alpha}$  for both curves

$$u_3^{(123)} = u_1^{(123)}|_{m_1 \leftrightarrow m_3}$$
 and  $u_3^{(345)} = u_4^{(345)}|_{m_4 \leftrightarrow m_3}$ . (7.23)

It is linearly dependent on the other two punctures:  $z_1^{(123)}+z_2^{(123)}+z_3^{(123)}=1=z_3^{(345)}+z_4^{(345)}+z_5^{(345)}$ . All of the punctures can be obtained in at least two ways:

- 1. One way to obtain an elliptic curve related to the sunrise graph is via its second graph polynomial  $F_{\alpha}$ . This curve is isogenic to the one we obtain from the maximal cuts for details we refer to the literature, e.g., [8, 92]. The marked points can then be obtained as the intersection points of the domain of integration in Feynman parameter space with the zero set of the second graph polynomial. One can map these points to the marked points on the curve obtained from the maximal cut.
- 2. One can obtain a marked point on the sunrise's torus by considering one of its eyeball super-topologies and integrating its maximal cut along the additional coordinate of the eyeball. Certain kinematic limits then allow us to recover the two sunrise punctures from this new punctures. We discuss this approach in detail in Section 7.2.2.

The canonical differential equation is then the  $\varepsilon$ -form differential equation whose entries can be written as quasi-modular forms on the respective tori. More specifically, they can be written as Kronecker forms with the  $z^{\alpha}$ -arguments being linear combinations of the punctures  $z_i^{\alpha}$ . There are different ways to obtain this form. We use a known result from the literature, inserting the transformation obtained in [92]. In particular, we denote the canonical bases of master integrals by  $\mathbf{J}^{(123)} = \mathrm{diag}(\varepsilon^2 \times \mathbbm{1}_{3\times 3}, \mathbf{U}^{(123)}))\mathbf{I}^{(123)}$  and  $\mathbf{J}^{(345)} = \mathrm{diag}(\varepsilon^2 \times \mathbbm{1}_{3\times 4}, \mathbf{U}^{(345)})\mathbf{I}^{(345)}$  respectively. Their differential equations take the form

$$d\mathbf{J}^{(123)} = \varepsilon \mathbf{B}_{\Phi}^{(123)} \mathbf{J}^{(123)} \text{ and } d\mathbf{J}^{(345)} = \varepsilon \mathbf{B}_{\Phi}^{(345)} \mathbf{J}^{(345)}$$
 (7.24)

The canonical differential equation for the *dual* sunrise integral family (in the sense of a canonical basis for the dual relative twisted cohomology group) was derived in [308]. After a simple final rotation, this basis is orthogonal to the basis given in [92].

# 7.2.2 Eyeball subtopology

We move on to the first new non-trivial subtopology of the full kite family: The eyeballs. Those are the following four families with 13 master integrals each:

$$\mathbf{I}_{4,1}^{\mathsf{T}} = (I_{1,1,0,0,0}, I_{1,0,1,0,0}, I_{0,1,1,0,0}, I_{1,0,0,1,0}, I_{0,0,1,1,0}, I_{1,1,1,0,0}, I_{1,1,1,0,0}, I_{1,1,1,0,0}, I_{1,1,1,0,0}, I_{1,1,1,0,0}, I_{1,1,1,0,0}, I_{1,1,1,1,0}),$$
(7.25)

$$\mathbf{I}_{4,2}^{\mathsf{T}} = (I_{1,1,0,0,0}, I_{1,0,1,0,0}, I_{0,1,1,0,0}, I_{0,1,0,0,1}, I_{0,0,1,0,1}, I_{1,1,1,0,0}, I_{1,1,1,0,0}, I_{1,2,1,0,0}, I_{1,1,2,0,0}, I_{0,1,1,0,1}, I_{1,1,0,0,1}, I_{1,0,1,0,1}, I_{1,1,1,0,1}),$$
(7.26)

$$\mathbf{I}_{4,3}^{\mathsf{T}} = (I_{0,1,1,0,0}, I_{0,0,1,1,0}, I_{0,0,1,0,1}, I_{0,0,0,1,1}, I_{0,0,1,1,1}, I_{0,0,2,1,1}, I_{0,0,1,2,1}, I_{0,0,1,1,2}, (7.27))$$

$$I_{0,1,0,0,1}, I_{0,1,0,1,1}, I_{0,1,1,0,1}, I_{0,1,1,1,0}, I_{0,1,1,1,1}),$$

$$\mathbf{I}_{4,4}^{\mathsf{T}} = (I_{1,0,1,0,0}, I_{0,0,1,1,0}, I_{0,0,1,0,1}, I_{0,0,0,1,1}, I_{0,0,1,1,1}, I_{0,0,2,1,1}, I_{0,0,1,2,1}, I_{0,0,1,1,2}, (7.28)$$

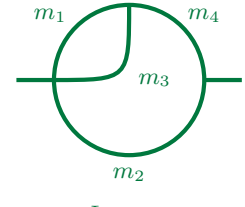
$$I_{1,0,0,1,0}, I_{1,0,1,1,0}, I_{1,0,0,1,1}, I_{1,0,1,0,1}, I_{1,0,1,1,1}).$$

The families  $\mathbf{I}_{4,1}$ ,  $\mathbf{I}_{4,2}$  are only associated to the (123)-torus, whereas the families  $\mathbf{I}_{4,3}$ ,  $\mathbf{I}_{4,4}$  are only associated to the (345)-torus. The eyeball integral families satisfy differential equations:

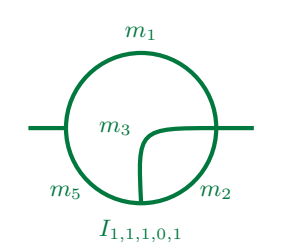
$$d\mathbf{I}_{4,i} = \mathbf{A}_{4,i} \cdot \mathbf{I}_{4,i} \,, \tag{7.29}$$

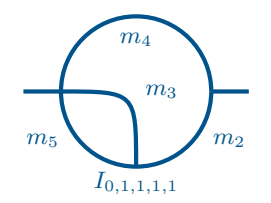


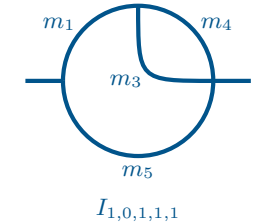
We review the algorithm in Section 6.1.1.



 $I_{1,1,1,1,0}$ 







197

where  $\mathbf{A}_{4,i}$  is a 13 × 13 submatrix of  $\mathbf{A}$ . We focus on the (1234)-eyeball, whose differential equation schematically takes the following form

# Four Punctures for an Eyeball

Each of the eyeball integral families has four parameters in kinematic space and we want to express these on the respective torus, i.e., as the moduli in their moduli spaces  $\mathcal{M}_{1,4}$ . In principle, the idea is to consider the moduli space of the sunrise integral family, that is a subtopology of the eyeball family, and systematically introduce an additional puncture. However, we see that this approach allows us to systematically identify *all* punctures. We demonstrate this in detail for the (1234)-eyeball and then summarize the results for all eyeballs in eq. (7.42). First, let us develop an intuitive understanding of what a *natural* additional puncture should look like:

- It should emerge naturally in the canonical differential equation<sup>4</sup> and, assuming that the equation can be expressed in quasi-modular Kronecker forms whose arguments contain the punctures, traces of the new puncture should appear in the form in eq. (7.20) even in kinematic coordinates. Practically, that means the punctures should appear as incomplete elliptic integrals after integrating out  $\varepsilon^0$  terms in the off-diagonal.
- For the (1234)-eyeball, it involves the kinematic parameter  $X_4$ , since expressions solely in  $X_0, X_1, X_2$  can already be written in terms of the sunrise's torus parameters.

By the first assumption, we expect that the punctures arise in the connection matrix after we integrate out the off-diagonal entries when the diagonal has already been brought in  $\varepsilon$ -form.<sup>5</sup> In general, the  $\varepsilon$ -form of the diagonal entries is achieved by dividing by the  $\varepsilon \to 0$  limit of the respective entry's maximal cut, i.e., by a transformation

$$\mathbf{U}_{4,1}^{\star} = \begin{pmatrix} \mathbf{1} & 0\\ 0 & \mathbf{MC}_{4,1}^{-1} \end{pmatrix}, \tag{7.31}$$

where we shortened  $MC_{4,1} = MC[I_{1,1,1,1,0}]_{\varepsilon \to 0}$ . After this transformation, we find

$$\mathbf{A}_{4,1}^{\star} = \begin{pmatrix} \varepsilon \cdot \boxplus & 0\\ \mathrm{MC}_{4,1}^{-1} \cdot (\boxminus_{0} + \varepsilon \cdot \boxminus_{1}) & \varepsilon \cdot \boxtimes \end{pmatrix}$$
 (7.32)

- <sup>4</sup>We confirm this in our computation of the eyeball's canonical differential equations, but we also present a simpler way to obtain them before computing the full canonical differential equation taking these assumptions into account. In fact, we use the punctures to compute the *kite's* full canonical differential equation.
- <sup>5</sup>Note that this does not mean the new puncture not appear on the diagonal when changing to the torus coordinates. We just argue that it can be more easily *found* as a new functions on the off-diagonal.

with  $\boxplus$ ,  $\boxtimes$ ,  $\boxminus_0$ ,  $\boxminus_1$  representing entries that are constant in  $\varepsilon$ . The remaining transformation to bring such a system in  $\varepsilon$ -form should look like

$$U_{4,1}^{\star\star} = \begin{pmatrix} \mathbf{1} & 0\\ \int \left( \operatorname{MC}_{4,1}^{-1} \cdot \boxminus_0 \right) & 1 \end{pmatrix}. \tag{7.33}$$

In principle, one can now define the entries of  $\int (MC_{4,1}^{-1} \cdot \boxminus_0)$  as a set of new functions and then potentially reduce them to a smaller set of new functions by finding which of them are linearly dependent or can be expressed in rational functions of known objects.<sup>6</sup> Note that in this case we assume that we find *at least one* actual *new* function, as we assume that we uncover a puncture. This also tells us about the structure we expect the new function to have: It should be proportional to an incomplete elliptic integral of the first kind, as it would naturally arise from Abel's map. In fact,  $\int (MC_{4,1}^{-1} \cdot \boxminus_0)$  for the specific problem at hand contains such a new object:

<sup>6</sup>Here we mean by *new* functions the objects introduced in step 4 of the algorithm from [24] presented in section 6.1.1.

$$z_{\phi}^{(123)} \sim \int dX_4 MC_{4,1} = \int \frac{dX_4}{\sqrt{\lambda(1, X_1, X_4)} \sqrt{\lambda(X_0, X_2, X_4)}},$$
 (7.34)

where  $\lambda(a,b,c) = a^2 + b^2 + c^2 - 2ab - 2ac - 2bc$  is the Källén function,  $\lambda_{abc} = \lambda(X_a,X_b,X_c)$  and  $X_3 = m_3^2/m_3^2 = 1$ . The integral in eq. (7.34) evaluates in an incomplete elliptic integral of the first kind and thus takes the form of a puncture obtained with Abel's map as defined in eq. (3.84). In particular, we integrate the maximal cut over  $X_4$ . We motivate the choice of integration variable from the observation that  $\mathcal{T}^{(123)}$  does not "know" about  $m_4^2$  and, consequently,  $X_4$  should be integrated out – which agrees with the second assumption given above. Explicitly, we obtain the puncture

$$z_{\phi}^{(123)} = \int \frac{\mathrm{d}X_4}{\sqrt{\lambda_{134}\lambda_{024}}} = \frac{1}{2c_4'} F\left(\arcsin\sqrt{u_{\phi}}, k_{\phi,(123)}^2\right), \qquad (7.35)$$

with

$$c_4' = -\frac{\sqrt{(+++)(+--)(-+-)(--+)}}{4}, \qquad (7.36a)$$

$$k_{\phi,(123)}^2 = \frac{(++-)(-++)(+-+)(---)}{(+++)(-+-)(--+)(+--)},$$
(7.36b)

$$u_{\phi} = \frac{(+++)(-+-)}{(+-+)(---)} \frac{1-2\sqrt{X_1} + X_1 - X_4}{1+2\sqrt{X_1} + X_1 - X_4}.$$
 (7.36c)

where

$$(\pm \pm \pm) = 1 \pm \sqrt{X_0} \pm \sqrt{X_1} \pm \sqrt{X_2}$$
. (7.37)

The choice of branch on the right-hand side of (7.35) is valid for  $0 < k_{\phi,(123)}^2 < 1$  and  $0 < X_4 < 1$ . Moreover, since  $k_{\phi,(123)}^2$  is a cross-ratio, it is manifestly invariant under any permutation of the kinematic variables. Though,  $k_{\phi,(123)}^2$  is still a distinct

elliptic modulus and we want to write all our punctures for the eyeball on the (123)-torus. We can rewrite eq. (7.35) to achieve this:

$$k_{\phi,(123)}^2 = \frac{1}{1 - k_{(123)}^2}$$
 and  $u_4^{(123)} = \frac{1}{1 - u_\phi}$ . (7.38)

Overall, we obtain using the identities from appendix C.1:

$$z_{\phi}^{(123)} = \frac{1}{2} \psi_1 \left[ \frac{F\left(\arcsin\sqrt{u_4}, k_{(123)}^2\right)}{K\left(k_{(123)}^2\right)} - 1 \right]$$

$$z_{\phi}^{(123)}$$
(7.39)

and we take  $z_4^{(123)}$  as our additional puncture. Note that due to the normalisation of the lattice in  $(1,\tau^{(123)})$ , we have the equivalence relation  $z_4^{(123)}\sim z_4^{(123)}\pm 1$ . We initially assumed that only one additional puncture is needed, with the sunrise punctures and period accounting for the other three degrees of freedom. However, we now argue that the two sunrise punctures can also be derived from the maximal cut argument. We start by noting that

$$u_4^{(123)} = u_2^{(123)} \frac{\left(1 + \sqrt{X_1}\right)^2 - X_4}{(\sqrt{X_0} + \sqrt{X_2})^2 - X_4}, \tag{7.40}$$

From this, we immediately see that the  $X_4 \to \infty$  limit (corresponding to an infinitely heavy  $m_4$  effectively pinching the (1234)-eyeball to the (123)-sunrise) gives

$$\lim_{X_4 \to \infty} u_4^{(123)} = u_2^{(123)} = u_1^{(123)}|_{X_1 \leftrightarrow X_2}. \tag{7.41}$$

The second equality is due to the symmetry of the sunrise itself. The key takeaway from this example is that one can identify *all* the necessary punctures to define the embedding of  $\mathcal{K}_{(1234)\text{-eyeball}}$  into  $\mathcal{M}_{1,4}^{(123)}$  simply by analysing the integral of the corresponding maximal cut.

In the same way, we can also identify a new puncture for the (1235)-eyeball on the (123)-torus and two punctures on the (345).torus from the (2345)- and the (1345)-eyeball. Note that each of these new punctures gives the corresponding sunrise punctures via the correct kinematic limits. We list all  $u_i^{\alpha}$  functions here:

$$u_{4}^{(123)} = u_{2}^{(123)} \frac{\left(1 + \sqrt{X_{1}}\right)^{2} - X_{4}}{(\sqrt{X_{0}} + \sqrt{X_{2}})^{2} - X_{4}}, \qquad u_{5}^{(123)} = u_{1}^{(123)} \frac{\left(1 + \sqrt{X_{2}}\right)^{2} - X_{5}}{(\sqrt{X_{0}} + \sqrt{X_{1}})^{2} - X_{5}},$$

$$(7.42a)$$

$$u_{1}^{(345)} = u_{5}^{(345)} \frac{\left(1 + \sqrt{X_{4}}\right)^{2} - X_{1}}{(\sqrt{X_{0}} + \sqrt{X_{5}})^{2} - X_{1}}, \qquad u_{2}^{(345)} = u_{4}^{(345)} \frac{\left(1 + \sqrt{X_{5}}\right)^{2} - X_{2}}{(\sqrt{X_{0}} + \sqrt{X_{4}})^{2} - X_{2}}.$$

$$(7.42b)$$

When combined with the sunrise punctures of each torus – which can be obtained through similar limits as in (7.41) – each torus  $\alpha = (123), (345)$  has four linearly independent punctures,  $\{z_1, z_2, z_4, z_5\}^{\alpha}$ . This allows for a complete embedding of  $\mathcal{K}_{\Phi}$ 

within  $\mathcal{M}_{1,5}^{(123)}$  or  $\mathcal{M}_{1,5}^{(345)}$  by analysing the maximal cuts of all eyeball subtopologies. The full set of punctures remains closed under specific mass permutations, which are collected in Appendix C.2. In the next section, we further show that these punctures align with the double integral of the maximal cut of the kite.

### The Transformation to Canonical Form

We transform the basis  $I_{4,1}$  to canonical form step-by-step, starting with the diagonal blocks.

1: The (123)-Sunrise Block We start by putting the upper left  $8 \times 8$  block that contains the seven (123)-sunrise subtopology's master integrals in canonical form. Thus, the first transformation matrix has the form

$$\mathbf{U}_{4,1}^{(1)} = \operatorname{diag}(\varepsilon^2 \times \mathbb{1}_{5 \times 5}, \mathbf{U}_{4,1}^{(123)}, \varepsilon^2 \times \mathbb{1}_{4 \times 4}). \tag{7.43}$$

The new basis  $\mathbf{J}_4^{(1)}$  satisfies the gauge transformed differential equation  $d\mathbf{J}_4^{(1)} = \mathbf{B}_4^{(1)} \cdot \mathbf{J}_4^{(1)}$  with

$$\mathbf{B}_{4}^{(1)} = d\mathbf{U}_{4,1}^{(1)} \cdot \left(\mathbf{U}_{4,1}^{(1)}\right)^{-1} + \mathbf{U}_{4,1}^{(1)} \cdot \mathbf{A}_{4,1} \cdot \left(\mathbf{U}_{4,1}^{(1)}\right)^{-1} . \tag{7.44}$$

The remaining entries that are not in  $\varepsilon$ -form are diagonal entries below the sunrise block as well as the off-diagonal entry  $\left(B_4^{(1)}\right)_{13,6}$ .

2: The Diagonal Entries The remaining master integrals all have have only a single entry in their sector and are polylogarithmic. Thus, the related diagonal entries can be brought to canonical form by leading singularity renormalisation[142]. That means, we solve the homogeneous differential equations

$$d \log u_{ii} = -\lim_{\epsilon \to 0} \left( B_{4,1}^{(1)} \right)_{ii} \quad \text{for } i \in \{10, 11, 12, 13\},$$
 (7.45)

and multiply the  $i^{\text{th}}$  basis element by the solution  $u_{ii}$ . As the fundamental solution of the diagonal blocks (in this case diagonal entries) of the differential equation are the maximal cuts, we effectively compute the inverse maximal cuts  $u_{i,i}$  (at  $\varepsilon \to 0$ ) or in other words, we normalise with the inverse maximal cuts at  $\varepsilon \to 0$ . The solutions are

$$u_{10,10} = \sqrt{\lambda_{134}} \,, \tag{7.46a}$$

$$u_{11,11} = u_{12,12} = \sqrt{\lambda_{024}}, \qquad (7.46b)$$

$$u_{13,13} = \sqrt{\lambda_{024}} \sqrt{\lambda_{134}} \,. \tag{7.46c}$$

The second transformation matrix takes the form

$$\mathbf{U}_{4,1}^{(2)} = \operatorname{diag}\left(\overline{1,\dots,1}, u_{10,10}, u_{11,11}, u_{12,12}, u_{13,13}\right), \tag{7.47}$$

We depict the entries of eq. (7.30) after the first transformation. The light entries are already in  $\varepsilon$ -form, the remaining entries need to be brought to  $\varepsilon$ -form in the subsequent steps:



$$= \begin{pmatrix} \mathbf{1} & 0 & 0 & 0 & 0 \\ \mathbf{0} & MC(I_{1,0,1,1,0})_{\varepsilon \to 0}^{-1} & 0 & 0 & 0 \\ \mathbf{0} & 0 & MC(I_{1,1,0,1,0})_{\varepsilon \to 0}^{-1} & 0 & 0 \\ \mathbf{0} & 0 & 0 & MC(I_{0,1,1,1,0})_{\varepsilon \to 0}^{-1} & 0 \\ \mathbf{0} & 0 & 0 & MC(I_{0,1,1,1,0})_{\varepsilon \to 0}^{-1} \end{pmatrix}$$

After this transformation, we obtain the basis  $\mathbf{J}_{4,1}^{(2)} = \mathbf{U}_{4,1}^{(2)} \cdot \mathbf{J}_{4,1}^{(1)}$  whose differential equation takes the form  $d\mathbf{J}_{4,1}^{(2)} = \mathbf{B}_{4,1}^{(2)} \cdot \mathbf{J}_{4,1}^{(2)}$  with connection matrix

$$\mathbf{B}_{4,1}^{(2)} = d\mathbf{U}_{4,1}^{(2)} \cdot \left(\mathbf{U}_{4,1}^{(2)}\right)^{-1} + \mathbf{U}_{4,1}^{(2)} \cdot \mathbf{B}_{4,1}^{(1)} \cdot \left(\mathbf{U}_{4,1}^{(2)}\right)^{-1}. \tag{7.48}$$

After this transformation, only the entry  $\left(B_{4,1}^{(2)}\right)_{13,6}$  is not in  $\varepsilon$ -form. To remove this entry, we follow the algorithm introduced in [308], which is based on the underlying  $SL(2,\mathbb{Z})$  covariance of the differential equation.

3: Removing  $\mathcal{O}(\varepsilon^0)$  off-diagonal terms At this point, the differential equation takes the form

$$\mathbf{B}_{4,1}^{(2)} = \mathbf{B}_{4,1}^{(2,0)} + \varepsilon \mathbf{B}_{4,1}^{(2,1)} \tag{7.49}$$

and we want to remove  $\mathbf{B}_{4,1}^{(2,0)}$  with the final gauge transformation. Its only non-vanishing entry is the entry (13,6). We make an ansatz for the final transformation, which takes the form<sup>8</sup>

$$\mathbf{U}_{4,1}^{(3)} = \mathbb{1}_{13 \times 13} + \begin{pmatrix} 0 & \dots & 0 & \dots & 0 \\ \vdots & & \vdots & & \\ 0 & \dots & u_{13,6} & \dots & 0 \end{pmatrix} \quad \text{with} \quad du_{13,6} + \left(B_{4,1}^{(2,0)}\right)_{13,6} = 0.$$

$$(7.50)$$

We decompose  $(B_{4,1}^{(2,0)})_{13.6}$  into terms proportional to  $\omega_1$  and  $\partial_0\omega_1$ 

$$\left(B_{4,1}^{(2,0)}\right)_{13,6} = \sigma(X_i, dX_i) \ \omega_1 + \rho(X_i, dX_i) \ \partial_0 \omega_1.$$
 (7.51)

The one-forms  $\sigma$  and  $\rho$  on  $\mathcal{K}_{\to}$  are invariant under modular transformations within the congruence subgroup  $\Gamma(2)$  of  $\mathrm{SL}(2,\mathbb{Z})$  [308]. That means we know how eq. (7.51) transforms and we can assume that  $\mathrm{d}u_{13,6}$  transforms in the same way. This is the idea of the "modular bootstrap" approach introduced in [308]. More specifically, the right hand side of eq. (7.51) transforms like the *derivative* of a modular form of weight one. Thus,  $u_{13,6}$  must transform as a modular form of weight one. Explicitly, applying a modular transformation to eq. (7.51) yields

$$\underbrace{\left(c\,\tau_{(123)} + d\right)\left[du_{13,6} + \left(B_{4,1}^{(2,0)}\right)_{13,6}\right]}_{=0} + c\left(u_{13,6}\,d\tau_{(123)} + \rho\left(\partial_0\tau_{(123)}\right)\,\omega_1\right) = 0. \quad (7.52)$$

We see that the differential equation for  $u_{13,6}$  in eq. (7.52) is easier to solve than the original one of eq. (7.50). But, as it is a differential equation in the coordinate

We depict the entries of eq. (7.30) after the second transformation. The light entries are already in  $\varepsilon$ -form, the remaining entries need to be brought to  $\varepsilon$ -form in the subsequent steps:



<sup>8</sup>Note that the inversion  $du_{13,6} = -(B_{4,1}^{(2,0)})_{13,6}$ is unambiguous only because it is closed. When  $\mathbf{B}_{4}^{(2,0)}$  is not closed, an additional gauge transformation is applied that renders it closed before this step. We see how to do this systematically when discussing the full kite family.

 $au_{(123)}$ , we want to solve it on the torus, i.e., we need to change to coordinates on the (123)-torus. At this point, we need the new parameter  $z_4^{(123)}$ , that we derived at the beginning of this section. In transforming from the coordinates  $(X_0, X_1, X_2, X_4)$  to the toric variables  $( au_{(123)}, z_1^{(123)}, z_2^{(123)}, z_4^{(123)})$  we find that  $\rho$  depends only on  $d au_{(123)}$  and not on punctures  $dz_i^{(123)}$ . In particular, the kinematic differentials are transformed to

$$dX_{i} = \frac{\partial X_{i}}{\partial \tau_{(123)}} d\tau_{(123)} + \sum_{i=1,2,4} \frac{\partial X_{i}}{\partial z_{i}^{(123)}} dz_{i}^{(123)}.$$
 (7.53)

Note that it is non-trivial to compute the partial derivatives of kinematic variables by the torus variables directly and thus we determine them from the inverse of the Jacobian matrix  $\mathcal{J}_{ij} = \partial \zeta_i/\partial X_j$  with  $\zeta_i \in \{\tau_{(123)}, z_1^{(123)}, z_2^{(123)}, z_4^{(123)}\}$ , for which we just need to compute the partial derivatives of torus variables by kinematic variables which is simpler. Substituting this into eq. (7.52) and extracting the  $d\tau_{(123)}$  component yields

$$u_{13,6} = -\omega_1 \frac{\partial \tau_{(123)}}{\partial X_0} \sum_{i=0,1,2,4} \rho_i \frac{\partial X_i}{\partial \tau_{(123)}}, \qquad (7.54)$$

where  $\rho = \sum_{i=0,1,2,4} \rho_i \, dX_i$  and  $\partial X_i/\partial \tau_{(123)} = \mathcal{J}_{i\tau_{(123)}}^{-1}$ . Inserting this solution for  $u_{13,6}$  into the ansatz eq. (7.50) for the transformation, we obtain an  $\varepsilon$ -form basis for the eyeball  $\mathbf{J}_{4,1} = \mathbf{U}_{4,1}^{(3)} \cdot \mathbf{J}_{4,1}^{(2)}$ . It satisfies the differential equation

$$d\mathbf{J}_{4,1} = \varepsilon \ \mathbf{B}_{4,1} \cdot \mathbf{J}_{4,1} \quad \text{where} \quad \mathbf{B}_{4,1} = \mathbf{U}_{4,1}^{(3)} \cdot \mathbf{B}_{4,1}^{(2,1)} \cdot \left(\mathbf{U}_{4,1}^{(3)}\right)^{-1}, \tag{7.55}$$

since  $d\mathbf{U}_{4,1}^{(3)} \cdot \left(\mathbf{U}_{4,1}^{(3)}\right)^{-1} + \mathbf{U}_{4,1}^{(3)} \cdot \mathbf{B}_{4,1}^{(2,0)} \cdot \left(\mathbf{U}_{4,1}^{(3)}\right)^{-1} = 0$  by construction.

All other eyeball-subtopologies can be transformed in an analogous way.

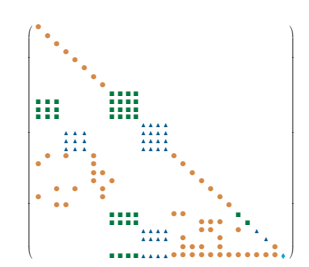
# 7.2.3 Full Kite Family

Our starting point is the initial differential equation of eq. (7.16) with the structure of the connection matrix in eq. (7.17). Note the two elliptic curves are completely decoupled from one another in all but the (30, 30)-entry, i.e. the top sector of the kite. Before we proceed with a step-by-step transformation of the differential equation to canonical form, we shortly discuss the kinematic space on the tori.

### Four Punctures on Each Torus

In Subsection 7.2.2, we explained how to derive coordinates for the kinematic space of an eyeball subtopology on its respective torus. These coordinates always consist of the torus period, two punctures associated to the respective sunrise subtopology and one *additional* puncture. Since there are two eyeballs associated to each torus, we have overall *two* such additional punctures on each torus and they are defined

Structure of the initial differential equation for the full kite integral family



in eq. (7.21). That means we already have five independent coordinates on each of the tori and we can express the kite's full kinematic space  $\mathcal{K}_{\rightarrow}$  in each of these:

We denote the moduli spaces defined in that way by  $\mathcal{M}_{1,5}^{(123)}$  and  $\mathcal{M}_{1,5}^{(345)}$ . Since there is a clear splitting of the entries of the differential equation in ones naturally associated to the (123)-torus (the entries  $\blacksquare$  in eq. (7.17)), ones naturally associated to the (345)-torus (the entries  $\triangle$  in eq. (7.17)) and ones naturally associated to neither or both tori (the entries  $\bullet$  and  $\diamond$  in eq. (7.17)), there is a natural prescription which torus and torus coordinates to work with for each entry. Entries associated to neither or both tori can of course be expressed on both tori equally. Besides this practical discussion on which torus and coordinates to use, we also want to use this paragraph to make some more comments on how one can obtain the additional punctures. We saw that the sunrise punctures can be obtained as a limit of the eyeball punctures – i.e., from the maximal cut of asupertopology. But of course, there is still a topology above the eyeballs: the full kite. A natural question is whether we could have obtained the punctures from the kite's maximal cut – which would be natural from the arguments we gave for our previous approach. To answer these questions, the most natural thing to do is to integrate the maximal cut of the kite, which takes the form  $MC(I_{11111}) = \frac{1}{\lambda_{01245}}$ , with respect to the variables exclusive to one elliptic curve

$$\int \frac{dX_i dX_j}{\lambda_{01245}} \text{ where } i, j \in \{1, 2\} \text{ or } i, j \in \{4, 5\} \text{ with } i \neq j.$$
 (7.58)

For example, suppose that we take i = 4 and j = 5. Then,

$$\int \frac{dX_4 dX_5}{\lambda_{01245}} = \int dX_4 \frac{2 \text{ MC}(I_{1,1,1,1,0})_{\varepsilon \mapsto 0}^{-1}}{X_0} \operatorname{arctanh} \left( Q \text{ MC}(I_{1,1,1,0})_{\varepsilon \mapsto 0}^{-1} \right), 
= \int dX_4 \frac{i \text{ MC}(I_{1,1,1,1,0})_{\varepsilon \mapsto 0}^{-1}}{X_0} \log \frac{Q + i \text{MC}(I_{1,1,1,1,0})_{\varepsilon \mapsto 0}^{-1}}{Q - i \text{MC}(I_{1,1,1,1,0})_{\varepsilon \mapsto 0}^{-1}},$$
(7.59)

where  $MC(I_{1,1,1,1,0})_{\varepsilon \mapsto 0}^{-1} = \sqrt{\lambda_{314}} \sqrt{\lambda_{024}}$  and

$$Q = X_0(1 - X_1 + X_4) + X_2(X_1 + X_4 - 1) + X_4(X_1 - X_4 - 2X_5 + 1).$$

At this point, the integrand in  $X_4$  is highly non-trivial: It takes the form of the Feynman parametric representation of the sunrise integral in 2-dimensions [276]. But, we already know that we can also obtain the new punctures in the eyeball subtopology. We can get to the subtopology by taking the  $X_5 \to \infty$  limit. In this limit,  $\log(\cdots) \to i\pi$  and we recover the integral (7.35) up to an overall factor. This remaining integral then gives us the new puncture from the (1234)-eyeball. So we see that we can indeed obtain the punctures also from a double integral of the full kite, but we need to consider the structure of the tori and take a limit to the subtopology where the new puncture would first appear.

<sup>9</sup>It would be interesting to also consider other examples for Feynman integrals with many parameters and see what kind of pattern one can observe there.

#### The Transformation to Canonical Form

As for the eyeball subtopology we obtain the transformation step by step.

1: The Sunrise Blocks As a first step, we apply the transformations to canonical form for both sunrise subtopologies, i.e., for the  $16 \times 16$  block in the upper left corner of the connection matrix:

$$\mathbf{U}^{(1)} = \operatorname{diag}(\varepsilon^2 \times \mathbb{1}_{8\times 8}, \mathbf{U}_{4\times 4}^{(123)}, \mathbf{U}_{4\times 4}^{(345)}, \varepsilon^2 \times \mathbb{1}_{14\times 14}). \tag{7.60}$$

Then, we define

$$\mathbf{J}^{(1)} = \mathbf{U}^{(1)} \cdot \mathbf{I} \quad \text{such that} \quad \mathbf{B}^{(1)} = d\mathbf{U}^{(1)} \cdot \left(\mathbf{U}^{(1)}\right)^{-1} + \mathbf{U}^{(1)} \cdot \mathbf{A} \cdot \left(\mathbf{U}^{(1)}\right)^{-1} \ . \quad (7.61)$$

Note that at this point:

$$\mathbf{B}^{(1)} = \mathbf{B}^{(1,0)} + \varepsilon \mathbf{B}^{(1,1)}. \tag{7.62}$$

2: The Diagonal Entries Again, the next step is to bring the diagonal entries below the  $16 \times 16$  block in canonical form. We do so by normalising with factors  $u_{ii}$  that can be obtained by solving homogeneous differential equations of the form

$$d\log u_{ii} = -\lim_{\varepsilon \to 0} \left( B^{(1)} \right)_{ii}. \tag{7.63}$$

as in eq. (7.45). In doing so, we obtain a transformation matrix of the form

$$\mathbf{U}^{(2)} = \text{diag}(\mathbb{1}_{1 \times 16}, \mathbf{u}_2), \qquad (7.64)$$

where

$$\mathbf{u}_{2} = \mathrm{MC}^{-1} \Big( \mathbf{I}_{1,0,1,1,0}, \mathbf{I}_{1,1,0,1,0}, \mathbf{I}_{1,0,0,1,1}, \mathbf{I}_{0,1,0,1,1}, \mathbf{I}_{0,1,1,0,1}, \mathbf{I}_{1,1,0,0,1}, \mathbf{I}_{1,0,1,0,1}, \mathbf{I}_{0,1,1,1,0}, \\ I_{1,1,1,1,0}, I_{1,1,1,0,1}, I_{0,1,1,1,1}, I_{1,0,1,1,1}, I_{1,1,0,1,1}, I_{1,1,1,1,1} \Big) |_{\varepsilon \to 0}, \\ = \Big( \sqrt{\lambda_{134}}, \sqrt{\lambda_{024}}, \sqrt{\lambda_{015}}, \sqrt{\lambda_{024}}, \sqrt{\lambda_{235}}, \sqrt{\lambda_{015}}, \sqrt{\lambda_{015}}, \sqrt{\lambda_{024}}, \sqrt{\lambda_{134}}, (7.65), \sqrt{\lambda_{024}}, \sqrt{\lambda_{134}}, \sqrt{\lambda_{015}}, \sqrt{\lambda_{024}}, \sqrt{\lambda_{015}}, \lambda_{01245} \Big).$$

We recall that  $\lambda_{ijk}$  is the Källen function and

$$\lambda_{01245} = X_1^2 X_2 + X_1 X_2^2 - X_1 X_2 - X_0 X_1 X_2 - X_4 X_1 X_2 - X_5 X_1 X_2 + X_4^2 X_5$$

$$+ X_5^2 X_4 - X_4 X_5 - X_0 X_4 X_5 - X_1 X_4 X_5 - X_2 X_4 X_5 + X_0^2 + X_0 - X_1 X_0$$

$$- X_2 X_0 - X_4 X_0 - X_5 X_0 + X_1 X_4 + X_0 X_1 X_5 + X_2 X_5 + X_0 X_2 X_4 .$$

$$(7.66)$$

After this transformation we obtain the basis  $\mathbf{J}^{(2)} = \mathbf{U}^{(2)} \cdot \mathbf{J}^{(1)}$  such that  $\mathbf{B}^{(2)} = d\mathbf{U}^{(2)} \cdot \left(\mathbf{U}^{(2)}\right)^{-1} + \mathbf{U}^{(2)} \cdot \mathbf{B}^{(1)} \cdot \left(\mathbf{U}^{(2)}\right)^{-1}$ . The connection matrix  $\mathbf{B}^{(2)}$  still has both an  $\mathcal{O}(\varepsilon^0)$  and an  $\mathcal{O}(\varepsilon)$  part:

$$\mathbf{B}^{(2)} = \mathbf{B}^{(2,0)} + \varepsilon \mathbf{B}^{(2,1)} \tag{7.67}$$

We depict the entries of eq. (7.16) after the first—transformation. The light entries are already in  $\varepsilon$ -form, the remaining entries need to be brought to  $\varepsilon$ -form in the subsequent steps:



We depict the entries of eq. (7.16) after the second transformation. The light entries are already in  $\varepsilon$ -form, the remaining entries need to be brought to  $\varepsilon$ -form in the subsequent steps:



but  $\mathbf{B}^{(2,0)}$  is now strictly lower-triangular. Next, we transform the off-diagonal entries to canonical form. We do so in two steps: In the first step, we remove the  $\varepsilon^0$  terms of the kite-eye ball entries. At the same time, this transformation makes the  $\mathbf{B}^{(2,0)}$  part of the connection matrix integrable. After that, we remove the remaining off-diagonal terms that are related to the sunrises and thus defined on the tori with the same approach we used for the eyeball's off-diagonal terms.

3: Off-diagonal Eveball-Kite Entries In the first step, we want to find a gauge transformation, that removes the  $\varepsilon^0$  terms of the (30, 25), (30, 26), (30, 27), (30, 28)entries and enforces  $\mathbf{B}^{(3,0)} \wedge \mathbf{B}^{(3,0)} = 0$ , so that the closure of  $\mathbf{B}^{(3,0)}$  is guaranteed. Given that  $d(\mathbf{B}^{(2,0)})_{30,i} \neq 0$  only for i = 9, 13, we use the following ansatz:

$$\mathbf{U}^{(3)} = \mathbb{1}_{30\times30} + \begin{pmatrix} \mathbf{0}_{29\times30} \\ (\mathbf{U}^{(3)})_{1\times30} \end{pmatrix} \quad \text{with} \quad \mathbf{U}^{(3)} = \begin{pmatrix} \mathbf{0}_{1\times24}, (\tilde{\mathbf{u}}_3)_{1\times4}, \mathbf{0}_{1\times2} \end{pmatrix}, (7.68)$$

and require that it fulfills:

$$du_j + (\mathbf{B}^{(2,0)})_{30,j} = 0$$
 for  $j = 25, 26, 27, 28$ . (7.69)

Solving these differential equations, we obtain:

$$(\tilde{\mathbf{u}}_3)_{1\times 4} = \frac{1}{2} \left( \frac{\Lambda_{01245}}{\sqrt{\lambda_{134}} \sqrt{\lambda_{024}}}, \frac{\Lambda_{02154}}{\sqrt{\lambda_{235}} \sqrt{\lambda_{015}}}, \frac{\Lambda_{05421}}{\sqrt{\lambda_{235}} \sqrt{\lambda_{015}}}, \frac{\Lambda_{04512}}{\sqrt{\lambda_{134}} \sqrt{\lambda_{015}}} \right), \tag{7.70}$$

where 
$$\Lambda_{abcde} = -X_d^2 - X_a X_b + X_a X_d + X_b X_c + X_b X_d + X_c X_d - 2X_d X_e + X_a - X_c + X_d$$
. Setting  $\mathbf{J}^{(3)} = \mathbf{U}^{(3)} \cdot \mathbf{J}^{(2)}$  we find  $\mathbf{B}^{(3)} = \mathrm{d}\mathbf{U}^{(3)} \cdot \left(\mathbf{U}^{(3)}\right)^{-1} + \mathbf{U}^{(3)} \cdot \mathbf{B}^{(2)} \cdot \left(\mathbf{U}^{(3)}\right)^{-1}$ .

4: Kite-Double-Bubble Entry The only remaining non-canonical entry that is a rational function of the  $X_i$  and does not contain periods  $\omega_1$  and their derivatives  $\partial_0 \omega_1$  is the entry  $B_{30,29}$ . The component  $(B^{(3,0)})_{30,29}$  describes how the differential of the kite couples to the (normalised) double-bubble integral  $I_{1,1,0,1,1}$ , which fully decouples from both sunrises. We can gauge away its  $\varepsilon^0$  component by a simple transformation that takes the form  $\mathbf{U}^{(4)} = \mathbb{1}_{30\times 30} + \tilde{\mathbf{U}}^{(4)}$  where the only non-zero component of  $\mathbf{U}^{(4)}$  is

$$\tilde{U}_{30,29}^{(4)} = \frac{-X_0^2 + X_1 X_0 + X_2 X_0 + X_4 X_0 + X_5 X_0 - 2X_0 + X_1 X_2 - X_1 X_4 - X_2 X_5 + X_4 X_5}{2\sqrt{\lambda_{024}}\sqrt{\lambda_{015}}}.$$
(7.71)

Setting 
$$\mathbf{J}^{(4)} = \mathbf{U}^{(4)} \cdot \mathbf{J}^{(3)}$$
, we have  $\mathbf{B}^{(4)} = d\mathbf{U}^{(4)} \cdot \left(\mathbf{U}^{(4)}\right)^{-1} + \mathbf{U}^{(4)} \cdot \mathbf{B}^{(3)} \cdot \left(\mathbf{U}^{(4)}\right)^{-1}$ .

5: Kite/Eveball-Sunrise Entries The only non-zero entries of  $\mathbf{B}^{(4,0)}$  are

(1345)- and (2345)-eyeball/(345)-sunrise:

(1234)- and (1235)-eyeball/(123)-sunrise: 
$$B_{25,9}^{(4,0)}$$
,  $B_{26,9}^{(4,0)}$ , (7.72a)  
(1345)- and (2345)-eyeball/(345)-sunrise:  $B_{27,13}^{(4,0)}$ ,  $B_{28,13}^{(4,0)}$ , (7.72b)

$$B_{27,13}^{(4,0)}, B_{28,13}^{(4,0)},$$
 (7.72b)

We depict the entries of eq. (7.16) after the third transformation. The light entries are already in  $\varepsilon$ -form, the remaining entries need to be brought to  $\varepsilon$ form in the subsequent steps:



We depict the entries of eq. (7.16) after the fourth transformation. The light entries are already in  $\varepsilon$ -form, the remaining entries need to be brought to  $\varepsilon$ form in the subsequent steps:



kite/(123)-sunrise: 
$$B_{30.9}^{(4,0)}$$
, (7.72c)

kite/(345)-sunrise: 
$$B_{30,13}^{(4,0)}$$
. (7.72d)

These entries take the form

$$B_{i,j}^{(3,0)} = \psi_1^{(123)} \ \sigma_{i,j}^{(123)} + \partial_0 \psi_1^{(123)} \ \rho_{i,j}^{(123)} \quad \text{for} \quad (i,j) \in \{(25,9), (26,9), (30,9)\},$$

$$(7.73a)$$

$$B_{i,j}^{(3,0)} = \psi_1^{(345)} \ \sigma_{i,j}^{(345)} + \partial_0 \psi_1^{(345)} \ \rho_{i,j}^{(345)} \quad \text{for} \quad (i,j) \in \{(27,13), (28,13), (30,13)\},$$

$$(7.73b)$$

where  $\sigma_{ij}^{(a)}$  and  $\rho_{ij}^{(a)}$  are differential one-forms in the kinematic variables  $X_a$ . To gauge away these entries, we make the ansatz  $\mathbf{U}^{(5)} = \mathbbm{1}_{30\times 30} + \tilde{\mathbf{U}}^{(5)}$  where the only non-zero components of  $\tilde{\mathbf{U}}^{(5)}$  are

$$\tilde{U}_{25,9}^{(5)}, \tilde{U}_{26,9}^{(5)}, \tilde{U}_{27,13}^{(5)}, \tilde{U}_{28,13}^{(5)}, \tilde{U}_{30,9}^{(5)}$$
 and  $\tilde{U}_{30,13}^{(5)}$ . (7.74)

Then, requiring that

$$d\tilde{U}_{i,j}^{(5)} + B_{i,j}^{(4,0)} = 0, (7.75)$$

ensures that  $\mathbf{B}^{(5)} = d\mathbf{U}^{(5)} \cdot (\mathbf{U}^{(5)})^{-1} + \mathbf{U}^{(5)} \cdot \mathbf{B}^{(4)} \cdot (\mathbf{U}^{(5)})^{-1}$  is in  $\varepsilon$ -form.

To obtain the entries to remove the kite/eyeball terms at  $\mathcal{O}(\varepsilon^0)$  in  $\mathbf{B}^{(4,0)}$ , we solve the differential equations

$$d\tilde{U}_{i,j}^{(4)} + B_{i,j}^{(3,0)} = 0 \quad \text{for} \quad (i,j) = (25,9), (26,9), (27,13), (28,13). \tag{7.76}$$

The entry (25,9) is the analogue of the (13,6) entry we discussed for the isolated (1234)-eyeball subtopology and we can remove it in the same way as well as treat the equivalent entries of the other three eyeballs similarly. That means we find the entries:

$$\tilde{U}_{25,9}^{(4)} = -\psi_1^{(123)} \frac{\partial \tau^{(123)}}{\partial X_0} \sum_i \left( \rho_{25,9}^{(123)} \right)_i \frac{\partial X_i}{\partial \tau^{(123)}}, \tag{7.77a}$$

$$\tilde{U}_{26,9}^{(4)} = -\psi_1^{(123)} \frac{\partial \tau^{(123)}}{\partial X_0} \sum_i \left( \rho_{26,9}^{(123)} \right)_i \frac{\partial X_i}{\partial \tau^{(123)}}, \tag{7.77b}$$

$$\tilde{U}_{27,13}^{(4)} = -\psi_1^{(345)} \frac{\partial \tau^{(345)}}{\partial X_0} \sum_i \left( \rho_{27,13}^{(345)} \right)_i \frac{\partial X_i}{\partial \tau^{(345)}}, \tag{7.77c}$$

$$\tilde{U}_{28,13}^{(4)} = -\psi_1^{(345)} \frac{\partial \tau^{(345)}}{\partial X_0} \sum_i \left( \rho_{28,13}^{(345)} \right)_i \frac{\partial X_i}{\partial \tau^{(345)}}, \tag{7.77d}$$

where i = 0, 1, 2, 4, 5 in the sums above and  $(\rho_{p,q}^{\alpha})_i$  is the  $dX_i$  component of  $\rho_{p,q}^{\alpha}$ . The derivatives of the kinematic parameters with respect to the moduli are computed from the inverses of the Jacobians

$$\mathcal{J}_{ij}^{(123)} = \frac{\partial \zeta_j^{(123)}}{\partial X_i} \quad \text{and} \quad \mathcal{J}_{ij}^{(345)} = \frac{\partial \zeta_j^{(345)}}{\partial X_i},$$
(7.78)

where  $\boldsymbol{\zeta}^{(123)} = \{\tau_{(123)}, z_{i=1,2}^{(123)}, z_{i=4,5}^{(123)}\}$ ,  $\boldsymbol{\zeta}^{(345)} = \{\tau_{(345)}, z_{i=1,2}^{(345)}, z_{i=4,5}^{(345)}\}$ . Note that at this point we explicitly needed all of the punctures on each torus that we derived before. As a consistency check, one can verify that the expressions in eq. (7.77) for the gauge transformations are numerically identical to the integrals.

$$\int_0^{X_4} dX_4' \left( B_{i,j}^{(3,0)} \right)_4 \quad \text{or} \quad \int_0^{X_5} dX_5' \left( B_{i,j}^{(3,0)} \right)_5, \tag{7.79}$$

where  $(B_{i,j}^{(3,0)})_a$  is the  $dX_a$  component of  $B_{i,j}^{(3,0)}$ . We can obtain the remaining two entries in the ansatz for the final transformation in the same way, namely as:

$$\tilde{U}_{30,9}^{(4)} = -\psi_1^{(123)} \frac{\partial \tau^{(123)}}{\partial X_0} \sum_i \left( \rho_{30,9}^{(123)} \right)_i \frac{\partial X_i}{\partial \tau^{(123)}}, \tag{7.80a}$$

$$\tilde{U}_{30,13}^{(4)} = -\psi_1^{(345)} \frac{\partial \tau^{(345)}}{\partial X_0} \sum_i \left( \rho_{30,13}^{(345)} \right)_i \frac{\partial X_i}{\partial \tau^{(345)}}. \tag{7.80b}$$

**Full Transformation** Finally, we apply all transformations

$$\mathbf{U} = \mathbf{U}^{(4)} \cdot \mathbf{U}^{(3)} \cdot \mathbf{U}^{(2)} \cdot \mathbf{U}^{(1)}, \tag{7.81}$$

to obtain an  $\varepsilon$ -form differential equation

$$d\mathbf{J} = \varepsilon \mathbf{B} \cdot \mathbf{J}$$
 with  $\mathbf{J} = \mathbf{U} \cdot \mathbf{I}$  and  $\mathbf{B} = d\mathbf{U} \cdot \mathbf{U}^{-1} + \mathbf{U} \cdot \mathbf{A} \cdot \mathbf{U}^{-1}$ . (7.82)

Both **U** and **B** are provided in a MATHEMATICA format in the ancillary file accompanying the paper [50].

## 7.3 Pullback on the Tori

After performing the transformation as detailed in the preceding sections, the differential equation is in  $\varepsilon$ -form and the  $\varepsilon$ -independent part of the connection matrix **B** contains only the following objects:

$$\left\{ X_{i}, \omega_{1}^{(123)}, \omega_{1}^{(345)}, \frac{\partial \omega_{1}^{(123)}}{\partial X_{0}}, \frac{\partial \omega_{1}^{(345)}}{\partial X_{0}}, \frac{\partial X_{i}}{\partial \tau_{(123)}}, \frac{\partial X_{i}}{\partial \tau_{(345)}} \right\}.$$
 (7.83)

The objects related to the tori were introduced throughout the transformation. Whilst we could easily check, that the connection is in  $\varepsilon$ -form (for example numerically), we know that the *canonical* form should have properties that go beyond just being  $\varepsilon$ -factorised. In particular, we show that when we express the connection matrix on the two tori, we can write every entry in quasi-modular forms as well as the modular forms  $\eta_2$ ,  $\eta_4$  of eq. (3.86). Then, we can show, that our result is also in C-form, as a further example for the discussion in Section 5.2.1.

#### Algorithmic Pullback 7.3.1

To determine the expansion of a given entry of **B** in terms of (quasi-)modular forms we use the following bootstrap algorithm:

- 1. Choose which torus to express  $B_{ij}$  on.
- 2. Use the modular properties of the entry  $B_{ij}$  to establish the modular weight of the differential forms that are allowed to appear. We assume all appearing forms to be Kronecker-Eisenstein and modular forms.
- 3. Make an ansatz of Kronecker- and  $\eta$  forms with a finite set of arguments in their z-variable. This set of arguments is determined beforehand by analysing the pole structure (of the diagonal entries).
- 4. Determine the coefficients in the ansatz numerically  $^{10}$ , assuming they lie in  $^{10}$ This can be done, e.g.,  $\mathbb{O} + i\mathbb{O}$ .

using Mathematica's FindIntegerNullVector[

Below we give details of the steps in this procedure.

#### 1. Choosing a torus

To choose which torus to work on for a given entry, we can follow a simple rule (that is basically already spelled out by the colour-coding in eq. (7.17)): If the entry couples to any of the sunrises (i.e., if it belongs to either the ■- or ▲-blocks in the matrix in eq. (7.17)), then we consider its pullback on  $\mathcal{M}_{1,5}^{(123)}$  or  $\mathcal{M}_{1,5}^{(345)}$ respectively. If the entry either couples to none of the sunrises (the entries • in the matrix in eq. (7.17)) or to both (the entry  $\bullet$  in the matrix in eq. (7.17)), it is a d log form and we can express it on either torus. Thus, for these entries we are in principle free to choose which torus to work on. But, we want to avoid that objects defined on  $\mathcal{M}_{1,5}^{(123)}$  and  $\mathcal{M}_{1,5}^{(345)}$  couple in the differential equation solution at a given order in  $\varepsilon$ . So we always choose them such that the iterated integrals are over only one torus order by order and entry by entry.

#### 2. Determining Forms

The modular transformation behaviour of the forms  $\omega_k$  can be derived from the behaviour of the g-kernels which we gave in eq. (3.173): The  $\omega_k$  transform as a quasi-modular form of weight k. On the other hand, we can compute the behaviour of an entry  $B_{ij}$  under a modular transformation – which is simple as it contains only the building blocks from eq. (7.83) whose modular transformation behaviour we know – and determine its quasi-modular weight.

Then we assume that the entry must be a  $(\mathbb{Q}+i\mathbb{Q})$ -linear combination of quasimodular forms of this weight and modular forms  $\eta_i$  of at most this weight. To make an ansatz for this linear combination, we need to determine, which z-arguments can appear and we do this in step three. As an example, for the modular weights, we display here the weights of the kite row (30), commenting also on the choice of torus:

Quasi-modular weights of the kite row The entries in the kite row have the following modular structure

The entries denoted by  $\cdot$  vanish, the ones labelled by dl are d log forms in the kinematic variables and the ones labelled with numbers are quasi-modular forms with the quasi-modular weight<sup>11</sup> indicated by the number. The colour indicates which torus we pull the entry back to, with (123) and (345) as before. The d log entries can be pulled back on either torus and the colour indicated here corresponds to the choice for which we give the explicit expressions in eq. (7.106). Though other choices might be more beneficial to avoid mixing of the tori when computing a specific  $\varepsilon$  order for some entry as mentioned before.

<sup>11</sup>Note that we use the definition of weight from definition 3.29 here.

### 3. All poles from the diagonal $d \log terms$

We observe that all poles of the matrix **B** can be determined by considering a smaller subset of matrix entries, namely the diagonal entries. More specifically, since we already know the poles appearing in the sunrise subtopologies from [92], we just need to consider the diagonal entries  $B_{ii}$  for  $i \in \{17, ..., 30\}$ . All of these are d log forms

$$d \log \left( d \frac{A_{i_1} \dots A_{i_n}}{A_{j_1} \dots A_{j_n}} \right) = d \log A_{i_1} + \dots + d \log A_{i_n} - d \log A_{j_1} - \dots - d \log A_{j_n}.$$
 (7.85)

Initially the arguments  $A_{i_j}$  are given in the kinematic coordinates  $X_i$ , which we can write in the torus coordinates  $\tau_{\alpha}, z_i^{\alpha}$  on the respective torus. At the same time, the diagonal d log forms are modular invariant objects that pull back to specific linear combinations of  $\omega_{\rm EK}^{(2)}(z,\tau)$ , often in a combination of the form

$$\Omega_{\rm EK}^{(2)}(z,\tau) = \omega_{\rm EK}^{(2)}(z,\tau) - 2\omega_{\rm EK}^{(2)}(z,2\tau).$$
(7.86)

The forms  $\omega_{\rm EK}^{(2)}(z,\tau_{\alpha})$  have the following  $q_{\alpha}$ -expansion:

$$\omega_{\text{EK}}^{(2)}(z, \tau_{\alpha}) = d \log \frac{\theta_1(\pi z, \tau_{\alpha})}{\eta(\tau_{\alpha})} = d \log \sin(\pi z) + \mathcal{O}(q^2), \qquad (7.87)$$

where  $\eta(\tau)$  is the Dedekind eta function.<sup>12</sup> Thus, any linear combination of  $\omega_0$ 's at leading order in  $q_{\alpha}$  take the form

$$\sum_{j} c_{j} \,\omega_{\text{EK}}^{(2)}(f_{j}(\boldsymbol{z}), \tau_{\alpha}) = d\log\left(\prod_{j} \sin^{c_{j}} \pi f_{j}(\boldsymbol{z})\right) + \mathcal{O}(q_{\alpha}^{2}), \qquad (7.88)$$

where  $c_j \in \mathbb{Q} + i\mathbb{Q}$ . Now, we can read off the appearing z-arguments by directly comparing eq. (7.85) and eq. (7.88): Each algebraic function  $A_i$  in eq. (7.85) can be expanded in  $q_{\alpha}$ . Then, expressing the leading-order terms of these expansions as the d log of a product of sines gives an efficient way of reading off the z-arguments  $f_j(z)$  appearing in (7.88). In the following we give examples for this procedure, again working our way up from the sunrise subtopologies to the eyeballs and then the full kite and we also comment on the relation of the singularities we find to the Landau singularities in kinematic space.

<sup>12</sup>From the *q*-expansion one can see that  $\omega_{\text{EK}}^{(2)}(z, \tau_{\alpha})$  diverges at z = 0

The (123)-sunrise subtopology Even thought the procedure above does not exactly apply to the sunrise, as its top sector is elliptic, and we specifically stated that we get the singularities of the sunrise from [92], those can also be deduced in a very similar way, which at the same time serves as a connection to the Landau singularities in kinematic parameters.

Instead of considering the top sector's d log forms as we do for the kite and eyeball topologies, let us just consider the simple d log forms in the diagonal connection entries corresponding to the three master integrals of the (123)-sunrise that are not in the top sector:

$$\left(\mathbf{B}_{\Leftrightarrow}^{(123)}\right)_{11} = \mathrm{d}\log X_1 \tag{7.89}$$

$$\left(\mathbf{B}_{\oplus}^{(123)}\right)_{22} = \mathrm{d}\log X_2$$
 (7.90)

$$\left(\mathbf{B}_{\oplus}^{(123)}\right)_{33} = d\log X_1 + d\log X_2.$$
 (7.91)

Noting  $that^{13}$ 

$$q_{(123)} = \exp(i\pi\tau_{(123)}).$$

<sup>13</sup>Here we use

$$X_1 = \sin^2(\pi z_1^{(123)}) \sin^{-2}(\pi (z_1^{(123)} + z_2^{(123)})) + \mathcal{O}(q_{(123)}), \tag{7.92a}$$

$$X_2 = \sin^2(\pi z_2^{(123)}) \sin^{-2}(\pi(z_1^{(123)} + z_2^{(123)})) + \mathcal{O}(q_{(123)}), \tag{7.92b}$$

and comparing with the general expression of eq. (7.88), we can directly read off that the arguments  $z_1^{(123)}, z_2^{(123)}, z_1^{(123)} + z_2^{(123)}$  should appear. Recalling that  $z_3^{(123)} = 1 - z_1^{(123)} - z_2^{(123)} \simeq z_1^{(123)} + z_2^{(123)} \mod \Lambda_{(1,\tau)}$  we see that this already covers all appearing arguments by comparing with the results of [92]. We gather the *letters* in

$$\mathcal{L}_{\oplus}^{(123)} = \left\{ z_1^{(123)}, z_2^{(123)}, z_1^{(123)} + z_2^{(123)} \right\} . \tag{7.93}$$

Now we interpret this result in the context of Landau singularities, keeping the discussion rather short and referring to [50] for more detail. The sub-leading Landau singularities are given by  $X_{0,1,2}=0,\infty$ . For any of these points we find  $\tau_{(123)}\to i\infty$  due to eq. (7.11) and  $z_i^{(123)}\to 0$  due to the above discussion. Thus, we have rediscovered the sub-leading Landau singularities from the diagonal analysis. The first type Landau singularities of the sunrise graph are given by the set of all  $(\pm,\pm,\pm)$  as defined in eq. (7.37). One can still access them by considering similar limits of the  $k_{(123)}^2$  modulus. The analysis for the (345)-sunrise subtopology is equivalent and one obtains

$$\mathcal{L}_{\oplus}^{(345)} = \left\{ z_4^{(345)}, z_5^{(345)}, z_4^{(345)} + z_5^{(345)} \right\} . \tag{7.94}$$

The (1234)-Eyeball The independent building block – i.e., the  $B_{i,j}$  of eq. (7.85) – of the diagonal d log entries in the (1234)-eyeball's differential equation below the sunrise sector are

$$\{X_0, X_4, \lambda_{024}^K, \lambda_{314}^K\},$$
 (7.95)

where  $\lambda_{ijk}^K = \lambda_K(X_i, X_j, X_k)$  is defined below (7.46c). Upon changing to the (123)-torus variables and performing the  $q_{(123)}$  expansion, the leading order terms in  $q_{(123)}$  are  $^{14}$ 

<sup>&</sup>lt;sup>14</sup>In the following expression we omit the labels (123) for the punctures  $z_i$ .

$$d \log \left( X_{0}|_{q^{2}} \right) = d \log \left( \sin^{2} \left( \pi z^{(3)} \right) \sin^{2} \left( \pi z_{2} \right) \right), \tag{7.96a}$$

$$d \log \left( X_{4}|_{q^{0}} \right) = d \log d \frac{\sin \left( \frac{\pi}{2} (2z_{1} + z_{2} + z_{4}) \right) \sin \left( \frac{\pi}{2} (2z_{1} + z_{2} - z_{4}) \right) \sin^{2} \left( \pi z_{2} \right)}{\sin^{2} \left( \pi (z_{1} + z_{2}) \right) \sin \left( \frac{\pi}{2} (z_{2} + z_{4}) \right) \sin \left( \frac{\pi}{2} (z_{2} - z_{4}) \right)}, \tag{7.96b}$$

$$d \log \left( \lambda_{024}^{K}|_{q^{0}} \right) = d \log d \frac{\sin^{2} \left( \pi (z_{1} + z_{2}) \right) \sin^{2} \left( \frac{\pi}{2} (z_{2} + z_{4}) \right) \sin^{2} \left( \frac{\pi}{2} (z_{2} - z_{4}) \right)}{\sin^{2} \left( \pi (z_{1} + z_{2}) \right) \sin^{2} \left( \frac{\pi}{2} (z_{2} + z_{4}) \right) \sin^{2} \left( \frac{\pi}{2} (z_{2} - z_{4}) \right)}. \tag{7.96c}$$

$$d \log \left( \lambda_{134}^{K}|_{q^{0}} \right) = d \log d \frac{\sin^{2} \left( \pi (z_{1} + z_{2}) \right) \sin^{2} \left( \frac{\pi}{2} (z_{2} + z_{4}) \right) \sin^{2} \left( \frac{\pi}{2} (z_{2} - z_{4}) \right)}{\sin^{2} \left( \frac{\pi}{2} (z_{2} + z_{4}) \right) \sin^{2} \left( \frac{\pi}{2} (z_{2} - z_{4}) \right)}. \tag{7.96d}$$

<sup>15</sup>In the following expression we omit the labels (123) for the punctures  $z_i$ .

From the arguments of the sin functions in these expressions we can read off all letters for the (1234)-eyeball:  $^{15}$ 

$$\mathcal{L}_{(1234)}^{(123)} = \left\{ z_1, z_2, z_4, z_1 + z_2, \frac{z_2 + z_4}{2}, \frac{z_2 - z_4}{2}, z_1 + \frac{z_2 + z_4}{2}, z_1 + \frac{z_2 - z_4}{2} \right\}. \quad (7.97)$$

Note that this set contains also the set  $\mathcal{L}_{\oplus}^{(123)}$ . Similarly one can find the letters for the three other eyeballs,  $\mathcal{L}_{(1235)}^{(123)}$ ,  $\mathcal{L}_{(2345)}^{(345)}$  and  $\mathcal{L}_{(1345)}^{(345)}$ .

**The Kite** Since only the last line (30) of the differential equation **B** is not included in any of the eyeball subtopologies, the set of letters for the full kite can be obtained as

$$\mathcal{L}^{(123)} = \mathcal{L}^{(1234)}_{(1234)} \cup \mathcal{L}^{(1235)}_{(1235)} \cup \{\text{Letters from entry } (30,30) \text{ on } (123) - \text{torus}\}, (7.98)$$

$$\mathcal{L}^{(345)} = \mathcal{L}^{(345)}_{(2345)} \cup \mathcal{L}^{(345)}_{(1345)} \cup \{\text{Letters from entry } (30,30) \text{ on } (345) - \text{torus}\}.$$
 (7.99)

We made explicit that each entry can be expressed on either  $\mathcal{M}_{1,5}^{\alpha=(123),(345)}$  and that the eyeball letters all come from analysing the set of arguments

$$\{X_0, X_1, X_2, X_4, X_5, \lambda_{024}^K, \lambda_{314}^K, \lambda_{315}^K, \lambda_{325}^K\}.$$
 (7.100)

The additional argument in the (30, 30) entry takes the form  $\lambda_{01245}^{K}$ . We find that it introduces introduces four new Z-arguments. Overall, we find:

$$\begin{split} & \left\{ \mathcal{L}_{i}^{(123)} \right\}_{i=1}^{17} = & \left\{ z_{1}^{(123)}, z_{2}^{(123)}, z_{4}^{(123)}, z_{5}^{(123)}, z_{1}^{(123)} + z_{2}^{(123)}, z_{2}^{(123)} + z_{4}^{(123)}, \frac{z_{2}^{(123)} + z_{4}^{(123)}}{2}, \frac{z_{2}^{(123)} - z_{4}^{(123)}}{2}, \\ & z_{1}^{(123)} + \frac{z_{2}^{(123)} + z_{4}^{(123)}}{2}, z_{1}^{(123)} + \frac{z_{2}^{(123)} - z_{4}^{(123)}}{2}, \frac{z_{1}^{(123)} + z_{5}^{(123)}}{2}, \frac{z_{1}^{(123)} - z_{5}^{(123)}}{2}, \frac{z_{1}^{(123)} - z_{5}^{(123)}}{2}, \\ & z_{2}^{(123)} + \frac{z_{1}^{(123)} + z_{5}^{(123)}}{2}, z_{2}^{(123)} + \frac{z_{1}^{(123)} - z_{5}^{(123)}}{2}, \frac{z_{1}^{(123)} + z_{2}^{(123)} + z_{4}^{(123)} + z_{5}^{(123)}}{2}, \end{split}$$

$$\frac{z_{1}^{(123)} + z_{2}^{(123)} + z_{4}^{(123)} - z_{5}^{(123)}}{2}, \frac{z_{1}^{(123)} + z_{2}^{(123)} - z_{4}^{(123)} + z_{5}^{(123)}}{2}, \frac{z_{1}^{(123)} + z_{2}^{(123)} - z_{4}^{(123)} - z_{5}^{(123)}}{2} \right\},$$

$$\left\{ \mathcal{L}_{i}^{(345)} \right\}_{i=1}^{17} = \left\{ z_{4}^{(345)}, z_{5}^{(345)}, z_{1}^{(345)}, z_{2}^{(345)}, z_{2}^{(345)}, z_{4}^{(345)} + z_{5}^{(345)}, \frac{z_{5}^{(345)} + z_{1}^{(345)}}{2}, \frac{z_{5}^{(345)} - z_{1}^{(345)}}{2}, \\ z_{4}^{(345)} + \frac{z_{5}^{(345)} + z_{1}^{(345)}}{2}, z_{4}^{(345)} + \frac{z_{5}^{(345)} - z_{1}^{(345)}}{2}, \frac{z_{4}^{(345)} + z_{2}^{(345)} + z_{2}^{(345)}}{2}, \frac{z_{4}^{(345)} - z_{2}^{(345)}}{2}, \frac{z_{4}^{(345)} + z_{5}^{(345)} + z_{1}^{(345)} + z_{2}^{(345)}}{2}, \\ z_{2}^{(345)} + z_{5}^{(345)} + z_{1}^{(345)} - z_{2}^{(345)}, \frac{z_{4}^{(345)} - z_{2}^{(345)} + z_{5}^{(345)} + z_{5}^{(345)} + z_{1}^{(345)} + z_{2}^{(345)}}{2}, \frac{z_{4}^{(345)} + z_{5}^{(345)} + z_{5}^{(345)} + z_{5}^{(345)} - z_{1}^{(345)} - z_{2}^{(345)}}{2}, \\ z_{2}^{(345)} + z_{5}^{(345)} + z_{1}^{(345)} - z_{2}^{(345)}, \frac{z_{4}^{(345)} + z_{5}^{(345)} - z_{1}^{(345)} + z_{5}^{(345)} - z_{1}^{(345)} - z_{2}^{(345)}}{2}, \frac{z_{4}^{(345)} + z_{5}^{(345)} - z_{1}^{(345)} - z_{1$$

Having analysed the modular properties of each entry and found a complete set of letters on each torus, one can make an ansatz for each entry and determine the coefficients in  $\mathbb{Q} + i\mathbb{Q}$  numerically.

#### 4. Determining the linear combination numerically

We list below the results for the (1234)-eyeball line (25) as well as the kite line (30). The other entries can be found in the ancillary file accompanying the paper [50].

The (1234)-eyeball pullback—Ordered by modular weight, we obtain the following expressions for the entries of B in Kronecker-Eisenstein and modular forms: <sup>16</sup> Modular weight 1

$$B_{25,12}^{(123)} = 2\omega_{\text{EK}}^{(1)} \left(\mathcal{L}_3^{(123)}, \tau\right).$$
 (7.102)

<sup>16</sup>Note that we do not label the  $\tau$  here, as the choice of torus is already indicated by the z-argument  $\mathcal{L}^{\alpha}$  with  $\alpha \in \{(123), (345)\}.$ 

## Modular weight 2

$$B_{25,10}^{(123)} = \frac{1}{2} \left[ \omega_{\text{EK}}^{(2)} \left( \mathcal{L}_{6}^{(123)}, \tau \right) - \omega_{\text{EK}}^{(2)} \left( \mathcal{L}_{7}^{(123)}, \tau \right) + \omega_{\text{EK}}^{(2)} \left( \mathcal{L}_{8}^{(123)}, \tau \right) - \omega_{\text{EK}}^{(2)} \left( \mathcal{L}_{9}^{(123)}, \tau \right) \right],$$

$$(7.103a)$$

$$B_{25,11}^{(123)} = \frac{1}{2} \left[ 3\omega_{\text{EK}}^{(2)} \left( \mathcal{L}_{7}^{(123)}, \tau \right) - 3\omega_{\text{EK}}^{(2)} \left( \mathcal{L}_{6}^{(123)}, \tau \right) + \omega_{\text{EK}}^{(2)} \left( \mathcal{L}_{8}^{(123)}, \tau \right) - \omega_{\text{EK}}^{(2)} \left( \mathcal{L}_{9}^{(123)}, \tau \right) \right],$$

$$(7.103b)$$

$$B_{25,17}^{(123)} = \Omega_{\text{EK}}^{(2)} \left( \mathcal{L}_{6}^{(123)}, \tau \right) + \Omega_{\text{EK}}^{(2)} \left( \mathcal{L}_{7}^{(123)}, \tau \right) + \Omega_{\text{EK}}^{(2)} \left( \mathcal{L}_{8}^{(123)}, \tau \right) + \Omega_{\text{EK}}^{(2)} \left( \mathcal{L}_{9}^{(123)}, \tau \right),$$

$$(7.103c)$$

$$B_{25,18}^{(123)} = \Omega_{\text{EK}}^{(2)} \left( \mathcal{L}_{7}^{(123)}, \tau \right) - \Omega_{\text{EK}}^{(2)} \left( \mathcal{L}_{6}^{(123)}, \tau \right) - \Omega_{\text{EK}}^{(2)} \left( \mathcal{L}_{8}^{(123)}, \tau \right) + \Omega_{\text{EK}}^{(2)} \left( \mathcal{L}_{9}^{(123)}, \tau \right),$$

$$(7.103d)$$

$$B_{25,24} = -\Omega_{\text{EK}}^{(2)} \left( \mathcal{L}_{6}^{(123)}, \tau \right) + \Omega_{\text{EK}}^{(2)} \left( \mathcal{L}_{7}^{(123)}, \tau \right) + \Omega_{\text{EK}}^{(2)} \left( \mathcal{L}_{8}^{(123)}, \tau \right) - \Omega_{\text{EK}}^{(2)} \left( \mathcal{L}_{9}^{(123)}, \tau \right),$$

$$(7.103e)$$

$$B_{25,25}^{(123)} = -2\omega_{\text{EK}}^{(2)} \left( \mathcal{L}_{1}^{(123)}, 2\tau \right) - 2\omega_{\text{EK}}^{(2)} \left( \mathcal{L}_{2}^{(123)}, 2\tau \right) - 2\omega_{\text{EK}}^{(2)} \left( \mathcal{L}_{3}^{(123)}, \tau \right) - 4\omega_{\text{EK}}^{(2)} \left( \mathcal{L}_{5}^{(123)}, \tau \right)$$

$$+6\omega_{\rm EK}^{(2)}(\mathcal{L}_5^{(123)}, 2\tau) + 3\omega_{\rm EK}^{(2)}(\mathcal{L}_6^{(123)}, \tau) + 3\omega_{\rm EK}^{(2)}(\mathcal{L}_7^{(123)}, \tau) + \omega_{\rm EK}^{(2)}(\mathcal{L}_8^{(123)}, \tau) + \omega_{\rm EK}^{(2)}(\mathcal{L}_9^{(123)}, \tau) + 6\eta_2(\tau).$$

The mass-permutation symmetry of the eyeball graph indicates that  $B_{25,18}$  must satisfy the relation  $B_{25,18} = B_{25,24}|_{m_1 \leftrightarrow m_3}$ .

#### See also:

In Appendix C.2, we discuss symmetries of the punctures.

### Modular weight 3

$$B_{25,9}^{(123)} = 4\omega_{\text{EK}}^{(3)} \left(\mathcal{L}_{3}^{(123)}, \tau\right) - 12\omega_{\text{EK}}^{(3)} \left(\mathcal{L}_{6}^{(123)}, \tau\right) + 12\omega_{\text{EK}}^{(3)} \left(\mathcal{L}_{7}^{(123)}, \tau\right) - 4\omega_{\text{EK}}^{(3)} \left(\mathcal{L}_{8}^{(123)}, \tau\right) + 4\omega_{\text{EK}}^{(3)} \left(\mathcal{L}_{9}^{(123)}, \tau\right).$$

$$(7.104)$$

The kite pullback We have given the choice of torus and the corresponding modular weight of the entries in line (30) for which we give the explicit expressions here in eq. (7.84). We list them by modular weight again. We use the shorthand  $\tilde{B}_{i,j} = B_{i,j}^{(123)}|_{(123)\mapsto(345)}$ .

#### Modular weight 0

$$B_{30,12}^{(123)} = \omega_{\text{EK}}^{(1)} \left( \mathcal{L}_1^{(123)}, \tau \right) + \omega_{\text{EK}}^{(1)} \left( \mathcal{L}_2^{(123)}, \tau \right), \tag{7.105a}$$

$$B_{30,16}^{(345)} = \tilde{B}_{30,12} = \omega_{\text{EK}}^{(1)} \left( \mathcal{L}_1^{(345)}, \tau \right) + \omega_{\text{EK}}^{(1)} \left( \mathcal{L}_2^{(345)}, \tau \right). \tag{7.105b}$$

#### Modular weight 1

$$B_{30,10}^{(123)} = \frac{1}{4} \left[ \sum_{k=8,9,12,13} \omega_{\text{EK}}^{(2)} \left( \mathcal{L}_k^{(123)}, \tau \right) - \sum_{\ell=6,7,10,11} \omega_{\text{EK}}^{(2)} \left( \mathcal{L}_\ell^{(123)}, \tau \right) \right], \tag{7.106a}$$

$$B_{30,14}^{(345)} = \tilde{B}_{30,10} \,, \tag{7.106b}$$

$$B_{30,11}^{(123)} = \frac{1}{4} \left[ \sum_{k=8,9,10,11} \omega_{\text{EK}}^{(2)} \left( \mathcal{L}_k^{(123)}, \tau \right) - \sum_{\ell=6,7,12,13} \omega_{\text{EK}}^{(2)} \left( \mathcal{L}_\ell^{(123)}, \tau \right) \right], \tag{7.106c}$$

$$B_{30,15}^{(345)} = \tilde{B}_{30,11} \,,$$
 (7.106d)

$$B_{30,17}^{(123)} = \frac{1}{2} \left[ \Omega_{\text{EK}}^{(2)} \left( \mathcal{L}_6^{(123)}, \tau \right) - \Omega_{\text{EK}}^{(2)} \left( \mathcal{L}_7^{(123)}, \tau \right) + \Omega_{\text{EK}}^{(2)} \left( \mathcal{L}_8^{(123)}, \tau \right) - \Omega_{\text{EK}}^{(2)} \left( \mathcal{L}_9^{(123)}, \tau \right) \right], \tag{7.106e}$$

$$B_{30,18}^{(123)} = -\frac{1}{2} \left[ \Omega_{\rm EK}^{(2)} \left( \mathcal{L}_6^{(123)}, \tau \right) + \Omega_{\rm EK}^{(2)} \left( \mathcal{L}_7^{(123)}, \tau \right) + \Omega_{\rm EK}^{(2)} \left( \mathcal{L}_8^{(123)}, \tau \right) + \Omega_{\rm EK}^{(2)} \left( \mathcal{L}_9^{(123)}, \tau \right) \right], \tag{7.106f}$$

$$B_{30,19}^{(123)} = \Omega_{\text{EK}}^{(2)} \left( \mathcal{L}_{10}^{(123)}, \tau \right) + \Omega_{\text{EK}}^{(2)} \left( \mathcal{L}_{11}^{(123)}, \tau \right), \tag{7.106g}$$

$$B_{30,20}^{(123)} = \Omega_{\text{EK}}^{(2)} \left( \mathcal{L}_6^{(123)}, \tau \right) + \Omega_{\text{EK}}^{(2)} \left( \mathcal{L}_7^{(123)}, \tau \right), \tag{7.106h}$$

$$B_{30,21}^{(123)} = \frac{1}{2} \left[ \Omega_{\rm EK}^{(2)} \left( \mathcal{L}_{10}^{(123)}, \tau \right) - \Omega_{\rm EK}^{(2)} \left( \mathcal{L}_{11}^{(123)}, \tau \right) + \Omega_{\rm EK}^{(2)} \left( \mathcal{L}_{12}^{(123)}, \tau \right) - \Omega_{\rm EK}^{(2)} \left( \mathcal{L}_{13}^{(123)}, \tau \right) \right], \tag{7.106i}$$

$$\begin{split} B_{30,22}^{(123)} &= -\frac{1}{2} \Big[ \Omega_{\rm EK}^{(2)} \Big( \mathcal{L}_{10}^{(123)}, \tau \Big) + \Omega_{\rm EK}^{(2)} \Big( \mathcal{L}_{11}^{(123)}, \tau \Big) + \Omega_{\rm EK}^{(2)} \Big( \mathcal{L}_{12}^{(123)}, \tau \Big) + \Omega_{\rm EK}^{(2)} \Big( \mathcal{L}_{13}^{(123)}, \tau \Big) \Big] \,, \\ &(7.106i) \\ B_{30,23}^{(123)} &= \frac{1}{2} \Big[ \Omega_{\rm EK}^{(2)} \Big( \mathcal{L}_{12}^{(123)}, \tau \Big) + \Omega_{\rm EK}^{(2)} \Big( \mathcal{L}_{13}^{(123)}, \tau \Big) - \Omega_{\rm EK}^{(2)} \Big( \mathcal{L}_{10}^{(123)}, \tau \Big) - \Omega_{\rm EK}^{(2)} \Big( \mathcal{L}_{11}^{(123)}, \tau \Big) - \Omega_{\rm EK}^{(2)} \Big( \mathcal{L}_{11}^{(123)}, \tau \Big) - \Omega_{\rm EK}^{(2)} \Big( \mathcal{L}_{10}^{(123)}, \tau \Big) - \Omega_{\rm EK}^{(2)} \Big( \mathcal{L}_{11}^{(123)}, \tau \Big) \Big] \,, \\ &(7.106k) \\ B_{30,24}^{(123)} &= \frac{1}{2} \Big[ \Omega_{\rm EK}^{(2)} \Big( \mathcal{L}_{8}^{(123)}, \tau \Big) + \Omega_{\rm EK}^{(2)} \Big( \mathcal{L}_{9}^{(123)}, \tau \Big) - \Omega_{\rm EK}^{(2)} \Big( \mathcal{L}_{6}^{(123)}, \tau \Big) \Big] \,, \\ &(7.106h) \\ B_{30,25}^{(123)} &= \frac{1}{2} \Big[ \sum_{k=6,8,16,17} \omega_{\rm EK}^{(2)} \Big( \mathcal{L}_{k}^{(123)}, \tau \Big) - \sum_{\ell=7,9,14,15} \omega_{\rm EK}^{(2)} \Big( \mathcal{L}_{\ell}^{(123)}, \tau \Big) \Big] \,, \\ &(7.106n) \\ B_{30,26}^{(123)} &= \frac{1}{2} \Big[ \Omega_{\rm EK}^{(2)} \Big( \mathcal{L}_{14}^{(123)}, \tau \Big) - \Omega_{\rm EK}^{(2)} \Big( \mathcal{L}_{15}^{(123)}, \tau \Big) + \Omega_{\rm EK}^{(2)} \Big( \mathcal{L}_{\ell}^{(123)}, \tau \Big) \Big] \,, \\ &(7.106n) \\ B_{30,27}^{(123)} &= \frac{1}{2} \Big[ \Omega_{\rm EK}^{(2)} \Big( \mathcal{L}_{14}^{(123)}, \tau \Big) - \Omega_{\rm EK}^{(2)} \Big( \mathcal{L}_{15}^{(123)}, \tau \Big) + \Omega_{\rm EK}^{(2)} \Big( \mathcal{L}_{16}^{(123)}, \tau \Big) - \Omega_{\rm EK}^{(2)} \Big( \mathcal{L}_{17}^{(123)}, \tau \Big) \Big] \,, \\ &(7.106e) \\ B_{30,28}^{(123)} &= \frac{1}{2} \Big[ \Omega_{\rm EK}^{(2)} \Big( \mathcal{L}_{14}^{(123)}, \tau \Big) + \Omega_{\rm EK}^{(2)} \Big( \mathcal{L}_{15}^{(123)}, \tau \Big) - \Omega_{\rm EK}^{(2)} \Big( \mathcal{L}_{16}^{(123)}, \tau \Big) - \Omega_{\rm EK}^{(2)} \Big( \mathcal{L}_{17}^{(123)}, \tau \Big) \Big] \,, \\ &(7.106e) \\ B_{30,29}^{(123)} &= -\frac{1}{2} \Big[ \Omega_{\rm EK}^{(2)} \Big( \mathcal{L}_{14}^{(123)}, \tau \Big) - \Omega_{\rm EK}^{(2)} \Big( \mathcal{L}_{15}^{(123)}, \tau \Big) - \Omega_{\rm EK}^{(2)} \Big( \mathcal{L}_{16}^{(123)}, \tau \Big) - \Omega_{\rm EK}^{(2)} \Big( \mathcal{L}_{17}^{(123)}, \tau \Big) \Big] \,, \\ &(7.106e) \\ B_{30,30}^{(123)} &= -\frac{1}{2} \Big[ \Omega_{\rm EK}^{(2)} \Big( \mathcal{L}_{14}^{(123)}, \tau \Big) - \Omega_{\rm EK}^{(2)} \Big( \mathcal{L}_{15}^{(123)}, \tau \Big) - \Omega_{\rm EK}^{(2)} \Big( \mathcal{L}_{15}^{(123)}, \tau \Big) - \Omega_{\rm EK}^{(2)} \Big( \mathcal{L}_{17}^{(123)}, \tau \Big) - \Omega_{\rm EK}^{(2)} \Big( \mathcal{L}_{17}^{(123)}, \tau \Big)$$

#### Modular weight 2

$$B_{30,9}^{(123)} = 2\left[\sum_{\ell=14}^{17} \omega_{\text{EK}}^{(3)} \left(\mathcal{L}_{\ell}^{(123)}, \tau\right) - \sum_{\ell=5}^{13} \omega_{\text{EK}}^{(3)} \left(\mathcal{L}_{\ell}^{(123)}, \tau\right)\right], \tag{7.107a}$$

$$B_{30,13}^{(345)} = \tilde{B}_{30,9} \,. \tag{7.107b}$$

#### 7.3.2 Comments on the Forms

The the differential equation in eq. (7.82) provides another example for a differential equation in C-form as discussed in Section 5.2.1. In principle, the arguments for this claim rely on recognising, that the function space just consists of two copies of the sunrises's function space with additional letters. So, we start by discussing just the sunrise and then consider the extension to the full kite, highlighting specific features due to the relation to two tori.

**Example 7.1** (Unequal-mass sunrise integral). We first consider the (123)-sunrise integral and its canonical differential equation eq. (7.24) with connection matrix

 $\varepsilon \mathbf{B}_{\oplus}^{(123)}$ , following the example given in [226]. As discussed in [198, 321],  $\mathbf{B}_{\oplus}^{(123)}$  can be written in terms of Eisenstein-Kronecker forms  $\omega_{\mathrm{EK}}^{(k)}$  with z-arguments  $z=z_1^{(123)},z_2^{(123)},z_3^{(123)}=1-z_1^{(123)}-z_2^{(123)}\sim z_1^{(123)}+z_2^{(123)}$  as well as two modular forms  $\eta_2(\tau)\mathrm{d}\tau_{(123)},\eta_4(\tau)\mathrm{d}\tau_{(123)}$  for  $\Gamma_0(2)$  and  $\mathrm{SL}(2,\mathbb{Z})$ . These forms span the  $\mathbb{Q}[i\pi^{\pm}]$  vector space  $\mathbb{V}_{\oplus}^{(123)}$ , i.e.,

$$\mathbb{V}_{\oplus}^{(123)} = \left\langle \omega_{\text{EK}}^{(k)}(Z), \eta_2(\tau_{(123)}), \eta_4(\tau_{(123)}) \,|\, k = 1, 2, 3 \text{ and } Z \in \mathcal{L}_{\oplus}^{(123)} \right\rangle_{\mathbb{Q}[i\pi^{\pm}]} \quad (7.108)$$

Similarly, the  $\mathbb{Q}[i\pi^{\pm}]$ -algebra of functions can be defined as

$$\mathbb{A}_{\oplus}^{(123)} = \mathbb{Q}[i\pi^{\pm 1}] \otimes_{\mathbb{Q}} \mathrm{QM}(\Gamma_0(2)) \otimes_{\mathbb{Q}} \mathrm{G}_{\oplus}^{(123)}, \qquad (7.109)$$

where

$$G_{\oplus}^{(123)} = \left\langle \partial_Z^k g^{(m)}(Z, j \cdot \tau_{(123)}) \mid m \ge 0, k \ge 0 \text{ and } Z \in \mathcal{L}_{\oplus}^{(123)} \right\rangle_{\mathbb{O}}. \tag{7.110}$$

Note that the algebra's only constants are in  $\mathbb{Q}[i\pi^{\pm}]$  and it is differentially closed. Iterated integrals of the forms in  $\mathbb{V}_{\oplus}^{(123)}$  evaluate to elliptic polylogarithms and iterated integrals of modular forms. One can show that these are linearly independent over  $\mathcal{F}_{\oplus}^{(123)} = \operatorname{Frac}(\mathbb{C} \otimes_{\mathbb{Q}} \mathbb{A} \oplus^{(123)})$  (cf., e.g., refs. [314, 315, 322, 323]), from which it follows that  $\mathbb{V}_{\oplus}^{(123)} \cap d\mathcal{F}_{\oplus}^{(123)} = \{0\}$ . So the system is in C-form.

Since the sectors that we need to express on a specific torus ( $\blacksquare$  and  $\blacktriangle$ ) decouple from each other and only couple to themselves and the entries that can be written on either torus ( $\bullet$  and  $\blacklozenge$ ), one can iteratively express the one-forms such that upon evaluating the iterated integrals at each order in  $\varepsilon$  are only elliptic polylogarithms and integrals over modular forms related to the same torus. We can make the choice such that there are no iterated integrals over Kronecker-Eisenstein kernels related to different tori. Though this is a local choice and needs to be done separately for every integral and order. This allows us to easily extend the C-form discussion to the full kite integral family.

**Example 7.2** (The Kite Integral Family in C-form). The forms appearing in the connection matrix  $\bf B$  of the full kite integral family are the same as the ones in the (123) and (345) sunrise integral's connection matrices albeit with additional Z arguments and we can organise them in two vector spaces:

$$\mathbb{V}^{(123)} = \left\langle \omega_{\text{EK}}^{(k)}(Z), \eta_2(\tau_{(123)}), \eta_4(\tau_{(123)}) \mid k = 1, 2, 3 \text{ and } Z \in \mathcal{L}^{(123)} \right\rangle_{\mathbb{O}[i\pi^{\pm}]}$$
(7.111)

$$\mathbb{V}^{(345)} = \left\langle \omega_{\text{EK}}^{(k)}(Z), \eta_2(\tau_{(345)}), \eta_4(\tau_{(345)}) \mid k = 1, 2, 3 \text{ and } Z \in \mathcal{L}^{(345)} \right\rangle_{\mathbb{Q}[i\pi^{\pm}]}$$
(7.112)

Additionally, we define

$$\mathbb{V}_{-} = \mathbb{V}^{(123)} \oplus \mathbb{V}^{(345)}. \tag{7.113}$$

Similarly, we define the  $\mathbb{Q}[i\pi^{\pm}]$  algebras of functions:

$$\mathbb{A}^{(123)} = \mathbb{Q}[i\pi^{\pm 1}] \otimes_{\mathbb{Q}} \mathrm{QM}(\Gamma_0(2)) \otimes_{\mathbb{Q}} \mathrm{G}^{(123)}$$

$$(7.114)$$

$$\mathbb{A}^{(345)} = \mathbb{Q}[i\pi^{\pm 1}] \otimes_{\mathbb{Q}} \mathrm{QM}(\Gamma_0(2)) \otimes_{\mathbb{Q}} \mathrm{G}^{(123)}, \qquad (7.115)$$

where

$$G^{(123)} = \left\langle \partial_Z^k g^{(m)}(Z, j \cdot \tau_{(123)}) \mid m \ge 0, k \ge 0, j = 1, 2 \text{ and } Z \in \mathcal{L}^{(123)} \right\rangle_{\mathbb{Q}}$$
 (7.116)

$$G^{(345)} = \left\langle \partial_Z^k g^{(m)}(Z, j \cdot \tau_{(345)}) \mid m \ge 0, k \ge 0 \\ j = 1, 2 \text{ and } Z \in \mathcal{L}^{(345)} \right\rangle_{\mathbb{O}}. \quad (7.117)$$

Finally, we define

$$\mathbb{A}_{-\Phi} = \mathbb{Q}[i\pi^{\pm 1}] \otimes_{\mathbb{Q}} \mathrm{QM}(\Gamma_0(2)) \otimes_{\mathbb{Q}} \mathrm{G}^{(123)} \otimes_{\mathbb{Q}} \mathrm{G}^{(345)} \subseteq \mathbb{A}^{(123)} \oplus \mathbb{A}^{(345)}. \tag{7.118}$$

From this it follows immediately, that

This implies, that

$$\mathbb{V}_{-} \cap d\mathcal{F}_{-} \subseteq (\mathbb{V}^{(123)} \oplus \mathbb{V}^{(345)}) \cap (d\mathcal{F}_{(123)} \oplus d\mathcal{F}_{(345)})$$
 (7.120)

and the right-hand side of this can be decomposed into:

$$\left(\mathbb{V}^{(123)} \oplus \mathbb{V}^{(345)}\right) \cap \left(d\mathcal{F}_{(123)} \oplus d\mathcal{F}_{(345)}\right) =$$

$$\left(\mathbb{V}^{(123)} \cap d\mathcal{F}_{(123)}\right) \oplus \left(\mathbb{V}^{(123)} \cap d\mathcal{F}_{(345)}\right) \oplus \left(\mathbb{V}^{(345)} \cap d\mathcal{F}_{(123)}\right) \oplus \left(\mathbb{V}^{(345)} \cap d\mathcal{F}_{(345)}\right).$$

The arguments of Example 7.1 still apply to the objects defined on the same torus, as they did not rely on the specific value of the considered Z values, so:

$$\left(\mathbb{V}^{(123)} \cap d\mathcal{F}_{(123)}\right) = \left(\mathbb{V}^{(345)} \cap d\mathcal{F}_{(345)}\right) = \{0\}. \tag{7.122}$$

On the other hand, the mixed-torus intersections can only contain  $\{0\}$ , as they are intersections between forms in different coordinates

$$\left(\mathbb{V}^{(345)} \cap d\mathcal{F}_{(123)}\right) = \left(\mathbb{V}^{(123)} \cap d\mathcal{F}_{(345)}\right) = \{0\}. \tag{7.123}$$

We conclude  $\mathbb{V}_{-} \cap d\mathcal{F}_{-} \subseteq \{0\}$  and since these spaces must contain 0:

$$\mathbb{V}_{-} \cap d\mathcal{F}_{-} = 0 \tag{7.124}$$

Due to the splitting of the two tori, we trivially find that the forms split into ones defined on either torus. We see that in this example the  $\varepsilon$ -form differential equation we obtain is in C-form. This is what we would expect, as it can fully be expressed in terms of multiple polylogarithms. It would be interesting to look at an example, where we can not prevent mixing and have iterated integrals over both tori.

# 7.4 Boundary Value and Integration

In the remainder of the chapter, we provide a boundary value and comment on the solution of the canonical differential equation we obtained. This includes checking some of our results numerically but also comments on obstacles in existing numerical implementations.

## Boundary value

For the boundary value  $X_0 \in \mathcal{K}_{\rightarrow}$ , we choose a point in kinematic space, where all master integrals are finite, namely:

$$m_i = m > 0 \text{ and } p^2 \to 0^+ \quad \forall i.$$
 (7.125)

In the neighbourhood of this point, our coordinates approach  $X_i \to 1$  for  $i \neq 0$  and  $X_0 \to 0^+$ . In the torus variables, this means:

$$\begin{split} \tau^{(123)} &= \tau^{(345)} = i \infty \,, \\ z_1^{(123)} &= z_2^{(123)} = z_4^{(345)} = z_5^{(345)} = \frac{1}{3} \,, \\ z_4^{(123)} &= z_5^{(123)} = z_1^{(345)} = z_2^{(345)} = \frac{1}{2} - i \infty \,. \end{split} \tag{7.126}$$

Explicitly, the vector of master integrals at  $\boldsymbol{X}^0$  evaluates to:

$$\mathbf{J}_{0} = \varepsilon^{2} \left( \underbrace{J_{1}}_{\stackrel{\sim}{\sim} 8}, \underbrace{\frac{\sqrt{3}J_{2}}{2}}_{\stackrel{\sim}{\sim} 2}, \underbrace{0}_{\stackrel{\sim}{\sim} 2}, -\frac{\sqrt{3}J_{2}}{4}, \underbrace{\frac{\sqrt{3}J_{2}}{2}}_{\stackrel{\sim}{\sim} 2}, \underbrace{0}_{\stackrel{\sim}{\sim} 2}, -\frac{\sqrt{3}J_{2}}{4}, i\sqrt{3}J_{2}, \underbrace{0}_{\stackrel{\sim}{\sim} 3}, i\sqrt{3}J_{2}, \underbrace{0}_{\stackrel{\sim}{\sim} 9} \right), \quad (7.127)$$

where  $J_1 = I_{1,1,0,0,0}$  and  $J_2 = I_{1,1,1,0,0}$ . We find that all 30 of the master integrals in (2.46) can be found by evaluating the following two

$$J_{1} = I_{1,1,0,0,0}(2 - 2\varepsilon; \mathbf{X}_{0}) = e^{2\gamma_{\text{EM}}\varepsilon} \Gamma^{2}(\varepsilon)$$

$$J_{2} = I_{1,1,1,0,0}(2 - 2\varepsilon; \mathbf{X}_{0}) = \mathcal{N}\left[\left(-e^{\frac{2i\pi}{3}}\right)^{-\varepsilon} F_{\varepsilon}\left(\frac{2i\pi}{3}\right) - \left(-e^{-\frac{2i\pi}{3}}\right)^{-\varepsilon} F_{\varepsilon}\left(-\frac{2i\pi}{3}\right) + \frac{\pi}{\varepsilon}\right],$$

$$(7.128)$$

near  $\mathbf{X}_0$ . Here,  $\mathcal{N} = \frac{e^{2\gamma_{\mathrm{EM}}\varepsilon}\Gamma(1+2\varepsilon)}{(-1)^{1+2\varepsilon}3^{\frac{1}{2}+\varepsilon}}$  and  $F_{\varepsilon}(z) = \frac{3i\Gamma^2(\varepsilon+1)}{2\varepsilon^2\Gamma(2\varepsilon+1)} {}_2F_1(-2\varepsilon, -\varepsilon, 1-\varepsilon, e^z)$ . An explicit  $\varepsilon$ -expansion of these integrals (7.128) and (7.129) is known and can be obtained from the identity

$${}_{2}F_{1}\left(-2\varepsilon,-\varepsilon;1-\varepsilon;x\right) = 1 + 2\varepsilon^{2}\operatorname{Li}_{2}\left(x\right) + \varepsilon^{3}\left[2\operatorname{Li}_{3}\left(x\right) - 4\operatorname{Li}_{2,1}\left(x,1\right)\right] + \varepsilon^{4}\left[2\operatorname{Li}_{4}\left(x\right) - 4\operatorname{Li}_{3,1}\left(x,1\right) + 8\operatorname{Li}_{2,1,1}\left(x,1,1\right)\right] + \mathcal{O}\left(\varepsilon^{5}\right).$$
(7.130)

<sup>17</sup>This leads to

$$\begin{split} \frac{\partial X_i}{\partial \tau^\alpha} &= \left. \frac{\partial X_0}{\partial \tau^\alpha} \right|_{\mathbf{X}_0} = 0 \\ \text{for} \quad i \neq 0 \quad . \end{split}$$

## Elliptic multiple polylogarithms

As we have already expressed the canonical differential equation in Eisenstein-Kronecker forms, it is straightforward to integrate them to elliptic polylogarithms. On the other hand, numerical evaluation of these functions is less straightforward due to a lack of efficient packages. Another challenge is that similar to Feynman integrals that evaluate to MPLs, we often want to evaluate the integrals at points near or beyond the boundary of their region of convergence (see, for example, [200]). For the kite master integral, this situation appears when the differential equation is solved for finite  $\tau$  values starting from (7.126). Since  $z_4^{(123)} = z_5^{(123)} = z_1^{(345)} = z_2^{(345)} = z$ 

$$J_{30}^{(2)} = \sum_{j=6}^{9} \Delta_{6,7}^{j} \left( \left[ \Omega_{2,j,1}^{(123)}, \Omega_{2,1,1}^{(123)} \right] - 2 \left[ \Omega_{2,j,1}^{(123)}, \Omega_{2,1,2}^{(123)} \right] - \left[ \Omega_{2,j,1}^{(123)}, \Omega_{2,5,1}^{(123)} \right] + 2 \left[ \Omega_{2,j,1}^{(123)}, \Omega_{2,5,2}^{(123)} \right] \right)$$

$$(7.131)$$

$$+\sum_{j=10}^{13} \Delta_{10,11}^{j} \left( \left[ \Omega_{2,j,1}^{(123)}, \Omega_{2,2,1}^{(123)} \right] - 2 \left[ \Omega_{2,j,1}^{(123)}, \Omega_{2,2,2}^{(123)} \right] - \left[ \Omega_{2,j,1}^{(123)}, \Omega_{2,5,1}^{(123)} \right] + 2 \left[ \Omega_{2,j,1}^{(123)}, \Omega_{2,5,2}^{(123)} \right] \right) + \left( (123) \leftrightarrow (345) \right),$$

where  $\Delta_{n,m}^j = (-1)^{\delta_{j,n}+\delta_{j,m}}$ ,  $\Omega_{a,b,c}^d = \omega_a(\mathcal{L}_b^d, c \, \tau_d)$  and

$$[w_1, w_2, ..., w_k] = \int_{i\infty}^{\tau} w_1(t_1) \int_{i\infty}^{t_1} w_2(t_2) ... \int_{i\infty}^{t_{k-1}} w_k(t_k) , \qquad (7.132)$$

Any singularities due to the endpoints can be treated with tangential base point regularisation [19, 172, 193, 324]. Once rewritten, for instance, in terms of ELiseries (see (3.172b)) – in order to evaluate the result numerically – the expression fails to numerically converge. This divergence naturally occurs because the solution involves a series expansion that extends beyond its radius of convergence. In this specific case, the issue is resolved by leveraging the quasiperiodicity of the g-kernels in  $\tau$  (see [8, eq. (13.200)]). Moreover, such divergences do not appear in subtopologies with three or fewer propagators, as these correspond to master integrals that do not depend on the additional punctures  $z_4^{(123)} = z_5^{(123)} = z_1^{(345)} = z_2^{(345)} = \frac{1}{2} - i\infty$ . Specifically, we observe that the sunrise contributions, after performing the  $\tau$  integrations, align with [92, eq. (106)], as expected.

Numerical checks in the soft  $(p^2=0^+)$  regime To avoid this need for analytic continuation, we choose to perform the numerical integration in the soft region, i.e., within the limit  $p^2=0^+$ . We first integrate the differential equation from (7.126) to finite values of  $z_4^{(123)}, z_5^{(123)}, z_1^{(345)}$  and  $z_2^{(345)}$ , for example, setting  $z_4^{(123)}=z_5^{(123)}=z_1^{(345)}=z_2^{(345)}=\frac{1}{2}$ , while keeping everything else constant. A practical advantage of evaluating the integral at fixed  $\tau^{(123)}=\tau^{(345)}=i\infty$  is that along the path  $\gamma_0$ , which follows the straight-line parametrisation  $z_4^{(123)}=z_5^{(123)}=z_1^{(345)}=z_1$ 

#### See also:

We define and discuss elliptic polylogarithms in Section 3.4.3.

 $z_2^{(345)}=t$  with t ranging from  $\frac{1}{2}-i\infty$  to  $\frac{1}{2}$ , the matrix elements take on a purely trigonometric form, and the resulting iterated integrals combine in a *non-trivial* manner to yield finite expressions. This allows for an efficient numerical evaluation using MATHEMATICA's NIntegrate[] function.

The mapping between the space  $\mathfrak{M}=\mathcal{M}_{1,5}^{(123)}\times\mathcal{M}_{1,5}^{(345)}$ , which is parametrised by the moduli spaces of the two tori, and the kinematic space  $\mathcal{K}_{\multimap}$  is not globally invertible. One reason for this is that the mapping is not surjective: while  $\mathfrak{M}$  is a 10-dimensional space,  $\mathcal{K}_{\multimap}$  has only five dimensions. Thus, the transformation to the tori is not an isomorphism. For example, the point

$$\begin{split} \tau^{(123)} &= \tau^{(345)} = i\infty \,, \\ z_1^{(123)} &= z_2^{(123)} = z_4^{(345)} = z_5^{(345)} = \frac{1}{3} \,, \\ z_4^{(123)} &= z_5^{(123)} = z_1^{(345)} = z_2^{(345)} = \frac{1}{2} \,, \end{split} \tag{7.133}$$

which is reached after integrating along  $\gamma_0$ , does *not* correspond to any (complex) point in  $\mathcal{K}_{\to}$ . As a result, the numerical outcome differs from the master integrals evaluated over  $\mathcal{K}_{\to}$ , instead representing their extensions to  $\mathfrak{M}$ . This practical limitation makes direct comparisons with software such as PySecDec [325] infeasible for certain coordinate values in  $\mathfrak{M}$ , including (7.133). Nevertheless, we can validate our results by going from (7.133) to points in  $\mathfrak{M}$  that are contained within  $\mathcal{K}_{\to}$ . By constraining ourselves to the submanifold of  $\mathfrak{M}$  where  $\tau^{(123)} = \tau^{(345)} = i\infty$ , we can obtain numerical values efficiently using the same method as described earlier, namely by successively integrating along straight-line paths in  $\mathfrak{M}$  with NIntegrate[]. For example, evaluating the master integrals at the specific point

$$\tau^{(123)} = \tau^{(345)} = i\infty, \quad z_1^{(123)} = z_4^{(345)} = \frac{1}{4}, \quad z_2^{(123)} = z_5^{(345)} = \frac{1}{2},$$

$$z_4^{(123)} = z_1^{(345)} = -\frac{2i\log(i\sqrt{2+\sqrt{3}})}{\pi}, \quad z_5^{(123)} = z_2^{(345)} = \frac{i\log(8+3\sqrt{7})}{2\pi},$$

$$(7.134)$$

which corresponds to  $\mathbf{X} = \{X_0, X_1, X_2, X_4, X_5\} = \{0^+, 1, 2, 1, 2\}$  in  $\mathcal{K}_{\Phi}$ , yields results that match the PySecDec predictions at both leading and sub-leading order in  $\varepsilon$ . Similar consistency checks were performed successfully for multiple points within the soft region.

# Massless Feynman Integrals in 2D

See also:

- In Section 2.4.3 we introduced fishnet integrals.
- In Section 3.5 we explained how to relate a Calabi-Yau variety to a conformal fishnet integral.
- In Chapter 4 we study twisted cohomology groups. In particular we discuss the construction of single-valued versions of twisted periods in Subsection 4.2.2 and Aomoto-Gelfand hypergeometric functions in Subsection 4.3.
- In Chapter 3 we discuss basic geometric objects needed to understand the Feynman integrals of this chapter that are related to Calabi-Yau varieties. In particular, we briefly review CY geometries in Subsection 3.3.

In this chapter we consider massless Feynman integrals in D=2 dimensions expressed in complex coordinates as in eq. (2.20). The integrand is holomorphically separable, i.e., it can be written as a product of a holomorphic and an anti-holomorphic form in the complex spacetime coordinates  $\boldsymbol{x}$  and their complex conjugates  $\overline{\boldsymbol{x}}$ . Explicitly, we define the L-form

$$\varphi_G = \left(\bigwedge_{j=1}^L \mathrm{d}x_j\right) \prod_{j=1}^{n_{\text{int}}} \frac{1}{q_j(\boldsymbol{x}, \boldsymbol{\lambda})^{\nu_j}}$$
(8.1)

and write the two-dimensional integral of eq. (2.20) as

$$I_{\nu}^{G}(\lambda) = (-1)^{\frac{L(L-1)}{2}} \left( -\frac{1}{2\pi i} \right)^{L} \int_{\mathbb{C}^{L}} \varphi_{G} \wedge \overline{\varphi}_{G}. \tag{8.2}$$

For generic exponents  $\nu_j$ , the form  $\varphi_G$  is multi-valued but due to the combination with its anti-holomorphic version in eq. (8.2), the integrals are single-valued. Consequently, such Feynman integrals should be expressible in single-valued versions of twisted periods. The functions  $q_j$  that constitute the propagators are linear in the complex internal spacetime variables  $\boldsymbol{x}$ . Thus, the varieties defined by  $q_j(\boldsymbol{x}, \boldsymbol{y}) = 0$  are hyperplanes in the complex affine space  $\mathbb{C}^L$ . The Feynman integrals of eq. (8.2) are single-valued versions of Aomoto-Gelfand hypergeometric functions.

We discuss this interpretation in detail in Section 8.1 and illustrate it with several examples. In Section 8.2, we explain how specific two-dimensional integrals – the conformal fishnet integrals – can be computed with tools from the study of Calabi-Yau manifolds.

- ♠ Section 8.1 is based on published results [36], which were obtained in collaborations with Claude Duhr.
- ♠ Section 8.2 briefly summarises previously published results [35, 37, 38], which were obtained in collaborations with Claude Duhr, Florian Loebbert, Christoph Nega and Albrecht Klemm.

## Contents of this Chapter

8.1	Sing	le-valued Hypergeometric Functions 22	24
8.2	Conformal Fishnets as Kähler Potentials		29
	8.2.1	Conformal Fishnets in $2D$ as Kähler Potentials	29
	8.2.2	Fishnets as Quantum Volumes	34
	8.2.3	Relations Between One-Parameter Fishnets 2	35

## 8.1 Single-valued Hypergeometric Functions

As noted above, Feynman integrals in two dimensions can be interpreted as single-valued versions of twisted periods. More specifically, they are related to single-valued analogues of Aomoto-Gelfand hypergeometric functions and we make this relation explicit in Theorem 8.1, first presented in [36].

**Theorem 8.1.** Let G be an L-loop Feynman graph with massless propagators that defines an integral  $I^G_{\nu}(\lambda)$  of the form given in eq. (8.2), in D=2 dimensions, with non-integer propagator weights  $\nu_j$  that satisfy  $\nu_{\infty} = -\sum_j \nu_j$ . Then G determines twisted de Rham (co-)homology groups and the value of the integral  $I^G_{\nu}(\lambda)$  is given by the single-valued version of a twisted period of these (co-)homology groups which is a single-valued analogue of an Aomoto-Gelfand hypergeometric function.

We start by explaining how to extract the relevant data to define the twisted (co-)homology groups. We already explained how to associate a relative twisted cohomology group with a Feynman integral family in Baikov representation in Section 4.4. The approach here is different: The dimension is integer, so the multivaluedness does not arise from the dimensional regulator  $\varepsilon$  but instead from the non-integer (or even generic) propagator weights. Due to these, the integrand has no unregulated poles. This choice of dimension and parameters also allows us to simply deduce the twisted (co-)homology groups associated to the Feynman integral directly from its momentum (or respectively position space) representation.

The two-dimensional Feynman integral of eq. (8.2) is fully characterised by the multi-valued (L,0)-form  $\varphi_G$  defined by the graph. All factors  $q_j(\boldsymbol{x})$  of  $\varphi_G$  define hyperplanes in the affine complex space  $\mathbb{C}^L$  and thus  $\varphi_G$  is the integrand of an Aomoto-Gelfand hypergeometric function. We split off the multi-valued part as the twist and write

$$\varphi_G = \Phi_G \, \varphi_L \text{ with } \varphi_L = \bigwedge_{j=1}^L \mathrm{d}x_j \text{ and } \Phi_G = \prod_{j=1}^{n_{\mathrm{int}}} \frac{1}{q_j(\boldsymbol{x}, \boldsymbol{\lambda})^{\nu_j}}.$$
 (8.3)

Based on this data, we define

$$X_G = \mathbb{C}^L - \bigcup_j \left\{ q_j(\boldsymbol{x}, \boldsymbol{\lambda}) = 0 \right\}, \tag{8.4}$$

and

$$\nabla_G = d + d\log \Phi_G \wedge \cdot . \tag{8.5}$$

This data defines the twisted cohomology group  $H^L_{dR}(X_G, \nabla_G)$  associated to  $I^G_{\nu}(\lambda)$  and we can write the integral of eq. (8.2) as

$$I_{\nu}^{G}(\boldsymbol{\lambda}) = (-1)^{\frac{L(L-1)}{2}} \left( -\frac{1}{2\pi i} \right)^{L} \int_{X_{G}} \left| \Phi_{G} \right|^{2} \varphi_{L} \wedge \overline{\varphi}_{L}. \tag{8.6}$$

This is a single-valued Aomoto-Gelfand hypergeometric function as defined in eq. (4.191).

Theorem 8.1 implies that every Feynman integral with massless propagators of non-integer weight in two dimensions can be expressed as a bilinear in holomorphic and anti-holomorphic Aomoto-Gelfand hypergeometric functions. This follows from the double copy construction for single-valued versions of twisted periods that was given in eq. (4.139) based on [7, 248, 249]. This was observed in several special cases before. For instance, four-point functions in conformal field theories [326] and Feynman integrals emerging from a specific two-dimensional conformal field theory [327] commonly evaluate to single-valued versions of hypergeometric functions. In [328] specific fishnet integrals in two dimensions are expressed as single-valued combinations of hypergeometric functions. The D-dimensional massless kite integral in position space was computed in [329] and this computation revealed that in two dimensions, the integral is holomorphically separable. Theorem 8.1 explains all these findings from the literature and extends them. Specifically, it establishes that holomorphic separability and single-valuedness are generic properties of Feynman integrals with massless propagators in two dimensions not limited to certain Feynman integrals in conformal field theories. This observation aligns with results from string theory, where certain closed-string integrals evaluate to single-valued versions of twisted periods [6, 266]. In [330] a recursion is presented that allows one to lift such two-dimensional results to four dimensions.

## Examples

We illustrate the above discussion with several examples.

**Example 8.1** (Massless Banana Integrals). As a first class of examples we consider massless banana integrals in two dimensions, i.e. the integrals of Example 2.10 with  $m_i \mapsto 0$  for all i:

$$I_{\nu}^{\text{banana,L}}(p) = \left(-\frac{1}{2\pi i}\right)^{L} \int_{\mathbb{C}^{L}} \left(\bigwedge_{j=1}^{L} d\ell_{j} \wedge d\overline{\ell}_{j}\right) \prod_{j=1}^{L+1} \frac{1}{|\ell_{j-1} - \ell_{j}|^{2\nu_{j}}}, \quad (8.7)$$

with  $\ell_0 = 0$  and  $\ell_{L+1} = p$ . For L = 1 we find:

$$I_{\nu}^{\text{banana},1}(p) = |p|^{2-2\nu_{12}} \beta^{sv}(1-\nu_1, 1-\nu_2)$$
(8.8)

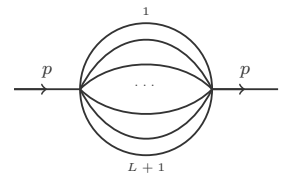
with  $\nu_{i_1\cdots i_k} = \nu_{i_1} + \ldots + \nu_{i_k}$  and  $\beta^{\text{sv}}$  the single-valued Beta function of eq. (4.144). Using (4.145) one can express the massless one-loop banana integral as a ratio of Gamma functions.<sup>1</sup> To obtain higher-loop banana integrals, one can integrate the loops recursively and obtains

$$I_{\nu}^{\text{banana,L}}(p) = |p|^{2L - 2\nu_{1\cdots L}} \prod_{j=1}^{L} \beta^{sv}(j - \nu_{1\cdots j}, 1 - \nu_j).$$
 (8.9)

All massless banana integrals in two dimensions are products of single-valued  $\beta$  functions.

#### See also:

We also presented many examples for this construction in Section 4.3.2.



<sup>1</sup>Of course, this result for the massless bubble is well-known and we just include it as a first example.

**Example 8.2** (Planar One-loop Integrals in Position Space). We have already found an expression for the one-loop bubble in two dimensions in eq. (8.8), but one can in fact determine all one-loop massless integrals in two dimensions. We consider graphs in position space that are given by a star with N external vertices (see figure 8.1).

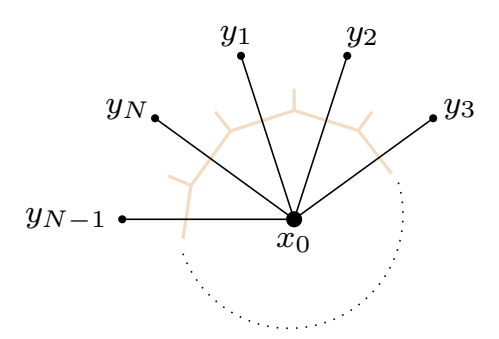


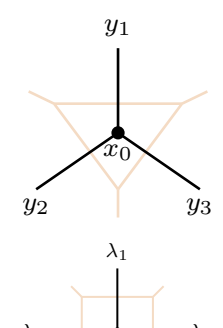
Figure 8.1: A star integral in position space corresponds to a one-loop integral in momentum space.

The corresponding integrals are

$$Star_{\boldsymbol{\nu}}^{N}(\boldsymbol{y}) = -\frac{1}{2\pi i} \int_{\mathbb{C}} dx_{0} \wedge d\overline{x}_{0} \prod_{j=1}^{N} \frac{1}{|x_{0} - y_{j}|^{2\nu_{j}}}.$$
 (8.10)

Note that in this case, the momentum space integrals take the same form [331]. The half-integrand

$$\varphi_{\text{Star}}^{N} = \frac{\mathrm{d}x_0}{\prod_{j=1}^{N} (x_0 - y_j)^{\nu_j}}$$
 (8.11)



resembles the integrand of a Lauricella's  $F_D^{(N-2)}$  as defined in eq. (4.174). In order to write the integrals in eq. (8.10) as single-valued Lauricella functions, one needs to perform a coordinate change that generates a constant prefactor and we find:

$$Star_{\boldsymbol{\nu}}^{N}(\boldsymbol{y}) =$$
 (8.12)

$$= \mathcal{F}_D^{sv} (1 - \nu_1, \nu_3, \dots, \nu_N, 2 - \nu_{12}; \tilde{y}_1, \dots, \tilde{y}_{N-2}) \frac{1}{|y_1 - y_2|^{2\nu_{12} - 2}} \prod_{j=3}^N \frac{1}{|y_1 - y_j|^{2\nu_j}},$$

with  $\tilde{y}_i = \frac{y_1 - y_2}{y_1 - y_{i+2}}$ . Thus, every one-loop integral can be expressed as a bilinear in Lauricella  $\mathcal{F}_D^{(N-2)}$  functions via eq. (4.139). Examples for N=3,4 are the triangle and box integrals, which are expressible as single-valued hypergeometric  ${}_2F_1$  and Appell  $F_1$  functions.

$$Star_{\nu}^{3}(\mathbf{y}) = |y_{1} - y_{2}|^{2-2\nu_{12}} |y_{1} - y_{3}|^{-2\nu_{3}} {}_{2}\mathcal{F}_{1}^{sv}(1 - \nu_{1}, \nu_{3}, 2 - \nu_{12}; \tilde{y}_{1}), \qquad (8.13)$$

$$Star_{\boldsymbol{\nu}}^{4}(\boldsymbol{y}) = |y_{1} - y_{2}|^{2-2\nu_{12}} |y_{1} - y_{3}|^{-2\nu_{3}} |y_{1} - y_{4}|^{-2\nu_{4}} \mathcal{F}_{1}^{sv} (1 - \nu_{1}, \nu_{3}, \nu_{4}, 2 - \nu_{12}; \tilde{y}_{1}, \tilde{y}_{2}).$$

$$(8.14)$$

The single-valued versions of these functions are given in eq. (4.193) and (4.196) as bilinears in the respective hypergeometric functions. As noted in Section 2.4.3, if  $\sum_{j=1}^{N} \nu_j = D = 2$  the integral transforms under the conformal algebra in two Euclidean spacetime dimensions with conformal weight  $\nu_j$  at each external point. Then, the Lauricella  $F_D^{(N-2)}$  functions that one initially associates to the one-loop integral can be written as Lauricella  $F_D^{(N-3)}$  functions. As an example for this, we consider the five-point integral

$$y_4$$
 $y_3$ 
 $y_3$ 
 $y_4$ 
 $y_1$ 

$$Star_{\nu}^{5}(\boldsymbol{y}) = -\frac{1}{2\pi i} \int_{\mathbb{C}} \frac{\mathrm{d}x_{0} \wedge \mathrm{d}\bar{x}_{0}}{\left(\prod_{i=1,2,4,5} |x_{0} - y_{i}|^{2}\right)^{\frac{2}{3}} |x_{0} - y_{3}|^{\frac{4}{3}}}.$$
 (8.15)

This integral arises in the computation of conformally invariant fishnet integrals with cubic vertices [37]. If we multiply the integral by the factor  $|y_1 - y_3|^{\frac{2}{3}}|y_2 - y_3|^{\frac{2}{3}}|y_4 - y_5|^{\frac{2}{3}}$ , it becomes conformally invariant. We may then use a conformal transformation to fix  $(y_3, y_4, y_5) = (\infty, 0, 1)$ , and obtain:

$$Star_{\nu}^{5}(\mathbf{y}) = -\frac{1}{2\pi i} |y_{1} - y_{3}|^{\frac{2}{3}} |y_{2} - y_{3}|^{\frac{2}{3}} |y_{4} - y_{5}|^{\frac{2}{3}} \int_{\mathbb{C}} \frac{\mathrm{d}x_{0} \wedge \mathrm{d}\bar{x}_{0}}{(|x_{0}|^{2}|1 - x_{0}|^{2}|x_{0} - u_{1}|^{2}|x_{0} - u_{2}|^{2})^{\frac{2}{3}}}$$

$$= \left| \frac{(y_{1} - y_{3})(y_{2} - y_{3})(y_{4} - y_{5})^{3}}{(y_{1} - y_{4})^{2}(y_{2} - y_{4})^{2}(y_{3} - y_{5})^{4}} \right|^{\frac{2}{3}} \mathcal{F}_{1}^{\text{sv}} \left( \frac{1}{3}, \frac{2}{3}, \frac{2}{3}; u_{1}^{-1}, u_{2}^{-1} \right) \qquad (8.16)$$

$$= \frac{\sqrt{3}u_{1}^{\frac{3}{3}}u_{2}^{\frac{1}{3}}}{2} \left| \frac{(y_{1} - y_{3})(y_{2} - y_{3})(y_{4} - y_{5})^{3}}{(y_{1} - y_{4})^{2}(y_{2} - y_{4})^{2}(y_{3} - y_{5})^{4}} \right|^{\frac{2}{3}} \left\{ 2i \mathcal{F}_{1} \left( \frac{1}{3}, \frac{2}{3}, \frac{2}{3}; \overline{u}_{1}^{-1}, \overline{u}_{2}^{-1} \right) \right.$$

$$\times \left[ e^{-\frac{i\pi}{3}} u_{2}^{-\frac{1}{3}} \mathcal{F}_{1} \left( \frac{1}{3}, \frac{2}{3}, \frac{2}{3}; \frac{2}{3}; u_{1}, \frac{u_{1}}{u_{2}} \right) - u_{1}^{-\frac{1}{3}} \mathcal{F}_{1} \left( \frac{1}{3}, \frac{2}{3}, \frac{2}{3}; u_{2}, \frac{u_{2}}{u_{1}} \right) \right]$$

$$+ 2e^{\frac{i\pi}{6}} \mathcal{F}_{1} \left( \frac{1}{3}, \frac{2}{3}, \frac{2}{3}; \overline{u}_{1}, \overline{u}_{2} \right)$$

$$\times \left[ e^{\frac{2i\pi}{3}} u_{2}^{-\frac{1}{3}} \mathcal{F}_{1} \left( \frac{1}{3}, \frac{2}{3}, \frac{2}{3}; \overline{u}_{1}, \overline{u}_{2} \right) + \mathcal{F}_{2} \left( \frac{1}{3}, \frac{2}{3}, \frac{2}{3}; u_{2}, \frac{u_{2}}{u_{1}} \right) \right]$$

$$- 2i \mathcal{F}_{1} \left( \frac{1}{3}, \frac{2}{3}, \frac{2}{3}; u_{2}, \frac{u_{2}}{u_{1}} \right)$$

$$\left[ e^{\frac{i\pi}{3}} \mathcal{F}_{1} \left( \frac{1}{3}, \frac{2}{3}, \frac{2}{3}; u_{1}, \frac{u_{1}}{u_{2}} \right) - u_{1}^{-\frac{1}{3}} \mathcal{F}_{1} \left( \frac{1}{3}, \frac{2}{3}, \frac{2}{3}; u_{1}^{-1}, u_{2}^{-1} \right) \right] \right\},$$

where we defined the cross ratios

$$u_i = \frac{(y_i - y_4)(y_3 - y_5)}{(y_i - y_3)(y_4 - y_5)},$$
(8.17)

and assume  $u_1, u_2 > 0$ .

**Example 8.3** (Ladder integrals). For a last example we consider the ladder graphs in position space as depicted in figure 8.2.

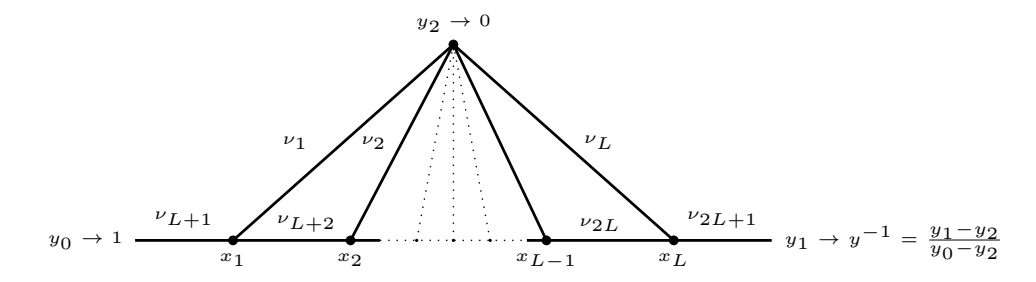


Figure 8.2: Ladder integrals in position space constitue an L-loop class of one-parameter fishnet graphs.

Their integral representation is

$$Lad_{\nu}^{L}(y_0, y_1, y_2) = |y_0 - y_2|^{2(2 - \sum_{i=1}^{2L+1} \nu_i)} |y|^{2\nu_{2L+1}}$$
(8.18)

$$\times \left( -\frac{1}{2\pi i} \right)^{L} \int_{\mathbb{C}^{L}} \left( \bigwedge_{i=1}^{L} \mathrm{d}x_{i} \wedge \mathrm{d}\bar{x}_{i} \right) |1 - yx_{L}|^{-2\nu_{2L+1}} \prod_{j=1}^{L} |x_{j}|^{-2\nu_{j}} |x_{j-1} - x_{j}|^{-2\nu_{L+j}},$$

where we defined  $y = \frac{y_0 - y_2}{y_1 - y_2}$ . In the one-loop case, L = 1, the ladder integral is the three point function  $Star_3$ . Comparing to eq. (4.197), we find that the ladder integrals in two dimensions amount to single-valued  $_p\mathcal{F}_q^{sv}$  functions and in particular

$$Lad_{\nu}^{L}(y_{0}, y_{1}, y_{2}) = (-1)^{\frac{L(L-1)}{2}} |y_{0} - y_{2}|^{2(2 - \sum_{i=1}^{2L+1} \nu_{i})} |y|^{2\nu_{2L+1}} L_{+1} \mathcal{F}_{L}^{sv}(\boldsymbol{a}, \boldsymbol{b}, y), \quad (8.19)$$

where the  $a_i$  and  $b_i$  are given by:

$$a_0 = \nu_{2L+1} \text{ and } a_i = L - i + 1 - \sum_{j=i}^{2L} \nu_j + \sum_{j=L+1}^{L+i} \nu_j \text{ for } i > 0,$$
 (8.20)

$$b_1 = L + 1 - \sum_{j=1}^{2L} \nu_j \text{ and } b_i = L - i + 2 - \sum_{j=i}^{2L} \nu_j + \sum_{j=L+1}^{L+i-1} \nu_j \text{ for } i > 1.$$
 (8.21)

A particular type of ladder integrals, originating from conformal four-point functions, was explored in ref. [328]. The two-loop ladder integral was computed in ref. [329] under the condition  $y_0 = y_1$  for any dimension D, and we confirm this result specifically for D = 2. Interestingly, it was noted that in D = 2, the outcome can be expressed as a bilinear in  $_3F_2$  functions. Our findings demonstrate that this observation is not merely coincidental but rather a direct consequence of our general Theorem 8.1, which, when applied to this particular graph, yields the expression:

$$Lad_{\nu}^{2}(y_{1}, y_{2}) = \tag{8.22}$$

= 
$$-|y_1 - y_2|^{2(2-\sum_{i=1}^5 \nu_i)} {}_3\mathcal{F}_2^{sv}(\nu_5, 2 - \nu_{124}, 1 - \nu_2, 3 - \nu_{1234}, 2 - \nu_{24}, 1)$$
. (8.23)

Furthermore, eq. 8.19 extends the results of refs. [328, 329] to ladder integrals with an arbitrary number of loops and general propagator powers.

## 8.2 Conformal Fishnets as Kähler Potentials

For the remainder of this chapter, we consider specific massless two-dimensional Feynman integrals: The conformal fishnet integrals of Section 2.4.3. In particular, these integrals take the form given in eq. (2.79) and as discussed in the second part of Section 3.5, their conformality allows us to associate a CY varieties to these fishnet integrals.

#### 8.2.1 Conformal Fishnets in 2D as Kähler Potentials

Our goal is to compute the integrals of eq. (2.20), which can be written as

$$I_{\nu}^{G}(\lambda) \sim \int \frac{\prod_{i} dx_{i}}{\sqrt{P_{G}(\boldsymbol{x}, \lambda)}} \wedge \frac{\prod_{i} d\bar{x}_{i}}{\sqrt{\overline{P_{G}(\boldsymbol{x}, \lambda)}}}.$$
 (8.24)

with  $P_G(\boldsymbol{x}, \boldsymbol{\lambda})$  the polynomial of eq. (3.217). Of course, these specific conformal fishnet integrals are still just a special class of two-dimensional integrals as discussed in section 8.1 and thus, computing them still just means computing single-valued versions of periods. The specific class of integrals considered here is related to Calabi-Yau families defined by the polynomial equation in eq. (3.217). This polynomial  $P_G(\boldsymbol{x}, \boldsymbol{\lambda})$  is a function of the external parameters  $\boldsymbol{\lambda}$  and the CY family is labelled by these parameters.<sup>2</sup> Due to conformal invariance, we expect the integrals to evaluate to non-trivial functions  $\phi(\boldsymbol{\chi})$  in cross ratios  $\boldsymbol{\chi}$ , up to an algebraic function  $F_G(\boldsymbol{\lambda})$  that carries the conformal weight, as stated in eq. (2.86). This split is not unique. We define  $\Omega_G(\boldsymbol{x}, \boldsymbol{\chi})$  to be a normalised version of the the (L, 0)-form  $\Omega(\boldsymbol{x})$  of eq. (3.219) – where the normalisation is chosen as in Definition 4.3. of ref. [332] – such that  $\Omega_G(\boldsymbol{x}, \boldsymbol{\chi})$  only depends on the cross ratios  $\boldsymbol{\chi}$ . The function  $F(\boldsymbol{\lambda}) \in \overline{\mathbb{Q}(\boldsymbol{\lambda})}$  lives in an algebraic extension of  $\mathbb{Q}(\boldsymbol{\lambda})$  and is determined by the chosen normalisation. Then the non-trivial part of the integral in eq. (2.86) is

$$\phi(\boldsymbol{\chi}) = \int_{\mathcal{M}} (-1)^{L(L-1)/2} \left(\frac{i}{2}\right)^{\ell} \Omega(\boldsymbol{\chi}) \wedge \overline{\Omega}(\boldsymbol{\chi}) = e^{-K(\boldsymbol{\chi})}, \qquad (8.25)$$

where  $\mathcal{M}$  denotes the fiber over the point  $\chi$  and  $K(\chi)$  is the Kähler potential on the complex moduli space  $\mathcal{M}_{cs}$  of the CY family parametrised by  $\chi$ . For a family of CY L-folds parametrised by  $\chi$ , the single-valued function  $\phi(\chi)$  can be computed as a bilinear of the periods  $\Pi(\chi)$  of the CY variety:

$$\phi(\mathbf{\chi}) = (-i)^{L^2} \mathbf{\Pi}(\mathbf{\chi})^{\dagger} \mathbf{\Sigma} \mathbf{\Pi}(\mathbf{\chi}) . \tag{8.26}$$

Here, this vector of periods  $\Pi(\chi)$  is

$$\mathbf{\Pi}(\boldsymbol{\chi}) = 2^{-\frac{L}{2}} \left( \int_{\Gamma_0} \Omega_G(\boldsymbol{x}, \boldsymbol{\chi}), \dots, \int_{\Gamma_{b_L - 1}} \Omega_G(\boldsymbol{x}, \boldsymbol{\chi}) \right) \text{ with } b_L = \dim[\mathbf{H}_L(\mathcal{M}, \mathbb{Z})], \quad (8.27)$$

where the  $\Gamma_j$  label an integral basis of the middle homology  $H_L(\mathcal{M}, \mathbb{Z})$ . Additionally, we denote by  $\Sigma$  the integral intersection form. Note the similarity to the

<sup>2</sup>More specifically, right below we will also label the family by cross ratios of the  $\lambda_i$  instead.

bilinear expression for the single-valued periods in eq. (4.139). Thus, to compute the fishnet integrals of eq. (8.24), we just need to compute the periods and the intersection matrix and we summarise this finding in the following claim:

Claim 1: For every L-loop fishnet graph G, there exists a family of CY L-folds  $\mathcal{M}_G$  with a holomorphic (L,0)-form  $\Omega_G$  such that

$$I_G(\lambda) = (-i)^{\ell} \,\tilde{\Pi}_G^{\dagger} \,\Sigma \,\tilde{\Pi}_G \,, \tag{8.28}$$

with  $\tilde{\mathbf{\Pi}}_G = F_G(\boldsymbol{\lambda})\mathbf{\Pi}(\boldsymbol{\chi})$  and the PFI is generated by  $\operatorname{Aut}(G) \cdot Y(\mathfrak{sl}_2(\mathbb{R}))$ .

Determining the PFI for a fishnet integral from the physical and graph symmetries is a central part of using this expression to compute fishnet integrals. The periods can be computed as solutions of this PFI, as described in Section 3.4. Since the generators of the Yangian operators annihilate the periods, they should also be contained in the PFI of the fishnet integral family. In many cases these generators by themselves are not sufficient to generate the full PFI. Yet, we find that we can supplement them with additional operators to obtain the PFI in many cases: The group Aut(G) of automorphisms of G acts on  $Y(\mathfrak{sl}_2(\mathbb{R}))$  by permuting the external points  $\lambda_i$  and the PFI also contains these operators. Those are the ones needed to generate the full PFI. In simpler cases, we can also find the PFI constructively from the integral representation of one period: We make an ansatz for its generators and then solve for their coefficients by requiring that the operators annihilate the period. For our examples, we find that the two approaches agree, though the information from the symmetries is invaluable for more complicated graphs. Every solution vector  $\Pi(\chi)$  satisfies a set of quadratic relations eq. (3.106). From these relations one can obtain the intersection matrix  $\Sigma$ . We illustrate this approach with several examples, particularly in the single-variable case. More examples can be found in [37, 38].

### Four-point Square (V = 4) Fishnet Integrals

We focus on the special case, where we have V=4, i.e. a square tiling, and just four external points and respectively one external cross-ratio  $\chi=\chi$ , which we choose to be

$$\chi = \frac{(\lambda_2 - \lambda_3)(\lambda_1 - \lambda_4)}{(\lambda_2 - \lambda_1)(\lambda_3 - \lambda_4)}.$$
(8.29)

These fishnet graphs are depicted in figure 8.3.

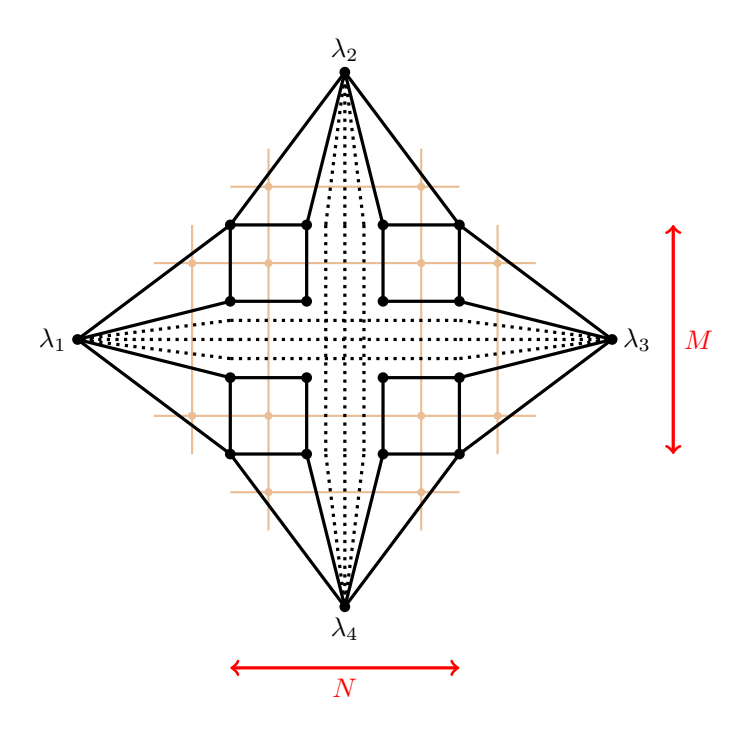


Figure 8.3: A generic one-parameter fishnet graph in position space with a square tiling has four external points.

Besides the value of their external points and in particular of the associated cross-ratio, they are characterised by the number of internal vertices on the horizontal axis (denoted N here) and on the vertical axis (denoted M here). We label objects associated to these specific fishnet graphs with the indices M, N, e.g.,  $P_{M,N}$  for the polynomial formerly denoted  $P_G$  and similarly  $F_{M,N}(\lambda)$ ,  $\Omega_{M,N}(\chi)$ ,  $\Pi_{M,N}(\chi)$  and  $\phi_{M,N}(\chi)$ . As indicated in eq. (8.26), we can then compute the non-trivial part of the integral by

$$\phi_{M,N}(\chi) = (-i)^{L^2} \mathbf{\Pi}_{M,N}(\chi)^{\dagger} \mathbf{\Sigma}_{M,N} \mathbf{\Pi}_{M,N}(\chi). \tag{8.30}$$

Determining the Picard-Fuchs Ideal Here, we explain how to find the Picard-Fuchs ideal for a one-parameter family given a single period in integral representation obtained from the graph. First, we perform a conformal transformation in the parameter space to set  $\lambda_1 = 1, \lambda_2 = 0, \lambda_4 = \infty$ . Then, we can identify the cross ratio in eq. (8.29) as  $\lambda := \lambda_3 = \chi$ . To obtain the integral representation of a specific period, we choose a cycle and a differential. In particular, we choose the differential  $\Omega_{M,N}$ , which is the unique holomorphic differential defined from the Feynman integral. For the cycle, we can choose an L-dimensional torus and thus we have to compute an L-dimensional residue:

$$\Pi_{M,N,0}(z) = \oint_{T^{\ell}} \Omega_{M,N} \xrightarrow{\text{conf.}} \oint_{T^{\ell}} \prod_{i=1}^{\ell} dx_i \frac{1}{\sqrt{\hat{P}_{M,N}(x,\chi)}}.$$
 (8.31)

Here,  $\hat{P}_{M,N}(x,\chi)$  denotes the polynomial after the conformal transformation that sets the external parameters to  $0, 1, \infty$  and  $\chi$ . This integral can be calculated as a

Laurent series by using the Taylor expansion of a square root

$$\frac{1}{\sqrt{1-u}} = \sum_{i=0}^{\infty} {2i \choose i} \left(\frac{u}{4}\right)^i, \quad |u| < 1 \tag{8.32}$$

on every linear factor of the polynomial  $\tilde{P}_{M,N}(x,\lambda)$  separately and then computing the residue. In this way we obtain a Taylor series representation for the period close to  $\lambda = 0$ :

$$\Pi_{M,N,0}(\chi) = \sum_{i=0}^{\infty} r_{M,N}^{(i)} \chi^i.$$
 (8.33)

Now we can determine the Picard Fuchs operator by constructing<sup>3</sup> the operator  $\mathbb{O}_{M,N}$  of minimal degree that annihilates  $\Phi_{M,N,0}(\chi)$ . In this case, we know, that the Picard-Fuchs ideal consists of a single operator..

**Example 8.4** (L = 1 loop Fishnet Integral). For L = 1, we consider the graph depicted in figure 8.4.

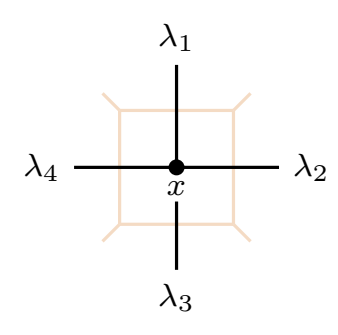


Figure 8.4: The one-loop fishnet integral in position space is a cross and its momentum space version is a box.

The corresponding integral falls under the category of the star integrals of eq. (8.10) and we explicitly computed it as the multiple of a single-valued hypergeometric  ${}_2F_1$  function for generic propagator weights in eq. (8.13). For the specific parameter choice of this section (i.e. with propagator weights  $\frac{1}{2}$  for conformality), we can also consider the integral family as a family of Kähler potentials of Legendre elliptic curves. Their periods can be expressed in terms of elliptic integrals. In particular, if we take a normalised version<sup>4</sup> of the basis of example 3.1, we find  $\Pi_{1,1,0} = \frac{2}{\pi}(K(\chi), K(1-\chi))^T$  and  $\Sigma = \begin{pmatrix} 0 & 1 \\ 1 & 0 \end{pmatrix}$ . Then the conformally invariant part takes the form [328, 333]:

$$\phi_{1,1}(\chi) = \frac{4}{\pi^2} \left[ K(\chi) \overline{K(1-\chi)} + \overline{K(\chi)} K(1-\chi) \right] = \frac{8}{\pi^2} |K(\chi)|^2 \operatorname{Im} \tau , \qquad (8.34)$$

and F\_{1,1}\!(a) =  $\pi/\sqrt{\lambda_{12}\lambda_{34}}$ . Here  $\tau = iK(1-\chi)/K(\chi)$ .

<sup>3</sup>That means, we make an ansatz for this operator and then solve for the coefficients by requiring that it annihilates the period we have determined.

<sup>4</sup>In particular, we take  $\lambda = \chi^{-1}$  and we normalise with  $\frac{1}{2\pi\sqrt{\chi}}$ .

As a second class of examples, let us consider the *ladder integrals*, i.e., one-parameter fishnet integrals with M=1 as depicted in figure 8.5.

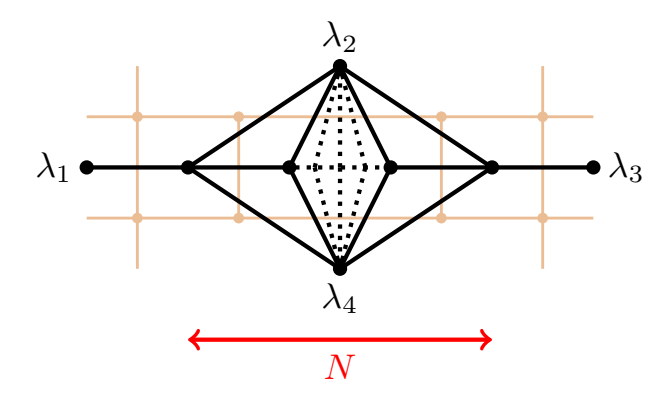


Figure 8.5: Ladder integrals in position space.

**Example 8.5** (Ladder Integrals). For ladder integrals, the loop number is equal to the dimension of the CY varieties they are associated with:

$$L = N = \dim_{\mathbb{C}}(\mathcal{M}_{1,N}). \tag{8.35}$$

In the one-parameter limit that we consider here, a ladder integral corresponds to the hypergeometric system defined by the Picard-Fuchs operator (see also ref. [334])

$$\mathbb{O}_N := \mathbb{O}_{1,N} = \theta_z^{N+1} - z \left(\theta_z + \frac{1}{2}\right)^{N+1}, \tag{8.36}$$

with the Riemann  $\mathcal{P}$ -Symbol

$$\mathcal{P} = \begin{cases} \frac{z & 1 & \infty}{0 & 0 & \frac{1}{2} \\ 0 & 1 & \frac{1}{2} \\ \vdots & \vdots & \vdots \\ 0 & N - 1 & \frac{1}{2} \\ 0 & \frac{N+1}{2} - 1 & \frac{1}{2} \end{cases} . \tag{8.37}$$

This differential operator  $\mathbb{O}_N$  has a MUM point at  $\chi = 0$  and the holomorphic solution at this MUM point is

$$\Pi_{N,0}(\chi) := \sum_{i=0}^{\infty} {\binom{-\frac{1}{2}}{i}}^{N+1} \chi^{i} = {}_{N+1}F_{N}\left(\frac{1}{2},\dots,\frac{1}{2};1,\dots,1;\chi\right) . \tag{8.38}$$

We formally introduce

$$\Pi_{0,0}(\chi) = \sum_{i=0}^{\infty} {2i \choose i} \left(\frac{\chi}{4}\right)^i = \frac{1}{\sqrt{1-\chi}}.$$
(8.39)

Note that  $b_N(\mathcal{M}_{1,N}) = N+1$  and the Hodge numbers are:

$$h^{N-k,k}(\mathcal{M}_{1,N}) = 1, \quad k = 0, \dots, N.$$
 (8.40)

We choose the rank N+1 intersection matrix of  $\mathcal{M}_{1,N}$  as

$$\Sigma_{N} = \begin{pmatrix} \mathbf{0} & \mathbf{K}_{\frac{N+1}{2}} \\ -\mathbf{K}_{\frac{N+1}{2}} & \mathbf{0} \end{pmatrix}, \quad N \text{ odd}, \qquad \Sigma_{N} = \begin{pmatrix} \mathbf{0} & 0 & \mathbf{K}_{\frac{N}{2}} \\ 0 & m & 0 \\ \mathbf{K}_{\frac{N}{2}} & 0 & \mathbf{0} \end{pmatrix}, \quad N \text{ even} ,$$

$$(8.41)$$

From this information, we can compute the ladder integrals using eq. (8.28). Our results agree with known results and numerical evaluations of these integrals.

For example of multi-parameter fishnet integrals and different tilings, see also [37, 38]. Note that the tilings with 3 and 6 edges entering the vertices are related by star-triangle relations.

## 8.2.2 Fishnets as Quantum Volumes

Here, we briefly summarise how to interpret the fishnet integrals expressed as multiples of the exponential of the Kähler potential as volumes. An obstacle for this interpretation is that we do not have a distinguished metric on  $\mathcal{M}_G$ . While a point  $\lambda$  fixes  $\Omega_G$ , and thus the complex structure, there is still freedom to define a Kähler form, and thus a metric, on  $\mathcal{M}_G$ . We now demonstrate that a volume interpretation can be achieved through mirror symmetry. As G determines a complex structure on  $\mathcal{M}_G$  via  $\Omega_G$ , mirror symmetry associates a Kähler form  $\omega_G \in \mathrm{H}^{1,1}(\mathcal{W}_G)$  to the mirror. By choosing the coordinates  $\lambda$  such that  $\mathcal{M}_G$  has a MUM-point at  $\lambda = 0$ , we obtain

$$\omega_G = \sum_i t_{G,i}^{\mathbb{R}}(z) \,\omega^{(i)} \,, \tag{8.42}$$

where  $\omega^{(i)}$  forms a basis of  $H^{1,1}(\mathcal{W}_G)$ , and the  $t_i^{\mathbb{R}}(z) = \operatorname{Im} t_i(z)$  are determined by the *mirror map* of Definition 3.15. The Kähler form can then be used to define a volume form  $\omega_G^L/L!$  on  $\mathcal{W}_G$ , and the *classical* volume of  $W_G$  is given by

$$\operatorname{Vol}_{\operatorname{cl}}(\mathcal{W}_G) = \int_{\mathcal{W}_G} \frac{\omega_G^L}{L!}$$
(8.43)

$$= \frac{1}{L!} \sum_{i_1, \dots, i_L} C^{\text{cl}}_{i_1, \dots, i_L} t^{\mathbb{R}}_{i_1}(z) \cdots t^{\mathbb{R}}_{i_L}(z) , \qquad (8.44)$$

where the  $C^{\text{cl}}_{i_1,\dots,i_L}$  are the (classical) intersection numbers of  $\mathcal{M}_G$ , which can be computed explicitly.

**Example 8.6** (One Loop Fishnet Graph – Volume Interpretation). In the way described here, we can interpret the one-loop fishnet integral of example 8.4 as a

normalised volume. In particular,  $Vol_{cl}(W_{1,1}) = t_{G_{1,1}^1}^{\mathbb{R}}(z) = Im \tau_1$ , which corresponds to the area of the fundamental parallelogram (with sides  $(1, \tau_1)$ ) defining the elliptic curve  $W_{G_{1,1}^1}$  associated with the one-loop fishnet graph. Comparing this with eq. (8.34) we find that the one-loop ladder integrals are proportional to the classical volume of the mirror CY:

$$\phi_{1,1}(\lambda) = \frac{4}{\pi^2} |K(\chi)|^2 Vol_{cl}(W_{1,1}), \qquad (8.45)$$

The prefactor, which is proportional to  $\Pi_{1,1,0}$ , sets the overall scale.

The same observation holds for multi-loop (and even multi-parameter) traintrack integrals<sup>5</sup> However, starting from three loops, the exponential of the Kähler potential is no longer proportional to  $\operatorname{Vol}_{\operatorname{cl}}(\mathcal{W}_G)$ . This is expected, as it is well established in string theory and mirror symmetry that for L > 2, the volumes of CY L-folds receive instanton corrections of the form  $e^{-t_i^{\mathbb{R}}}$ . These corrections are incorporated in the quantum volume of  $\mathcal{W}_G$ :

Claim 2: The function  $\phi_G(\chi)$  is determined by the *quantum* volume of the mirror CY  $\mathcal{W}_G$  of the graph's CY  $\mathcal{M}_G$ :

$$\phi_G(\boldsymbol{\chi}) = |\Pi_{G,0}(\boldsymbol{\chi})|^2 \operatorname{Vol}_{\mathbf{q}}(\mathcal{W}_G). \tag{8.46}$$

One can pose the following requirements for a volume

- 1. It is real and positive.
- 2. In the limit  $\lambda_i \to 0$  (or equivalently, in the large volume limit  $t_i^{\mathbb{R}} \to \infty$ ), it approaches the classical volume given in (8.43).
- 3. It is monodromy-invariant, meaning it extends uniquely over the complex moduli space the distinguishing quality of the single valued version of a period.

In (8.46),  $\operatorname{Vol}_{\mathbf{q}}(W_G)$  satisfies 1. and 2. but not 3. In the normalization  $\widetilde{\Pi}_{G,0}(\boldsymbol{\lambda}) = 1 + \mathcal{O}(\boldsymbol{\lambda})$ , one could alternatively define  $\phi_G$  itself as the quantum volume, fulfilling 1.-3.. Thus, we interpret  $\phi_G$  as the *calibrated volume*, as it has all three properties.

#### 8.2.3 Relations Between One-Parameter Fishnets

We focus here again on four-point square (V=4) fishnet integrals, as depicted in figure 8.3. We briefly sketch how the properties of the associated CY families and in particular their PFI can be used to obtain relations between these integrals. For a detailed discussion we refer to [37].

#### Periods and Operators for Ladder Integrals

The ladder integral operators  $\mathbb{O}_{1,N} = \mathbb{O}_N$  are given in (8.36). The holomorphic periods annihilated by these operators take the form given in (8.38).

<sup>5</sup>Traintrack integrals are the multi-parameter versions of the ladder integrals, with M=1but possibly with several distinct external parameters.

**Hadamard products** With the Hadamard product \* defined as in (3.116), we see that

$$\Pi_{N,0} = \Pi_{p,0} * \Pi_{N-p-1,0}, \quad 0 \le p \le N-1,$$
(8.47)

Thus, the Picard-Fuchs operators can also be constructed iteratively as Hadamard products:

$$\mathbb{O}_N = \mathbb{O}_p * \mathbb{O}_{N-p-1} = \mathbb{O}_0 * \mathbb{O}_{N-1} = \mathbb{O}_0^{*(N+1)}, \quad 0 \le p \le N-1.$$
 (8.48)

**Symmetric Square** Every CY operator of degree 3 is equivalent to the symmetric square of a CY operator of degree 2 [321, 335, 336]. In that sense, we find

$$\mathbb{O}_2 = \operatorname{Sym}^2(\mathbb{O}_1). \tag{8.49}$$

In particular, we can deduce from this result that the periods of the two-loop traintracks can be written as symmetric products of the on-loop traintrack periods, which are functions of elliptic integrals K.

#### Periods and Operators for One-Parameter Fishnets with M > 1

We find empirically – by computing the holomorphic periods up to (M, N) = (2, 4) and (3, 3) – that

$$\Pi_{M,N,0}(z) = D_{01\cdots(M-1)}^{(W)}(z),$$
(8.50)

where we set W := M + N - 1 and – as in eq. (3.18) – define

$$D_{I}^{(W)}(z) := \det \begin{pmatrix} \Pi_{W,i_{1}}(z) & \dots & \Pi_{W,i_{M}}(z) \\ \theta_{z}\Pi_{W,i_{1}}(z) & & \theta_{z}\Pi_{W,i_{M}}(z) \\ \vdots & \ddots & \vdots \\ \theta_{z}^{M-1}\Pi_{W,i_{1}}(z) & \dots & \theta_{z}^{M-1}\Pi_{W,i_{M}}(z) \end{pmatrix} \text{ with } I = (i_{1}, \dots, i_{M}).$$

$$(8.51)$$

Thus, the Picard-Fuchs operator of the CY  $\mathcal{M}_{M,N}$  is the  $M^{\text{th}}$  exterior power of a certain ladder operator  $\mathbb{O}_W$ ,

$$\mathbb{O}_{M,N} \sim \wedge^M \mathbb{O}_W \sim \wedge^M \mathbb{O}_0^{*(W+1)}. \tag{8.52}$$

This relation also shows that  $\mathbb{O}_{M,N}$  and  $\mathbb{O}_{N,M}$  are equivalent:

$$\mathbb{O}_{M,N} \sim \wedge^M \mathbb{O}_W \sim \wedge^{W-M+1} \mathbb{O}_W = \wedge^N \mathbb{O}_W \sim \mathbb{O}_{N,M},$$
 (8.53)

This implies that two one-parameter fishnet graphs that are just rotated versions of each other differ by a simple prefactor – as one would expect:  $\mathcal{M}_{M,N}$  and  $\mathcal{M}_{N,M}$  share the same periods, differing only by multiplication with an algebraic function of  $\chi$ . Furthermore, this symmetry allows us to focus solely on the cases where  $M \leq N$ . Finally, from eq. (8.52) and eq. (8.53), we deduce that

$$\mathbb{O}_{M,N} \sim \wedge^M \mathbb{O}_{1,M+N-1} , \qquad (8.54)$$

where without restriction of generality  $M \leq N$ .

#### **Intersection Matrices**

We have now seen, how the Picard-Fuchs operators and periods obtained from different one-parameter fishnet graphs can be related. The fishnet integrals themselves are by (8.30) computed as bilinears of periods with the intersection matrix  $\Sigma$ . Thus, in order to understand what the aforementioned relations imply for the fishnet integrals, we also need to understand how the intersection matrices  $\Sigma_{M,N}$  for  $\mathcal{M}_{M,N}$  of different graphs are related. The intersection matrices of ladder integrals take the form given in (8.41). In fact, even for M > 1, we can obtain an object that in our applications takes the role of the intersection matrices from intersection matrices of smaller graphs and in particular ladders:

$$\left(\widetilde{\Sigma}_{M,N}\right)_{IJ} = \det\left[\Sigma_W(I,J)\right] = \det\left[\left(\Sigma_W\right)_{ij}\right]_{\substack{i \in I \\ i \in J}}.$$
 (8.55)

The derivation of this relation can be found in [37] and relies on understanding the relations between the respective periods.

#### **Basso-Dixon Relations**

From the objects defined above, we write down the following expression:

$$\phi_{M,N}(\chi) = (-i)^{(MN)^2} D_I^{(W)}(\bar{\chi}) \left( \tilde{\Sigma}_{M,N} \right)_{IJ} D_J^{(W)}(\chi) . \tag{8.56}$$

We find experimentally, that for all tested cases, these expression agrees with the one obtained directly from (8.26). Thus, we can express fishnet integrals as bilinears of determinants of periods. On the other hand, the Basso-Dixon (BD) formula states, that they can be expressed as determinants of ladder integrals, i.e. as determinants of bilinears of periods. We now demonstrate how the BD formula in D=2 dimensions emerges from the CY geometry. In the following  $\varepsilon_{a_1\cdots a_M}$  denotes the Levi-Civita tensor of rank M, i.e., the totally antisymmetric tensor in M indices. We compute

$$\det \left(\theta_{\bar{\chi}}^{i-1}\theta_{z}^{j-1}\phi_{W}(\chi)\right)_{1\leq i,j\leq M}$$

$$= \frac{1}{M!}\varepsilon_{a_{1}\cdots a_{M}}\varepsilon_{b_{1}\cdots b_{M}} \left[\theta_{\bar{\chi}}^{a_{1}-1}\theta_{\chi}^{b_{1}-1}\phi_{W}(\chi)\right] \cdots \left[\theta_{\bar{\chi}}^{a_{M}-1}\theta_{\chi}^{b_{M}-1}\phi_{W}(\chi)\right]$$

$$= \frac{(-i)^{MW^{2}}}{M!}\varepsilon_{a_{1}\cdots a_{M}}\varepsilon_{b_{1}\cdots b_{M}} \left[\theta_{\bar{\chi}}^{a_{1}-1}\Pi_{W,i_{1}}(\bar{\chi})\left(\Sigma_{W}\right)_{i_{1}j_{1}}\theta_{\chi}^{b_{1}-1}\Pi_{W,j_{1}}(\chi)\right] \times \cdots$$

$$\times \left[\theta_{\bar{\chi}}^{a_{M}-1}\Pi_{W,i_{M}}(\bar{\chi})\left(\Sigma_{W}\right)_{i_{M}j_{M}}\theta_{\chi}^{b_{M}-1}\Pi_{W,j_{M}}(\chi)\right]$$

$$= \frac{(-i)^{MW^{2}}}{M!}\left[\varepsilon_{a_{1}\cdots a_{M}}\theta_{\bar{\chi}}^{a_{1}-1}\Pi_{W,1}(\bar{\chi})\cdots\theta_{\bar{\chi}}^{a_{M}-1}\Pi_{W,i_{M}}(\bar{\chi})\right]\left(\Sigma_{W}\right)_{i_{1}j_{1}}\cdots\left(\Sigma_{W}\right)_{i_{M}j_{M}} \times$$

$$\times \left[\varepsilon_{b_{1}\cdots b_{M}}\theta_{\chi}^{b_{1}-1}\Pi_{W,j_{1}}(\chi)\cdots\theta_{\chi}^{b_{M}-1}\Pi_{W,j_{M}}(\chi)\right].$$

$$(8.57)$$

We have, with  $J = (j_1, \ldots, j_M)$ ,

$$\varepsilon_{b_1\cdots b_M}\theta_{\chi}^{b_1-1}\Pi_{W,j_1}(\chi)\cdots\theta_{\chi}^{b_M-1}\Pi_{W,j_M}(\chi) = \varepsilon_{j_1\cdots j_M}\det\left(\theta_{\chi}^b\Pi_{W,j}(\chi)\right)_{1\leq b\leq M,j\in J} \quad (8.58)$$

$$= \varepsilon_{j_1 \cdots j_M} D_J^{(W)}(\chi), \qquad (8.59)$$

and similarly for the anti-holomorphic contribution. Hence,

$$\det \left(\theta_{\bar{\chi}}^{i-1}\theta_{\chi}^{j-1}\phi_{W}(\chi)\right)_{1\leq i,j\leq M}$$

$$= (-i)^{MW^{2}} D_{I}^{(W)}(\bar{\chi}) \left[\frac{1}{M!} \varepsilon_{i_{1}\cdots i_{M}} \varepsilon_{j_{1}\cdots j_{M}} \left(\Sigma_{W}\right)_{i_{1}j_{1}} \cdots \left(\Sigma_{W}\right)_{i_{M}j_{M}}\right] D_{J}^{(W)}(\chi)$$

$$= (-i)^{MW^{2}} D_{I}^{(W)}(\bar{\chi}) \det \left[\left(\Sigma_{W}\right)_{ij}\right]_{i\in I,j\in J} D_{J}^{(W)}(\chi)$$

$$= (-i)^{MW^{2}} D_{I}^{(W)}(\bar{\chi}) \left(\widetilde{\Sigma}_{M,N}\right)_{IJ} D_{J}^{(W)}(\chi)$$

$$= (-i)^{MW^{2}} i^{(MN)^{2}} \phi_{M,N}(\chi) .$$
(8.60)

To summarize, we see that we have the relation:

$$\phi_{M,N}(\chi) = (-i)^{(MN)^2 - M(M+N-1)^2} \det \left(\theta_{\bar{\chi}}^{i-1} \theta_{\chi}^{j-1} \phi_{M+N-1}(\chi)\right)_{1 \le i,j \le M} . \tag{8.61}$$

<sup>6</sup>We emphasize that, a priori, the final equality is directly justified only for the lower-loop cases, where we explicitly verified the determinant representation of the Basso-Dixon periods; see the discussion around (8.50). However, since it is established in [328] that the 2D Basso-Dixon formula holds universally, it follows that this equality must also hold in full generality.

The above relation allows the fishnet integral  $\phi_{M,N}(\chi)$  to be expressed,<sup>6</sup> up to an overall constant factor, as an  $M \times M$  determinant involving the derivatives of the ladder integral with W = M + N - 1 loops. This expression is, in fact, identical to the BD formula for 2D fishnet integrals presented in ref. [328]. The only apparent differences arise from our normalization of the ladder integrals and the specific choice of the conformal cross ratio. Equation (8.61) demonstrates that the BD formula for  $\phi_{M,N}(z)$  in two dimensions is equivalent to the assertion that  $\mathbb{O}_{M,N} = \wedge^M \mathbb{O}_W$ . However, this statement has only been explicitly verified for low loop orders and remains conjectural in the general case. Nevertheless, since the BD formula was independently proven in ref. [328], it follows that  $\mathbb{O}_{M,N} = \wedge^M \mathbb{O}_W$  holds for all values of (M,N). This relation also allows to find relations for the quantum volume of the associated CY families due to (8.46).

## Chapter 9

## Conclusion

The unifying objective of the projects presented in this thesis is to develop a deeper understanding of the mathematical structures underlying Feynman integrals. The two central classes of objects investigated throughout are the geometries and twisted (co-)homology groups related to these integrals. In particular, we are interested in the interplay between these structures. We explore this both through general considerations and through concrete examples of integral families that illustrate interesting key features.

We summarise here the key points of the new results presented in this thesis, which were obtained during the time of my PhD in varying collaborations:

- The twisted Riemann bilinear relations and (cuts of) Feynman integrals [Chapter 5]: We explored for the first time explicitly and in detail the role of the twisted Riemann bilinear relations for cuts of Feynman integrals. This study revealed that one can always find bilinear relations for maximal cuts of Feynman integrals from these TRBRs and that many of the existing bilinear relations in the literature are just manifestations of these. Additionally, we found that for a basis of differentials in  $\varepsilon$  and C-form the intersection matrix becomes constant in the external parameters. This finding constitutes as step forward in understanding generic properties of canonical bases for Feynman integrals. Additionally, it provides a tool for finding this basis in general, which we illustrate with several specific examples, most prominently the hyperelliptic Lauricella functions.
- Canonical bases for hyperelliptic Lauricella functions [Chapter 6]: We constructed canonical differential equations for Lauricella hypergeometric functions associated with genus-one and genus-two curves using the algorithm of [24] supplemented with our findings on the related intersection matrices. Additionally we analyse the resulting function space. As these Lauricella functions serve as a general model for maximal cuts of hyperelliptic Feynman integrals, such as the non-planar crossed box family, this result is a first step for the analytic computation of such Feynman integrals.
- Unequal-mass kite family [Chapter 7]: We analytically computed the

five-parameter kite integral family in  $D = 2 - 2\varepsilon$ , which constitutes the most generic two-point two-loop scalar integral family that one can write down. In particular we solved the problem of how to parametrise the kinematic space of this integral family on the two related tori by integrating over maximal cuts. Additionally, we systematically write the connection matrix in forms on these tori.

• (Fishnet) integrals in two dimensions [Chapter 8]: We explored how 2D Feynman integrals can be computed as single-valued versions of Aomoto-Gelfand hypergeometric functions and in particular as double copies of hypergeometric functions. Additionally, we found that conformal fishnet integrals in two dimensions, which are related to Calabi-Yau families, can be computed from periods of these Calabi-Yau varieties. This result allows us to study fishnet integrals with geometric tools and properties of Calabi-Yau periods.

Whilst reviewing iterated integrals on the discussed varieties, we also briefly mentioned ongoing work on a coaction-like map for iterated Eisenstein integrals. Together, all of these results highlight the mentioned mathematical structures (can) play for the computation of Feynman integrals. They provide new tools for identifying relations, constructing the canonical form and finding deeper algebraic and modular structures. This is not only relevant for high-precision particle physics, but also for amplitudes in gravity, cosmology, and string theory. Naturally, in the computation of real world or phenomenological observables provides a variety of different obstacles and the computation of multi-loop massive Feynman integrals is merely a small piece of the puzzle.

At the same time there is a variety of interesting questions building on the results presented here.

- There are many examples for canonical bases of Feynman integrals in the literature. In particular, we have employed the algorithm of [24] supplemented with our results on intersection matrices for several examples. This suggests that it should always be possible to find a canonical basis, but it would be interesting to prove this existence and in doing so to understand the generic properties beyond well-understood examples.
- Beyond theoretical considerations, it would be interesting use the results on the intersection matrix to find the canonical basis for more complicated examples.
- The parametrisation of Feynman integral families on complex geometries is non-trivial but can be crucial as we saw for the unequal mass kite integral family. It would be interesting to see whether the ideas applied there are also applicable for other multi-mass Feynman integral families associated to one or more complicated geometries.
- Having understood how to find a canonical basis for a model of the nonplanar crossed box maximal cut, it would be interesting to solve the full

#### Chapter 9

integral family, using the understanding on hyperelliptic canonical bases we developed.

Thus, connection between mathematics and physics in theoretical particle physics and specifically the integrals appearing in this field remains an interesting area of study. With the results presented in this thesis, we made some specific contributions to this field and hope they will be useful for future researchers.

## Appendix A

## Basic Objects in Mathematics

In this appendix, we collect definitions for some basic objects in mathematics that appear in the main part of the thesis and are assumed to be basic knowledge.

**Definition A.1** (Algebraic number field). An algebraic number field  $\mathbb{K}$  is a finite-degree field extension of the rational numbers  $\mathbb{Q}$ . Every element of  $\mathbb{K}$  is algebraic over  $\mathbb{Q}$ , meaning it satisfies a non-zero polynomial equation with coefficients in  $\mathbb{Q}$ .

**Definition A.2** (Sheaf). A sheaf  $\mathcal{F}$  on a topological space X is a functor from the category of open sets of X (with inclusions as morphisms) to a category (typically sets, groups, or rings), satisfying the following conditions:

- 1. <u>Locality</u>: If  $\{U_i\}$  is an open cover of U and two sections  $s, t \in \mathcal{F}(U)$  satisfy  $\overline{s|_{U_i} = t|_{U_i}}$  for all i, then s = t in  $\mathcal{F}(U)$ .
- 2. Gluing: If  $s_i \in \mathcal{F}(U_i)$  are sections over an open cover  $\{U_i\}$  such that  $s_i$  and  $s_j$  agree on overlaps  $U_i \cap U_j$ , then there exists a unique  $s \in \mathcal{F}(U)$  such that  $s|_{U_i} = s_i$  for all i.

In the context of twisted (co-)homology groups, we need specific sheaves:

**Definition A.3** (Local System). A sheaf  $\mathcal{F}$  is a local system local system if it is locally constant and finitely generated, i.e., for every  $x \in X$  there is a neighbourhood  $x \in U$  such that  $\mathcal{F}_U \cong \underline{V}_U$  for some finitely generated k-module V. We denote the category of local systems of X by  $Loc_k(X)$ .

In fact, the so-called *geometries* we study in this thesis are in many cases actually *algebraic varieties*, defined by some polynomials. In the simplest (and in this thesis most common) case that means we consider algebraic curves.

**Definition A.4** (Algebraic Curve). A function f(z) defined on a domain  $\mathcal{D}$  is called **algebraic** if there exists a polynomial function P(w, z), such that P(f(z), z) = 0 for  $z \in \mathcal{D}$ . The locus

$$C := \{ (w, z) \in \mathbb{C}^2 | P(w, z) = 0 \}$$
(A.1)

is called an algebraic curve. Here, we consider mostly (hyper-)elliptic curves, which are defined on  $\mathbb{C}$  or on  $\mathbb{PC}$  with homogenous coordinates. In the latter case, the polynomial of course also needs to be homogenous to have a well-defined zero set.

**Definition A.5** (Branch point). Let  $f: M \to N$  be a holomorphic covering. A point  $P \in M$  is called a branch point of f if it has no neighbourhood V such that  $f|_V$  is injective. A covering without branch points is called unramified.

The number of branch points of a holomorphic covering of a compact Riemann surface is generally finite. One can assign different notions of genus to algebraic curves.

**Definition A.6.** Arithmetic Genus If d is the degree of the polynomials, the arithmetic genus of the algebraic curve is

$$g = \frac{1}{2}(d-1)(d-2). \tag{A.2}$$

For smooth curves the arithmetic genus equals the geometric genus.

**Definition A.7** (Lattice). A subgroup U of a finite dimensional real vector space V is a lattice, if it is discrete and if V/U is compact.

**Definition A.8** (Euler Number). The Euler number  $\chi$  of a topological space X, denoted by  $\chi(X)$ , is a topological invariant defined as the alternating sum of the ranks of its homology groups:

$$\chi(X) = \sum_{i=0}^{\dim X} (-1)^i \dim H^i(X, \mathbb{Q}).$$

The Calabi-Yau manifolds we review in section 3.3 and used to compute fishnet integrals in chapter 8 are special instances of Kähler manifolds. We will introduce the basic objects related to these, that are used in definition 3.14 of a Calabi-Yau manifold.

We already introduced complex coordinates on a complex manifold in (3.1). Here we give the basic definitions for these objects. A complex manifold can be obtained from an even dimensional real one by attaching a complex structure, requiring the existence of certain structures.

**Definition A.9** (Almost complex manifold). An even dimensional real manifold is an almost complex manifold, if it has a differentiable endomorphism of tangent bundles:  $J: TM \to TM$  with  $J^2 = -1$ .

**Definition A.10** (Hermitian metric). A hermitian metric is a positive-definite inner product  $TM \otimes TM \to \mathbb{C}$ . In local coordinates, it can be written as  $ds^2 = \sum_{i,j}^n G_{ij}(w) dz_i \otimes d\bar{z}_j$ . The fundamental form of the metric is defined as

$$\omega = i \sum_{i,j=1}^{n} G_{ij} dz_i \wedge d\bar{z}_j.$$
 (A.3)

For a complex manifold to be Kähler, its metric must satisfy the Kähler condition:

**Definition A.11** (Kähler metric). An hermitian metric  $G_{ij}$  whose fundamental form is closed  $d\omega$  is called a Kähler metricand the form  $\omega$  is called the Kähler form.

## Appendix B

## Computing Intersection Matrices

In this appendix, we give details on the computation of intersection numbers for twisted (co-)homology groups in practice. In particular, in Section B.1, we explain basic algorithms and methods for their computation in standard cases. In Section B.2, we give more examples and in particular ones we need throughout the main part of the thesis. In the final section B.3, we give a proof for the dependence of specific intersection numbers on a parameter  $\mu$  appearing in the exponent of the twist. This proof is needed for Theorem 4.1.

#### **B.1** Review: Computing Intersection Numbers

Here, we provide a review on how to practically compute intersection numbers for twisted (co-)homology groups as introduced in [40, 41] in the physics literature. Note that by now improvements of this algorithm for specific cases as well as different methods to compute these intersection numbers have been developed in the physics literature [42, 43, 234–237].

#### **B.1.1** Twisted Cohomology Intersection Numbers

The basic algorithm for computing intersection numbers for a twisted cohomology group, where the restriction eq. (4.14) holds<sup>1</sup> is performed iteratively over the integration variables [39, 41, 232]. We first review the univariate case and then explain the iterative process.

Univariate Case Let  $\varphi_L \in H^1_{dR}(X, \nabla_{\Phi})$  and  $\check{\varphi}_R \in H^1_{dR}(X, \check{\nabla}_{\Phi})$  for some twist  $\Phi$  in one variable and an appropriately defined space X. As given in eq. (4.36) the intersection number between these forms is an integral over the full space X. This integral can also be expressed as a sum of residues

$$\langle \varphi_L | \check{\varphi}_R \rangle := \frac{1}{2\pi i} \int_X \varphi_L \wedge \check{\varphi}_R = \sum_{p \in \mathcal{P}_{\Phi}} \operatorname{Res}_{z=p} \left[ \psi_p \check{\varphi}_R \right] ,$$
 (B.1)

<sup>1</sup>We briefly comment on intersection numbers for relative twisted cohomology groups where eq. (4.14) does not need to hold in the end of this Section.

where  $\psi_p$  is the local solution of

$$\nabla_{\Phi}\psi_p = \varphi_L \tag{B.2}$$

around z = p. Thus, a crucial part of computing the intersection number consists of solving the differential equation eq. (B.2) for  $\psi_p$ . Though, since  $\psi_p$  only appears inside a residue in eq. (B.1) we do not need a closed solution but rather a few terms of its Laurent series are sufficient. More specifically, we makes an ansatz of the form

$$\psi_p = \sum_{k=\min}^{\max} c_{p,k} x_p^k, \tag{B.3}$$

with  $x_p$  a local coordinate at p and

$$\min = \operatorname{ord}_{p}(\varphi_{L}) + 1 \text{ and } \max = -\operatorname{ord}_{p}(\check{\varphi}_{R}) - 1,$$
(B.4)

where  $\operatorname{ord}_p$  denotes the lowest non-vanishing order of the expansion in p. If  $\max < \min$ , the local solution  $\psi_p$  does not contribute to eq. (B.1).

**Example B.1** ( $_2F_1$ : Intersection Numbers). We consider as an example the hypergeometric  $_2F_1$  function of Examples 4.2 and 4.5. For the basis and the dual basis we choose eq. (4.46) and eq. (4.47). By expanding these forms in local coordinates, we obtain the following lowest orders and respective minimal and maximal orders we need to compute of the  $\psi_p$ :

Form	$\operatorname{ord}_0$	$\operatorname{ord}_1$	$\operatorname{ord}_{\lambda}$	$\operatorname{ord}_{\infty}$
$\varphi_1$	0	0	0	-2
$\varphi_2$	0	0	0	-3
$\check{\varphi}_1$	-1	-1	-1	1
$\check{arphi}_2$	-1	-1	-1	0

p	0	1	λ	$\infty$
$\min_1$	1	1	1	-1
$\min_2$	1	1	1	-2
$\max_1$	0	0	0	-2
$\max_2$	0	0	0	-1

Table B.1: Lowest orders in the local expansion of the bases eq. (4.46) and eq. (4.47) and the corresponding values for min and max.

Most contributions to the intersection numbers vanish, which simplifies the calculation.

 $\langle \varphi_1 | \check{\varphi}_1 \rangle$ : Reading off from table B.1, we find, that  $min_1 > max_1$  for all poles. Thus, we immediately see:

$$\langle \varphi_1 | \check{\varphi}_1 \rangle = 0.$$
 (B.5)

 $\langle \varphi_2 | \check{\varphi}_2 \rangle$ : Reading off from table B.1, we find, that  $min_2 > max_2$  is true only for the pole at  $\infty$ . With the differential equation of eq. (B.2) we find the series

$$\psi_{\infty}^{22} = \left(\frac{1}{2 - a + c}\right) \frac{1}{z_{\infty}^{2}} + \left(\frac{b - c + a\lambda}{(a - 2 - c)(a - c - 1)}\right) \frac{1}{z_{\infty}} + \mathcal{O}\left(z_{\infty}^{0}\right)$$
(B.6)

in the local coordinate  $z_{\infty}$  near  $\infty$ . Consequently, we obtain:

$$\langle \varphi_2 | \check{\varphi}_2 \rangle = Res_{z=\infty} \left[ \psi_{\infty}^{22} \check{\varphi}_2 \right] = \frac{1 - a + b + \lambda (1 + c)}{(1 - a + c)(2 - a + c)}. \tag{B.7}$$

Similarly, we obtain the off-diagonal intersection numbers and overall the intersection matrix is

$$\mathbf{C}(\lambda) = \begin{pmatrix} 0 & \frac{1}{1-a+c} \\ \frac{1}{2-a+c} & \frac{1-a+b+\lambda(1+c)}{(1-a+c)(2-a+c)} \end{pmatrix}.$$
 (B.8)

Multivariate Case We follow here the algorithm given in [41] based on [46] and also refer to these sources for more details and many instructive examples. This algorithm relies on computing the intersection numbers recursively integration variable by integration variable and the univariate intersection numbers are obtained by the formulae already given above. In that sense, we now consider a generic twisted cohomology group  $H^n_{dR}(X, \nabla_{\Phi})$  and its dual  $H^n_{dR}(X, \check{\nabla}_{\Phi})$ . Elements from these cohomology groups can be decomposed into components of a n-1 dimensional space and a one-dimensional space:

$$\langle \varphi_L | = \sum_{i=1}^{d_{n-1}} \langle e_i^{(n-1)} | \wedge \langle \varphi_{L,i}^n | \in H^n_{dR}(X, \nabla_{\Phi})$$
 (B.9)

$$|\check{\varphi}_R\rangle = \sum_{i=1}^{d_{n-1}} |\check{h}_i^{(n-1)}\rangle \wedge |\check{\varphi}_{R,i}^n\rangle \in \mathrm{H}^{\mathrm{n}}_{\mathrm{dR}}(\mathrm{X}, \check{\nabla}_{\Phi}),$$
 (B.10)

where  $d_{n-1}$  denotes the dimension of the subspace of the twisted cohomology group in variables  $z_1, \ldots, z_{n-1}$ . The forms  $e_i^{(n-1)}$ ,  $\check{h}_i^{(n-1)}$  are basis elements<sup>2</sup> of these (n-1)-variable subspaces and  $\varphi_{L,i}^n$ ,  $\check{\varphi}_{R,i}^n$  are one-forms in the variable  $z_n$ . We assume, that we have already calculated the intersection numbers of the n-1-variable subspace and the intersection matrix with entries

$$(\mathbf{C}_{(n-1)})_{ij} = \langle e_i^{(n-1)} | \check{h}_j^{(n-1)} \rangle \tag{B.11}$$

and compute the projection onto the (n-1)-variable subspaces as

$$\langle \varphi_{L,i}^n | = \langle \varphi_L | h_j^{(n-1)} \rangle \left( \mathbf{C}_{(n-1)}^{-1} \right)_{ii}$$
 (B.12)

$$|\check{\varphi}_{R,i}^n\rangle = \left(\mathbf{C}_{(n-1)}^{-1}\right)_{ij} \langle e_j^{(n-1)} | \check{\varphi}_R \rangle.$$
 (B.13)

Then the recursive formula for the intersection number is

$$\langle \varphi_L | \check{\varphi}_R \rangle = \sum_{p \in \mathcal{P}_n} \operatorname{Res}_{z_n = p} \left( \psi_i^{(n)} \left( \mathbf{C}_{(n-1)} \right)_{ij} \varphi_{R,j}^{(n)} \right),$$
 (B.14)

where the functions  $\psi_i^{(n)}$  are defined as the solutions of the system of differential equations

$$\partial_{z_n} \psi_i^{(n)} + \psi_j^{(n)} \hat{\boldsymbol{B}}_{ji}^{(n)} = \varphi_{L,i}^{(n)} \text{ with } \hat{\boldsymbol{B}}_{ji}^{(n)} = \langle (\partial_{z_n} + \omega_{\Phi,n}) e_j^{(n-1)} | \check{h}_k^{(n-1)} \rangle \left( \mathbf{C}_{(n-1)}^{-1} \right)_{ki}.$$
(B.15)

<sup>2</sup>Note that a suitable choice for these *inter-mediate* bases greatly simplifies the computation in praxis.

and  $\mathcal{P}_n$  is the set of poles of  $\hat{\boldsymbol{B}}^{(n)}$ . We refer to the literature mentioned above for more details.

Relative Twisted Cohomology Intersection Numbers The only significant difference when considering forms from relative twisted cohomology groups in the framework discussed in this thesis is the appearance of the forms  $\delta(...)$  in the dual forms. In the univariate case, the local intersection numbers of  $\delta$  forms are given by simple residue

$$\langle \varphi | \delta_{z_i}(1) \rangle = \operatorname{Res}_{z=z_i} \left( \frac{\Phi}{\Phi|_{z=z_i}} \varphi \right)$$
 (B.16)

and the intersection numbers twisted of co-cycles that do not involve these objects are computed exactly like in the non-relative case of eq. (B.1):

$$\langle \varphi | [\phi_{\text{reg}}]_c \rangle = \sum_k \text{Res}_{z=z_k}(\psi_k \varphi).$$
 (B.17)

The multi-variate case generalises in a similar way: The multivariate intersection number between a twisted co-cycle  $\varphi_L$  in n variables and a twisted dual cocycle that takes the form

$$\delta_{z_1,\dots,z_m} \left( \check{\varphi}_R \right) = \delta_{z_1,\dots,z_m} \left( f_R \, \mathrm{d} z_{m+1} \wedge \dots \wedge \mathrm{d} z_n \right) \tag{B.18}$$

is computed by the prescription

$$\langle \varphi_L | \delta_{z_1, \dots, z_m} (\check{\varphi}_R) \rangle = \left\langle \operatorname{Res}_{z_1 = 0, \dots, z_m = 0} \left( \frac{\Phi}{\Phi|_{z_1, \dots, z_m \to 0}} \varphi_L \right) | \check{\varphi}_R \right\rangle.$$
 (B.19)

The outer n - m-variate intersection number can be computed in the non-relative framework. For further details and examples we refer to [49, 239].

#### B.1.2 Twisted Homology Intersection Numbers

♠ The review and examples presented here closely follow 8.1 is based on published results [36], which were obtained in collaborations with Claude Duhr.

The discussion we give in the following Section is applicable for cases, where all factors  $L_i(z)$  of the twist are linear in the internal variables z, meaning the  $\Sigma_i$  are hyperplanes defined by linear equations and where the condition in eq. (4.14) holds. We comment on what changes if eq. (4.14) does not hold and also briefly comment on degenerate arrangements at the end of this Section. We follow the notations and definitions introduced in Example 4.3. We aim to give a pedagogical introduction, following [228, 231, 233, 281, 337–345]. The following factors commonly appear in the computation of homology intersection numbers due to analytic continuations of the multi-valued twist:

$$\mathfrak{c}_j = \exp(2\pi i \alpha_j) \text{ and } \mathfrak{d}_j = \mathfrak{c}_j - 1.$$
(B.20)

#### See also:

Relative twisted cohomology groups are discussed in Subsection 4.2.

#### See also:

The computation of homology intersection numbers plays an important role for computing single-valued versions of twisted periods (e.g. single-valued hypergeometric functions of Section 4.3.2 and thus for computing single-valued Feynman integrals which are the topic of Chapter 8).

#### Chapter B

Their products are denoted by

$$\mathfrak{c}_{jk\dots} = \mathfrak{c}_j \mathfrak{c}_k \dots \text{ and } \mathfrak{d}_{jk\dots} = \mathfrak{c}_{jk\dots} - 1.$$
 (B.21)

Let  $|\gamma_B| \in H_n(X, \check{\mathcal{L}}_{\Phi})$  and  $[\check{\gamma}_A| \in H_n^{lf}(X, \mathcal{L}_{\Phi})$  with the local systems defined by a twist  $\Phi$  with only linear factors. Both of these cycles can be decomposed in embedded simplices as in eqs. (4.21) and eq. (4.28). The intersection number of these cycles is

$$[\check{\gamma}_A|\gamma_B] = \sum_{v} [\check{\gamma}_A|\gamma_B]_v = \sum_{\triangle,\square} \sum_{\{v\} \in \triangle \cap \square} c_\triangle d_\square \Phi_\triangle|_v \Phi_\square^{-1}|_v I_v(\triangle,\square)$$
 (B.22)

with the sum taken over all topological intersection points v of the simplices  $\triangle$  and  $\square$  and  $I_v(\triangle,\square)$  the local topological intersection number at an intersection v:

$$I_{v}(\triangle, \square) = \begin{cases} +1 & \triangle \text{ and } \square \text{ intersect with positive orientation at } v : \\ -1 & \triangle \text{ and } \square \text{ intersect with negative orientation } v : \end{cases}$$
(B.23)

We also denote  $[\tilde{\gamma}_A|\gamma_B]_v$  the local intersection number at v. In the following, we illustrate the computation of uni- and multivariate intersection numbers with this formula.

Univariate intersection numbers There are three distinct configurations in which the twisted cycle and the dual locally finite cycle can intersect. We examine each case individually, as outlined in ref. [233].

Local intersection with agreeing branches of the twist.

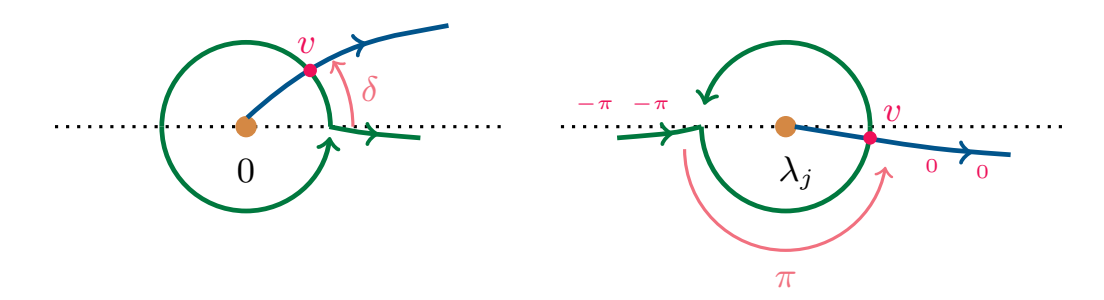


Figure B.1: Illustration of two configurations where the cycle and the dual cycle intersect with agreeing branches of the twist near a point 0 or  $\lambda_i$ .

We consider first a local intersection at a point  $v_{C1}$  near a puncture, where the branches assigned to the cycle and the dual cycle agree. In this configuration, the local intersection number is simply

$$[\check{\gamma}_A|\gamma_B]_{v_{C1}} = \pm \frac{1}{\mathfrak{d}_k}, \tag{B.24}$$

with the factor  $\frac{1}{\delta_k}$  from the regularisation in eq. (4.32). One such configuration is depicted in the left panel of figure B.1 with the cycle  $\gamma_j$  and dual cycles  $\check{\gamma}_j$ : The interval  $\Delta_{\check{\gamma}_j} = (0, \lambda_j)$  meets its regularised version  $\Delta_{\gamma_j}^c$  at the point  $v_{C1}$  near the branch point  $0 \in \Sigma$ . At this point, the twist (more specifically its factor  $L_0^{\alpha_0}(z)$ ) was analytically continued for both, the twisted cycle  $\gamma_j$  and its dual  $\check{\gamma}_j$ . Thus,

$$[\check{\gamma}_j|\gamma_j]_v = \frac{1}{\mathfrak{d}_0} e^{i\delta a_0} e^{-i\delta a_0} (-1) = -\frac{1}{\mathfrak{d}_0}.$$
 (B.25)

A second such configuration is depicted in the right panel of figure B.1. Here, the intersection  $v_{C1}$  is actually the only one between the locally finite dual twisted cycle  $\check{\eta}_{j+1}$  and the twisted cycle  $\eta_j$  (as defined in eq. (4.30)). Apart from the factor  $L_j$ , all factors of the twist agree on the intervals  $(\lambda_j, \lambda_{j+1})$  and  $(\lambda_{j-1}, \lambda_j)$ . Following the choice in eq. (4.31), the arguments of the factor  $L_j(z)$  are given by:

$$\arg[L_j(x)] = \begin{cases} 0 & \text{on the interval } (\lambda_j, \lambda_{j+1}), \\ -\pi & \text{on the interval } (\lambda_{j-1}, \lambda_j). \end{cases}$$
(B.26)

Since the twist is analytically continued along  $S_{\epsilon}(\lambda_{j+1})$ , the argument of its factor  $L_j(z)$  picks up an extremely factor of  $\pi$  at  $v_{C1}$  on  $\Delta_{\eta_j}^c$ . Consequently, the branches of the twist assigned to the two cycles agree again at  $v_{C1}$  and we obtain:

$$[\check{\eta}_{j+1}|\eta_j]_{v_{C1}} = \frac{1}{\mathfrak{d}_j}.$$
 (B.27)

Local intersection near a point  $y_i^{-1}$  with disagreeing branches of the twist.

If the branches of the two cycles disagree at a given point, we generally pick up factors  $\mathfrak{c}_j$  due to the analytic continuation of the twist. An example for this configuration is given in figure B.2, where we depict the intersection between the cycles  $\eta_j$  and  $\check{\eta}_{j-1}$  as defined in eq. (4.30) near  $\lambda_j$ .

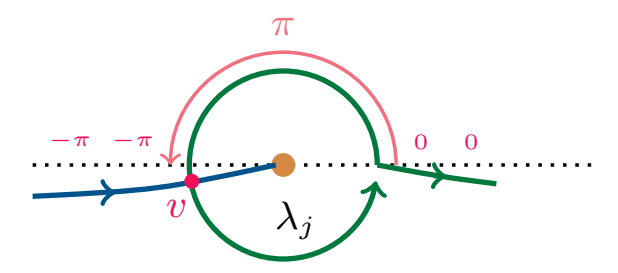


Figure B.2: Illustration of a configuration where the cycle and the dual cycle intersect with disagreeing branches of the twist near a point  $\lambda_i$ .

The arguments of  $L_j$  on the respective intervals are as given in eq. (B.26). In regularising the dual cycle, we additionally perform an analytic continuation of the

#### Chapter B

twist along  $S_{\epsilon}(\lambda_j)$  through the upper half-plane, which gives an extra argument of  $\pi$  at  $v_{C2}$  on  $\Delta_{\eta_j}^c$  for the factor  $L_j$  of  $\Phi$ . Consequently, the twists at this point contribute the factor

$$\Phi|_{v_{C2} \in \Delta_{\eta_j}^c} \Phi^{-1}|_{v_{C2} \in \Delta_{\eta_{j-1}}} = e^{2\pi i \alpha_j} = \mathfrak{c}_j,$$
 (B.28)

and overall, the local intersection number at  $v_{C2}$  is

$$[\check{\eta}_{j-1}|\eta_j]_v = \frac{\mathfrak{c}_j}{\mathfrak{d}_j}.$$
 (B.29)

The latter two examples illustrate why the choice of arguments as indicated in eq. (4.31) is equivalent to saying that the functions are defined on the lower half-plane: As long as we only analytically continue in the lower half-plane, we follow the analytical continuation indicated by this choice of arguments and stay on the same branch. If we analytically continue through the upper half-plane, we land on different branches.

#### Local intersection on the interval between two points

The local intersection number at a point on the interval between two punctures  $\lambda_i$  and  $\lambda_{i\pm 1}$ , where the regularised cycle has not been analytically continued, is just the topological intersection number  $\pm 1$ .

We can now compute the self-intersection of  $\gamma_j$  as defined in eq. (4.29) in two ways:

**Example B.2** (Self-intersection of  $\gamma_j$ ). We generally deform the dual contour  $\Delta_{\gamma_j}$  and depending on the chosen deformation, we get different intersection points, but we see that for the two natural deformations the overall intersection number agrees. Deformation 1: We depict the first possible deformation in figure B.3.

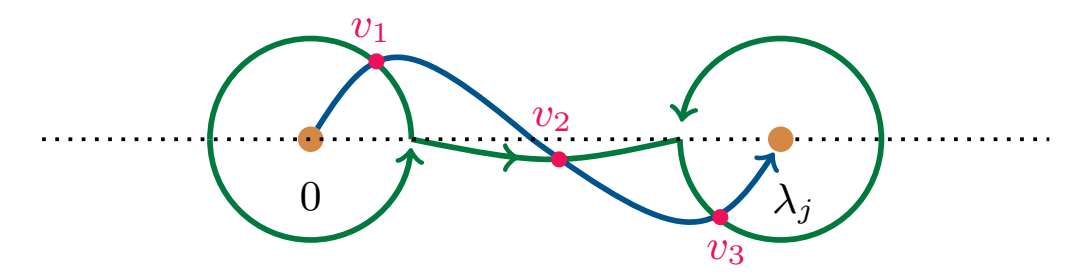


Figure B.3: The self-intersection of the cycle  $\gamma_j$  as defined in eq. (4.29) with three local intersection points  $v_1, v_2$  and  $v_3$  marked.

We already saw how to compute the local intersection number at each of these local intersection points. At  $v_1$  and  $v_3$ , the twist is analytically continued but the branches chosen for both the cycle and the dual cycle agrees. At  $v_2$  we are far away from the branch points. Overall, we find:

$$[\check{\gamma}_j|\gamma_j]_{v_1} + [\check{\gamma}_j|\gamma_j]_{v_2} + [\check{\gamma}_j|\gamma_j]_{v_3} = -\frac{1}{\mathfrak{d}_0} - 1 - \frac{1}{\mathfrak{d}_{j+1}} = -\frac{\mathfrak{d}_{0,j+1}}{\mathfrak{d}_0\mathfrak{d}_{j+1}}.$$
 (B.30)

<u>Configuration 2:</u> We depict the second configuration in figure B.4 and in this case, there are only two local intersection points.

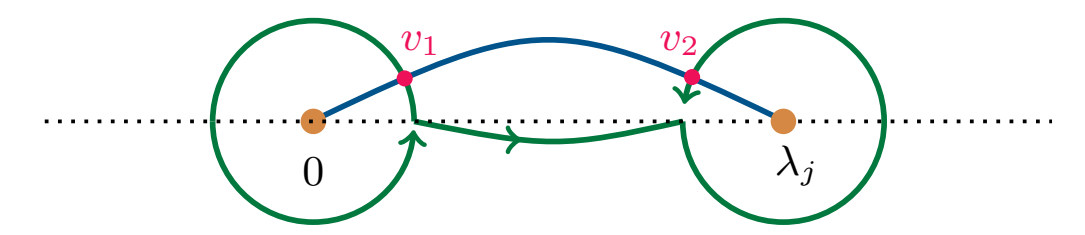


Figure B.4: The self-intersection of the cycle  $\gamma_j$  as defined in eq. (4.29) with two local intersection points  $v_1, v_2$  marked.

At  $v_1$ , the branches of the twist assigned to the cycle and the dual cycle agree and at  $v_2$  they don't, as the branch assigned to the regularised cycle is continued around  $S_{\varepsilon}(\lambda_i)$ . Consequently, we find:

$$[\check{\gamma}_j|\gamma_j] = -\frac{1}{\mathfrak{d}_0} - \frac{\mathfrak{c}_j}{\mathfrak{d}_i} = -\frac{\mathfrak{d}_{0,j+1}}{\mathfrak{d}_0\mathfrak{d}_{j+1}}.$$
 (B.31)

Multi-variate case In general, intersection numbers in multi-variate spaces can be computed recursively as described in refs. [228, 231, 338]. As in the cohomology case, the computation relies on a recursive decomposition of the *n*-variable problem into lower variable computations with the univariate case being computed as already explained above. We do not review this process in detail here but instead just give the resulting formula [228] for the twisted cycles that are supported on chambers bounded by hyperplanes.

As in the univariate case, keeping track of the branch choices is of particular relevance. In diagrams, we indicate with "+" that we choose  $\arg [L_j] = 2n\pi$  in a given region and with "-" that we choose an uneven multiple of  $\pi$  for  $\arg [L_j]$  in that region. Let  $\gamma_D \in \mathrm{H_n}(\mathrm{X}, \check{\mathcal{L}}_\Phi)$  be a twisted cycle supported on the regulated chamber  $\Delta_D$  and  $\check{\gamma}_E \in \mathrm{H_n}(\mathrm{X}, \mathcal{L}_\Phi)$  a dual twisted cycle supported on  $\Delta_E$ . Let  $\Sigma_{D,i_1}, \ldots \Sigma_{D,i_q}$  be the hyperplanes meeting normally along the topological intersection of  $\Delta_E$  and  $\Delta_D$  and  $\Sigma_{i_1} \cap \cdots \cap \Sigma_{i_p}$  the boundary of its interior. In general, we choose the branches

$$\arg[L_{i_1}(\underline{x})] = \dots = \arg[L_{i_q}(\underline{x})] = 0 \text{ on } \Delta_D,$$
 (B.32)

$$\arg[L_{i_1}(\underline{x})] = \dots = \arg[L_{i_p}(\underline{x})] = -\pi \text{ on } \Delta_E$$
 (B.33)

and 
$$\arg[L_{i_{p+1}}(\underline{x})] = \cdots = \arg[L_{i_q}(\underline{x})] = 0 \text{ on } \Delta_E.$$
 (B.34)

For this branch choice, the intersection number is [228]

$$[\check{\gamma}_E|\gamma_D] = (-1)^{n-p} \frac{\mathfrak{c}_{i_1} \dots \mathfrak{c}_{i_p}}{\mathfrak{d}_{i_1} \dots \mathfrak{d}_{i_p}} \left( 1 + \sum_{k=1}^{n-p} \sum_{i_{p+1} \le j_1 \le \dots \le j_k \le i_q} \frac{1}{\mathfrak{d}_{j_1} \dots \mathfrak{d}_{j_k}} \right).$$
(B.35)

#### Chapter B

The summation over the  $j_i$  is taken such that we only consider  $j_1 \leq \cdots \leq j_k$  with

$$\Delta_D \cap \Delta_E \cap \bigcap_{j_i \in j_1 \dots j_k} \Sigma_{j_i} \neq 0, \qquad (B.36)$$

meaning, we are now summing over intersection planes instead of intersection points. Note that in the two-variable case, we can simply read off the self-intersection number from a graphical depiction of the intersecting cycles via the following simple set of rules:

- assign to the barycentre a 1
- assign to each edge a factor  $\frac{1}{\mathfrak{d}_i}$
- $\bullet$  assign to each vertex between two lines ^3 a factor of  $\frac{1}{\mathfrak{d}_i\mathfrak{d}_j}$

The self-intersection number is then the sum of all these contributions assigned to the chamber. Additionally, note that the intersection number of any other choice of arguments, different from eq. (B.32) can be computed by attaching an appropriate prefactor of powers of  $\mathfrak{c}_i$  to eq. (B.35). For the self-intersection number, this prefactor is always one, since we change the branch in the same way for the cycle and its dual. Thus, it is convenient to work in a homology basis where the cycles do not intersect each other and the intersection matrix is diagonal.

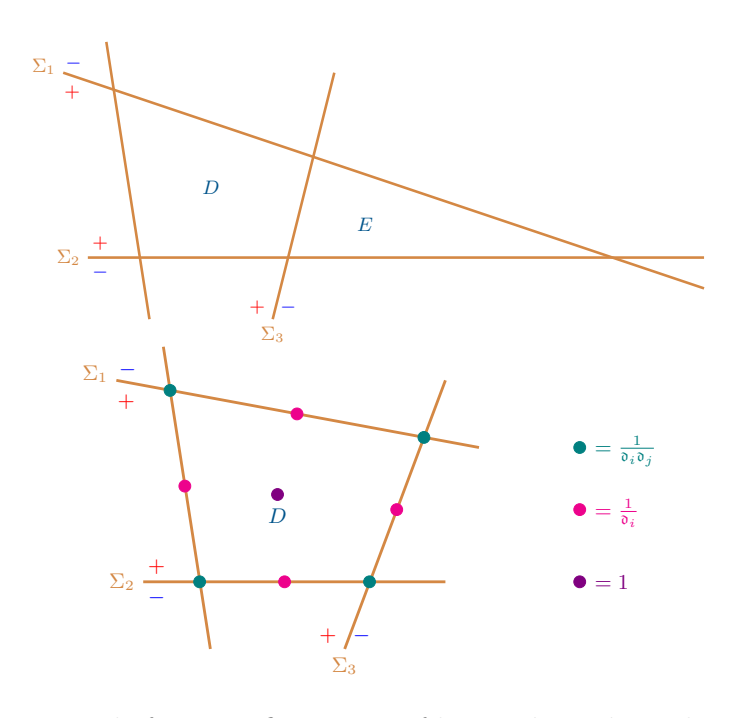


Figure B.5: An example for a configuration of hyperplanes bounding two chambers D and E. The upper panel depicts the configuration of hyperplanes with both chambers and the branch choices of the  $L_i(z)$  indicated by + and -. The lower panel shows just the chamber D and put points on each crossing, boundary and plane to indicate what they contribute to the self-intersection of the chamber labelled D.

<sup>3</sup>The case where more than two lines meet is degenerate and discussed below. **Example B.3.** As an example we consider the arrangement depicted in figure B.5. We consider a cycle and dual cycle supported on D and E respectively and the interior of their topological intersection is just the boundary  $\Sigma_3$ , which is intersected by the hyperplanes  $\Sigma_1$  and  $\Sigma_2$ . We assign to these hyperplanes the following branches of the twist:

$$arg[L_1(\underline{x})] = arg[L_2(\underline{x})] = arg[L_3(\underline{x})] = 0 \text{ on } \Delta_D,$$
 (B.37)

$$arg[L_1(\underline{x})] = arg[L_2(\underline{x})] = 0 \text{ and } arg[L_3(\underline{x})] = -\pi \text{ on } \Delta_E.$$
 (B.38)

Then, by eq. (B.35):

$$[\check{\gamma}_E|\gamma_D] = -\frac{\mathfrak{c}_3}{\mathfrak{d}_3} \left( 1 + \frac{1}{\mathfrak{d}_1} + \frac{1}{\mathfrak{d}_2} \right) = -\frac{\mathfrak{c}_3 \mathfrak{d}_{12}}{\mathfrak{d}_1 \mathfrak{d}_2 \mathfrak{d}_3}. \tag{B.39}$$

Similarly, one obtains the self intersection number of  $\gamma_D$ :

$$[\check{\gamma}_D|\gamma_D] = 1 + \frac{1}{\mathfrak{d}_1} + \frac{1}{\mathfrak{d}_2} + \frac{1}{\mathfrak{d}_3} + \frac{1}{\mathfrak{d}_4} + \frac{1}{\mathfrak{d}_1\mathfrak{d}_2} + \frac{1}{\mathfrak{d}_2\mathfrak{d}_4} + \frac{1}{\mathfrak{d}_4\mathfrak{d}_3} + \frac{1}{\mathfrak{d}_3\mathfrak{d}_4} = \frac{\mathfrak{d}_{13}\mathfrak{d}_{24}}{\mathfrak{d}_1\mathfrak{d}_2\mathfrak{d}_3\mathfrak{d}_4}.$$
(B.40)

As illustrated in the lower panel of figure B.5 one can also obtain this result graphically by adding up contributions from different kinds of boundaries  $(\bullet, \bullet, \bullet)$ .

**Degenerate arrangements** The preceding discussion excluded degenerate arrangements, e.g., with vertices where more than two hyperplanes meet. We briefly comment on these cases and give an example, but for a more detailed discussion, we refer to the literature e.g. ref. [346].

In general, one can consider degenerate arrangements with more than two hyperplanes meeting in a point by blowing up the degenerate vertex into an arrangement in general position. In figure B.6, we show how this would look for a case where m lines meet.

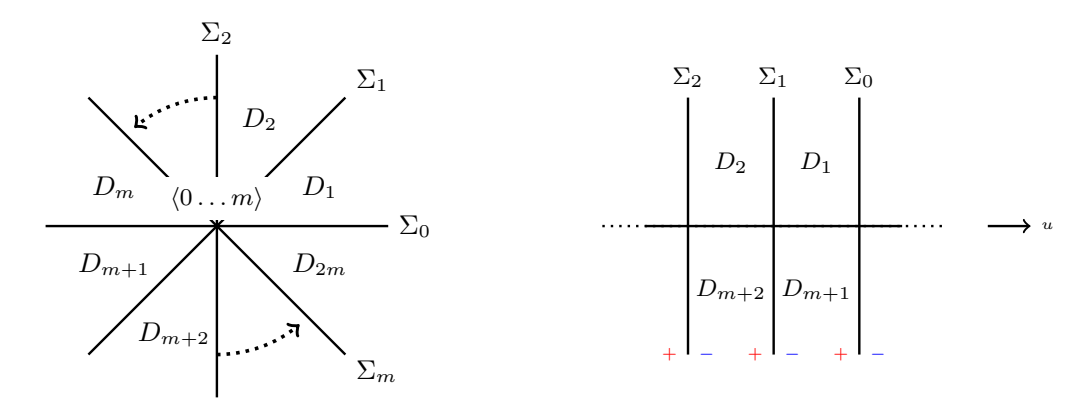


Figure B.6: An illustration of the blow-up of a vertex where m hyperplanes meet.

In that case, one can blow-up the vertex  $\langle 1 \dots m \rangle$  into a hyperplane  $\Sigma_u$  along which a new coordinate u is introduced as depicted in the right panel of figure B.6.

#### Chapter B

The hyperplane  $\Sigma_u$  is loaded with  $\sum_{i=0}^m \alpha_i$ , i.e.  $\mathfrak{c}_u = \mathfrak{c}_{0...m}$ . Then we can compute intersection numbers of cycles supported on the chambers depicted on the right-hand side as sums of their local intersection numbers along the hyperplane  $H_u$ .

**Example B.4.** As an example we consider the local intersection number contributing to the self-intersection of the twisted cycle supported on  $D_1$  (of the left panel of figure B.6). It has a contributions from the barycentre  $B_1$  of  $D_1$  and from the two vertices  $\langle u, 0 \rangle$  and  $\langle u, 1 \rangle$  which sum up to

$$[\check{\gamma}_D|\gamma_D]_{\langle 0,\dots,m\rangle} = \frac{1}{\mathfrak{d}_u} + \frac{1}{\mathfrak{d}_u\mathfrak{d}_0} + \frac{1}{\mathfrak{d}_u\mathfrak{d}_1} = \frac{\mathfrak{d}_{01}}{\mathfrak{d}_0\mathfrak{d}_1} \frac{1}{\mathfrak{d}_u} = \frac{\mathfrak{d}_{01}}{\mathfrak{d}_0\mathfrak{d}_1} \frac{1}{\mathfrak{d}_{0\dots m}}.$$
 (B.41)

Relative Twisted Homology Intersection Numbers The preceding discussion on computing intersection numbers between twisted cycles is in principle already sufficient to compute intersection numbers between relative twisted cycles (at least in non-degenerate arrangements of (regularised) chambers bounded by hyperplanes). Thus, we do not discuss this in detail but instead give an example.

**Example B.5.** We consider the cycles of Example 4.8 and in particular briefly explain how to compute the homology intersection matrix of eq. (4.103). One can clearly see from figure eq. (??) that the only non-zero intersections are self-intersections. The intersection between  $\gamma_1$  and  $\check{\gamma}_1$  is as computed in eq. (B.31) – with appropriate exponents – for the non-relative case. Since the twist is not multivariate near  $\lambda$ , the computation of the intersection number between  $\gamma_2$  and  $\check{\gamma}_2$  is even similar: In principle it is just the topological intersection number, i.e.,  $\pm 1$ . Taking into account the normalisation of  $\Delta_{\gamma_2}$  in eq. (4.101), we find:

$$\left[\check{\gamma}_2|\gamma_2\right] = -\frac{i}{2\pi} \,. \tag{B.42}$$

#### **B.2** Examples (Intersection Matrices)

In this section of the appendix, we give examples for the intersection matrices whose computation was reviewd in the previous section of the appendix. In particular, we consider Aomoto-Gelfand hypergeometric functions as those are needed for the computation of single-valued Feynman integrals in chapter 8.

#### Lauricella Functions

First, we consider the Lauricella  $F_D$  functions as introduced in eq. (4.173). For certain parameters  $(a, \boldsymbol{b}, c; \boldsymbol{y})$  those define (r+1)-dimensional twisted (co-)homology groups  $\mathrm{H}^1_{\mathrm{dR}}(\mathbb{C} - \Sigma_r, \nabla_{\Phi})$  and  $\mathrm{H}_1(\mathbb{C} - \Sigma_r, \check{\mathcal{L}}_{\Phi})$  with  $\Phi$  as in eq. (4.181). For simplicity, we assume here that the parameters are such that all exponents in the twist eq. (4.181) are non-integer and lie between zero and one. Configurations with non-integer exponents that are larger than one can be treated the same way by

splitting off non-integer parts and using these for the exponents. Additionally we denote  $\lambda_j = y_j^{-1}$  and  $\lambda_0 = 1$ . We choose the basis

$$\varphi_{r,j} = \operatorname{dlog}\left(\frac{z}{z - \lambda_{j-1}}\right) \text{ for } 1 \le j \le r+1$$
(B.43)

for  $H^1_{dR}(\mathbb{C} - \Sigma_r, \nabla_{\Phi})$  and the basis

$$\gamma_{r,j} = \Delta^c_{\gamma_{j-1}} \otimes \Phi|_{\Delta_{\gamma_{j-1}}} \tag{B.44}$$

for  $H_1(\mathbb{C} - \Sigma_r, \check{\mathcal{L}}_{\Phi})$ , where  $\Delta_{\gamma_{j-1}}^c$  denotes the regularised version of the open interval  $\Delta_{\gamma_{j-1}} = (0, \lambda_{j-1})$  (see eq. (4.29) in example 4.3. Then:

$$\mathcal{F}_D^{(r)}(a, \boldsymbol{b}, c; \boldsymbol{y}) = \langle \varphi_{r,1} | \gamma_{r,1} ]. \tag{B.45}$$

For the remainder of this section, we use the following notation:

$$\boldsymbol{\alpha} = (a, \boldsymbol{b}, c), \tag{B.46}$$

$$\mathbf{y}^{(k)} = \left(\frac{y_1}{y_k}, \dots, \frac{y_{k-1}}{y_k}, \frac{1}{y_k}, \frac{y_{k+1}}{y_k}, \dots, \frac{y_r}{y_k}\right). \tag{B.47}$$

The period matrix  $P_{\alpha}$ . From eq. (B.45), we find:

$$(\mathbf{P}_{\boldsymbol{\alpha}})_{11} = \langle \varphi_{r,1} | \gamma_{r,1} \rangle = \mathcal{F}_D^{(r)}(\boldsymbol{\alpha}; \boldsymbol{y}).$$
 (B.48)

Integrating  $\langle \varphi_{r,1} |$  over another cycle  $\gamma_{r,k}$  we obtain the period

$$\left(\mathbf{P}_{\alpha}\right)_{1k} = \langle \varphi_{r,1} | \gamma_{r,k} \rangle \tag{B.49}$$

$$= \lambda_{k-1}^{a} \mathcal{F}_{D}^{(r)} \left( \alpha, b_{1}, \dots, 1 + \alpha - c, \dots, b_{r}, 1 - b_{k-1} + a; \boldsymbol{y}^{(k-1)} \right), \quad (B.50)$$

whereas integrating another co-cycle  $\varphi_{r,k}$  over  $\gamma_{r,1}$  we obtain

$$(\mathbf{P}_{\alpha})_{k1} = \langle \varphi_{r,k} | \gamma_{r,1} \rangle = \mathcal{F}_D^{(r)}(a, b_1, \dots, b_{k-2}, b_{k-1} + 1, b_k, \dots, b_r, c+1; \boldsymbol{y})$$
. (B.51)

In the most general case we obtain:

$$y_{k-1}^{a} \left( \mathbf{P}_{\alpha} \right)_{lk} = y_{k-1}^{a} \left\langle \varphi_{r,l} \middle| \gamma_{r,k} \right] \tag{B.52}$$

$$= \begin{cases} \mathcal{F}_{D}^{(r)}\left(a, b_{1}, \dots, b_{l-1} + 1, \dots, b_{k-2}, a - c, b_{k}, \dots, b_{r}, 1 - b_{k-1} + a; \boldsymbol{y}^{(k-1)}\right) & l \neq k, \\ \mathcal{F}_{D}^{(r)}\left(a, b_{1}, \dots, b_{k-2}, a - c, b_{k}, \dots, b_{r}, -b_{k-1} + a; \boldsymbol{y}^{(k-1)}\right) & l = k. \end{cases}$$

The cohomology intersection matrix  $C_{\alpha}$ . The intersection matrix for the twisted co-cycles of eq. (B.43) is

$$\mathbf{C}_{\alpha} = \begin{pmatrix} \frac{1}{a} + \frac{1}{c-a} & \dots & \frac{1}{a} & \frac{1}{a} \\ \frac{1}{a} & \frac{1}{a} - \frac{1}{b_{1}} & \dots & \frac{1}{a} \\ \vdots & \ddots & \ddots & \vdots \\ \frac{1}{a} & \dots & \dots & \frac{1}{a} - \frac{1}{b_{n}} \end{pmatrix} . \tag{B.53}$$

#### Chapter B

The homology intersection matrix  $\mathbf{H}_{\alpha}$ . The homology intersection matrix for the chosen basis of twisted cycles as in eq. (B.44), is

$$\mathbf{H}_{\alpha} = \begin{pmatrix} -\frac{\delta_{01}}{\delta_{0}\delta_{1}} & -\frac{\epsilon_{0}}{\delta_{0}} & \dots & -\frac{\epsilon_{0}}{\delta_{0}} \\ -\frac{1}{\delta_{0}} & -\frac{\delta_{02}}{\delta_{0}\delta_{2}} & \dots & \vdots \\ \vdots & \ddots & \ddots & \vdots \\ -\frac{1}{\delta_{0}} & \dots & \dots & -\frac{\delta_{0r}}{\delta_{r}\delta_{0}} \end{pmatrix} = \begin{pmatrix} \frac{i}{2}(\mathfrak{C}(a)+\mathfrak{C}(c-a)) & \frac{i}{2}(\mathfrak{C}(a)+i) & \dots & \frac{i}{2}(\mathfrak{C}(a)+i) \\ \frac{1}{2}(1+i\mathfrak{C}(a)) & \frac{i}{2}(\mathfrak{C}(a)-\mathfrak{C}(b_{1})) & \dots & \vdots \\ \vdots & \ddots & \ddots & \vdots \\ \frac{1}{2}(1+i\mathfrak{C}(a)) & \dots & \dots & \frac{i}{2}(\mathfrak{C}(a)-\mathfrak{C}(b_{r})) \end{pmatrix},$$

$$(B.54)$$

where we introduced the shorthand  $\mathfrak{C}(x) = \cot(\pi x)$ . The diagonal entries of the intersection matrix are calculated as in eq. (B.30). The off-diagonal intersection numbers can be computed from one local intersection number each and those have the form of either  $v_1$  or  $v_2$  in figure B.4. We have numerically confirmed that the Riemann bilinear relations from eq. (4.58) are satisfied for the period and intersection matrices presented in this section for r=0,1,2. Note that to evaluate the period matrix for the Appell  $F_1$  function (r=2) numerically, analytical continuations as given in ref. [286] are necessary. We can use these matrices to express the single-valued analogues of Lauricella's  $F_D^{(r)}$  functions as bilinears in  $F_D^{(r)}$  function. For r=1, we reproduce the results for the single-valued analogue of Gauss'  ${}_2F_1$  function of ref. [253]. Note that ref. [253] works with a different basis of cycles where the homology intersection matrix  $\mathbf{H}_{\alpha}$  is diagonal.

#### $_{p+1}F_p$ function

We consider here the  $_{p+1}F_p$  functions of eq. (4.183), following the discussion in [285]. For certain parameters  $(\boldsymbol{a}, \boldsymbol{b}; y)$  those functions define twisted (co-)homology groups  $\mathrm{H}^1_{\mathrm{dR}}(\mathbb{C} - \Sigma, \nabla_{\Phi})$  and  $\mathrm{H}_1(\mathbb{C} - \Sigma, \check{\mathcal{L}}_{\Phi})$  with  $\Phi$  as in eq. (4.190). The  $\Sigma$  are defined by the twist as usual.

For p = 2, eq. (4.186) reduces to

$${}_{3}\mathcal{F}_{2}\left(\boldsymbol{a},\boldsymbol{b};y\right)$$

$$= \int_{0}^{1} \int_{0}^{1} t_{2}^{a_{2}-1} (1-t_{2})^{b_{2}-a_{2}-1} t_{1}^{a_{1}-1} (1-t_{1})^{b_{1}-a_{1}-1} (1-yt_{1}t_{2})^{-a_{0}} dt_{1} \wedge dt_{2}$$

$$= \int_{D_{1}} z_{1}^{a_{1}-b_{2}} z_{2}^{a_{2}-1} (1-z_{1})^{b_{1}-a_{1}-1} (1-yz_{2})^{-a_{0}} (z_{1}-z_{2})^{b_{2}-a_{2}-1} dz_{1} \wedge dz_{2},$$
(B.55)

where the last step follows is due to the change of variables in eq. (4.188). The integration region  $D_1$  is defined in (B.61). From eq. (B.55) we extract the twist

$$\Phi = z_1^{a_1 - b_2} z_2^{a_2} (1 - z_1)^{b_1 - a_1} (1 - y z_2)^{-a_0} (z_1 - z_2)^{b_2 - a_2},$$
(B.56)

where  $a_i, b_i$  are the non-integer parts of  $\alpha_i, b_i$ , and  $\mathbf{a} = (a_1 - b_2, a_2, b_1 - a_1, -a_0, b_2 - a_2)$ . It defines the following collection of hyperplanes:

$$\Sigma_{3F_2} = \{z_1 = 0\} \cup \{z_2 = 0\} \cup \{z_1 = 1\} \cup \{z_2 = y^{-1}\} \cup \{z_1 = z_2\}.$$
 (B.57)

Let  $X_{3F_2} = \mathbb{C}^2 - \Sigma_{3F_2}$ . We depict a projection of  $X_{3F_2}$  in  $\mathbb{R}^2$  for y < 1 in figure B.7. We choose the following basis for  $H^2_{dR}(X_{3F_2}, \nabla_a)$ :

$$\varphi_1 = \frac{\mathrm{d}z_1 \wedge \mathrm{d}z_2}{z_2(1-z_1)(z_1-z_2)},$$
 (B.58)

$$\varphi_2 = \frac{y \, \mathrm{d}z_1 \wedge \mathrm{d}z_2}{(1 - yz_2)(z_1 - z_2)}, \tag{B.59}$$

$$\varphi_3 = \frac{y \, \mathrm{d}z_1 \wedge \mathrm{d}z_2}{z_1 (1 - z_1)(1 - y z_2)}. \tag{B.60}$$

For the homology basis we choose cycles  $\gamma_i$  supported on the (regularisations of) the following chambers (see figure B.7):

$$D_1 = \{0 < x_2 < x_1 < 1\}, \tag{B.61}$$

$$D_2 = \{ y^{-1} < x_2 < x_1 < \infty \}, \tag{B.62}$$

$$D_3 = \{0 < x_1 < 1, y^{-1} < x_2 < \infty\}.$$
 (B.63)

Then:

$$_{3}\mathcal{F}_{2}(a_{0}, a_{1}, a_{2}, b_{1}, b_{2}, y) = \langle \varphi_{1} | \gamma_{1} \rangle.$$
 (B.64)

It is obvious how to generalise these p=2 bases for the case with a generic p>2. For the remainder of this discussion we use the following notation

$$\boldsymbol{\alpha} = (\boldsymbol{a}, \boldsymbol{b}), \tag{B.65}$$

$$\mathbf{a}_k = (1 + a_k - b_k, 1 + a_1 - b_k, \dots, 1 + a_p - b_k, 1 + a_0 - b_k),$$
(B.66)

$$\boldsymbol{b}_{k} = (1 - b_{k} + b_{1}, \dots, 1 - b_{k} + b_{k-1}, 1 - b_{k} + b_{k+1}, \dots, 1 - b_{k} + b_{p}, 2 - b_{k}),$$
(B.67)

$$\boldsymbol{a}_{kl} = (1 + a_l - b_l - \delta_{kl}, 1 + a_1 - b_l - \delta_{kl}, \dots, 1 + a_p - b_l - \delta_{kl}, 1 + a_0 - b_l - \delta_{kl}),$$
(B.68)

$$\mathbf{b}_{kl} = (1 - b_l + b_1 - \delta_{lk}, \dots, 1 - b_l + b_{l-1} - \delta_{lk}, 1 - b_l + b_{l+1} - \delta_{lk},$$
(B.69)

..., 
$$2 - b_l + b_k$$
, ...,  $1 - b_l + b_p - \delta_{lk}$ ,  $2 - b_l - 2\delta_{lk}$ ). (B.70)

The periods matrix  $P_{\alpha}$ . We reproduce the period matrix for the generalized hypergeometric function  $_{p+1}F_p$  given in ref. [285]. The first row (i.e., integrals of the first basis co-cycle over various cycles) and the first column (i.e., integrals of the different basis co-cycles over the first basis cycle) of the intersection matrix are

$$(\mathbf{P}_{\alpha})_{11} = {}_{p+1}\mathcal{F}_{p}(\boldsymbol{a}, \boldsymbol{b}; y) ,$$

$$(\mathbf{P}_{\alpha})_{1k} = (-1)^{k} e^{-i\pi(1+a_{0}+a_{k-1}-b_{k-1})} y^{1-b_{k-1}} {}_{p+1}\mathcal{F}_{p}(\boldsymbol{a}_{k-1}, \boldsymbol{b}_{k-1}; y) ,$$

$$(\mathbf{P}_{\alpha})_{k1} = y_{p+1}\mathcal{F}_{p}(1+a_{0}, 1+a_{1}, \dots, 1+a_{p}, 1+b_{1}, \dots, 2+b_{k-1}, \dots, 1+b_{p}; y) .$$
(B.71)

Most generally, we obtain:

$$(\mathbf{P}_{\boldsymbol{\alpha}})_{kl} = (-1)^{l} y^{1-b_{l-1}-\delta_{lk}} e^{-i\pi(2+a_0+a_{l-1}-b_{l-1}-\delta_{kl})} {}_{p+1} \mathcal{F}_p(\boldsymbol{a}_{k-1,l-1}, \boldsymbol{b}_{k-1,l-1}; y) . \quad (B.72)$$

The cohomology intersection matrix  $C_{\alpha}$ . The intersection matrix is

$$\mathbf{C}_{\alpha} = \begin{pmatrix} \prod_{i=1}^{p} \frac{b_{i}}{a_{i}(a_{i}-b_{i})} & 0 & 0 & 0 \\ 0 & -\frac{b_{1}}{a_{0}(a_{0}-b_{1})} \prod_{i=1,i\neq 1}^{p} \frac{b_{1}-b_{i}}{(b_{1}-a_{i})(a_{i}-b_{i})} & 0 & 0 \\ 0 & 0 & \ddots & 0 \\ 0 & 0 & 0 & -\frac{b_{p}}{a_{0}(a_{0}-b_{p})} \prod_{i=1,i\neq p}^{p} \frac{b_{p}-b_{i}}{(b_{p}-a_{i})(a_{i}-b_{i})} \end{pmatrix}$$

$$(B.73)$$

The homology intersection matrix  $\mathbf{H}_{\alpha}$ . The homology intersection matrices for  $_{p+1}F_p$  functions is discussed in refs. [284, 285] and we review it here. In the case p=1 we have the  $_2F_1$  function and this function was already discussed in the context of Lauricella's  $F_D^{(r)}$  function. Here, we derive the homology intersection matrix for the  $_3F_2$  function explicitly and deduce from it the generalisation to p>2. The case p=2: The projection of  $X_{3F_2}$  onto  $\mathbb{R}^2$ , along with a qualitative depiction of its parallel lines intersecting the hyperplane at infinity, is shown in figure B.7.

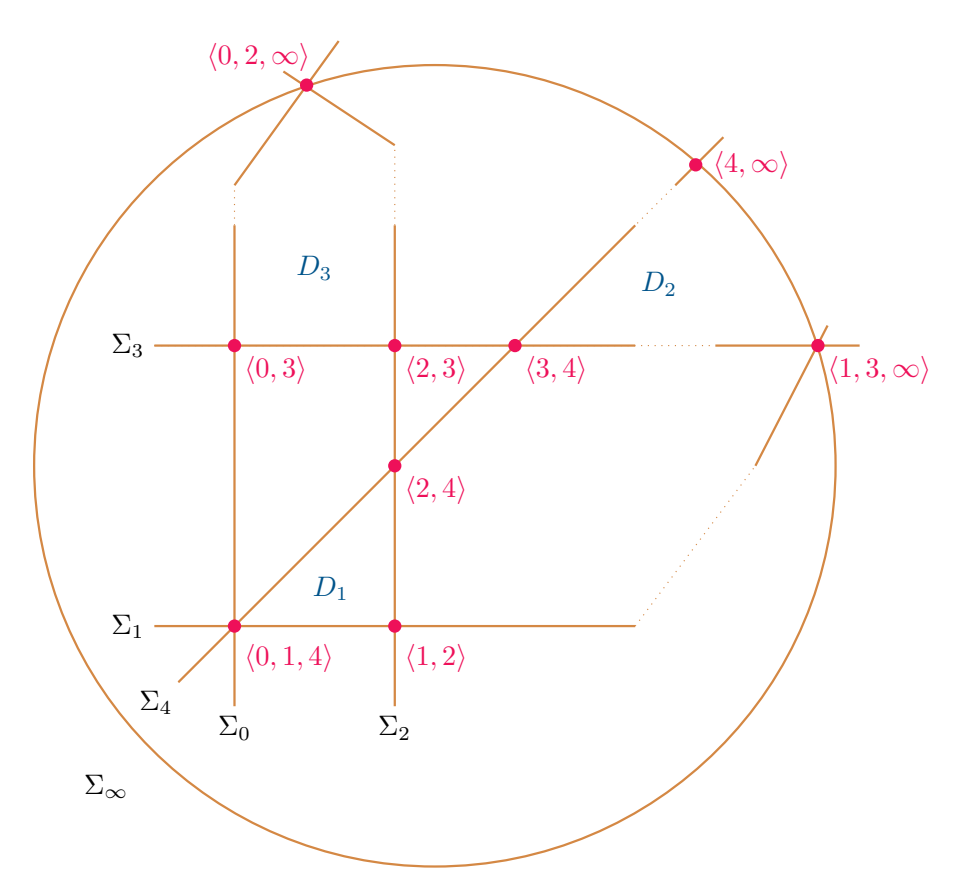


Figure B.7: A depiction of the hyperplanes defined by the twist of the  $_{p+1}F_p$  function and the bounded chambers  $D_1, D_2, D_3$  that we choose to support the basis of the corresponding homology group.

The three chambers from eq. (B.61) that support the basis of cycles are labelled as  $D_1, D_2, D_3$ . Since these chambers do not meet, the intersection matrix is

diagonal. Some local intersection numbers are degenerate (i.e., there exist points where three lines meet) and to compute them we need to use eq. (B.41). A similar configuration was studied in ref. [338]. From these considerations, we obtain the three non-zero elements of  $\mathbf{H}_{\alpha}$ :

$$(\mathbf{H}_{\alpha})_{11} = 1 + \frac{1}{\mathfrak{d}_{1}} + \frac{1}{\mathfrak{d}_{2}} + \frac{1}{\mathfrak{d}_{4}} + \frac{1}{\mathfrak{d}_{1}\mathfrak{d}_{2}} + \frac{1}{\mathfrak{d}_{2}\mathfrak{d}_{4}} + \frac{\mathfrak{d}_{14}}{\mathfrak{d}_{1}\mathfrak{d}_{4}} \frac{1}{\mathfrak{d}_{014}} = \frac{\mathfrak{d}_{14}\mathfrak{d}_{0124}}{\mathfrak{d}_{1}\mathfrak{d}_{2}\mathfrak{d}_{4}\mathfrak{d}_{014}}$$

$$(\mathbf{H}_{\alpha})_{22} = 1 + \frac{1}{\mathfrak{d}_{3}} + \frac{1}{\mathfrak{d}_{4}} + \frac{1}{\mathfrak{d}_{\infty}} + \frac{1}{\mathfrak{d}_{3}\mathfrak{d}_{4}} + \frac{1}{\mathfrak{d}_{4}\mathfrak{d}_{\infty}} + \frac{\mathfrak{d}_{3\infty}}{\mathfrak{d}_{3}\mathfrak{d}_{\infty}} \frac{1}{\mathfrak{d}_{13\infty}} = \frac{\mathfrak{c}_{3}\mathfrak{c}_{4}\mathfrak{d}_{022}\mathfrak{d}_{0124}}{\mathfrak{d}_{3}\mathfrak{d}_{4}\mathfrak{d}_{024}\mathfrak{d}_{01234}}$$

$$(\mathbf{H}_{\alpha})_{33} = 1 + \frac{1}{\mathfrak{d}_{0}} + \frac{1}{\mathfrak{d}_{2}} + \frac{1}{\mathfrak{d}_{3}} + \frac{1}{\mathfrak{d}_{3}\mathfrak{d}_{0}} + \frac{1}{\mathfrak{d}_{2}\mathfrak{d}_{3}} + \frac{\mathfrak{d}_{02}}{\mathfrak{d}_{0}\mathfrak{d}_{2}} \frac{1}{\mathfrak{d}_{02\infty}} = \frac{\mathfrak{c}_{3}\mathfrak{d}_{02}\mathfrak{d}_{14}}{\mathfrak{d}_{002}\mathfrak{d}_{3}\mathfrak{d}_{134}} .$$

As  $\alpha_{\infty} = -\sum_{i=0}^{4} \alpha_i$ , we have  $\mathfrak{c}_{\infty} = \mathfrak{c}_{01234}^{-1}$ . The full intersection matrix for the hypergeometric function  ${}_{3}\mathcal{F}_{2}(a_{0}, a_{1}, a_{2}, b_{1}, b_{2}; y)$  is

$$\mathbf{H}_{\alpha} = \begin{pmatrix} -\frac{\mathfrak{s}(b_{1})\mathfrak{s}(b_{2})}{4\,\mathfrak{s}(a_{1})\mathfrak{s}(a_{2})\mathfrak{s}(a_{1}-b_{1})\mathfrak{s}(a_{2}-b_{2})} & 0 & 0 \\ 0 & -\frac{\mathfrak{s}(b_{1})\mathfrak{s}(b_{1}-b_{2})}{4\,\mathfrak{s}(a_{0})\mathfrak{s}(a_{0}-b_{1})\mathfrak{s}(a_{2}-b_{1})\mathfrak{s}(a_{2}-b_{2})} & 0 \\ 0 & 0 & \frac{\mathfrak{s}(b_{1}-b_{2})\mathfrak{s}(b_{2})}{4\,\mathfrak{s}(a_{0})\mathfrak{s}(a_{1}-b_{1})\mathfrak{s}(a_{0}-b_{2})\mathfrak{s}(a_{1}-b_{2})} \end{pmatrix},$$

$$(B.75)$$

with  $\mathfrak{s}(x) = \sin(\pi x)$ . We numerically verified that the intersection matrix  $\mathbf{H}_{\alpha}$ , along with the period matrix  $P_{\alpha}$  and the intersection matrix  $C_{\alpha}$ , satisfies the twisted Riemann bilinear relations in eq. (4.58).

The case p > 2: Extending the result from eq. (B.74), we obtain the following nonzero entries of the homology intersection matrix for p > 2:

$$(\mathbf{H}_{\alpha})_{11} = (-2i)^{-p} \prod_{i=1}^{p} \frac{\mathfrak{s}(b_i)}{\mathfrak{s}(a_i)\mathfrak{s}(a_i - b_i)},$$
(B.76)

$$(\mathbf{H}_{\alpha})_{kk} = -(-2i)^{-p} \frac{\mathfrak{s}(b_{k-1})}{\mathfrak{s}(a_0)\mathfrak{s}(a_0 - b_{k-1})} \prod_{i=1}^{p} \frac{\mathfrak{s}(b_{k-1} - b_i)}{\mathfrak{s}(b_{k-1} - a_i)\mathfrak{s}(a_i - b_i)}$$
(B.77)

$$(\mathbf{H}_{\alpha})_{ik} = 0 \text{ for } i \neq k \tag{B.78}$$

#### **Unequal Mass Sunrise**

With these choices for the bases of the (co-)homology groups and their duals as given in eq. (4.211), eq. (4.215), and eq. (4.216), we obtain the following expressions for the intersection matrices (with  $\mathbf{x} = (p^2, m_1^2, m_2^2, m_3^2)$ ):

$$\mathbf{C}_{\Theta}(\boldsymbol{x},\varepsilon) = \begin{pmatrix} 0 & \frac{1}{-3\varepsilon-1} & 0 & 0\\ \frac{1}{1-3\varepsilon} & -\frac{\varepsilon(\lambda_{2}+\lambda_{2}+\lambda_{3}+\lambda_{4})^{2}}{12(9\varepsilon^{2}-1)} & \frac{\lambda_{1}+\lambda_{2}+\lambda_{3}+\lambda_{4}}{6-18\varepsilon} & 0\\ 0 & -\frac{\lambda_{1}+\lambda_{2}+\lambda_{3}+\lambda_{4}}{18\varepsilon+6} & -\frac{1}{3\varepsilon} & 0\\ 0 & 0 & 0 & -\frac{1}{\lambda_{1}\lambda_{2}\lambda_{3}\lambda_{4}\varepsilon} \end{pmatrix}, \quad (B.79)$$

$$\mathbf{H}_{\Theta}(\varepsilon) = \begin{pmatrix} i\tan(\pi\varepsilon) & -1 + \frac{1}{1+e^{2i\pi\varepsilon}} & i\tan(\pi\varepsilon) & 0\\ \frac{1}{1+e^{2i\pi\varepsilon}} & i\tan(\pi\varepsilon) & -i\tan(\pi\varepsilon) & 0\\ i\tan(\pi\varepsilon) & -i\tan(\pi\varepsilon) & 2i\tan(\pi\varepsilon) & -1 + \frac{1}{1+e^{2i\pi\varepsilon}}\\ 0 & 0 & \frac{1}{1+e^{2i\pi\varepsilon}} & i\csc(2\pi\varepsilon) \end{pmatrix}. \quad (B.80)$$

$$\mathbf{H}_{\oplus}(\varepsilon) = \begin{pmatrix} i \tan(\pi \varepsilon) & -1 + \frac{1}{1 + e^{2i\pi \varepsilon}} & i \tan(\pi \varepsilon) & 0\\ \frac{1}{1 + e^{2i\pi \varepsilon}} & i \tan(\pi \varepsilon) & -i \tan(\pi \varepsilon) & 0\\ i \tan(\pi \varepsilon) & -i \tan(\pi \varepsilon) & 2i \tan(\pi \varepsilon) & -1 + \frac{1}{1 + e^{2i\pi \varepsilon}}\\ 0 & 0 & \frac{1}{1 + e^{2i\pi \varepsilon}} & i \csc(2\pi \varepsilon) \end{pmatrix} .$$
 (B.80)

### B.3 The $\varepsilon$ -Dependence of Specific Intersection Numbers

♠ The statement and proof given here were already given in [50], which resulted from collaborations with Claude Duhr, Cathrin Semper and Sven Stawinski. We only changed the notation and some of the wording to fit with the remainder of the thesis.

In the remainder of this thesis, we focus specifically on cohomology intersection numbers of d log forms and prove that eq. (4.73) fully captures the  $\mu$ -dependence of the intersection between a d log form and its derivative with respect to exterior parameters. This result is essential for the proof of Theorem 4.1. Additionally, we require a theorem from ref. [238], which provides a formula for the intersection numbers of d log-forms (see eq. (4.71)). We begin by reviewing this theorem before proceeding to the proof of eq. (4.73). The latter follows a similar structure to the proof of eq. (4.71) presented in [238]. We assume here that the twist is given by

$$\Phi = \prod_{i=0}^{r+1} L_i(\boldsymbol{z}, \boldsymbol{\lambda})^{\alpha_i}, \qquad (B.81)$$

where the  $L_i(\mathbf{z}, \boldsymbol{\lambda}) = 0$  define hyperplanes  $\Sigma_i$ . We assume that a d log basis of the cohomology group as given in eq. (4.67) is chosen. We introduce some local notation for this appendix: First, we define the index sets  $P_m = (q_1, \ldots, q_m), P_{m+1} = (p_0, \ldots, p_m)$  with  $p_0 < p_1 < \cdots < p_m$  and similarly for the  $q_i$ 

$$\delta(P_m, P_{m+1}) = \begin{cases} (-1)^{\mu}, & \text{if } P_m \subset P_{m+1}, \\ 0, & \text{if } P_m \not\subset P_{m+1}, \end{cases}$$
(B.82)

where  $\mu$  is determined as  $\{p_{\mu}\}=P_{m+1}-P_m$  in the case  $P_m\subset P_{m+1}$ . The intersection number between d log forms can be computed with the following theorem from ref. [238]:

Theorem B.1. For multi-indices

$$I = (i_0, \dots, i_n)$$
, with  $0 \le i_0 < i_1 < \dots < i_n \le r + 1$ ,  $J = (j_0, \dots, j_n)$ , with  $0 \le j_0 < j_1 < \dots < j_n \le r + 1$ ,

the intersection pairing of the corresponding dlog-forms is

$$\langle \varphi_J | \check{\varphi}_I \rangle = \begin{cases} (2\pi i)^n \frac{\sum_{i \in I} \alpha_i}{\prod_{i \in I} \alpha_i}, & \text{if } I = J, \\ (2\pi i)^n \frac{(-1)^{\beta_1 + \beta_2}}{\prod_{i \in (I \cap J)} \alpha_i}, & \text{if } |I \cap J| = n, \\ 0, & \text{otherwise}. \end{cases}$$
(B.83)

The exponents  $\beta_i$  are defined by  $\{i_{\beta_1}\} = I - (I \cap J)$  and  $\{i_{\beta_2}\} = J - (I \cap J)$ .

This theorem can be proven constructively, i.e. one explicitly constructs the bases and computes the residua.

**Theorem B.2.** We consider a dlog-form  $\varphi_I$  and a covariant derivative of a dlog-form  $\varphi_J$ , namely  $\eta_J = (d_{\text{ext}} + d_{\text{ext}} \log \Phi \wedge) \varphi_J$  defined by the multi-indices I, J. Then, the intersection pairing between these differentials exhibits the following  $\mu$ -dependence:

$$\langle \eta_J | \varphi_I \rangle \sim \frac{1}{\mu^{n-1}} \,.$$
 (B.84)

We perform the proof similarly as it was done for Theorem B.1 in ref. [238] and consider first the case n = 1.

*Proof.* The case n = 1. Since  $\varphi_I$  is a dlog-form, all steps in the proof of Theorem B.1 that involve only this form remain the same. Thus, we already know its compactly supported version as it is provided in ref. [238]. Thus, we can proceed to the next step of the proof, at which point our argument deviates slightly. First, we write explicitly:

$$\langle \eta_J | \varphi_I \rangle = -2\pi i \sum_{p=0}^{r+1} \operatorname{Res}_{\Sigma_p} (\psi^p \eta_J) ,$$
 (B.85)

where  $\psi^p$  is a holomorphic primitive of  $\varphi_I$  that has the following expansion in local coordinates near  $\Sigma_p$  [238]:

$$\psi^p = \frac{\delta(p, I)}{\alpha_p} + \mathcal{O}(z). \tag{B.86}$$

In particular, the form  $\eta_J$  contains the following expressions in local coordinates near the  $\Sigma_p$ :

$$d_{\text{ext}}\varphi_{J} = \frac{d_{\text{ext}}(dL_{j_{0}})}{L_{j_{0}}} - \frac{d_{\text{ext}}(dL_{j_{1}})}{L_{j_{1}}} - \frac{(d_{\text{ext}}L_{j_{0}}) \wedge (dL_{j_{0}})}{L_{j_{0}}^{2}} + \frac{(d_{\text{ext}}L_{j_{1}}) \wedge (dL_{j_{1}})}{L_{j_{1}}^{2}},$$
(B.87)

$$d_{\text{ext}} \log \Phi \wedge \varphi_J = \sum_{l=0}^{r+1} \frac{\alpha_l d_{\text{ext}} L_l}{L_l} \wedge d \log \frac{L_{j_0}}{L_{j_1}}$$

$$= \left( \frac{\alpha_{j_0} (d_{\text{ext}} L_{j_0}) \wedge (d L_{j_0})}{L_{j_0}^2} + \sum_{l \neq j_0} \frac{\alpha_l d_{\text{ext}} L_l}{L_l} \wedge \frac{d L_{j_0}}{L_{j_0}} \right) - (j_0 \leftrightarrow j_1).$$

If we were to insert this form into eq. (B.85), we would not be able to immediately deduce the scaling with  $\mu$ , as eq. (B.87) still contains double poles and terms that do not scale with  $\mu$ . This arises because the residue is neither 1 nor zero, unlike in the case of logarithmic forms. While a full residue computation would ultimately yield the same scaling, we adopt an alternative strategy that allows us to extract

#### Chapter B

the scaling of the intersection pairing more directly. Specifically, we modify  $\eta_J$  by adding an exact form, rewriting it in a simpler form from which the scaling can be easily determined. Consider the following exact form:

$$\chi_{j_0}^1 = \nabla \left( \frac{\mathrm{d}_{\text{ext}} L_{j_0}}{L_{j_0}} - \frac{\mathrm{d}_{\text{ext}} L_{j_1}}{L_{j_1}} \right) 
= \left( \frac{-\mathrm{d}_{\text{ext}} \left( \mathrm{d} L_{j_0} \right)}{L_{j_0}} + \frac{\left( \mathrm{d}_{\text{ext}} L_{j_0} \right) \wedge \left( \mathrm{d} L_{j_0} \right)}{L_{j_0}^2} - \frac{\alpha_{j_0} (\mathrm{d}_{\text{ext}} L_{j_0}) \wedge \left( \mathrm{d} L_{j_0} \right)}{L_{j_0}^2} \right) 
+ \sum_{l \neq j_0} \frac{\alpha_l \mathrm{d} L_l}{L_l} \wedge \frac{\mathrm{d}_{\text{ext}} L_{j_0}}{L_{j_0}} - \left( j_0 \leftrightarrow j_1 \right).$$
(B.88)

We than have:

$$\eta_{J} \sim \eta_{J} + \chi_{j_{0}}^{1} =: \tilde{\eta}_{J} = \sum_{l \neq j_{0}} \alpha_{l} \left( \frac{\mathrm{d}_{\mathrm{ext}} L_{l}}{L_{l}} \wedge \frac{\mathrm{d} L_{j_{0}}}{L_{j_{0}}} + \frac{\mathrm{d} L_{l}}{L_{l}} \wedge \frac{\mathrm{d}_{\mathrm{ext}} L_{j_{0}}}{L_{j_{0}}} \right) - (j_{0} \leftrightarrow j_{1}).$$
(B.89)

Each term in the sum in eq. (B.89) has only simple poles at the hyperplanes  $\mathcal{L}_j$ . Setting  $\alpha_j = a_j \mu$ , the  $\mu$ -dependence of the sum manifests as an overall factor of  $\mu$ . Consequently, in local coordinates  $z^p$  near  $\mathcal{L}_p$ , we obtain:

$$\psi^p \eta_J = \frac{\delta_{p,I}}{\mu a_p} \frac{\mu a_p C_p \, \mathrm{d} z^p}{z^p} + \mathcal{O}(1) \,,$$

where  $C_p$  is a  $\mu$ -independent factor that can be determined from eq. (B.89). Ultimately, we arrive at:

$$\langle \eta_J | \varphi_I \rangle = -2\pi i \sum_{p=0}^{r+1} \operatorname{Res}_{\mathcal{L}_p} (\psi^p \eta_J) \sim \mu^0$$
 (B.90)

is independent of  $\mu$ .

The case of generic n We now outline how the previous argument can be extended to arbitrary n. Once again, we begin with a residue computation, as all preceding steps follow from the same compactification of the dlog form  $\varphi_J$  as given in ref. [238]:

$$\langle \eta_J | \varphi_I \rangle = (-2\pi i)^n \sum_P \operatorname{Res}_{z_n} \left( \operatorname{Res}_{z_{n-1}} \left( \dots \operatorname{Res}_{z_1} \left( \tilde{\psi}^P \eta_J \right) \dots \right) \right) .$$
 (B.91)

Here,  $z_i^P$  represents the local coordinates near  $\mathcal{L}_P$ , and  $\tilde{\psi}^P$  is a holomorphic primitive with a leading-order term proportional to  $\prod_{i \in P} \frac{1}{\alpha_i}$ . Once again, we begin by expressing the form  $\eta_J$ :

$$\eta_J = \sum_{l=0}^{n-1} (-1)^l \operatorname{dlog}\left(\frac{L_{j_0}}{L_{j_1}}\right) \wedge \dots \wedge \operatorname{d}_{\operatorname{ext}} \operatorname{dlog}\left(\frac{L_{j_l}}{L_{j_{l+1}}}\right) \wedge \dots \wedge \operatorname{dlog}\left(\frac{L_{j_{n-1}}}{L_{j_n}}\right) \quad (B.92)$$

$$+\sum_{l=0}^{r+1} \alpha_l \mathrm{d}_{\mathrm{ext}} \mathrm{log} \, L_l \wedge \varphi_J \,.$$

Furthermore, we define the exact form

$$\chi_{j_{l-1}}^{n} = \nabla \left( \varphi_{j_0 j_1} \wedge \dots \wedge \varphi_{j_{l-2}, j_{l-1}} \wedge \left( \operatorname{d_{ext} log} L_{j_{l-1}} - \operatorname{d_{ext} log} L_{j_l} \right) \wedge \varphi_{j_l, j_{l+1}} \wedge \dots \wedge \varphi_{j_{n-1}, n} \right) .$$
(B.93)

where we use the fact that  $\varphi_{j_{k-1}j_k}$  are defined according to eq. (4.67). Then

$$\eta_J \sim \eta_J + \sum_{l=1}^n \chi_{j_{l-1}}^n =: \tilde{\eta}_J$$
(B.94)

It has only simple poles in each set of local coordinates  $z^P$  and exhibits an overall scaling with  $\mu$ . As in the n=1 case, the terms with double poles cancel. Thus:

$$\langle \tilde{\eta}_J | \varphi_I \rangle \sim \frac{\mu}{\mu^n} = \frac{1}{\mu^{n-1}}.$$
 (B.95)

## Appendix C

# Additional Relations for Kite Punctures

#### See also:

We compute the kite integral family and derive the punctures discussed here in Chapter 7 In this appendix, we give definitions and relation of elliptic integrals needed to compute elliptic Feynman integrals and in particular the kite integral family. Additionally we collect relations of the punctures defined by the kite integral family.

#### C.1 Elliptic Integrals

We repeat here the definition of the elliptic integrals also given in (3.70):

$$K(\lambda) = \int_0^1 \frac{dx}{\sqrt{(1 - \lambda x^2)(1 - x^2)}}$$
 and  $E(\lambda) = \int_0^1 dx \sqrt{\frac{1 - \lambda x^2}{1 - x^2}}$ . (C.1)

We summarise the relations we use in Chapter 7 to relate elliptic integrals with different moduli k. For  $0 \le k^2 \le 1$  and  $0 \le \phi \le \pi/2$ , the following relations hold

(i) 
$$F(-\phi, k^2) = -F(\phi, k^2)$$

(ii) 
$$F(\phi, k^2) + F(\psi, k^2) = \pm K(k^2)$$
 for  $\psi = \pm \arccos\left(\pm \sin(\phi)\sqrt{1 - k^2}/\sqrt{1 - k^2\sin^2(\phi)}\right)$ ,

(iii) 
$$F(\phi, k^2) + F(\psi, k^2) = iK(1 - k^2)$$
 for  $\psi = \arcsin(-1/(k\sin(\phi)))$ ,

(iv) 
$$F(\phi, 1/k^2) = kF(\psi, k^2)$$
 for  $\psi = \arcsin(\sin(\phi)/k)$ ,

$$\text{(v) } F(\phi, 1-k^2) = iF(\psi, k^2) - iK(k^2) \quad \text{for} \quad \psi = \arcsin\left(1/\sqrt{1-(1-k^2)\sin^2(\phi)}\right).$$

Modular transformations and shifts In Chapter 7 we define the normalized period and the punctures in elliptic integrals, namely:

$$\tau = \frac{iK(1-k^2)}{K(k^2)}$$
 and  $z = \frac{F(\phi, k^2)}{K(k^2)}$ . (C.2)

These objects transform under S-transformations as:

$$S(z) = \frac{z}{\tau} = \frac{F(\phi, k^2)}{iK(1 - k^2)} = \frac{F(\psi_1, 1 - k^2) - K(1 - k^2)}{K(1 - k^2)} = \frac{F(\psi_2, 1 - k^2)}{K(1 - k^2)}, \quad (C.3)$$

where  $\psi_1 = \arcsin\left(1/\sqrt{1-k^2\sin^2(\phi)}\right)$  and  $\psi_2 = -\operatorname{arccot}(k\tan(\psi_1))$ . Similarly, we have for the *a*-cycle shift

$$z' = z + 1 = \frac{F(\phi, k^2)}{K(k^2)} + \frac{K(k^2)}{K(k^2)} = \frac{F(\psi, k^2)}{K(k^2)},$$
 (C.4)

where  $\psi = \arccos\left(-\sin(\phi)\sqrt{1-k^2}/\sqrt{1-k^2\sin^2(\phi)}\right)$ . The *b*-cycle shift can be used to cast a given elliptic integral back into the range  $0 \le \phi \le \pi/2$  by writing

$$z' = z + \tau = \frac{F(\psi, k^2)}{K(k^2)} + \frac{iK(1 - k^2)}{K(k^2)} = \frac{F(\phi, k^2)}{K(k^2)},$$
 (C.5)

where  $\psi = \arcsin(1/(k\sin(\phi)))$ .

Example: extracting  $z_4^{(123)}$  from the maximal cut of the eyeball Integrating the maximal cut of the eyeball yields

$$\frac{1}{2c_4'}F\left(\arcsin\sqrt{u_\phi},k_\phi^2\right),\tag{C.6}$$

with  $k_{(123)}^2 = 1 - 1/k_{\phi}^2$ . Using successively relation (iv) and (v), we find

$$\frac{1}{2c_4'}F(\arcsin\sqrt{u_{\phi}}, k_{\phi}^2) = \frac{1}{2c_4'k_{\phi}} = \frac{i}{2c_4'k_{\phi}} \left[ F\left(\arcsin\left(\frac{1}{\sqrt{1-u_{\phi}}}\right), 1 - \frac{1}{k_{\phi}^2}\right) - K\left(1 - \frac{1}{k_{\phi}^2}\right) \right]. \tag{C.7}$$

Consequently, we see that  $u_{(123)} = 1/(1 - u_{\phi})$  and  $c_4 = -ic'_4 k_{\phi}$ . Finally, plugging in  $\psi_1 = 2K(k^2_{(123)})/c_4$ , we find:

$$\frac{1}{2c_4'}F\left(\arcsin\sqrt{u_\phi}, k_\phi^2\right) = \frac{1}{2}\psi_1\left[\frac{F\left(\arcsin\sqrt{u_4}, k_{(123)}^2\right)}{K\left(k_{(123)}^2\right)} - 1\right]. \tag{C.8}$$

#### C.2 Relations Between the Punctures

In this appendix, we present several examples illustrating how the discrete symmetries of the sunrise, eyeball, and kite topologies act on the punctures and Z-arguments. The (123)- and (345)-sunrise configurations remain invariant under the action of the respective symmetric groups  $S_3(\{m_1, m_2, m_3\})$  and  $S_3(\{m_3, m_4, m_5\})$ . In contrast, the (1234)-, (1235)-, (2345)-, and (1345)-eyeball diagrams exhibit symmetry only under specific mass exchanges:  $m_1 \leftrightarrow m_3$ ,  $m_2 \leftrightarrow m_3$ ,  $m_2 \leftrightarrow m_5$ ,

#### Chapter C

and  $m_3 \leftrightarrow m_4$ , respectively. The kite topology possesses two discrete symmetries, namely the transformations  $m_1 \leftrightarrow m_4$ ,  $m_2 \leftrightarrow m_5$ , as well as  $m_1 \leftrightarrow m_5$ ,  $m_2 \leftrightarrow m_4$ . A partial summary of how these symmetries influence the punctures and Z-arguments is provided in table C.1.

Mass permutations	Puncture permutations	Z-argument permutations
$m_1 \leftrightarrow m_2$	$z_1^{(123)} \leftrightarrow z_2^{(123)}$	$\mathcal{L}_1^{(123)} \leftrightarrow \mathcal{L}_2^{(123)}$
$m_1 \leftrightarrow m_3$	$z_1^{(123)} \leftrightarrow 1 - z_1^{(123)} - z_2^{(123)}$	$\mathcal{L}_1^{(123)} \leftrightarrow -\mathcal{L}_5^{(123)}$
$m_2 \leftrightarrow m_3$	$z_2^{(123)} \leftrightarrow 1 - z_1^{(123)} - z_2^{(123)}$	$\mathcal{L}_2^{(123)} \leftrightarrow -\mathcal{L}_5^{(123)}$

Mass permutations	Puncture permutations	Z-argument permutations	
$m_1 \leftrightarrow m_3$	$z_1^{(123)} \leftrightarrow 1 - z_1^{(123)} - z_2^{(123)}$	$\mathcal{L}_1^{(123)} \leftrightarrow -\mathcal{L}_5^{(123)},  \mathcal{L}_8^{(123)} \leftrightarrow -\mathcal{L}_9^{(123)}$	

Mass permutations	Puncture permutations	Z-argument permutations
$m_1 \leftrightarrow m_2, m_4 \leftrightarrow m_5$	$z_1^{(123)} \leftrightarrow z_2^{(123)}, \ z_4^{(123)} \leftrightarrow z_5^{(123)}$	$\begin{array}{c} \mathcal{L}_{1}^{(123)} \leftrightarrow \mathcal{L}_{2}^{(123)},  \mathcal{L}_{4}^{(123)} \leftrightarrow \mathcal{L}_{5}^{(123)}, \\ \mathcal{L}_{6}^{(123)} \leftrightarrow \mathcal{L}_{10}^{(123)},  \mathcal{L}_{7}^{(123)} \leftrightarrow \mathcal{L}_{11}^{(123)}, \\ \mathcal{L}_{8}^{(123)} \leftrightarrow \mathcal{L}_{12}^{(123)},  \mathcal{L}_{9}^{(123)} \leftrightarrow \mathcal{L}_{13}^{(123)}, \\ \mathcal{L}_{15}^{(123)} \leftrightarrow \mathcal{L}_{16}^{(123)},  \mathcal{L}_{17}^{(123)} \leftrightarrow -\mathcal{L}_{17}^{(123)} \end{array}$
$m_1 \leftrightarrow m_4, m_2 \leftrightarrow m_5$	$ \begin{array}{c} \tau^{(123)} \leftrightarrow \tau^{(345)}, \\ z_1^{(123)} \leftrightarrow z_4^{(345)}, z_2^{(123)} \leftrightarrow z_5^{(345)}, \\ z_4^{(123)} \leftrightarrow z_1^{(345)}, z_5^{(123)} \leftrightarrow z_2^{(345)} \end{array} $	$\mathcal{L}_i^{(123)} \leftrightarrow \mathcal{L}_i^{(345)}$
$m_1 \leftrightarrow m_5, m_2 \leftrightarrow m_4$	$ \begin{array}{c} \tau^{(123)} \leftrightarrow \tau^{(345)}, \\ z_1^{(123)} \leftrightarrow z_5^{(345)}, \ z_2^{(123)} \leftrightarrow z_4^{(345)}, \\ z_4^{(123)} \leftrightarrow z_2^{(345)}, \ z_5^{(123)} \leftrightarrow z_1^{(345)} \end{array} $	$ \begin{array}{c} \mathcal{L}_{1}^{(123)} \leftrightarrow \mathcal{L}_{2}^{(345)},  \mathcal{L}_{4}^{(123)} \leftrightarrow \mathcal{L}_{5}^{(345)}, \\ \mathcal{L}_{6}^{(123)} \leftrightarrow \mathcal{L}_{10}^{(345)},  \mathcal{L}_{7}^{(123)} \leftrightarrow \mathcal{L}_{11}^{(345)}, \\ \mathcal{L}_{8}^{(123)} \leftrightarrow \mathcal{L}_{12}^{(345)},  \mathcal{L}_{9}^{(123)} \leftrightarrow \mathcal{L}_{13}^{(345)}, \\ \mathcal{L}_{15}^{(123)} \leftrightarrow \mathcal{L}_{16}^{(345)},  \mathcal{L}_{17}^{(123)} \leftrightarrow -\mathcal{L}_{17}^{(345)}, \\ \mathcal{L}_{3}^{(123)} \leftrightarrow \mathcal{L}_{3}^{(345)},  \mathcal{L}_{14}^{(123)} \leftrightarrow \mathcal{L}_{14}^{(345)} \end{array} $

Table C.1: **(Top)** Symmetries of the sunrise  $I_{1,1,1,0,0}$  and its implications on punctures and Z-arguments. **(Middle)** Symmetries of the eyeball  $I_{1,1,1,1,0}$  and its implications on punctures and Z-arguments. **(Bottom)** Symmetries of the kite  $I_{1,1,1,1,1}$  and its implications on punctures and Z-arguments.

## Appendix D

## **Extended Calculations**

## D.1 Laurent Expansion of Differentials on a Hyperelliptic Curve

In this appendix we give the Laurent expansions for simple differentials on a hyperelliptic curve, that we need in section 3.2 of the main part.

**Odd Hyperelliptic Curve.** Let us first examine the case of an *odd* hyperelliptic curve. To expand around  $\infty$ , we introduce a change of coordinates via  $u = \frac{1}{x^2}$ . The square in this transformation is necessary because  $\infty$  is a branch point of the square root appearing in the differential. The expansion of the relevant differentials around u = 0 is then given by

$$\frac{x^{k-1}dx}{\sqrt{(x-\lambda_1)\dots(x-\lambda_{2g+1})}} = -2\sum_{N=g-k}^{\infty} \mathcal{S}_{N+k-g} u^{2N} du, \qquad (D.1)$$

where

$$S_N = (-1)^N \sum_{\sigma \subset \Sigma(N)} (-1)^{|\sigma|} \frac{(2|\sigma|)!}{(2^{|\sigma|}|\sigma|!)^2} s(\sigma), \qquad (D.2)$$

with the definition  $S_0 = 1$ . The sum runs over all ordered integer partitions of N, for instance,

$$\Sigma(3) = \{\{3\}, \{2, 1\}, \{1, 2\}, \{1, 1, 1\}\}. \tag{D.3}$$

We denote by  $|\sigma|$  the cardinality of the ordered set  $\sigma$ , and

$$s(\sigma) = \prod_{i=1}^{|\sigma|} s_{\sigma_i}(\vec{\lambda}) \tag{D.4}$$

represents a product of symmetric polynomials in the  $\lambda_i$ .<sup>1</sup>

<sup>1</sup>Undefined symmetric polynomials are considered to be zero.

#### Chapter D

**Even Hyperelliptic Curve.** Let us now examine the case of an *even* hyperelliptic curve. In this case, the differentials

$$\frac{x^k \mathrm{d}x}{y}, \quad k \ge g, \tag{D.5}$$

have non-vanishing residues at  $\infty$ . To expand around  $\infty$ , we introduce the variable transformation x = 1/u. This yields

$$\frac{x^{k-1}dx}{\sqrt{(x-\lambda_1)\dots(x-\lambda_{2g+2})}} = -\sum_{N=g-k}^{\infty} \mathcal{S}_{N+k-g} u^N du.$$
 (D.6)

This allows us to explicitly construct linear combinations of differentials that have only a pole of order k+1. To this end, we define the functions  $\tilde{\Psi}_k$  as

$$\tilde{\Psi}_k = \sum_{i=0}^k \sum_{\sigma \subset \Sigma(i)} (-1)^{|\sigma|} \mathcal{S}(\sigma) x^{g+k-i}, \quad \mathcal{S}(\sigma) = \prod_{i=1}^{|\sigma|} \mathcal{S}_{\sigma_i}. \tag{D.7}$$

Then, the differential

$$\frac{\tilde{\Psi}_k \mathrm{d}x}{y} = -\frac{1}{u^{k+1}} \mathrm{d}u + \mathcal{O}(1) \tag{D.8}$$

has a pole of order k + 1 and no higher-order singularities.

Naturally, we can add any linear combination of holomorphic differentials without affecting this pole structure. We will make such adjustments in a way that simplifies the bilinear relations between (quasi-)periods, as illustrated in examples 3.1 and 3.6.

## D.2 Proof for the Linear Independence of Certain Iterated Integrals

♠ The statement and proof given here were already given in [50], which resulted from collaborations with Claude Duhr, Cathrin Semper and Sven Stawinski. We only changed the notation and some of the wording to fit with the remainder of the thesis.

We repeat here the proof of theorem 5.1. It was given in [226] and closely follows the proof for the single-variable version of the statement given in [309].

*Proof.*  $\underline{1. \Rightarrow 2.:}$  Showing that the J(w) are linearly independent over  $\mathcal{F}_{\mathbb{C}}$  is equivalent to showing that for a finite subset  $S \subset \mathcal{B}_{\mathbf{B}}$  and  $f_w \in \mathcal{F}_{\mathbb{C}}$ :

$$\sum_{w \in \mathcal{S}} f_w J(w) = 0 \Rightarrow f_w = 0. \tag{D.9}$$

We define  $\mathbb{E}_{\mathcal{F}} = \mathcal{F}_{\mathbb{C}} \otimes \mathbb{E}_{\mathbf{B}}$ , the  $\mathcal{F}_{\mathbb{C}}$  vector space generated by the basis of  $\mathbb{E}_{\mathbf{B}}$ , and its dual  $\mathbb{E}_{\mathcal{F}}^* = \mathcal{F}_{\mathbb{C}} \otimes_{\mathbb{K}} \mathbb{E}_{\mathbf{B}}^*$ . Any dual element  $p^*$  can be decomposed in a basis  $w^*$  dual to w and in particular we define the dual vector

$$w^*(\tilde{w}) = \begin{cases} 1 & w = \tilde{w} \\ 0 & \text{else} \end{cases}$$

$$p^* = \sum_{w \in S} f_w w^* \,. \tag{D.10}$$

. Furthermore, we define a map

$$\phi_{\mathbb{G}_I} : \mathbb{E}_{\mathcal{F}}^* \to \mathcal{F}_{\mathbb{C}} \otimes_{\mathbb{K}} \mathcal{V}_{\mathbf{B}}, \ p^* \mapsto p^*(\mathbb{G}_I) = \sum_{w \in \mathcal{S}} f_w J(w).$$
 (D.11)

Then, the condition in eq. (D.9) is equivalent to  $\operatorname{Ker} [\phi_{\mathbb{G}_{\mathbb{I}}}] = \{0\}$ . Let us assume  $\operatorname{Ker} [\phi_{\mathbb{G}_{\mathbb{I}}}] \neq \{0\}$  and let  $q^*$  be the non-zero element of  $\operatorname{Ker} [\phi_{\mathbb{G}_{\mathbb{I}}}]$  with the smallest leading monomial in some monomial ordering  $^2$ , which we denote by  $\operatorname{Im}(q^*) = w_0^*$ . We can write

$$q^* = f_{w_0} w_0^* + \sum_{\substack{w \in \mathcal{B}_{\mathbf{B}} \\ w_0^* \prec w^*}} f_w w^*, \qquad f_{w_0} \neq 0.$$
 (D.12)

Note that we must have  $|w_0| > 0$ . Indeed, if  $|w_0| = 0$ , then  $w_0 = 1$  is the empty word, and we have  $\phi_{\mathbb{G}_I}(q^*) = f_{w_0}$ . Since  $q^* \in \text{Ker }\phi_{\mathbb{G}_I}$ , this implies  $f_{w_0} = 0$ , but then  $q^* = 0$ , and we assumed that  $q^*$  is not zero. So, since  $f_{w_0} \neq 0$ , we can define  $\tilde{q}^* = \frac{1}{f_{w_0}}q^*$ . Using eq. (5.92) we obtain:

$$0 = d\phi_{\mathbb{G}}(\tilde{q}^*) = d\tilde{q}^*(\mathbb{G}) + \tilde{q}^*(d\mathbb{G})$$
(D.13)

$$= d\tilde{q}^*(\mathbb{G}) + \sum_{i=1}^p \varpi_i \, \tilde{q}^*(e_{I,i}\mathbb{G})$$
 (D.14)

$$= d\tilde{q}^*(\mathbb{G}) + \sum_{i=1}^p \varpi_i e_{I,i}^{\dagger} \tilde{q}^*(\mathbb{G}).$$
 (D.15)

Inserting (D.12), we find

$$d\tilde{q}^* + \sum_{i=1}^p \varpi_i e_{\mathbf{I},i}^{\dagger} \tilde{\mathbf{q}}^* = \sum_{\substack{w \in \mathcal{B}_{\mathbf{B}} \\ w \neq w_0}} \left[ df_w w^* + \sum_{i=1}^p \varpi_i e_{\mathbf{I},i}^{\dagger} w^* \right] + \sum_{i=1}^p \omega_i e_{\mathbf{I},i}^{\dagger} w_0^*. \tag{D.16}$$

Observe that the action of the Hermitian conjugate  $e_{I,i}^{\dagger}$  reduces the length of a word. Specifically, for any words  $w_1, w_2$ , we have

$$e_{I,i}^{\dagger} w_1^*(w_2) = w_1^*(e_{I,i} w_2) = 0$$

unless

$$|w_1| = |e_{I,i}w_2| = |w_2| + 1,$$

which implies that

$$|e_{L_i}^{\dagger}w_1| = |w_2| = |w_1| - 1.$$

#### Chapter D

Since our monomial ordering respects word length, it follows that all monomials are smaller than  $w_0$ . Since  $q^*$  was the nonzero element in the kernel with the smallest value of  $\text{lm}(q^*)$ , we must have

$$d\tilde{q}^* + \sum_{i=1}^p \varpi_i e_{\mathbf{I},i}^{\dagger} \tilde{\mathbf{q}}^* = 0.$$
 (D.17)

Thus, for all words w (not just those in  $\mathcal{B}_{\mathbf{B}}$ ), it follows that

$$d(\tilde{q}^{*}(w)) = -\sum_{i=1}^{p} \varpi_{i} e_{I,i}^{\dagger} \tilde{q}^{*}(w) = -\sum_{i=1}^{p} \varpi_{i} \tilde{q}^{*}(e_{I,i}w).$$
 (D.18)

Now, assume that  $|w| = |w_0|$ , so that  $|e_{I,i}w| = |w| + 1 > |w_0|$ . Since all monomials in  $\tilde{q}^*$  have length at most  $|w_0|$  (as  $w_0$  is the leading monomial and therefore the largest in our ordering), we must have  $\tilde{q}^*(e_{I,i}w) = 0$ . Consequently, we obtain:

$$d\tilde{q}^*(w) = 0$$
, for all  $|w| = |w_0|$ . (D.19)

Since  $w_0$  is the shortest non-empty word, it must contain at least one letter  $e_{I,k}$  and can be written as  $w_0 = e_{I,k}v_0$ , where  $v_0$  may be the empty word. Due to the normalization of  $\tilde{q}$ , we also note that  $\tilde{q}^*(e_{I,k}v_0) = \tilde{q}^*(w_0) = 1$ . Substituting  $w = v_0$  in eq. (D.18) yields:

$$d\tilde{q}^*(v_0) = -\sum_{i=1}^p \varpi_i \,\alpha_i \quad \text{with} \quad \alpha_i = -\tilde{q}^*(e_{I,i}v_0).$$
 (D.20)

Since  $|\mathbf{e}_{\mathbf{I},i}\mathbf{v}_0| = |\mathbf{w}_0|$ , equation eq. (D.19)) implies that  $\mathrm{d}\tilde{q}^*(\mathbf{e}_{\mathbf{I},i}\mathbf{v}_0) = 0$ , and thus the  $\alpha_i$  must be constants. By definition (or condition 1), the constants of  $\mathbb{A}_{\mathbf{B}}$  belong to  $\mathbb{K}$ , so  $\alpha_i \in \mathbb{K}$  for all i, meaning the right-hand side of eq. (D.20)) lies in  $\mathbb{V}_{\mathbf{B}}$ . At the same time, by definition,  $\tilde{q}^*(v_0) \in \mathcal{F}_{\mathbb{C}}$ , so the left-hand side of eq. (D.20)) belongs to  $\mathrm{d}\mathcal{F}_{\mathbb{C}}$ . This implies that eq. (D.20)) must lie in  $\mathrm{d}\mathcal{F}_{\mathbb{C}} \cap \mathbb{V}_{\mathbf{B}} = \{0\}$ . Since the  $\varpi_i$  form a basis of  $\mathbb{V}_{\mathbf{B}}$ , it follows that  $\alpha_i = 0$  for all i. This leads to a contradiction, as we also know that for some i = k,  $\tilde{q}^*(\mathbf{e}_{\mathbf{I},\mathbf{k}}\mathbf{v}_0) = \tilde{q}^*(\mathbf{w}_0) = 1$ .

 $\underline{2. \Rightarrow 1...}$  Let us assume, that there are  $\alpha_1, \ldots, \alpha_p \in \mathbb{K}$  and  $f \in \mathcal{F}_{\mathbb{C}}$  such that

$$-\sum_{i=1}^{p} \alpha_i \overline{\omega}_i = \mathrm{d}f, \qquad (D.21)$$

Again, we define a dual vector as in eq. (D.10)), in this case, we denote:

$$p_f^* = -f\mathbf{1}^* + \sum_{i=1}^p \alpha_i e_{I,i}^*.$$
 (D.22)

Then:

$$p_f^*(\mathbb{G}_I) = -f\mathbf{1}^*(\mathbb{G}_I) + \sum_{i=1}^p \alpha_i e_{I,i}^*(\mathbb{G}_I) = -f + \sum_{i=1}^p \alpha_i I_{\gamma}(\overline{\omega}_i).$$
 (D.23)

Equation (D.21) implies  $\mathrm{d} p_f^*(\mathbb{G}_I)=0$ , so  $p_f^*(\mathbb{G}_I)$  must be some constant  $\lambda$ . We define

$$q_f^* = p_f^* - \lambda \mathbf{1}^*$$
 (D.24)

Then:

$$0 = q_f^*(\mathbb{G}_I) = -(f+\lambda) + \sum_{i=1}^p \alpha_i I_\gamma(\overline{\omega}_i).$$
 (D.25)

Since 1 and  $I_{\gamma}(\varpi_i)$  are linearly independent over  $\mathcal{F}_{\mathbb{C}}$  by hypothesis, we must have

$$\alpha_1 = \ldots = \alpha_p = 0 \quad \text{and} \quad f = -\lambda.$$
 (D.26)

## Appendix E

## Representation Theory

<sup>1</sup>Note, that the notation GL(g, K) for a general linear group GL(V) implies, that we have chosen some basis for the g dimensional vector space and the group is the group of  $g \times g$  matrices over K.

We repeat here the basic definition of a representation of a Lie group and then discuss different representations for the group  $GL(g, \mathbb{C})$ . We will also comment on what the role of these representations is in the context of Siegel modular forms.

**Definition E.1** (Group Representation). A representation  $\rho = (\rho, V)$  of group G on a vector space V over a field K is a group homomorphism from G to GL(V), the general linear group on V:

$$\rho: G \to GL(V)$$
(E.1)

such that

$$\rho(g_1g_2) = \rho(g_1)\rho(g_2) \text{ for all } g_1, g_2 \in G.$$

The dimension of the representation space V is called the dimension or degree of the representation.

**Definition E.2** (Irreducibility). A representation  $(\rho, V)$  is called irreducible if it is non-zero and V has no non-trivial subspace W, such that  $(\rho|_W, W)$  is closed under the group action.

We recall that a Lie algebra representation  $\rho$  is called *reducible* if there is a matrix  $\mathbf{M} \in \mathrm{GL}(N,\mathbb{C})$  such that  $\mathbf{M}\rho\mathbf{M}^{-1}$  is block upper-triangular and an irreducible representation is one that is not reducible.

**Lemma 2** (Schur's Lemma). Let  $\rho: G \to \operatorname{GL}(V)$  be an irreducible representation of a finite group G. If a matrix  $\mathbf{A}$  commutes with  $\rho(g)$  for all  $g \in G$ , then  $\mathbf{A} = \lambda \mathbf{1}$  for some  $\lambda \in \mathbb{C}$ .

#### Irreducible Representations of $GL(g, \mathbb{C})$ .

↑ The discussion here was already given in [34], which resulted from collaborations with Claude Duhr, and Sven Stawinski. We only changed the notation and some of the wording to fit with the remainder of the thesis.

#### See also:

The Siegel modular group, is a subgroup  $\operatorname{Sp}(2g,\mathbb{Z}) \subset \operatorname{GL}(g,\mathbb{C}).$ We consider Siegel modular forms that transform under certain representations of this group in section 3.4.4 and discuss the appearance of such forms in the canonical differential equation a hyperelliptic Feynman integral family in section 6.2.

**Trivial Representation** Since we are considering a general linear group, the trivial representation is

$$\rho_{\rm id}: {\rm GL}(g,\mathbb{C}) \to {\rm GL}(1,\mathbb{C}), \mathbf{M} \mapsto \mathbf{1}.$$
(E.2)

**Determinant Representation** The determinant representation with index k is a one-dimensional irreducible representation defined by

$$\rho_{\text{det,k}} = \det^k : \text{GL}(g,\mathbb{C}) \to \text{GL}(1,\mathbb{C}), \, \mathbf{M} \mapsto (\det \mathbf{M})^k.$$
(E.3)

A group element in this representation acts by multiplication, i.e.

$$(\det \mathbf{M})^k : \mathbb{C} \to \mathbb{C}, z \mapsto (\det \mathbf{M})^k z.$$
 (E.4)

Siegel modular forms with weight  $\rho = \det^k$  are referred to as classical Siegel modular forms of weight k and degree g.

Fundamental and Dual Representation The fundamental representation is an irreducible representation of dimension g defined by:

$$\rho_{\rm F}: {\rm GL}({\rm g},\mathbb{C}) \to {\rm GL}({\rm g},\mathbb{C}), \boldsymbol{M} \mapsto \boldsymbol{M}.$$
(E.5)

The dual representation is an irreducible representation of dimension g defined by:

$$\rho_{\mathcal{F}}: \mathrm{GL}(\mathcal{G}, \mathbb{C}) \to \mathrm{GL}(\mathcal{G}, \mathbb{C}), \mathcal{M} \mapsto (\mathbf{M}^{-1})^{\mathrm{T}}.$$
(E.6)

Both of these representations  $\rho_{\rm D}(\boldsymbol{M})$  and  $\rho_{\rm F}(\boldsymbol{M})$  act by multiplication.

 $\underline{g=2}$  For g=2 the fundamental and dual representations are related. Note, that for  $M\in \mathrm{GL}(2,\mathbb{C})$ 

$$\epsilon(\mathbf{M}^{-1})^T \epsilon^{-1} = \det(\mathbf{M})^{-1} \mathbf{M} \quad \text{with} \quad \epsilon = \begin{pmatrix} 0 & 1 \\ -1 & 0 \end{pmatrix},$$
 (E.7)

This implies, that

$$\rho_{\rm D} \simeq \rho_{\rm F} \otimes \rho_{\rm det,-1} \,.$$
(E.8)

Symmetric Tensor Representation The symmetric tensor representations are a class of irreducible representations of dimension g, which are defined by

$$\rho_{\text{Sym,k}}: \text{GL}(g,\mathbb{C}) \to \text{GL}(\text{Sym}^k V), \mathbf{M} \mapsto \text{Sym}^k(\mathbf{M})$$
(E.9)

with

$$\operatorname{Sym}^{k} V = V^{\otimes k} / S_{k} \,, \tag{E.10}$$

with the symmetric group  $S_k$  permuting the k copies of the space V, which is here given by the representation space of the fundamental representation  $V = \mathbb{C}^g$ . The representation acts on tensor of rank k as

$$\operatorname{Sym}^{k}(\mathbf{M}): \operatorname{Sym}^{k}V \to \operatorname{Sym}^{k}V, T_{i_{1},\dots,i_{k}} \mapsto M_{i_{1},j_{1}}\dots M_{i_{k},j_{k}}T_{j_{1},\dots,j_{k}}. \tag{E.11}$$

# Acknowledgements

One of the best of aspects of doing my PhD were the people I got to meet and I really want to thank all of you for enriching my scientific journey and life.<sup>2</sup> There is no way to rank these connections in any way, so I will order these remarks by location – starting at home, in Bonn.

Of course, I want to start by thanking **Claude Duhr**, for all the support and opportunities I had during my PhD. I am very grateful for the variety of mathematical topics related to Feynman integrals I got to explore during my PhD: Thank you for sharing your broad knowledge on all of these with me at home but also letting me travel extensively to broaden my horizon. I learned a lot over the years, and I really appreciate the guidance and trust along the way. It was a great pleasure for me to work in a large group with many different member that greatly enriched my time in the office<sup>3</sup>:

Ani, Andres, Cathrin, Chandra, Chi, Ekta, Franka, Guideon, Paarth, Paul, Pooja, Sara, Sven, Yashasvee, Yoann and Yu.

Of course besides our group, I also thank the other Bethe center members with whom I spent many lunches and a few Christmas parties. Within the wider physics community in Bonn, I am very thankful for the

"Women\* in Physics" group, particularly my co-organizers Amelie, Cathrin, Elli, Hannah, Luna and Yashasvee.

All of you are great people in general and I am very curious to see what you will organise the next few years. During my PhD I learned that I really enjoy teaching and so I am also grateful for all students in my tutorials, who generally asked great questions. In particular to *Cathrin*, who kept doing that during her Master's thesis<sup>4</sup> and didn't let me get away with any half-knowledge. Without you, I would know far less about twisted cohomology and the last two years would also have been far less fun! Additionally I want to thank everyone who helped in any organisational matters, specifically

Christa, Lora, Nadine and Patricia as well as Oliver and Andreas.

And finally (amongst people in Bonn) of course I owe many thanks to my thesis committee:

Valentin Blomer, Lena Funcke, Claude Duhr, Albrecht Klemm.

Finally, I owe thanks to the people who gave comments on earlier versions of this thesis: Pooja Mukherjee, Sven Stawinski, Cathrin Semper, Franca Lippert and Amelie Mierau.

The place that has felt like my second (scientific) home has been Uppsala, not only for the last three and a half years but actually since my Erasmus semester

<sup>2</sup>This will just be a repetitive list of "names, I learned so much from you". But it in all cases, this is just true!.

<sup>3</sup>Whenever I wasn't too lazy for my three minute commute to the university and worked from home.

<sup>4</sup>And of course also now as a PhD student.

there in 2019. I will always be thankful to **Oliver Schlotterer** for the warm welcome back then, but also for being welcomed back in Uppsala again for a shorter time nearly every year. Thank you for always having a (virtual) open door for any questions or need of advise and the many enjoyable hours spent in front of blackboards in various places. Despite Oli being phenomenal in creating a welcoming atmoshphere, my fond memories of Uppsala are also due to some other people: Thanks for that also go to

Carlos, Henrik, Lucile<sup>5</sup>, Maor, Paolo and Yoann

as well as all the other people in the mathematical physics group. I am very grateful for the NORDITA for hosting me for a month within the *Visiting PhD fellowship*.

But I also spent a lot of time at neither of these places I called homes, visiting conferences and schools. Those were very enriching experience where I learned a lot. Specicically, this implies all participants (and of course organizers) that I got to interact with in any way at the following events

Elliptics ('22,'23,'24), Amplitudes '24, Holonomic Techniques for Feynman Integrals, Beyond Elliptic Polylogarithms, Fall Bonn HEP Meeting 2024, Geometries and Special Functions for Physics and Mathematics, the Amplitudes School '22, the Elliptics School '23 and the School in Atrani in '23.

Additionally, I am grateful for the invitations I got to visit other groups and the interesting discussions I had there: To Lorenzo for inviting me to Munich, Mathias for inviting me to Odense and Bernd for inviting me to Leipzig. In some way every one of these visits and events changed my perspective on some aspect of my research . In that sense, I should also specifically thank Matija and Clement who spent some time patiently explaining maths to me.

Between the coffee room in Bonn, blackboards all over the world and endless (often enjoyable) Zoom calls, I was lucky to work with many different people on a variety of projects during my PhD which allowed me to see many different viewpoints. So I want to thank all my collaborators

Claude Duhr, Andrzej Pokraka, Mathieu Giroux, Yoann Sohnle, Albrecht Klemm, Florian Loebbert, Christoph Nega, Giacomo Brunello, Sven Stawinski, Cathrin Semper, Robin Marzucca, Oliver Schlotterer, Axel Kleinschmidt, Matija Tapuskovic, Sebastian Pögel, Gaia Fontana, Sara Maggio

I really learned a lot from every single one of you. Some of you have also become good friends and I hope no matter where life takes us, our pathes will cross again and again somehow!

I will keep my thanks to people outside of academia generic and primarily deliver them in person, but I want to explicitly give my thanks to the person who inspired me start this journey more than 10 years ago, my school physics teacher Daniel Seeharsch. And now, ten years later, I also owe as much thanks for the people who reminded me of all the things in life that are important in life besides physics, particularly in the last year.

<sup>5</sup>Who made me especially proud, by claiming me as an honorary member of the Uppsala group.

#### Chapter E

And still, finally, thanks to all the theoretical physicists and mathematicians of the past, present and future, for building an abstract framework for how we can think of the world and other structures as humans. Having the background to admire and enjoy these things will surely add a sense of wonder and a source of pleasure to the rest of my life no matter what.

My work was funded by the European Union (ERC Consolidator Grant LoCo-Motive 101043686). Views and opinions expressed are however those of the author only and do not necessarily reflect those of the European Union or the European Research Council. Neither the European Union nor the granting authority can be held responsible for them.

# List of Figures

2.1	The bubble integral family has three master integrals, one in each sector. The top sector contains the unequal mass bubble [left] and the other two sectors contain tadpoles, each with one of the two	
2.2	masses of the full bubble integral [middle and right]  The upper graph is the kite graph with five propagators to which we associate distinct masses. Upon setting certain propagator weights to zero (or graphically <i>pinching</i> the propagators) one obtains two distinct sunrise graphs	28 35
2.3	We illustrate the loop-by-loop approach for computing the Baikov representation of the sunrise integral family. The first loop has loop	
2.4	momentum $\ell_1$ and the second loop has loop momentum $\ell_2$ We illustrate the loop-by-loop approach for computing the Baikov representation of the sunrise integral family. The first loop has loop	36
2.5	momentum $\ell_2$ and the second loop has loop momentum $\ell_1$ An illustration of how one obtains a fishnet graph by cutting along a closed contour in a regular tiling. In this example, a 6-loop graph is cut from a rectangular tiling, where the black graph depicts the position space representation and the light-orange graph depicts the dual momentum space representation	38 40
3.1 3.2	Varieties appearing in Feynman integrals	52
3.3	handles	59
3.4	replaced by $\infty$	60
3.5	around the holes	66
3.6	The periods $\omega_1$ and $\omega_2$ define the lattice $\Lambda_{\omega_1,\omega_2}$	68
4.1	The dual cycle $\check{\gamma}_j$ of eq. (4.29) is supported on the interval $(0, \lambda_j)$ as illustrated here	101

## LIST OF FIGURES

4.2	The dual cycle $\check{\eta}_j$ of eq. (4.30) is supported on the interval $(\lambda_{j-1}, \lambda_j)$ as illustrated here	101
4.3	The cycle $\gamma_j$ of eq. (4.32) is supported on a regularised version of the interval $(0, \lambda_j)$ as illustrated here	102
4.4	There are four twisted (co-)homology groups we can associate to a space $X$ and a twist $\Phi$ and for each pair of them we can associate a	103
4.5	pairing	103
4.6	The basis cycles of basis cycles of eq. (4.101) are depicted on a regularized interval $(0,1)^c$ and a $\epsilon$ -ball around $\lambda$ . The dual basis cycles of eq. (4.102) are supported on the intervals $(0,1)$ and $(\lambda,\infty)$	112
4.7	The single-valued map (lower-right) and coaction (upper-right) for the generating series of multiple polylogarithms as well as their relation is well understood. Additionally there exists a single-valued map for the generating series of iterated Eisenstein integrals. By analogy, we define a map $\Delta$ acting on the generating series for iter-	
	ated Eisenstein integrals.	122
4.8	The unequal mass sunrise integral family has seven master integrals and four of these are in the top sector	134
4.9	We derive the twisted cycles that we choose for the basis of the sunrise's homology group by choosing the intervals related to the sunrise's elliptic curve's $a$ and $b$ cycles	135
7.1	The Kite integral with its two sunrises and two tori	188
7.2	Graphical representation of all Feynman diagrams from the basis eq. (7.3) that have two propagators	191
7.3	Graphical representation of all Feynman diagrams from the basis in eq. $(7.3)$ that are in the sunrises' top sectors	191
7.4	Graphical representation of all Feynman diagrams from the basis in eq. (7.3) that are not the sunrises' top sectors but have three	
7.5	propagators	192
7.6	propagators and no sunrise subtopologies	192
1.0	A diagrammatic representation of the top sector of the kite integral family, which contains only $I_{1,1,1,1,1}$	192
8.1	A star integral in position space corresponds to a one-loop integral in momentum space	226
8.2	Ladder integrals in position space constitue an L-loop class of one-	∠∠U
	parameter fishnet graphs	228

## LIST OF FIGURES

8.3	A generic one-parameter fishnet graph in position space with a square	001
	tiling has four external points.	231
8.4	The one-loop fishnet integral in position space is a cross and its	
	momentum space version is a box	232
8.5	Ladder integrals in position space	233
В.1	Illustration of two configurations where the cycle and the dual cycle	
	intersect with agreeing branches of the twist near a point 0 or $\lambda_j$ .	250
B.2	Illustration of a configuration where the cycle and the dual cycle	
	intersect with disagreeing branches of the twist near a point $\lambda_j$	251
B.3	The self-intersection of the cycle $\gamma_j$ as defined in eq. (4.29) with three	
	local intersection points $v_1, v_2$ and $v_3$ marked	252
B.4	The self-intersection of the cycle $\gamma_j$ as defined in eq. (4.29) with two	
	local intersection points $v_1, v_2$ marked	253
B.5	An example for a configuration of hyperplanes bounding two cham-	
	bers $D$ and $E$ . The upper panel depicts the configuration of hy-	
	perplanes with both chambers and the branch choices of the $L_i(z)$	
	indicated by $+$ and $-$ . The lower panel shows just the chamber $D$	
	and put points on each crossing, boundary and plane to indicate	
	what they contribute to the self-intersection of the chamber labelled	
	D	254
B.6	An illustration of the blow-up of a vertex where $m$ hyperplanes meet	255
B.7	A depiction of the hyperplanes defined by the twist of the $_{p+1}F_p$	
	function and the bounded chambers $D_1, D_2, D_3$ that we choose to	
	support the basis of the corresponding homology group	260

# Bibliography

- [1] Gustav Uhre Jakobsen, Gustav Mogull, Jan Plefka, and Benjamin Sauer. "All things retarded: radiation-reaction in worldline quantum field theory". In: *JHEP* 10 (2022), p. 128. DOI: 10.1007/JHEP10(2022)128. arXiv: 2207. 00569 [hep-th].
- [2] Gustav Mogull, Jan Plefka, and Jan Steinhoff. "Classical black hole scattering from a worldline quantum field theory". In: *JHEP* 02 (2021), p. 048. DOI: 10.1007/JHEP02(2021)048. arXiv: 2010.02865 [hep-th].
- [3] Hjalte Frellesvig, Roger Morales, and Matthias Wilhelm. "Classifying post-Minkowskian geometries for gravitational waves via loop-by-loop Baikov". In: *JHEP* 08 (2024), p. 243. DOI: 10.1007/JHEP08(2024)243. arXiv: 2405. 17255 [hep-th].
- [4] Mathias Driesse et al. "High-precision black hole scattering with Calabi-Yau manifolds". In: (Nov. 2024). arXiv: 2411.11846 [hep-th].
- [5] Albrecht Klemm, Christoph Nega, Benjamin Sauer, and Jan Plefka. "Calabi-Yau periods for black hole scattering in classical general relativity". In: *Phys. Rev. D* 109.12 (2024), p. 124046. DOI: 10.1103/PhysRevD.109.124046. arXiv: 2401.07899 [hep-th].
- [6] Rishabh Bhardwaj, Andrzej Pokraka, Lecheng Ren, and Carlos Rodriguez. "A double copy from twisted (co)homology at genus one". In: *Journal of High Energy Physics* 2024.7 (July 2024). ISSN: 1029-8479. DOI: 10.1007/jhep07(2024)040. URL: http://dx.doi.org/10.1007/JHEP07(2024)040.
- [7] Francis Brown and Clément Dupont. "Single-valued integration and double copy". In: J. Reine Angew. Math. 2021.775 (2021), pp. 145–196. DOI: 10. 1515/crelle-2020-0042. arXiv: 1810.07682 [math.NT].
- [8] Stefan Weinzierl. Feynman Integrals. 2022. arXiv: 2201.03593 [hep-th]. URL: https://arxiv.org/abs/2201.03593.
- [9] Samuel Abreu, Ruth Britto, and Claude Duhr. "The SAGEX review on scattering amplitudes Chapter 3: Mathematical structures in Feynman integrals". In: *Journal of Physics A: Mathematical and Theoretical* 55.44 (Nov. 2022), p. 443004. ISSN: 1751-8121. DOI: 10.1088/1751-8121/ac87de. URL: http://dx.doi.org/10.1088/1751-8121/ac87de.

- [10] Jacob L. Bourjaily et al. "Functions Beyond Multiple Polylogarithms for Precision Collider Physics". In: *Snowmass 2021*. Mar. 2022. arXiv: 2203. 07088 [hep-ph].
- [11] Francis Brown and Oliver Schnetz. "A K3 in  $\phi^4$ ". In: *Duke Math. J.* 161.10 (2012), pp. 1817–1862. DOI: 10.1215/00127094–1644201. arXiv: 1006.4064 [math.AG].
- [12] Spencer Bloch, Matt Kerr, and Pierre Vanhove. "A Feynman integral via higher normal functions". In: *Compos. Math.* 151.12 (2015), pp. 2329–2375.
   DOI: 10.1112/S0010437X15007472. arXiv: 1406.2664 [hep-th].
- [13] Spencer Bloch, Matt Kerr, and Pierre Vanhove. "Local mirror symmetry and the sunset Feynman integral". In: Adv. Theor. Math. Phys. 21 (2017), pp. 1373–1453. DOI: 10.4310/ATMP.2017.v21.n6.a1. arXiv: 1601.08181 [hep-th].
- Jacob L. Bourjaily, Andrew J. McLeod, Matt von Hippel, and Matthias Wilhelm. "Bounded Collection of Feynman Integral Calabi-Yau Geometries".
   In: Phys. Rev. Lett. 122.3 (2019), p. 031601. DOI: 10.1103/PhysRevLett. 122.031601. arXiv: 1810.07689 [hep-th].
- [15] Jacob L. Bourjaily et al. "Embedding Feynman Integral (Calabi-Yau) Geometries in Weighted Projective Space". In: JHEP 01 (2020), p. 078. DOI: 10.1007/JHEP01(2020)078. arXiv: 1910.01534 [hep-th].
- [16] Albrecht Klemm, Christoph Nega, and Reza Safari. "The *l*-loop Banana Amplitude from GKZ Systems and relative Calabi-Yau Periods". In: *JHEP* 04 (2020), p. 088. DOI: 10.1007/JHEP04(2020)088. arXiv: 1912.06201 [hep-th].
- [17] Cristian Vergu and Matthias Volk. "Traintrack Calabi-Yaus from Twistor Geometry". In: *JHEP* 07 (2020), p. 160. DOI: 10.1007/JHEP07(2020)160. arXiv: 2005.08771 [hep-th].
- [18] Kilian Bönisch, Fabian Fischbach, Albrecht Klemm, Christoph Nega, and Reza Safari. "Analytic structure of all loop banana integrals". In: *JHEP* 05 (2021), p. 066. DOI: 10.1007/JHEP05(2021)066. arXiv: 2008.10574 [hep-th].
- [19] Kilian Bönisch, Claude Duhr, Fabian Fischbach, Albrecht Klemm, and Christoph Nega. "Feynman integrals in dimensional regularization and extensions of Calabi-Yau motives". In: *JHEP* 09 (2022), p. 156. DOI: 10.1007/JHEP09(2022) 156. arXiv: 2108.05310 [hep-th].
- [20] Claude Duhr, Albrecht Klemm, Christoph Nega, and Lorenzo Tancredi. "The ice cone family and iterated integrals for Calabi-Yau varieties". In: *JHEP* 02 (2023), p. 228. DOI: 10.1007/JHEP02(2023)228. arXiv: 2212.09550 [hep-th].

- [21] Sebastian Pögel, Xing Wang, and Stefan Weinzierl. "The three-loop equalmass banana integral in  $\varepsilon$ -factorised form with meromorphic modular forms". In: *JHEP* 09 (2022), p. 062. DOI: 10.1007/JHEP09(2022)062. arXiv: 2207. 12893 [hep-th].
- [22] Sebastian Pögel, Xing Wang, and Stefan Weinzierl. "Taming Calabi-Yau Feynman Integrals: The Four-Loop Equal-Mass Banana Integral". In: *Phys. Rev. Lett.* 130.10 (2023), p. 101601. DOI: 10.1103/PhysRevLett.130.101601. arXiv: 2211.04292 [hep-th].
- [23] Andrew J. McLeod and Matt von Hippel. "Traintracks All the Way Down". In: (June 2023). arXiv: 2306.11780 [hep-th].
- [24] Lennard Görges, Christoph Nega, Lorenzo Tancredi, and Fabian J. Wagner. "On a procedure to derive  $\epsilon$ -factorised differential equations beyond polylogarithms". In: *JHEP* 07 (2023), p. 206. DOI: 10.1007/JHEP07(2023)206. arXiv: 2305.14090 [hep-th].
- [25] Hjalte Frellesvig, Roger Morales, Sebastian Pögel, Stefan Weinzierl, and Matthias Wilhelm. "Calabi-Yau Feynman integrals in gravity:  $\varepsilon$ -factorized form for apparent singularities". In: (Dec. 2024). arXiv: 2412.12057 [hep-th].
- [26] Hjalte Frellesvig, Roger Morales, and Matthias Wilhelm. "Calabi-Yau Meets Gravity: A Calabi-Yau Threefold at Fifth Post-Minkowskian Order". In: *Phys. Rev. Lett.* 132.20 (2024), p. 201602. DOI: 10.1103/PhysRevLett. 132.201602. arXiv: 2312.11371 [hep-th].
- [27] Hans Jockers et al. "A Calabi-Yau-to-curve correspondence for Feynman integrals". In: *JHEP* 01 (2025), p. 030. DOI: 10.1007/JHEP01(2025)030. arXiv: 2404.05785 [hep-th].
- [28] Claude Duhr, Federico Gasparotto, Christoph Nega, Lorenzo Tancredi, and Stefan Weinzierl. "On the electron self-energy to three loops in QED". In: *JHEP* 11 (2024), p. 020. DOI: 10.1007/JHEP11(2024)020. arXiv: 2408. 05154 [hep-th].
- [29] Rijun Huang and Yang Zhang. "On Genera of Curves from High-loop Generalized Unitarity Cuts". In: *JHEP* 04 (2013), p. 080. DOI: 10.1007/JHEP04(2013)080. arXiv: 1302.1023 [hep-ph].
- [30] Jonathan D. Hauenstein, Rijun Huang, Dhagash Mehta, and Yang Zhang. "Global Structure of Curves from Generalized Unitarity Cut of Three-loop Diagrams". In: *JHEP* 02 (2015), p. 136. DOI: 10.1007/JHEP02(2015)136. arXiv: 1408.3355 [hep-th].
- [31] Robin Marzucca, Andrew J. McLeod, Ben Page, Sebastian Pögel, and Stefan Weinzierl. "Genus drop in hyperelliptic Feynman integrals". In: *Phys. Rev. D* 109.3 (2024), p. L031901. DOI: 10.1103/PhysRevD.109.L031901. arXiv: 2307.11497 [hep-th].

- [32] Mathieu Giroux, Andrzej Pokraka, Franziska Porkert, and Yoann Sohnle. "The soaring kite: a tale of two punctured tori". In: *JHEP* 05 (2024), p. 239. DOI: 10.1007/JHEP05(2024)239. arXiv: 2401.14307 [hep-th].
- [33] Mathieu Giroux, Andrzej Pokraka, Franziska Porkert, and Yoann Sohnle. "Looping the loops: a tale of elliptic dual Feynman integrals". In: *PoS* RAD-COR2023 (2024), p. 033. DOI: 10.22323/1.432.0033. arXiv: 2309.04592 [hep-th].
- [34] Claude Duhr, Franziska Porkert, and Sven F. Stawinski. "Canonical differential equations beyond genus one". In: *JHEP* 02 (2025), p. 014. DOI: 10.1007/JHEP02(2025)014. arXiv: 2412.02300 [hep-th].
- [35] Claude Duhr, Albrecht Klemm, Florian Loebbert, Christoph Nega, and Franziska Porkert. "Yangian-Invariant Fishnet Integrals in Two Dimensions as Volumes of Calabi-Yau Varieties". In: *Phys. Rev. Lett.* 130.4 (2023), p. 041602. DOI: 10.1103/PhysRevLett.130.041602. arXiv: 2209.05291 [hep-th].
- [36] Claude Duhr and Franziska Porkert. "Feynman integrals in two dimensions and single-valued hypergeometric functions". In: *JHEP* 02 (2024), p. 179. DOI: 10.1007/JHEP02(2024)179. arXiv: 2309.12772 [hep-th].
- [37] Claude Duhr, Albrecht Klemm, Florian Loebbert, Christoph Nega, and Franziska Porkert. "The Basso-Dixon formula and Calabi-Yau geometry". In: *JHEP* 03 (2024), p. 177. DOI: 10.1007/JHEP03(2024)177. arXiv: 2310. 08625 [hep-th].
- [38] Claude Duhr, Albrecht Klemm, Florian Loebbert, Christoph Nega, and Franziska Porkert. "Geometry from integrability: multi-leg fishnet integrals in two dimensions". In: *JHEP* 07 (2024), p. 008. DOI: 10.1007/JHEP07(2024) 008. arXiv: 2402.19034 [hep-th].
- [39] Pierpaolo Mastrolia and Sebastian Mizera. "Feynman integrals and intersection theory". In: *Journal of High Energy Physics* 2019.2 (Feb. 2019). ISSN: 1029-8479. DOI: 10.1007/jhep02(2019)139. URL: http://dx.doi.org/10.1007/JHEP02(2019)139.
- [40] Pierpaolo Mastrolia and Sebastian Mizera. "Feynman Integrals and Intersection Theory". In: JHEP 02 (2019), p. 139. DOI: 10.1007/JHEP02(2019)139. arXiv: 1810.03818 [hep-th].
- [41] Hjalte Frellesvig et al. "Decomposition of Feynman Integrals on the Maximal Cut by Intersection Numbers". In: *JHEP* 05 (2019), p. 153. DOI: 10.1007/JHEP05(2019)153. arXiv: 1901.11510 [hep-ph].
- [42] Giacomo Brunello, Vsevolod Chestnov, and Pierpaolo Mastrolia. "Intersection Numbers from Companion Tensor Algebra". In: (Aug. 2024). arXiv: 2408.16668 [hep-th].

- [43] Gaia Fontana and Tiziano Peraro. "Reduction to master integrals via intersection numbers and polynomial expansions". In: *JHEP* 08 (2023), p. 175. DOI: 10.1007/JHEP08(2023)175. arXiv: 2304.14336 [hep-ph].
- [44] Sebastian Mizera. "Scattering Amplitudes from Intersection Theory". In: *Phys. Rev. Lett.* 120.14 (2018), p. 141602. DOI: 10.1103/PhysRevLett. 120.141602. arXiv: 1711.00469 [hep-th].
- [45] Sebastian Mizera. "Status of Intersection Theory and Feynman Integrals". In: PoS MA2019 (2019), p. 016. DOI: 10.22323/1.383.0016. arXiv: 2002. 10476 [hep-th].
- [46] Sebastian Mizera. "Aspects of Scattering Amplitudes and Moduli Space Localization". PhD thesis. Princeton, Inst. Advanced Study, 2020. DOI: 10. 1007/978-3-030-53010-5. arXiv: 1906.02099 [hep-th].
- [47] Simon Caron-Huot and Andrzej Pokraka. "Duals of Feynman integrals. Part
   I. Differential equations". In: JHEP 12 (2021), p. 045. DOI: 10.1007/
   JHEP12(2021)045. arXiv: 2104.06898 [hep-th].
- [48] Federico Gasparotto, Pouria Mazloumi, and Xiaofeng Xu. "Differential equations for tree–level cosmological correlators with massive states". In: (Nov. 2024). arXiv: 2411.05632 [hep-th].
- [49] Simon Caron-Huot and Andrzej Pokraka. "Duals of Feynman Integrals. Part II. Generalized unitarity". In: *JHEP* 04 (2022), p. 078. DOI: 10.1007/JHEP04(2022)078. arXiv: 2112.00055 [hep-th].
- [50] Claude Duhr, Franziska Porkert, Cathrin Semper, and Sven F. Stawinski. "Twisted Riemann bilinear relations and Feynman integrals". In: *JHEP* 03 (2025), p. 019. DOI: 10.1007/JHEP03(2025)019. arXiv: 2407.17175 [hep-th].
- [51] Michael E. Peskin and Daniel V. Schroeder. An Introduction to quantum field theory. Reading, USA: Addison-Wesley, 1995. ISBN: 978-0-201-50397-5, 978-0-429-50355-9, 978-0-429-49417-8. DOI: 10.1201/9780429503559.
- [52] Steven Weinberg. The Quantum theory of fields. Vol. 1: Foundations. Cambridge University Press, June 2005. ISBN: 978-0-521-67053-1, 978-0-511-25204-4. DOI: 10.1017/CB09781139644167.
- [53] Matthew D. Schwartz. Quantum Field Theory and the Standard Model. Cambridge University Press, Mar. 2014. ISBN: 978-1-107-03473-0, 978-1-107-03473-0.
- [54] Simon Badger, Johannes Henn, Jan Plefka, and Simone Zoia. Scattering Amplitudes in Quantum Field Theory. 2023. arXiv: 2306.05976 [hep-th]. URL: https://arxiv.org/abs/2306.05976.
- [55] Henriette Elvang and Yu-tin Huang. Scattering Amplitudes. 2014. arXiv: 1308.1697 [hep-th]. URL: https://arxiv.org/abs/1308.1697.

- [56] F. J. Dyson. "Divergence of Perturbation Theory in Quantum Electrodynamics". In: *Phys. Rev.* 85 (4 Feb. 1952), pp. 631–632. DOI: 10.1103/PhysRev.85.631. URL: https://link.aps.org/doi/10.1103/PhysRev.85.631.
- [57] G. Passarino and M. J. G. Veltman. "One Loop Corrections for e+ e- Annihilation Into mu+ mu- in the Weinberg Model". In: *Nucl. Phys. B* 160 (1979), pp. 151–207. DOI: 10.1016/0550-3213(79)90234-7.
- [58] P. Nogueira. "Automatic Feynman Graph Generation". In: Journal of Computational Physics 105.2 (1993), pp. 279–289. ISSN: 0021-9991. DOI: https://doi.org/10.1006/jcph.1993.1074. URL: https://www.sciencedirect.com/science/article/pii/S0021999183710740.
- [59] Thomas Hahn. "Generating Feynman diagrams and amplitudes with FeynArts 3". In: Computer Physics Communications 140.3 (Nov. 2001), pp. 418–431. ISSN: 0010-4655. DOI: 10.1016/s0010-4655(01)00290-9. URL: http://dx.doi.org/10.1016/S0010-4655(01)00290-9.
- [60] J. A. M. Vermaseren. "New features of FORM". In: (2000). arXiv: math-ph/0010025 [math-ph]. URL: https://arxiv.org/abs/math-ph/0010025.
- [61] J. Kuipers, T. Ueda, J.A.M. Vermaseren, and J. Vollinga. "FORM version 4.0". In: *Computer Physics Communications* 184.5 (May 2013), pp. 1453–1467. ISSN: 0010-4655. DOI: 10.1016/j.cpc.2012.12.028. URL: http://dx.doi.org/10.1016/j.cpc.2012.12.028.
- [62] Ben Ruijl, Takahiro Ueda, and Jos Vermaseren. "FORM version 4.2". In: (2017). arXiv: 1707.06453 [hep-ph]. URL: https://arxiv.org/abs/1707.06453.
- [63] R. Mertig, M. Bohm, and Ansgar Denner. "FEYN CALC: Computer algebraic calculation of Feynman amplitudes". In: *Comput. Phys. Commun.* 64 (1991), pp. 345–359. DOI: 10.1016/0010-4655(91)90130-D.
- [64] Vladyslav Shtabovenko, Rolf Mertig, and Frederik Orellana. "New Developments in FeynCalc 9.0". In: *Comput. Phys. Commun.* 207 (2016), pp. 432–444. DOI: 10.1016/j.cpc.2016.06.008. arXiv: 1601.01167 [hep-ph].
- [65] Vladyslav Shtabovenko, Rolf Mertig, and Frederik Orellana. "FeynCalc 9.3: New features and improvements". In: Comput. Phys. Commun. 256 (2020), p. 107478. DOI: 10.1016/j.cpc.2020.107478. arXiv: 2001.04407 [hep-ph].
- [66] J.H. Schwarz M.B. Green and E. Witten. *Superstring Theory*. Cambridge University Press, 2012.
- [67] J. Polchinski. String theory. Vol. 1: An introduction to the bosonic string. Cambridge University Press, 2007.
- [68] H. Kawai, D. C. Lewellen, and S. H. H. Tye. "A Relation Between Tree Amplitudes of Closed and Open Strings". In: *Nucl. Phys. B* 269 (1986), pp. 1–23. DOI: 10.1016/0550-3213(86)90362-7.

- [69] B. P. Abbott et al. "Observation of Gravitational Waves from a Binary Black Hole Merger". In: *Phys. Rev. Lett.* 116.6 (2016), p. 061102. DOI: 10.1103/PhysRevLett.116.061102. arXiv: 1602.03837 [gr-qc].
- [70] R. Abbott et al. "GWTC-3: Compact Binary Coalescences Observed by LIGO and Virgo during the Second Part of the Third Observing Run". In: *Phys. Rev. X* 13.4 (2023), p. 041039. DOI: 10.1103/PhysRevX.13.041039. arXiv: 2111.03606 [gr-qc].
- [71] Pau Amaro-Seoane et al. "Laser Interferometer Space Antenna". In: (Feb. 2017). arXiv: 1702.00786 [astro-ph.IM].
- [72] M. Punturo et al. "The Einstein Telescope: A third-generation gravitational wave observatory". In: *Class. Quant. Grav.* 27 (2010). Ed. by Fulvio Ricci, p. 194002. DOI: 10.1088/0264-9381/27/19/194002.
- [73] N. E. J. Bjerrum-Bohr, P. H. Damgaard, L. Plante, and P. Vanhove. "The SAGEX review on scattering amplitudes Chapter 13: Post-Minkowskian expansion from scattering amplitudes". In: *J. Phys. A* 55.44 (2022), p. 443014. DOI: 10.1088/1751-8121/ac7a78. arXiv: 2203.13024 [hep-th].
- [74] David A. Kosower, Ricardo Monteiro, and Donal O'Connell. "The SAGEX review on scattering amplitudes Chapter 14: Classical gravity from scattering amplitudes". In: *J. Phys. A* 55.44 (2022), p. 443015. DOI: 10.1088/1751-8121/ac8846. arXiv: 2203.13025 [hep-th].
- [75] Alessandra Buonanno et al. "Snowmass White Paper: Gravitational Waves and Scattering Amplitudes". In: *Snowmass 2021*. Apr. 2022. arXiv: 2204. 05194 [hep-th].
- [76] Shounak De and Andrzej Pokraka. "Cosmology meets cohomology". In: JHEP 03 (2024), p. 156. DOI: 10.1007/JHEP03(2024)156. arXiv: 2308. 03753 [hep-th].
- [77] Shounak De and Andrzej Pokraka. "A physical basis for cosmological correlators from cuts". In: (Nov. 2024). arXiv: 2411.09695 [hep-th].
- [78] Jiaqi Chen, Bo Feng, and Yi-Xiao Tao. "Multivariate hypergeometric solutions of cosmological (dS) correlators by d log-form differential equations". In: (Nov. 2024). arXiv: 2411.03088 [hep-th].
- [79] Daniel Baumann, Harry Goodhew, and Hayden Lee. "Kinematic Flow for Cosmological Loop Integrands". In: (Oct. 2024). arXiv: 2410.17994 [hep-th].
- [80] Thomas W. Grimm and Arno Hoefnagels. "Reductions of GKZ Systems and Applications to Cosmological Correlators". In: (Sept. 2024). arXiv: 2409. 13815 [hep-th].
- [81] Song He, Xuhang Jiang, Jiahao Liu, Qinglin Yang, and Yao-Qi Zhang. "Differential equations and recursive solutions for cosmological amplitudes". In: (July 2024). arXiv: 2407.17715 [hep-th].
- [82] Nima Arkani-Hamed et al. "Differential Equations for Cosmological Correlators". In: (Dec. 2023). arXiv: 2312.05303 [hep-th].

- [83] Shounak De and Andrzej Pokraka. "A physical basis for cosmological correlators from cuts". In: (Nov. 2024). arXiv: 2411.09695 [hep-th].
- [84] Charalampos Anastasiou, Diogo P. L. Bragança, Leonardo Senatore, and Henry Zheng. "Efficiently evaluating loop integrals in the EFTofLSS using QFT integrals with massive propagators". In: *JHEP* 01 (2024), p. 002. DOI: 10.1007/JHEP01(2024)002. arXiv: 2212.07421 [astro-ph.C0].
- [85] Hjalte Frellesvig and Costas G. Papadopoulos. "Cuts of Feynman Integrals in Baikov representation". In: Journal of High Energy Physics 2017.4 (Apr. 2017). ISSN: 1029-8479. DOI: 10.1007/jhep04(2017)083. URL: http://dx. doi.org/10.1007/JHEP04(2017)083.
- [86] Hjalte Frellesvig and Costas G. Papadopoulos. "Cuts of Feynman Integrals in Baikov representation". In: *JHEP* 04 (2017), p. 083. DOI: 10.1007/JHEP04(2017)083. arXiv: 1701.07356 [hep-ph].
- [87] Hjalte Frellesvig. "The Loop-by-Loop Baikov Representation Strategies and Implementation". In: (Dec. 2024). arXiv: 2412.01804 [hep-th].
- [88] Ruth Britto, Claude Duhr, Holmfridur S. Hannesdottir, and Sebastian Mizera. "Cutting-Edge Tools for Cutting Edges". In: Feb. 2024. DOI: 10.1016/B978-0-323-95703-8.00097-5. arXiv: 2402.19415 [hep-th].
- [89] Samuel Abreu, Ruth Britto, Claude Duhr, and Einan Gardi. "Cuts from residues: the one-loop case". In: *JHEP* 06 (2017), p. 114. DOI: 10.1007/JHEP06(2017)114. arXiv: 1702.03163 [hep-th].
- [90] Charalampos Anastasiou and Kirill Melnikov. "Higgs boson production at hadron colliders in NNLO QCD". In: Nucl. Phys. B 646 (2002), pp. 220– 256. DOI: 10.1016/S0550-3213(02)00837-4. arXiv: hep-ph/0207004.
- [91] Charalampos Anastasiou, Lance J. Dixon, Kirill Melnikov, and Frank Petriello. "Dilepton rapidity distribution in the Drell-Yan process at NNLO in QCD". In: *Phys. Rev. Lett.* 91 (2003), p. 182002. DOI: 10.1103/PhysRevLett.91. 182002. arXiv: hep-ph/0306192.
- [92] Christian Bogner, Stefan Müller-Stach, and Stefan Weinzierl. "The unequal mass sunrise integral expressed through iterated integrals on  $\overline{\mathcal{M}}_{1,3}$ ". In: (2019). arXiv: 1907.01251 [hep-th].
- [93] Afaf Sabry. "Fourth order spectral functions for the electron propagator". In: Nuclear Physics 33 (1962), pp. 401-430. ISSN: 0029-5582. DOI: https://doi.org/10.1016/0029-5582(62)90535-7. URL: https://www.sciencedirect.com/science/article/pii/0029558262905357.
- [94] Ina Hönemann, Kirsten Tempest, and Stefan Weinzierl. "Electron self-energy in QED at two loops revisited". In: *Physical Review D* 98.11 (Dec. 2018). ISSN: 2470-0029. DOI: 10.1103/physrevd.98.113008. URL: http://dx. doi.org/10.1103/PhysRevD.98.113008.
- [95] Felix Forner, Christoph Nega, and Lorenzo Tancredi. "On the photon self-energy to three loops in QED". In: (Nov. 2024). arXiv: 2411.19042 [hep-th].

- [96] S. Bauberger, Frits A. Berends, M. Bohm, and M. Buza. "Analytical and numerical methods for massive two loop selfenergy diagrams". In: Nucl. Phys. B 434 (1995), pp. 383–407. DOI: 10.1016/0550-3213(94)00475-T. arXiv: hep-ph/9409388.
- [97] Arttu K. Rajantie. "Feynman diagrams to three loops in three-dimensional field theory". In: *Nucl. Phys. B* 480 (1996). [Erratum: Nucl.Phys.B 513, 761–762 (1998)], pp. 729–752. DOI: 10.1016/S0550-3213(96)00474-9. arXiv: hep-ph/9606216.
- [98] S. Bauberger, M. Böhm, G. Weiglein, Frits A. Berends, and M. Buza. "Calculation of two-loop self-energies in the electroweak Standard Model". In: Nucl. Phys. B Proc. Suppl. 37.2 (1994). Ed. by T. Riemann and Johannes Blümlein, pp. 95–114. DOI: 10.1016/0920-5632(94)90665-3. arXiv: hep-ph/9406404.
- [99] Michele Caffo, H. Czyz, S. Laporta, and E. Remiddi. "The Master differential equations for the two loop sunrise selfmass amplitudes". In: *Nuovo Cim.* A 111 (1998), pp. 365–389. arXiv: hep-th/9805118.
- [100] S. Laporta and E. Remiddi. "Analytic treatment of the two loop equal mass sunrise graph". In: Nuclear Physics B 704.1-2 (Jan. 2005), pp. 349-386. ISSN: 0550-3213. DOI: 10.1016/j.nuclphysb.2004.10.044. URL: http://dx.doi.org/10.1016/j.nuclphysb.2004.10.044.
- [101] B. A. Kniehl, A. V. Kotikov, A. Onishchenko, and O. Veretin. "Two-loop sunset diagrams with three massive lines". In: *Nucl. Phys. B* 738 (2006), pp. 306–316. DOI: 10.1016/j.nuclphysb.2006.01.013. arXiv: hep-ph/0510235.
- [102] Luise Adams, Christian Bogner, and Stefan Weinzierl. "The two-loop sunrise graph with arbitrary masses". In: *J. Math. Phys.* 54 (2013), p. 052303. DOI: 10.1063/1.4804996. arXiv: 1302.7004 [hep-ph].
- [103] Luise Adams, Christian Bogner, and Stefan Weinzierl. "The two-loop sunrise graph in two space-time dimensions with arbitrary masses in terms of elliptic dilogarithms". In: *J. Math. Phys.* 55.10 (2014), p. 102301. DOI: 10.1063/1. 4896563. arXiv: 1405.5640 [hep-ph].
- [104] Luise Adams, Christian Bogner, and Stefan Weinzierl. "The two-loop sunrise integral around four space-time dimensions and generalisations of the Clausen and Glaisher functions towards the elliptic case". In: *J. Math. Phys.* 56.7 (2015), p. 072303. DOI: 10.1063/1.4926985. arXiv: 1504.03255 [hep-ph].
- [105] Matija Tapušković. "The cosmic Galois group, the sunrise Feynman integral, and the relative completion of  $\Gamma^1(6)$ ". In: Commun. Num. Theor. Phys. 18.2 (2024), pp. 261–326. DOI: 10.4310/CNTP.2024.v18.n2.a1. arXiv: 2303.17534 [math.AG].

- [106] Spencer Bloch and Pierre Vanhove. "The elliptic dilogarithm for the sunset graph". In: J. Number Theor. 148 (2015), pp. 328-364. DOI: 10.1016/j.jnt.2014.09.032. arXiv: 1309.5865 [hep-th].
- [107] Sebastian Pögel, Xing Wang, and Stefan Weinzierl. "Bananas of equal mass: any loop, any order in the dimensional regularisation parameter". In: *JHEP* 04 (2023), p. 117. DOI: 10.1007/JHEP04(2023)117. arXiv: 2212.08908 [hep-th].
- [108] Rijun Huang and Yang Zhang. "On genera of curves from high-loop generalized unitarity cuts". In: *Journal of High Energy Physics* 2013.4 (Apr. 2013). ISSN: 1029-8479. DOI: 10.1007/jhep04(2013)080. URL: http://dx.doi.org/10.1007/JHEP04(2013)080.
- [109] Alessandro Georgoudis and Yang Zhang. "Two-loop integral reduction from elliptic and hyperelliptic curves". In: *Journal of High Energy Physics* 2015.12 (Dec. 2015), pp. 1–26. ISSN: 1029-8479. DOI: 10.1007/jhep12(2015)086. URL: http://dx.doi.org/10.1007/JHEP12(2015)086.
- [110] Omer Gürdoğan and Vladimir Kazakov. "New Integrable 4D Quantum Field Theories from Strongly Deformed Planar  $\mathcal{N}=4$  Supersymmetric Yang-Mills Theory". In: *Phys. Rev. Lett.* 117.20 (2016). [Addendum: Phys.Rev.Lett. 117, 259903 (2016)], p. 201602. DOI: 10.1103/PhysRevLett.117.201602. arXiv: 1512.06704 [hep-th].
- [111] Vladimir Kazakov and Enrico Olivucci. "Biscalar Integrable Conformal Field Theories in Any Dimension". In: *Phys. Rev. Lett.* 121.13 (2018), p. 131601. DOI: 10.1103/PhysRevLett.121.131601. arXiv: 1801.09844 [hep-th].
- [112] Florian Loebbert, Julian Miczajka, Dennis Müller, and Hagen Münkler. "Yangian Bootstrap for Massive Feynman Integrals". In: *SciPost Phys.* 11 (2021), p. 010. DOI: 10.21468/SciPostPhys.11.1.010. arXiv: 2010.08552 [hep-th].
- [113] Florian Loebbert and Julian Miczajka. "Massive Fishnets". In: *JHEP* 12 (2020), p. 197. DOI: 10.1007/JHEP12(2020) 197. arXiv: 2008.11739 [hep-th].
- [114] Florian Loebbert and Julian Miczajka. "Massive Integrability: From Fishnet Theories to Feynman Graphs and Back". In: *PoS* EPS-HEP2021 (2022), p. 733. DOI: 10.22323/1.398.0733. arXiv: 2109.11937 [hep-th].
- [115] Florian Loebbert. "Integrability for Feynman integrals". In: SciPost Phys. Proc. 14 (2023), p. 008. DOI: 10.21468/SciPostPhysProc.14.008. arXiv: 2212.09636 [hep-th].
- [116] Johannes M. Henn. "Multiloop Integrals in Dimensional Regularization Made Simple". In: *Phys. Rev. Lett.* 110 (25 June 2013), p. 251601. DOI: 10.1103/PhysRevLett.110.251601. URL: https://link.aps.org/doi/10.1103/PhysRevLett.110.251601.

- [117] Johannes M Henn. "Lectures on differential equations for Feynman integrals". In: Journal of Physics A: Mathematical and Theoretical 48.15 (Mar. 2015), p. 153001. ISSN: 1751-8121. DOI: 10.1088/1751-8113/48/15/153001. URL: http://dx.doi.org/10.1088/1751-8113/48/15/153001.
- [118] A.V. Kotikov. "Differential equations method. New technique for massive Feynman diagram calculation". In: *Physics Letters B* 254.1 (1991), pp. 158–164. ISSN: 0370-2693. DOI: https://doi.org/10.1016/0370-2693(91) 90413-K. URL: https://www.sciencedirect.com/science/article/pii/037026939190413K.
- [119] Ettore Remiddi. "Differential equations for Feynman graph amplitudes". In: *Nuovo Cim. A* 110 (1997), pp. 1435–1452. DOI: 10.1007/BF03185566. arXiv: hep-th/9711188.
- [120] T. Gehrmann and E. Remiddi. "Differential equations for two-loop four-point functions". In: *Nucl. Phys. B* 580 (2000), pp. 485–518. DOI: 10.1016/S0550-3213(00)00223-6. arXiv: hep-ph/9912329.
- [121] F. V. Tkachov. "A theorem on analytical calculability of 4-loop renormalization group functions". In: *Phys. Lett. B* 100 (1981), pp. 65–68. DOI: 10.1016/0370-2693(81)90288-4.
- [122] K. G. Chetyrkin and F. V. Tkachov. "Integration by parts: The algorithm to calculate  $\beta$ -functions in 4 loops". In: *Nucl. Phys. B* 192 (1981), pp. 159–204. DOI: 10.1016/0550-3213(81)90199-1.
- [123] S. Laporta. "High-precision calculation of multiloop Feynman integrals by difference equations". In: *Int. J. Mod. Phys. A* 15 (2000), pp. 5087–5159. DOI: 10.1142/S0217751X00002159. arXiv: hep-ph/0102033.
- [124] S. Laporta. "Calculation of Feynman integrals by difference equations". In: *Acta Phys. Polon. B* 34 (2003). Ed. by M. Awramik, M. Czakon, and J. Gluza, pp. 5323–5334. arXiv: hep-ph/0311065.
- [125] A. von Manteuffel and C. Studerus. "Reduze 2 Distributed Feynman Integral Reduction". In: (2012). arXiv: 1201.4330 [hep-ph]. URL: https://arxiv.org/abs/1201.4330.
- [126] Roman N Lee. "LiteRed 1.4: a powerful tool for reduction of multiloop integrals". In: Journal of Physics: Conference Series 523 (June 2014), p. 012059. ISSN: 1742-6596. DOI: 10.1088/1742-6596/523/1/012059. URL: http://dx.doi.org/10.1088/1742-6596/523/1/012059.
- [127] A.V. Smirnov and F.S. Chukharev. "FIRE6: Feynman Integral REduction with modular arithmetic". In: Computer Physics Communications 247 (Feb. 2020), p. 106877. ISSN: 0010-4655. DOI: 10.1016/j.cpc.2019.106877. URL: http://dx.doi.org/10.1016/j.cpc.2019.106877.

- [128] Jonas Klappert, Fabian Lange, Philipp Maierhöfer, and Johann Usovitsch. "Integral reduction with Kira 2.0 and finite field methods". In: Computer Physics Communications 266 (Sept. 2021), p. 108024. ISSN: 0010-4655. DOI: 10.1016/j.cpc.2021.108024. URL: http://dx.doi.org/10.1016/j.cpc.2021.108024.
- [129] R.N Lee. "Group structure of the integration-by-part identities and its application to the reduction of multiloop integrals". In: *Journal of High Energy Physics* 2008.07 (July 2008), pp. 031–031. ISSN: 1029-8479. DOI: 10.1088/1126-6708/2008/07/031. URL: http://dx.doi.org/10.1088/1126-6708/2008/07/031.
- [130] O. V. Tarasov. "Computation of Grobner bases for two loop propagator type integrals". In: *Nucl. Instrum. Meth. A* 534 (2004). Ed. by S. Kawabata and D. Perret-Gallix, pp. 293–298. DOI: 10.1016/j.nima.2004.07.104. arXiv: hep-ph/0403253.
- [131] Vladimir P. Gerdt and Daniel Robertz. "A Maple package for computing Grobner bases for linear recurrence relations". In: *Nucl. Instrum. Meth. A* 559 (2006). Ed. by J. Blumlein et al., pp. 215–219. DOI: 10.1016/j.nima. 2005.11.171. arXiv: cs/0509070.
- [132] A. V. Smirnov and Vladimir A. Smirnov. "Applying Grobner bases to solve reduction problems for Feynman integrals". In: *JHEP* 01 (2006), p. 001. DOI: 10.1088/1126-6708/2006/01/001. arXiv: hep-lat/0509187.
- [133] A. V. Smirnov. "An Algorithm to construct Grobner bases for solving integration by parts relations". In: JHEP 04 (2006), p. 026. DOI: 10.1088/1126-6708/2006/04/026. arXiv: hep-ph/0602078.
- [134] A. V. Smirnov and V. A. Smirnov. "S-bases as a tool to solve reduction problems for Feynman integrals". In: *Nucl. Phys. B Proc. Suppl.* 160 (2006). Ed. by J. Blumlein, S. Moch, and T. Riemann, pp. 80–84. DOI: 10.1016/j.nuclphysbps.2006.09.032. arXiv: hep-ph/0606247.
- [135] Mohamed Barakat, Robin Brüser, Claus Fieker, Tobias Huber, and Jan Piclum. "Feynman integral reduction using Gröbner bases". In: *JHEP* 05 (2023), p. 168. DOI: 10.1007/JHEP05(2023) 168. arXiv: 2210.05347 [hep-ph].
- [136] Mohamed Barakat, Robin Brüser, Tobias Huber, and Jan Piclum. "IBP reduction via Gröbner bases in a rational double-shift algebra". In: *PoS* LL2022 (2022), p. 043. DOI: 10.22323/1.416.0043. arXiv: 2207.09275 [hep-ph].
- [137] Matt von Hippel and Matthias Wilhelm. "Refining Integration-by-Parts Reduction of Feynman Integrals with Machine Learning". In: (Feb. 2025). arXiv: 2502.05121 [hep-th].

- [138] Roman N. Lee and Andrei A. Pomeransky. "Critical points and number of master integrals". In: *Journal of High Energy Physics* 2013.11 (Nov. 2013). ISSN: 1029-8479. DOI: 10.1007/jhep11(2013)165. URL: http://dx.doi.org/10.1007/JHEP11(2013)165.
- [139] Thomas Bitoun, Christian Bogner, René Pascal Klausen, and Erik Panzer. "Feynman integral relations from parametric annihilators". In: Letters in Mathematical Physics 109.3 (Aug. 2018), pp. 497–564. ISSN: 1573-0530. DOI: 10.1007/s11005-018-1114-8. URL: http://dx.doi.org/10.1007/s11005-018-1114-8.
- [140] O. V. Tarasov. "Connection between Feynman integrals having different values of the space-time dimension". In: *Phys. Rev. D* 54 (1996), pp. 6479–6490. DOI: 10.1103/PhysRevD.54.6479. arXiv: hep-th/9606018.
- [141] R. N. Lee. "Space-time dimensionality D as complex variable: Calculating loop integrals using dimensional recurrence relation and analytical properties with respect to D". In: *Nucl. Phys. B* 830 (2010), pp. 474–492. DOI: 10.1016/j.nuclphysb.2009.12.025. arXiv: 0911.0252 [hep-ph].
- [142] Johannes M. Henn. "Multiloop integrals in dimensional regularization made simple". In: *Phys. Rev. Lett.* 110 (2013), p. 251601. DOI: 10.1103/PhysRevLett. 110.251601. arXiv: 1304.1806 [hep-th].
- [143] Luise Adams and Stefan Weinzierl. "The ε-form of the differential equations for Feynman integrals in the elliptic case". In: *Phys. Lett.* B781 (2018), pp. 270–278. DOI: 10.1016/j.physletb.2018.04.002. arXiv: 1802.05020 [hep-ph].
- [144] Johannes Broedel, Claude Duhr, Falko Dulat, Brenda Penante, and Lorenzo Tancredi. "From modular forms to differential equations for Feynman integrals". In: KMPB Conference: Elliptic Integrals, Elliptic Functions and Modular Forms in Quantum Field Theory. 2019, pp. 107–131. DOI: 10.1007/978-3-030-04480-0\_6. arXiv: 1807.00842 [hep-th].
- [145] Luise Adams, Ekta Chaubey, and Stefan Weinzierl. "Planar Double Box Integral for Top Pair Production with a Closed Top Loop to all orders in the Dimensional Regularization Parameter". In: Phys. Rev. Lett. 121.14 (2018), p. 142001. DOI: 10.1103/PhysRevLett.121.142001. arXiv: 1804.11144 [hep-ph].
- [146] Christoph Dlapa, Johannes M. Henn, and Fabian J. Wagner. "An algorithmic approach to finding canonical differential equations for elliptic Feynman integrals". In: *JHEP* 08 (2023), p. 120. DOI: 10.1007/JHEP08(2023)120. arXiv: 2211.16357 [hep-ph].
- [147] Hildegard Müller and Stefan Weinzierl. "A Feynman integral depending on two elliptic curves". In: *JHEP* 07 (2022), p. 101. DOI: 10.1007/JHEP07(2022) 101. arXiv: 2205.04818 [hep-th].

- [148] Roman N. Lee. "Reducing differential equations for multiloop master integrals". In: *JHEP* 04 (2015), p. 108. DOI: 10.1007/JHEP04(2015)108. arXiv: 1411.0911 [hep-ph].
- [149] Oleksandr Gituliar and Vitaly Magerya. "Fuchsia: a tool for reducing differential equations for Feynman master integrals to epsilon form". In: *Comput. Phys. Commun.* 219 (2017), pp. 329–338. DOI: 10.1016/j.cpc.2017.05.004. arXiv: 1701.04269 [hep-ph].
- [150] Christoph Meyer. "Algorithmic transformation of multi-loop master integrals to a canonical basis with CANONICA". In: *Comput. Phys. Commun.* 222 (2018), pp. 295–312. DOI: 10.1016/j.cpc.2017.09.014. arXiv: 1705.06252 [hep-ph].
- [151] Roman N. Lee. "Libra: A package for transformation of differential systems for multiloop integrals". In: *Comput. Phys. Commun.* 267 (2021), p. 108058. DOI: 10.1016/j.cpc.2021.108058. arXiv: 2012.00279 [hep-ph].
- [152] Christoph Dlapa, Johannes Henn, and Kai Yan. "Deriving canonical differential equations for Feynman integrals from a single uniform weight integral". In: *JHEP* 05 (2020), p. 025. DOI: 10.1007/JHEP05(2020)025. arXiv: 2002.02340 [hep-ph].
- [153] H.M. Farkas and I. Kra. Riemann Surfaces. Springer New York, NY, 1992.
- [154] Alexander I. Bobenko and Christian Klein. Computational approach to Riemann surfaces. Springer Berlin, Heidelberg, 2011.
- [155] J.D. Fay. Theta Functions on Riemann Surfaces. 1st ed. Springer Berlin, Heidelberg, 1973.
- [156] D. Mumford. Tata Lectures on Theta II. Birkhäuser Boston, 1984.
- [157] D. Mumford. Tata Lectures on Theta I. Birkhäuser Boston, 1983.
- [158] Eric D'Hoker, Martijn Hidding, and Oliver Schlotterer. "Cyclic products of Szegö kernels and spin structure sums. Part I. Hyper-elliptic formulation". In: *JHEP* 05 (2023), p. 073. DOI: 10.1007/JHEP05(2023)073. arXiv: 2211. 09069 [hep-th].
- [159] Konstantin Baune, Johannes Broedel, Egor Im, Artyom Lisitsyn, and Federico Zerbini. "Schottky-Kronecker forms and hyperelliptic polylogarithms". In: *J. Phys. A* 57.44 (2024), p. 445202. DOI: 10.1088/1751-8121/ad8197. arXiv: 2406.10051 [hep-th].
- [160] V. M. Buchstaber, V. Z. Enolski, and D. V. Leykin. "Multi-Dimensional Sigma-Functions". In: arXiv:1208.0990 (2012). DOI: 10.48550/arXiv.1208. 0990. arXiv: 1208.0990 [math-ph].
- [161] H.F. Baker. Abelian Functions: Abel's Theorem and the Allied Theory of Theta Functions. Cambridge University Press, 1996.
- [162] Joseph H. Silverman. *The Arithmetic of Elliptic Curves*. Springer-Verlag New York, 2009.

- [163] Johannes Broedel, Claude Duhr, Falko Dulat, Brenda Penante, and Lorenzo Tancredi. "Elliptic Feynman integrals and pure functions". In: *JHEP* 01 (2019), p. 023. DOI: 10.1007/JHEP01(2019)023. arXiv: 1809.10698 [hep-th].
- [164] M. Bertola. Riemann Surfaces and Theta Functions. http://mypage.concordia.ca/mathstat/bertola/ThetaCourse/ThetaCourse.pdf. 2010.
- [165] Yongbin Ruan Emily Clader. B-Model Gromov-Witten Theory.
- [166] Daniel Huybrechts Mark Gross Dominic Joyce. Calabi-Yau Manifolds and Related Geometries. Heidelberg: Springer Berlin, 2001.
- [167] Claude Duhr. "Mathematical aspects of scattering amplitudes". In: *Theoretical Advanced Study Institute in Elementary Particle Physics: Journeys Through the Precision Frontier: Amplitudes for Colliders.* 2015, pp. 419–476. DOI: 10.1142/9789814678766\_0010. arXiv: 1411.7538 [hep-ph].
- [168] Claude Duhr. "Hopf algebras, coproducts and symbols: an application to Higgs boson amplitudes". In: *JHEP* 08 (2012), p. 043. DOI: 10.1007/JHEP08(2012)043. arXiv: 1203.0454 [hep-ph].
- [169] Claude Duhr, Herbert Gangl, and John R. Rhodes. "From polygons and symbols to polylogarithmic functions". In: *JHEP* 10 (2012), p. 075. DOI: 10.1007/JHEP10(2012)075. arXiv: 1110.0458 [math-ph].
- [170] Hadleigh Frost et al. "Motivic coaction and single-valued map of polylogarithms from zeta generators". In: *J. Phys. A* 57.31 (2024), 31LT01. DOI: 10.1088/1751-8121/ad5edf. arXiv: 2312.00697 [hep-th].
- [171] Par P. Deligne. "Le Groupe Fondamental de la Droite Projective Moins Trois Points". In: *Galois Groups over* Q. New York, NY: Springer US, 1989, pp. 79–297. ISBN: 978-1-4613-9649-9.
- [172] Erik Panzer. "Feynman integrals and hyperlogarithms". PhD thesis. Humboldt U., 2015. DOI: 10.18452/17157. arXiv: 1506.07243 [math-ph].
- [173] Samuel Abreu, Ruth Britto, and Claude Duhr. "The SAGEX review on scattering amplitudes Chapter 3: Mathematical structures in Feynman integrals". In: *J. Phys. A* 55.44 (2022), p. 443004. DOI: 10.1088/1751-8121/ac87de. arXiv: 2203.13014 [hep-th].
- [174] Michael B. Green and Pierre Vanhove. "The Low-energy expansion of the one loop type II superstring amplitude". In: *Phys. Rev. D* 61 (2000), p. 104011. DOI: 10.1103/PhysRevD.61.104011. arXiv: hep-th/9910056.
- [175] Eric D'Hoker, Michael B. Green, and Pierre Vanhove. "On the modular structure of the genus-one Type II superstring low energy expansion". In: *JHEP* 08 (2015), p. 041. DOI: 10.1007/JHEP08(2015)041. arXiv: 1502.06698 [hep-th].
- [176] Francis Brown. "Multiple modular values and the relative completion of the fundamental group of  $\mathcal{M}_{1,1}$ ". In: (2014). arXiv: 1407.5167v4 [math.NT].

- [177] Daniele Dorigoni et al. "Non-holomorphic modular forms from zeta generators". In: *JHEP* 10 (2024), p. 053. DOI: 10.1007/JHEP10(2024)053. arXiv: 2403.14816 [hep-th].
- [178] P. P. Deligne. "Le groupe fondamental de la droite projective moins trois points". In: (Aug. 1989).
- [179] Y. Ihara. "Braids, Galois groups, and some arithmetic functions". In: *Proceedings of the International Congress of Mathematicians* I,II (1991), pp. 99–120.
- [180] N. Takao Y. Ihara. Seminar talk. 1993.
- [181] Hiroshi Tsunogai. "On Some Derivations of Lie Algebras Related to Galois Representations". In: *Publ. Res. Inst. Math. Sci. 31* (1995), pp. 113–134.
- [182] A. B. Goncharov. "Multiple ζ-values, Galois groups, and geometry of modular varieties". In: European Congress of Mathematics, C. Casacuberta, R. M. Miro-Roig, J. Verdera, and S. Xambo-Descamps (2001), pp. 361–392.
- [183] H. Gangl, M. Kaneko, and D. Zagier. "Double zeta values and modular forms". In: *Automorphic forms and zeta functions* (2006), pp. 71–102.
- [184] L.Schneps. "On the Poisson bracket on the free Lie algebra in two generators". In: *J. Lie Theory* 16 (), pp. 19–37.
- [185] Johannes Broedel, Nils Matthes, and Oliver Schlotterer. "Relations between elliptic multiple zeta values and a special derivation algebra". In: *J. Phys.* A49.15 (2016), p. 155203. DOI: 10.1088/1751-8113/49/15/155203. arXiv: 1507.02254 [hep-th].
- [186] Aaron Pollack. Relations between derivations arising from modular forms. https://dukespace.lib.duke.edu/dspace/handle/10161/1281. Undergraduate thesis, Duke University. 2009.
- [187] F. Brown. Talk "Anatomy of the motivic Lie algebra, given at the program "Grothendieck-Teichm" uller Groups, Deformation and Operads" (Newton Institute, Cambridge, UK). https://sms.cam.ac.uk/media/1459610.2013.
- [188] Richard Hain. "Notes on the universal elliptic KZB connection". In: *Pure Appl. Math. Q.* 16.2 (2020), pp. 229–312. ISSN: 1558-8599. DOI: 10.4310/PAMQ.2020.v16.n2.a2. arXiv: 1309.0580 [math.AG].
- [189] Francis Brown. "Zeta elements in depth 3 and the fundamental Lie algebra of the infinitesimal Tate curve". In: Forum Math. Sigma 5 (2017), Paper No. e1, 56. DOI: 10.1017/fms.2016.29. arXiv: 1504.04737 [math.NT].
- [190] Samuel Baumard and Leila Schneps. "On the derivation representation of the fundamental Lie algebra of mixed elliptic motives". In: (2015). arXiv: 1510.05549 [math.QA]. URL: https://arxiv.org/abs/1510.05549.

- [191] Richard Hain and Makoto Matsumoto. "Universal Mixed Elliptic Motives". In: Journal of the Institute of Mathematics of Jussieu 19.3 (Apr. 2018), pp. 663–766. ISSN: 1475-3030. DOI: 10.1017/s1474748018000130. URL: http://dx.doi.org/10.1017/S1474748018000130.
- [192] Jean-Gabriel Luque, Jean-Christophe Novelli, and Jean-Yves Thibon. "Period polynomials and Ihara brackets". In: *J. Lie Theory* 17 (2007), pp. 229–239. arXiv: math/0606301 [math.CO,math.NT].
- [193] Francis Brown. "Multiple Modular Values and the relative completion of the fundamental group of  $M_{1,1}$ ". In: (July 2014). arXiv: 1407.5167 [math.NT].
- [194] Francis C. S. Brown and Andrey Levin. "Multiple Elliptic Polylogarithms". In: (Oct. 2011). arXiv: 1110.6917 [math.NT].
- [195] Johannes Broedel, Carlos R. Mafra, Nils Matthes, and Oliver Schlotterer. "Elliptic multiple zeta values and one-loop superstring amplitudes". In: *JHEP* 07 (2015), p. 112. DOI: 10.1007/JHEP07(2015)112. arXiv: 1412. 5535 [hep-th].
- [196] Johannes Broedel, Claude Duhr, Falko Dulat, and Lorenzo Tancredi. "Elliptic polylogarithms and iterated integrals on elliptic curves. Part I: general formalism". In: *JHEP* 05 (2018), p. 093. DOI: 10.1007/JHEP05(2018)093. arXiv: 1712.07089 [hep-th].
- [197] Moritz Walden and Stefan Weinzierl. "Numerical evaluation of iterated integrals related to elliptic Feynman integrals". In: (Oct. 2020). arXiv: 2010. 05271 [hep-ph].
- [198] Johannes Broedel, Claude Duhr, Falko Dulat, Brenda Penante, and Lorenzo Tancredi. "Elliptic symbol calculus: from elliptic polylogarithms to iterated integrals of Eisenstein series". In: *JHEP* 08 (2018), p. 014. DOI: 10.1007/JHEP08(2018)014. arXiv: 1803.10256 [hep-th].
- [199] Johannes Broedel, Claude Duhr, Falko Dulat, and Lorenzo Tancredi. "Elliptic polylogarithms and iterated integrals on elliptic curves II: an application to the sunrise integral". In: *Phys. Rev. D* 97.11 (2018), p. 116009. DOI: 10.1103/PhysRevD.97.116009. arXiv: 1712.07095 [hep-ph].
- [200] Claude Duhr and Lorenzo Tancredi. "Algorithms and tools for iterated Eisenstein integrals". In: *JHEP* 02 (2020), p. 105. DOI: 10.1007/JHEP02(2020) 105. arXiv: 1912.00077 [hep-th].
- [201] E. Freitag. Siegelsche Modulfunktionen. Springer Berlin, Heidelberg, 1983.
- [202] G. van der Geer. "Siegel Modular Forms and Their Applications". In: *The* 1-2-3 of Modular Forms. Ed. by K. Ranestad. Springer, Berlin, Heidelberg, 2008, pp. 181–245.
- [203] H. Klingen. *Introductory Lectures on Siegel Modular Forms*. Cambridge University Press, 2009.
- [204] A. Andrianov. Introduction to Siegel Modular Forms and Dirichlet Series. Springer New York, NY, 2009.

- [205] Ameya Pitale. Siegel modular forms: Classical approach and representation theory. URL: http://www2.math.ou.edu/~apitale/LNM-pitale.pdf.
- [206] J.-i. Igusa. Theta Functions. Springer Berlin, 1972.
- [207] J.-i. Igusa. "Modular Forms and Projective Invariants". In: Am. J. Math. 89 (1967), p. 817.
- [208] J. Thomae. "Beitrag zur Bestimmung  $\theta(0, ..., 0)$  durch die Klassenmoduln algebraischer Funktionen". In: J. für Reine Angew. Math. 71 (1870), p. 201.
- [209] V. Enolski and P. Richter. "Periods of hyperelliptic integrals expressed in terms of  $\theta$ -constants my means of Thomae formulae". In: *Phil. Trans. R. Soc. A* 366 (2008), p. 1005. DOI: 10.1098/rsta.2007.2059.
- [210] Keno Eilers. "Rosenhain-Thomae formulae for higher genera hyperelliptic curves". In: (2017). DOI: 10.48550/arXiv.1707.08855. arXiv: 1707.08855.
- [211] N. A'Campo. "Tresses, monodromie et le groupe symplectique". In: Comment. Math. Helv. 54.2 (1979), pp. 318–327.
- [212] Hossein Movasati. "Quasi-modular forms attached to Hodge structures". In: (2010). DOI: 10.48550/arXiv.1009.5038. arXiv: 1009.5038.
- [213] Georg Rosenhain. "Abhandlung ueber die Functionen Zweier Variablen mit Vier Perioden, welche die Inversen sind der ultra-elliptischen Integrale erster Klasse". In: Ostwald's Klassiker der Exakten Wissenschaften. Vol. 65. Wilhelm Engelmann, Leipzig, 1895, pp. 1–96.
- [214] Eric D'Hoker and Oliver Schlotterer. "Meromorphic higher-genus integration kernels via convolution over homology cycles". In: (Feb. 2025). arXiv: 2502. 14769 [hep-th].
- [215] Eric D'Hoker, Martijn Hidding, and Oliver Schlotterer. "Constructing polylogarithms on higher-genus Riemann surfaces". In: (June 2023). arXiv: 2306. 08644 [hep-th].
- [216] F. Schottky. "Ueber eine specielle Function, welche bei einer bestimmten linearen Transformation ihres Arguments unverändert bleibt." In: Journal für die reine und angewandte Mathematik 101 (1887), p. 227.
- [217] P.J. Myrberg. "Über die numerische Ausführung der Uniformisierung". In: *Acta Soc. scient. Fenn.* 48 (1920).
- [218] K.-D. Semmler and M. Seppälä. "Numerical Uniformization of Hyperelliptic Curves". In: *Proceedings of the 1995 International Symposium on Symbolic and Algebraic Computation*. ISSAC '95. 1995, p. 208.
- [219] M. Seppälä. "Myrberg's Numerical Uniformization of Hyperelliptic Curves". In: Ann. Acad. Sci. Fenn 29 (2004), p. 3.
- [220] R. A. Hidalgo and M. Seppälä. "Numerical Schottky Uniformizations: Myrberg's Opening Process". In: *Computational Approach to Riemann Surfaces*. Ed. by A. I. Bobenko and C. Klein. Springer Berlin Heidelberg, 2011, p. 195.

- [221] Xin Li. "Myrberg's Numerical Uniformization". en. In: ().
- [222] E. D'Hoker and D.H. Phong. "The geometry of string perturbation theory". In: Rev. Mod. Phys. 60 (1998), p. 917.
- [223] E. D'Hoker, M. B. Green, and B. Pioline. "Higher genus modular graph functions, string invariants, and their exact asymptotics". In: *Commun. Math. Phys.* 366 (2019), p. 927. arXiv: 1712.06135.
- [224] Charles F. Doran, Andrew Harder, Pierre Vanhove, and Eric Pichon-Pharabod. "Motivic Geometry of two-Loop Feynman Integrals". In: *Quart. J. Math. Oxford Ser.* 75.3 (2024), pp. 901–967. DOI: 10.1093/qmath/haae015. arXiv: 2302.14840 [math.AG].
- [225] Francis Brown. "Motivic periods and the projective line minus three points". In: *Proceedings of the ICM 2014*. 2014. arXiv: 1407.5165 [math.NT]. URL: https://api.semanticscholar.org/CorpusID:118359180.
- [226] Claude Duhr, Franziska Porkert, Cathrin Semper, and Sven F. Stawinski. "Self-duality from twisted cohomology". In: *JHEP* 03 (2025), p. 053. DOI: 10.1007/JHEP03(2025)053. arXiv: 2408.04904 [hep-th].
- [227] Axel Kleinschmidt, Franziska Porkert, and Oliver Schlotterer. "UUITP-xx/24 Towards Motivic Coactions at Genus One from Zeta Generators [In Progress]". In: (2025).
- [228] Masaaki Yoshida. Hypergeometric Functions, My Love. en. Ed. by Klas Diederich. Vol. 32. Aspects of Mathematics. Wiesbaden: Vieweg+Teubner Verlag, 1997. ISBN: 978-3-322-90168-2 978-3-322-90166-8. DOI: 10.1007/978-3-322-90166-8. URL: http://link.springer.com/10.1007/978-3-322-90166-8 (visited on 01/06/2023).
- [229] Keiji Matsumoto. "Relative twisted homology and cohomology groups associated with Lauricella's  $F_D$ ". In: (2019). arXiv: 1804.00366 [math.AG]. URL: https://arxiv.org/abs/1804.00366.
- [230] Koji Cho and Keiji Matsumoto. "Intersection theory for twisted cohomologies and twisted Riemann's period relations I". In: *Nagoya Mathematical Journal* 139 (1995), pp. 67–86. DOI: 10.1017/S0027763000005304.
- [231] Kazuhiko Aomoto and Michitake Kita. Theory of Hypergeometric Functions. Springer Monographs in Mathematics. Springer Japan, 2011.
- [232] Hjalte Frellesvig et al. "Decomposition of Feynman Integrals by Multivariate Intersection Numbers". In: Journal of High Energy Physics 2021.3 (Mar. 2021). arXiv:2008.04823 [hep-ph, physics:hep-th], p. 27. ISSN: 1029-8479. DOI: 10.1007/JHEP03(2021)027. URL: http://arxiv.org/abs/2008.04823 (visited on 05/10/2023).
- [233] Michitake Kita and Masaaki Yoshida. "Intersection Theory for Twisted Cycles". en. In: *Math. Nachr.* 166.1 (1994), pp. 287–304. ISSN: 0025584X, 15222616. DOI: 10.1002/mana.19941660122. URL: https://onlinelibrary.wiley.com/doi/10.1002/mana.19941660122 (visited on 09/23/2022).

- [234] Vsevolod Chestnov, Hjalte Frellesvig, Federico Gasparotto, Manoj K. Mandal, and Pierpaolo Mastrolia. "Intersection numbers from higher-order partial differential equations". In: *JHEP* 06 (2023), p. 131. DOI: 10.1007/JHEP06(2023)131. arXiv: 2209.01997 [hep-th].
- [235] Vsevolod Chestnov. "Recent progress in intersection theory for Feynman integrals decomposition." In: *PoS* LL2022 (2022), p. 058. DOI: 10.22323/1.416.0058. arXiv: 2209.01464 [hep-th].
- [236] Vsevolod Chestnov et al. "Macaulay matrix for Feynman integrals: linear relations and intersection numbers". In: *JHEP* 09 (2022), p. 187. DOI: 10. 1007/JHEP09(2022)187. arXiv: 2204.12983 [hep-th].
- [237] Vsevolod Chestnov, Saiei J. Matsubara-Heo, Henrik J. Munch, and Nobuki Takayama. "Restrictions of Pfaffian systems for Feynman integrals". In: *JHEP* 11 (2023), p. 202. DOI: 10.1007/JHEP11(2023)202. arXiv: 2305.01585 [hep-th].
- [238] Keiji Matsumoto. "Intersection numbers for logarithmic k-forms". In: Osaka Journal of Mathematics 35.4 (1998), pp. 873–893.
- [239] Giacomo Brunello et al. "Intersection numbers, polynomial division and relative cohomology". In: *JHEP* 09 (2024), p. 015. DOI: 10.1007/JHEP09(2024) 015. arXiv: 2401.01897 [hep-th].
- [240] Francis Brown. "Periods and Feynman amplitudes". In: (2015). arXiv: 1512. 09265 [math-ph]. URL: https://arxiv.org/abs/1512.09265.
- [241] Francis Brown. "Notes on Motivic Periods". In: (2017). arXiv: 1512.06410 [math.NT]. URL: https://arxiv.org/abs/1512.06410.
- [242] A. B. Goncharov. "Galois symmetries of fundamental groupoids and non-commutative geometry". In: *Duke Math. J.* 128 (2005), p. 209. DOI: 10. 1215/S0012-7094-04-12822-2. arXiv: math/0208144.
- [243] Francis Brown. "Mixed Tate motives over Z". In: *Ann. of Math. (2)* 175.2 (2012), pp. 949–976. ISSN: 0003-486X. DOI: 10.4007/annals.2012.175.2. 10.
- [244] Francis Brown. "On the decomposition of motivic multiple zeta values". In: Galois-Teichmüller theory and arithmetic geometry. Vol. 63. Adv. Stud. Pure Math. Math. Soc. Japan, Tokyo, 2012, pp. 31–58. arXiv: 1102.1310 [math.NT].
- [245] Daniele Dorigoni et al. "Canonicalizing zeta generators: genus zero and genus one". In: (June 2024). arXiv: 2406.05099 [math.QA].
- [246] Vittorio Del Duca et al. "Amplitudes in the Multi-Regge Limit of  $\mathcal{N}{=}4$  SYM". In: *Acta Phys. Polon. Supp.* 12.4 (2019). Ed. by Wojciech Bruzda, Agata Górz-Kudłacz, Krystyna Stankiewicz, and Elżbieta Zachorowska-Such, pp. 961–966. DOI: 10.5506/APhysPolBSupp.12.961. arXiv: 1811.10588 [hep-th].

- [247] Vittorio Del Duca et al. "The seven-gluon amplitude in multi-Regge kinematics beyond leading logarithmic accuracy". In: *JHEP* 06 (2018), p. 116. DOI: 10.1007/JHEP06(2018)116. arXiv: 1801.10605 [hep-th].
- [248] Francis Brown and Clément Dupont. "Single-Valued Integration and Superstring Amplitudes in Genus Zero". In: Communications in Mathematical Physics 382.2 (Feb. 2021), pp. 815–874. ISSN: 1432-0916. DOI: 10.1007/s00220-021-03969-4. URL: http://dx.doi.org/10.1007/s00220-021-03969-4.
- [249] Francis Brown and Clément Dupont. "Lauricella hypergeometric functions, unipotent fundamental groups of the punctured Riemann sphere, and their motivic coactions". In: Nagoya Math. J. 249 (2023), pp. 148–220. DOI: 10. 1017/nmj.2022.27. arXiv: 1907.06603 [math.AG].
- [250] Oliver Schnetz. "Graphical functions and single-valued multiple polylogarithms". In: Commun. Num. Theor. Phys. 08 (2014), pp. 589–675. DOI: 10.4310/CNTP.2014.v8.n4.a1. arXiv: 1302.6445 [math.NT].
- [251] Francis Brown. "Single-valued Motivic Periods and Multiple Zeta Values". In: SIGMA 2 (2014), e25. DOI: 10.1017/fms.2014.18. arXiv: 1309.5309 [math.NT].
- [252] Francis Brown. "A class of non-holomorphic modular forms II: equivariant iterated Eisenstein integrals". In: Forum of Mathematics, Sigma 8 (2020), p. 1. DOI: 10.1017/fms.2020.24. arXiv: 1708.03354 [math.NT].
- [253] Francis Brown and Clément Dupont. "Lauricella Hypergeometric Functions, Unipotent Fundamental Groups of the Punctured Riemann Spehere, and their Motivic Coactions". In: Nagoya Mathematical Journal 249 (Sept. 2022), pp. 148–220. ISSN: 2152-6842. DOI: 10.1017/nmj.2022.27. URL: http://dx.doi.org/10.1017/nmj.2022.27.
- [254] Alexander B. Goncharov, Marcus Spradlin, C. Vergu, and Anastasia Volovich. "Classical Polylogarithms for Amplitudes and Wilson Loops". In: *Phys. Rev. Lett.* 105 (2010), p. 151605. DOI: 10.1103/PhysRevLett.105.151605. arXiv: 1006.5703 [hep-th].
- [255] O. Schlotterer and S. Stieberger. "Motivic Multiple Zeta Values and Super-string Amplitudes". In: J. Phys. A46 (2013), p. 475401. DOI: 10.1088/1751-8113/46/47/475401. arXiv: 1205.1516 [hep-th].
- [256] J. M. Drummond and E. Ragoucy. "Superstring amplitudes and the associator". In: *JHEP* 08 (2013), p. 135. DOI: 10.1007/JHEP08(2013)135. arXiv: 1301.0794 [hep-th].
- [257] Samuel Abreu, Ruth Britto, Claude Duhr, and Einan Gardi. "From multiple unitarity cuts to the coproduct of Feynman integrals". In: *JHEP* 10 (2014), p. 125. DOI: 10.1007/JHEP10(2014)125. arXiv: 1401.3546 [hep-th].

- [258] Erik Panzer and Oliver Schnetz. "The Galois coaction on  $\phi^4$  periods". In: Commun. Num. Theor. Phys. 11 (2017), pp. 657–705. DOI: 10.4310/CNTP. 2017.v11.n3.a3. arXiv: 1603.04289 [hep-th].
- [259] Samuel Abreu, Ruth Britto, Claude Duhr, and Einan Gardi. "Algebraic Structure of Cut Feynman Integrals and the Diagrammatic Coaction". In: *Phys. Rev. Lett.* 119.5 (2017), p. 051601. DOI: 10.1103/PhysRevLett.119. 051601. arXiv: 1703.05064 [hep-th].
- [260] Samuel Abreu, Ruth Britto, Claude Duhr, and Einan Gardi. "Diagrammatic Hopf algebra of cut Feynman integrals: the one-loop case". In: *JHEP* 12 (2017), p. 090. DOI: 10.1007/JHEP12(2017)090. arXiv: 1704.07931 [hep-th].
- [261] Oliver Schnetz. "The Galois coaction on the electron anomalous magnetic moment". In: Commun. Num. Theor. Phys. 12 (2018), pp. 335–354. DOI: 10.4310/CNTP.2018.v12.n2.a4. arXiv: 1711.05118 [math-ph].
- [262] Simon Caron-Huot et al. "The Cosmic Galois Group and Extended Steinmann Relations for Planar  $\mathcal{N}=4$  SYM Amplitudes". In: *JHEP* 09 (2019), p. 061. DOI: 10.1007/JHEP09(2019)061. arXiv: 1906.07116 [hep-th].
- [263] Samuel Abreu, Ruth Britto, Claude Duhr, Einan Gardi, and James Matthew. "Generalized hypergeometric functions and intersection theory for Feynman integrals". In: *PoS* RACOR2019 (2019), p. 067. DOI: 10.22323/1.375.0067. arXiv: 1912.03205 [hep-th].
- [264] Matija Tapušković. "Motivic Galois coaction and one-loop Feynman graphs". In: *Commun. Num. Theor. Phys.* 15.2 (2021), pp. 221–278. DOI: 10.4310/CNTP.2021.v15.n2.a1. arXiv: 1911.01540 [math.AG].
- [265] Omer Gürdoğan. "From integrability to the Galois coaction on Feynman periods". In: *Phys. Rev. D* 103.8 (2021), p. L081703. DOI: 10.1103/PhysRevD. 103.L081703. arXiv: 2011.04781 [hep-th].
- [266] Ruth Britto, Sebastian Mizera, Carlos Rodriguez, and Oliver Schlotterer. "Coaction and double-copy properties of configuration-space integrals at genus zero". In: *JHEP* 05 (2021), p. 053. DOI: 10.1007/JHEP05(2021)053. arXiv: 2102.06206 [hep-th].
- [267] Lance J. Dixon, Omer Gurdogan, Andrew J. McLeod, and Matthias Wilhelm. "Folding Amplitudes into Form Factors: An Antipodal Duality". In: *Phys. Rev. Lett.* 128.11 (2022), p. 111602. DOI: 10.1103/PhysRevLett. 128.111602. arXiv: 2112.06243 [hep-th].
- [268] Michael Borinsky and Oliver Schnetz. "Recursive computation of Feynman periods". In: JHEP 22 (2022), p. 291. DOI: 10.1007/JHEP08(2022) 291. arXiv: 2206.10460 [hep-th].

- [269] Lance J. Dixon, Ömer Gürdoğan, Yu-Ting Liu, Andrew J. McLeod, and Matthias Wilhelm. "Antipodal Self-Duality for a Four-Particle Form Factor". In: *Phys. Rev. Lett.* 130.11 (2023), p. 111601. DOI: 10.1103/PhysRevLett. 130.111601. arXiv: 2212.02410 [hep-th].
- [270] Lance J. Dixon and Yu-Ting Liu. "An eight loop amplitude via antipodal duality". In: *JHEP* 09 (2023), p. 098. DOI: 10.1007/JHEP09(2023)098. arXiv: 2308.08199 [hep-th].
- [271] Lance J. Dixon and Claude Duhr. "Antipodal self-duality of square fishnet graphs". In: (Feb. 2025). arXiv: 2502.00862 [hep-th].
- [272] Pierre Cartier. "La folle journée, de Grothendieck à Connes et Kontsevich. Évolution des notions d'espace et de symétrie". fr. In: *Publications Mathématiques de l'IHÉS* S88 (1998), pp. 23–42. URL: http://www.numdam.org/item/PMIHES\_1998\_\_S88\_\_23\_0/.
- [273] Yasutaka Ihara. "The Galois representation arising from  $\mathbb{P}^1 \{0, 1, \infty\}$  and Tate twists of even degree". In: 1989. URL: https://api.semanticscholar.org/CorpusID:118731503.
- [274] A. B. Goncharov. "Multiple polylogarithms and mixed Tate motives". In: (Mar. 2001). arXiv: math/0103059.
- [275] Francis Brown. "Feynman amplitudes, coaction principle, and cosmic Galois group". In: *Commun. Num. Theor. Phys.* 11 (2017), pp. 453–556. DOI: 10. 4310/CNTP.2017.v11.n3.a1. arXiv: 1512.06409 [math-ph].
- [276] Matthias Wilhelm and Chi Zhang. "Symbology for elliptic multiple polylogarithms and the symbol prime". In: (June 2022). arXiv: 2206.08378 [hep-th].
- [277] Andreas Forum and Matt von Hippel. "A symbol and coaction for higher-loop sunrise integrals". In: *SciPost Phys. Core* 6 (2023), p. 050. DOI: 10. 21468/SciPostPhysCore.6.3.050. arXiv: 2209.03922 [hep-th].
- [278] Alexander Kristensson, Matthias Wilhelm, and Chi Zhang. "Elliptic Double Box and Symbology Beyond Polylogarithms". In: *Phys. Rev. Lett.* 127.25 (2021), p. 251603. DOI: 10.1103/PhysRevLett.127.251603. arXiv: 2106. 14902 [hep-th].
- [279] Andrew McLeod, Roger Morales, Matt von Hippel, Matthias Wilhelm, and Chi Zhang. "An infinite family of elliptic ladder integrals". In: *JHEP* 05 (2023), p. 236. DOI: 10.1007/JHEP05(2023) 236. arXiv: 2301.07965 [hep-th].
- [280] Anne Spiering, Matthias Wilhelm, and Chi Zhang. "All planar two-loop amplitudes in maximally supersymmetric Yang-Mills theory". In: (June 2024). arXiv: 2406.15549 [hep-th].
- [281] I. M. Gelfand. "General theory of hypergeometric functions". In: *Dokl. Akad. Nauk SSSR* 288.1 (1986), pp. 14–18. ISSN: 0002-3264.

- [282] I. M. Gel'fand and A. V. Zelevinskii. "Algebraic and combinatorial aspects of the general theory of hypergeometric functions". In: Functional Analysis and Its Applications 20.3 (July 1986), pp. 183–197. ISSN: 1573-8485. DOI: 10.1007/BF01078470. URL: https://doi.org/10.1007/BF01078470.
- [283] Kazuhiko Aomoto. "Equations aux différences linéaires et les intégrales des fonctions multiformes, I.Théorème d'existence". In: *Proceedings of the Japan Academy* 50.7 (1974), pp. 413–415. DOI: 10.3792/pja/1195518895. URL: https://doi.org/10.3792/pja/1195518895.
- [284] K. Mimachi. "Intersection Numbers for Twisted Cycles and the Connection Problem Associated with the Generalized Hypergeometric Function  $_{n+1}F_n$ ". en. In: International Mathematics Research Notices (July 2010), rnq131. ISSN: 1073-7928, 1687-0247. DOI: 10.1093/imrn/rnq131. URL: https://academic.oup.com/imrn/article-lookup/doi/10.1093/imrn/rnq131 (visited on 07/14/2023).
- [285] Yoshiaki Goto. "Intersection numbers and twisted period relations for the generalized hypergeometric function  $_{m+1}F_m$ ". In: (). arXiv: 1406.7464 [math.AG].
- [286] S. I. Bezrodnykh. "Analytic continuation of the Appell function F 1 and integration of the associated system of equations in the logarithmic case". en. In: Computational Mathematics and Mathematical Physics 57.4 (Apr. 2017), pp. 559–589. ISSN: 0965-5425, 1555-6662. DOI: 10.1134/S0965542517040042. URL: http://link.springer.com/10.1134/S0965542517040042 (visited on 06/01/2023).
- [287] Samuel Abreu, Ruth Britto, Claude Duhr, Einan Gardi, and James Matthew. "Diagrammatic Coaction of Two-Loop Feynman Integrals". In: *PoS* RAD-COR2019 (2020), p. 065. DOI: 10.22323/1.375.0065. arXiv: 1912.06561 [hep-th].
- [288] Mathieu Giroux, Andrzej Pokraka, Franziska Porkert, and Yoann Sohnle. "Looping the loops: a tale of elliptic dual Feynman integrals". In: *PoS* RAD-COR2023 (2024), p. 033. DOI: 10.22323/1.432.0033. arXiv: 2309.04592 [hep-th].
- [289] Sergio L. Cacciatori and Pierpaolo Mastrolia. "Intersection Numbers in Quantum Mechanics and Field Theory". In: (2022). arXiv: 2211.03729 [hep-th]. URL: https://arxiv.org/abs/2211.03729.
- [290] Amedeo Primo and Lorenzo Tancredi. "On the maximal cut of Feynman integrals and the solution of their differential equations". In: *Nucl. Phys. B* 916 (2017), pp. 94–116. DOI: 10.1016/j.nuclphysb.2016.12.021. arXiv: 1610.08397 [hep-ph].
- [291] Amedeo Primo and Lorenzo Tancredi. "Maximal cuts and differential equations for Feynman integrals. An application to the three-loop massive banana graph". In: *Nucl. Phys. B* 921 (2017), pp. 316–356. DOI: 10.1016/j.nuclphysb.2017.05.018. arXiv: 1704.05465 [hep-ph].

- [292] Jorrit Bosma, Mads Sogaard, and Yang Zhang. "Maximal Cuts in Arbitrary Dimension". In: *JHEP* 08 (2017), p. 051. DOI: 10.1007/JHEP08(2017)051. arXiv: 1704.04255 [hep-th].
- [293] R. P. Feynman. "Quantum Theory of Gravitation". In: *Acta Physica Polonica* 24 (Dec. 1963). URL: https://www.osti.gov/biblio/4077804.
- [294] R. P. Feynman. "Closed Loop and Tree Diagrams". In: Magic Without Magic. Ed. by J. R. Klauder. Reprinted in Selected Papers of Richard Feynman, ed. L. M. Brown, World Scientific, Singapore, 2000, p. 867. San Francisco: Freeman, 1972, p. 355.
- [295] David Broadhurst and David P. Roberts. "Quadratic relations between Feynman integrals". In: *PoS* LL2018 (2018), p. 053. DOI: 10.22323/1.303.0053.
- [296] Yajun Zhou. "Wronskian factorizations and Broadhurst-Mellit determinant formulae". In: *Commun. Num. Theor. Phys.* 12 (2018), pp. 355–407. DOI: 10.4310/CNTP.2018.v12.n2.a5. arXiv: 1711.01829 [math.CA].
- [297] Yajun Zhou. "Wick rotations, Eichler integrals, and multi-loop Feynman diagrams". In: Commun. Num. Theor. Phys. 12 (2018), pp. 127–192. DOI: 10.4310/CNTP.2018.v12.n1.a5. arXiv: 1706.08308 [math.NT].
- [298] Yajun Zhou. "Some algebraic and arithmetic properties of Feynman diagrams". In: KMPB Conference: Elliptic Integrals, Elliptic Functions and Modular Forms in Quantum Field Theory. 2019, pp. 485–509. DOI: 10.1007/978-3-030-04480-0\_19. arXiv: 1801.05555 [math.NT].
- [299] Yajun Zhou. "On Laporta's 4-loop sunrise formulae". In: *Ramanujan J.* 50.3 (2019), pp. 465–503. DOI: 10.1007/s11139-018-0090-z. arXiv: 1801.02182 [math.CA].
- [300] Javier Fresán, Claude Sabbah, and Jeng-Daw Yu. "Quadratic relations between Bessel moments". In: *Algebra and Number Theory* 17.3 (Apr. 2023), pp. 541–602. ISSN: 1937-0652. DOI: 10.2140/ant.2023.17.541. URL: http://dx.doi.org/10.2140/ant.2023.17.541.
- [301] Jacob L. Bourjaily, Yang-Hui He, Andrew J. Mcleod, Matt Von Hippel, and Matthias Wilhelm. "Traintracks through Calabi-Yau Manifolds: Scattering Amplitudes beyond Elliptic Polylogarithms". In: *Phys. Rev. Lett.* 121.7 (2018), p. 071603. DOI: 10.1103/PhysRevLett.121.071603. arXiv: 1805.09326 [hep-th].
- [302] Roman N. Lee. "Symmetric  $\epsilon$  and ( $\epsilon$  + 1/2)-forms and quadratic constraints in "elliptic" sectors". In: *JHEP* 10 (2018), p. 176. DOI: 10.1007/JHEP10(2018)176. arXiv: 1806.04846 [hep-ph].
- [303] Roman N. Lee and Andrei A. Pomeransky. "Differential equations, recurrence relations, and quadratic constraints for *L*-loop two-point massive tadpoles and propagators". In: *JHEP* 08 (2019), p. 027. DOI: 10.1007/JHEP08(2019) 027. arXiv: 1904.12496 [hep-ph].

- [304] Jiaqi Chen, Bo Feng, and Li Lin Yang. "Intersection theory rules symbology". In: *Sci. China Phys. Mech. Astron.* 67.2 (2024), p. 221011. DOI: 10.1007/s11433-023-2239-8. arXiv: 2305.01283 [hep-th].
- [305] Jiaqi Chen and Bo Feng. "Notes on Selection Rules of Canonical Differential Equations and Relative Cohomology". In: (Sept. 2024). arXiv: 2409.12663 [hep-th].
- [306] Pierre Deligne. "Le groupe fondamental de la droite projective moins trois points". In: *Galois Groups over* Q. Vol. 16. Math. Sci. Res. Inst. Publ. Springer, 1989, pp. 79–297.
- [307] Shounak De and Andrzej Pokraka. "Cosmology meets cohomology". In: *JHEP* 03 (2024), p. 156. DOI: 10.1007/JHEP03(2024)156. arXiv: 2308.03753 [hep-th].
- [308] Mathieu Giroux and Andrzej Pokraka. "Loop-by-loop differential equations for dual (elliptic) Feynman integrals". In: *JHEP* 03 (2023), p. 155. DOI: 10.1007/JHEP03(2023)155. arXiv: 2210.09898 [hep-th].
- [309] Matthieu Deneufchâtel, Gérard H.E. Duchamp, Vincel Hoang Ngoc Minh, and Allan I. Solomon. "Independence of hyperlogarithms over function fields via algebraic combinatorics." In: Lecture Notes in Computer Science, Volume 6742 (2011). May 2011. URL: https://hal.science/hal-00558773.
- [310] Sebastian Pögel, Xing Wang, Stefan Weinzierl, Konglong Wu, and Xiaofeng Xu. "Self-dualities and Galois symmetries in Feynman integrals". In: (July 2024). arXiv: 2407.08799 [hep-th].
- [311] Claude Duhr and Sara Maggio. "Feynman integrals, elliptic integrals and two-parameter K3 surfaces". In: (Feb. 2025). arXiv: 2502.15326 [hep-th].
- [312] Taushif Ahmed, Ekta Chaubey, Mandeep Kaur, and Sara Maggio. "Two-loop non-planar four-point topology with massive internal loop". In: *JHEP* 05 (2024), p. 064. DOI: 10.1007/JHEP05(2024)064. arXiv: 2402.07311 [hep-th].
- [313] Johannes Broedel et al. "An analytic solution for the equal-mass banana graph". In: *JHEP* 09 (2019), p. 112. DOI: 10.1007/JHEP09(2019)112. arXiv: 1907.03787 [hep-th].
- [314] Pierre Lochak, Nils Matthes, and Leila Schneps. "Elliptic Multizetas and the Elliptic Double Shuffle Relations". In: *International Mathematics Research Notices* 2021.1 (Apr. 2020), pp. 695–753. ISSN: 1073-7928. DOI: 10.1093/imrn/rnaa060. URL: https://doi.org/10.1093/imrn/rnaa060.
- [315] Nils Matthes. "On the algebraic structure of iterated integrals of quasimodular forms". In: Algebra & Number Theory 11.9 (2017), pp. 2113–2130. DOI: 10.2140/ant.2017.11.2113. URL: https://doi.org/10.2140/ant.2017.11.2113.

- [316] Yongbin Ruan, Yingchun Zhang, and Jie Zhou. "Genus Two Siegel Quasi-Modular Forms and Gromov-Witten Theory of Toric Calabi-Yau Three-folds". In: (2023). DOI: 10.1007/s00220-022-04534-3. arXiv: 1911.07204.
- [317] R.N. Lee. "Space-time dimensionality D as complex variable: Calculating loop integrals using dimensional recurrence relation and analytical properties with respect to D". In: Nuclear Physics B 830.3 (2010), pp. 474-492. ISSN: 0550-3213. DOI: https://doi.org/10.1016/j.nuclphysb.2009. 12.025. URL: https://www.sciencedirect.com/science/article/pii/S0550321309006828.
- [318] O. V. Tarasov. "Connection between Feynman integrals having different values of the space-time dimension". In: *Phys. Rev. D* 54 (1996), pp. 6479–6490. DOI: 10.1103/PhysRevD.54.6479. arXiv: hep-th/9606018.
- [319] O. V. Tarasov. "Generalized recurrence relations for two loop propagator integrals with arbitrary masses". In: *Nucl. Phys. B* 502 (1997), pp. 455–482. DOI: 10.1016/S0550-3213(97)00376-3. arXiv: hep-ph/9703319.
- [320] Sebastian Mizera and Simon Telen. "Landau discriminants". In: *JHEP* 08 (2022), p. 200. DOI: 10.1007/JHEP08(2022) 200. arXiv: 2109.08036 [math-ph].
- [321] Michael Bogner. "On differential operators of Calabi-Yau type". PhD thesis. Johannes Gutenberg-Universität Mainz, 2012.
- [322] Johannes Broedel, Claude Duhr, Falko Dulat, and Lorenzo Tancredi. "Elliptic polylogarithms and iterated integrals on elliptic curves. Part I: general formalism". In: *Journal of High Energy Physics* 2018.5 (May 2018). ISSN: 1029-8479. DOI: 10.1007/jhep05(2018)093. URL: http://dx.doi.org/10.1007/JHEP05(2018)093.
- [323] Benjamin Enriquez and Federico Zerbini. "Elliptic Hyperlogarithms". In: (2023). arXiv: 2307.01833 [math.AG].
- [324] Par P Deligne. "Le groupe fondamental de la droite projective moins trois points". In: Galois Groups over Q: Proceedings of a Workshop Held March 23–27, 1987. Springer. 1989, pp. 79–297.
- [325] G. Heinrich et al. "Numerical scattering amplitudes with pySecDec". In: Comput. Phys. Commun. 295 (2024), p. 108956. DOI: 10.1016/j.cpc. 2023.108956. arXiv: 2305.19768 [hep-ph].
- [326] Katsuhisa Mimachi and Masaaki Yoshida. "Intersection numbers of twisted cycles and the correlation functions of the conformal field theory. 2." In: Commun. Math. Phys. 234 (2003), pp. 339–358. DOI: 10.1007/s00220-002-0766-4. arXiv: math/0208097.
- [327] Indranil Halder and Daniel L. Jafferis. "Double winding condensate CFT". In: JHEP 05 (2024), p. 189. DOI: 10.1007/JHEP05(2024)189. arXiv: 2308. 11702 [hep-th].

- [328] Sergei Derkachov, Vladimir Kazakov, and Enrico Olivucci. "Basso-Dixon Correlators in Two-Dimensional Fishnet CFT". In: *JHEP* 04 (2019), p. 032. DOI: 10.1007/JHEP04(2019)032. arXiv: 1811.10623 [hep-th].
- [329] S. E. Derkachev, A. V. Ivanov, and L. A. Shumilov. "Mellin-Barnes Transformation for Two-Loop Master-Diagram". In: *J. Math. Sci.* 264.3 (2022), pp. 298–312. DOI: 10.1007/s10958-022-05998-3. arXiv: 2303.09203 [hep-th].
- [330] Florian Loebbert and Sven F. Stawinski. "Conformal four-point integrals: recursive structure, Toda equations and double copy". In: *JHEP* 11 (2024), p. 092. DOI: 10.1007/JHEP11(2024)092. arXiv: 2408.15331 [hep-th].
- [331] J. M. Drummond, J. Henn, V. A. Smirnov, and E. Sokatchev. "Magic identities for conformal four-point integrals". In: *JHEP* 01 (2007), p. 064. DOI: 10.1088/1126-6708/2007/01/064. arXiv: hep-th/0607160.
- [332] M. Gross, D. Huybrechts, and D. Joyce. Calabi-Yau manifolds and related geometries. Universitext. Lectures from the Summer School held in Nordfjordeid, June 2001. Springer-Verlag, Berlin, 2003, pp. viii+239. ISBN: 3-540-44059-3. DOI: 10.1007/978-3-642-19004-9. URL: https://doi.org/10.1007/978-3-642-19004-9.
- [333] Luke Corcoran, Florian Loebbert, and Julian Miczajka. "Yangian Ward identities for fishnet four-point integrals". In: *JHEP* 04 (2022), p. 131. DOI: 10.1007/JHEP04(2022)131. arXiv: 2112.06928 [hep-th].
- [334] F. Beukers and G. Heckman. "Monodromy for the hypergeometric function  $_nF_{n-1}$ ". In: *Invent. Math.* 95.2 (1989), pp. 325–354. ISSN: 0020-9910,1432-1297. DOI: 10.1007/BF01393900. URL: https://doi.org/10.1007/BF01393900.
- [335] Chuck Doran. "Picard–Fuchs Uniformization and Modularity of the Mirror Map". In: Comm. Math. Phys. 212 (2000), pp. 625–647.
- [336] Michael Bogner. "Algebraic characterization of differential operators of Calabi-Yau type". In: (2013). arXiv: 1304.5434 [math.AG].
- [337] Saiei-Jaeyeong Matsubara-Heo, Sebastian Mizera, and Simon Telen. Four Lectures on Euler Integrals. 2023. arXiv: 2306.13578 [math-ph].
- [338] Michitake Kita and Masaaki Yoshida. "Intersection Theory for Twisted Cycles II Degenerate Arrangements". en. In: *Math. Nachr.* 168.1 (Nov. 2006), pp. 171–190. ISSN: 0025584X, 15222616. DOI: 10.1002/mana.19941680111. URL: https://onlinelibrary.wiley.com/doi/10.1002/mana.19941680111 (visited on 09/23/2022).
- [339] Katsuhisa Mimachi, Hiroyuki Ochiai, and Masaaki Yoshida. "Intersection theory for loaded cycles IV— resonant cases". en. In: *Math. Nachr.* 260.1 (Nov. 2003), pp. 67–77. ISSN: 0025-584X, 1522-2616. DOI: 10.1002/mana. 200310105. URL: https://onlinelibrary.wiley.com/doi/10.1002/mana.200310105 (visited on 09/28/2022).

- [340] Yoshiaki Goto. "Intersection Numbers and Twisted Period Relations for the Generalized Hypergeometric Function  $_{m+1}F_m$ ". en. In: Kyushu Journal of Mathematics 69.1 (2015), pp. 203-217. ISSN: 1340-6116, 1883-2032. DOI: 10.2206/kyushujm.69.203. URL: https://www.jstage.jst.go.jp/article/kyushujm/69/1/69\_203/\_article (visited on 07/14/2023).
- [341] Yoshiaki Goto and Kenji Koike. Picard-Vessiot groups of Lauricella's hypergeometric systems  $E_C$  and Calabi-Yau varieties arising integral representations. arXiv:1807.10890 [math]. July 2018. DOI: 10.1112/jlms.12311. URL: http://arxiv.org/abs/1807.10890 (visited on 09/19/2023).
- [342] Yoshiaki Goto. "Intersection numbers of twisted cycles and cocycles for degenerate arrangements". In: (2018). arXiv: 1805.01714 [math.AG]. URL: https://arxiv.org/abs/1805.01714.
- [343] Yoshiaki Goto. "Lauricella's  $F_C$  with finite irreducible monodromy group". In: (2020). arXiv: 1905.00250 [math.CA]. URL: https://arxiv.org/abs/1905.00250.
- [344] YOSHIAKI GOTO. "Twisted Cycles and Twisted Period Relations for Lauricella's Hypergeometric Function FC". In: *International Journal of Mathematics* 24.12 (Nov. 2013), p. 1350094. ISSN: 1793-6519. DOI: 10.1142/s0129167x13500948. URL: http://dx.doi.org/10.1142/s0129167X13500948.
- [345] Yoshiaki Goto and Kenji Koike. "Picard-Vessiot groups of Lauricella's hypergeometric systems EC and Calabi-Yau varieties arising integral representations". In: *Journal of the London Mathematical Society* 102.1 (Apr. 2020), pp. 22–42. ISSN: 1469-7750. DOI: 10.1112/jlms.12311. URL: http://dx.doi.org/10.1112/jlms.12311.
- [346] Masaaki Yoshida. "Intersection Theory for Twisted Cycles III Determinant Formulae". de. In: *Mathematische Nachrichten* 214.1 (June 2000), pp. 173–185. ISSN: 0025-584X, 1522-2616. DOI: 10.1002/1522-2616(200006) 214:1<173::AID-MANA173>3.0.CO; 2-0. URL: https://onlinelibrary.wiley.com/doi/10.1002/1522-2616(200006) 214:1%3C173::AID-MANA173%3E3.0.CO; 2-0 (visited on 09/28/2022).